frontiers | Research Topics

# Halophytes: Salt stress tolerance mechanisms and potential use

**Edited by**
Raoudha Abdellaoui, Esmaeil Bakhshandeh, Fayçal Boughalleb, Ali El-Keblawy, Amr Adel Elkelish and Hedi Mighri

**Published in**
Frontiers in Plant Science

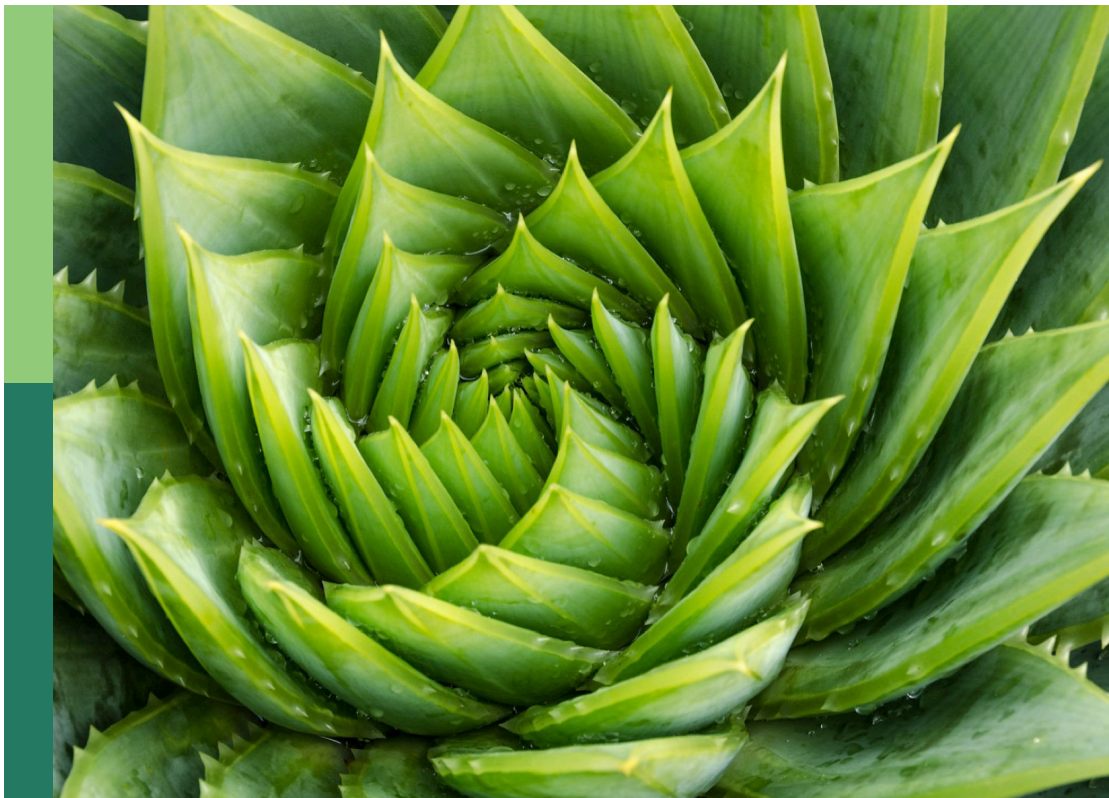

ISSN 1664-8714
ISBN 978-2-8325-2930-0
DOI 10.3389/978-2-8325-2930-0

## About Frontiers

Frontiers is more than just an open access publisher of scholarly articles: it is a pioneering approach to the world of academia, radically improving the way scholarly research is managed. The grand vision of Frontiers is a world where all people have an equal opportunity to seek, share and generate knowledge. Frontiers provides immediate and permanent online open access to all its publications, but this alone is not enough to realize our grand goals.

## Frontiers journal series

The Frontiers journal series is a multi-tier and interdisciplinary set of open-access, online journals, promising a paradigm shift from the current review, selection and dissemination processes in academic publishing. All Frontiers journals are driven by researchers for researchers; therefore, they constitute a service to the scholarly community. At the same time, the *Frontiers journal series* operates on a revolutionary invention, the tiered publishing system, initially addressing specific communities of scholars, and gradually climbing up to broader public understanding, thus serving the interests of the lay society, too.

## Dedication to quality

Each Frontiers article is a landmark of the highest quality, thanks to genuinely collaborative interactions between authors and review editors, who include some of the world's best academicians. Research must be certified by peers before entering a stream of knowledge that may eventually reach the public - and shape society; therefore, Frontiers only applies the most rigorous and unbiased reviews. Frontiers revolutionizes research publishing by freely delivering the most outstanding research, evaluated with no bias from both the academic and social point of view. By applying the most advanced information technologies, Frontiers is catapulting scholarly publishing into a new generation.

## What are Frontiers Research Topics?

Frontiers Research Topics are very popular trademarks of the *Frontiers journals series*: they are collections of at least ten articles, all centered on a particular subject. With their unique mix of varied contributions from Original Research to Review Articles, Frontiers Research Topics unify the most influential researchers, the latest key findings and historical advances in a hot research area.

Find out more on how to host your own Frontiers Research Topic or contribute to one as an author by contacting the Frontiers editorial office: frontiersin.org/about/contact

# Halophytes: Salt stress tolerance mechanisms and potential use

**Topic editors**

Raoudha Abdellaoui — Institut des Régions Arides, Tunisia
Esmaeil Bakhshandeh — Sari Agricultural Sciences and Natural Resources University, Iran
Fayçal Boughalleb — Institut des Régions Arides, Tunisia
Ali El-Keblawy — University of Sharjah, United Arab Emirates
Amr Adel Elkelish — Suez Canal University, Egypt
Hedi Mighri — Institut des Régions Arides, Tunisia

**Citation**

Abdellaoui, R., Bakhshandeh, E., Boughalleb, F., El-Keblawy, A., Elkelish, A. A., Mighri, H., eds. (2023). *Halophytes: Salt stress tolerance mechanisms and potential use*. Lausanne: Frontiers Media SA. doi: 10.3389/978-2-8325-2930-0

# Table of contents

frontiers | Frontiers in Plant Science

TYPE Editorial
PUBLISHED 22 June 2023
DOI 10.3389/fpls.2023.1218184



OPEN ACCESS

EDITED AND REVIEWED BY
Oscar Vicente,
Universitat Politècnica de València, Spain

*CORRESPONDENCE
Raoudha Abdellaoui
raoudhamabdellaoui@yahoo.com

RECEIVED 06 May 2023
ACCEPTED 05 June 2023
PUBLISHED 22 June 2023

CITATION
Abdellaoui R, Elkelish A, El-Keblawy A, Mighri H, Boughalleb F and Bakhshandeh E (2023) Editorial: Halophytes: salt stress tolerance mechanisms and potential use. *Front. Plant Sci.* 14:1218184. doi: 10.3389/fpls.2023.1218184



# Editorial: Halophytes: salt stress tolerance mechanisms and potential use

Raoudha Abdellaoui [1]*, Amr Elkelish [2,3], Ali El-Keblawy [4], Hedi Mighri [1], Fayçal Boughalleb [1] and Esmaeil Bakhshandeh [5]

[1]Laboratory of Rangeland Ecosystems and Valorization of Spontaneous Plants LR16IRA03, Arid Regions Institute, University of Gabès, Médenine, Tunisia, [2]Biology Department, College of Science, Imam Mohammad Ibn Saud Islamic University (IMSIU), Riyadh, Saudi Arabia, [3]Botany and Microbiology Department, Faculty of Science, Suez Canal University, Ismailia, Egypt, [4]Department of Applied Biology, College of Sciences, University of Sharjah, Sharjah, United Arab Emirates, [5]Genetics and Agricultural Biotechnology Institute of Tabarestan & Sari Agricultural Sciences and Natural Resources University, Sari, Iran

KEYWORDS

**soil salinization, osmotic stress-associated traits, biochemical adaptation, phenotypic plasticity and resilience, salinity stress alleviation, biosaline agriculture**

Editorial on the Research Topic
Halophytes: salt stress tolerance mechanisms and potential use

## 1 Introduction

Drought and salinity are among the principal environmental factors restricting plant growth, reducing productivity in numerous plant species. Both rising sea levels and increasing temperature contribute to this salinization; a common problem predicted to become more widespread worldwide. About 3.6 billion of the 5.2 billion hectares of arid lands used for agriculture suffer from erosion, salinization, and soil degradation (Riadh et al., 2010).

In addition, climate change over the coming decades is expected to decrease annual precipitation in semi-arid, arid, and desert regions. As a result, good quality water would be increasingly reserved for urban and drinking purposes, so brackish and saline water could be an alternative for irrigation (Shabala, 2013). Moreover, it is estimated that by 2050, the world population will increase to 9.7 billion, which would necessitate more than 70% of food production, causing additional pressure on the arable lands (Calone et al., 2021).

To achieve such goal the salt-affected, degraded, and marginalized regions should be valorized and used as promising areas for valuable resources, especially in arid lands. The restoration and rehabilitation of salt-affected lands for crop production can be achieved through several methods, including halophytes and extremophiles that respond to salt stress factors in the short term by complex accommodation processes and in the long term by developing adaptation strategies.

Halophytes have strong potential for developing saline agriculture strategies and could later improve the natural ecosystem. These plants are adapted to growing in high-salt environments; they have unique mechanisms that allow them to survive and thrive in extreme saline conditions. Planting halophytes in salt-affected areas can improve soil quality, restore biodiversity, produce valuable products, such as animal feeds and renewable

energy sources, and save freshwater, scarce depleted natural resources. They have been used successfully to restore wetlands, salt marshes, and other coastal habitats. Halophytes capable of growing and reproducing in extremely saline conditions could depict a treasure trove of genes used to improve the production of crops in saline lands and to develop biosaline agriculture (Cheeseman, 2015; Ventura et al., 2015).

This Research Topic is to promote biosaline agriculture and maximize the value of their products by identifying relevant traits that can be used to understand and investigate halophytes' salt tolerance mechanisms. Furthermore, despite knowledge gaps, exploring the genetic potential of halophytes seems an important tactic to enlighten on the adaptive mechanisms and unveil the threshold environment of halophytes for survival and strengthen plant productivity under saline conditions.

In this special Research Topic of Frontiers in Plant Science, the articles concentrated on three main themes: (1) mechanisms and strategies for adaptations to salinity, (2) alleviation of salinity stress, and (3) sustainable utilization of halophytes for restoration of salt-affected lands.

## 2 Mechanisms and strategies of plant adaptations to salinity

### 2.1 Metabolomic approaches

Plants adopt several strategies for survival the salt-affected lands. For example, the multipurpose tree *Gliricidia sepium* adopts a salt-excluding strategy through leaf defoliation and limiting salt absorption in the roots. Besides, the metabolomics analysis helped postulate that lignin accumulation in the cell wall, accumulation of some phytosterols that adjust membrane structure and characteristics, and lysine biosynthesis play a role in promoting the salinity adaptation response (Braga et al.). In another article, morpho-physiological approaches revealed the main survival strategy of the Semi-mangrove *Clerodendrum inerme* to salinity through reshaping its metabolic and ion profiles. Besides, this species adapted to salinity stress at the seedling stages by altering its metabolism of nucleotides, enzymes, transcription factors, amino acids, plant hormones, and carbohydrates. By rebalancing the energy allocation between growth and stress tolerance, *C. inerme* moderates its development rate to withstand both short- and long-term salt adversity (Liang et al.).

### 2.2 Molecular and genomic approaches

Salinity stress is a major environmental factor that negatively affects plant growth and productivity. In response to salt stress, plants undergo a range of physiological, molecular, and genomic changes. Molecular and genomic approaches have been employed to study the mechanisms underlying the response of plants to salinity stress.

Wang et al. investigated *Sesuvium portulacastrum*'s salt tolerance mechanism. RNA-Seq identified DEGs in salt-stressed plant roots and leaves. Na is taken in by cyclic nucleotide-gated channels (CNGCs), whereas $Na^+/H^+$ exchangers (NHXs) push it out and store it. Glutathione metabolism scavenged reactive oxygen species and osmoprotected soluble sugar and proline.

On the other hand, Jiang et al. studied *Chenopodium quinoa*, which is categorized as a halophyte with exceptional nutritional qualities. Quinoa had 26 CqCrRLK1L and 18 CqRALF genes. After salt treatment, three CqCrRLK1L genes were substantially up-regulated by transcriptomic profiling. Biochemical analysis showed that CqRALF15 physically interacts with CrRLK1L, CqFER, and AtFER proteins. Arabidopsis overexpressing CqRALF15 bleaches leaves more under salt stress.

The molecular and genomic approaches on economic crops are fulfilled in two successive years by evaluating 30 cotton genotypes under drought and/or heat stresses. Results showed that all the morphological and quality characteristics, for instance, boll weight, fiber fineness, fiber strength, and fiber length are significantly decreased under drought and heat. However, superoxide dismutase (SOD), ginning out turn percentage (GOT %), and flavonoids increased particularly (Farooq et al.).

Finally, Rice, a salt-sensitive plant, was extensively studied by Wang et al. and using a Genome-wide association study (GWAS). They identified 65 Quantitative Trait Locus (QTLs) associated with salt tolerance. They found that LOC_Os06g47970, LOC_Os06g47820, LOC_Os06g47720, and LOC_Os06g47850 were found to be related to salinity stress. They suggested that these candidate genes are helpful in rice breeding programs.

Overall, molecular and genomic approaches have provided valuable insights into the mechanisms underlying the response of plants to salt stress. These approaches have identified key genes and pathways that are involved in response to salt stress, which could be targeted to improve plant tolerance to salinity stress.

### 2.3 Alleviation of salinity stress

Several types of phytohormones and endophytic microbes, and arbuscular mycorrhizal fungi can help plants alleviate salinity stress. Jasmonic acid (JA), a phytohormone, alleviated salinity stress in wheat by regulating morphological, biochemical, and genetic attributes (Sheteiwy et al.). The authors demonstrated that JA modulates the salinity effect in wheat plants through different pathways, including improving ion homeostasis that reduces ion toxicity, recovering chloroplast ultrastructure that increases the photosynthesis efficiency, and stimulating antioxidant defense machinery that scavengers ROS accumulation. In another study, Al-Elwany et al. reported that the foliar spraying folic acid (FA) mitigated the salinity effect in the medicinal plant *Plectranthus amboinicus*. FA played a key role in enhancing photosynthetic efficiency, pigment contents, leaf osmoprotectant compounds, and the concentrations of soluble sugars, free amino acids, proline, and total phenolics in *Plectranthus amboinicus* plants subjected to salinity stress. Such improvement in the physiological and biochemical attributes improved the growth and production of essential oil content of salt-stressed plants.

In an interesting approach, Selim et al. used magnetically treated seawater to reduce the salt effect on wheat plants. Such treatment improved wheat's seed germination, growth, and yield attributes under saline conditions by modulating physiological and anatomical attributes. Wheat irrigated with magnetic-treated seawater improved leaf water deficit, abscisic acid content, and transpiration rate. Irrigation with seawater treated with a magnetic field is a promising way to mitigate the salinity effects. However, further studies are needed to explore possible mechanisms behind this technology.

## 3 Sustainable utilization of halophytes

The salinization of soil and water severely restricts sustainable agricultural development in semiarid and arid regions. Halophytes irrigated with seawater and cultivated in salt-affected soils could be a promising solution for freshwater scarcity, soil salinization, and fodder shortages. For example, Wang et al. assessed the forage nutritional value and salt removal capacity of the halophyte *Salsola salsa* under varied salinity levels in the arid lands of China. The researchers found that salinity increased the crude protein content and mineral nutrition and decreased the fiber concentration, increasing the forage nutritional value of *S. salsa*. Interestingly, this halophyte can bioconcentrates salts in its tissues, rehabilitating salt-affected soil. The study concluded that *S. salsa* could be a potential crop in saline soils irrigated with brackish water. In addition, it provides a possible additional source of fodder in arid regions where non-saline arable lands and freshwater are limited.

Moreover, Abideen et al. reviewed potential halophytes and algal species as alternatives for food biomass used in producing renewable energy sources. The review summarizes the pitfalls and precautions for producing biomass in an environmentally friendly way that does not harm coastal ecosystems. Several species with great potential as sources of bioenergy were highlighted. Despite the tremendous advantages of their use as non-food biomass for producing renewable energy, some negative impacts are associated with their introduction in new environments, such as ecosystem alteration, the introduction of invasive species, and transmissible plant diseases.

Furthermore, in an interesting systematic review article, Ashilenje et al. studied crop species mechanisms and ecosystems services for sustainable cropping systems in salt-affected arid regions using data obtained from the results of 20 studies published in peer-reviewed journals between the years 2000 and 2021. This paper examined the mechanisms and synergies of species that can be incorporated into cropping systems to alleviate soil salinity problems and maintain forage productivity in dry lands. Clearly, halophyte and non-halophyte forages have converging mechanisms of salinity tolerance manifested through increased photosynthesis and productivity. Indicators of the ubiquity of ecosystem services of both halophyte and non-halophyte species exist along a continuum soil salinity increase. Possible synergies among perennials, halophytes, herbaceous plants, fungi, and bacteria to combat the effects of soil salinity have been identified. These synergies can be used to develop sustainable forage cropping systems that improve saline soils and nutrient cycling to maintain optimal forage productivity.

Besides, more research is needed to overcome seed availability, germination, dormancy problems, and propagation techniques. In this context, Chen et al. assessed the germination requirements (e.g., light and temperature), salinity, and drought tolerance of naked and winged (i.e., with the attached perianth structures) seeds of several *Salsola* species. Detailed germination information was provided for cultivating four *Salsola* species in degraded saline soils.

In perspective, we believe that this Research Topic highlights interesting avenues for using halophytes as food, feed, and source of secondary metabolites and to understand better how we can improve crops' tolerance to saline stress.

## Author contributions

All authors listed have made a substantial, direct, and intellectual contribution to the work and approved it for publication.

## Acknowledgments

The guest editors of this Research Topic would like to thank Chief Editors of Plant Abiotic Stress section, Luisa Sandalio, and Functional Plant Ecology section, Boris Rewald. Our thanks also go to Journal Specialist Frontiers in Plant Science, DR. Deborah Oluwasanya, and Journal manager, Dr. Liudmila Efremova. We can't forget also to thank all the authors that contributed with their research and review articles to achieve the goal of our Research Topic.

## Conflict of interest

The authors declare that the research was conducted in the absence of any commercial or financial relationships that could be construed as a potential conflict of interest.

## Publisher's note

## References

Calone, R., Bregaglio, S., Sanoubar, R., Noli, E., Lambertini, C., and Barbanti, L. (2021). Physiological adaptation to water salinity in six wild halophytes suitable for Mediterranean agriculture. *Plants* 10 (2), 309. doi: 10.3390/plants10020309

Cheeseman, J. M. (2015). The evolution of halophytes, glycophytes and crops, and its implications for food security under saline conditions. *New Phytol.* 206, 557–570. doi: 10.1111/nph.13217

Riadh, K., Wided, M., Koyro, H.W., and Chedly, A. (2010). Responses of halophytes to environmental stresses with special emphasis to salinity. *Adv. Botan. Res.* 53, 117–145. doi: 10.1016/S0065-2296(10)53004-0

Shabala, S. (2013). Learning from halophytes: physiological basis and strategies to improve abiotic stress tolerance in crops. *Ann. Bot.* 112, 1209–1221. doi: 10.1093/aob/mct205

Ventura, Y., Eshel, A., Pasternak, D., and Sagi, M. (2015). The development of halophyte-based agriculture: past and present. *Ann. Bot.* 115, 529–540. doi: 10.1093/aob/mcu173

frontiers | Frontiers in Plant Science

ORIGINAL RESEARCH
published: 26 April 2022
doi: 10.3389/fpls.2022.847863

# Mining Beneficial Genes for Salt Tolerance From a Core Collection of Rice Landraces at the Seedling Stage Through Genome-Wide Association Mapping

*Xiaoliang Wang[1], Jinquan Li[2,3], Jian Sun[1], Shuang Gu[1], Jingbo Wang[1], Chang Su[1], Yueting Li[1], Dianrong Ma[1], Minghui Zhao[1]*and Wenfu Chen[1]*

[1]Rice Research Institute, Shenyang Agricultural University, Shenyang, China, [2]State Key Laboratory for Conservation and Utilization of Subtropical Agro-Bioresources, South China Agricultural University, Guangzhou, China, [3]Strube Research GmbH & Co. KG, Söllingen, Germany

OPEN ACCESS

**Edited by:**
*Ali El-Keblawy, University of Sharjah, United Arab Emirates*

**Reviewed by:**
*Xinghai Yang, Guangxi Academy of Agricultural Sciences, China*
*Kareem A. Mosa, University of Sharjah, United Arab Emirates*
*Amr Adel Elkelish, Suez Canal University, Egypt*

***Correspondence:**
*Minghui Zhao*
*mhzhao@syau.edu.cn*

**Specialty section:**
*This article was submitted to Plant Abiotic Stress, a section of the journal Frontiers in Plant Science*

**Received:** *03 January 2022*
**Accepted:** *08 April 2022*
**Published:** *26 April 2022*

**Citation:**
*Wang X, Li J, Sun J, Gu S, Wang J, Su C, Li Y, Ma D, Zhao M and Chen W (2022) Mining Beneficial Genes for Salt Tolerance From a Core Collection of Rice Landraces at the Seedling Stage Through Genome-Wide Association Mapping. Front. Plant Sci. 13:847863. doi: 10.3389/fpls.2022.847863*

Rice is a salt-sensitive plant. High concentration of salt will hinder the absorption of water and nutrients and ultimately affect the yield. In this study, eight seedling-stage salt-related traits within a core collection of rice landraces were evaluated under salinity stress (100 mM NaCl) and normal conditions in a growth chamber. Genome-wide association study (GWAS) was performed with the genotypic data including 2,487,353 single-nucleotide polymorphisms (SNPs) detected in the core collection. A total of 65 QTLs significantly associated with salt tolerance (ST) were identified by GWAS. Among them, a co-localization QTL *qTL4* associated with the SKC, RN/K, and SNC on chromosome 6, which explained 14.38–17.94% of phenotypic variation, was selected for further analysis. According to haplotype analysis, qRT-PCR analysis, and sequence alignment, it was finally determined that 4 candidate genes (*LOC_Os06g47720*, *LOC_Os06g47820*, *LOC_Os06g47850*, *LOC_Os06g47970*) were related to ST. The results provide useful candidate genes for marker assisted selection for ST in the rice molecular breeding programs.

**Keywords: rice, salinity tolerance, candidate gene, GWAS, QTL**

## INTRODUCTION

Soil salinization is one of the important abiotic stresses that limits agricultural food production, because it reduces crop yields and restricts land use. With the modernization of industry and the continuous deterioration of the ecological environment, the area of arable land is gradually decreasing, while the area of soil salinization continues to increase because of unreasonable irrigation to the farmland (Qadir et al., 2014). It is estimated that about 950 million hectares of arable land in the world, including 250 million hectares of irrigated land, are affected by salinization (Solis et al., 2020). Rice (*Oryza sativa*) is a salt-sensitive plant, and salt stress seriously affects its growth, development, and yield (Wang et al., 2018a). Therefore, it is of great significance to mine and utilize the novel salt-tolerant (ST) genes in rice and breed ST varieties (Li et al., 2014).

A large number of studies have shown that ST is a complex trait controlled by quantitative trait loci (QTL; Roy et al., 2011). In recent years, with the development of modern science and technology, sequencing technology has become more and more mature. A lot of researches have been done on QTL mapping of ST in rice, and many QTLs related to ST have been identified. Using the $F_2$ population derived from the parent Dianjingyou1 as the recipient parent and SR86 as the donor parent, a huge segregation analysis library was constructed and a QTL named *qst1.1* related to ST was identified on chromosome 1, which can explain 62.6% of the phenotypic variation (Wu et al., 2020). Using the RIL population, 38 QTLs related to ST were identified and a new QTL affecting stem length was found on chromosome 7, which could explain 6.8% of the phenotypic variation (Jahan et al., 2020). Takehisa et al. (2004) identified 12 QTLs for stem length under salt stress on chromosomes 1, 3, and 7, explaining 12–30% of the phenotypic variation. Wang et al. (2012) used the IR26/Jucaiqing recombinant inbred line (RIL) population and found 16 QTLs related to the swelling rate and germination rate under salt stress. Prasad et al. (2000) used the DH population and identified a QTL for seed root length under salt stress on chromosome 6, which explained 18.9% of the phenotypic variation. Zeng et al. (2021) used the $BC_1F_2$ population and performed QTL mapping for the seed germination rate (GR) and germination index (GI). A total of 13 QTLs were identified, which explained 7.32–24.39% of the phenotypic variation.

GWAS can be used to perform association analysis on the genetic variation of complex traits at the genome-wide level (Hirschhorn and Daly, 2005). It is an effective method for in-depth understanding of the genetic structure of complex traits of crops. With GWAS, several researchers have identified many QTLs and candidate genes related to ST traits. Yuan et al. (2020) used 664 rice varieties and different statistical models to conduct GWAS for ST, and a total of 21 QTLs were identified. Using 208 rice varieties from a core collection, Naveed et al. (2018) identified 20 quantitative trait nucleotides (QTNs) for one salt related trait through GWAS, including 6 QTNs affecting ST at the germination stage and 14 QTNs at the seedling stage, and identified 22 candidate genes. Using 708 rice varieties, Liu et al. (2019) identified 7 candidate genes through GWAS, which were significantly associated with grain yield and its related traits under saline stress conditions. Zhang et al. (2017) used GWAS to identify salt-tolerant loci and favorable alleles for iron and zinc resistance and detected 60 salt-tolerant loci as well as 22 candidate genes in 10 important QTLs regions. An et al. (2020) used a core collection which consisted of 181 varieties and detected 17 loci significantly associated with dry weight ratio (DWR) for ST through GWAS.

The seedling stage is the key stage for ST in rice, and it is highly sensitive to salt stress (Nayyeripasand et al., 2021). High concentration of salt will hinder the absorption of water and nutrients in the rice seedling stage, inhibit the growth of seedlings, and ultimately reduce rice yield (Ruan et al., 2011). To a certain extent, it can be used as a reference for ST during the whole growth period. The ST identification at the seedling stage is easy to operate with short cycle and high efficiency and can be widely used in screening germplasm resources for ST and breeding selection (Walia et al., 2005).

Abundant germplasm resources for ST are available in the Asian cultivated rice, especially in rice landraces. As early as in 1920–1964, a total of 7,128 accessions of rice landraces had been collected by Prof. Ying Ting, which was named as Ting's rice collection (Li et al., 2011). They were from all over China as well as from some main rice cultivation countries. Based on 48 phenotypic data, Li et al. (2011) have constructed a rice core collection consisting of 150 accessions. The large variation within the core collection provides an important gene pool of genetic diversity and beneficial genes for rice breeding. Therefore, it is worth to perform GWAS with such a core collection for ST in rice. Population structure analysis for the core collection indicated that there existed two subgroups mainly corresponding to *indica* and *japonica* subspecies and the linkage disequilibrium (LD) decay distance was about 200–500 kb (Zhang et al., 2011; Li and Zhang, 2012; Zhao et al., 2018). Using this core collection, several researches have been performed to identify resistant QTLs for aluminum (Al) tolerance and cold tolerance. With the mixed linear model, GWAS identified a total of 30 QTLs for Al tolerant traits which explained 7.73 to 13.30% of the phenotypic variation (Zhao et al., 2018). A total of 26 QTLs were found to be significantly associated with cold tolerance, which explained 26–33% of the phenotypic variation (Song et al., 2018). These results indicated that these landraces are importance sources for stress tolerance in rice and the mapping results could provide important information to breed stress tolerant rice cultivars through marker-assisted selection. However, to our knowledge, no previous research was performed for ST at the seedling stage with the core collection. Moreover, no previous research was performed to map QTLs for ST and further identify candidate genes with the core collection. Therefore, the objectives for this study were: (1) to screen the performance of ST in the in the core collection; (2) to map the QTLs for ST through GWAS; and (3) to identify some candidate genes for ST in rice for better understanding the genetic basis of ST at the seedling stage in rice and providing new genetic resources for improvement of ST in rice cultivars.

# MATERIALS AND METHODS

## Plant Materials

The Ting's rice core collection, i.e., a total of 150 accessions of rice landraces, was used to screen their salt tolerance (**Supplementary Table S9**). These landraces were mainly collected from 20 different provinces in China as well as from North Korea, Japan, Philippines, Brazil, Celebes, Java, Oceania, and Vietnam. These regions are distributed across the north latitude 55° to south latitude 10° and including regions with temperate, tropical, and subtropical climate. The core collection was constructed from 150 accessions of 2,262 based on a strategy of stepwise clustering and preferred sampling on adjusted Euclidean distances and weighted pair-group average method using integrated qualitative and quantitative

traits (Li et al., 2007). Of the 150 landraces, 32 were classified as *japonica* rice (24 were typical *japonica* rice, and 8 were *japonica*-clined rice), and 118 were classified as *indica* rice (16 were *indica*-clined rice, and 102 were typical *indica* rice), according to Cheng's index criterion (Li et al., 2011).

## ST Evaluation at the Seedling Stage

The seeds of the 150 landraces were placed in an oven at 50°C for 48 h to break dormancy. From each landrace, 40 seeds with uniform size and full rice grains were selected, and then the seeds were soaked in 75% alcohol for 15–20 min for disinfection treatment. Then, the seeds were rinsed with sterile water for three times. The rinsed seeds were put in a net bag, soaked in distilled water, and placed in a thermostat at 30°C for 48 h to incubate germination. Then, the seeds were transferred to 96-well PCR plates with cut wells and distilled water. The PCR plates were placed in a culture room with light at 28°C for cultivation and later cultivated with 12 h of light and 12 h of darkness. After 7 days, the distilled water was changed to the standard nutrition of the International Rice Research Institute (IRRI) but with only 0.5-fold concentration (Yoshida et al., 1976), while keeping the PH value of Yoshida's solution at 5.5. The nutrient solution was changed once per 3 days. After culturing for 7 days, the cultivation was changed to 0.5-fold Yoshida's solution and later changed to one-fold Yoshida's solution with regularly replacing the nutrient solution. When the seedlings grew to the three-leaf stage, the samples of both the control and the salt treated were extracted in 25 ml acetic acid (100 mm) at 90°C for 2 h, and 2 ml extraction was divided into two groups for sodium and potassium, respectively. 100 mm NaCl solution was added to the nutrient solution for salt stress treatment, while the control group continued to grow in the nutrient solution. Each treatment was set with three repetitions. After 10 days of treatment, samples were taken to measure the phenotypic traits. Shoot and root $Na^+$ and $K^+$ concentrations (RNC, SKC, and SNC) of each sample were determined by atomic absorption spectrometry (AAS, Series 2, Thermo Electron Corporation). Concentrations of sodium and potassium in shoots and roots were expressed in millimoles per gram ($mMg^{-1}$; Qi et al., 2005; An et al., 2020). The $K^+/Na^+$ ratios in roots (RN/K) were calculated subsequently. A root scanner (Expression 1100XL) was used to analyze root traits. To reduce errors, 10 seedlings were scanned for each material, and each seedling was scanned 3 times, and the average values of TRSA (total root surface area), TRV (total root volume), and TRL (total root length) were calculated. Set up 3 biological replicates. RTRSA (relative total root surface area), RTRV (relative total root volume), RTRL (relative total root length), and RSN/K (relative ratio of $Na^+$ to $K^+$ concentrations in shoots) were calculated according to the following formula: relative trait value (%) = (trait value under salt stress) / (trait value under control) × 100.

## RNA Extraction and Real-Time PCR

In this study, to further determine whether candidate genes are related to ST, we first screened extreme salt-tolerant (S125) and extreme salt-sensitive (S87) rice landraces, RT-PCR of candidate genes was performed in salt-tolerant (S125) and sensitive (S87) rice landraces. Under the condition of salt stress, the time for rice seedlings to appear stress phenotype lags behind the response time of related genes. Under salt stress, the expression levels of some salt-related genes will change rapidly and then return to their original levels, resulting in undetectable changes in expression levels. Using high concentration and short time salt stress for gene expression analysis can more accurately analyze the changes of related gene expression. Therefore, in this study, the 20-day-old seedlings were treated with 200 mm NaCl for a short time (0, 3, 6 and 12 h) for gene expression analysis (Xiaoxue et al., 2019). The expression of genes at 0 h of salt stress in this study is as control data for non-stress (without salt stress). The total RNA from the shoots tissues of landraces was extracted using *steadyPure* Plsant RNA Extraction Kit (Accurate Biotechnology; An et al., 2020). The cDNA for real-time PCR was reverse-transcribed from 2 μg of total RNA using *Evo M-MLV* Reverse Transcription Reagent Master Mix (Accurate Biotechnology). According to the manufacturer's instructions, real-time PCR was performed using SYBR Green *Pro Taq* HS kit (Accurate Biotechnology) in a real-time PCR machine (QuanStudio). Relative gene expression levels were determined using the $2^{-\Delta\Delta Ct}$ method (Livak and Schmittgen, 2002). Data analysis and graphing were performed using GraphPad Prism 6.02 software, and Duncan's test was performed using SPSS. The rice actin was selected as the internal control. Primers used for qRT-PCR analysis are listed in (**Supplementary Table S10**).

## DNA Extraction and Candidate Gene Sequence Alignment

DNA Quick Plant System (Tiangen Biotechnology, Beijing, China) was used to extract plant genomic DNA. The target sequence was amplified with specific primers. The amplified product was purified with EasyPure PCR purification kit (Tiangen Biotech, China) and quantified with NanoDrop 8,000 spectrophotometer (Thermo Fisher Science, Waltham, MA, United States). Sequence alignment was performed with the DNAMAN software using the genes in the Nipponbare genome as a reference.

## GWAS Analysis and Haplotype Analysis

GWAS was performed by using the compressed MLM program in the Tassel5.0 software, where the model was as follows: $Y = X\alpha + Q\beta + K\mu + e$, where Q represents the kinship, X is genotype, Y is phenotype, while $X\alpha$ and $Q\beta$ considered as fixed effects and $K\mu$ and e as random effects. The population structure K was calculated by the Admixture software, and the kinship between samples was calculated by the SPAGeDi software. The significant SNPs were identified by $p$ value. To obtain high-density SNPs, we encrypted the original 67,511 SNPs and obtained 2,487,353 SNPs by the following method: the user uploads input files in oxford format (.gen/.sample) per chromosome. The imputation server utilizes chromosome recombination maps and the Rice Reference Panel (RICE-RP)

haplotypes to impute the user's data out to 5.2 M SNPs with IMPUTE2 and returns imputed results in plink binary format. The user can filter the imputed data using plink1.9 to produce a final data set of desired SNP density and composition (Wang et al., 2018b).[1] Manhattan scatter plots and QQ plots are drawn using the "qqman" package in R software. LD heatmaps surrounding peaks in the GWAS were constructed using "LD heatmaps" in the R package (Shin et al., 2006). The haplotypes of at least three rice landraces were analyzed for phenotypic comparison. Differences in phenotypic values between alleles of each non-synonymous SNP were assessed by Student's t tests. The sequence alignment of each gene was determined using non-synonymous SNPs associated with ST, and differences in phenotypic value between haplotypes of each gene were calculated by one-way ANOVA or Student's *t* tests.

# RESULTS

## Phenotypic Variation

In order to evaluate the phenotypic variation of ST in the core collection at the seedling stage, a statistical analysis was performed on 8 ST-related traits: RNC (root $Na^+$ concentration), SKC (shoot $K^+$ concentration), SNC (shoot $Na^+$ concentration), RN/K (ratio of $Na^+$ to $K^+$ concentrations in roots), RTRSA (relative total root surface area), RTRV (relative total root volume), RTRL (relative total root length), and RSN/K (relative ratio of $Na^+$ to $K^+$ concentrations in shoots; **Supplementary Table S1**). The results showed that all traits showed tremendous phenotypic variation in the population. In particular, RN/K had the highest coefficient of variation, and RTRSA had the lowest coefficient of variation. Correlation analysis showed that most traits were significantly positively correlated. Significant negative correlations were observed only between SKC and RSN/K, SKC, and RN/K (**Supplementary Table S2**). The results showed that salt stress has different degrees of influence on the 8 ST-related traits at rice seedling stage.

## GWAS Results

In previous studies, the rice core collection was sequenced using the Specific-Locus Amplified Fragment Sequencing(SLAF-seq)approach and 67,511 SNPs were obtained (Zhao et al., 2018). Based on them, 2,487,353 SNPs were further obtained by the imputation method of (Wang et al., 2018b). With consideration of the population structure and kinship, the MLM (+Q + K) model and 2,487,353 SNPs were used to perform GWAS on eight traits related to ST with the high density SNPs set, and the results are presented in the form of Manhattan plots (**Figure 1**) and QQ plots (**Supplementary Figure S1**). With a significant threshold of $p < 0.0001$, 843 significant SNPs were detected (**Supplementary Table S3**), which were unevenly distributed on the 12 chromosomes. The most significant position with the largest contribution rate is located on chromosome 1, which can explain 28.11% of the phenotypic variation.

## QTLs for ST at the Seedling Stage

ST-related QTLs are defined by the decay distance of linkage disequilibrium (LD). Previous studies had shown that the decay distance of LD is 500 kb (Zhao et al., 2018). Therefore, a region was considered as one QTL if it had more than one SNP with $p < 0.0001$ within the LD decay distance. We named salt tolerance QTLs with reference to the method proposed by Mccouch et al. (1997). In total, 65 QTLs were identified significantly associated with ST (**Figure 2**). There are 1–13 of QTLs on each chromosome, and each QTL contains 1–379 SNPs. These QTLs explained 13.47 to 28.11% of the phenotype variation (**Supplementary Table S4**).

For RNC, we detected 8 QTLs located on chromosomes 1, 3, 5, 8, 9, 10, and 12 under salt stress, which could explain 14.83–23.96% of the phenotypic variation. Under salt stress, we detected 14 QTLs for SNC on chromosomes 1, 2, 3, 5, 6, 7, 9, 11, and 12, which can explain 13.91–23.61% of the phenotypic variation. For RN/K under salt stress, ten QTLs were detected on chromosomes 1, 3, 5, 6, 8, 9, 10, and 11, which could explain 13.75–27.74% of the phenotypic variation. For RTRV under salt stress, 8 QTLs were detected on chromosomes 3, 6, 8, 9, and 11, which could explain 13.47–20.52% of the phenotypic variation. Under salt stress, we detected 13 QTLs for SN/K on chromosomes 1, 2, 3, 4, 5, 8, and 9, which could explain 13.67–21.14% of the phenotypic variation. For SKC under salt stress, two QTLs were detected on chromosomes 6 and 8, which could explain 14.38–17.94% of the phenotypic variation. Under salt stress, we detected 5 QTLs for SKC on chromosomes 1 and 12, which can explain 14.46–28.11% of the phenotypic variation. For TRSA under salt stress, 5 QTLs were detected on chromosomes 1, 7, 9, 10, and 11, which can explain 14.33–23.10% of the phenotypic variation.

## Co-localization of QTLs Under Salinity Stress Conditions

Through association mapping analysis, there are 6 genomic regions containing co-localization QTLs. We defined co-localization QTLs as *qTL1*, *qTL2*, *qTL3*, *qTL4*, *qTL5,* and *qTL6*, respectively (**Table 1**). The most complicated is the co-localization region of chromosome 6, i.e., *qTL4*, which is composed of 3 QTLs and has a large overlap region. The remaining 5 co-localization regions are all composed of 2 QTLs.

## Identification of Candidate Genes for ST

Since *qTL4* is composed of 3 QTLs with 14 significant SNPs, it was chosen for further analysis. The *qTL4* contains the highest peak SNP (Chr6_28930159) at approximately 28.93Mbp, which can explain 14.38–17.94% of the phenotypic variation. According to the LD decay analysis of the population, the 250 kb upstream and downstream around the peak SNP were designated as the searching range of candidate genes as shown by the LD heat map (**Figure 3**). Through the Rice Annotation

[1]http://rice-impute.biotech.cornell.edu

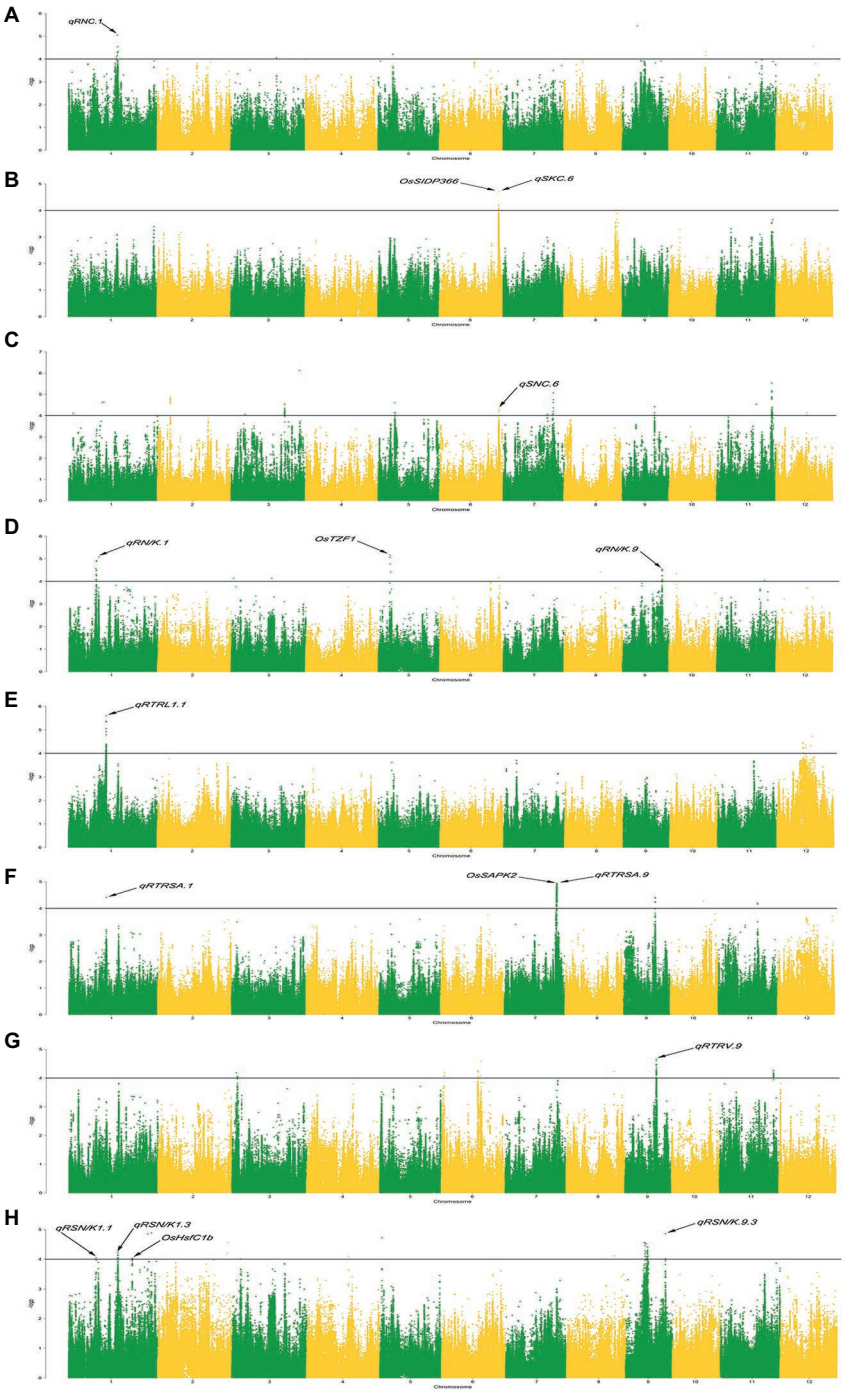


**FIGURE 1 |** Manhattan plots of genome-wide association studies. **(A-H):** Manhattan plots for the RNC (root $Na^+$ concentration), SKC (shoot $K^+$ concentration), SNC (shoot $Na^+$ concentration), RN/K (ratio of $Na^+$ to $K^+$ concentrations in roots), RTRSA (relative total root surface area), RTRV (relative total root volume), RTRL (relative total root length), and RSN/K (relative ratio of $Na^+$ to $K^+$ concentrations in shoots).

Project database,[2] ninety-four genes were found in this region (**Supplementary Table S5**). It includes 50 functional annotation genes, 24 expressed proteins, 17 transposon proteins, and 3 hypothetical proteins. Among them, a known salt tolerant gene (*OsSIDP366*) was found in this region, which was located in the interval between *qSKC.6* and *qSNC.6*. Besides it, *qRN/K1.1* and *qRSN/K1.1* also were co-localization, which were detected in the interval of *qTL6* and related to ratio of $Na^+$ to

[2]http://rice.uga.edu

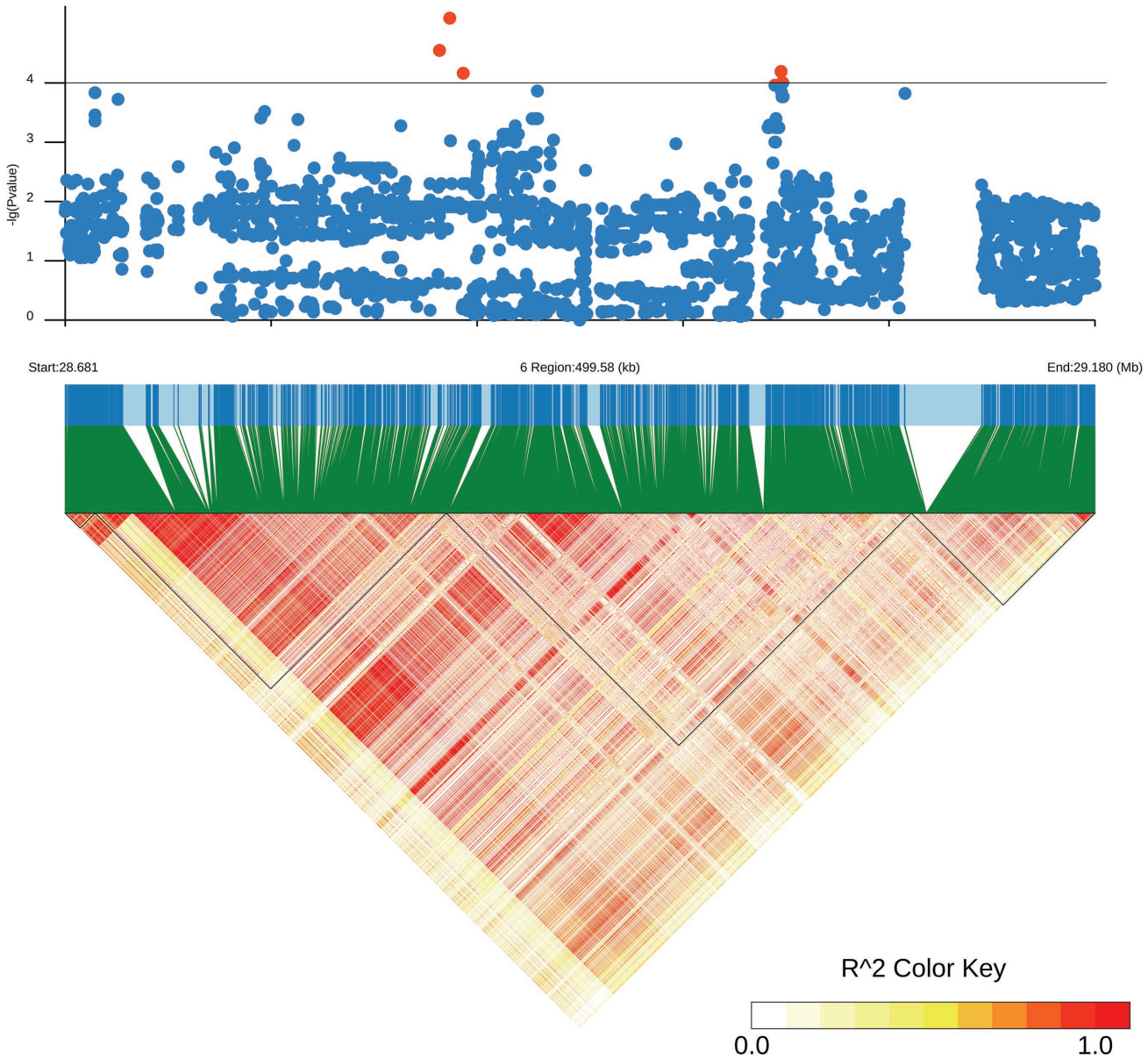


**FIGURE 2 |** Local Manhattan plot (upper) and LD heatmap (lower) surrounding the lead SNP for SKC on chromosome 6.

**TABLE 1 |** Co-localization of QTLs at seeding stage.

| QTL | Chr | Position/interval (Mbp) | No. of Co-located QTLs | No. of Associated SNPs | Co-located QTLs |
|---|---|---|---|---|---|
| *qTL1* | 1 | 12.98–13.34 | 2 | 18 | *qRN/K.1,qRSN/K1.1* |
| *qTL2* | 1 | 18.01–18.26 | 2 | 73 | *qRTRL1.1,qRTRSA.1* |
| *qTL3* | 1 | 23.28–24.03 | 2 | 17 | *qRNC.1,qRSN/K1.3* |
| *qTL4* | 6 | 28.76–29.01 | 3 | 14 | *qSKC.6,qRN/K.6,qSNC.6* |
| *qTL5* | 9 | 15.43–15.53 | 2 | 67 | *qRTRV.9,qRTRSA.9* |
| *qTL6* | 9 | 19.50–19.54 | 2 | 11 | *qRN/K.9,qRSN/K.9.3* |

$K^+$ concentrations. The *qTL6* contains the highest peak SNP (Chr9_19518843) at approximately 19.51Mbp, which can explain 13.75–16.92% of the phenotypic variation. In addition, we also found a SNP Chr6_28822519 in the *qRN/K.6* interval with a significant threshold of $p = 0.000069293$, which could explain 17.49% of the phenotypic variation, indicating that there may

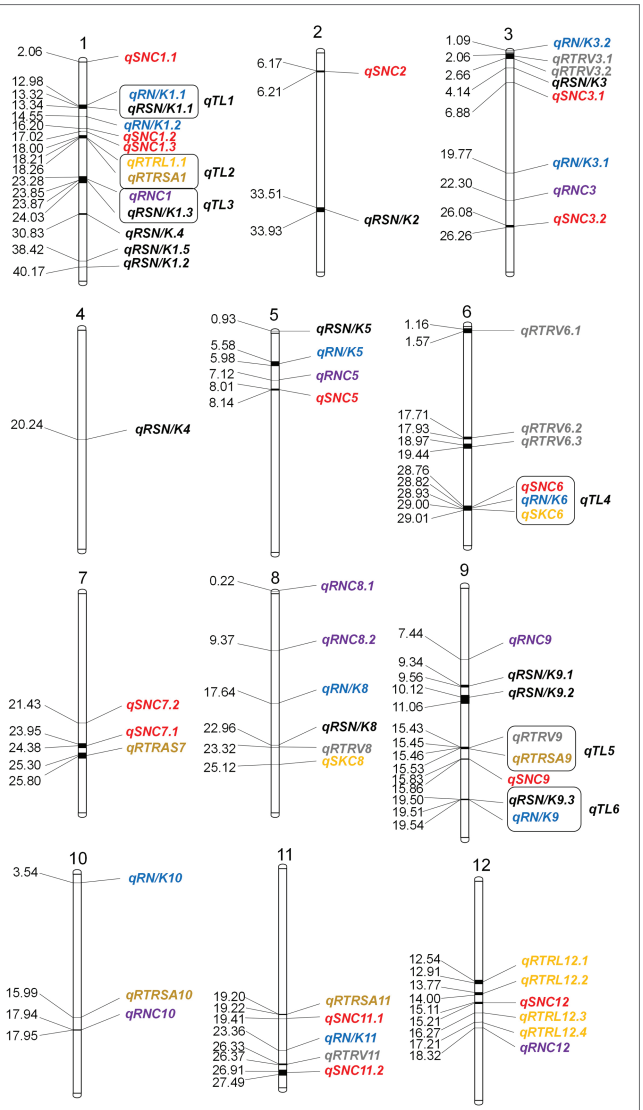


**FIGURE 3 |** Distribution of GWAS-based detected QTLs on 12 chromosomes in rice. Distances on the map are in Mbp.

be new salt resistance-related genes in this interval. Based on gene functional annotation and GO enrichment analysis[3] (**Supplementary Table S6**), we screened and found 11 out of 50 functional genes which are related to stress response or metabolism process-related genes were salt tolerance-related candidate genes (**Supplementary Table S7**).

## Haplotype Analysis of Candidate Genes

We further performed haplotype analysis on the non-synonymous mutant SNPs and the promoter SNPs in the exon region of the 11 candidate genes and detected significant differences among different major haplotypes based on the haplotypes with all non-synonymous SNPs. It was found that the haplotypes of the 4 candidate genes had significant differences (**Table 2**), and each candidate gene had a different number of non-synonymous SNPs (**Supplementary Table S8**). The haplotype analysis showed that the four candidate genes were significantly associated with SKC (shoot $K^+$ concentration), and the SKC of different haplotypes were also significantly different (**Figure 4**). These findings suggest that the four candidate genes (*LOC_Os06g47720*, *LOC_Os06g47820*, *LOC_Os06g47850, and LOC_Os06g47970*) may be involved in the regulation of salt tolerance at seedling stage in rice.

**TABLE 2 |** Candidate genes.

| Related traits | Gene ID | Position (Mbp) | Gene description |
|---|---|---|---|
| SKC | LOC_Os06g47720 | 28,874,838–28,878,068 | Serine/threonine-protein kinase BRI1-like 2 precursor, putative, expressed |
| | LOC_Os06g47820 | 28,941,271–28,943,703 | Protein kinase domain containing protein, expressed |
| | LOC_Os06g47850 | 28,958,626–28,960,418 | Zinc finger family protein, putative, expressed |
| | LOC_Os06g47970 | 29,002,279–29,003,541 | Protein of unknown function DUF1517 domain containing protein |

## Identification of Candidate Genes by Gene Expression

To further determine whether the aforementioned 4 candidate genes are related to ST, gene expression assays for the 4 candidate genes were conducted in salt tolerant (S125) and sensitive (S87) rice landraces. We performed a statistical analysis on the dead seedling rates in S87 and S125 under salt stress to further verify their differences in salt tolerance (**Figure 5**). There were significant differences in the dead seedling rates of S87 and S125 under the two salt stress concentrations, indicating that they had significant differences in salt tolerance. Therefore, S87 and S125 were selected for subsequent analysis of candidate genes expression. The gene expression level of *LOC_Os06g47720* in S87 showed a continuous increase trend from 0–12 h and was higher than S125 for all tested time points. The gene expression level of *LOC_Os06g47720* in S87 was nearly 10-fold higher than that in S125 after 12 h of salt stress treatment. The opposite expression pattern was observed for *LOC_Os06g47820*, *LOC_Os06g47850,* and *LOC_Os06g47970*, where the gene expression levels in S125 were higher than those in S87 for all tested time points after salt stress treatment. Among them, the gene expression levels of *LOC_Os06g47850* and *LOC_Os06g47970* in S125 were nearly 10-fold higher than those in S87 after 12 h of salt stress treatment.

## Sequence Analysis of the Candidate Genes

To determine the association between candidate genes and ST phenotypes, four candidate genes were sequenced for the two rice landraces S125 and S87 (**Supplementary Figure S1**) and the sequence alignment was generated using DNAMAN.

[3]http://www.bioinformatics.com.cn

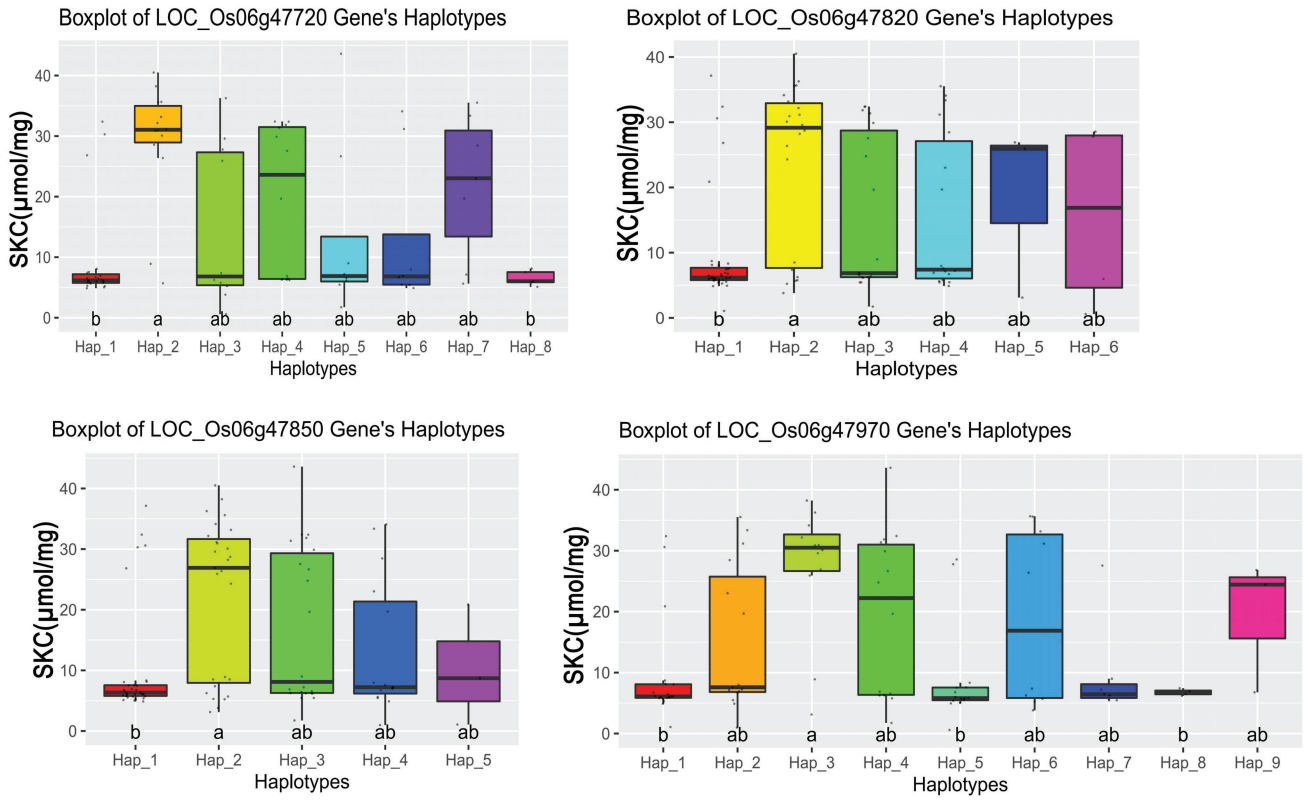


**FIGURE 4 |** Boxplots for the entire population based on the haplotypes (Hap) for four candidate genes, where the a and b are ranked by Duncan's test at $p < 0.05$.

*LOC_Os06g47720* has 29 mutation sites in the two ST extreme genotypes, which lead to 11 amino acids changed in the S125, while translation was terminated early in the S125. For *LOC_Os06g47820*, it showed that the two genotypes had 17 mutation sites and 14 amino acids changed. *LOC_Os06g47970* has a pair of base substitutions in S125, which caused the glycine to change into the asparagine. *LOC_Os06g47850* has no sequence difference between the two genotypes.

# DISCUSSION

## Phenotypic Variation and Prospects of the Core Collection of Rice Landraces

Artificial directional domestication and selection have led to the reduction of genetic diversity in many crops such as rice, and many excellent resistance gene resources have been gradually lost in common cultivated rice. Some landraces are less affected by artificial selection and contain more genetic diversity and resistance genes. The core collection of rice landraces was constructed from a total of 7,128 accessions of rice landraces from the Ting's rice collection (Li et al., 2011) and came from all over China as well as some main rice cultivation countries. It provides an important gene pool of genetic diversity and beneficial genes for rice breeding. For example, several QTLs for aluminum tolerance and cold tolerance were identified in the core collection (Song et al., 2018; Zhao et al., 2018). In this study，8 traits related to ST showed tremendous phenotypic variation in the core collection, which suggested that salt stress has different degrees of influence on the ST-related traits at the seedling stage, and these phenotypes could be used for GWAS. Furthermore, a total of 65 QTLs significantly associated with salt tolerance were identified by GWAS. These results further verified that the core collection of rice landraces contains abundant resistance gene resources to biotic stress and abiotic stress and is a precious germplasm resource with great prospect for mining and utilization of beneficial genes for rice breeding.

## Comparison of QTLs With Previous Studies

GWAS is a promising method for QTL fine-mapping in plants in response to abiotic stress. At present, many QTLs related to salt stress have been identified. We compared the previously reported QTLs and found that a total of 12 previously reported QTLs for ST in this study were overlapped or close to the range of previously mapped QTLs for ST.

For example, under stress conditions 151 trait–marker associations were identified that were scattered in 29 genomic regions on 10 chromosomes of rice (Nayyeripasand et al., 2021). Some of the QTLs are consistent with or close to our mapped QTL regions. The QTL *qSNC1.1* on chromosome 1 coincides with the reported QTL *qRDWn1.1* (root dry weight);

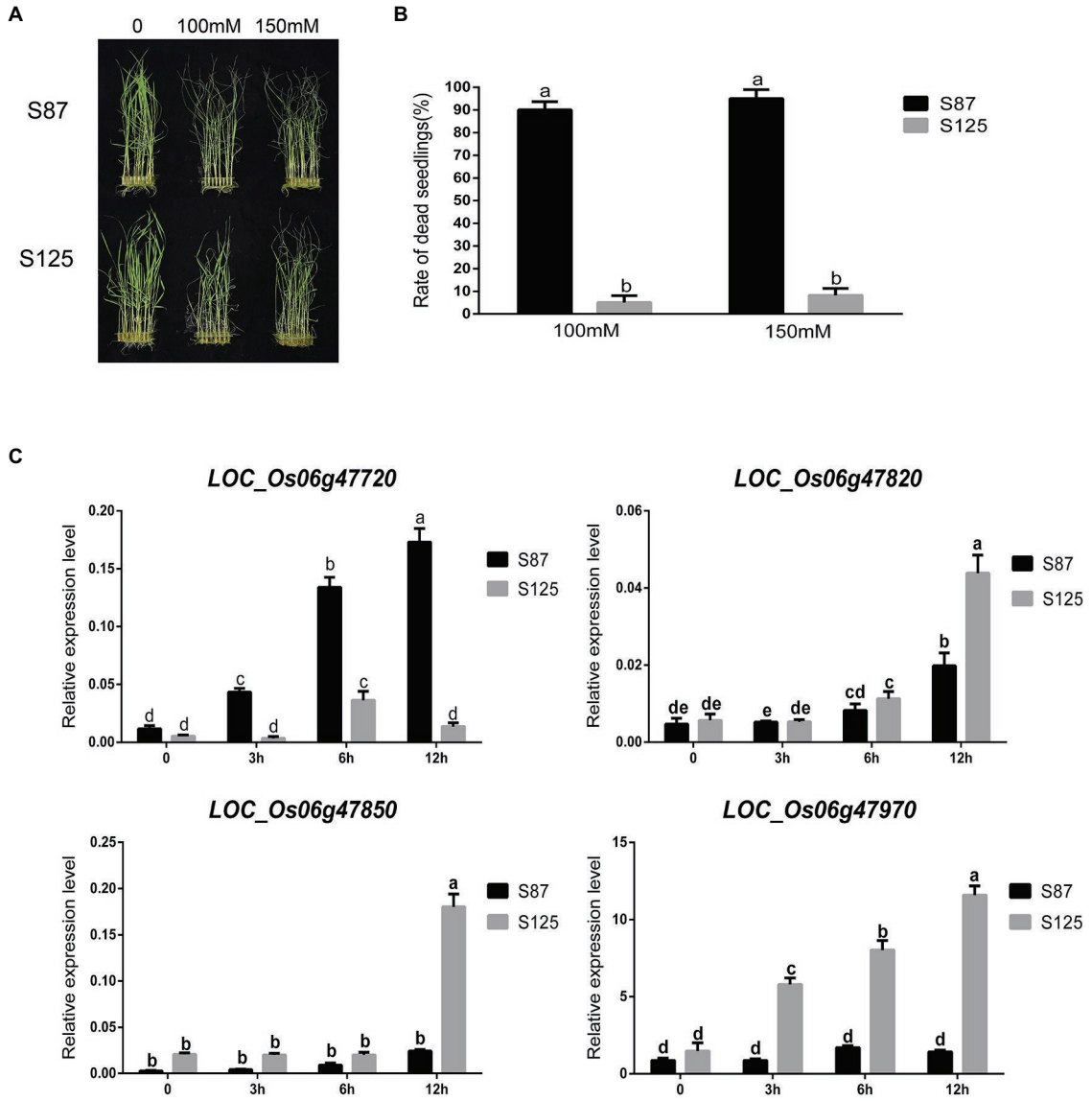


**FIGURE 5 | (A)** Phenotypes of S87 (salt sensitive variety) and S125 (salt tolerant variety) at different salt concentrations. **(B)** Statistical analysis of S87 and S125 for dead seedling rate, where the a and b are ranked by Duncan's test at $p < 0.05$. **(C)** changes in relative gene expression level of four candidate genes at different times (0, 3 h, 6 h, 12 h) after salinity stress in different rice cultivars, where the a, b, c, d, and e are ranked by Duncan's test at $p < 0.05$.

the QTL *qRNC1* is located in the region of the reported QTL *qRDWs1.1* (root dry weight). The QTLs *qRTRL12.1* and *qRTRL12.2* on chromosome 12 are located in the region of the reported QTL *qSLn12.1* (shoot length). The QTL *qRTRL12.4* is 320kbp away from the previously reported QTL *qRDWs12.1* (root dry weight), and the QTL *qRNC12.1* (root fresh weight) is 140 kb apart from the previously reported QTL *qRFWs12*. The QTL *qRN/K8* on chromosome 8 is located in the previously reported QTL *qRFWn8.1* (root fresh weight) interval. Chen et al. (2020) identified 23 QTLs with different salt tolerance indexes through GWAS. Some of the QTLs coincide with our regions. The QTL *qRSN/K1.2* is located in the region of previously reported QTL *qSIS1* (salt injury score) and *qSNaC1.2* (shoot $Na^+$ concentration), while the QTL *qSNC2* on chromosome 2 is within the interval of previously reported *qRRDW2* (relative root dry weight). The QTL *qSKC8* is located in the interval of previously reported *qRSKC8* (relative shoot $K^+$ concentration) and *qRNaC8* (root $Na^+$ concentration). Zhang et al. (2020) used the 55 K rice SNP array to genotype the entire population and four parents, and a total of 7 salt-tolerant QTLs were detected. Some of the QTLs coincide with or close to our regions. The QTL *qRSN/K1.5* is about 174kbp away from the previously reported QTL *qSLST1* (shoot length under salt stress treatment) and is located in the intervals of previously reported QTL *qRDSW1* (relative dry shoot weight) and *qRB1* (relative bio-mass). The QTL *qSNC9* on chromosome 9 is 430 kb away

**TABLE 3** | Known ST genes surrounding the mapped QTLs.

| Related traits | QTLs | Chr | Position (Mbp) | Known genes |
|---|---|---|---|---|
| RNC | *qRNC5* | 5 | 7.13 | *OsCYP51G3* Xia et al. 2015 |
| | | | | *OsPYL* Tian et al. 2015 |
| | *qRNC9* | 9 | 7.44 | *OsMYBc* Wang et al. 2015 |
| SNC | *qSNC1.1* | 1 | 2.07 | *OsRAV2* Duan et al. 2016 |
| | | | | *HSP17.0* Ham et al. 2013 |
| | *qSNC2* | 2 | 6.18–6.21 | *OsGlRL1* Park et al. 2014 |
| | *qSNC3.1* | 3 | 6.88 | *DSM3* Du et al. 2011 |
| | *qSNC9* | 9 | 15.83–15.86 | *OsDSG1* Park et al. 2010 |
| | | | | *OsBlERF1* Cao et al. 2006 |
| | *qSNC11.2* | 11 | 26.92–27.49 | *OsJAMyb* Yang et al. 2020 |
| RN/K | *qRN/K5* | 5 | 5.59–5.98 | *OsTZF1* Jan et al. 2013 |
| RTRV | *qRTRV3.1* | 3 | 2.06 | *ONAC022* Hong et al. 2016 |
| | *qRTRV3.2* | 3 | 2.66–2.67 | *OsAP23* Zhuang et al. 2013 |
| | *qRTRV6.1* | 6 | 1.16–1.58 | *OsSlK1* Ouyang et al. 2010 |
| RSN/K | *qRSN/K1.4* | 1 | 30.84 | *OsHsfC1b* Schmidt et al. 2012 |
| | *qRSN/K1.5* | 1 | 38.43 | *OsNAC6* Chung et al. 2009 |
| | *qRSN/K2* | 2 | 33.52–33.93 | *OsEREBP1* Jisha et al. 2015 |
| | *qRSN/K3* | 3 | 4.15 | *OsJAZ9* Wu et al. 2015 |
| SKC | *qSKC6* | 6 | 28.76–29.01 | *OsSIDP366* Guo et al. 2016 |
| | *qSKC8* | 8 | 25.12 | *OsDOG* Giri et al. 2011 |
| | | | | *OsXylT* Takano et al. 2015 |
| RTRL | *qRTRL1.1* | 1 | 18.01–18.26 | *OsMEK1* Wen et al. 2002 |
| RTRAS | *qRTRAS7* | 7 | 25.30–25.80 | *OsSAPK2* Xu et al. 2013 |

from the previously reported QTL *qRL-R9.1* (root length), and the QTL *qRNC9* is 430kbp away from the previously reported QTL *qDSW9* (dry shoot weight) and *qBST9* (biomass under salt treatment). It can be seen that some of the QTLs we mapped by GWAS were overlapped with or were close to the previously reported QTLs, which demonstrates that our GWAS mapping results are rather accurate.

In addition, 52 newly identified QTLs for ST were also found in this study. Among them, *qRN/K1.1* and *qRSN/K1.1* were located on chromosome 1 between 12.98–13.34Mbp and can explain 13.75–16.92% of phenotypic variation. The QTL *qRTRV.9* and *qRTRSA.9* between 15.43–15.53Mbp on chromosome 9 can explain 13.47–17.14% of the phenotypic variation. The QTL *qRN/K.9* and *qRSN/K9.3* between 19.50 and 19.54 Mb on chromosome 9 can explain 16.65–21.14% of phenotypic variation. These QTLs are newly discovered and need to be further examined in the future.

Moreover, we also compared the cold-tolerant and aluminum-tolerant QTLs previously mapped using the same core collection. Some QTLs are overlapped or are similar to the QTL regions for ST in this study. Compared with the previously located QTLs for cold tolerance, the QTL *qRSN/K4* in this study on chromosome 4 is about 200kbp away from the previously located cold-tolerant SNP (Chr4_20440388). The QTL *qRTRV6.1* on chromosome 6 contains the previously located cold-tolerant SNP (Chr6_1320300). The QTL *qRNC8.1* on chromosome 8 is about 151kbp away from the previously located cold-tolerant SNP (Chr8_374729). The QTL *qRN/K10* on chromosome 10 is about 18kbp away from the previously located cold-tolerant SNP (Chr10_3365663; Song et al., 2018). Compared with the previously located QTLs for aluminum tolerance, the QTL *qRN/K1.1* and *qRSN/K1.1* on chromosome 1 are about 330kbp away from the previously located QTL *qALT1.3*. The QTL *qRNC1* and *qRSN/K1.3* on chromosome 1 are about 400kbp away from the previously located QTL *qALT1.5*. The QTL *qRTRSA7* on chromosome 7 is about 84kbp away from the previously located QTL *qALT7.2*. The QTL region for *qRSN/K9.2* contains the previously located QTL *qALT9.1* (Zhao et al., 2018). These results indicate that the candidate genes in these intervals may have pleiotropic effects. It also indicates that the core collection contains a wealth of excellent resistance genes to biotic and abiotic stress.

## Comparison of the QTL Locations With the ST Genes

We also compared the QTL locations with the genes known to be related to ST.[4] Twenty-three ST genes were found to co-localize with our QTLs (**Table 3**). Three ST genes were found close to the mapped QTLs related to RNC in this study. Seven ST genes were found close to the mapped QTLs related to SNC. One ST gene was found in the QTL interval related to RN/K. Three ST genes were found close to the QTLs related to RTRV. Four ST genes were found close to the mapped QTLs related to RSN/K. Three ST genes were found close to the mapped QTLs related to SKC. One ST gene was found close to the QTLs related to RTRL. One ST gene was found close to the QTLs related to RTRAS. In short, these ST genes are located in or close to the relevant QTLs interval (with a searching range of +/− 250 kb). Among them, the QTL *qTL4* region is composed of *qSKC.6*, *qRN/K.6,* and *qSNC.6* and the

[4]http://qtaro.abr.affrc.go.jp

overlapping regions are dense. A known ST gene *OsSIDP366* was found in the region of *qTL4*, where a candidate gene and *OsSIDP366* both contain the DUF domain. These findings support the reliability of the mapping results in this study.

## Promising Candidate Genes for ST in Rice

The salinity tolerance in rice seedling is majorly governed by root and shoots $Na^+/K^+$ ratio. The lower $Na^+/K^+$ ratio provides protection against the toxic effects of $Na^+$, hence, tolerant to salt stress. Therefore, maintaining intracellular $Na^+/K^+$ homeostasis is a key factor in determining the survival ability of plants in response to salt stress (Yang and Yan, 2018). In this study, we found that *qSKC6*, *qSNC6,* and *qRN/K.6* were co-localization and 4 candidate genes (*LOC_Os06g47720*, *LOC_Os06g47820*, *LOC_Os06g47850*, and *LOC_Os06g47970*) were detected in the interval of *qTL4* which are all related to ratio of $Na^+$ to $K^+$ concentrations; therefore, we chose the four candidate genes for further study. Besides, *qRN/K1.1* and *qRSN/K1.1* also were co-localization and detected in the interval of *qTL6* which are related to $Na^+$ and $K^+$, the *qTL6* contains the highest peak SNP (Chr9_19518843). Therefore, searching for candidate genes in the interval of *qTL6* is also the focus of our next study.

To do it, we first checked the expression profiles of these four candidate genes from the Encyclopedia of Rice Transcriptome (TENOR) database.[5] According to the TENOR database (**Supplementary Figure S2**), the candidate gene *LOC_Os06g47720* has a higher expression level under salt stress conditions. The gene annotation of *LOC_Os06g47720* is a serine threonine protein kinase BRI1-like 2 precursor. BRI1 (protein brassinosteroid insensitive 1) is the receptor kinase of BR (brassinosteroids), located on the cell membrane, and is a leucine-rich repeat (LRR) receptor-like serine/threonine kinase on the cell surface, which is crucial in the BR signaling pathway. BR is a plant steroid hormone, which plays a key role in growth and response to abiotic and biotic stress (Zhao et al., 2019; Ma et al., 2021). The plants adapt to various environmental stresses by changing their physiological and molecular processes, which are coordinated with changes of the levels on hormones (including brassinosteroids) in plant externally and internally (Bilal et al., 2021). The response of BR under salt stress may be mediated by BRI1, inhibiting the degradation of the endoplasmic reticulum to combat salt stress (Cui et al., 2012). BR signaling also counters salt stress by signaling cascades or initiating ethylene biosynthesis (Planas-Riverola et al., 2019). In this study, the expression level of *LOC_Os06g47720* in S87 is much higher than that in S125, and *LOC_Os06g47720* had far more mutation sites in S87 than in S125. By comparison of amino acid sequences, it also revealed that only the amino acids in S87 were changed and the translation was terminated in S125. These findings suggest that *LOC_Os06g47720* may be involved in the regulation of ST through the BR pathway.

The candidate gene *LOC_Os06g47820* is receptor-like kinases, which has the highest expression level under ABA treatment conditions (**Supplementary Figure S2**). ABA can coordinate with hormones such as auxin, gibberellin (GA) and cytokinin (CK) to regulate the response of plants to salt stress (Yu et al., 2020). Receptor-like kinases (RLKs) are a large family of proteins that exist on the surface of plant cell membranes. Their basic function is to transmit regulatory signals on the cell surface. Plant receptor-like protein kinases occupy important metabolic positions, and rice has about 1,130 RLK genes (Quynh-Nga et al., 2015). Plant RLKs are composed of intracellular, extracellular, and transmembrane regions (Ye et al., 2017). Receptor-like protein kinase RLK is widely involved in cell signal transduction and plant response to stress (Lemmon and Schlessinger, 2010). In recent years, several researchers studied the important role of RLKs in optimizing the response of plants to salt stress and other abiotic stresses (Zhou et al., 2018; Lin et al., 2020). In this study, the expression level of *LOC_Os06g47820* in S125 was found much higher than that in S87. The gene had much more mutation sites in S125 than in S87. There are more changes in amino acids in S125 than in S87. These findings indicate that *LOC_Os06g47820* is a candidate gene that may be involved in the regulation of ST in rice.

The candidate gene *LOC_Os06g47850* encodes a zinc finger family protein. The zinc finger protein (ZFP) family is widely distributed in eukaryotic genomes and is one of the most important transcription factors, which plays an important role in plant growth and development and abiotic stress response (Mukhopadhyay et al., 2004; Sakamoto, 2004). More than 60 transcription factor families have been reported in plants (Iuchi, 2001). *LOC_Os06g47850* has the highest expression level under cold stress conditions (**Supplementary Figure S2**). In our study, the expression level of *LOC_Os06g47820* in S125 was much higher than that in S87. DNA sequence alignment results showed that the gene has no mutation sites. Therefore, the mechanism of this candidate gene remains to be elucidated.

The candidate gene *LOC_Os06g47970* encodes a DUF1517 (domains of unknown function, DUF) which are a class of proteins whose functions have not been characterized and account for about 25% of the total protein family (Mudgal et al., 2015). According to the TENOR database (**Supplementary Figure S2**), *LOC_Os06g47970* has the highest expression level under drought stress and as we know that salinity usually occurs at the same time as drought stress (Hu et al., 2006). In recent years, an increasing number of studies were conducted on the regulation of different DUFs family genes involved in plant growth and development and plant response to stress (biotic and abiotic stress; Li et al., 2018; Lv et al., 2019). We found a DUFs gene in the *qTL4*, i.e., *OsSIDP366*, which is a stress-induced DUF1644 protein and contains a DUF1644 domain, a C2H2 and a ring finger domain. *OsSIDP366* is expressed in multiple tissues. The expression is higher in young roots, mature leaves, and leaf sheaths, but lower or no expression in internodes, mature seeds, lemmas and glumes. High salt and drought treatments can induce the expression of *OsSIDP366*. *OsSIDP366* may positively regulate salt and drought resistance in rice (Guo et al., 2016). In addition, we also found that the homologous gene *AT5G57345* in *Arabidopsis*, a single copy gene, is localized to ER and expressed in the whole plant and induced expression in response

[5]http://tenor.dna.affrc.go.jp/

to abiotic stress. Although the function of *AT5G57345* is unclear, overexpression can lead to increased tolerance to abiotic stress and increased ascorbic acid content (Bu et al., 2016). In addition, we also found that the expression level of *LOC_Os06g47970* in S125 was much higher than that in S87. Sequence analysis found that *LOC_Os06g47970* only had a pair of base substitutions in S125, i.e., one amino acid was changed in S125, while no change in S87. Therefore, *LOC_Os06g47970* might be involved in the regulation of ST in rice.

This study lays a foundation for the functional analysis of the candidate genes in the regulation of salt tolerance in rice and the enrichment of the rice salt tolerance regulatory network. In addition, our newly discovered QTLs also lay the foundation for further research on the ST mechanism in rice in the future. The salt tolerance-related candidate genes and QTLs would provide important resources for molecular breeding and functional analysis of the salt tolerance during the seedling stage of rice. However, the four candidate genes identified in this study which involved in the regulation of salt stress in rice need further research and verification. In addition, the mechanism and the regulation pathway for these genes under salt stress in rice still need to be clarified. In future, the function of candidate genes related to salt tolerance will be studied by Crispr-Cas9 technology, which will help to precisely uncover the mechanisms of salinity tolerance at molecular level.

## CONCLUSION

Eight seedling-stage salt-related traits within a core collection of rice landraces were evaluated under salinity stress (100 mm NaCl) in a growth chamber, and abundant phenotypic variations were observed for these traits. With 2,487,353 SNPs derived from an enrichment of 67,511 SNPs from SLAF-seq, GWAS was performed for the eight traits related to ST with a mixed linear model. In total, 65 QTLs were identified significantly associated with eight ST traits. These QTLs explained 13.47 to 28.11% of the phenotype variation. There are 8 QTLs for RNC, 14 QTLs for SNC, 10 QTLs for RN/K, 8 QTLs for RTRV, 13 QTLs for SN/K, 2 QTLs for SKC, 5 QTLs for SKC, and 5 QTLs for TRSA. Several QTLs in this study were overlapped with or were close to the previously reported candidate genes or QTLs related to ST. There are 6 genomic regions containing co-localization QTLs (qTL1 – qTL6). Among them, a co-localization QTL qTL4 associated with the SKC, RN/K and SNC on chromosome 6, which explained 14.38–17.94% of phenotypic variation, was selected for further analysis. According to haplotype analysis, qRT-PCR analysis, and sequence alignment, it was finally determined that 4 candidate genes (*LOC_Os06g47720*, *LOC_Os06g47820*, *LOC_Os06g47850*, and *LOC_Os06g47970*) were related to ST. The results provide useful candidate genes for marker-assisted selection for ST in the rice molecular breeding programs.

## DATA AVAILABILITY STATEMENT

The datasets presented in this study can be found in online repositories. The names of the repository/repositories and accession number(s) can be found in the article/**Supplementary Material**.

## AUTHOR CONTRIBUTIONS

MZ and WC designed the study. MZ, XW, SG, CS, YL, and DM performed data analyses. XW and JS performed GWAS and statistical analyses. MZ, XW, and CS performed searching candidate genes/QTLs. XW wrote the paper. JL provided the rice core collection. MZ and JL revised the manuscript. All authors read and approved the final manuscript.

## FUNDING

This work was supported by LiaoNing Revitalization Talents Program (XLYC2008025).

## SUPPLEMENTARY MATERIAL

The Supplementary Material for this article can be found online at: https://www.frontiersin.org/articles/10.3389/fpls.2022.847863/full#supplementary-material

**Supplementary Figure S1 |** QQ plots of genome-wide association studies for the eight traits related to ST. A-H: QQ plots for RNC, SKC, SNC, RN/K, RTRL, RTRSA, RTRV, and RSN/K.

**Supplementary Figure S2 | (A–C)** DNA sequence analysis and amino acid sequence analysis for three candidate genes.

**Supplementary Figure S3 |** Expression profiles in rice seedling under the various environmental conditions.

## REFERENCES

An, H., Liu, K., Wang, B., Tian, Y., Ge, Y., Zhang, Y., et al. (2020). Genome-wide association study identifies QTLs conferring salt tolerance in rice. *Plant Breed.* 139, 73–82. doi: 10.1111/pbr.12750

Bilal, H. M., Noreen, Z., Kiran, Z., Ali, R., Aaliya, K., Kanval, S., et al. (2021). Brassinosteroids: molecular and physiological responses in plant growth and abiotic stresses. *Plant Stress* 2:100029. doi: 10.1016/j.stress.2021.100029

Bu, Y., Sun, B., Zhou, A., Zhang, X., Takano, T., and Liu, S. (2016). Overexpression of AtOxR gene improves abiotic stresses tolerance and vitamin C content in *Arabidopsis thaliana*. *BMC Biotechnol.* 16:69. doi: 10.1186/s12896-016-0299-0

Cao, Y., Song, F., Goodman, R. M., and Zheng, Z. (2006). Molecular characterization of four rice genes encoding ethylene-responsive transcriptional factors and their expressions in response to biotic and abiotic stress. *J. Plant Physiol.* 163, 1167–1178. doi: 10.1016/j.jplph.2005.11.004

Chen, T., Zhu, Y., Chen, K., Shen, C., Zhao, X., Shabala, S., et al. (2020). Identification of new QTL for salt tolerance from rice variety Pokkali. *J. Agron. Crop Sci.* 206, 202–213. doi: 10.1111/jac.12387

Chung, P. J., Kim, Y. S., Jeong, J. S., Park, S.-H., Nahm, B. H., and Kim, J.-K. (2009). The histone deacetylase OsHDAC1 epigenetically regulates the OsNAC6 gene that controls seedling root growth in rice. *Plant J.* 59, 764–776. doi: 10.1111/j.1365-313X.2009.03908.x

Cui, F., Liu, L., Li, Q., Yang, C., and Xie, Q. (2012). UBC32 mediated oxidative tolerance in Arabidopsis. *J. Genet. Genomics* 39, 415–417. doi: 10.1016/j.jgg.2012.05.005

Du, H., Liu, L., You, L., Yang, M., He, Y., Li, X., et al. (2011). Characterization of an inositol 1,3,4-trisphosphate 5/6-kinase gene that is essential for drought and salt stress responses in rice. *Plant Mol. Biol.* 77, 547–563. doi: 10.1007/s11103-011-9830-9

Duan, Y. B., Li, J., Qin, R. Y., Xu, R. F., Li, H., Yang, Y. C., et al. (2016). Identification of a regulatory element responsible for salt induction of rice OsRAV2 through ex situ and in situ promoter analysis. *Plant Mol. Biol.* 90, 49–62. doi: 10.1007/s11103-015-0393-z

Giri, J., Vij, S., Dansana, P. K., and Tyagi, A. K. (2011). Rice A20/AN1 zinc-finger containing stress-associated proteins (SAP1/11) and a receptor-like cytoplasmic kinase (OsRLCK253) interact via A20 zinc-finger and confer abiotic stress tolerance in transgenic Arabidopsis plants. *New Phytol.* 191, 721–732. doi: 10.1111/j.1469-8137.2011.03740.x

Guo, C., Luo, C., Guo, L., Li, M., Guo, X., Zhang, Y., et al. (2016). OsSIDP366, a DUF1644 gene, positively regulates responses to drought and salt stresses in rice. *J. Integr. Plant Biol.* 58, 492–502. doi: 10.1111/jipb.12376

Ham, D.-J., Moon, J.-C., Hwang, S.-G., and Jang, C. S. (2013). Molecular characterization of two small heat shock protein genes in rice: their expression patterns, localizations, networks, and heterogeneous over expressions. *Mol. Biol. Rep.* 40, 6709–6720. doi: 10.1007/s11033-013-2786-x

Hirschhorn, J. N., and Daly, M. J. (2005). Genome-wide association studies for common diseases and complex traits. *Nat. Rev. Genet.* 6, 95–108. doi: 10.1038/nrg1521

Hong, Y., Zhang, H., Huang, L., Li, D., and Song, F. (2016). Overexpression of a stress-responsive NAC transcription factor gene ONACO22 improves drought and salt tolerance in Rice. *Front. Plant Sci.* 7:4. doi: 10.3389/fpls.2016.00004

Hu, Y., Burucs, Z., and Schmidhalter, U. (2006). Short-term effect of drought and salinity on growth and mineral elements in wheat seedlings. *J. Plant Nutr.* 29, 2227–2243. doi: 10.1080/01904160600975111

Iuchi, S. (2001). Three classes of C2H2 zinc finger proteins. *Cell. Mol. Life Sci.* 58, 625–635. doi: 10.1007/PL00000885

Jahan, N., Zhang, Y., Lv, Y., Song, M., Zhao, C., Hu, H., et al. (2020). QTL analysis for rice salinity tolerance and fine mapping of a candidate locus qSL7 for shoot length under salt stress. *Plant Growth Regul.* 90, 307–319. doi: 10.1007/s10725-019-00566-3

Jan, A., Maruyama, K., Todaka, D., Kidokoro, S., Abo, M., Yoshimura, E., et al. (2013). OsTZF1, a CCCH-tandem zinc finger protein, confers delayed senescence and stress tolerance in Rice by regulating stress-related genes. *Plant Physiol.* 161, 1202–1216. doi: 10.1104/pp.112.205385

Jisha, V., Dampanaboina, L., Vadassery, J., Mithoefer, A., Kappara, S., and Ramanan, R. (2015). Overexpression of an AP2/ERF type transcription factor OsEREBP1 confers biotic and abiotic stress tolerance in Rice. *PLoS One* 10:e0127831. doi: 10.1371/journal.pone.0127831

Lemmon, M. A., and Schlessinger, J. (2010). Cell signaling by receptor tyrosine kinases. *Cell* 141, 1117–1134. doi: 10.1016/j.cell.2010.06.011

Li, X. L., Li, J. Q., and Lu, Y. G. (2007). Research on the construction strategy of rice core collection. *J. Shenyang Agri. Univ.* 5, 681–687.

Li, X., Lu, Y., Li, J., Xu, H., and Shahid, M. Q. (2011). Strategies on Sample Size Determination and Qualitative and Quantitative Traits Integration to Construct Core Collection of Rice (Oryza sativa). *Rice Science* 18, 46–55. doi: 10.1016/S1672-6308(11)60007-3

Li, L. H., Lv, M. M., Li, X., Ye, T. Z., He, X., Rong, S. H., et al. (2018). The Rice OsDUF810 family: OsDUF810.7 may be involved in the tolerance to salt and drought. *Mol. Biol.* 52, 567–575. doi: 10.1134/S0026898418040122

Li, J., Pu, L., Han, M., Zhu, M., Zhang, R., and Xiang, Y. (2014). Soil salinization research in China: advances and prospects. *J. Geogr. Sci.* 24, 943–960. doi: 10.1007/s11442-014-1130-2

Li, J., and Zhang, P. (2012). "Assessment and utilization of the genetic diversity in rice," in *Genetic Diversity in Plants.* ed M. Caliskan (London: InTech-Open Access Publisher), 87–102.

Lin, F., Li, S., Wang, K., Tian, H., and Du, C. (2020). A Leucine-rich repeat receptor-like kinase, OsSTLK, modulates salt tolerance in rice. *Plant Sci.* 296:110465. doi: 10.1016/j.plantsci.2020.110465

Liu, C., Chen, K., Zhao, X., Wang, X., Shen, C., Zhu, Y., et al. (2019). Identification of genes for salt tolerance and yield-related traits in rice plants grown hydroponically and under saline field conditions by genome-wide association study. *Rice* 12:88. doi: 10.1186/s12284-019-0349-z

Livak, K. J., and Schmittgen, T. D. (2002). Analysis of Relative Gene Expression Data using Real-Time Quantitative PCR. *Methods* 25, 402–408. doi: 10.1006/meth.2001.1262

Lv, M., Hou, D., Zhang, L., Fan, J., Li, C., Chen, W., et al. (2019). Molecular characterization and function analysis of the rice OsDUF1191 family. *Biotechnol. Equipment* 33, 1608–1615. doi: 10.1080/13102818.2019.1684843

Ma, X., Yuan, Y., Li, C., Wu, Q., He, Z., Li, J., et al. (2021). Brassinosteroids suppress ethylene-induced fruitlet abscission through LcBZR1/2-mediated transcriptional repression of LcACS1/4 and LcACO2/3 in litchi. *Hortic. Res.* 8:105. doi: 10.1038/s41438-021-00540-z

Mccouch, S., Cho, Y., Yano, M., Paul, E., Blinstrub, M., Morishima, H., et al. (1997). Report on QTL nomenclature. *Rice Genet Newsl* 14.

Mudgal, R., Sandhya, S., Chandra, N., and Srinivasan, N. (2015). De-DUFing the DUFs: deciphering distant evolutionary relationships of domains of unknown function using sensitive homology detection methods. *Biol. Direct* 10:38. doi: 10.1186/s13062-015-0069-2

Mukhopadhyay, A., Vij, S., and Tyagi, A. K. (2004). Overexpression of a zinc-finger protein gene from rice confers tolerance to cold, dehydration, and salt stress in transgenic tobacco. *Proc. Natl. Acad. Sci. U. S. A.* 101, 6309–6314. doi: 10.1073/pnas.0401572101

Naveed, S. A., Zhang, F., Zhang, J., Zheng, T. Q., Meng, L. J., Pang, Y. L., et al. (2018). Identification of QTN and candidate genes for salinity tolerance at the germination and seedling stages in Rice by genome-wide association analyses. *Sci. Rep.* 8:6505. doi: 10.1038/s41598-018-24946-3

Nayyeripasand, L., Garoosi, G. A., and Ahmadikhah, A. (2021). Genome-wide association study (GWAS) to identify salt-tolerance QTLs carrying novel candidate genes in Rice During early vegetative stage. *Rice* 14:9. doi: 10.1186/s12284-020-00433-0

Ouyang, S.-Q., Liu, Y.-F., Liu, P., Lei, G., He, S.-J., Ma, B., et al. (2010). Receptor-like kinase OsSIK1 improves drought and salt stress tolerance in rice (*Oryza sativa*) plants. *Plant J.* 62, 316–329. doi: 10.1111/j.1365-313X.2010.04146.x

Park, S., Moon, J.-C., Park, Y. C., Kim, J.-H., Kim, D. S., and Jang, C. S. (2014). Molecular dissection of the response of a rice leucine-rich repeat receptor-like kinase (LRR-RLK) gene to abiotic stresses. *J. Plant Physiol.* 171, 1645–1653. doi: 10.1016/j.jplph.2014.08.002

Park, G.-G., Park, J.-J., Yoon, J., Yu, S.-N., and An, G. (2010). A RING finger E3 ligase gene, *Oryza sativa* delayed seed germination 1 (OsDSG1), controls seed germination and stress responses in rice. *Plant Mol. Biol.* 74, 467–478. doi: 10.1007/s11103-010-9687-3

Planas-Riverola, A., Gupta, A., Betegon-Putze, I., Bosch, N., Ibanes, M., and Cano-Delgado, A. I. (2019). Brassinosteroid signaling in plant development and adaptation to stress. *Development* 146:dev.151894. doi: 10.1242/dev.151894

Prasad, S. R., Bagali, P. G., Hittalmani, S., and Shashidhar, H. E. (2000). Molecular mapping of quantitative trait loci associated with seedling tolerance to salt stress in rice (*Oryza sativa* L.). *Curr. Sci.* 78, 162–164.

Qadir, M., Quillerou, E., Nangia, V., Murtaza, G., Singh, M., Thomas, R. J., et al. (2014). Economics of salt-induced land degradation and restoration. *Nat. Res. Forum* 38, 282–295. doi: 10.1111/1477-8947.12054

Qi, D. L., Han, L. Z., and Zhang, S. Y. (2005). Methods of Characterization and Evaluation of Salt or Alkaline Tolerance in Rice. *Journal of Plant Genetic Resources* 6, 226–231.

Quynh-Nga, N., Lee, Y.-S., Cho, L.-H., Jeong, H.-J., An, G., and Jung, K.-H. (2015). Genome-wide identification and analysis of *Catharanthus roseus* RLK1-like kinases in rice. *Planta* 241, 603–613. doi: 10.1007/s00425-014-2203-2

Roy, S. J., Tucker, E. J., and Tester, M. (2011). Genetic analysis of abiotic stress tolerance in crops. *Curr. Opin. Plant Biol.* 14, 232–239. doi: 10.1016/j.pbi.2011.03.002

Ruan, S.-L., Ma, H.-S., Wang, S.-H., Fu, Y.-P., Xin, Y., Liu, W.-Z., et al. (2011). Proteomic identification of OsCYP2, a rice cyclophilin that confers salt tolerance in rice (*Oryza sativa* L.) seedlings when overexpressed. *BMC Plant Biol.* 11:34. doi: 10.1186/1471-2229-11-34

Sakamoto, H. (2004). Arabidopsis Cys2/His2-type zinc-finger proteins function as transcription repressors under drought, cold, and high-salinity stress conditions. *Plant Physiol.* 136, 2734–2746. doi: 10.1104/pp.104.046599

Schmidt, R., Schippers, J. H. M., Welker, A., Mieulet, D., Guiderdoni, E., and Mueller-Roeber, B. (2012). Transcription factor OsHsfC1b regulates salt tolerance and development in *Oryza sativa* ssp japonica. *AOB Plants.* 2012:pls011. doi: 10.1093/aobpla/pls011

Shin, J.-H., Blay, S., Mcneney, B., and Graham, J. (2006). LDheatmap: An R function for graphical display of pairwise linkage disequilibria between single nucleotide polymorphisms. *J. Stat. Softw.* 16, 1–9. doi: 10.18637/jss.v016.c03

Solis, C. A., Yong, M. T., Vinarao, R., Jena, K., and Chen, Z. H. (2020). Back to the wild: on a quest for donors toward salinity tolerant Rice. *Front. Plant Sci.* 11:323. doi: 10.3389/fpls.2020.00323

Song, J., Jinqun, L., Jian, S., Tao, H., Aiting, W., Sitong, L., et al. (2018). Genome-wide association mapping for cold tolerance in a Core collection of Rice (*Oryza sativa* L.) landraces by using high-density single nucleotide polymorphism markers from specific-locus amplified fragment sequencing. *Front. Plant Sci.* 9:875. doi: 10.3389/fpls.2018.00875

Takano, S., Matsu Da, S., Unabiki, A. F., Furukawa, J. I., Yamauchi, T., Tokuji, Y., et al. (2015). The rice RCN11 gene encodes β1,2-xylosyltransferase and is required for plant responses to abiotic stresses and phytohormones. *Plant Sci.* 236, 75–88. doi: 10.1016/j.plantsci.2015.03.022

Takehisa, H., Shimodate, T., Fukuta, Y., Ueda, T., Yano, M., Yamaya, T., et al. (2004). Identification of quantitative trait loci for plant growth of rice in paddy field flooded with salt water. *Field Crop Res.* 89, 85–95. doi: 10.1016/j.fcr.2004.01.026

Tian, X., Wang, Z., Li, X., Lv, T., and Liu, H. (2015). Characterization and functional analysis of Pyrabactin resistance-Like Abscisic acid receptor family in Rice. *Rice.* 8:28. doi: 10.1186/s12284-015-0061-6

Walia, H., Wilson, C., Condamine, P., Liu, X., Ismail, A. M., Zeng, L., et al. (2005). Comparative transcriptional profiling of two contrasting rice genotypes under salinity stress during the vegetative growth stage. *Plant Physiol.* 139, 822–835. doi: 10.1104/pp.105.065961

Wang, D. R., Agosto-Pérez, F. J., Chebotarov, D., Shi, Y., Marchini, J., Fitzgerald, M., et al. (2018a). An imputation platform to enhance integration of rice genetic resources. *Nat. Commun.* 9:3519. doi: 10.1038/s41467-018-05538-1

Wang, Z., Chen, Z., Cheng, J., Lai, Y., Wang, J., Bao, Y., et al. (2012). QTL analysis of Na+ and K+ concentrations in roots and shoots under different levels of NaCl stress in Rice (*Oryza sativa* L.). *PLoS One* 7:e51202. doi: 10.1371/journal.pone.0051202

Wang, R., Jing, W., Xiao, L., Jin, Y., Shen, L., and Zhang, W. (2015). The Rice high-affinity potassium Transporter1;1 is involved in salt tolerance and regulated by an MYB-type transcription factor. *Plant Physiol.* 168:1076. doi: 10.1104/pp.15.00298

Wang, W., Mauleon, R., Hu, Z., Chebotarov, D., Tai, S., Wu, Z., et al. (2018b). Genomic variation in 3,010 diverse accessions of Asian cultivated rice. *Nature* 557:43. doi: 10.1038/s41586-018-0063-9

Wen, J.-Q., Oono, K., and Imai, R. (2002). Two novel mitogen-activated protein signaling components, OsMEK1 and OsMAP1, are involved in a moderate low-temperature signaling pathway in rice. *Plant Physiol.* 129, 1880–1891. doi: 10.1104/pp.006072

Wu, F., Yang, J., Yu, D., and Xu, P. (2020). Identification and validation a major QTL from "sea Rice 86," seedlings conferred salt tolerance. *Agronomy* 10:410. doi: 10.3390/agronomy10030410

Wu, H., Ye, H., Yao, R., Zhang, T., and Xiong, L. (2015). OsJAZ9 acts as a transcriptional regulator in jasmonate signaling and modulates salt stress tolerance in rice. *Plant Sci.* 232, 1–12. doi: 10.1016/j.plantsci.2014.12.010

Xia, K., Ou, X., Tang, H., Ren, W., Ping, W., Jia, Y., et al. (2015). Rice microRNA Osa-miR1848 targets the obtusifoliol 14α-demethylase gene OsCYP51G3 and mediates the biosynthesis of phytosterols and brassinosteroids during development and in response to stress. *New Phytol.* 208, 790–802. doi: 10.1111/nph.13513

Xiaoxue, P., Mingyu, H., Xiaoying, J., Wenqin, B., Ling, G., Hong, W., et al. (2019). Overexpression of the Thellungiella salsuginea TsIPK2 gene enhances salt tolerance of transgenic rice. *J. Plant Nutrit. Fertiliz* 25, 741–747. doi: 10.11674/zwyf.18144

Xu, M.-R., Huang, L.-Y., Zhang, F., Zhu, L.-H., Zhou, Y.-L., and Li, Z.-K. (2013). Genome-wide phylogenetic analysis of stress-activated protein kinase genes in Rice (OsSAPKs) and expression profiling in response to *Xanthomonas oryzae* pv. Oryzicola infection. *Plant Mol. Biol. Report.* 31, 877–885. doi: 10.1007/s11105-013-0559-2

Yang, Z., Huang, Y., Yang, J., Yao, S., Zhao, K., Wang, D., et al. (2020). Jasmonate signaling enhances RNA silencing and antiviral defense in Rice. *Cell Host Microbe* 28:89. doi: 10.1016/j.chom.2020.05.001

Yang, Y., and Yan, G. (2018). Unraveling salt stress signaling in plants. *J. Integr. Plant Biol.* 60, 796–804. doi: 10.1111/jipb.12689

Ye, Y., Ding, Y., Jiang, Q., Wang, F., Sun, J., and Zhu, C. (2017). The role of receptor-like protein kinases (RLKs) in abiotic stress response in plants. *Plant Cell Rep.* 36, 235–242. doi: 10.1007/s00299-016-2084-x

Yoshida, S., Forno, D. A., Cock, J. H., and Gomez, K. A. (1976). *Laboratory Manual for Physiological Studies of Rice. 3rd Edn.* The International Rice Research Institute, Manila.

Yu, Z., Duan, X., Luo, L., Dai, S., and Xia, G. (2020). How plant hormones mediate salt stress responses. *Trends Plant Sci.* 25, 1117–1130. doi: 10.1016/j.tplants.2020.06.008

Yuan, J., Wang, X., Zhao, Y., Khan, N. U., Zhao, Z., Zhang, Y., et al. (2020). Genetic basis and identification of candidate genes for salt tolerance in rice by GWAS. *Sci. Rep.* 10:9958. doi: 10.1038/s41598-020-66604-7

Zeng, P., Zhu, P., Qian, L., Qian, X., Mi, Y., Lin, Z., et al. (2021). Identification and fine mapping of qGR6.2, a novel locus controlling rice seed germination under salt stress. *BMC Plant Biol.* 21:36. doi: 10.1186/s12870-020-02820-7

Zhang, J., Chen, K., Pang, Y., Naveed, S. A., Zhao, X., Wang, X., et al. (2017). QTL mapping and candidate gene analysis of ferrous iron and zinc toxicity tolerance at seedling stage in rice by genome-wide association study. *BMC Genomics* 18:828. doi: 10.1186/s12864-017-4221-5

Zhang, P., Li, J., Li, X., Liu, X., Zhao, X., and Lu, Y. (2011). Population Structure and Genetic Diversity in a Rice Core Collection (Oryza sativa L.) Investigated with SSR Markers. *PLoS One* 6:e27565. doi: 10.1371/journal.pone.0027565

Zhang, Y., Ponce, K., Meng, L., Chakraborty, P., and Ye, G. (2020). QTL identification for salt tolerance related traits at the seedling stage in indica rice using a multi-parent advanced generation intercross (MAGIC) population. *Plant Growth Regul.* 92, 365–373. doi: 10.1007/s10725-020-00644-x

Zhao, X., Dou, L., Gong, Z., Wang, X., and Mao, T. (2019). BES1 hinders ABSCISIC ACID INSENSITIVE5 and promotes seed germination in Arabidopsis. *New Phytol.* 221, 908–918. doi: 10.1111/nph.15437

Zhao, M., Song, J., Wu, A., Hu, T., and Li, J. (2018). Mining beneficial genes for aluminum tolerance Within a Core collection of Rice landraces Through genome-wide association mapping With high density SNPs From specific-locus amplified fragment sequencing. *Front. Plant Sci.* 9:1838. doi: 10.3389/fpls.2018.01838

Zhou, Y.-B., Liu, C., Tang, D.-Y., Yan, L., Wang, D., Yang, Y.-Z., et al. (2018). The receptor-Like cytoplasmic kinase STRK1 phosphorylates and activates CatC, thereby regulating H2O2 homeostasis and improving salt tolerance in Rice. *Plant Cell* 30, 1100–1118. doi: 10.1105/tpc.17.01000

Zhuang, J., Jiang, H.-H., Wang, F., Peng, R.-H., Yao, Q.-H., and Xiong, A.-S. (2013). A Rice OsAP23, functioning as an AP2/ERF transcription factor, reduces salt tolerance in transgenic Arabidopsis. *Plant Mol. Biol. Report.* 31, 1336–1345. doi: 10.1007/s11105-013-0610-3

**Conflict of Interest:** JL is employed by Strube Research GmbH & Co.

The remaining authors declare that the research was conducted in the absence of any commercial or financial relationships that could be construed as a potential conflict of interest.

**Publisher's Note:** All claims expressed in this article are solely those of the authors and do not necessarily represent those of their affiliated organizations, or those of the publisher, the editors and the reviewers. Any product that may be evaluated in this article, or claim that may be made by its manufacturer, is not guaranteed or endorsed by the publisher.

frontiers | Frontiers in Plant Science

ORIGINAL RESEARCH
published: 19 May 2022
doi: 10.3389/fpls.2022.892667

# Seed Germination Response and Tolerance to Different Abiotic Stresses of Four *Salsola* Species Growing in an Arid Environment

*Pengyou Chen*[1,2,3,4†], *Li Jiang*[1†], *Weikang Yang*[1,2,3,4], *Lei Wang*[1,4*] and *Zhibin Wen*[1,3,4,5*]

[1] State Key Laboratory of Desert and Oasis Ecology, Xinjiang Institute of Ecology and Geography, Chinese Academy of Sciences, Urumqi, China, [2] Sino-Tajikistan Joint Laboratory for Conservation and Utilization of Biological Resources, Urumqi, China, [3] The Specimen Museum of Xinjiang Institute of Ecology and Geography, Chinese Academy of Sciences, Urumqi, China, [4] University of Chinese Academy of Sciences, Beijing, China, [5] Xinjiang Key Lab of Conservation and Utilization of Plant Gene Resources, Urumqi, China

OPEN ACCESS

**Edited by:**
Ali El-Keblawy,
University of Sharjah,
United Arab Emirates

**Reviewed by:**
Sanjay Gairola,
EPAA, United Arab Emirates
Mohsin Tanveer,
University of Tasmania, Australia
Salman Gulzar,
University of Karachi, Pakistan

***Correspondence:**
Lei Wang
egiwang@ms.xjb.ac.cn
Zhibin Wen
zhibinwen@ms.xjb.ac.cn

[†]These authors have contributed equally to this work

**Specialty section:**
This article was submitted to Plant Abiotic Stress, a section of the journal Frontiers in Plant Science

**Received:** 09 March 2022
**Accepted:** 15 April 2022
**Published:** 19 May 2022

**Citation:**
Chen P, Jiang L, Yang W, Wang L and Wen Z (2022) Seed Germination Response and Tolerance to Different Abiotic Stresses of Four Salsola Species Growing in an Arid Environment.
Front. Plant Sci. 13:892667.
doi: 10.3389/fpls.2022.892667

Land degradation caused by soil salinization and wind erosion is the major obstruction to sustainable agriculture in the arid region. *Salsola* species have the potential to prevent land degradation. However, there is limited information about seed germination requirements and tolerance to salinity and drought for representative *Salsola* species. This study aimed to assess the effects of the winged perianth (seed structural features) and abiotic factors (light, temperature, salinity, and drought) on the seed germination of these species. These *Salsola* species varied considerably in seed germination characteristics. Compared with naked seeds, winged seeds had lower germination percentages for *S. heptapotamica S. rosacea,* and *S. nitraria* species. Darkness decreased the germination percentage of winged and naked seeds of *S. rosacea*, however, for *S. heptapotamica* and *S. nitraria*, decreased seed germination was only when the winged perianth existed. Germination of *S. heptapotamica*, *S. rosacea,* and *S. nitraria* seeds depended on the perianth and light conditions. The naked seeds of these three species could germinate at a wide range of temperatures, especially in light. The presence of perianth, light, and temperature did not significantly influence the germination of *S. ruthenica* seeds. When cultivating these species, it is beneficial to remove the winged perianth of seeds and sow it on the soil surface when the temperature is above 5/15°C. In addition, seed germination of *Salsola* displayed high tolerance to salinity and drought. Compared with winged seeds, naked seeds showed lower recovery germination under high salinity but had a similar recovery of germination under high PEG concentration. Our study provides detailed germination information for the cultivation of these four representative *Salsola* species in degraded saline soils of the arid zone.

**Keywords: light, salinity, *Salsola*, seed germination, winged perianth, land rehabilitation**

## INTRODUCTION

Land degradation refers to the succession process in which unfavorable natural factors or inappropriate land use leads to the gradual loss of production potential (Prince et al., 2009). The arid land in Central Asia is the largest dry area located in the temperate and warm temperate zone of the northern hemispheric earth, where land degradation is quite serious because of climatic

variations and human activities resulting from population increase (Kuang et al., 2014). It is reported that the land degradation area in Central Asia is about $58.78 \times 10^4$ km$^2$, accounting for 10.37% of the total land area (Kuang et al., 2014). Salinity and drought are two abiotic factors resulting in land degradation in the arid region in Central Asia, which increasingly threaten sustainable agriculture with global climate change (Negrão et al., 2017). Currently, ∼10% of the total land is degraded by salinity (Ruan et al., 2010) and up to 41% by drought (D'Odorico et al., 2013). Therefore, it is not unexpected that a large effort is devoted to repairing or restoring the deteriorating land (Zhang et al., 2015; Wang et al., 2020).

Cultivation of native plant species could be a viable alternative to rehabilitating such degraded land (El-Keblawy and Ksiksi, 2005). The use of suitable candidate plants is a vital step in any recovery program (El-Keblawy, 2017). One of the most important selection criteria to choose plants for land rehabilitation is their capacity of seeds to germinate under complex conditions, especially under stress (Lu et al., 2016). Therefore, a thorough knowledge of seed germination requirements for light and temperature, and tolerance to salinity or drought stress of native plants is the key aspect to understanding the role of the plants in the restoration and rehabilitation strategies (Qian et al., 2016).

Temperature is a determining factor for seed germination of most plants, which can break seed dormancy and stimulate germination (Probert, 1992; Baskin and Baskin, 2014). Seed germination of native plants in arid regions is often limited by the temperature though the other conditions are suitable (Evans and Etherington, 1990). Light is another important regulatory environmental signal for seed germination of desert plants (Katerina et al., 2014). In the desert and semi-desert areas, plants vary in their requirement for light during germination. Some germinate strictly in need of light (Sen and Chatterji, 1968), while others can germinate well in light or dark (Huang et al., 2003), and some even germinate better in dark than in light (Sekmen et al., 2004). In addition, the actual germination requirements of seeds to light depend on the interaction with other environmental factors such as temperature (El-Keblawy et al., 2011). Many desert plants germinate only when the combinations of light and temperature are suitable for seedling establishment (Naidoo and Naicker, 1992).

In arid and semi-arid regions, reduction in water potential of soil caused by salinity or drought is common stress that affects seed imbibition and thereby germination (Rasheed et al., 2019). Seed germination percentage is generally decreased with the increase in salinity or PEG concentration (Khan and Gulzar, 2003; Xing et al., 2013). Most ungerminated seeds remain viable under harsh conditions (e.g., high salinity and drought) by entering a state of conditional or enforced dormancy and can recover germination on the provision of sufficient moisture (Rasheed et al., 2015). Such germination inhibition may be a survival strategy for plants in arid regions, which could reduce seedling mortality (Khan and Gul, 2006).

There are a large group of plants in nature, whose seed structure has additional appendages such as winged perianth or bracteole (Jurado et al., 1991). Seeds with winged perianth take the advantage in dispersal (Baskin et al., 2014). Moreover, the presence of perianth-inhibited seed germination is seen in many plants, such as *Haloxylon stocksii* (Rasheed et al., 2019), *Salsola ikonnikovii* (Xing et al., 2013), and *S. schweinfurthii* (Bhatt et al., 2016). In general, inhibition of perianth on seeds germination could occur through many different pathways, such as induction of a light requirement for germination, mechanical inhibition, chemical inhibitors, and specific ion effects (Wei et al., 2008). In addition, the presence of perianth affected the germination response of seeds to different environmental factors, such as increased germination requirements to light of *S. rubescens* seed (El-Keblawy et al., 2013); change optimal temperature ranges of *H. stocksii* seed (Rasheed et al., 2019); and aggravate the inhibitive effect of salinity on seed germination of *S. ikonnikovii* (Xing et al., 2013), and of drought on seed germination of *S. ferganica* (Maimaitijiang et al., 2019).

*Salsola* L. belongs to the family Amaranthaceae and includes ∼130 species occurring in the arid desert of Africa, Asia, and Europe (Zhu et al., 2003). There are ∼37 species in China, 33 species of which distribute in Xinjiang. The typical feature of this genus is that perianth segments are abaxially winged in fruit (Zhu et al., 2003). Many plants of this genus have good effects on soil and water conservation, diminish wind- and sand-shifting (Wang et al., 2008), and thus have great potential for restoration of deteriorated land in arid regions. Some scholars have studied germination response to different environmental factors of seeds for *Salsola* plants (e.g., El-Keblawy et al., 2013; Elnaggar et al., 2019). The effects of winged perianth on seed germination are also considered (Wei et al., 2008; Ma et al., 2017). However, most of the researches only consider the effects of one

**TABLE 1 |** The habitat characteristics of four representative annual *Salsola* plants.

| Species | Habitat | Accompanying plants | Latitude and longitude | Altitude /m |
|---|---|---|---|---|
| *S. heptapotamica* Iljin | Gobi desert, and sandy land | *S. affinis* C.A. Mey., *Haloxylon ammodendron* (C. A. Mey.) Bunge, *Kalidium foliatum* (Pall.) Moq. | N44°45'E87°53' | 370 |
| *S. rosacea* Linn. | Gravelly soil before the mountain | *S. collina* Pall., *Anabasis salsa* (C. A. Mey.) Benth. ex Volkens, *Atriplex* | N43°44'E82°55' | 810 |
| *S. nitraria* Pall | Gravelly soil | *H. ammodendron* (C. A. Mey.) Bunge, *Halogeton glomeratus* (Bieb.) C. A. Mey. | N44°48'E86°37' | 320 |
| *S. ruthenica* Iljin | Sandy soil of valley and gravel gobi | *Artemisia*, *S. affinis* C.A. Mey., *A. micrantha* C. A. Mey. | N44°19'E87°57' | 400 |

or at most two factors between perianth, temperature and light on seed germination (Chang et al., 2008; Wang et al., 2013), comprehensive evaluation of the effects of these three factors are absent, which is vital to assess the true germination condition of seed in the arid desert. In addition, studies on the effect of perianth on seed germination tolerance to salinity or drought of *Salsola* plants are also limited (Xing et al., 2013; Maimaitijiang et al., 2019).

In this study, we collected seeds of four representative *Salsola* species, including three endemic species *S. heptapotamica Iljin*,

**TABLE 2 |** The characteristics of winged seed and naked seed of the four annual *Salsola* plants.

| Species | Radius of winged seed (mm) | Diameter of naked seed (mm) | Mass/100 winged seeds (g) | Mass/100 naked seeds (g) |
|---|---|---|---|---|
| *S. heptapotamica* | 5.627±0.154$^{a}$ | 2.671 ± 0.088$^{a}$ | 0.751 ± 0.009$^{a}$ | 0.391 ± 0.005$^{a}$ |
| *S. rosacea* | 4.894 ± 0.106$^{b}$ | 2.387 ± 0.111$^{b}$ | 0.514 ± 0.004$^{b}$ | 0.307 ± 0.005$^{a}$ |
| *S. nitraria* | 3.674 ± 0.151$^{c}$ | 1.024 ± 0.037$^{c}$ | 0.192 ± 0.002$^{c}$ | 0.064 ± 0.001$^{b}$ |
| *S. ruthenica* | 2.339 ± 0.214$^{d}$ | 1.116 ± 0.025$^{c}$ | 0.155 ± 0.002$^{c}$ | 0.083 ± 0.001$^{b}$ |

*Data are the mean of seven replicates (± SE). Different letters in columns indicate significant differences ($p < 0.05$) among the four Salsola plants.*

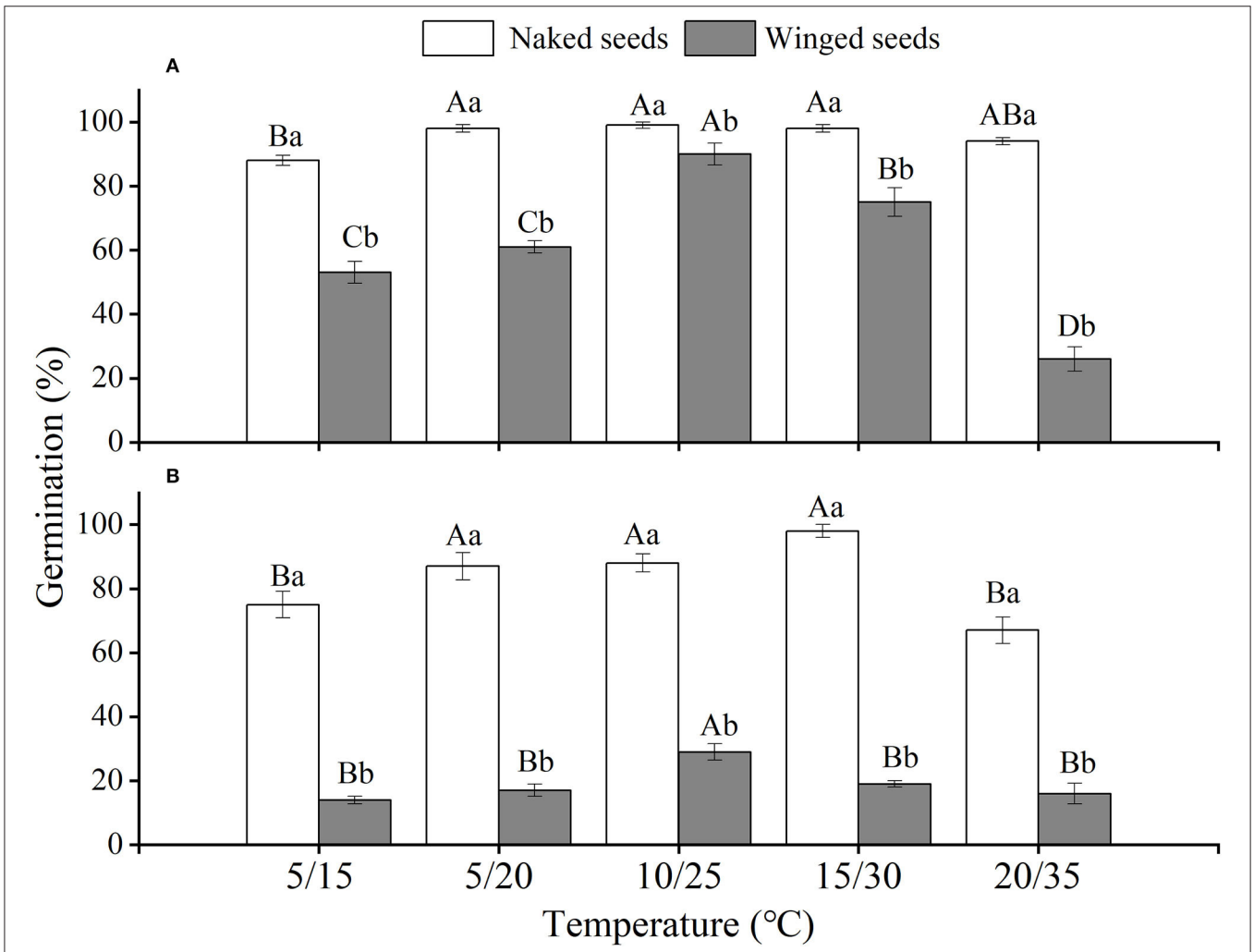


**FIGURE 1 |** The effects of winged perianth, light, and temperature on seed germination percentage (mean ± SE) of *Salsola heptapotamica*. **(A)** germination in light, **(B)** germination in dark. Different uppercase letters denote a significant difference ($p < 0.05$) in germination percentage at different temperatures for the same perianth treatment, and different lowercase letters indicate a significant difference ($p < 0.05$) of germination percentage for different treatments of perianth at the same temperature.

*S. rosacea Linn*., and *S. nitraria Pall*, mainly distributed in northern Xinjiang in China, and one widespread species *S. ruthenica Iljin*. distributed in many places in China (Zhu et al., 2003). We performed laboratory germination tests and aimed to provide detailed germination information for better screening of suitable *Salsola* plants in rehabilitating deteriorated lands in arid lands in Central Asia. We hypothesize that (1) the presence of winged perianth inhibits seed germination of these species; (2) the germination responses to light and temperature of endemic species are more sensitive than that of widespread species; (3) all these *Salsola* species have a high tolerance to salinity and drought.

## MATERIALS AND METHODS

### Seed Collection and Habitat Characteristics

Freshly matured fruits of the four *Salsola* species were collected from natural populations growing at the edge of Junggar Basin in Xinjiang during September–October 2020. This area is arid to semi-arid with a typical temperate continental climate. Annual precipitation is around 167 mm with minimum precipitation in winter and maximum in summer. Annual potential evaporation is 2,300 mm. The mean annual temperature is 6.7°C with a minimum temperature of −34.4°C in January and a maximum temperature 41.7°C in August. The soil is saline soil and the pH is above 8. Fruits of each species were randomly collected from about 50 plants and taken to the laboratory. Fruits were air-dried under room temperature (18–25°C) for 2 weeks and then were stored at 4°C for about 1 month until used in this experiment. The specific habitat characteristics are shown in **Table 1**.

### Seed Characteristics

The size, shape, and color of the four *Salsola* seeds with and without winged perianth (hereafter as winged seeds and naked seeds) were recorded using the stereomicroscope

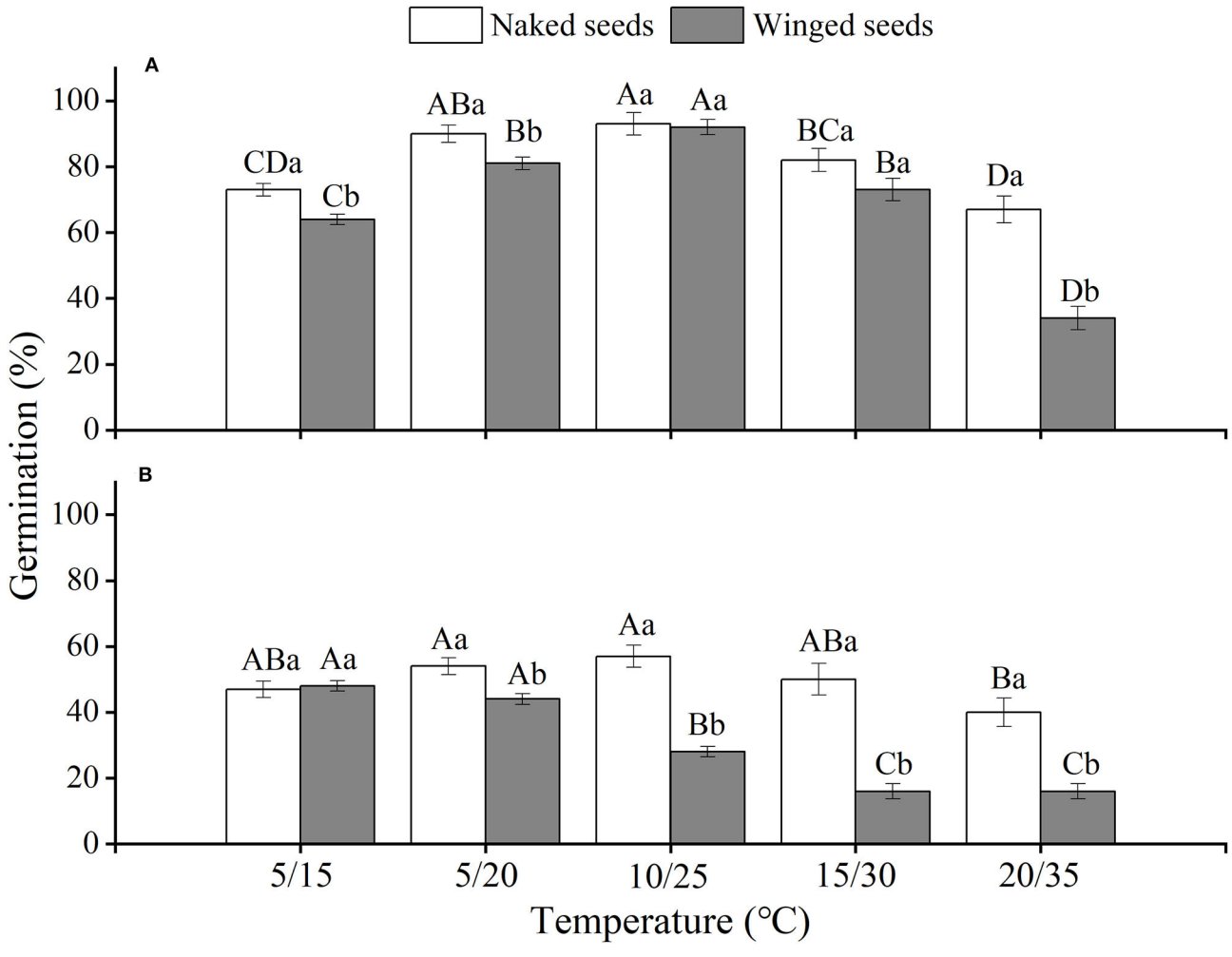


**FIGURE 2 |** The effects of winged perianth, light, and temperature on seed germination percentage (mean ± SE) of *Salsola rosacea*. **(A)** germination in light, **(B)** germination in dark. Different uppercase letters denote a significant difference ($p < 0.05$) in germination percentage at different temperatures for the same perianth treatment, and different lowercase letters indicate a significant difference ($p < 0.05$) of germination percentage for different treatments of perianth at the same temperature.

(Olympus SZX10, Tokyo, Japan). Winged perianth-enclosed seeds were removed manually. Seven groups of 100 winged seeds or naked seeds were weighed using an analytical balance (precision 0.001 g). The sizes of winged seeds or naked seeds were determined using Image J Analysis Software (National Institutes of Mental Health, America). Each determination had seven replicates.

## Seed Germination

### Winged Perianth, Light, and Temperature Effects

The winged seeds or naked seeds were incubated in five incubators adjusted to a temperature regime of 5/15, 5/20, 10/25, 15/30, and 20/35°C (common temperature regimes of the region) in both continuous darkness and alternating 12 h darkness/12 h light, hereafter referred as dark and light, respectively. Seeds were placed in 9-cm-diameter Petri dishes on two layers of Whatman no. 1 filter paper moistened with 7 ml of distilled water. The Petri dishes were sealed with parafilm. For the dark treatment, the Petri dishes were wrapped in two layers of aluminum foil to prevent any exposure to light. Each treatment had four replicates with 25 seeds. Radicle protrusion from the seed was the criterion for germination of winged seeds, and naked seeds were germinated when the radicle length was $\geq$ 2 mm. Seed germination was monitored every day, germinated seeds were discarded at each counting, and the experiment lasted for 14 d. The seeds incubated in dark were checked only after 14 d. The rate of germination was estimated by using a modified Timson's index of germination velocity = $\Sigma G/t$, where G is the percentage of seed germination every day and t is the total germination period (Khan and Ungar, 1984).

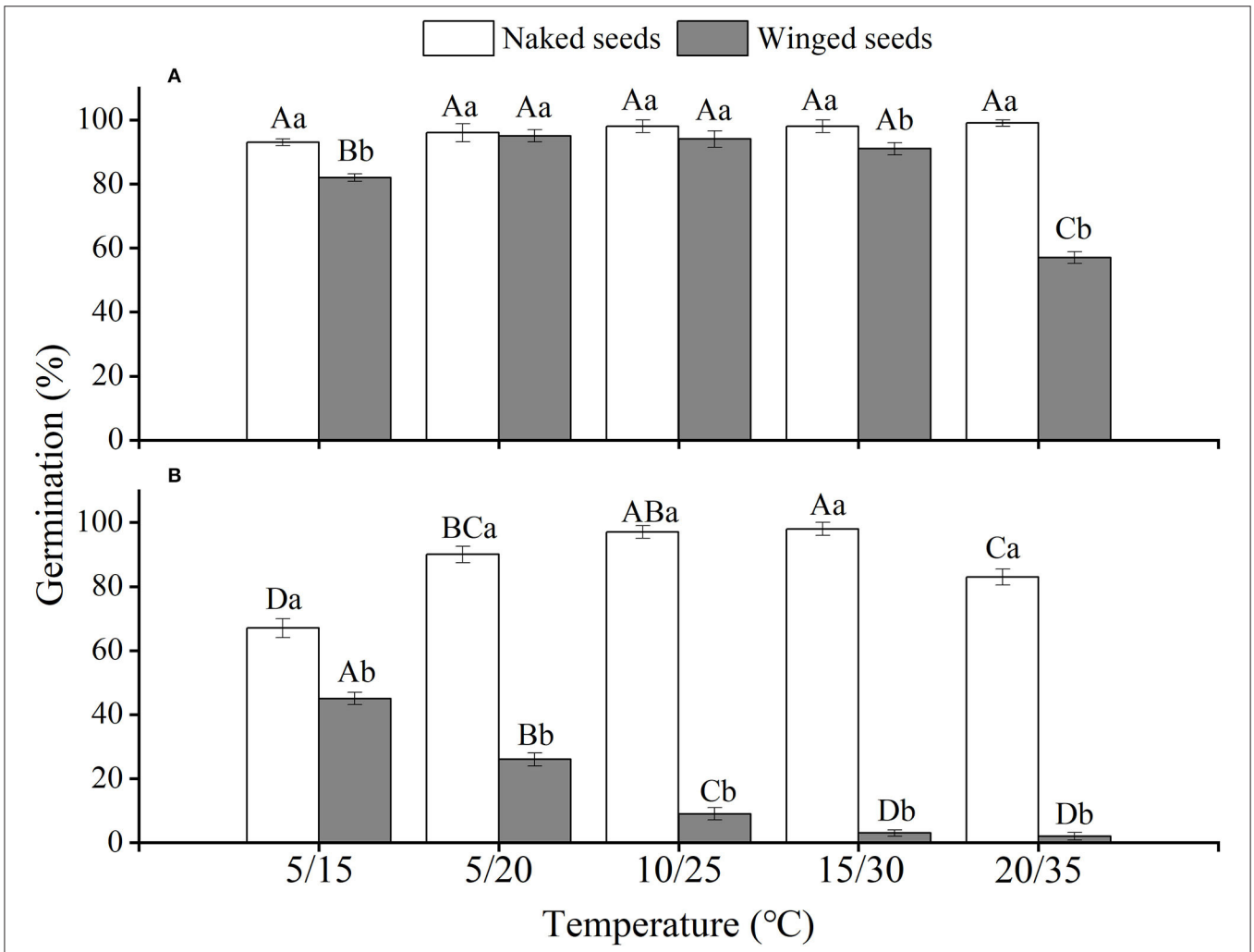


**FIGURE 3 |** The effects of winged perianth, light, and temperature on seed germination percentage (mean ± SE) of *Salsola nitraria*. **(A)** germination in light, **(B)** germination in dark. Different uppercase letters denote a significant difference ($p < 0.05$) in germination percentage at different temperatures for the same perianth treatment, and different lowercase letters indicate a significant difference ($p < 0.05$) of germination percentage for different treatments of perianth at the same temperature.

### Winged Perianth and Salinity Effects

Due to the relatively higher germination percentages of the four *Salsola* species in light and at 10/25°C, winged seeds and naked seeds were sown in different NaCl concentrations (0, 50, 100, 300, 500, and 700 mM, based on preliminary results) and incubated at this condition. Each dish was wrapped with parafilm against loss of water by evaporation. Germination was monitored after 14 d of incubation. All the seeds that failed to germinate were rinsed with distilled water and then incubated in distilled water for another 7 d. Recovery percentages (RP) were calculated using the formula: RP = [(a – b)/c] × 100, where a is the sum of the number of seeds germinated in NaCl solutions plus those that recovered to germinate in the distilled water; b is the total number of seeds germinated in NaCl solutions, and c is the total number of seeds tested. The total germination percentage was recorded as (a/c) ×100.

### Winged Perianth and Drought Effects

Winged seeds or naked seeds were germinated in Petri dishes with six levels of polyethylene glycol (PEG) concentrations (0, 50, 100, 150, 200, 300 $g \cdot L^{-1}$, based on preliminary results), which correspond to osmotic potential ($\Psi_S$) of 0, −0.05, −0.15, −0.3, −0.5 and −1.03 MPa (Michel and Kaufmann, 1973). The light and temperature conditions were the same as in the salinity experiment. Recovery percentage and total germination were also calculated.

## Statistical Analysis

Seed germination data are of binomial type (i.e., germination is 1, not germination is 0). The forward stepwise (Wald) in binary logistic regression models was used to analyze the effect of winged perianth, light, temperature, and their interactions on seed germination. The same method was used to determine

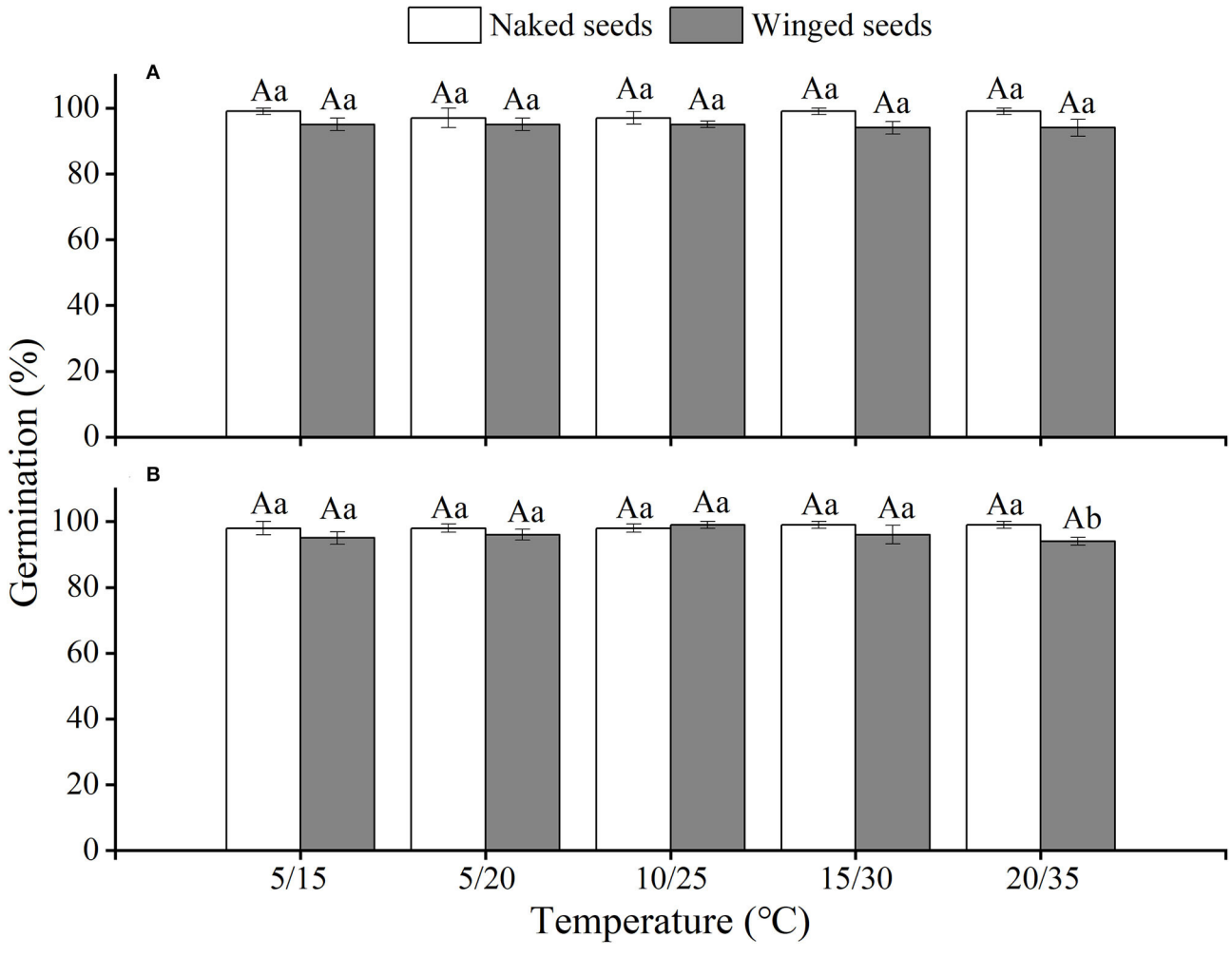


**FIGURE 4 |** The effects of winged perianth, light, and temperature on seed germination percentage (mean ± SE) of *Salsola ruthenica*. **(A)** germination in light, **(B)** germination in dark. Different uppercase letters denote a significant difference ($p < 0.05$) of germination percentage at different temperatures for the same perianth treatment, and different lowercase letters indicate a significant difference ($p < 0.05$) of germination percentage for different treatments of perianth at the same temperature.

the effect of the winged perianth, salinity and their interactions, winged perianth, PEG and their interactions on seed germination and total germination. This method will automatically eliminate the parameters with a low probability of Wald statistics in the equation, to ensure the accuracy of the regression curve to a great extent (Li and Luo, 2003). In addition, for parameters that have significant effects on germination, Turkey's multiple comparison tests were used to test the differences that existed among groups. The same method was also used to determine the effect of winged perianth and temperature on the germination index of these *Salsola* species. Non-parametric tests were also performed to test the differences among the recovery percentages that did not meet the homogeneity of variance in different concentrations of NaCl or PEG solution. The difference between perianth treatments at the same temperature of seed germination was analyzed by Student's test at 95% confidence level. Data were expressed as mean ± standard error. All statistical tests were analyzed using the IBM SPSS Statistics 20 (IBM Corp., Armonk, New York, United States).

# RESULTS

## Seed Characteristics

The winged seeds of the four *Salsola* plants are all utricle and surrounded by fan-shaped and membranous wings (**Supplementary Figures 1B–K**). The naked seeds of the four plants are slightly flattened to slightly conical and have the typical spiral embryo (**Supplementary Figures 1C–L**). Winged seeds and naked seeds of *S. heptapotamica* and *S. rosacea* are significantly larger and heavier than those of *S. nitraria* and *S. ruthenica* (**Supplementary Figure 1**; **Table 2**).

## Winged Perianth, Light, and Temperature Effects

The effects of winged perianth, light, and temperature on seed germination of *S. heptapotamica*, *S. rosacea,* and *S. nitraria* were significant. The interactive effect of winged perianth, light, and temperature on seed germination of *S. heptapotamica* and *S. nitraria* were also significant but

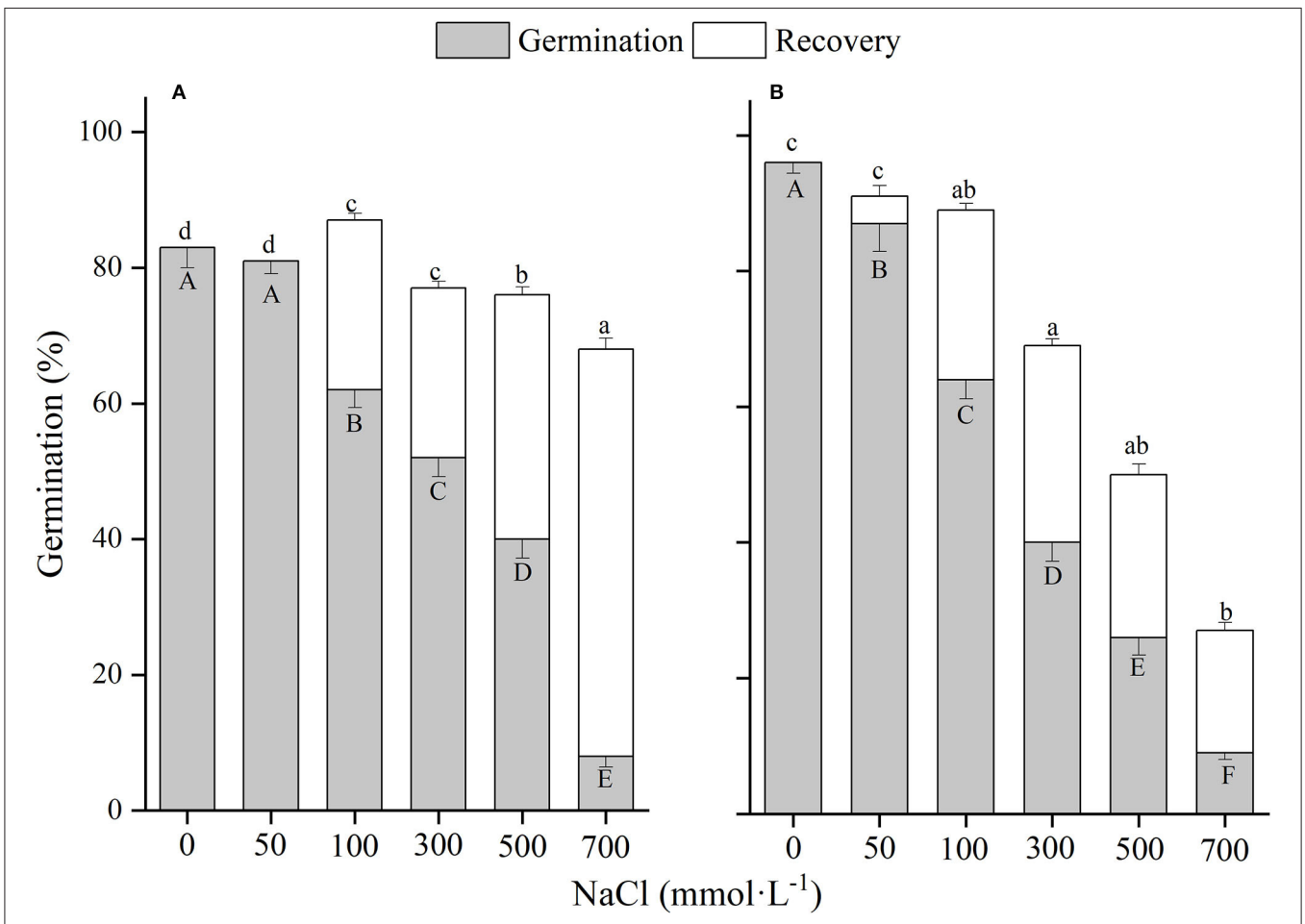


**FIGURE 5 |** The effects of winged perianth and NaCl concentration on seed germination and recovery germination of *Salsola heptapotamica*. **(A)** winged seeds, **(B)** naked seeds. Different uppercase letters denote a significant difference ($p < 0.05$) in germination percentage among different NaCl concentration. Different lowercase letters indicate a significant difference ($p < 0.05$) in recovery germination among different NaCl concentration.

were not for *S. rosacea* (**Supplementary Table 1**). For the three *Salsola* plants, germinations of winged seeds were all significantly lower than those of naked seeds (**Figures 1–3**). Germination percentages of winged and naked seeds of *S. rosacea* were significantly lower in dark than those in the light (**Figures 2A,B**). While for *S. heptapotamica* and *S. nitraria*, only winged seeds performed significantly lower germination percentages in dark than in light (**Figures 1A,B**, **3A,B**). At the five temperature ranges, germination percentages of naked seeds for the three *Salsola* plants were all up to 40% whether in light or dark. For winged seeds germinated in dark, germination percentages were all no more than 43%, and winged seeds of *S. nitraria* were even <5% at 15/30–20/35°C (**Figures 1–3**). For *S. ruthenica*, except winged perianth ($p < 0.001$), other factors and their interactions had no significant effect on seed germination (**Supplementary Table 1**). Besides, germination percentages of winged and naked seeds were both more than 90% at the five temperatures whether in light or dark (**Figures 4A,B**).

For *S. heptapotamica*, *S. rosacea*, and *S. nitraria*, germination indices of winged seeds were significantly lower than those of naked seeds (**Supplementary Figures 2A–C**). Germination indices of naked seeds for these three *Salsola* plants were increased with the raising of temperature, but those for winged seeds were increased initially and then decreased (**Supplementary Figures 2A–C**). For *S. ruthenica*, there was no significant difference in germination indices between winged and naked seeds at the five temperatures (**Supplementary Figure 2D**).

## Winged Perianth and Salinity Effects

There was a significant ($p < 0.01$) interaction of winged perianth and salinity on seed germination and total germination for the four *Salsola* plants (**Supplementary Table 2**). Germination percentages and total germinations of winged and naked seeds of the four *Salsola* plants were all decreased with the increase of NaCl concentration (**Figures 5–8**). Germination percentages of naked seeds were all higher than those of winged seeds, except

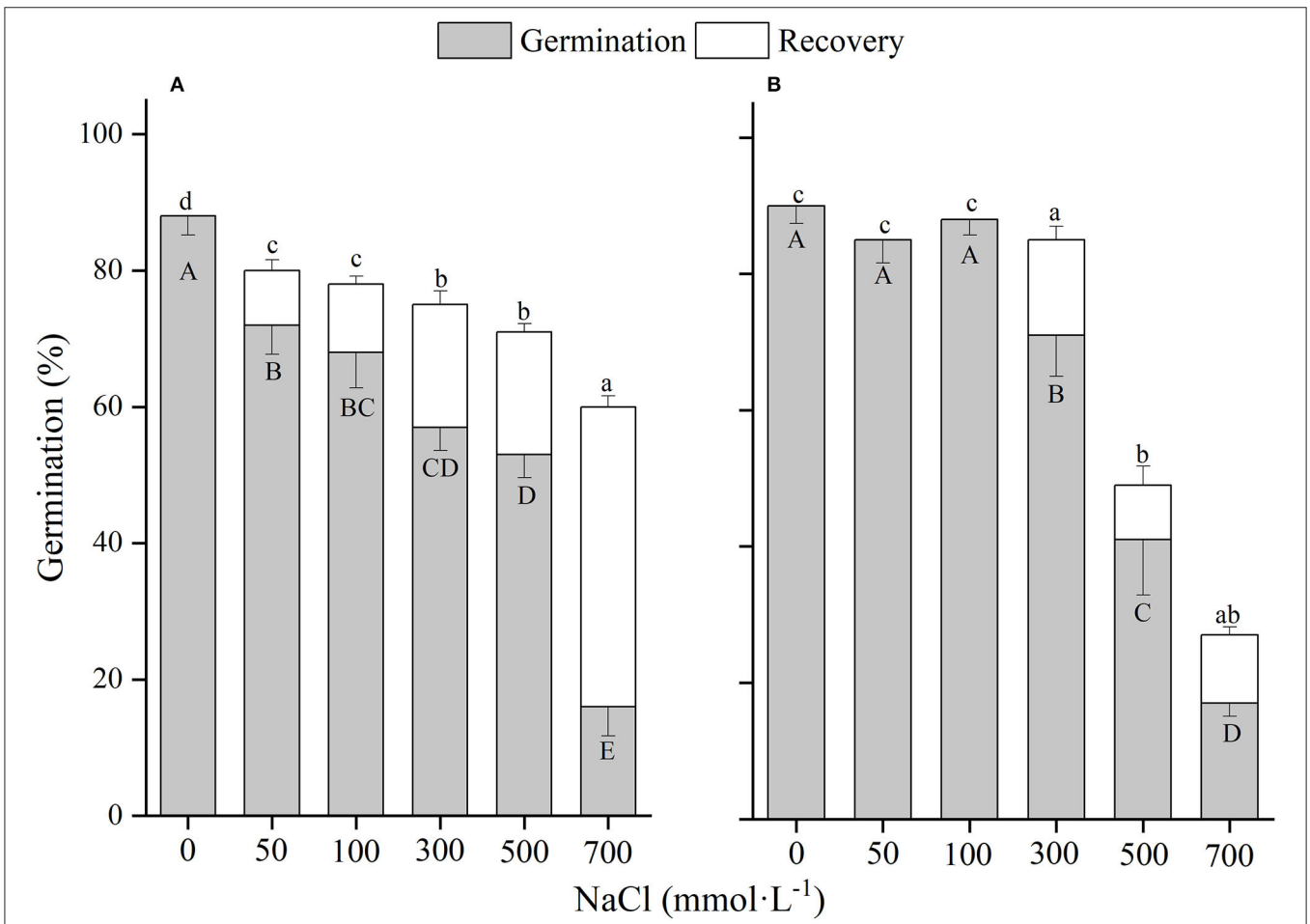


**FIGURE 6 |** The effects of winged perianth and NaCl concentration on seed germination and recovery germination of *Salsola rosacea*. **(A)** winged seeds, **(B)** naked seeds. Different uppercase letters denote a significant difference ($p < 0.05$) in germination percentage among different NaCl concentrations. Different lowercase letters indicate a significant difference ($p < 0.05$) in recovery germination among different NaCl concentrations.

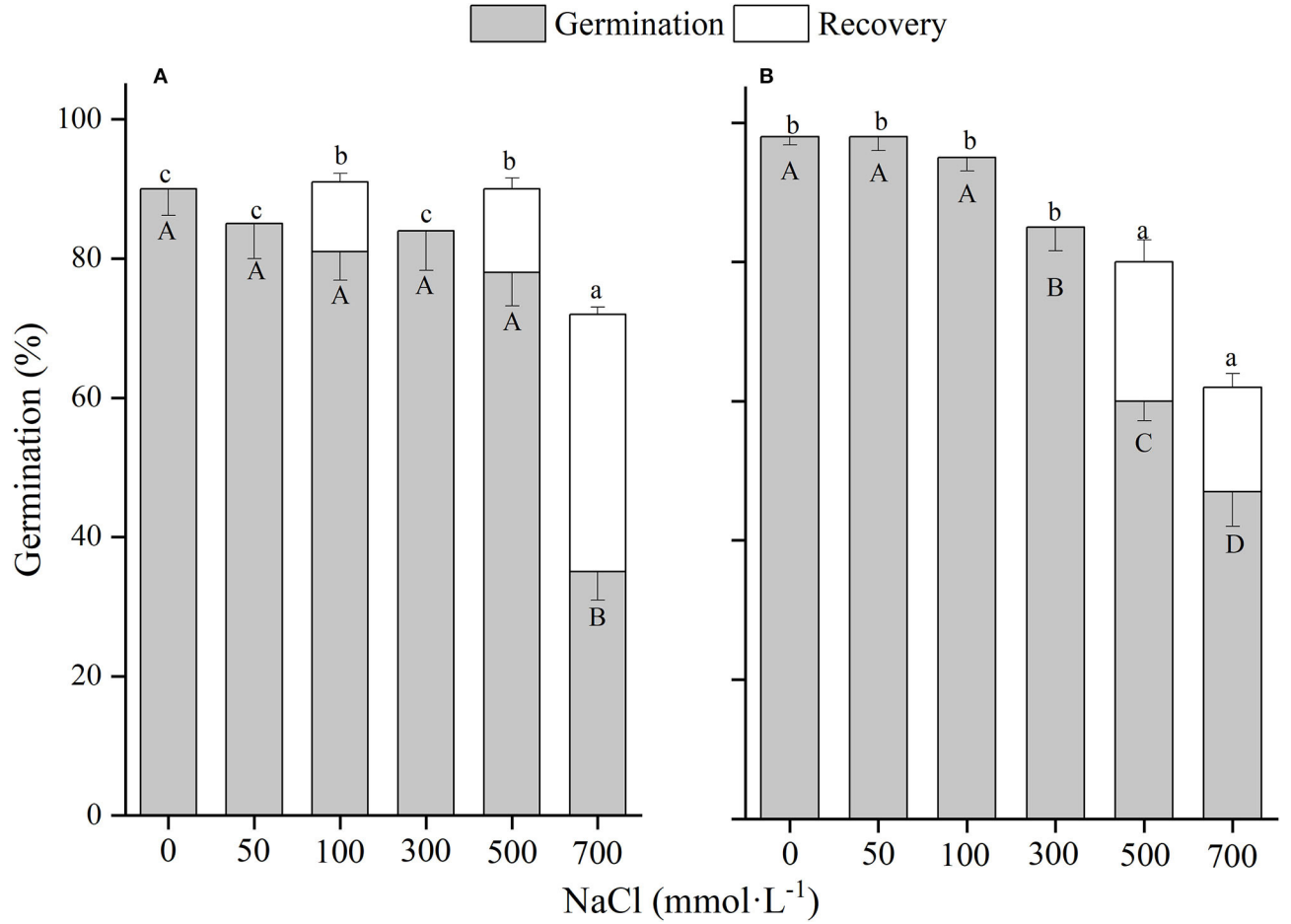


**FIGURE 7 |** The effects of winged perianth and NaCl concentration on seed germination and recovery germination of *Salsola nitraria*. **(A)** winged seeds, **(B)** naked seeds. Different uppercase letters denote a significant difference ($p < 0.05$) in germination percentage among different NaCl concentrations. Different lowercase letters indicate a significant difference ($p < 0.05$) of recovery germination among different NaCl concentrations.

at 500 mM, in which germination percentages of naked seeds for *S. heptapotamica, S. rosacea,* and *S. nitraria* were lower than those of winged seeds (**Figures 5–7**). The recovery percentages of winged seeds for the four *Salsola* were all increased with the raising of NaCl concentration, while those of naked seeds were increased initially and then decreased. At 0–300 mM NaCl concentration, the total germinations of naked seeds for the four *Salsola* plants were higher than those of winged seeds or there were no significant differences, but at 500–700 mM, the results were opposite (**Figures 5–8**).

## Winged Perianth and Drought Effects

There were significant ($p < 0.05$) effects of winged perianth and drought on seed germination of the four *Salsola* species, but were not for their interactive effects. There was no significant interaction of winged perianth and drought on total germinations of the four *Salsola* plants either (**Supplementary Table 3**). Germination percentages and total germination of winged and naked seeds for the four *Salsola* plants were all decreased with the decline in $\Psi_S$ of PEG solution (**Figures 9–12**). Germination percentages and total germinations of naked seeds were all higher or there were no significant differences than those of winged seeds. The winged seeds of *S. heptapotamica* even had no germination at $\Psi_S$ of −1.03 MPa (**Figure 9A**). The recovery percentages of winged and naked seeds for *S. heptapotamica, S. nitraria,* and *S. ruthenica* were all increased with the decrease of $\Psi_S$, while those for *S. rosacea* seeds were increased initially and then decreased (**Figure 10B**).

# DISCUSSION

Although there is some information about the germination characteristics of *Salsola* seeds, our data provide a thorough knowledge of the seed germination ecology of four representative *Salsola* species to complex abiotic conditions and the potential interactions with the winged perianth. These data also indicate that the presence of winged perianth inhibits seed germination of *S. heptapotamica*, *S. rosacea,* and *S. nitraria*. In addition, all

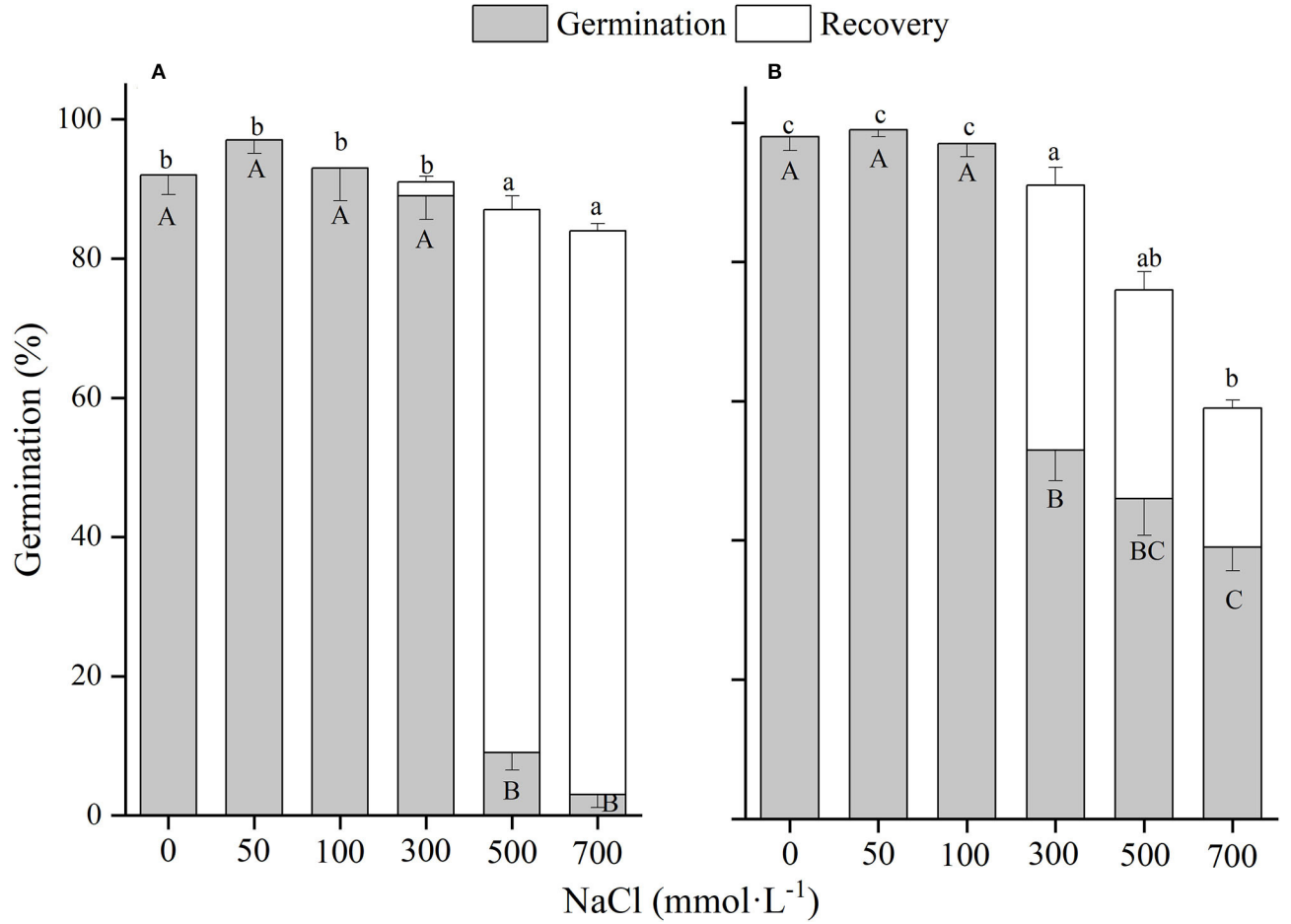


**FIGURE 8 |** The effects of winged perianth and NaCl concentration on seed germination and recovery germination of *Salsola ruthenica*. **(A)** winged seeds, **(B)** naked seeds. Different uppercase letters denote a significant difference ($p < 0.05$) in germination percentage among different NaCl concentrations. Different lowercase letters indicate a significant difference ($p < 0.05$) of recovery germination among different NaCl concentrations.

these *Salsola* species have a high tolerance to salinity and drought. The results indicate that the germination responses to light and temperature conditions of endemic species are more sensitive than that of widespread species.

Perianth-enclosed seeds are a characteristic feature of the *Salsola* species, which helps in the dispersal of seeds by wind. But the presence of winged perianth usually inhibit seed germination (El-Keblawy et al., 2013). In this study, germination percentages and germination indices of winged seeds of *S. heptapotamica, S. rosacea,* and *S. nitraria* were significantly inhibited. Removal of winged perianth significantly increased the germination percentages and germination indices of the three *Salsola* plants. A similar effect of perianth on seeds germination was also found in *H. persicum* (Wei and Wang, 2006), *S. affinis* (Wei et al., 2008), and *H. stocksii* (Rasheed et al., 2019). Previous studies reported that perianth-inhibited seed germination by acting as a mechanical barrier for radicle emergence or due to the presence of inhibitor substances, which caused low germinability of seeds (El-Keblawy et al., 2013; Xing et al., 2013). In addition, our results showed that inhibitory effects of winged perianth on seed germination could be alleviated at some specific combination of temperature and light, such as germinating at 10/25°C and light, indicating winged perianth has complex effects on germination requirements to light and temperature.

For *S. rosacea*, germination percentages of winged and naked seeds were all significantly lower in dark than in light at the five temperatures, which indicated the positive photoblastic nature of the seeds. Light requirement of seed ensures germination at or near soil surface that facilitates seedling survival and growth (Rasheed et al., 2019). For *S. heptapotamica* and *S. nitraria*, compared with naked seeds, only germinations of winged seeds showed high light requirement, indicating that presence of winged perianth enhanced seeds germination requirements to light for these two *Salsola* plants. Light-filtering properties of the winged perianth surrounding the

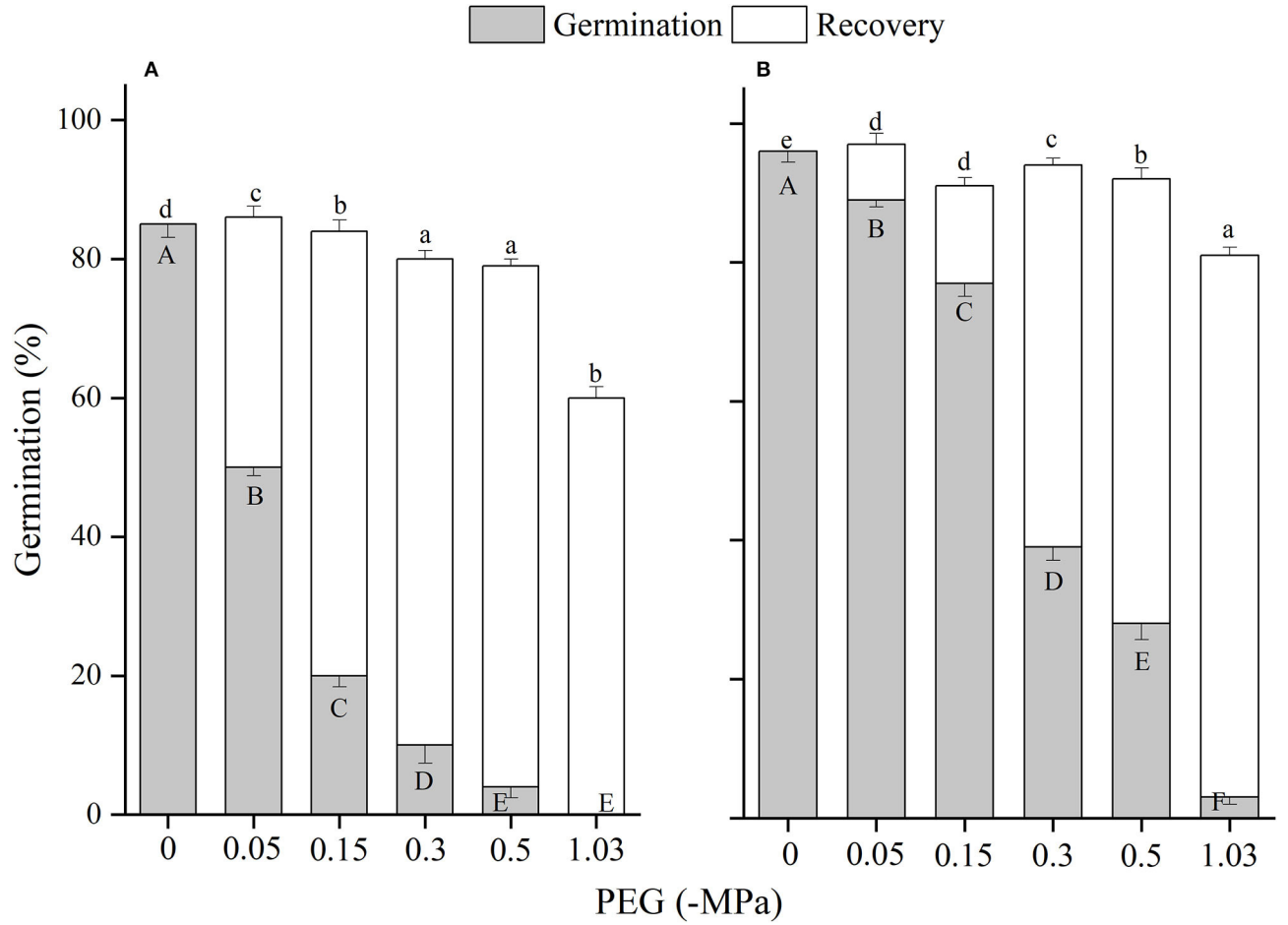


**FIGURE 9 |** The effects of winged perianth and PEG concentration on seed germination and recovery germination of *Salsola heptapotamica*. **(A)** winged seeds, **(B)** naked seeds. Different uppercase letters denote a significant difference ($p < 0.05$) in germination percentage among different PEG concentrations. Different lowercase letters indicate a significant difference ($p < 0.05$) of recovery germination among different PEG concentrations.

seeds might be responsible for the sensitivity of germination to light (Cresswell and Grime, 1981). The color of the winged perianth of *S. nitraria* was yellow-green. The relative lower light absorbance by winged perianth of *S. nitraria* might be the reason for greater light requirement during seeds germination. However, the winged perianth of *S. heptapotamica* has a variety of colors in the wild (Zhu et al., 2003), and the absorption of pigments to light is not enough to explain the high light requirement for seed germination, which is needed to further research.

The naked seeds of *S. heptapotamica, S. rosacea,* and *S. nitraria* had up to 60% germination percentages in light, and had more than 40% germination percentages in dark at all tested temperature regimes. While winged seeds for these three *Salsola* plants were hard to germinate in dark, with <5% germination percentage for *S. nitraria* at high temperatures. These results indicated significant interaction among winged perianth, light, and temperature for seeds germination. In many species, interactions among different factors are often more inhibitory for seed germination than their individual effects (Rasheed et al., 2019). In this study, the inhibitory effect of winged perianth on seed germination aggravated further in dark at unsuitable temperatures.

Germination percentage of winged and naked seeds for *S. ruthenica* was almost 100% at wide temperature regimes from 5/15 to 20/35°C whether in light or dark. This indicated that *S. ruthenica* seeds may have an "opportunistic" germination strategy that allowed them to highly germinate in relatively wide environmental conditions (Wei et al., 2007), which might be the reason for its wide distribution in the Central Asia region (Zhu et al., 2003). In a changing climate, a wide adaptation range of environments confers an advantage for the species to be used in rehabilitation. Besides, germination indices of *S. ruthenica* seeds were more than 90% at the five temperatures, which allowed them to rapidly develop into seedlings in early spring when

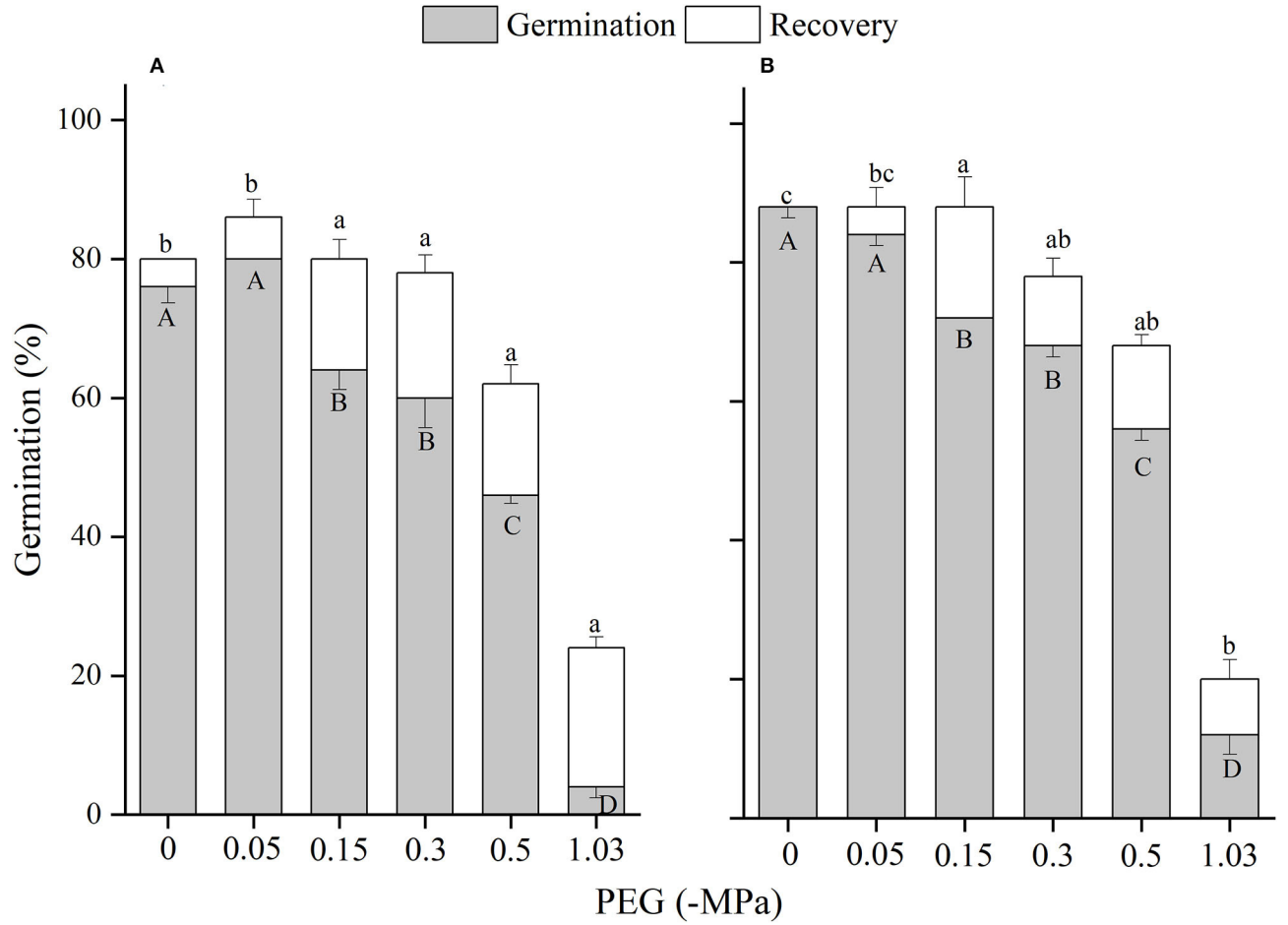


**FIGURE 10 |** The effects of winged perianth and NaCl concentration on seed germination and recovery germination of *Salsola rosacea*. **(A)** winged seeds, **(B)** naked seeds. Different uppercase letters denote a significant difference ($p < 0.05$) in germination percentage among different PEG concentrations. Different lowercase letters indicate a significant difference ($p < 0.05$) in recovery germination among different PEG concentrations.

the soil is sufficiently moist, to occupy favorable habitats and complete colonization in arid deserts. By contrast, germination percentages and germination indices of *S. heptapotamica*, *S. rosacea,* and *S. nitraria* seeds were relatively low due to their interaction of winged perianth, light, and temperatures, which prevented germination of all the seeds at one time. Retention of a fraction of ungerminated seeds in the seed bank could be considered a bet-hedging strategy to share the risk of seed germination and improve chances for survival (Saatkamp et al., 2011). However, it also prevents these three species from being widely distributed as *S. ruthenica* in different habitats (Zhu et al., 2003).

These four *Salsola* plants decreased germination percentages with the increase of NaCl concentrations. Similar results are also found in other species, such as *Suaeda salsa* (Song et al., 2008) and *S. iberica* (Khan et al., 2002). This effect might be caused by salinity-induced osmotic stress and/or ion toxicity (Song et al., 2005). Seeds of the four *Salsola* plants can germinate at 700 mM NaCl solution with >10% germination percentages, which showed higher tolerance to salinity than other halophytes, such as *S. vermiculata* 600 mM (Guma et al., 2010), *Atriplex triangularis* 510 mM (Khan and Ungar, 1984), and *Halogenton glomeratus* 400 mM (Ahmed and Khan, 2010). Besides, El-Keblawy et al. (2020) found that seeds germination of *S. drummondii* collected in non-salty habitats had a lower germination percentage than those in salty habitats, indicating that maternal environment played an important role in seed tolerance to salinity. In our study, seeds of the four *Salsola* plants were all collected from non-salty habitats, which may be underestimated of their salt tolerance. In addition, the presence of winged perianth aggravated the inhibition effect of NaCl on germination percentage, especially for *S. ruthenica*, of which germination of naked seeds (39%) was significantly higher than that of winged seeds (3%) at 700 mM NaCl concentration. However, the recovery germinations and total germinations of winged

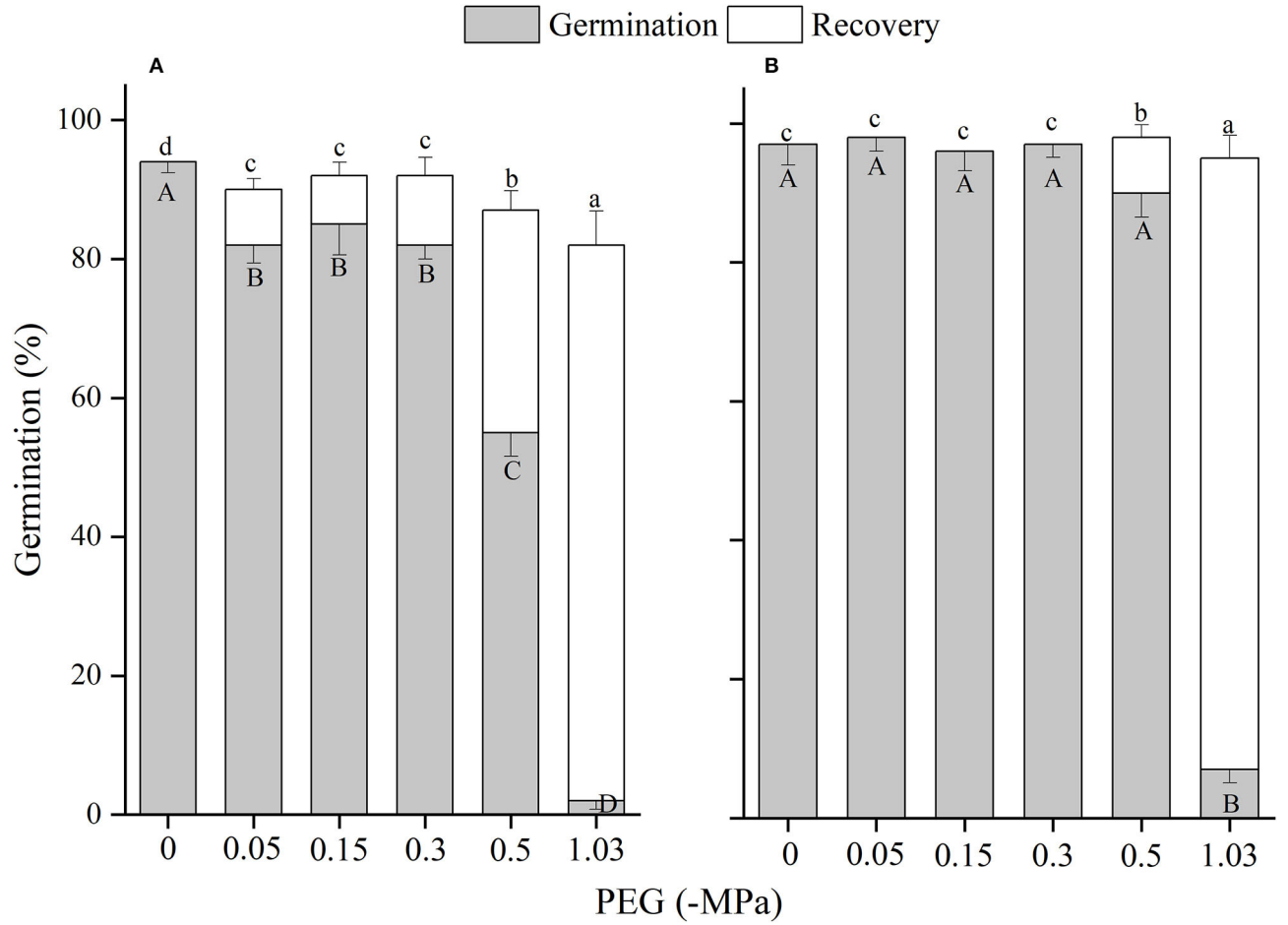


**FIGURE 11 |** The effects of winged perianth and NaCl concentration on seed germination and recovery germination of *Salsola nitraria*. **(A)** winged seeds, **(B)** naked seeds. Different uppercase letters denote a significant difference ($p < 0.05$) in germination percentage among different PEG concentration. Different lowercase letters indicate a significant difference ($p < 0.05$) in recovery germination among different PEG concentrations.

seeds for the four *Salsola* plants at higher NaCl concentrations were significantly higher than those of naked seeds, suggesting that winged perianth also plays a positive role in the protection of seeds during exposure to high salinity (Xing et al., 2013).

Drought stress also caused a reduction in seed germination percentage and total germination of the four *Salsola* plants, which might be ascribed to a reduction in the osmotic potential of the solution that restricts sufficient imbibition of seeds (Tobe et al., 2000). At $\Psi_S$ of −1.03 MPa, except for *S. heptapotamica* with the least germination percentage of 3%, the other three *Salsola* plants can germinate ∼10%, which were more tolerant to drought than *Agropyron mongolicum* and *Caragana korshinskii* (Yu et al., 2021), *S. vermiculata* (Al-Shamsi et al., 2018), and *Lachnoloma lehmannii* (Mamut et al., 2019). Moreover, the inhibitive effect of drought was performed more significantly by the presence of winged perianth. The germination of winged seed for *S. heptapotamica* was no germination at $\Psi_S$ of −1.03 MPa. It is reported that the perianth-enclosed seed confined germination occurrence only after sufficient rainfall, which will dilute soil salinity and can also soften the perianth and leach the inhibitors (Rasheed et al., 2019).

## CONCLUSIONS

Seed germination of endemic species *S. heptapotamica*, *S. rosacea,* and *S. nitraria* were significantly inhibited by perianth and darkness and showed high sensitivity to different abiotic conditions. For better germination and seedling emergence, the perianth in these three species should be removed before sowing the seeds on the topsoil when the temperature is above 5/15°C. However, widespread species *S. ruthenica* seeds germinate equally well in light or dark in a wide range of temperatures. Considering the high tolerance of these *Salsola* species to salinity and drought, they could be cultivated for rehabilitating degraded arid-saline lands.

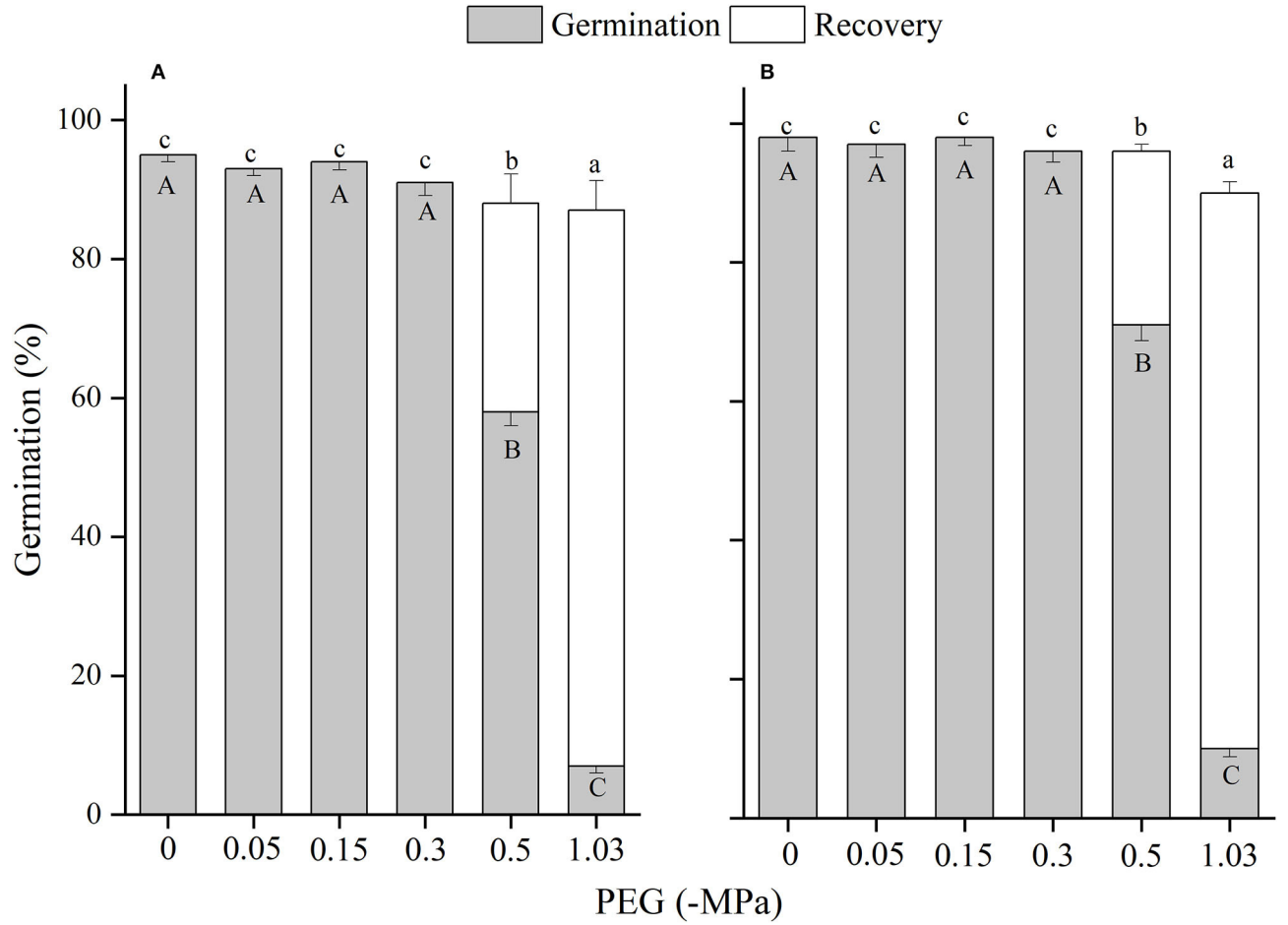


**FIGURE 12 |** The effects of winged perianth and NaCl concentration on seed germination and recovery germination of *Salsola ruthenica*. **(A)** winged seeds, **(B)** naked seeds. Different uppercase letters denote a significant difference ($p < 0.05$) in germination percentage among different PEG concentrations. Different lowercase letters indicate a significant difference ($p < 0.05$) in recovery germination among different PEG concentrations.

## DATA AVAILABILITY STATEMENT

The raw data supporting the conclusions of this article will be made available by the authors, without undue reservation.

## AUTHOR CONTRIBUTIONS

ZW and LW conceived the topic. PC and LJ performed the experiments and analyzed all statistical data. PC, LJ, WY, ZW, and LW wrote the manuscript. ZW and LW revised the manuscript. All authors contributed to the article and approved the submitted version.

## FUNDING

This work was supported by the Tianshan elite program of Xinjiang Uygur Autonomous Region (no. Y970000335), the National Natural Science Foundation of China (no. 31970354), and the Youth Innovation Promotion Association of Chinese Academy of Sciences (no. 2018479).

## SUPPLEMENTARY MATERIAL

The Supplementary Material for this article can be found online at: https://www.frontiersin.org/articles/10.3389/fpls.2022.892667/full#supplementary-material

## REFERENCES

Ahmed, M. Z., and Khan, M. A. (2010). Tolerance and recovery responses of playa halophytes to light, salinity and temperature stresses during seed germination. *Flora* 205, 764–771. doi: 10.1016/j.flora.2009.10.003

Al-Shamsi, N., El-Keblawy, A., Mosa, K. A., and Navarro, T. (2018). Drought tolerance and germination response to light and temperature for seeds of saline and non-saline habitats of the habitat-indifferent desert halophyte *Suaeda vermiculata*. *Acta Physiol. Plant.* 40, 200. doi: 10.1007/s11738-018-2771-z

Baskin, C. C., and Baskin, J. M. (2014). *Seeds: Ecology, Biogeography, and Evolution of Dormancy and Germination*. 2nd ed. San Diego, CA: Academic Press.

Baskin, J. M., Lu, J. J., Baskin, C. C., Tan, D. Y., and Wang, L. (2014). Diaspore dispersal ability and degree of dormancy in heteromorphic species of cold deserts of northwest China: a review. *Perspect. Plant Ecol. Evol. Syst.* 16, 93–99. doi: 10.1016/j.ppees.2014.02.004

Bhatt, A., Perez-Garcia, F., Caron, M. M., and Gallacher, D. (2016). Germination response of *Salsola schweinfurthii* (Chenopodiaceae) to salinity and winged perianth removal. *Seed Sci. Technol.* 44, 1–7. doi: 10.15258/sst.2016.44.2.14

Chang, S. J., Zuo, B., Wang, X. W., and Huang, J. H. (2008). Influence of light, temperature and salt on the germination of *Salsola nitraria* Pall. *Arid Land Geogr.* 31, 897–903. doi: 10.13826/j.cnki.cn65-1103/x.2008.06.002

Cresswell, E. G., and Grime, J. P. (1981). Induction of a light requirement during seed development and its ecological consequences. *Nature* 291, 583–585. doi: 10.1038/291583a0

D'Odorico, P., Bhattachan, A., Davis, K. F., Ravi, S., and Runyan, C. W. (2013). Global desertification: drivers and feedbacks. *Adv. Water Resour.* 51, 326–344. doi: 10.1016/j.advwatres.2012.01.013

El-Keblawy, A. (2017). Light and temperature requirements during germination of potential perennial grasses for rehabilitation of degraded sandy Arabian deserts. *Land Degrad. Dev.* 28, 1687–1695. doi: 10.1002/ldr.2700

El-Keblawy, A., Al-Ansari, F., and Al-Shamsi, N. (2011). Effects of temperature and light on salinity tolerance during germination in two desert glycophytic grasses, *Lasiurus scindicus* and *Panicum turgidum*. *Grass Forage Sci.* 66, 173–182. doi: 10.1111/j.1365-2494.2010.00773.x

El-Keblawy, A., Bhatt, A., and Gairola, S. (2013). Perianths color affects germination behaviour in wind-pollinated Salsola rubescens in Arabian deserts. *Botany* 92, 69–75. doi: 10.1139/cjb-2013-0183

El-Keblawy, A., Elnaggar, A., Tammam, A., and Mosa, K. A. (2020). Seed provenance affects salt tolerance and germination response of the habitat-indifferent *Salsola drummondii* halophyte in the arid Arabian deserts. *Flora* 266, 151592. doi: 10.1016/j.flora.2020.151592

El-Keblawy, A., and Ksiksi, T. (2005). Artificial forests as conservation sites for the native flora of the UAE. *Forest Ecol. Manag.* 213, 288–296. doi: 10.1016/j.foreco.2005.03.058

Elnaggar, A., El-Keblawy, A., Mosa, K. A., and Navarro, T. (2019). Adaptive drought tolerance during germination of *Salsola drummondii* seeds from saline and nonsaline habitats of the arid Arabian deserts. *Botany* 97, 122–123. doi: 10.1139/cjb-2018-0174

Evans, C. E., and Etherington, J. R. (1990). The effect of soil water potential on seed germination of some British plants. *New Phytol.* 115, 539–548. doi: 10.1111/j.1469-8137.1990.tb00482.x

Guma, I. R., Padron-Mederos, M. A., Santos-Guerra, A., and Reyes-Betancort, J. A. (2010). Effect of temperature and salinity on germination of *Salsola vermiculata* L. (Chenopodiaceae) from Canary Islands. *J. Arid Environ.* 74, 708–711. doi: 10.1016/j.jaridenv.2009.10.001

Huang, Z. Y., Zhang, X. S., Zheng, G. H., and Gutterman, Y. (2003). Influence of light, temperature, salinity and storage on seed germination of *Haloxylon ammodendron*. *J. Arid Environ.* 55, 453–464. doi: 10.1016/S0140-1963(02)00294-X

Jurado, E., Westoby, M., and Nelson, D. (1991). Diaspore weight, dispersal, growth form and perenniality of central Australian plants. *J. Ecol.* 79, 811–828. doi: 10.2307/2260669

Katerina, K., Daws, M. I., and Thanos, C. A. (2014). Campanulaceae: A family with small seeds that require light for germination. *Ann. Bot-London* 113, 135–143. doi: 10.1093/aob/mct250

Khan, M. A., and Gul, B. (2006). "Halophyte seed germination," in *Ecophysiology of High Salinity Tolerant Plants* eds M. A. Khan, and D. J. Weber (Dordrecht: Springer Press), 11–30. doi: 10.1007/1-4020-4018-0_2

Khan, M. A., Gul, B., and Weber, D. J. (2002). Seed germination in the great basin halophyte *Salsola iberica*. *Can. J. Bot.* 80, 650–655. doi: 10.1139/b02-046

Khan, M. A., and Gulzar, S. (2003). Germination responses of *Sporobolus ioclados*: a saline desert grass. *J. Arid Environ.* 53, 387–394. doi: 10.1006/jare.2002.1045

Khan, M. A., and Ungar, I. A. (1984). The effect of salinity and temperature on the germination of polymorphic seeds and growth of *Atriplex triangularis* Willd. *Am. J. Bot.* 71, 481–489. doi: 10.1002/j.1537-2197.1984.tb12533.x

Kuang, W., Yonggang, M. A., Hong, L. I., and Liu, C. (2014). Analysis of land degradation intensity and trend in Central Asia from 1999 to 2012. *Remote Sens. Environ.*, 26, 163–169. doi: 10.6046/gtzyyg.2014.04.26

Li, Z. H., and Luo, P. (2003). *SPSS for Windows: Statistical Analysis Tutorial*. 2nd ed. Beijing: Electronic Industry Press, 257–265.

Lu, Y. H., Ranjitkar, S., Xu, J. C., Ou, X. K., and Zhou, Y. Z. (2016). Propagation of native tree species to restore subtropical evergreen broad-leaved forests in SW China. *Forests* 7, 12. doi: 10.3390/f7010012

Ma, Y. L., Wang, J., Zhang, J. H., Zhang, S. Y., Liu, Y. X., and Lan, H. Y. (2017). Seed heteromorphism and effects of light and abiotic stress on germination of a typical annual halophyte *Salsola ferganica* in cold desert. *Front. Plant Sci.* 8, 2257. doi: 10.3389/fpls.2017.02257

Maimaitijiang, T., Ma, Y. L., and Lan, H. Y. (2019). Effect of saltm coupled with drought stress on seed germination and seedling growth of *Salsola ferganica*. *Arid Zone Res.* 36, 878–885. doi: 10.13866/j.azr.2019.04.11

Mamut, J., Tan, D. Y., Baskin, C. C., and Baskin, J. M. (2019). Effects of water stress and NaCl stress on different life cycle stages of the cold desert annual *Lachnoloma lehmannii* in China. *J. Arid Land* 11, 774–784. doi: 10.1007/s40333-019-0015-8

Michel, B. E., and Kaufmann, M. R. (1973). The osmotic potential of polyethylene glycol 6000. *Plant Physiol.* 51, 914–916. doi: 10.1104/pp.51.5.914

Naidoo, G., and Naicker, K. (1992). Seed germination in the coastal halophytes *Triglochin bulbosa* and *Triglochin striata*. *Aquat. Bot.* 42, 217–229. doi: 10.1016/0304-3770(92)90023-C

Negrão, S., Schmöckel, S. M., and Tester, M. (2017). Evaluating physiological responses of plants to salinity stress. *Ann. Bot-London* 119, 1–11. doi: 10.1093/aob/mcw191

Prince, S. D., Becker-Reshef, I., and Rishmawi, K. (2009). Detection and mapping of long-term land degradation using local net production scaling: application to Zimbabwe. *Remote Sens. Environ.* 113, 1046–1057. doi: 10.1016/j.rse.2009.01.016

Probert, R. J. (1992). "The role of temperature in germination ecophysiology," in *Seeds: the Ecology of Regeneration in plant Communities*, ed M. Fenner (Wallingford: CABI Publishing), 410.

Qian, J. Q., Liu, Z. M., Hatier, J. H. B., and Liu, B. (2016). The vertical distribution of soil seed bank and its restoration implication in an active sand dune of Northeastern inner Mongolia, China. *Land Degrad. Dev.* 27, 305–315. doi: 10.1002/ldr.2428

Rasheed, A., Hameed, A., Gul, B., and Khan, M. A. (2019). Perianth and abiotic factors regulate seed germination of *Haloxylon stocksii*—a cash crop candidate for degraded saline lands. *Land Degrad. Dev.* 30, 1468–1478. doi: 10.1002/ldr.3334

Rasheed, A., Hameed, A., Khan, M. A., and Gul, B. (2015). Effects of salinity, temperature, light and dormancy regulating chemicals on seed germination of *Salsola drummondii* Ulbr. *Pak. J. Bot.* 47, 11–19.

Ruan, C. J., da Silva, J. A. T., Mopper, S., Qin, P., and Lutts, S. (2010). Halophyte improvement for a salinized world. *Crit. Rev. Plant Sci.* 29, 329–359. doi: 10.1080/07352689.2010.524517

Saatkamp, A., Affre, L., Baumberger, T., Dumas, P. J., Gasmi, A., Gachet, S., et al. (2011). Soil depth detection by seeds and diurnally fluctuating temperatures: different dynamics in 10 annual plants. *Plant Soil* 349, 331–340. doi: 10.1007/s11104-011-0878-8

Sekmen, A. H., Ozdemir, F., and Turkan, I. (2004). Effects of salinity, light, and temperature on seed germination in a Turkish endangered halophyte, *Kalidiopsis wagenitzii* (Chenopodiaceae). *Isr. J. Plant Sci.* 52, 21–30. doi: 10.1560/NXAR-71FB-CND5-E8FJ

Sen, D. N., and Chatterji, U. N. (1968). Ecology of desert plants and observations on their seedlings. II. germination behaviour of seeds in Asclepiadaceae. *Plant Syst. Evol.* 115, 18–27. doi: 10.1007/BF01373525

Song, J., Fan, H., Zhao, Y., Jia, Y., Du, X., and Wang, B. (2008). Effect of salinity on germination, seedling emergence, seedling growth and ion accumulation of a euhalophyte Suaeda salsa in an intertidal zone and on saline inland. *Aquat. Bot.* 88, 331–337. doi: 10.1016/j.aquabot.2007.11.004

Song, J., Feng, G., Tian, C. Y., and Zhang, F. S. (2005). Strategies for adaptation of *Suaeda physophora*, *Haloxylon ammodendron* and *Haloxylon persicum* to a saline environment during seed-germination stage. *Ann. Bot-London* 96, 399–405. doi: 10.1093/aob/mci196

Tobe, K., Li, X., and Omasa, K. (2000). Effects of sodium chloride on seed germination and growth of two Chinese desert shrubs, *Haloxylon ammodendron* and *H. persicum (Chenopodiaceae). Aust. J. Bot.* 48, 455–460. doi: 10.1071/BT99013

Wang, C., Wang, S., Fu, B. J., Lu, Y. H., Liu, Y. X., and Wu, X. (2020). Integrating vegetation suitability in sustainable revegetation for the Loess Plateau, China. *Sci. Total Environ.* 11, 559–564. doi: 10.1016/j.scitotenv.2020.143572

Wang, Y., Jiang, G. Q., Han, Y. N., and Liu, M. M. (2013). Effects of salt, alkali and salt–alkali mixed stresses on seed germination of the halophyte *Salsola ferganica* (Chenopodiaceae). *Acta Ecol. Sini.* 33, 354–360. doi: 10.1016/j.chnaes.2013.09.010

Wang, Y., Zhang, X. M., Li, L., and Li, H. X. (2008). Seed on response of germination of four species of *Salsola* L. to main ecology factors. *Seed* 27, 58–63, 67. doi: 10.16590/j.cnki.1001-4705.2008.08.061

Wei, Y., Dong, M., and Huang, Z. Y. (2007). Seed polymorphism, dormancy and germination of *Salsola affinis* (Chenopodiaceae), a dominant desert annual inhabiting the Junggar Basin of Xinjiang, China. *Aust. J. Bot.* 55, 464–470. doi: 10.1071/BT06016

Wei, Y., Dong, M., Huang, Z. Y., and Tan, D. Y. (2008). Factors influencing seed germination of *Salsola affinis* (Chenopodiaceae), a dominant annual halophyte inhabiting the deserts of Xinjiang, China. *Flora* 203, 134–140. doi: 10.1016/j.flora.2007.02.003

Wei, Y., and Wang, X. Y. (2006). Role of winged perianth in germination of *Haloxylon* (Chenopodiaceae) seeds. *Acta Ecol. Sin.* 26, 4014–4018.

Xing, J. J., Cai, M., Chen, S. S., Chen, L., and Lan, H. Y. (2013). Seed germination, plant growth and physiological responses of *Salsola ikonnikovii* to short-term NaCl stress. *Plant Biosyst.* 147, 285–297. doi: 10.1080/11263504.2012.731017

Yu, L., Guo, T. D., Sun, Z. C., Ma, Y. P., Li, Z. L., Zhao, Y. N., et al. (2021). The seed germination characteristics and thresholds of two dominant plants in desert grassland-shrubland transition of the eastern Ningxia, China. *Acta Ecol. Sin.* 41, 4160–4169. doi: 10.5846/stxb201910152147

Zhang, K., Zheng, H., Chen, F. L., Ouyang, Z. Y., Wang, Y., Wu, Y. F., et al. (2015). Changes in soil quality after converting *Pinus* to *Eucalyptus* plantations in southern China. *Solid Earth* 6, 115–123. doi: 10.5194/se-6-115-2015

Zhu, G. L., Mosyakin, S. L., and Clemants, S. E. (2003). "Chenopodiaceae," in *Flora of China*, eds Z. Y. Wu, and P. H. Raven (Beijing: Science Press), 351–414.

**Conflict of Interest:** The authors declare that the research was conducted in the absence of any commercial or financial relationships that could be construed as a potential conflict of interest.

**Publisher's Note:** All claims expressed in this article are solely those of the authors and do not necessarily represent those of their affiliated organizations, or those of the publisher, the editors and the reviewers. Any product that may be evaluated in this article, or claim that may be made by its manufacturer, is not guaranteed or endorsed by the publisher.

frontiers | Frontiers in Plant Science

ORIGINAL RESEARCH
published: 19 May 2022
doi: 10.3389/fpls.2022.869105

# Deep Untargeted Metabolomics Analysis to Further Characterize the Adaptation Response of *Gliricidia sepium* (Jacq.) Walp. to Very High Salinity Stress

*Ítalo de Oliveira Braga*[1], *Thalliton Luiz Carvalho da Silva*[1], *Vivianny Nayse Belo Silva*[1], *Jorge Candido Rodrigues Neto*[2], *José Antônio de Aquino Ribeiro*[3], *Patrícia Verardi Abdelnur*[2,3], *Carlos Antônio Ferreira de Sousa*[4] *and Manoel Teixeira Souza Jr.*[1,3]*

[1] Graduate Program of Plant Biotechnology, Federal University of Lavras, Lavras, Brazil, [2] Institute of Chemistry, Federal University of Goiás, Campus Samambaia, Goiânia, Brazil, [3] Brazilian Agricultural Research Corporation, Embrapa Agroenergy, Brasília, Brazil, [4] Brazilian Agricultural Research Corporation, Embrapa Mid-North, Teresina, Brazil

OPEN ACCESS

**Edited by:**
*Amr Adel Elkelish,*
*Suez Canal University, Egypt*

**Reviewed by:**
*Atsushi Fukushima,*
*Kyoto Prefectural University, Japan*
*Caifeng Li,*
*Northeast Agricultural University, China*

***Correspondence:**
*Manoel Teixeira Souza Jr.*
*manoel.souza@embrapa.br*

**Specialty section:**
*This article was submitted to Plant Abiotic Stress, a section of the journal Frontiers in Plant Science*

**Received:** *03 February 2022*
**Accepted:** *28 March 2022*
**Published:** *19 May 2022*

**Citation:**
*Braga ÍO, Carvalho da Silva TL, Belo Silva VN, Rodrigues Neto JC, Ribeiro JAA, Abdelnur PV, de Sousa CAF and Souza MT Jr (2022) Deep Untargeted Metabolomics Analysis to Further Characterize the Adaptation Response of Gliricidia sepium (Jacq.) Walp. to Very High Salinity Stress. Front. Plant Sci. 13:869105. doi: 10.3389/fpls.2022.869105*

The multipurpose tree *Gliricidia sepium* (Jacq.) Walp. adapts to a very high level of salt stress (≥20 dS $m^{-1}$) and resumes the production of new leaves around 2 weeks after losing all leaves due to abrupt salinity stress. The integration of metabolome and transcriptome profiles from gliricidia leaves points to a central role of the phenylpropanoid biosynthesis pathway in the short-term response to salinity stress. In this study, a deeper untargeted metabolomics analysis of the leaves and roots of young gliricidia plants was conducted to characterize the mechanism(s) behind this adaptation response. The polar and lipidic fractions from leaf and root samples were extracted and analyzed on a UHPLC.ESI.Q-TOF.HRMS system. Acquired data were analyzed using the XCMS Online, and MetaboAnalyst platforms, *via* three distinct and complementary strategies. Together, the results obtained first led us to postulate that these plants are salt-excluding plants, which adapted to high salinity stress *via* two salt-excluding mechanisms, starting in the canopy—severe defoliation—and concluding in the roots—limited entry of Na. Besides that, it was possible to show that the phenylpropanoid biosynthesis pathway plays a role throughout the entire adaptation response, starting in the short term and continuing in the long one. The roots metabolome analysis revealed 11 distinct metabolic pathways affected by salt stress, and the initial analysis of the two most affected ones—steroid biosynthesis and lysine biosynthesis—led us also to postulate that the accumulation of lignin and some phytosterols, as well as lysine biosynthesis—but not degradation, play a role in promoting the adaptation response. However, additional studies are necessary to investigate these hypotheses.

**Keywords: abiotic stress, salt tolerance, chemometrics, high-resolution mass spectrometry, phenylpropanoids, phytosterols, lignin**

## INTRODUCTION

Soil salinity is an environmental limiting factor for plant biomass production worldwide, with approximately 20% of all agricultural land in the world having either saline or sodic soils, and between 25 and 30% of the irrigated land area is affected by salt (Negrão et al., 2017; Shahid et al., 2018). The annual global cost of salt-induced land degradation in irrigated areas can reach US$ 27.3 billion due to a decrease in productivity (Pan et al., 2020). Salinity imposes adverse effects on plant growth by causing water imbalance, oxidative stress, and $Na^+$ toxicity (Zarei et al., 2020). Besides that, it also compromises germinative processes, photosynthetic pigmentation, and photosynthesis.

Metabolomics (the study of modification in metabolites) is a comprehensive and quantitative analysis of all small molecules in a biological system (Belinato et al., 2019). It is one promising approach used to detect and quantify primary and secondary metabolites of low molecular weight, generally <1,500 Da (Bueno and Lopes, 2020). Recent studies show that some metabolites are present in metabolic changes induced by salt stress, and they can act as effectors of osmotic readjustment or antioxidant response (Arbona et al., 2013). The presence of specific metabolites may be associated with tolerance to stress and serve as biomarkers for salt-tolerant genotypes selection in plant breeding programs (D'amelia et al., 2018).

*Gliricidia sepium* (Jacq.) Walp., a medium-sized legume (10–15 m) from the Fabaceae family, is originally from Central America. It is one of the most well-known multipurpose trees, known for its ability to adapt very well to a wide range of soils, from eroded acidic soils, sandy soils, heavy clay, limestone, and alkaline soils (Rahman et al., 2019). As pointed out by Rahman et al. (2019), Gliricidia salinity tolerance limits alongside the morphophysiological responses to salt stress are not yet well-understood. Rahman and colleagues reported a study where seawater from the southern coastal area of Bangladesh induced salinity stress in 1-month-old gliricidia seedlings for 90 days and showed that seawater-induced salinity negatively affected several growth-related attributes. They also showed enhanced accumulation of proline, the proteinogenic secondary amino acid that participates in metabolic signaling and is known to be metabolized by its own family of enzymes responding to stress (Phang et al., 2010), postulating that it might help adjust the plant to water deficit conditions (Rahman et al., 2019).

In a previous study done by our group, we described two distinct responses of gliricidia plants—tolerance and adaptation—to salt stress, depending on the amount of NaCl used (Carvalho da Silva et al., 2021). Additionally, when employing single and integrative transcriptomic and metabolomic analysis approaches, it showed that the phenylpropanoid biosynthesis pathway was the most salt stress-affected pathway in the leaves of young gliricidia plants, with 15 metabolites and three genes differentially expressed, and that this pathway role was more evident at the beginning of the stress, not in the long-term.

Ho et al. (2020) characterized the transcriptomes, metabolomes, and lipidomes of domesticated and landrace barley plants with distinct seedling root growth responses under salt stress. The phenylpropanoid biosynthesis was the most statistically enriched biological pathway among all salinity responses observed, based on pathway over-representation of the differentially expressed genes and metabolites (Ho et al., 2020). Zhu et al. (2021) also performed a combined transcriptomic and metabolomic analysis of salt-stressed *Sophora alepecuroide* plants, a leguminous perennial herb found mainly in the desert and semi-desert areas of the China northwest region, and also showed that the differentially expressed genes and metabolites in the phenylpropanoid biosynthesis pathway significantly correlated under salt stress. A difference between the work done by Carvalho da Silva et al. (2021) and the ones by Ho et al. (2020) and Zhu et al. (2021) is that it used leaves and the later ones used roots.

The current study is a follow-up to our previous study (Carvalho da Silva et al., 2021). Hence, the objective of this present study was to carry out a deeper metabolome analysis not only of the leaves but also the roots of *G. sepium* plants submitted to very high salt stress. For this purpose, gliricidia plants were under salinity stress, and leaves and root samples were collected from control and stressed plants at 2 and 55 days after the onset of the stress for untargeted metabolomics (UM) analysis.

## MATERIALS AND METHODS

### Plant Material, Growth Conditions, Experimental Design, and Saline Stress

The accession of gliricidia [*Gliricidia sepium* (Jacq.) Steud.] used in this study belongs to the Gliricidia Collection at Embrapa Tabuleiros Costeiros (www.embrapa.br/en/tabuleiros-costeiros). After soaking the seeds in 2% sodium hypochlorite and Tween® 20 for 5 min under slow agitation, we washed them with sterile water and dried them on sterilized filter paper. Then they were placed in a Petri dish with filter paper moistened with sterilized water until the radicle emission. Subsequently, each germinated seed was transferred individually to a 5 L plastic pot (about 20 cm × 25 cm × 15 cm in size, top × height × bottom) containing 4 kg of substrate previously prepared by mixing sterile soil, vermiculite, and a commercial substrate (Bioplant®), in the ratio 2/1/1 (v/v/v); and kept in a greenhouse for 3 months.

Groups of five and a half-month-old gliricidia plants were kept under control conditions or subjected to saline stress (27 dS/m of electric conductivity) for 2 (short-term stress) or 55 (long-term stress) days. The experimental design was completely randomized with 12 replicates (plants) per treatment.

The NaCl was dissolved in deionized water to salinize the substrate. We replaced the water lost by evapotranspiration with deionized water on a daily basis, and the amount of deionized water used corresponded to the difference between the amount of water previously present in the substrate and the amount of water necessary for the substrate to reach field capacity, as described in Vieira et al. (2020), Carvalho da Silva et al. (2021). Applying the right amount of water—up to the substrate field capacity—was a means of ensuring no leakage of the solution out of the pot and no loss of $Na^+$ or $Cl^-$. The electric conductivity and water potential in the substrate solution were monitored at 0 and 25 days after imposing the stress treatment for all replicates. The

electric conductivity in the soil was measured at field capacity (ECfc) and not in the saturated paste extract (ECe), as also described in (Vieira et al., 2020; Carvalho da Silva et al., 2021).

## Mineral Analysis

Samples were collected for determination of mineral content; as well as samples of the substrate before and after plant growth. Dried samples were ground in a Wiley mill Tecnal Mod. TE 680 (Tecnal, Piracicaba, SP, Brazil), passed through a 1 mm (20 mesh) sieve and then subjected to the extraction of minerals by the standard methods used in laboratory routine at Soloquímica (www.soloquimica.com.br).

Initially, mineral analysis data were examined for normality using the Shapiro-Wilk test. Then, parametric and non-parametric data were compared using the *T*-tests ($p < 0.05$) and Mann-Whitney test ($p < 0.05$), respectively, and biomass data were examined by linear regression analysis.

## Metabolomics Analysis

Leaves and roots from control and stressed plants—five replicates per treatment—were collected at 2 and 55 days after stress treatment (DAT), immediately immersed in liquid nitrogen, and then stored at −80°C until extraction of metabolites.

### Chemicals and Metabolites Extraction

Samples were grounded in liquid nitrogen before solvent extraction. The solvents methanol grade ultra-high performance liquid chromatography (UHPLC), acetonitrile grade liquid chromatography-mass-spectrometry (LC-MS), formic acid grade LC-MS and sodium hydroxide American Chemical Society (ACS) grade LC-MS were from Sigma-Aldrich (St. Louis, MO, USA), and the water was treated in a Milli-Q system (Millipore, Bedford, MA, USA).

We employed a well-known protocol (Vargas et al., 2016; Rodrigues-Neto et al., 2018) to extract the metabolites through a mixture of polar solvents. After transferring aliquots of 50 mg of grounded sample to 2 ml microtubes, 1 ml of a 1:3 (v:v) methanol: methyl tert-butyl ether mixture was added, and then left for homogenization at 4°C on an orbital shaker for 10 min, followed by an ultrasound treatment in an ice bath for another 10 min. Next, 500 µl of a 1:3 (v:v) methanol: water mixture (1:3) was added to each microtube before centrifugation (12,000 rpm, 4°C for 5 min). After centrifugation, three phases were obtained: a non-polar phase for lipid analysis, a polar phase for secondary metabolism analysis and a pellet for protein analysis. The lipidic and polar fractions were transferred separately to 1.5 ml microtubes and vacuum dried overnight in room temperature in a Speed vac system (Centrivap, Labconco, Kansa, MO, USA). Polar and lipidic fractions samples were resuspended in a 500 µl of 1:3 (v:v) methanol: water mixture and transferred to vials prior to chemical analysis.

### UHPLC-MS and UHPLC-MS/MS

A UHPLC chromatographic system was used (Nexera X2, Shimadzu Corporation, Japan) equipped with an Acquity UPLC HSS T3 (1.8 µm, 2.1 × 150 mm) reverse phase column (Waters Technologies, Milford, MA), maintained at 35°C. A polar mobile phase was used, composed by water (solvent A) and acetonitrile/methanol (70/30, v/v) (solvent B), both in 0.1% formic acid. The gradient elution used, with a flow rate of 0.4 mL $min^{-1}$, was as follows: isocratic from 0 to 1 min (0% B), linear gradient from 1 to 3 min (5% B), from 3 to 10 min (50% B), and 10 to 13 min (100% B), isocratic from 13 to 15 min (100% B), followed by rebalancing in the initial conditions for 5 min.

A high-resolution mass spectrometry equipment (HRMS) (MaXis 4G Q-TOF MS, Bruker Daltonics, Germany), coupled to the UHPLC system, performed the chemical mass to charge ratio (m/z) detection using an electrospray source in positive [ESI (+)—MS] and negative [ESI (–)—MS] ionization modes. Final plate offset, 500 V; capillary voltage, 3,800 V; nebulizer pressure, 4 bar; dry gas flow, 9 L $min^{-1}$, and dry temperature, 200°C. The rate of acquisition spectra was 3.00 Hz, monitoring a mass range of 70–1,200 m/z. A sodium formate solution (10 mM HCOONa solution in 50/50 v/v isopropanol/water containing 0.2% formic acid) was injected directly through a 6-way valve at the beginning of each chromatographic run for external calibration. Ampicillin ([M+H] + *m/z* 350.11867 and [M-H]— *m/z* 348.10288) was added to each sample as an internal standard for peak normalization.

Tandem mass spectrometry (MS/MS) parameters have been adjusted to improve mass fragmentation, with collision energy ranging from 20 to 50 eV, using a step method. Precursor ions were acquired using the 3.0 s cycle time. The general AutoMS settings were: mass range, *m/z* 70–1,000 (polar fraction) and *m/z* 300–1,600 (lipidic fraction); spectrum rate, 3 Hz; ionic, positive polarity; pre-pulse storage, 8 µs; funnel 1 RF, 250.0 Vpp. The UHPLC-MS and UHPLC-MS/MS data were acquired by HyStar Application version 3.2 (BrukerDaltonics, Germany).

### Metabolomics Data Analysis

The raw data from UHPLC-MS were exported as mzMXL files, using DataAnalysis 4.2 software (Bruker Daltonics, Germany). During data pre-processing, peak detection, retention time correction, and metabolites alignment were performed using XCMS Online (Tautenhahn et al., 2012; Gowda et al., 2014). Peak detection was performed using centWave peak detection ($\Delta$m/z = 10 ppm; minimum peak width, 5 s; maximum peak width, 20 s) and mzwid =0.015, minfrac =0.5, bw = 5 for the alignment of retention time. The unpaired parametric *t*-test (Welch *t*-test) was used for statistical analysis.

The processed data (csv file) were exported to MetaboAnalyst 5.0, and submitted to analysis in the Statistical Analysis module (Chong et al., 2019; Chong and Xia, 2020). Before the chemometric analysis, all data variables from the polar fraction were normalized by internal standard (ampicillin-rT = 7.9 min; [M+H], *m/z* = 350.1169509; sodium formate adduct-r T = 0.1 min, [M-H], *m/z* = 112.9854317), and all data variables from the lipidic fraction were also normalized by internal standard (1,2-diheptadecanoyl-sn-glycero-3-phosphocholine = 4.85 min; [M+H] + *m/z* = 762.6002192). Prior to the multivariate analysis, no data transformation was applied to the data matrices containing m/z and intensities values. All three sets of data were scaled using the Pareto scaling, which reduced the relative importance of large values, keeping data structure partially intact,

and although sensitive to large fold changes, it stays closer to the original measurement than Autoscaling.

The differentially expressed peaks (DEP) were selected according to the following criteria: adjusted *P*-value (FDR) $\leq$ 0.050, of the Welch *t*-test. The selected DEPs were then submitted to analysis in the MS Peaks to Pathway module (Chong et al., 2019; Chong and Xia, 2020) and analyzed using the following parameters: molecular weight tolerance of 5 ppm; mixed ion mode; analysis using the mummichog algorithm (Li et al., 2013) with the default *p*-value cutoff, ranked by *p*-values, and the latest KEGG version of the *Arabidopsis thaliana* pathway library.

In the case of a DEP with two or more matched forms (isotopes) and later a matched compound with two or more DEPs, the criterion of metabolite selection applied was the mass difference comparing to the metabolite database—choosing the smallest one. Then, we used the formula and exact mass data from KEGG to perform the putative annotation of the metabolites of interest, with just one candidate on each detected ion.

The KEGG IDs of the matched compounds were then submitted to pathway analysis (integrating enrichment analysis and pathway topology analysis) and visualization in the Pathway Analysis module (Chong et al., 2019; Chong and Xia, 2020) and analyzed using the Scatter plot (testing significant features) as visualization method, the Hypergeometric Test as the enrichment method, the relative-betweenness centrality as topology analysis, and the latest KEGG version of the *A. thaliana* pathway library as reference metabolome (from October 2019).

## METABOLOMICS DOWNSTREAM ANALYSIS

Initially, correlation analyses were done between pairs of differentially expressed metabolites—a pairwise combination of the different scenarios evaluated—using homemade python scripts. The input data for the correlation analysis was the $Log_2$(FC).

Then, the Omics Fusion web platform (Brink et al., 2016) was used to verify which pathways the metabolites selected in the correlation analysis belonged to. The input data on the platform were the KEGG IDs and the $Log_2$(FC) of the metabolites and an enrichment analysis was initially carried out to discover the metabolic pathways to which they belong. The "KEGG feature distribution" module was used, which showed the metabolic pathways and the amount of metabolites differentially expressed in each pathway. To verify which were these metabolites, for each pathway, the module "Map data on the KEGG pathway" was then used.

## RESULTS

### Gliricidia Sepium Morphophysiological Responses to Salt Stress

The evapotranspiration rates of the control (**Figure 1A**) were higher than salt-stressed treatment (**Figure 1B**) throughout the experiment. However, the shape of the curve was similar in both treatments. In addition to the temporal fluctuation in transpiration rates, it was observed that as the plants got older, more water was demanded.

The young gliricidia plants submitted to a very high level of salinity in this study showed the adaptation response previously reported by Carvalho da Silva et al. (2021). Immediately after adding salt to the substrate, the gliricidia plants were fully leafy, with completely green leaves (**Figure 2A**), but went on to lose all leaves before the end of the first week under salt stress (**Figure 2B**). Approximately 3 weeks after the onset of stress, new leaves started to emerge and continued to emerge and grow in the following weeks (**Figures 2C,D**).

The addition of NaCl to the substrate led to a significant increase in the concentration of exchangeable $Na^+$, $Mg^{2+}$, and $K^+$. As a consequence, there was an increase in the sum of bases, cation exchange capacity, base saturation, and sodium saturation index. Additionally, a significant increase in organic matter and C was observed (**Supplementary Table 1**). The plants under salt stress accumulated significantly more $Na^+$ and $Cl^-$ than control in both the canopy and the roots. P, Cu, and Zn ions were significantly increased in the canopy under salt stress, while Fe was significantly increased in the roots.

### Gliricidia Metabolome Under Salinity Stress

Before submitting the data for analysis in the statistics module of MetaboAnalyst 5.0, the data got separated into leaf and root data and organized as follows: all in treatments dataset (control and stressed plants at 2 and 55 days after treatment—DAT); age effect—AE (samples from the control plants at 2 and 55 DAT); short-term stress—STS (the control and the stressed plants at 2 DAT); long-term stress 1—LTS1 (control and stressed plants at 55 DAT); and long-term stress 2—LTS2 (the stressed plants at 2 and 55 DAT). Each dataset had five biological replicates per treatment.

#### Leaves

Partial least squares discriminant analysis (PLS-DA) permutation tests were performed using the leaves all treatment data set to validate the model, applying permutation number = 2,000. PLS-DA is an important and widespread classification model for untargeted metabolomics, where model tendencies are described based on group separation. Groups and samples behavior can be studied through the insights given by PLS-DA on outliers, intragroup separation tendencies, and explained variance used, which add the visualization aspect to the metabolomics model. When evaluated by group separation distance, the probability that the model was created by chance was 0.06 for the lipidic-positive fraction and <0.0005 for the other two fractions (**Supplementary Figure 1**).

The ANOVA analysis using the leaves all treatments data set generated 4,464 peaks with a *p*-value cutoff of 8.0E-5 that were submitted to functional interpretation *via* analysis in the MS Peaks to Pathway module. After applying the initial criteria of metabolite selection, 367 peaks with a hit to just one known compound were submitted to the pathway topology analysis module, resulting in 13 pathways with a Raw $p \leq 0.05$; they were: ubiquinone and other terpenoid-quinone biosynthesis;

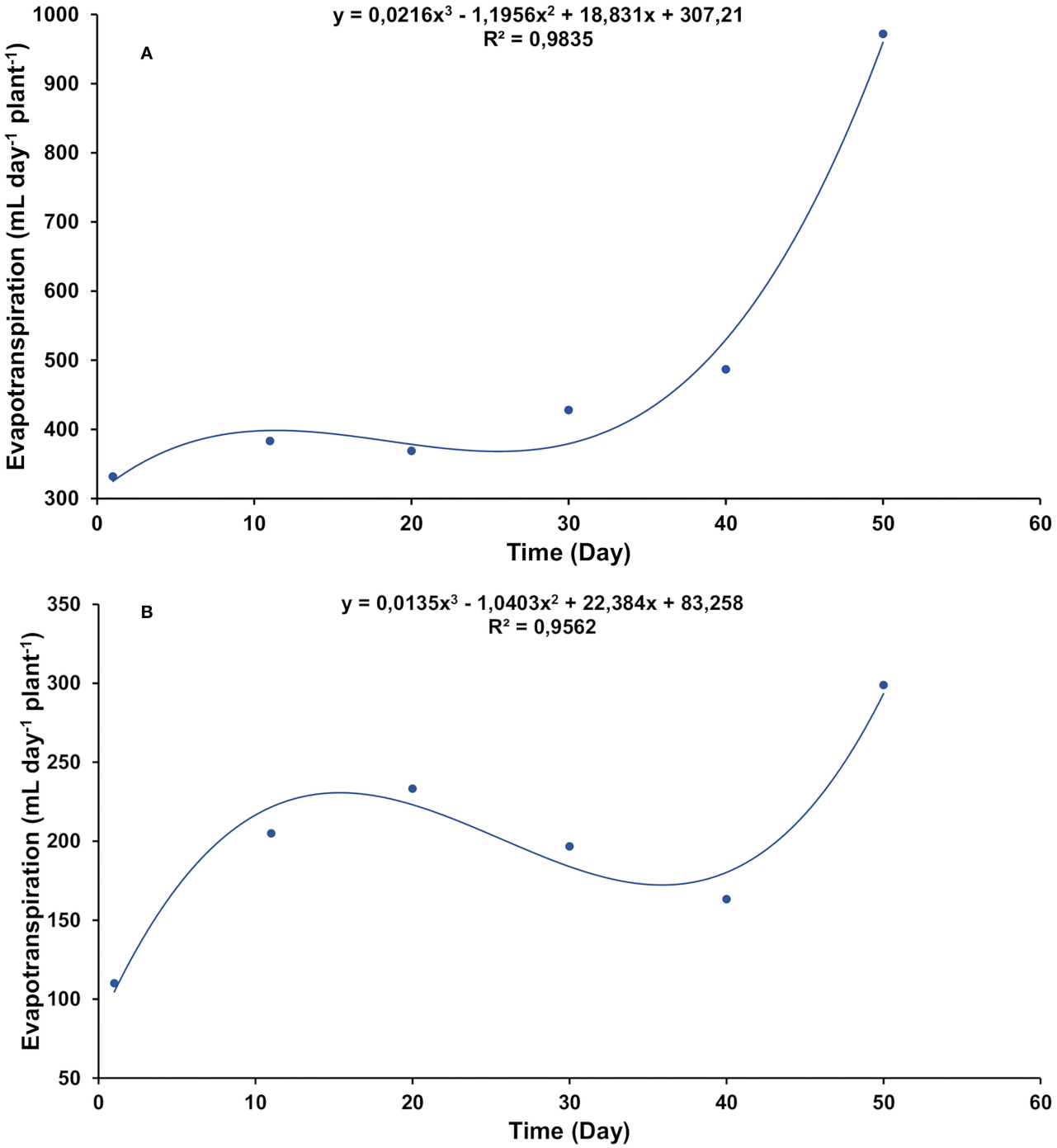


**FIGURE 1 |** Daily evapotranspiration rate in gliricidia plants at 0.0 **(A)** and 0.8 **(B)** g of NaCl per 100 g of the substrate. The values represent the average of 11 replicates, in a timeline starting from 1 day up to 50 days of treatment.

arginine biosynthesis; lysine biosynthesis; phenylpropanoid biosynthesis; monobactam biosynthesis; steroid biosynthesis; carotenoid biosynthesis; flavone and flavonol biosynthesis; tyrosine metabolism; valine, leucine, and isoleucine biosynthesis; porphyrin and chlorophyll metabolism, and Indole alkaloid biosynthesis. These pathways came out with 19, 11, 7, 20, 6, 19, 18, 6, 8, 10, 18, and 3 differentially expressed metabolites with the highest level of significance within the set of matched metabolites submitted to analysis, respectively (data not shown).

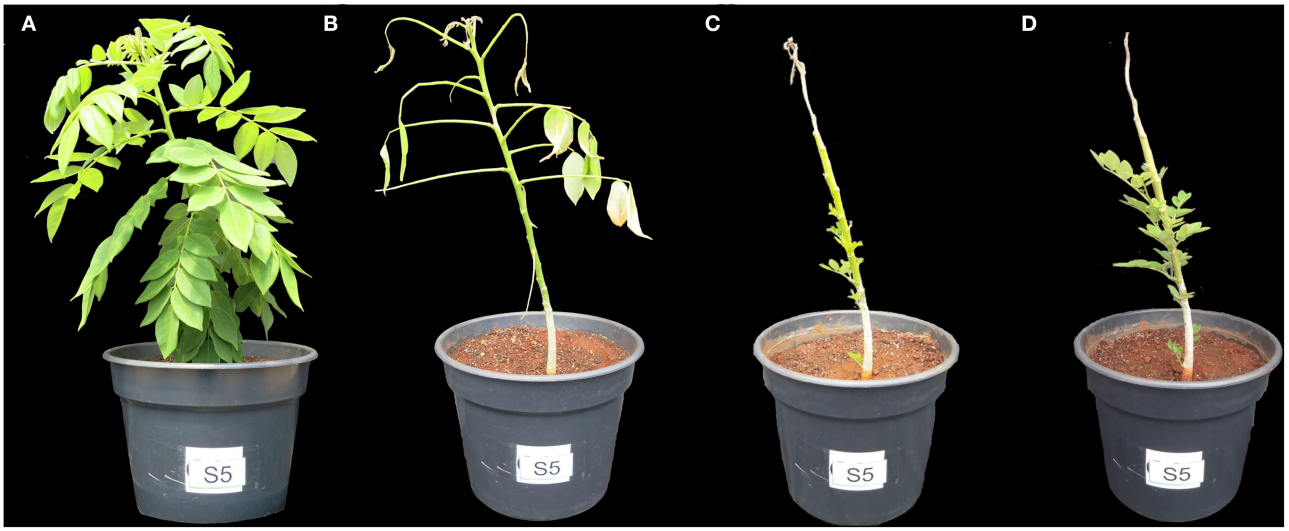


**FIGURE 2 |** Timeline of the adaptation response in gliricidia plant under salinity stress. Plants at 0.8 g of NaCl per 100 g of the substrate. After 1 **(A)**, 5 **(B)**, 23 **(C)**, and 34 **(D)** days of stress.

The changes in the metabolic profile due to the age effect, once there is a 53-day gap between the two assessments, were measured using the AE data set. The AE data set from leaves contained 816, 550, and 4,010 peaks, respectively, in the polar-positive, polar-negative, and lipidic-positive fractions; and a total of 3,168 (58.93%) peaks out of the 5,376 seen in the three fractions were differentially expressed—a differentially expressed peak (DEP) is a peak with an adjusted *P*-value (FDR) $\leq 0.05$, and $Log_2$ (FC) $> 0$ (up-regulated) or $Log_2$ (FC) $< 0$ (down-regulated) (**Table 1**).

The short-term stress dataset from leaves was employed to evaluate how distinct are the metabolome profiles of the control and stressed plants at 2 DAT, just 1 day before the leaves started to wilt. The samples applied to evaluate the STS scenario in the leaves contained 829, 589, and 4,010 peaks, respectively, and a total of 1,550 (28.56%) peaks out of the 5,428 seen in the three fractions were differentially expressed (**Table 1**).

The LTS1 dataset from leaves was employed to evaluate how distinct are the metabolome profiles of the control and stressed plants at 55 DAT. The samples applied contained 788, 580, and 4,001 peaks, respectively, and a total of 1,285 (23.93%) peaks out of the 5,369 seen in the three fractions were differentially expressed (**Table 1**). The LTS2 dataset from leaves was employed to evaluate how distinct are the metabolome profiles of the stressed plants at two and 55 DAT. The samples applied contained 827, 573, and 4,010 peaks, respectively, and a total of 2,615 (48.34%) peaks out of the 5,410 seen in the three fractions were differentially expressed (**Table 1**).

All 1,550 peaks differentially expressed in the STS were submitted to functional interpretation *via* analysis in the MS Peaks to Pathway module, with a *p*-value cutoff of 1.0E-5. After applying the initial criteria of metabolite selection, 197 DEPs with a hit to just one known compound were submitted to the pathway topology analysis module, resulting in 16 pathways with a raw $p \leq 0.05$; they were: valine, leucine, and isoleucine biosynthesis; phenylpropanoid biosynthesis; arginine biosynthesis; monobactam biosynthesis; flavone and flavonol biosynthesis; indole alkaloid biosynthesis; pyruvate metabolism; lysine biosynthesis; glycine, serine, and threonine metabolism; beta-alanine metabolism; pantothenate and CoA biosynthesis; glyoxylate and dicarboxylate metabolism; C5-branched dibasic acid metabolism; fructose and mannose metabolism, anthocyanin biosynthesis, and tyrosine metabolism (**Figure 3A**). These pathways came out with 10, 15, 8, 5, 5, 3, 7, 4, 9, 6, 7, 8, 3, 6, 4, and 5 differentially expressed metabolites with the highest level of significance within the set of matched metabolites submitted to analysis, respectively (data not shown).

The 2,615 peaks differentially expressed in the LTS2 were also submitted to functional interpretation *via* analysis in the MS Peaks to Pathway module, with a *p*-value cutoff of 1.0 E-5. After applying the initial criteria of metabolite selection, 258 DEPs with a hit to just one known compound were submitted to the pathway topology analysis module, resulting in nine pathways with a raw $p \leq 0.05$; they were: ubiquinone and other terpenoid-quinone biosynthesis; steroid biosynthesis; monobactam biosynthesis; lysine biosynthesis; phenylpropanoid biosynthesis; porphyrin and chlorophyll metabolism; tyrosine metabolism; arginine biosynthesis; and brassinosteroid biosynthesis (**Figure 3B**). These pathways came out with 17, 18, 6, 6, 15, 15, 7, 7, and 9 differentially expressed metabolites with the highest level of significance within the set of matched metabolites submitted to analysis, respectively (data not shown).

## Roots

Partial least squares discriminant analysis permutation tests were performed using the roots all treatments data set (control and stressed plants at 2 and 55 DAT) to validate the model, applying permutation number = 2,000. When evaluated by group

**TABLE 1 |** Differentially expressed peaks and features in the leaves and roots of gliricidia plants submitted to salinity stress in four distinct scenarios: age effect—AE (control plants at 2 and 55 days under salinity stress—DAT); short-term stress—STS (control and the stress plants at 2 DAT); long-term stress 1—LTS1 (control and stressed plants at 55 DAT); and long-term stress 2—LTS2 (stressed plants at 2 and 55 DAT).

| | # of peaks | Up | Down | Non-DE |
|---|---|---|---|---|
| **Leaves** | | | | |
| Age effect | Control plants at 55 DAT vs. control plants at 02 DAT | | | |
| Polar-positive | 816 | 29 | 483 | 304 |
| Polar-negative | 550 | 8 | 346 | 196 |
| Lipidic-positive | 4,010 | 1,629 | 673 | 1,708 |
| Total | 5,376 | 1,666 | 1,502 | 2,208 |
| Short-term stress | Stressed plants at 02 DAT vs. control plants at 02 DAT | | | |
| Polar-positive | 829 | 70 | 185 | 574 |
| Polar-negative | 589 | 3 | 472 | 114 |
| Lipidic-positive | 4,010 | 203 | 617 | 3,190 |
| Total | 5,428 | 276 | 1,274 | 3,878 |
| Long-term stress 1 | Stressed plants at 55 DAT vs. control plants at 55 DAT | | | |
| Polar-positive | 788 | 186 | 97 | 505 |
| Polar-negative | 580 | 8 | 516 | 56 |
| Lipidic-positive | 4,001 | 75 | 403 | 3,523 |
| Total | 5,369 | 269 | 1,016 | 4,084 |
| Long-term stress 2 | Stressed plants at 55 DAT vs. stressed plants at 02 DAT | | | |
| Polar-positive | 827 | 99 | 313 | 415 |
| Polar-negative | 573 | 36 | 181 | 356 |
| Lipidic-positive | 4,010 | 1,393 | 593 | 2,024 |
| Total | 5,410 | 1,528 | 1,087 | 2,795 |
| **Roots** | | | | |
| Age effect | Control plants at 55 DAT vs. control plants at 02 DAT | | | |
| Polar-positive | 636 | 49 | 356 | 231 |
| Polar-negative | 392 | 22 | 78 | 292 |
| Lipidic-positive | 3,976 | 1,570 | 513 | 1,893 |
| Total | 5,004 | 1,641 | 947 | 2,416 |
| Short-term stress | Stressed plants at 02 DAT vs. control plants at 02 DAT | | | |
| Polar-positive | 666 | 104 | 6 | 556 |
| Polar-negative | 429 | 36 | 216 | 177 |
| Lipidic-positive | 3,993 | 0 | 28 | 3,965 |
| Total | 5,088 | 140 | 250 | 4.698 |
| Long-term stress 1 | Stressed plants at 55 DAT vs. control plants at 55 DAT | | | |
| Polar-positive | 561 | 0 | 0 | 561 |
| Polar-negative | 380 | 12 | 148 | 220 |
| Lipidic-positive | 3,748 | 0 | 0 | 3,748 |
| Total | 4,689 | 12 | 148 | 4,529 |
| Long-term stress 2 | Stressed plants at 55 DAT vs. stressed plants at 02 DAT | | | |
| Polar-positive | 671 | 37 | 342 | 292 |
| Polar-negative | 421 | 14 | 124 | 283 |
| Lipidic-positive | 3,990 | 1,992 | 546 | 1,452 |
| Total | 5,082 | 2,043 | 1,012 | 2,027 |

*The differentially expressed peaks are those with an adjusted P-value (FDR) ≤ 0.05, of the Welch t-test; and $Log_2$ (Fold Change) ≠ 1.*

separation distance, the probability that the model was created by chance was 0.011 (polar-positive), 0.0005 (polar-negative), and 0.0415 (lipidic-positive) (**Supplementary Figure 1**).

The ANOVA analysis using the roots all in treatments dataset generated 3,600 peaks with a $p \leq 0.05$, submitted to functional interpretation *via* analysis in the MS Peaks to Pathway module, with a *p*-value cutoff of 1.0E-5. After applying the initial criteria of metabolite selection, 326 peaks with a hit to just one known compound were submitted to the pathway topology analysis module, resulting in 10 pathways with a raw $p \leq 0.05$; they were: steroid biosynthesis; lysine biosynthesis, ubiquinone, and other terpenoid-quinone biosynthesis; arginine biosynthesis; monobactam biosynthesis; carotenoid biosynthesis; valine, leucine, and isoleucine biosynthesis; tyrosine metabolism; phenylpropanoid biosynthesis; and porphyrin and chlorophyll metabolism. These pathways came out with 20, 7, 17, 10, 6, 18, 10, 8, 16, and 16 differentially expressed metabolites with the highest level of significance within the set of matched metabolites submitted to analysis, respectively (data not shown).

The age effect data set from roots was employed to evaluate how distinct are the metabolome profiles of the control plants at 2 and 55 DAT, a 53-day gap between the two assessments. The AE data set contained 636, 392, and 3,976 peaks, respectively, in the polar-positive, polar-negative, and lipidic-positive fractions; and a total of 2,588 (51.72%) peaks out of the 5,004 seen in the three fractions were differentially expressed (**Table 1**).

The STS dataset from roots was employed to evaluate how distinct are the metabolome profiles of the control and stressed plants at 2 DAT, just 1 day before the leaves started to wilt. The samples applied to evaluate the STS scenario in the leaves contained 666, 429, and 3,993 peaks, respectively, and a total of 390 (7.67%) peaks out of the 5,088 seen in the three fractions were differentially expressed (**Table 1**).

The LTS1 data set from roots was employed to evaluate how distinct are the metabolome profiles of the control and stressed plants at 55 DAT. The samples applied contained 561, 380, and 3,748 peaks, respectively, and a total of 160 (3.41%) peaks out of the 4,689 seen in the three fractions were differentially expressed (**Table 1**). A principal component analysis (PCA), an unsupervised method commonly used to identify patterns between multivariate samples, was applied to detect any inherent patterns within the data in the LTS1, and it was not able to completely separate the groups between the control and the stressed samples in the polar positive and lipidic positive fractions (**Figure 4**). The LTS2 data set from roots was employed to evaluate differences in the profiles from the stressed plants at two and 55 DAT. The samples applied contained 671, 421, and 3,990 peaks, respectively, and a total of 3,055 (60.11%) peaks out of the 5,082 seen in the three fractions were differentially expressed (**Table 1**).

All 390 peaks differentially expressed in the STS were submitted to functional interpretation *via* analysis in the MS Peaks to Pathway module, with a *p*-value cutoff of 1.0E-5. After applying the initial criteria of metabolite selection, 83 DEPs with a hit to just one known compound were submitted to the pathway topology analysis module, resulting in eight pathways with a raw $p \leq 0.05$. The indicated pathways were: galactose metabolism; valine, leucine, and isoleucine biosynthesis; glucosinolate biosynthesis; glycine, serine, and threonine metabolism; pantothenate and CoA biosynthesis;

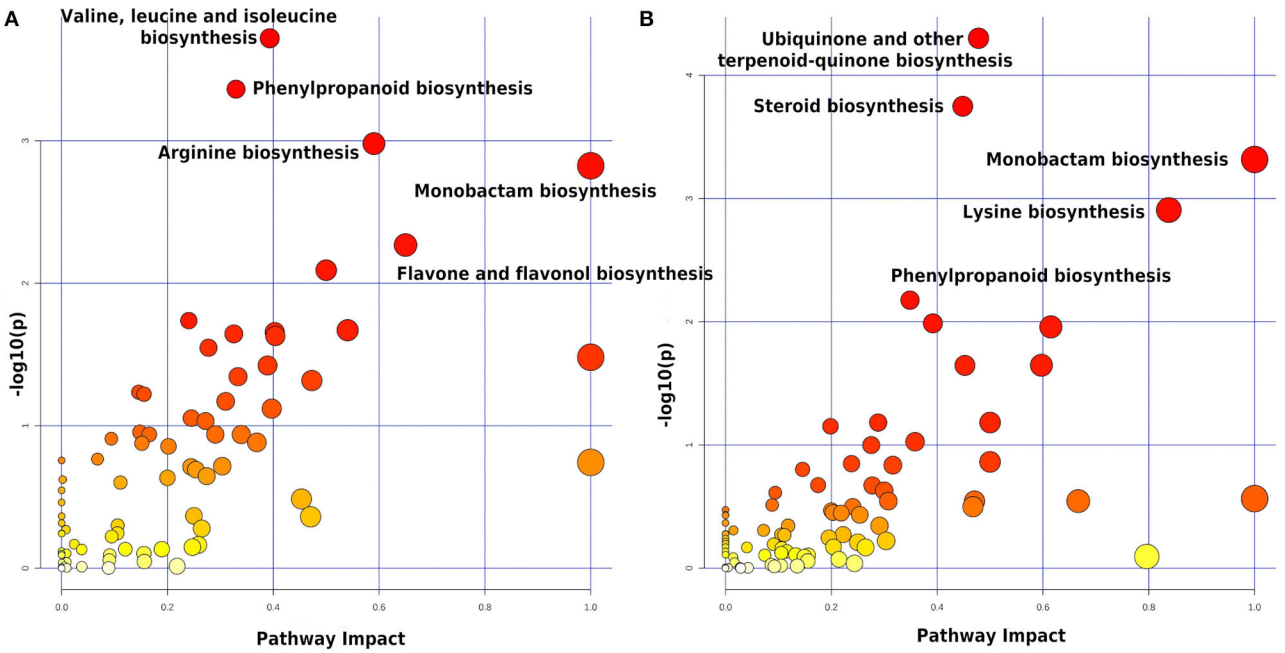


**FIGURE 3 |** Summary of the pathway analysis of the data from leaves—STS **(A)** and LTS2 **(B)**—using the Pathway Topology Analysis modules of MetaboAnalyst 5.0. The metabolome view resulted from the analysis in the Pathway Topology Analysis module using the Hypergeometric test, the relative betweenness centrality node importance measure, and the latest KEGG version of the *A. thaliana* pathway library. STS, Short-term stress (the control and the stressed plants at 2 DAT); LTS2, Long-term stress 2 (the stressed plants at 2 and 55 DAT). Pathway impact takes into account both node centrality parameters—betweenness centrality and degree centrality—and represents the importance of annotated compounds in a specific pathway.

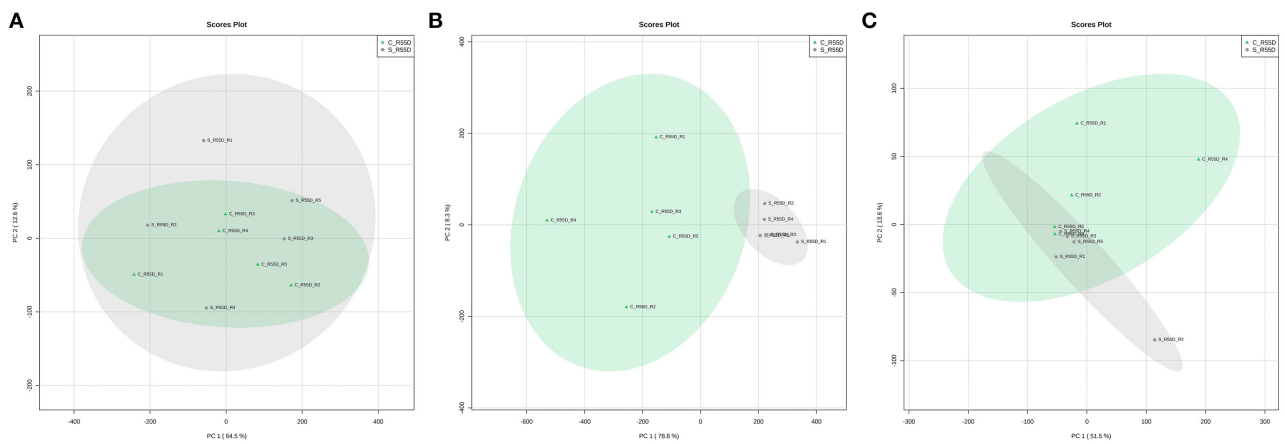


**FIGURE 4 |** PCA score plots comparing roots samples from control and stressed plants at 55 DAT—LTS1 (Long-term stress 1). Polar positive **(A)**, polar negative **(B)**, and lipidic positive **(C)** fractions.

arginine and proline metabolism; C5-branched dibasic acid metabolism; and biosynthesis of secondary metabolites—other antibiotics. These pathways came out with 6, 5, 9, 5, 6, 4, 5, 2, and 2 differentially expressed metabolites with the highest level of significance within the set of matched metabolites submitted to analysis, respectively (data not shown).

All 160 peaks differentially expressed in the LTS1 were submitted to functional interpretation *via* analysis in the MS Peaks to Pathway module, with a *p*-value cutoff of 1.0E-5. After applying the initial criteria of metabolite selection, 39 DEPs with a hit to just one known compound were submitted to the pathway topology analysis module, resulting in seven pathways with a raw $p \leq 0.05$; they were: glyoxylate and dicarboxylate metabolism; biosynthesis of secondary metabolites—other antibiotics; beta-alanine metabolism; citrate cycle (TCA cycle); monobactam biosynthesis; alanine, aspartate, and glutamate metabolism; and

pantothenate and CoA biosynthesis. These pathways came out with 5, 2, 3, 3, 2, 3, and 3 differentially expressed metabolites with the highest level of significance within the set of matched metabolites submitted to analysis, respectively (data not shown).

At last, all 3,055 peaks differentially expressed in the LTS2 were submitted to functional interpretation *via* analysis in the MS Peaks to Pathway module, with a *p*-value cutoff of 1.0E-5. After applying the initial criteria of metabolite selection, 262 DEPs with a hit to just one known compound were submitted to the pathway topology analysis module, resulting in 10 pathways with a raw $p \leq 0.05$; they were: steroid biosynthesis; lysine biosynthesis; carotenoid biosynthesis; valine, leucine, and isoleucine biosynthesis; ubiquinone and other terpenoid-quinone biosynthesis; monobactam biosynthesis; arginine biosynthesis; phenylpropanoid biosynthesis; porphyrin and chlorophyll metabolism; and glyoxylate and dicarboxylate metabolism. These pathways came out with 20, 7, 16, 10, 14, 5, 8, 15, 14, and 9 differentially expressed metabolites with the highest level of significance within the set of matched metabolites submitted to analysis, respectively (data not shown).

## Salt Effect in Metabolites Differentially Expressed Contributing to the Adaptation Response

As the goal of this study was to look for metabolites whose behavior could give insights into the salt resistance mechanisms behind the adaptation response, both in the leaves and the roots, a series of filters were applied to select peaks differentially expressed before undergoing analysis in the MS Peaks to Pathway module of the MetaboAnalyst 5.0.

First, the 5,354 peaks in the leaf samples common to the AE, STS, and LTS2 scenarios were selected. After that, the combined effect of the salt in the short and long-term stress—denominated LTS_Final—was calculated using the following equation: FC_LTS_Final = (FC_STS * FC_LTS2 * (1/FC_AE)); the log2(FC_LTS_Final) was then subsequently calculated. After removing those peaks non-differentially expressed in the AE and the LTS_Final scenarios, the remaining 4,126 ones underwent analysis in the MS Peaks to Pathway module. A total of 353 differentially expressed peaks with a single matched compound were submitted to the Pathway Topology Analysis module (**Supplementary Table 2**), resulting in 12 pathways with a raw $p \leq 0.05$; they were: ubiquinone and other terpenoid-quinone biosynthesis; phenylpropanoid biosynthesis; arginine biosynthesis; lysine biosynthesis; monobactam biosynthesis; steroid biosynthesis; flavone and flavonol biosynthesis; tyrosine metabolism; valine, leucine, and isoleucine biosynthesis; porphyrin and chlorophyll metabolism; indole alkaloid biosynthesis; and pyruvate metabolism. These pathways came out with 19, 21, 11, 7, 6, 19, 6, 8, 10, 17, 3, and 9 differentially expressed metabolites with the highest level of significance within the set of matched metabolites submitted to analysis, respectively (data not shown).

At last, there were 4,954 peaks in the root samples that were common to the AE, STS, and LTS2 scenarios. After submitting them to the same treatment mentioned above, a group of 3,557 peaks was left for analysis in the MS Peaks to Pathway module. A total of 309 differentially expressed peaks with a single matched compound were submitted to the Pathway Topology Analysis module (**Supplementary Table 2**), resulting in 11 pathways with a raw $p \leq 0.05$; they were: steroid biosynthesis; lysine biosynthesis; monobactam biosynthesis; ubiquinone and other terpenoid-quinone biosynthesis; arginine biosynthesis; valine, leucine, and isoleucine biosynthesis; carotenoid biosynthesis; phenylpropanoid biosynthesis; alanine, aspartate, and glutamate metabolism; porphyrin and chlorophyll metabolism; and tyrosine metabolism. These pathways came out with 20, 7, 6, 16, 9, 10, 16, 16, 9, 16, and 7 differentially expressed metabolites with the highest level of significance within the set of matched metabolites submitted to analysis, respectively (data not shown).

# DISCUSSION

One of the manners by which salt affects plants is through the osmotic effect. Salt reduces the osmotic potential and, consequently, diminishes the soil water potential, making it difficult for plants to absorb water (Sánchez-Blanco et al., 2004; Franco et al., 2011; Hanin et al., 2016). Under such conditions, there is a reduction in the stomatal opening (Acosta-Motos et al., 2017). As a result, the plants transpire less, and therefore less water is lost by evaporation, as occurred with the salt-stressed gliricidia plants. However, irrespective of salt stress, weather variables, such as radiation, temperature, and relative humidity, continue to exert their effects on evapotranspiration. For this, the shape of both evapotranspiration curves, stressed or unstressed by salt, was the same (**Figure 1**).

The gliricidia control plants exerted their maximum transpiration capacity, as there was no obstacle in the soil limiting water availability. They had full foliage and high rates of evapotranspiration (**Figures 1A**, **2A**). In the salt-stressed gliricidia plants, the osmotic shock caused by the abrupt addition of salt to the substrate led to severe defoliation (**Figure 2B**). This fact is a drastic artifice used by plants to reduce the transpiring surface and maintain water status (Alarcón et al., 2006), although it could also be a mechanism of salt exclusion (Acosta-Motos et al., 2017). The fact is that, after metabolic adjustment to that stressful situation, gliricidia plants developed new leaves and continue their development (**Figures 2C,D**).

The availability of exchangeable Na in the substrate represented 36% of the base saturation and was at least six times higher than K in the salt-stressed treatments. Even under these conditions, the gliricidia plants only absorbed a tiny part of the Na, while they absorbed Mg, Ca, and K just like the control ones (**Supplementary Table 1**), which suggests that it limited the entry of Na by the roots (Hanin et al., 2016) and maintain the nutritional balance. Therefore, it is a typical salt-excluding plant (Acosta-Motos et al., 2017).

The heatmaps generated out of the metabolome from the roots of young gliricidia plants submitted to salinity stress, using the all treatments datasets, revealed much closer proximity between treatments within the short-term scenario, as well as within the long-term one, but only for the polar positive and

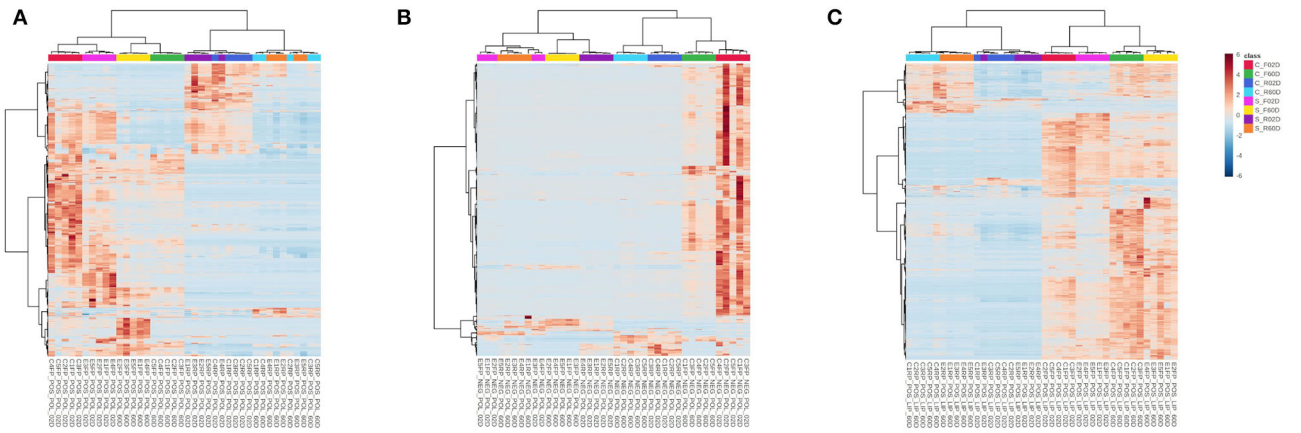


**FIGURE 5 |** Heatmap analysis of the all treatments data sets (control and stressed plants at 2 and 55 DAT). Blue color indicates low intensity and red color indicates high intensity. The upper row represents sample groups (C—Control, S—Stressed, F—Leaves, and R—Roots). Polar positive **(A)**, polar negative **(B)**, and lipidic positive **(C)** fractions.

lipidic positive fractions evaluated (**Figure 5**). The hierarchical clustering heatmaps were generated in MetaboAnalyst 5.0 using normalized data as data source, autoscale features as standardization, Pearson as distance measure, and Ward as a clustering method. To a certain extent, the same was true for the metabolome from the leaves (**Figure 5**). That led us to postulate that, once adapted to high salinity stress, most likely *via* a salt-excluding mechanism that limited the entry of Na in the roots, gliricidia plants resumed growth and went back to have almost the same metabolome profile as the control plants at the end of the experiment.

In the leaves, the phenylpropanoid biosynthesis pathway always appeared as one of the most affected pathways, independent of the strategy used to analyze the different data sets, with 21 metabolites differently expressed. When further evaluating the changes experienced by these metabolites in short-term and long-term stress, we found that 14 did downregulate and seven upregulate at 55 DAT in the stressed plants, in comparison with the control plants also at 55 DAT. Besides that, 12 were downregulated in the short-term but not long-term, two differentially regulated at short-term and long-term, and seven differentially regulated only at long-term (**Table 2**).

Taken together, the results that are shown in this study corroborate the previous work done by Carvalho da Silva et al. (2021), who showed that this pathway is highly affected in the leaves of young gliricidia plants by salt stress, but also that most of the salt effect occurs in the short-term. However, it goes forward and shows that most of those changes remained in the long-term, and also that some metabolites change in expression only during the process of adaptation to high salinity experienced by these plants. In summary, this pathway plays a role in the response of young gliricidia plants to high salinity throughout the entire adaptation response, starting in the short term and continuing in the long one.

Zhu et al. (2021) also applied an integrated transcriptomic and metabolomic analysis to show that the Phenylpropanoid biosynthesis pathway had genes and metabolites that show a significant correlation in the roots of salt-stressed *Sophora alopecuroides*, which is a leguminous perennial herb that is an excellent sand-fixing pioneer plant distributed mainly in the desert and semi-desert areas of Northwest China.

Phenylpropanoids, a class of secondary metabolites showing indispensable roles in plant survival, are synthesized from phenylalanine (or tyrosine) through a series of enzymatic reactions (Deng and Lu, 2017). Their biosynthesis includes a collection of the first two or three steps of the phenylpropanoid pathway, which redirects carbon flow from primary metabolism to phenylpropanoid metabolism; and after the generation of intermediates in the initial steps, the carbon flow is channeled into specific branch pathways to produce flavonoids, stilbenes, monolignols, phenolic acids, and coumarins (Deng and Lu, 2017).

In the present study, L-Phenylalanine (C00079) is one of the three metabolites from this pathway that only differentiated in the long-term stress, experiencing an increase of 3.56X in its peak intensity due exclusively to the salt effect. The other two differentiated metabolites were Sinapic acid (C00482) and N1,N5,N10-Tricaffeoyl spermidine (C18070), which experienced a decrease of 96 and 54%, respectively, also due exclusively to the salt effect.

Ferulic acid (C01494) and Coniferyl aldehyde (C02666) were the two metabolites that experienced the most increase in expression level in the long-term—due exclusively to the salt effect—among those 21 metabolites differentially expressed in this pathway, experiencing 9.11X and 20.45X increase in intensity, respectively (**Figure 6**). Ferulic acid belongs to the hydroxycinnamic acid group, which is one of the two major subgroups of phenolic acids, likely produced by the oxidation of coniferaldehyde under the catalysis by coniferyl-aldehyde dehydrogenase. Many steps of the phenolic acid pathway are unknown, and it is still

**TABLE 2 |** Differentially expressed peaks and features from the phenylpropanoid biosynthesis pathway (leaves), steroid biosynthesis (roots), and lysine biosynthesis (roots), in gliricidia plants submitted to salinity stress in three distinct scenarios: age effect—AE (control plants at 2 and 55 days under salinity stress—DAT), short-term stress—STS (control and the stress plants at 2 DAT); and long-term stress 2—LTS2 (stressed plants at 2 and 55 DAT).

| Pathway/ organ | m.z | Mode | Matched. Compound | Matched. Form | Mass. Diff | Fold_ Change_ AE | Log2(FC)_ AE | Profile_ AE | Fold_ Change_ STS | Log2(FC)_ STS | Profile_ STS | Fold_ Change_ LTS2 | Log2(FC)_ LTS2 | Profile_ LTS2 | Fold_ Change_ LTS_ Final | Log2(FC)_ LTS_ Final | Profile_ LTS_ Final |
|---|---|---|---|---|---|---|---|---|---|---|---|---|---|---|---|---|---|
| Phenylpropanoid biosynthesis/leaf | 163.0399 | Negative | C05608 | M-H+O[-] | 1.50E-04 | 0.32 | −1.63 | Down | 0.02 | −5.72 | Down | 1.00 | 0.00 | Non-DE | 0.06 | −4.08 | Down |
| | 165.0558 | Negative | C12206 | M-H[-] | 3.44E-05 | 0.15 | −2.75 | Down | 0.03 | −4.92 | Down | 1.00 | 0.00 | Non-DE | 0.22 | −2.18 | Down |
| | 179.0350 | Negative | C10945 | M-H+O[-] | 2.75E-05 | 0.15 | −2.71 | Down | 0.02 | −5.72 | Down | 1.00 | 0.00 | Non-DE | 0.12 | −3.01 | Down |
| | 223.0611 | Negative | C05610 | M-H+O[-] | 9.97E-05 | 0.24 | −2.06 | Down | 0.08 | −3.74 | Down | 1.00 | 0.00 | Non-DE | 0.31 | −1.67 | Down |
| | 250.0721 | Negative | C05619 | M+ACN-H[-] | 8.96E-06 | 0.03 | −5.24 | Down | 0.01 | −6.51 | Down | 1.00 | 0.00 | Non-DE | 0.42 | −1.27 | Down |
| | 309.0965 | Positive | C10434 | M-CO+H[1+] | 2.82E-04 | 0.52 | −0.94 | Down | 0.32 | −1.66 | Down | 1.00 | 0.00 | Non-DE | 0.61 | −0.72 | Down |
| | 338.0965 | Negative | C12208 | M(C13)-H[-] | 2.10E-04 | 0.08 | −3.63 | Down | 0.01 | −6.97 | Down | 1.00 | 0.00 | Non-DE | 0.10 | −3.33 | Down |
| | 341.0878 | Negative | C05839 | M-H+O[-] | 4.68E-05 | 0.05 | −4.25 | Down | 0.02 | −5.72 | Down | 1.00 | 0.00 | Non-DE | 0.36 | −1.46 | Down |
| | 401.1457 | Negative | C00761 | M+CH3COO[-] | 8.98E-04 | 1.00 | 0.00 | Non-DE | 0.03 | −5.16 | Down | 1.00 | 0.00 | Non-DE | 0.03 | −5.16 | Down |
| | 355.0673 | Negative | C02887 | M-H+O[-] | 2.13E-04 | 1.00 | 0.00 | Non-DE | 0.05 | −4.47 | Down | 1.00 | 0.00 | Non-DE | 0.05 | −4.47 | Down |
| | 327.1088 | Negative | C05855 | M-H+O[-] | 3.05E-04 | 0.13 | −2.91 | Down | 0.03 | −5.06 | Down | 2.76 | 1.47 | Up | 0.62 | −0.68 | Down |
| | 85.52103 | Positive | C00423 | M+H+Na[2+] | 1.80E-04 | 0.01 | −6.15 | Down | 1.00 | 0.00 | Non-DE | 0.01 | −6.62 | Down | 0.73 | −0.46 | Down |
| | 632.2630 | Positive | C18070 | M+H[1+] | 2.78E-03 | 1.00 | 0.00 | Non-DE | 1.00 | 0.00 | Non-DE | 0.46 | −1.11 | Down | 0.46 | −1.11 | Down |
| | 293.0632 | Positive | C00482 | M+HCOONa[1+] | 6.87E-05 | 1.00 | 0.00 | Non-DE | 1.00 | 0.00 | Non-DE | 0.04 | −4.48 | Down | 0.04 | −4.48 | Down |
| | 105.0697 | Positive | C00903 | M-CO+H[1+] | 1.34E-04 | 0.02 | −5.87 | Down | 0.03 | −5.32 | Down | 1.00 | 0.00 | Non-DE | 1.46 | 0.55 | Up |
| | 455.1160 | Positive | C01175 | M+HCOONa[1+] | 3.74E-05 | 0.10 | −3.26 | Down | 0.35 | −1.52 | Down | 1.00 | 0.00 | Non-DE | 3.32 | 1.73 | Up |
| | 108.0387 | Positive | C02947 | M(C13)+3H[3+] | 5.14E-04 | 0.31 | −1.71 | Down | 2.20 | 1.14 | Up | 0.31 | −1.70 | Down | 2.22 | 1.15 | Up |
| | 107.0488 | Positive | C02666 | M-C3H4O2+H[1+] | 3.25E-04 | 0.22 | −2.15 | Down | 1.00 | 0.00 | Non-DE | 4.60 | 2.20 | Up | 20.45 | 4.35 | Up |
| | 167.0701 | Positive | C01494 | M-CO+H[1+] | 1.29E-04 | 0.58 | −0.79 | Down | 1.00 | 0.00 | Non-DE | 5.26 | 2.39 | Up | 9.11 | 3.19 | Up |
| | 333.1531 | Positive | C00933 | M+Na[1+] | 1.63E-03 | 0.60 | −0.74 | Down | 1.00 | 0.00 | Non-DE | 0.63 | −0.66 | Down | 1.05 | 0.08 | Up |
| | 180.0664 | Negative | C00079 | M-H+O[-] | 2.50E-04 | 1.00 | 0.00 | Non-DE | 1.00 | 0.00 | Non-DE | 3.56 | 1.83 | Up | 3.56 | 1.83 | Up |
| Steroid biosynthesis/roots | 361.3266 | Positive | C15780 | M-H4O2+H[1+] | 1.28E-03 | 0.15 | −2.71 | Down | 1.00 | 0.00 | Non-DE | 0.18 | −2.44 | Down | 1.20 | 0.27 | Up |
| | 435.3599 | Positive | C15782 | M+Na[1+] | 1.42E-04 | 1.00 | 0.00 | Non-DE | 1.00 | 0.00 | Non-DE | 1.42 | 0.50 | Up | 1.42 | 0.50 | Up |
| | 397.3826 | Positive | C22121 | M-CO+H[1+] | 1.42E-04 | 1.00 | 0.00 | Non-DE | 1.00 | 0.00 | Non-DE | 1.95 | 0.97 | Up | 1.95 | 0.97 | Up |
| | 415.3940 | Positive | C01753 | M+H[1+] | 5.60E-04 | 5.83 | 2.54 | Up | 1.00 | 0.00 | Non-DE | 7.92 | 2.99 | Up | 1.36 | 0.44 | Up |
| | 449.3752 | Positive | C01054 | M+Na[1+] | 2.19E-04 | 2.24 | 1.16 | Up | 1.00 | 0.00 | Non-DE | 3.81 | 1.93 | Up | 1.70 | 0.77 | Up |
| | 441.4077 | Positive | C08830 | M+H[1+] | 1.35E-03 | 5.67 | 2.50 | Up | 1.00 | 0.00 | Non-DE | 9.43 | 3.24 | Up | 1.66 | 0.73 | Up |
| | 437.3754 | Positive | C15915 | M+Na[1+] | 6.85E-05 | 2.07 | 1.05 | Up | 1.00 | 0.00 | Non-DE | 2.08 | 1.05 | Up | 1.00 | 0.01 | Up |
| | 397.3830 | Positive | C01943 | M-HCOOH+H[1+] | 6.38E-05 | 3.64 | 1.86 | Up | 1.00 | 0.00 | Non-DE | 3.65 | 1.87 | Up | 1.00 | 0.01 | Up |
| | 465.3501 | Positive | C11523 | M+K[1+] | 1.11E-03 | 2.14 | 1.10 | Up | 1.00 | 0.00 | Non-DE | 2.21 | 1.14 | Up | 1.03 | 0.04 | Up |
| | 457.3674 | Positive | C22120 | M+H[1+] | 1.36E-04 | 3.96 | 1.99 | Up | 1.00 | 0.00 | Non-DE | 1.00 | 0.00 | Non-DE | 3.96 | 1.99 | Up |
| | 369.3516 | Positive | C01189 | M-H2O+H[1+] | 2.37E-05 | 1.00 | 0.00 | Non-DE | 1.00 | 0.00 | Non-DE | 4.14 | 2.05 | Up | 4.14 | 2.05 | Up |
| | 479.3861 | Positive | C00751 | M+HCOONa[1+] | 1.35E-04 | 5.13 | 2.36 | Up | 1.00 | 0.00 | Non-DE | 7.59 | 2.92 | Up | 1.48 | 0.56 | Up |
| | 489.3937 | Positive | C22116 | M+H2O+H[1+] | 1.72E-04 | 6.64 | 2.73 | Up | 1.00 | 0.00 | Non-DE | 5.29 | 2.40 | Up | 0.80 | −0.33 | Down |
| | 383.3671 | Positive | C11508 | M-CO+H[1+] | 5.36E-05 | 3.21 | 1.68 | Up | 1.00 | 0.00 | Non-DE | 2.99 | 1.58 | Up | 0.93 | −0.10 | Down |
| | 429.3728 | Positive | C22123 | M+H2O+H[1+] | 1.05E-05 | 3.00 | 1.58 | Up | 1.00 | 0.00 | Non-DE | 1.79 | 0.84 | Up | 0.60 | −0.74 | Down |
| | 445.3477 | Positive | C22119 | M(S34)+H[1+] | 7.31E-05 | 6.47 | 2.69 | Up | 1.00 | 0.00 | Non-DE | 3.53 | 1.82 | Up | 0.55 | −0.87 | Down |
| | 384.1425 | Positive | C00448 | M(C13)+H[1+] | 7.79E-04 | 0.61 | −0.72 | Down | 1.00 | 0.00 | Non-DE | 0.58 | −0.79 | Down | 0.95 | −0.07 | Down |
| | 443.3052 | Positive | C05437 | M+NaCl[1+] | 1.03E-04 | 44.02 | 5.46 | Up | 1.00 | 0.00 | Non-DE | 30.00 | 4.91 | Up | 0.68 | −0.55 | Down |
| | 400.3654 | Positive | C15777 | M(C13)+H[1+] | 1.86E-04 | 3.63 | 1.86 | Up | 1.00 | 0.00 | Non-DE | 3.12 | 1.64 | Up | 0.86 | −0.22 | Down |
| | 541.3193 | Positive | C03428 | M-HCOOH+H[1+] | 1.45E-03 | 27.03 | 4.76 | Up | 1.00 | 0.00 | Non-DE | 14.04 | 3.81 | Up | 0.52 | −0.95 | Down |

*(Continued)*

**TABLE 2** | Continued

| Pathway/ organ | m.z | Mode | Matched. Compound | Matched. Form | Mass. Diff | Fold_ Change_ AE | Log2(FC)_ AE | Profile_ AE | Fold_ Change_ STS | Log2(FC)_ STS | Profile_ STS | Fold_ Change_ LTS2 | Log2(FC)_ LTS2 | Profile_ LTS2 | Fold_ Change_ LTS_ Final | Log2(FC)_ LTS_ Final | Profile_ LTS_ Final |
|---|---|---|---|---|---|---|---|---|---|---|---|---|---|---|---|---|---|
| Lysine biosynthesis/roots | 88.0394 | Positive | C00049 | M-HCOOH+H[1+] | 5.11E-05 | 0.44 | −1.18 | Down | 1.00 | 0.00 | Non-DE | 0.46 | −1.12 | Down | 1.04 | 0.06 | Up |
| | 130.0497 | Positive | C03082 | M-HCOOK+H[1+] | 8.97E-05 | 0.46 | −1.11 | Down | 1.00 | 0.00 | Non-DE | 0.56 | −0.83 | Down | 1.21 | 0.28 | Up |
| | 256.0424 | Positive | C20258 | M+HCOONa[1+] | 3.00E-04 | 0.01 | −6.17 | Down | 1.00 | 0.00 | Non-DE | 0.16 | −2.65 | Down | 11.47 | 3.52 | Up |
| | 100.0393 | Positive | C00441 | M-H2O+H[1+] | 6.94E-06 | 0.36 | −1.49 | Down | 1.00 | 0.00 | Non-DE | 0.29 | −1.81 | Down | 0.80 | −0.32 | Down |
| | 144.0652 | Positive | C03972 | M-CO+H[1+] | 1.85E-04 | 0.16 | −2.61 | Down | 1.00 | 0.00 | Non-DE | 0.08 | −3.57 | Down | 0.51 | −0.96 | Down |
| | 191.1023 | Positive | C00666 | M+H[1+] | 3.22E-04 | 0.13 | −2.92 | Down | 1.00 | 0.00 | Non-DE | 0.01 | −7.02 | Down | 0.06 | −4.10 | Down |
| | 106.0384 | Positive | C00680 | M+H+Na[2+] | 3.20E-04 | 0.35 | −1.51 | Down | 1.00 | 0.00 | Non-DE | 0.29 | −1.81 | Down | 0.81 | −0.30 | Down |

*The differentially expressed peaks are those with an adjusted P-value (FDR) ≤ 0.05, of the Welch t-test; and $Log_2$ (Fold Change) ≠ 1. LTS_Final, Effect of salt stress in the long-term discounted the age effect; Down, Downregulated; Up, Upregulated; Non-DE, Non-Differentially Expressed. If False Discovery Rate (FDR) ≤ 0.05, then Profile was called Non-DE, and FC (Fold Change) became 1.0.*

*Down, Downregulated; Up, Upregulated; Non-DE, Non-Differentially Expressed. If False Discovery Rate (FDR) ≤ 0.05, then Profile = Non-De, and FC = 1. Scenarios: age effect—AE (samples from the control plants at 2 and 55 days after treatment—DAT); short-term stress—STS (the control and the stressed plants at 2 DAT); long-term stress 1—LTS1 (the control and the stressed plants at 55 DAT); long-term stress 2—LTS2 (the stressed plants at 2 and 55 DAT); and LTS_Final = Effect of salt stress in the long-term discounted the age effect.*

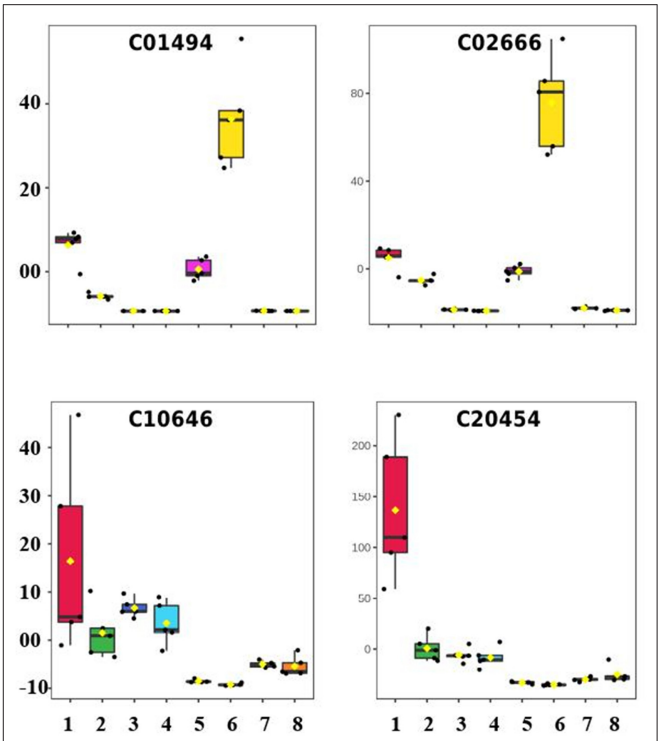


**FIGURE 6 |** Box plot showing the normalized concentration of metabolites in the leaves and roots of young gliricidia plants submitted to salt stress. (The expression profiles of Ferulic acid (C01494), Coniferyl aldehyde (C02666) (+)-Lariciresinol (C10646), and (–)-Lariciresinol (C20454) in the following treatments: 1—C_L02D, 2—C_L55D, 3—C_R02D, 4—C_R55D, 5—S_L02D, 6—S_L55D, 7—S_R02D, 8—S_R55D, where C—Control, S—Stressed, F—Leaves, R—Roots, 02D—short-term stress, and 60D—long-term stress).

under revision (Deng and Lu, 2017). Recently, Linić et al. (2021) showed that exogenous application of a 10.0 μM solution of ferulic acid attenuated effects on salt-stressed Chinese cabbage plants, causing a decrease in proline and salicylic acid.

Besides ferulic acid and coniferyl aldehyde, three other metabolites upregulated at 55 DAT in the stressed plants, in comparison with the control plants also at 55 DAT; they were: 1-O-Sinapoyl-beta-D-glucose (C01175), Cinnamaldehyde (C00903), and 4-Coumaroylshikimate (C02947), which experienced an increase of 3.32X, 1.46X, and 2.22X, respectively (data not shown). According to Chun et al. (2019), enzymes, such as phenylalanine ammonia-lyase (PAL), cinnamoyl CoA reductase (EC 1.2.1.44), ferulate 5-hydroxylase (F5H), caffeate 3-O-methyltransferase (EC 2.1.1.68), and cinnamyl alcohol dehydrogenase (EC 1.1.1.195)—to mention a few—take part in the synthesis of monolignols. Peroxidases and laccases polymerize monolignols to yield lignin as a final product. L-Phenylalanine, Ferulic acid, Coniferyl aldehyde, and Cinnamaldehyde, which the expression level increased due to the salt effect in this present study, are directly linked to these five enzymes.

When silencing the *CcoAOMT1* gene in *A. thaliana* and demonstrating that the mutants became phenotypically hypersensitive to salt stress, Chu and colleagues provided molecular and genetic evidence indicating the importance of enhanced lignin accumulation in the cell wall of this plant species during the responses to salt stress (Chun et al., 2019). The lignin accumulation and the strong expression of lignin biosynthetic genes are factors key to acquiring salt tolerance in plants, and, based on the results from our present study, we postulate that this phenomenon is playing a role in the adaptation of young gliricidia plants to high levels of salt stress. Additional studies are necessary to investigate this hypothesis.

Only 3.4% of the peaks show differential expression in the LTS1 scenario, in contrast to the AE (51.7%) and LTS2 (60.1%) ones, in the roots of gliricidia plants. The principal component analysis (PCA) did not completely separate the control and stressed samples in the polar positive and the lipidic positive fraction (**Figure 4**), and all 160 differentially expressed peaks in the subsequent analysis came from the negative one. Together, these results show that the young gliricidia plants did experience a metabolic adjustment that led their metabolic status in the roots to pretty much the same one of the control plants and that this adjustment most likely took place after the loss of the leaves.

Only 39 DEPs with a hit to just one known compound were found in LTS1 and submitted to the pathway topology analysis module, resulting in seven pathways with a raw $p \leq 0.05$. However, only the biosynthesis of secondary metabolites—other antibiotics one suffered the utmost impact seen, with two lignans downregulated in the short-term and kept at a low level in the long-term stress (+)-Lariciresinol (C10646), and (–)-Lariciresinol (C20454) (**Figure 6**). This finding opposes Xiao et al. (2020), who showed that the upregulation of lariciresinol biosynthesis in *Isatis indigotica*, particularly in tetraploids compared to diploids, improved root development, and enhanced salt and drought stress tolerance.

In the roots, the steroid biosynthesis is the most affected pathway in the long-term stress, with 20 differently expressed metabolites. Fourteen of them are from the phytosterol biosynthesis module (M00917—squalene 2,3-epoxide => campesterol/sitosterol). When evaluating the changes experienced by these 20 metabolites in the short-term and long-term stress, none of them expressed differentially at 02 DAT (**Table 2**). Lathosterol (C01189) had the utmost change in the expression level due exclusively to salt stress, with a 4.14X increase after the short-term. Cycloeucalenone (C22121), with 1.95X increase, and Squalene 2,3-epoxide (C01054) and 24-Methylidenecycloartanol (C08830), both with approximately 1.7X.

Over 250 different plant sterols are known, among which campesterol, sitosterol, and stigmasterol are the most abundant ones in most plants (Moreau et al., 2018). An overall summary of the enzymes involved in the biosynthesis of phytosterols is lacking, and very little research on the metabolism and regulation of phytosterols biosynthesis has been reported (Zhang et al., 2020). According to Zhang et al. (2020), sterol profiles vary greatly among plant species and seem to be accumulated more in plants with higher tolerance to salinity; these changes of phytosterols accumulation can indicate plant adaptability to stresses to a certain extent. Phytosterols may help plants adapt to environmental stresses by adjusting membrane structure and characteristics, including the recruitment of specific proteins attached to the plasma membrane to transduce signals (Zhang et al., 2020). Maintenance of membrane homeostasis represents one of the principal functions of sterols in plant cells (Rogowska and Szakiel, 2020), and phytosterols and their corresponding esters have a pivotal role in imparting tolerance to abiotic stresses by maintaining cell membrane integrity (Kumar et al., 2018).

In the roots of salt-stressed gliricidia plants, the Lysine biosynthesis appeared as the second most affected pathway in the long-term, with seven metabolites expressed differently; being all of them from the DAP aminotransferase pathway module (Hudson et al., 2006). When further evaluating the changes experienced by these seven metabolites in the short-term and long-term stress, four of them were downregulated (C00441, C00666, C00680, and C03972) and three upregulated (C00049, C03082, and C20258) in the long-term, due exclusively to salt stress. None of them expressed differentially at 02 DAT, short-term (**Table 2**).

In higher plants, the synthesis of Lysine (Lys) occurs in plastids *via* the diaminopimelate (DAP) pathway, and no evidence exists for its cytosolic synthesis (Hudson et al., 2006; Kishor et al., 2020). When accumulated in high concentrations, Lys may be toxic to the plants and must then undergo degradation *via* the cadaverine, the saccharopine, or the NHP pathway (Arruda and Barreto, 2020; Kishor et al., 2020). In the present study, Lys was not among the metabolites expressed differentially in the roots of gliricidia plants due to salt stress; so, it is not possible to say whether these plants are experiencing energy limitations or not. However, as six metabolites (C00026, C00042, C00164, C00408, C00449, and C04076) from the Lys degradation pathways were found in the roots of gliricidia plants after 55 days under stress, and all of them at levels similar to the ones in the control plants (data not shown), one can postulate that Lys degradation did not play a role in promoting the adaptation response.

The (2S,4S)-4-Hydroxy-2,3,4,5-tetrahydrodipicolinate—HTPA (C20258) metabolite experienced, by far, the utmost increase (11.47X) in expression level in the long-term after removing the age effect; and the LL-2,6-Diaminopimelic acid (C00666) the utmost decrease (94%). Since HTPA expression upregulates due to salt stress, one can infer that the protein expressed by a putative homolog of the *dapA* gene in *G. sepium* is Lys-insensitive or that the amount of Lys is not enough to trigger a feedback inhibition (Galili et al., 2001). The 4-hydroxy-tetrahydrodipicolinate synthase (EC 4.3.3.7), which catalyzes the production of HTPA, is coded by the *dapA* gene (Soares da Costa et al., 2021).

## CONCLUSION

In the salt-stressed gliricidia plants, the osmotic shock caused by the abrupt addition of salt to the substrate led to severe defoliation. After a metabolic adjustment to that stressful

situation, those plants released new leaves and continued their development. These salt-adapted gliricidia plants only absorbed a tiny part of the Na present in the substrate while absorbing Mg, Ca, and K just like the control ones. The limited entry of Na and the maintenance of the nutritional balance in the roots, plus the fact that the roots metabolome profiles of the control and adapted plants were very similar, led us to postulate that these plants are salt-excluding plants that are adapted to high salinity stress *via* two salt-excluding mechanisms, starting in the canopy—severe defoliation—and concluding in the roots—limited entry of Na.

This present study not only corroborates our previous study that indicated that the phenylpropanoid biosynthesis pathway has a role in the response of gliricidia plants to a very high level of salinity (Carvalho da Silva et al., 2021) but went forward and also showed that most of the changes experienced by this pathway in the leaves during the short-term stress, remained in the long-term. However, some metabolites from this pathway play a role only in the long-term response to this stress. In summary, this pathway plays a role throughout the entire adaptation process, starting in the short term and continuing in the long.

Based on the results from our present study—from leaves and roots—we can also postulate that the accumulation of lignin and some phytosterols, as well as lysine biosynthesis—but not degradation, play a role in promoting the adaptation response of gliricidia plants to a very high level of salinity. However, additional studies are necessary to investigate this hypothesis.

## DATA AVAILABILITY STATEMENT

The data-sets used and/or analyzed during the current study are available from the corresponding author on reasonable request.

## AUTHOR CONTRIBUTIONS

PA, CS, and MS designed the study. ÍB, TC, VB, JRo, and JRi performed the experiments and generated the data. ÍB and MS wrote first draft of the manuscript, which was extensively edited and approved the submitted version by all authors. MS was responsible for the funding acquisition, project administration, and group supervision. All authors contributed to the article and approved the submitted version.

## FUNDING

The grant (01.13.0315.00—DendePalm Project) for this study was awarded by the Brazilian Ministry of Science, Technology, and Innovation (MCTI) *via* the Brazilian Research and Innovation Agency (FINEP). The authors confirm that the funder had no influence over the study design, the content of the article, or the selection of this journal.

## ACKNOWLEDGMENTS

The authors acknowledge funding to ÍB by the Foundation for Research Support of the State of Minas Gerais (FAPEMIG), to VB, TC, and JRo by the Coordination for the Improvement of Higher Education Personnel (CAPES), *via* the Graduate Program in Plant Biotechnology at the Federal University of Lavras (UFLA) and the Graduate Program in Chemistry at the Federal University of Goiás (UFG).

## SUPPLEMENTARY MATERIAL

The Supplementary Material for this article can be found online at: https://www.frontiersin.org/articles/10.3389/fpls.2022.869105/full#supplementary-material

**Supplementary Figure 1 |** PLS-DA permutation validation evaluated by group separation distance, applying permutation number = 2,000. From the all treatments leaves **(A,C,E)** and roots **(B,D,F)** data sets (control and stressed plants at 2 and 55 DAT). Polar-positive **(A,B)**, polar-negative **(C,D)**, and lipidic-positive **(E,F)** fractions.

**Supplementary Table 1 |** Physicochemical properties of the substrate and the mineral composition of canopy and roots of gliricidia plants at the end of the experiment, according to the NaCl level (g of NaCl per 100 g of substrate) applied. The values represent an average of five samples, followed by the standard deviation of the mean. The asterisks indicate a significant difference between the two groups (*t*-test or Mann-Whitney test).*$p \leq 0.05$; **$p \leq 0.01$; ***$p \leq 0.001$; ****$p \leq 0.0001$. pH $H_2O$: pH of the soil in water; P, Phosphorus; $Ca^{2+}$, Calcium; $Mg^{2+}$, Magnesium; $K^{+}$, Potassium; $Na^{+}$, Sodium; $Al^{3+}$, Aluminum; CTC, Cation exchange capacity; V, Base saturation; m, Saturation by aluminum; ISNa, Sodium Saturation Index; OM, Organic Matter; B, Boron; Cu, Copper; Fe, Iron; Mn, Manganese; Zn, Zinc; S, Sulfur; N, Nitrogen; and Cl-, Chlorine. ND, Not Determined.

**Supplementary Table 2 |** List of differentially expressed peaks (mass to charge ratio—m/z) resulted from the pathway analysis using the MS Peaks to Pathway module of MetaboAnalyst 5.0, by organ—leaf or roots. Data set showing the m.z, the mode—positive or negative, the KEGG id of the matched compound, matched form, mass difference, fold change—FC, $Log_2$(FC), and profile, in each one of the three scenarios evaluated: age effect—AE (control plants at 2 and 55 days under salinity stress—DAT), short-term stress—STS (control and the stress plants at 2 DAT); and long-term stress 2—LTS2 (stressed plants at 2 and 55 DAT). The differentially expressed peaks are those with an adjusted *P*-value (FDR) $\leq$ 0.05, of the Welch *t*-test; and $Log_2$ (Fold Change) $\neq$ 1. LTS_Final, Effect of salt stress in the long-term discounted the age effect; Down, Downregulated; Up, Upregulated; Non-DE, Non-Differentially Expressed. If False Discovery Rate (FDR) $\leq$ 0.05, then Profile was called Non-DE, and FC (Fold Change) became 1.0.

## REFERENCES

Acosta-Motos, J. R., Ortuño, M. F., Bernal-Vicente, A., Diaz-Vivancos, P., Sanchez-Blanco, M. J., and Hernandez, J. A. (2017). Plant responses to salt stress: adaptive mechanisms. *Agronomy* 7, 18. doi: 10.3390/agronomy7010018

Alarcón, J. J., Morales, M. A., Ferrández, T., and Sánchez-Blanco, M. J. (2006). Effects of water and salt stresses on growth, water relations and gas exchange in *Rosmarinus officinalis*. *J. Hortic. Sci. Biotechnol.* 81, 845–853. doi: 10.1080/14620316.2006.11512148

Arbona, V., Manzi, M., Ollas, C. D., and Gómez-Cadenas, A. (2013). Metabolomics as a tool to investigate abiotic stress tolerance in plants. *Int. J. Mol. Sci.* 14, 4885–4911. doi: 10.3390/ijms14034885

Arruda, P., and Barreto, P. (2020). Lysine catabolism through the saccharopine pathway: enzymes and intermediates involved in plant responses to

abiotic and biotic stress. *Front. Plant Sci.* 11, 587. doi: 10.3389/fpls.2020.00587

Belinato, J. R., Bazioli, J. M., Sussulini, A., Augusto, F., and Fill, T. P. (2019). Metabolômica microbiana: inovações e aplicações. *Química Nova* 42, 546–559. doi: 10.21577/0100-4042.20170324

Brink, B. G., Seidel, A., Kleinbölting, N., Nattkemper, T. W., and Albaum, S. P. (2016). Omics fusion - a platform for integrative analysis of omics data. *J. Integr. Bioinform.* 13, 296. doi: 10.2390/biecoll-jib-2016-296

Bueno, P. C. P., and Lopes, N. P. (2020). Metabolomics to characterize adaptive and signaling responses in legume crops under abiotic stresses. *ACS Omega* 5, 1752–1763. doi: 10.1021/acsomega.9b03668

Carvalho da Silva, T. L., Belo Silva, V. N., Braga, Í. O., Rodrigues Neto, J. C., Leão, A. P., Ribeiro, J., et al. (2021). Integration of metabolomics and transcriptomics data to further characterize Gliricidia sepium (Jacq.) Kunth under high salinity stress. *Plant Geneom.* 15, e20182. doi: 10.1002/tpg2.20182

Chong, J., Wishart, D. S., and Xia, J. (2019). Using metaboanalyst 4.0 for comprehensive and integrative metabolomics data analysis. *Curr. Protocols Bioinformatics* 68, e86. doi: 10.1002/cpbi.86

Chong, J., and Xia, J. (2020). Using metaboanalyst 4.0 for metabolomics data analysis, interpretation, and integration with other omics data. *Methods Mol. Biol.* 2104, 337–360. doi: 10.1007/978-1-0716-0239-3_17

Chun, H. J., Baek, D., Cho, H. M., Lee, S. H., Jin, B. J., Yun, D. J., et al. (2019). Lignin biosynthesis genes play critical roles in the adaptation of arabidopsis plants to high-salt stress. *Plant Signal. Behav.* 14, 1625697. doi: 10.1080/15592324.2019.1625697

D'amelia, L., Dell'Aversana, E., Woodrow, P., Ciarmiello, L. F., and Carillo, P. (2018). "Metabolomics for crop improvement against salinity stress," in *Salinity Responses and Tolerance in Plants, Vol. 2* eds L. Vinay, H. W. Shabir, S. Penna, and P. T. Lam-son (Cham: Springer), 267–287.

Deng, Y., and Lu, S. (2017). Biosynthesis and regulation of phenylpropanoids in plants. *CRC. Crit. Rev. Plant Sci.* 36, 257–290. doi: 10.1080/07352689.2017.1402852

Franco, J. A., Bañón, S., Vicente, M. J., Miralles, J., and Martínez-Sánchez, J. J. (2011). Root development in horticultural plants grown under abiotic stress conditions—a review. *J. Hortic. Sci. Biotechnol.* 86, 543–556. doi: 10.1080/14620316.2011.11512802

Galili, G., Tang, G., Zhu, X., and Gakiere, B. (2001). Lysine catabolism: a stress and development super-regulated metabolic pathway. *Curr. Opin. Plant Biol.* 4, 261–266. doi: 10.1016/S1369-5266(00)00170-9

Gowda, H., Ivanisevic, J., Johnson, C. H., Kurczy, M. E., Benton, H. P., Rinehart, D., et al. (2014). Interactive xcms online: simplifying advanced metabolomic data processing and subsequent statistical analyses. *Anal. Chem.* 86, 6931–6939. doi: 10.1021/ac500734c

Hanin, M., Ebel, C., Ngom, M., Laplaze, L., and Masmoudi, K. (2016). New insights on plant salt tolerance mechanisms and their potential use for breeding. *Front. Plant Sci.* 7, 1787. doi: 10.3389/fpls.2016.01787

Ho, W. W. H., Hill, C. B., Doblin, M. S., Shelden, M. C., van de Meene, A., Rupasinghe, T., et al. (2020). Integrative multi-omics analyses of barley rootzones under salinity stress reveal two distinctive salt tolerance mechanisms. *Plant Commun.* 1, 100031. doi: 10.1016/j.xplc.2020.100031

Hudson, A. O., Singh, B. K., Leustek, T., and Gilvarg, C. (2006). An LL-diaminopimelate aminotransferase defines a novel variant of the lysine biosynthesis pathway in plants. *Plant Physiol.* 140, 292–301. doi: 10.1104/pp.105.072629

Kishor, P., Suravajhala, R., Rajasheker, G., Marka, N., Shridhar, K. K., Dhulala, D., et al. (2020). Lysine, lysine-rich, serine, and serine-rich proteins: link between metabolism, development, and abiotic stress tolerance and the role of ncRNAs in their regulation. *Front. Plant Sci.* 11, 546213. doi: 10.3389/fpls.2020.546213

Kumar, M. S., Mawlong, I., Ali, K., and Tyagi, A. (2018). Regulation of phytosterol biosynthetic pathway during drought stress in rice. *Plant Physiol. Biochem.* 129, 11–20. doi: 10.1016/j.plaphy.2018.05.019

Li, S., Park, Y., Duraisingham, S., Strobel, F. H., Khan, N., Soltow, Q. A., et al. (2013). Predicting network activity from high throughput metabolomics. *PLoS Comput. Biol.* 9, e1003123. doi: 10.1371/journal.pcbi.1003123

Linić, I., Mlinarić, S., Brkljačić, L., Pavlović, I., Smolko, A., and Salopek-Sondi, B. (2021). Ferulic acid and salicylic acid foliar treatments reduce short-term salt stress in chinese cabbage by increasing phenolic compounds accumulation and photosynthetic performance. *Plants* 10, 2346. doi: 10.3390/plants10112346

Moreau, R. A., Nyström, L., Whitaker, B. D., Winkler-Moser, J. K., Baer, D. J., Gebauer, S. K., et al. (2018). Phytosterols and their derivatives: Structural diversity, distribution, metabolism, analysis, and health-promoting uses. *Progress Lipid Res.* 70, 35–61. doi: 10.1016/j.plipres.2018.04.001

Negrão, S., Schmöckel, S. M., and Tester, M. (2017). Evaluating physiological responses of plants to salinity stress. *Ann. Bot.* 119, 1–11. doi: 10.1093/aob/mcw191

Pan, J., Tian, X., Huang, H., and Zhong, N. (2020). Proteomic study of fetal membrane: inflammation-triggered proteolysis of extracellular matrix may present a pathogenic pathway for spontaneous preterm birth. *Front. Physiol.* 11, 800. doi: 10.3389/fphys.2020.00800

Phang, J. M., Liu, W., and Zabirnyk, O. (2010). Proline metabolism and microenvironmental stress. *Annu. Rev. Nutr.* 30, 441–463. doi: 10.1146/annurev.nutr.012809.104638

Rahman, M., Das, A., Saha, S., Uddin, M., and Rahman, M. (2019). Morpho-physiological response of gliricidia sepium to seawater-induced salt stress. *Agriculturists* 17, 66–75. doi: 10.3329/agric.v17i1-2.44697

Rodrigues-Neto, J. C., Correia, M. V., Souto, A. L., Ribeiro, J., Vieira, L. R., Souza, Jr., et al. (2018). Metabolic fingerprinting analysis of oil palm reveals a set of differentially expressed metabolites in fatal yellowing symptomatic and non-symptomatic plants. *Metabolomics* 14, 142. doi: 10.1007/s11306-018-1436-7

Rogowska, A., and Szakiel, A. (2020). The role of sterols in plant response to abiotic stress. *Phytochem. Rev.* 19, 1525–1538. doi: 10.1007/s11101-020-09708-2

Sánchez-Blanco, M. J., Rodríguez, P., Olmos, E., Morales, M. A., and Torrecillas, A. (2004). Differences in the effects of simulated sea aerosol on water relations, salt content, and leaf ultrastructure of rock-rose plants. *J. Environ Qual.* 33, 1369–1375. doi: 10.2134/jeq2004.1369

Shahid, S. A., Zaman, M., and Heng, L. (2018). "Salinity and sodicity adaptation and mitigation options," in *Guideline for Salinity Assessment, Mitigation and adaptation Using Nuclear and Related Techniques*, eds M. Zaman, S. Shahid, and L. Heng (Cham: Springer), 43–53. doi: 10.1007/978-3-319-96190-3_3

Soares da Costa, T. P., Hall, C. J., Panjikar, S., Wyllie, J. A., Christoff, R. M., Bayat, S., et al. (2021). Towards novel herbicide modes of action by inhibiting lysine biosynthesis in plants. *Elife* 10, e69444. doi: 10.7554/eLife.69444

Tautenhahn, R., Patti, G. J., Rinehart, D., and Siuzdak, G. (2012). Xcms online: a web-based platform to process untargeted metabolomic data. *Anal. Chem.* 84, 5035–5039. doi: 10.1021/ac300698c

Vargas, L. H. G., Neto, J. C. R., De Aquino Ribeiro, J. A., Ricci-Silva, M. E., Souza, M. T. Jr, Rodrigues, C. M., et al. (2016). Metabolomics analysis of oil palm (elaeis guineensis) leaf: evaluation of sample preparation steps using UHPLC–MS/MS. *Metabolomics* 12, 153. doi: 10.1007/s11306-016-1100-z

Vieira, L. R., Silva, V. N. B., Casari, R. A. C. N., Carmona, P. A. O., Sousa, C. A. F., and Sousa, M. A. Jr. (2020). Morphophysiological responses of young oil palm plants to salinity stress. *Pesq Agrop Brasileira*. 55, e01835. doi: 10.1590/S1678-3921.pab2020.v55.01835

Xiao, Y., Feng, J., Li, Q., Zhou, Y., Bu, Q., Zhou, J., et al. (2020). IiWRKY34 positively regulates yield, lignan biosynthesis and stress tolerance in Isatis indigotica. *Acta Pharm. Sin. B* 10, 2417–2432. doi: 10.1016/j.apsb.2019.12.020

Zarei, M., Shabala, S., Zeng, F., Chen, X., Zhang, S., Azizi, M., et al. (2020). Comparing kinetics of xylem ion loading and its regulation in halophytes and glycophytes. *Plant Cell Physiol.* 61, 403–415. doi: 10.1093/pcp/pcz205

Zhang, X., Lin, K., and Li, Y. (2020). Highlights to phytosterols accumulation and equilibrium in plants: biosynthetic pathway and feedback regulation. *Plant Physiol. Biochem.* 155, 637–649. doi: 10.1016/j.plaphy.2020.08.021

Zhu, Y., Wang, Q., Wang, Y., Xu, Y., Li, J., Zhao, S., et al. (2021). Combined transcriptomic and metabolomic analysis reveals the role of phenylpropanoid biosynthesis pathway in the salt tolerance process of *Sophora alopecuroides*. *Int. J. Mol. Sci.* 22, 2399. doi: 10.3390/ijms22052399

**Conflict of Interest:** The authors declare that the research was conducted in the absence of any commercial or financial relationships that could be construed as a potential conflict of interest.

**Publisher's Note:** All claims expressed in this article are solely those of the authors and do not necessarily represent those of their affiliated organizations, or those of the publisher, the editors and the reviewers. Any product that may be evaluated in this article, or claim that may be made by its manufacturer, is not guaranteed or endorsed by the publisher.

frontiers | Frontiers in Plant Science

SYSTEMATIC REVIEW
published: 24 May 2022
doi: 10.3389/fpls.2022.899926

# Crop Species Mechanisms and Ecosystem Services for Sustainable Forage Cropping Systems in Salt-Affected Arid Regions

*Dennis S. Ashilenje, Erick Amombo, Abdelaziz Hirich, Lamfeddal Kouisni, Krishna P. Devkota, Ayoub El Mouttaqi and Abdelaziz Nilahyane**

*African Sustainable Agriculture Research Institute (ASARI), Mohammed VI Polytechnic University (UM6P), Laayoune, Morocco*

Soil salinity limits crop productivity in arid regions and it can be alleviated by crop synergies. A multivariate analysis of published data ($n$ = 78) from arid and semiarid habitats across continents was conducted to determine the crop species mechanisms of salinity tolerance and synergies relevant for designing adapted forage cropping systems. Halophyte [*Cynodon plectostachus* (K. Schum.) Pilg.] and non-halophyte grasses (*Lolium perenne* L. and *Panicum maximum* Jacq.) clustered along increasing soil salinity. Halophytic grasses [*Panicum antidotale* Retz. and *Dicanthum annulatum* (Forssk.) Stapf] congregated with *Medicago sativa* L., a non-halophytic legume along a gradient of increasing photosynthesis. Halophytic grasses [*Sporobolus spicatus* (Vahl) Kunth, and *Cynodon plectostachyus* (K. Schum.) Pilg.] had strong yield-salinity correlations. *Medicago sativa* L. and *Leptochloa fusca* L. Kunth were ubiquitous in their forage biomass production along a continuum of medium to high salinity. Forage crude protein was strongly correlated with increasing salinity in halophytic grasses and non-halophytic legumes. Halophytes were identified with mechanisms to neutralize the soil sodium accumulation and forage productivity along an increasing salinity. Overall, halophytes-non-halophytes, grass-forbs, annual-perennials, and plant-bacteria-fungi synergies were identified which can potentially form cropping systems that can ameliorate saline soils and sustain forage productivity in salt-affected arid regions.

**Keywords: species salinity tolerance, photosynthesis, relative yield, synergies, forage cropping systems**

OPEN ACCESS

***Edited by:***
*Raoudha Abdellaoui, Institut des Régions Arides, Tunisia*

***Reviewed by:***
*Jagdish Chander Dagar, Indian Council of Agricultural Research (ICAR), India*
*Mohamed Tarhouni, Institut des Régions Arides, Tunisia*

****Correspondence:***
*Abdelaziz Nilahyane*
*abdelaziz.nilahyane@um6p.ma*

***Specialty section:***
*This article was submitted to Functional Plant Ecology, a section of the journal Frontiers in Plant Science*

***Received:*** *19 March 2022*
***Accepted:*** *22 April 2022*
***Published:*** *24 May 2022*

***Citation:***
*Ashilenje DS, Amombo E, Hirich A, Kouisni L, Devkota KP, El Mouttaqi A and Nilahyane A (2022) Crop Species Mechanisms and Ecosystem Services for Sustainable Forage Cropping Systems in Salt-Affected Arid Regions. Front. Plant Sci. 13:899926. doi: 10.3389/fpls.2022.899926*

## INTRODUCTION

Forage crops and rangeland species have immense potential to rehabilitate and improve the natural ecosystem services besides providing forage supply to livestock and wildlife. They maintain soil health by regulating environments against the effect of climate change and pollution. In arid regions, these benefits from vegetation have been jeopardized by adverse environmental conditions, particularly endemically marginal precipitation (Antipolis, 2003). Traditional interventions such as selection and cultivation of drought-tolerant species and irrigation strategies have helped

to augment forage production in these areas (Qadir et al., 2007). However, these measures have implications in aggravating salt accumulation in soils and diminishing ecosystem services associated with forage crops.

Soil salinity is a major problem limiting forage productivity in a wide range of agroecosystems. An estimated 1,125 million ha of land distributed across different continents is degraded by salinity (Hossain, 2019). The problem of salinity is unique in different ecosystems with greater prevalence in arid and semi-arid zones (Antipolis, 2003). Salt accumulation from seawater intrusion is endemic to coastal areas. However, mismanagement of agronomic practices particularly over-irrigation using brackish water triggers capillary and evapotranspiration and as a result, unfavorable amounts of salts accumulate in the soil profile. Saline soils are characterized by electrical conductivity (EC) exceeding 4 dS $m^{-1}$ and sodium accumulation greater than 15% (Allison et al., 1954). Salinity can occur simultaneously with alkalinity, where accumulation and hydrolysis of Na and $NaCO_3$ release $OH^-$ ions which elevate pH above 8.5 and consequently phosphorus, calcium, magnesium, and zinc precipitate and are less available to plants (Choudhari and Kharche, 2018; Wahba et al., 2019). High pH (>9) and $Na^+$ ions relatively thicken the saline layer and mediate the enhanced repulsive force in soil intermicellar layer which causes soil particle dispersion (Zhou and Yu, 2016). Dispersion disaggregates soil layers and predisposes organic carbon to mineralization (Wong et al., 2010), enhances compaction, obstructs soil water infiltration and as consequence soils are easily swept off by runoff (Shrivastava and Kumar, 2015). The excess NaCl concentration in soil solution inhibits microbial enzymes and therefore limits C and N cycling (Rietz and Haynes, 2003), net primary production, and turnover of crop residues (Yannarell and Pearl, 2007). At the ecological scale, soil salinity can adversely limit species diversity and their ecological niches.

To be specific, salinity is associated with negative osmotic potential which inhibits seed germination (Patel et al., 2010) and debilitates cell turgidity (Patel and Pandey, 2009). As a consequence, reduced plant cell elongation and photosynthetic area retards growth and, in some circumstances, plants fail to reproduce. Plants in sodic soils absorb excessive amounts of sodium ($Na^+$) ions which replace potassium ($K^+$) ions in plant biochemical functions (Roy and Chowdhury, 2020). Sodium toxicity stunts plants, suppresses net primary productivity, and deteriorates the nutritive value of forage crops (Temel et al., 2015; Worku et al., 2019). Irrigation measures that eliminate salts (Hanson et al., 2006) and soil amendments with gypsum and manure (Matosic et al., 2018) are traditionally used to manage soil salinity. These physical techniques involve relatively higher costs and unsustainable effects compared to the alternative of salt tolerant crop species (Fita et al., 2015).

Salt tolerant crop species are relatively convenient and affordable compared to physical measures used to manage soil salinity. The salinity tolerance in plants involves mechanisms of maintaining favorable water potential, balanced nutrient uptake, net photosynthesis, and alleviating toxic effects of $Na^+$ and $Cl^-$ ions (Lambers et al., 2008). These mechanisms are illustrated in **Figure 1**. The primary purpose of characterizing crop species is to develop salt tolerant varieties with superior yields and forage nutritive value. The need for synergies among species is increasing with the particular focus to formulate wholistic cropping systems that can foster and sustain environmental and production benefits. Contemporary forage cropping systems in non-saline conditions are renowned for their provisioning of forage, regulating soil health and hydrology, and supporting microbial and animal communities (Rodriguez et al., 2006). Dagar (2018) highlighted the possible ways to augmented forage cropping systems in saline environments by incorporating salinity tolerant halophytic species with agronomic value and unique abilities to alleviate salinity and salt toxicity.

Soil salinity management is a long-standing topic particularly focusing on food and forage crops. The increasing need for ecologically sound crop and livestock production has prompted efforts to mimic natural ecosystems in cultivated systems. There is a tendency to focus on individual plant species tolerance to salinity to meet imminent production objectives with little regard for ecosystems. One of the major gaps in the management of salinity is to identify and harness ecosystem services of plant species in developing cropping systems that can rehabilitate saline soils and, in the process, sustain forage productivity and ecosystem health. This prompts the need to understand (i) how consistent are mechanisms of tolerance to salinity among forage species in different habitats, (ii) do species converge in their salinity tolerance mechanisms, (iii) what are the possible synergies among species in their adaptation to saline soils, and (iv) how can mechanisms of species tolerance and synergies be used to design forage cropping systems adapted to saline soils. Hence this article reviews and reanalyzes published data to determine crop yield loss to soil salinity, species mechanisms of salinity tolerance and ecosystem services, and their potential synergies which can be used to design forage cropping systems for sustainable and resilient agroecosystems.

# METHODS

## Conceptual Framework

This article provides a synthesis of correlations between salinity tolerance mechanisms and ecosystem services of forage crops. The first stage was to determine forage crop yield losses to soil salinity and discuss its tolerance. Thereafter, attempts were made to determine if forage crop species converge in their mechanisms of salinity tolerance and what this implies to forage productivity. In this regard, tolerance was considered the ability to maintain photosynthesis and dry matter yields with increasing salinity up to 200 mM NaCl concentrations in the propagation medium (Munns and Gillham, 2015). Salinity tolerance classes were according to the following: halophytes > 250 mM NaCl, marginal halophytes 100–250 mM NaCl, and non-halophytes < 100 mM NaCl (Munns et al., 2006). The data were obtained from 17 diverse experiments conducted under controlled greenhouse environments. The species were profiled according to crop duration, salinity tolerance classes, and their ecosystem services over a range of saline conditions (saturated soil extract EC > 4 dS $m^{-1}$). Subsequently, crop species were categorized according to their ecosystem services reported in saline

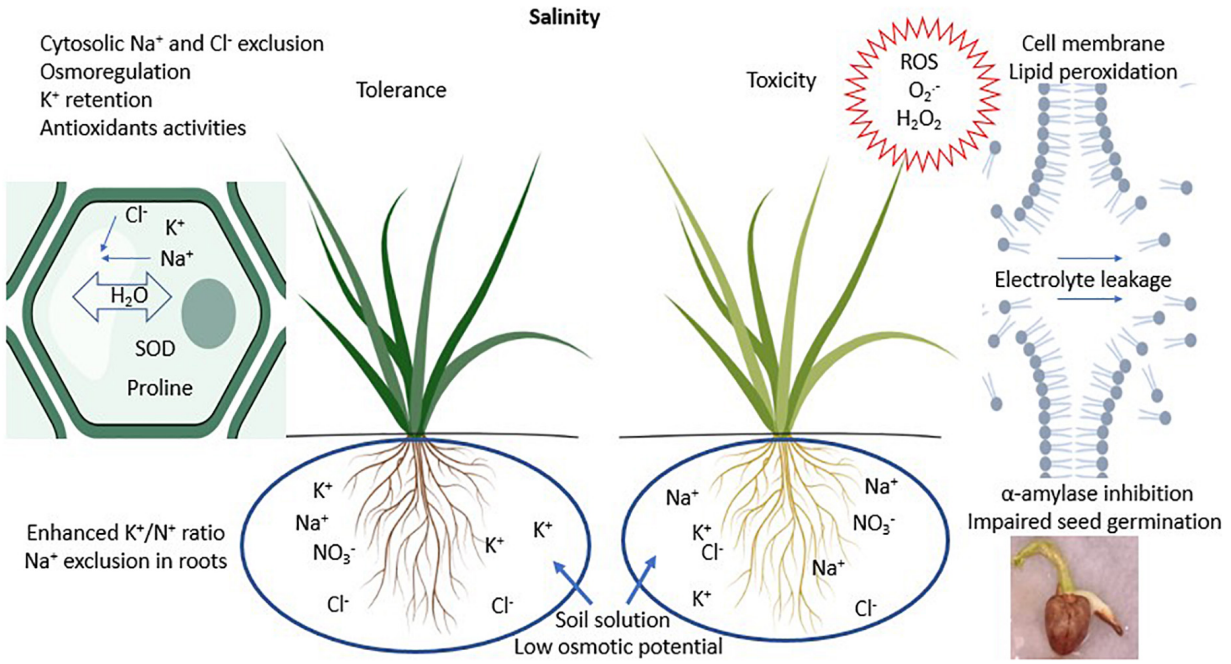


**FIGURE 1 |** Schematic illustration of salinity effects to plants and its tolerance. SOD stands for superoxide dismutase; ROS stands for reactive oxygen species. Illustrations were created with BioRender.com.

soils in arid and semi-arid habitats across continents. These involved studies spanning 1–5 years conducted in field conditions, each with a non-saline soil control besides an increasing magnitude of treatment to strongly saline soils. The criteria of Adhikari and Hartemink (2016) was used with some modifications to determine provisioning, regulating, and supporting ecosystem services of forage crops. **Figure 2** shows a schematic association between crop categories and their association with ecosystem services, key functions, and synergies. Consequently, provisioning services included forage dry matter biomass yield and nutritive value. Forage crude protein was consistently reported along with soil salinity treatments in a number of studies; hence, this was chosen as a measure of provisioning services for forage nutritional value. Regulating ecosystem services included soil organic carbon and $Na^+$ ion accumulation in crop biomass and their role in reducing soil salinity (bioremediation). Lastly, supporting services were crop microbe interactions that support nutrient cycling in forage cropping systems. The identified synergies were used as indicators to illustrate the model cropping systems that can alleviate soil salinity and enhance forage crop productivity and nutritive value.

## Data Acquisition and Analysis

The data for this review were obtained from the results of 20 studies published in peer-reviewed journals between the years 2000 and 2021. The literature search was done on the Google Scholar website. There is a sheer number of field investigations to identify physiological mechanisms of salinity tolerance because of their need for controlled environments. Hence, the relationship between salinity, photosynthesis and relative yield of seventeen crops in greenhouse studies was analyzed. Relative forage biomass was computed as the percentage forage accumulation of each crop in saline media against yield obtained in non-saline conditions. To determine crop ecosystem services, there were a total of 78 data entries representing crops evaluated in field trials whose details are recorded in **Supplementary Table S1**. Data was organized according to the location of study, crop name, cropping system (mono crop vs. polyculture), soil $EC_e$ (saturated paste extract), and crop duration and cited authors. Additional variables including accumulated soil organic carbon, forage dry biomass, forage crude protein, soil EC change, and $Na^+$ ion uptake. Data were subjected to the multivariate analysis procedure to determine correlations between variables and accordingly relationships among forage crop species. In doing so, the FactoMiner package was deployed to conduct principal component analysis (PCA) which also involved standardizing data according to the deviation of individual variates from the sample mean divided by sample standard deviation (R Core Team, 2019). The charts were visualized using the fviz_pca_biplot function in the R software version 3.6.3 (R Core Team, 2019).

# RESULTS AND DISCUSSION

## Yield Loss Due to Soil Salinity and Salinity Tolerance

The yield losses of selected forage crop reported in saline soils were on average 5.4 Mg $ha^{-1}$ and ranged from 1 Mg $ha^{-1}$ in arid subtropical conditions to 22 Mg $ha^{-1}$ in semi-arid tropical

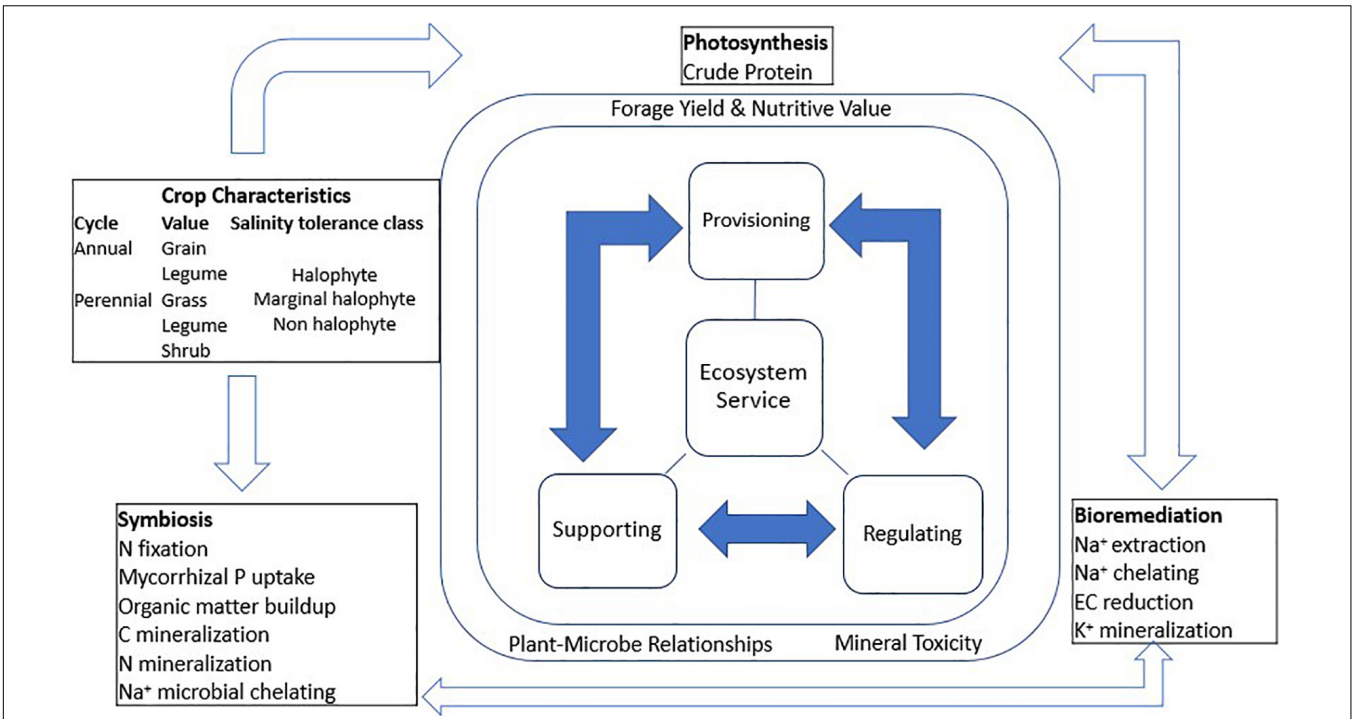


**FIGURE 2 |** Flow diagram of conceptual framework for evaluating ecosystem services and synergies among forage crop species. Filled arrows represent interacting mechanisms and open arrows represent synergies.

**TABLE 1 |** Forage crop losses to salinity in arid and semiarid environment.

| Location | Habitat | Species | Classification | EC dS $m^{-1}$ | ESP (%)† | Change in yield (Mg $ha^{-1}$)‡ | References |
|---|---|---|---|---|---|---|---|
| Turkey | Arid | *Medicago sativa* L. | Non-halophyte | 9.8 | 11.9 | −3 | Yalti and Aksu, 2019 |
| | | *Lotus corniculatus* L. | Non-halophyte | 9.8 | 11.9 | −3 | |
| | | *Onobrychis sativa* Lam. | Non-halophyte | 9.8 | 11.9 | −2 | |
| | | *Cynodon dactylon* (L.) Pers. | Non-halophyte | 10.0 | 12.0 | + 1 | Temel et al., 2015 |
| | | *Chloris gayana* Kunth. | Non-halophyte | 10.0 | 12.0 | + 1 | |
| | | *Festuca arundinacea* Schreb. | Non-halophyte | 10.0 | 12.0 | −1 | |
| Ethiopia | Semi arid | *Cenchrus ciliaris* L. | Non-halophyte | 16.0 | 25.0 | −7 | Worku et al., 2019 |
| | | *Sorghum sudanense* (Piper) Stapf | Non-halophyte | 10.0 | 21.0 | −22 | |
| | | *Chloris gayana* Kunth. | Non-halophyte | 18.0 | 27.0 | −6 | |
| Iran | Arid | *Sorghum bicolor* L. Moench | Non-halophyte | 11.0 | – | −3 | Tabatabaei et al., 2012 |
| | | *Kochia scoparia* (L.) Schrad. | Halophyte | 23.0 | – | −1 | Nabati et al., 2011 |
| California | Arid | *Pennisetum purpureum* Schumach. | Non-halophyte | 25.0 | - | −7.8 | Wang et al., 2002 |
| Iran | Arid | *Sorghum bicolor* L. Moench | Non-halophyte | 14 | – | −10 | Hedayati-Firoozabadi et al., 2020 |
| | | *Kochia scoparia* (L.) Schrad. | Halophyte | 14 | – | −4 | |
| Iran | Arid | *Brassica napus L.* | Non-halophyte | 10 | – | −0.6 | Shabani et al., 2013 |

†*ESP, Exchangeable sodium percentage.*
‡*Change in yield = forage yield in saline soils – forage yield in non-saline soils.*

environments (**Table 1**). These values corresponded to increasing exchangeable sodium percentage (ESP) from 12 to 27. Salinity is adversely compounded with sodicity creating a disequilibrium favoring $CaCO_3$ adsorption to cation exchange sites where $Na^+$ ion is displaced and released in the soil solution (Wong et al., 2010). An overaccumulation of sodium greater than 15% of exchangeable cation has serious consequences of diminishing plant water and potassium uptake. Although this threshold varies with crop species, the ESP at which yield losses exceed 50% distinguishes crops that are intolerant compared to those that tolerate salinity (Pal et al., 2006).

The ways by which some forage species tolerate salinity are summarized in **Figure 1** and **Table 2**. The $C_4$ grass species *Aeluropus lagopoides* (L.) Thwaites and *Panicum antidotales* Retz. have been reported to retain similar shoot moisture with increasing salinity levels from 0 to 140 mM NaCl (Rafay et al.,

**TABLE 2 |** Mechanisms of salinity tolerance in forage species.

| Enhanced mechanism | Salinity stress | Species | References |
|---|---|---|---|
| Water retention in shoots | 140 mM NaCl | *Aeluropus lagopoides* (L.) Thwaites | Rafay et al., 2021 |
| | | *Panicum antidotales* Retz. | |
| Retention of $K^+$ ions | 150 mM NaCl | *Lathyrus sativus* L. | Tokarz et al., 2020 |
| | 200 mM NaCl | *Festuca arundinacea* Schreb. | Xu and Fujiyama, 2013 |
| Membrane stability | 140 mM NaCl | *Aeluropus lagopoides* (L.) Thwaites | Rafay et al., 2021 |
| | | *P. antidotales* Retz. | |
| Rubisco activity | 100 mM NaCl | *P. antidotales* Retz. | Hussain et al., 2020 |
| Photosynthesis | 400 mM NaCl | *Sporobolus spicatus* (Vahl) Kunth | Hamilton et al., 2001 |
| Proline and soluble sugar content | 200 mM NaCl | *Imperata cylindrica* (L.) P. Beauv | Roy and Chakraborty, 2017 |
| | | *Eragrotis amabilis* (L.) Wight and Arn | |
| | | *Cynodon dactylon* (L.) Pers. | |
| | | *Digitaria ciliaris* (Retz.) Koeler | |
| | | *Festuca arundinacea* Schreb. | Xu and Fujiyama, 2013 |
| | | *Poa pratense* L. | |
| | 150 mM NaCl | *Agropyron desertorum* L. | Sheikh-Mohamadi et al., 2017 |
| Increased activity of SOD | 200 mM NaCl | *Festuca arundinacea* Schreb. | Xu and Fujiyama, 2013 |
| | | *Poa pratense* L. | |
| $Na^+$ and $Cl^-$ ion exudation | 400 mM NaCl | *Sporobolus spicatus* (Vahl) Kunth | Hamilton et al., 2001 |

2021). Maintenance of water balance in salt tolerant grasses is associated with the accumulation of organic osmolytes including proline and sugars which balance against negative osmotic pressure exerted by $Na^+$ ions in the media around roots (Xu and Fujiyama, 2013). This phenomenon is also evident in the grass species *Imperata cylindrica* (L.) P. Beauv., *Eragrotis amabilis* (L.) Wight and Arn., *Cynodon dactylon* (L.) Pers., and *Digitaria ciliaris* (Retz.) Koeler (Roy and Chakraborty, 2017), *Festuca arundinacea* Schreb. and *Poa pratense* L. at 200 mM NaCl (Xu and Fujiyama, 2013), and *Agropyron desertorum* L. exposed to 150 mM NaCl (Sheikh-Mohamadi et al., 2017). Under increasing salinity, the dominance of $Na^+$ uptake over $K^+$ adversely affects plant metabolism (Lambers et al., 2008). Potassium plays vital roles in plant metabolism and growth including maintaining osmotic potential and activity of enzymes involved in protein and carbohydrate synthesis (Hasanuzzaman et al., 2018). Potassium also enhances tolerance to salinity stress for instance by reducing activity of reactive oxygen species and their toxicity. $C_3$ species *Lathyrus sativus* L. and *Festuca arundinacea* Schreb. can maintain relatively constant shoot $K^+$ ion concentrations in non-saline conditions up to 150 and 200 mM NaCl concentrations, respectively (Xu and Fujiyama, 2013; Tokarz et al., 2020). In this case, *Festuca arundinacea* Schreb. limited $Na^+$ uptake and transport to the shoots (Xu and Fujiyama, 2013). In the leaves, halophytes suppress leakage of $K^+$ ions to the apoplasm by maintaining membrane stability as observed in halophytic grass *Panicum antidotales* Retz. and *Aeluropus lagopoides* (L.) Thwaites grown in saline environments up to 140 mM NaCl (Rafay et al., 2021). In addition, at moderate salinity (100 mM NaCl), *Panicum antidotales* Retz. is reported to retain activities of rubisco carboxylase similar to non-saline conditions. More pronounced effects have been recorded in *Sporobolus spicatus* (Vahl) Kunth which enhanced photosynthesis up to 400 mM NaCl (Hamilton et al., 2001). Maintaining similar or greater net photosynthesis with increasing salinity confers halophytes with relatively more shoot biomass accumulation compared to glycophytes (Bose et al., 2013). Species avert direct toxicity of $Na^+$ and $Cl^-$ ions as well as their role in generating reactive oxygen species. This is exemplified in enhanced exudation of $Na^+$ and $Cl^-$ ions by *Sporobolus spicatus* (Vahl) Kunth at 400 mM NaCl (Hamilton et al., 2001). *Festuca arundinacea* Schreb. and *Poa pratense* L. generate more antioxidant enzyme superoxide dismutase in response to 200 mM NaCl (Xu and Fujiyama, 2013), which degrade reactive oxygen species from photosystems I and II into less toxic $H_2O_2$ and $O_2$ (Gill and Tuteja, 2010). These mechanisms represent standalone species characterization which, if harnessed in cropping systems, can alleviate impacts of soil salinity to crops and the environment.

## Implications of Species Salinity Tolerance Mechanisms to Forage Productivity

It is of primary significance that grass and forb species mechanisms of salinity tolerance translate to sustainable forage biomass production and resilience to further exposure to salt stress. **Figure 3** shows a PCA of relative forage biomass of popular annual and perennial grass and legume species from different studies. Principle component 1 explained 54% of total variation associated with increasing photosynthesis, and relative biomass as salinity increased in the propagation media. Salinity was strongly correlated with relative yield, but no correlation with photosynthesis. It indicates improving forage yield is possible through improving photosynthetic capacity in those species or selecting photosynthetically efficient species. Star grass (*Cynodon plectostachyus* (K. Schum.) Pilg.), a halophytic grass, clustered together with non-halophytes including perennial ryegrass (*Lolium perenne* L.) and guinea grass (*Panicum maximum* Jacq.) and less proximately with *Setaria sphacelata* (Schum.) Stapf and Hubb. and *Pennisetum hybridus*, all of which had close associations with increasing soil salinity. Alfalfa which is a non-halophyte clustered with halophytes namely marvel grass (*Dicanthum annulatum* (Forssk.) Stapf) and blue panicum grass (*Panicum antidotales* Retz.) along increasing photosynthesis. Saltgrass (*Sporobolus spicatus* (Vahl)

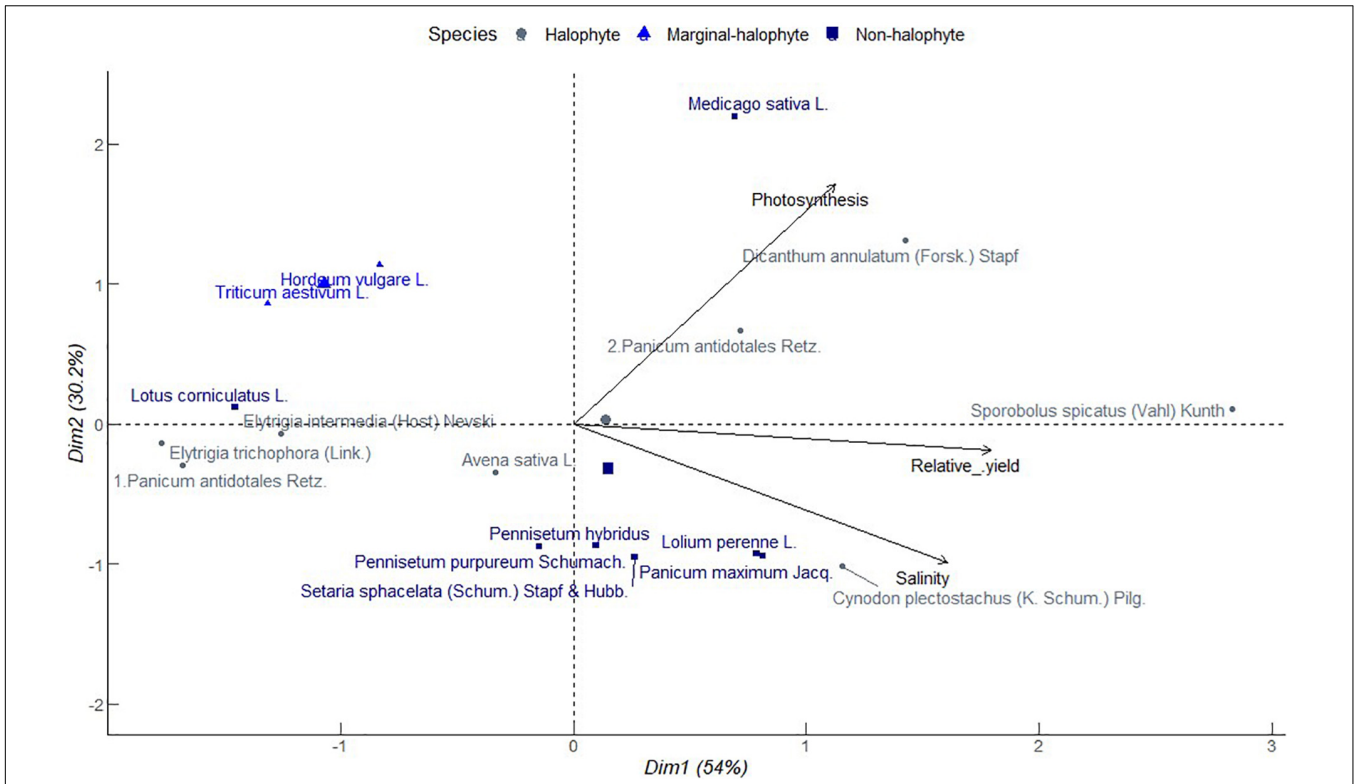


**FIGURE 3 |** Principal component analysis of relationship between soil salinity, photosynthesis, and relative biomass for different forage crop species obtained from different studies conducted in greenhouse environments from 2000 to 2021. Salinity tolerance class is in the order of halophytes > 250 mM NaCl, marginal halophytes 100–250 mM NaCl and non-halophytes < 100 mM NaCl (Munns et al., 2006).

Kunth) which is a halophyte, stood alone with strong and near equitable contribution to increasing relative yield, photosynthesis and salinity. Saltgrass is reported to restrict the $Na^+$ uptake with increasing soil salinity and secrete excess salts at night (Ramadan, 2001). This indicates the resilience of saltgrass to salinity, which is a potential attribute for sustaining net primary production in companion cropping. Birdsfoot trefoil (*Lotus corniculatus* L.), a non-halophytic legume, congregated with halophytic grasses including intermediate wheatgrass [*Elytrigia intermedia* (Host) Nevski, and *Elytrigia trichophora* (Link.)], and blue panicum grass (*Panicum antidotales* Retz.) associated with reducing salinity, photosynthesis, and relative yield. Intermediate wheatgrass has $C_3$ photosynthetic machinery (Jaikumar et al., 2016) and is likely to coexist with birdsfoot trefoil unlike blue panicum a vigorous $C_4$ grass. In this category, there was as well a cluster of barley (*Hordeum vulgare* L.) and wheat (*Triticum aestivum* L.) which are considered marginal halophytes. These annual grain crops are commonly diversified with annual legumes in time or space. Nevertheless, their proximal grouping with birdsfoot trefoil suggests a potential coexistence, for instance, in living mulch or in prolonged rotations. Living mulch refers to maintaining a perennial legume crop in an annual cropping system. Oat (*Avena sativa* L.), a halophytic annual grain, and *Pennisetum purpureum* Schumach., a non-halophytic grass, had near neutral contribution to salinity, photosynthesis, and relative yields hence potential candidates for long perennial annual rotations. Overall, the results of PC indicate a convergence of halophytes and non-halophytes in their physiology and yield response to salinity. This suggests possibilities for synchrony of diverse species functional groups in their adaptation to salinity stress which can support synergies that enhance overall forage productivity. In broad sense, such coexistence and facilitation can compensate for generally low forage productivity of halophytes as Dagar (2005) reports.

## Synergies Among Forage Crop Species in the Context of Soil Salinity

Synergies refer to the simultaneous increase or decrease in the provisioning of ecosystem services (Rodriguez et al., 2006). Forage crops are renowned for a wide range of ecosystem services. Among these, provisioning, regulating, and supporting services have been amplified in an effort to address escalating adversities of climate change, environmental degradation, and low agricultural productivity. In cultivated, non-saline conditions, perennial forage crops have gained attention due to their ability to reverse soil degradation. Perennial grasses are renowned for below-ground carbon sequestration, while legumes support nitrogen accretion in the agroecosystems. With this background, plants support microbial diversity with feedback to nutrient cycling, net primary production and sustainable

ecosystems. These crops regulate nutrient cycling, soil moisture retention, soil erosion while supporting the accretion of soil carbon and nitrogen.

Overboard, crop diversification to mimic the stability of primary production and resilience of natural vegetation to disturbances is increasingly appealing to the design of sustainable agroecosystems (Islam and Ashilenje, 2018). For example, recently, grass-legume mixtures maintained without fertilizers have been demonstrated to enhance forage yield and nitrogen and crude protein concentrations, and to buffer against nitrous oxide emissions in non-saline soils (Ashilenje, 2018). Islam and Ashilenje (2018) have discussed the benefits of diversified cropping systems in detail. In summary, mixtures assemble legumes and grasses that scavenge for excess soil mineral N, which, if left, serves as the substrate for denitrification. Accumulated mineral N inhibits nitrogenase enzyme activities of N fixation. Grasses amass carbon in their expansive root system and in the process alleviate losses through mineralization. These qualities of grasses recondition the soil in a gradual process that balances nutrient turnover from atmospheric nitrogen fixation, mineralization, and organic matter input from legume crops in mixtures. As a consequence, forage yields and soil health can be sustained while forfeiting shifts in ecosystem balance associated with fertilizers, tillage, and related anthropogenic factors. Intensified forage production on cultivated lands can support livestock health on less land resources unlike extensive systems associated with overgrazing and consequently, loss of plant canopy cover (Rutherford and Powrie, 2013). There are indicators that the agronomic and ecological benefits of diversified forage crop systems with halophytes can ameliorate soil salinity (Ghaffarian et al., 2021). In this light, ecosystem services reported in diverse forage crops growing in saline soils with EC ranging from 4.4 dS $m^{-1}$ (moderately saline) to 41 dS $m^{-1}$ (extremely saline) are analyzed in sections "Provisioning Ecosystem Services of Forage Production" to "Supporting Ecosystem Services for Soil and Animal Health."

## Provisioning Ecosystem Services of Forage Production

As shown in **Figure 4**, PC1 explained 47.9% of the total variation, which was positively correlated with high soil salinity and negatively so with forage biomass accumulation and duration of production. Annual forage grain monocrops including barley, finger millet, and Sudan grass clustered with alfalfa and kallar grass in close association with increasing soil salinity but decreasing forage biomass accumulation. At moderate soil salinity, perennial grasses including tall wheatgrass, blue panicum grass, paspalum, Bermuda grass, alkali sacaton, and kikuyu grass, grouped together with alfalfa and narrow leaf trefoil. Crops in this category, with exception of alfalfa and kikuyu grass, exhibit tolerance to salinity and indicate a wide variety of options for diversification against effects of soil salinity (Guo et al., 2014; Xiang et al., 2015). This cluster also included saltwort and salicornia which are eminent halophytes. On the other side, Sudan grass tied together with buffel grass, Rhodes grass, blue panicum grass, kallar grass, and millet rice in a cluster contributing to increasing forage accumulation. Sudan grass also formed a distinct group with Rhodes grass, buffel grass, and blue panicum grass which had intermediate contributions to forage accumulation and crop duration in PC2 (31.8%). Alfalfa again congregated with perennial legumes namely birdsfoot trefoil and sainfoin as well as Bermuda grass, tall wheat grass, tall fescue, and Rhodes grass associated with extended cropping period but decreasing forage accumulation and soil salinity. It is worthy to note that Sudan grass crop and alfalfa have an unrestricted pattern ranging from short duration of growth in high soil salinity with low yields and the inverse of high forage biomass at reducing salinity. Sudan grass-clitoria mixture had a profound contribution to forage biomass accumulation (Abusuwar, 2019). This implies that ineptness of annual species to saline conditions can be leveraged by mixtures. In annual cropping systems, adverse effects of soil salinity might be encouraged by water evaporation direct deposit of salts on the soil surface (Gabriel et al., 2012). This can be reversed by high crop density and retention of crop residues beyond one cropping season (Cuevas et al., 2019). Alfalfa and kallar grass displayed a wide range of influences from strong to negative correlation with soil salinity in a gradient of 6–41 dS $m^{-1}$. Blue panicum grass and Rhodes grass followed a similar pattern.

The ubiquity of grass and alfalfa indicates that these species can coexist and buffer against limitations of soil salinity to forage biomass accumulation. More specifically, a combination of species selective preference for uptake of $K^+$ over $Na^+$ ions in grass (Guo et al., 2014) and narrow leaf trefoil (Teakle et al., 2006) and the abilities of halophytic grass to alleviate salt accumulation in soil can avert stresses to legumes susceptible to salinity. Hence, these relationships can sustain overall crop ecosystem primary production. These associations can be exploited across a gradient of soil salinity up to extreme levels as revealed in the results of PCA. Alfalfa, blue panicum grass, and Rhodes grass distribution varied from longer growth period to shorter growth span associated with increasing forage accumulation. This indicates that the provisioning services of these perennial forage crops are not tied to the duration of growth. This trend further explains the potential to enhance forage biomass accumulation of the perennial grasses during the early years of establishment or complementarity in mixtures with perennial legumes beyond establishment. Halophytic crops including Salicornia, saltwort, and kochia tended to be neutral in their association with forage biomass accumulation and soil salinity. The same applied to saltwort-maize, saltwort-sorghum, kochia-guar, kochia-sesbania, and kochia-sesbania-guar mixtures. These results again suggest a facilitating role of halophytes to perpetuate growth of annuals normally susceptible to salinity. The characteristic ability of halophytes to extract $Na^+$ ions from soils, hence regulate salinity, are discussed in detail in section "Regulatory Ecosystem Services Against Soil Nutrient Imbalance and Phytotoxicity."

## Provisioning Ecosystem Services of Forage Nutritive Value

Together with yield, forage nutritive value determines animal health and production. The multivariate analysis revealed potential synergies among crops in their influence on forage crude protein in saline soils. As shown in **Figure 5**, PC1 explains

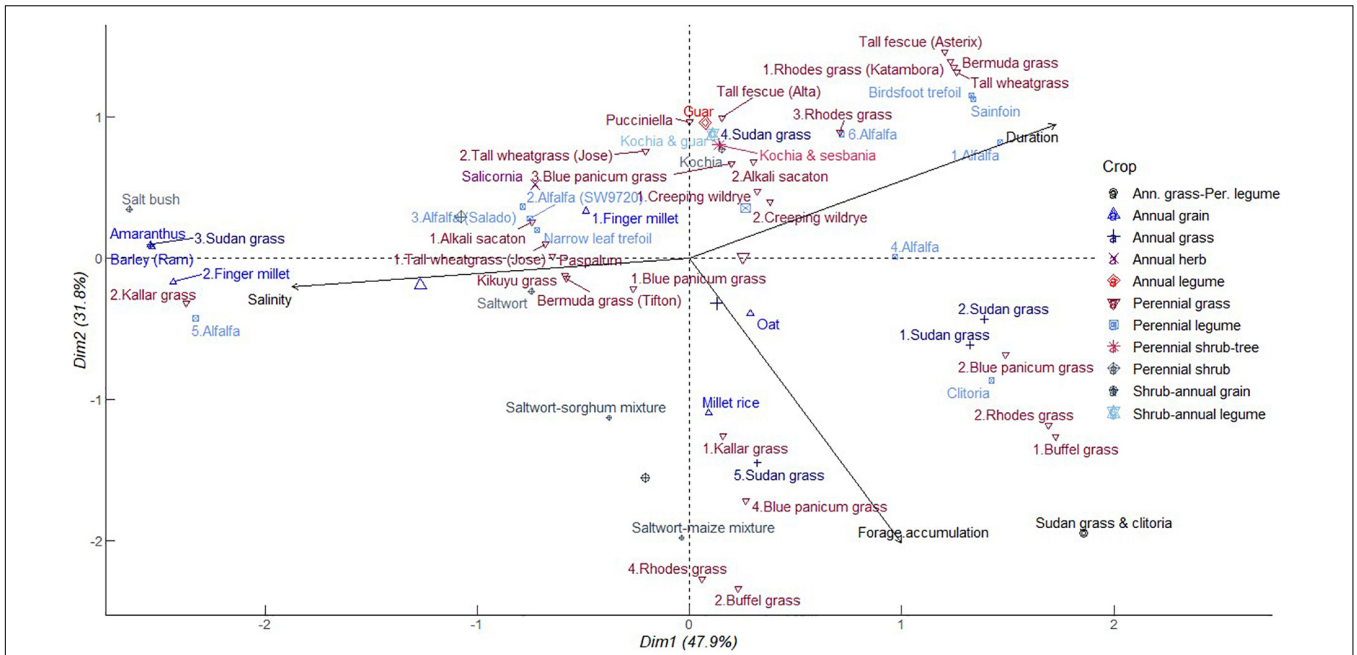


**FIGURE 4 |** Principal component analysis of dry biomass accumulation of different forage crops in saline conditions. The data points were obtained from seventeen different studies published from 2000 to 2021. Crops are numbered differently according to study and labels in parenthesis represent crop variety.

50.1% of the total variance. In this case, forage crude protein is correlated positively to soil salinity and negatively to crop duration. Tall wheatgrass, Bermuda grass, alkali sacaton, kikuyu grass, alfalfa, and narrow leaf trefoil contributed strongly in the cluster with increasing salinity and crude protein. This confounds the detriments of increasing soil salinity on nitrogen uptake and accumulation of proteins in forages as explained in the previous studies (Kumar et al., 2018; Kamran et al., 2020). Conversely, there are possible explanations supporting forage crude protein—soil salinity dependence. Certain amino acids may have osmoregulatory functions that alleviate the deleterious effects of $Na^+$ ions on plant proteins (Kamran et al., 2020). Alfalfa, Bermuda grass, and tall wheatgrass exhibited indeterminate patterns that extend from association with increasing salinity and forage crude protein to a counteractive effect when they grow for longer periods. This group also comprised Rhodes grass, tall fescue, sainfoin, and birdsfoot. Alfalfa, birdsfoot trefoil, and berseem clover formed a cluster that balances between duration, salinity, and forage crude protein. Forage kochia and creeping wildrye appeared intermediary with respect to duration, soil salinity, and forage crude protein. These crops are extremely tolerant to salinity (Suyama et al., 2007; Waldron et al., 2020). These results unbind the traditional profiling of the compatibility of common forage crops and identify commonalities in species traits that can overcome temporal effects of soil salinity to forage productivity and nutritive value.

Although not included in this analysis, grasses tend to accumulate more neutral detergent fiber (NDF) and lower crude protein than legumes. As depicted here, grasses are versatile in their range of crude protein concentration, some of which march that of legumes. A combination of grasses and forbs to generate forage of NDF $\leq$ 50% and crude protein $\geq$ 20% of dry matter is recommended to support animal and ruminal microbial energy needs which invigorate animal health and reproduction (Collins and Fritz, 2003). The balance of fiber and crude protein in crop residues also has implications on carbon-to-nitrogen ratio which influences soil microbial communities and their functions. These functions are discussed in detail in supporting ecosystem services in section "Supporting Ecosystem Services for Soil and Animal Health."

## Regulatory Ecosystem Services Against Soil Nutrient Imbalance and Phytotoxicity

As depicted in **Figure 6**, PC1 represented 69.3% of total variation with the positive correlation between accumulated soil organic carbon, soil salinity, and duration of cropping systems. This cluster had the sole contribution of one of the kallar grass crops. However, accumulated soil organic carbon was independent of the role of soil salinity or crop duration. The majority of the crops were clustered in the zone of declining contribution of duration, soil organic carbon, and salinity. It is less probable that crops adapted to salinity also promote soil organic carbon accumulation. This may be explained by depressed primary production and carbon sequestration (Lal, 2009). The reverse process of alleviating sodicity can help resuscitate plant growth in the process to improve soil carbon sequestration. A combination of species mechanisms and crop combinations that generate crop residues can help boost soil surface cover and soil organic matter accumulation. As a consequence, soil organic matter ameliorates against salinity primarily *via* improved soil structure and therefore enhanced infiltration of $Na^+$ ions down the soil

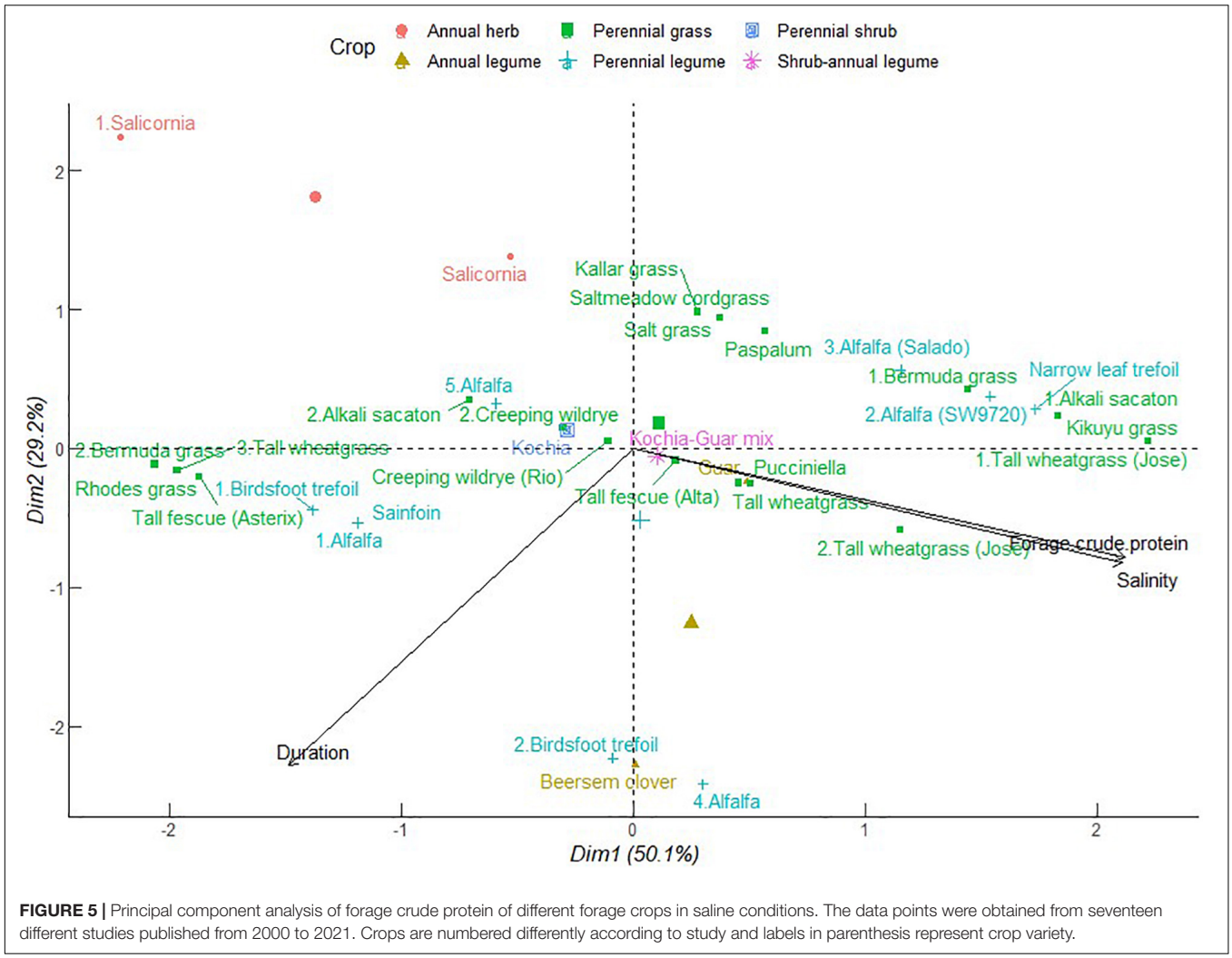


**FIGURE 5 |** Principal component analysis of forage crude protein of different forage crops in saline conditions. The data points were obtained from seventeen different studies published from 2000 to 2021. Crops are numbered differently according to study and labels in parenthesis represent crop variety.

profile (Bhuiyan et al., 2016). The confluence of soil carbon accumulation and salinity reduction have been demonstrated in tree-understory halophytic grass silvipastoral systems (Singh et al., 2022). The successful soil amelioration in this case was attributed to enhanced uptake of $Na^+$ ion by understory grass whose forage accumulation was facilitated by enhanced regime of photosynthetic active radiation, as influenced by the companion perennial tree canopy. Other possible mechanisms include organic matter decomposition and subsequent release of humic acids which can sequester $Na^+$ ions and help to reduce soil sodium exchangeable potential and electrical conductivity (Bhuiyan et al., 2016).

There is growing interest in the bioremediation of saline soils to sustain forage production. For example, Rabhi et al. (2010) determined that sea purslane (*Sesuvium portulacastrum* L.), a halophyte, can extract an estimated 1 ton of $Na^+$ ions $ha^{-1}$ $year^{-1}$. This subsequently enhanced plant water and $K^+$ ion retention together with shoot biomass in succeeding barley (*Hordeum vulgare* L.). Saltwort has similar potential, for instance, accumulating up to 125 g of $Na^+$ ion $kg^{-1}$ of dry matter within a span of 1 year (Toderich et al., 2008). In **Figure 7**, PC1 explained 52.7% of total variation strongly associated with increasing salinity as crop duration decreases. Salinity clustered tightly with barley, finger millet, amaranthus, Sudan grass, and alfalfa. Conversely, creeping wildrye, alkali sacaton, tall wheatgrass, tall fescue, and pucciniella clustered together along the increasing crop duration but decreasing salinity. In PC2 which explained 30.1% of the total variation, forage accumulation was correlated with sodium uptake profoundly associated with saltwort and to a lesser extend alfalfa. Enhanced shoot biomass and $Na^+$ ion accumulation are jointly classic qualities required for efficient bioremediation of saline soils by halophytes (Qadir et al., 2007). Nevertheless, species compatibility, forage value, and temporal effects of halophytic species are factors that count in the approach to integrate bioremediation in salt-affected cropping systems. The ability of common forage crops to reduce soil salinity is recorded in **Table 3**. Kallar grass is reported to have the highest influence of reducing soil salinity by 4 and 5 dS $m^{-1}$ annually (Akhter et al., 2004; Tawfik et al., 2013). This behavior is associated with altering of soil structure to support deep leaching of $Na^+$ ions (Akhter et al., 2004). Saltgrass (4 dS $m^{-1}$), saltmeadow cordgrass (3 dS $m^{-1}$), and blue panicum grass (2 dS $m^{-1}$) are reported to

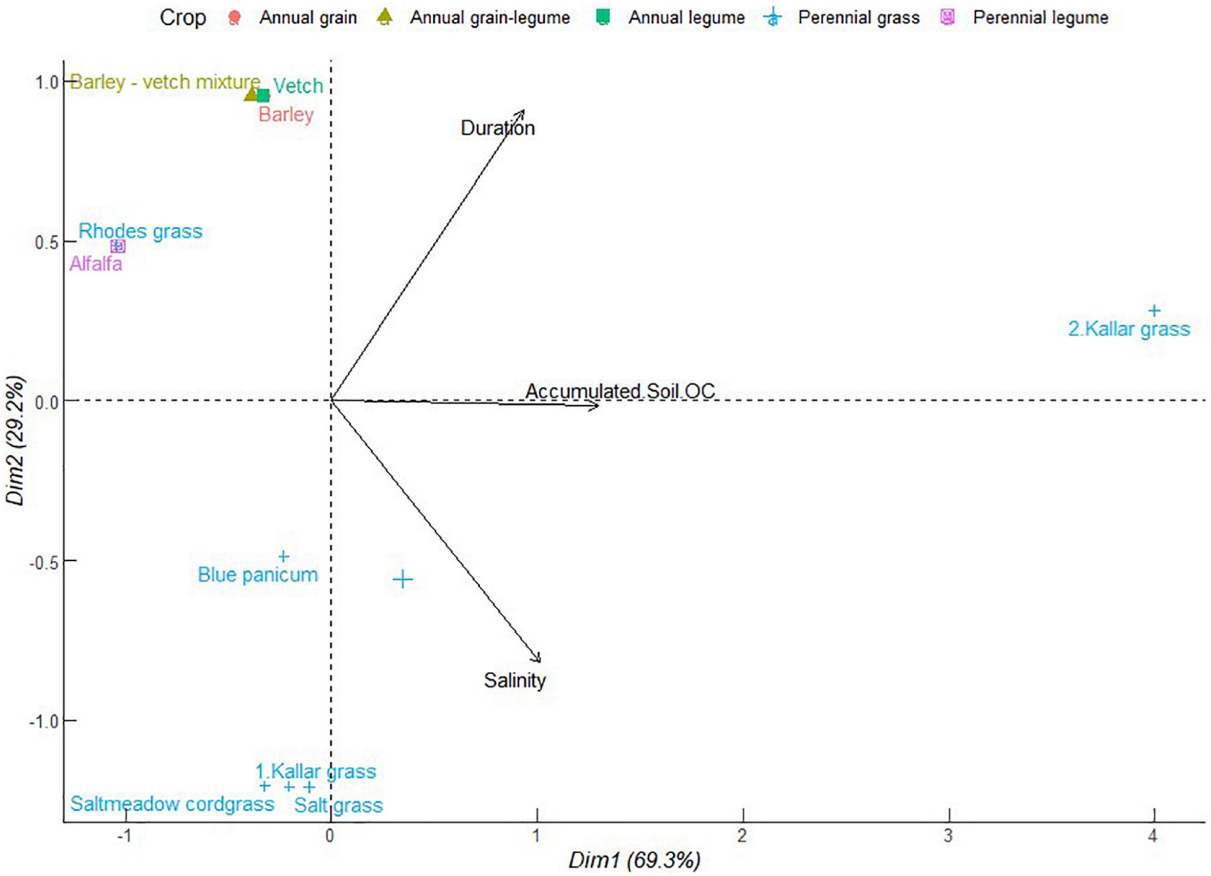


**FIGURE 6 |** Principal component analysis of accumulated soil organic carbon (OC) of different forage crops in saline conditions. The data points were obtained from four different studies published from 2000 to 2021. Crops are numbered differently according to study.

have intermediate effects (Tawfik et al., 2013; Gelaye et al., 2019). Rhodes grass, Sudan grass, and alfalfa rank on the lower range, each reducing the soil salinity by 1 dS $m^{-1}$ $year^{-1}$ (Gelaye et al., 2019). Unlike physical amendments to soil salinity, plant-based mechanisms of reducing salinity have inconsistent effects. Hence, the need for species- and site-specific determinations of optimum cropping systems to alleviate salinity.

## Supporting Ecosystem Services for Soil and Animal Health

Discussions of plant microbe interactions and their supporting ecosystem services are presented in this section. Biological nitrogen fixation, phosphorus solubilization and uptake, and nitrogen mineralization are important in this respect. Soil salinity has antagonistic mechanisms against mineral N, but a mixture of positive and negative influences on P uptake depending on plant species (Grattan and Grieve, 1999). Salinity can also suppress the availability of these minerals in the soils. Elevated levels of $Cl^{-}$ ions act against $NO_3{}^{-1}$ uptake and activity of nitrate reductase enzyme (Farissi et al., 2014). Increasing salinity also depresses N mineralization (Lodhi et al., 2009). Increasing salinity has particularly been associated with reducing P uptake in alfalfa (Farissi et al., 2014) and explained by the low solubility of P-Ca complexes (Grattan and Grieve, 1999). These important functions of crop N and P nutrition are mediated by soil microbes which are devastated by soil salinity (Kizildag et al., 2013). This challenge has traditionally been addressed by symbiosis between crops and salinity tolerant microorganisms. There are limited studies quantifying the $N_2$ fixation by forage crops in saline conditions. Among the few studies of this nature, Bruning et al. (2015) reported no significant effect of increasing soil salinity (1.7–16 dS $m^{-1}$) on biological N fixation by sweet clover (∼100%) and alfalfa (90–70%) except at 20 dS $m^{-1}$ (80 and 43%, respectively). It is suggested that N fixing bacteria release indole acetic acid at levels that safeguard the symbiotic process and plant growth from severe levels of soil salinity (William and Signer, 1990). This mechanism is pertinent to genus *Sinorhizobium* (Rejii and Mahdhi, 2014). The question arising is how these benefits can be maintained in cropping systems under saline conditions. The understanding of species diversity and their interactions with microbial communities in saline soils can help discern related ecosystem support services. Drawing a parallel from non-saline conditions, grass-legume mixtures can stimulate greater N2 fixation compared to legume monocrops and enrich grass crude protein compared to grass monoculture (Ashilenje, 2018). Nitrogen-fixing bacteria are more

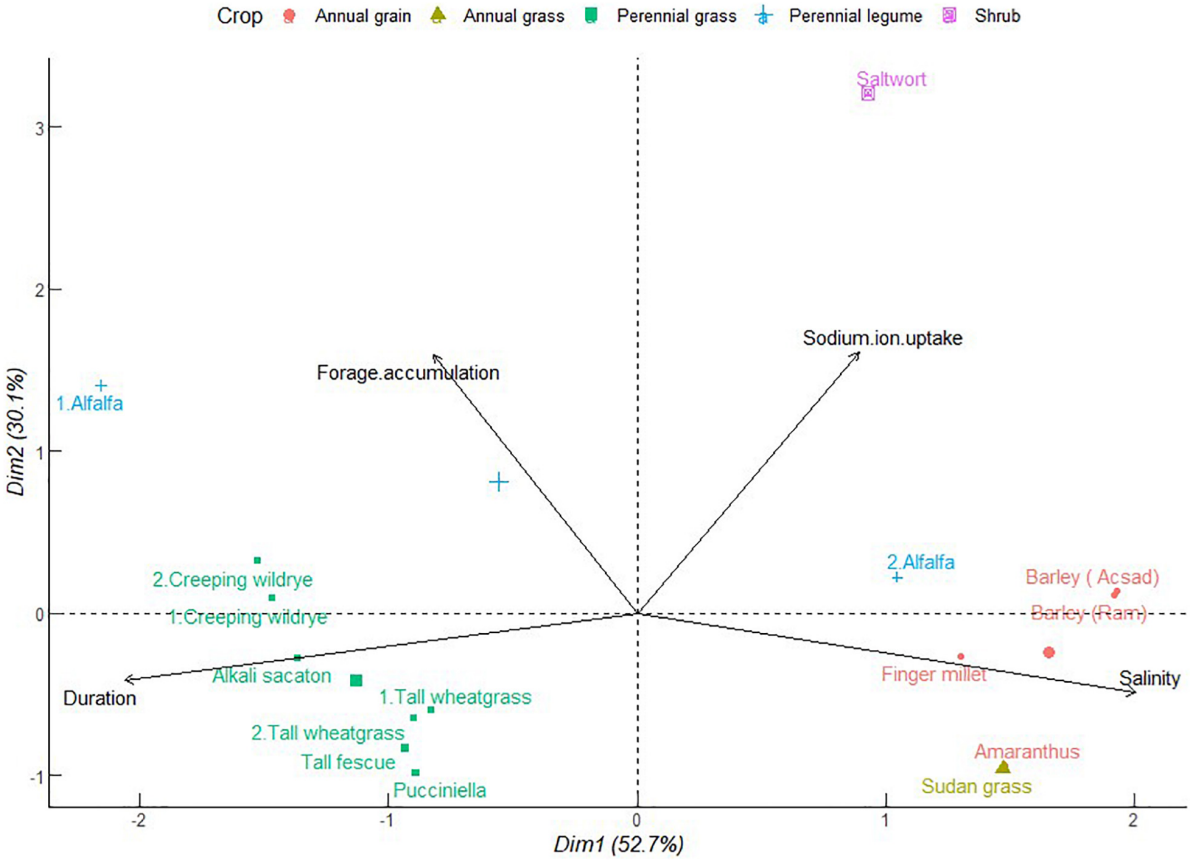


**FIGURE 7 |** Principal component analysis of sodium ($Na^+$) ion uptake of different forage crops in saline conditions. The data points were obtained from three different studies published from 2000 to 2021. Crops are numbered differently according to study and labels in parenthesis represent crop variety.

**TABLE 3 |** Ability of common forage crops to reduce soil salinity.

| Crop | | Soil Salinity | | | References |
|---|---|---|---|---|---|
| | Period | Initial | Change during entire period | Annual change | |
| | Years | | dS $m^{-1}$ | | |
| Blue panicum | 2 | 14 | −4 | −2 | Gelaye et al., 2019 |
| Alfalfa | 2 | 6 | −1 | −1 | |
| Sudan grass | 2 | 14 | −1 | −1 | |
| Rhodes grass | 2 | 6 | −1 | −1 | |
| Kallar grass | 1 | 15 | −5 | −5 | Tawfik et al., 2013 |
| Salt grass | 1 | 15 | −4 | −4 | |
| Saltmeadow cordgrass | 1 | 15 | −3 | −3 | |
| Kallar grass | 5 | 22 | −20 | −4 | Akhter et al., 2004 |

salt tolerant to soil salinity than their hosts (Zahran, 1999). This characteristic of plant growth promoting bacteria coupled with host species interactions that deescalate soil salinity and toxicity can potentially create environments for enhanced symbiosis in forage cropping systems. Soil microbe-mediated P uptake contrasts that of N. For instance, the role of mycorrhizae in augmenting P uptake and growth of grasses can be jeopardized by poor colonization of hosts as soil salinity increases (Pedranzani et al., 2016; Romero-Munar et al., 2019). Similarly, Arbuscular mycorrhiza fungi (AMF) have been observed to alleviate moderate effects of salinity on P uptake, photosynthesis, and plant growth in berseem clover and alfalfa (Shokri and Maadi, 2009; Shi-Chu et al., 2019). The role of AMF in alleviating the effect of salinity can be upmodulated in forage legumes. For example, co-inoculation with rhizobium can enhance AMF colonization of alfalfa roots (Ashrafi and Zahedi, 2014). As a

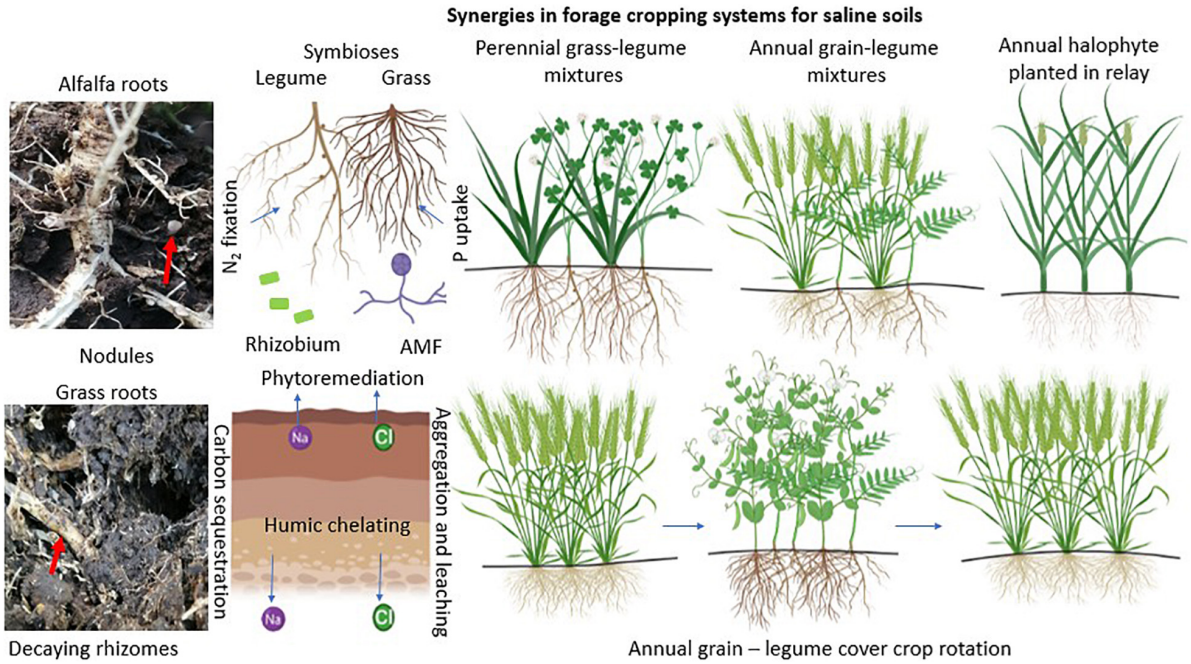


**FIGURE 8 |** Summary of plant-microbe synergies relevant for forage cropping systems designed to adapt to saline conditions. AMF stands for arbuscular mycorrhizal fungi. Illustrations were created with BioRender.com.

consequence, these microbes interact to step-up $N_2$ fixation, P uptake, photosynthesis, and shoot biomass yields.

### Designing Appropriate Forage Cropping Systems for Saline Soils

All of the above information showed that there is overwhelming evidence that soil microbes are ingredients of ecosystem sustainability by virtue of their roles in soil nutrient cycling. Soil microbial communities rely on energy from their plant hosts, and when established, they can revitalize crops against the effects of soil salinity and support forage productivity and nutritive value. This potential has not been fully exploited in orchestrated cropping systems to alleviate soil salinity and its effects on ecosystem health. **Figure 8** provides a synthesis of plant-microbe synergies that can be perpetuated in cropping systems designed to alleviate the effect of salinity on forages and sustain forage production and resilience. Annual and perennial cropping systems are depicted, premised on potential complementarities and symbioses. There are four scenarios with implications for designing forage cropping systems to exploit ecosystem services identified in this study. The first one is a perennial grass-legume mixture lasting for at least 3 years with an initial inoculum of nitrogen-fixing bacteria and AMF. This system might include a halophytic grass that extracts significant amounts of $Na^+$ ions from soils and allows legumes to thrive while entrenching microbial N and P uptakes. The second scenario is an annual grain legume mixture with the grain crop designed to reduce $Na^+$ ion contents in soils with repeated planting every year. Again, legumes in this case need to have the capacity to fix substantial amounts of N within the growing season. The third scenario is establishing annual halophytes in relay (before harvesting) with annual grain-legume mixtures in a sequence that extends through fallow periods. The halophyte is designed not only to adapt in marginal weather conditions but also able to absorb $Na^+$ ions and supply surface mulch for the next annual grain-legume crop mixture. The fourth system is an annual grain monocrop-legume monocrop in rotation. This system advances the benefits of optimum forage productivity and cover crops over at least 3 years of rotation. Overall, the cropping systems suggested here are designed to exploit the ecosystem services that enhance N and P supplies and optimize forage productivity and nutritive value. These systems are also developed to sequester carbon and alleviate salt buildup and toxicity in a gradual process that leads to sustainable forage production in areas prone to salinity.

## CONCLUSION

This article explored species mechanisms and synergies that can be incorporated in cropping systems to alleviate the challenges of soil salinity and sustain forage productivity in arid regions. It is clear that halophytic and non-halophytic forage crop species have convergent mechanisms of salinity tolerance manifested in enhanced photosynthesis and productivity. There are indicators of ubiquity of ecosystem services of both halophyte and non-halophytic species along a continuum of increasing soil salinity. Potential grass-forb, annual-perennial, halophytes-non-halophytes, and plant-bacteria-fungi synergies against effects of soil salinity were identified. These synergies can be harnessed in designing sustainable forage cropping systems that ameliorate

saline soils and improve nutrient cycling to sustain optimum forage productivity.

## DATA AVAILABILITY STATEMENT

The original contributions presented in the study are included in the article/ **Supplementary Material**, further inquiries can be directed to the corresponding author.

## AUTHOR CONTRIBUTIONS

DA and AN conceived and designed the study. AN supervised the work. DA, EA, AH, and AE collected and analyzed the data. DA drafted the manuscript. AH, LK, KD, and AN validated the data analysis and reviewed all the versions of the manuscript. All authors contributed to the article and approved the submitted version.

## FUNDING

We would like to thank the OCP Phosboucraa Foundation for funding this project (FPB_SPA002_2020).

## SUPPLEMENTARY MATERIAL

The Supplementary Material for this article can be found online at: https://www.frontiersin.org/articles/10.3389/fpls.2022.899926/full#supplementary-material

## REFERENCES

Abusuwar, A. O. (2019). Effect of fermented manures on intercropped Sudan grass (*Sorghum sudanese L.*) and clitoria (*Clitoria ternate*) grown in an arid saline environment. *J. Anim. Plant Sci.* 29, 269–277.

Adhikari, K., and Hartemink, A. E. (2016). Linking soils to ecosystem services –a global review. *Geoderma* 262, 101–111. doi: 10.1016/j.geoderma.2015.08.009

Akhter, J., Murray, R., Mahmood, K., Malik, K. A., and Ahmed, S. (2004). Improvement of degraded physical properties of a saline sodic soil by reclamation with kallar grass (*Leptochloa fusca*). *Plant Soil* 258, 207–216. doi: 10.1023/B:PLSO.0000016551.08880.6b

Allison, L. E., Bernstein, L., Bower, C. A., Brown, J. W., Fireman, M., Hatcher, J. T., et al. (1954). *Diagnosis and Improvement of Saline and Alkali Soils* Available online at https://www.ars.usda.gov/ARSUserFiles/20360500/hb60_pdf/hb60complete.pdf (Accessed September 9, 2021)

Antipolis, S. (2003). *Threat to soils in Mediterranean countries. Bibliographic studies*. Available online at http://citeseerx.ist.psu.edu/viewdoc/download?doi=10.1.1.460.6771&rep=rep1&type=pdf (Accessed July 9, 2021)

Ashilenje, D. S. (2018). *Plant Community Structure and Nitrogen Dynamics Affect Productivity and Environment of Meadow Bromegrass—Legume Cropping Systems. [Ph.D. Dissertation]*. Laramie (WY: University of Wyoming.

Ashrafi, E., and Zahedi, M. (2014). Co-inoculations of arbuscular mycorrhizal fungi and rhizobia under salinity in alfalfa. *Soil Sci. Plant Nutr.* 60, 619–629. doi: 10.1080/00380768.2014.936037

Bhuiyan, M. S. I., Raman, A., and Hodgkins, D. (2016). Plants in remediating salinity-affected agricultural landscapes. *Proc. Indian Nat. Sci. Acad.* 83, 51–66. doi: 10.16943/ptinsa/2016/48857

Bose, J., Rodrigo-Moreno, A., and Shabala, S. (2013). ROS homeostasis in halophytes in the context of salinity stress tolerance. *J. Exp. Bot.* 65, 1241–1257. doi: 10.1093/jxb/ert430

Bruning, B., van Logtestijn, R., Broekman, R., de Vos, A., Gonzalez, A. P., and Rozena, J. (2015). Growth and nitrogen fixation of legumes at increasing salinity under field conditions: Implications for the use of green manures in saline environments. *AoB Plants* 7:lv010. doi: 10.1093/aobpla/plv010

Choudhari, O. P., and Kharche, V. K. (2018). "Soil salinity and sodicity," in *Soil Science: An introduction*, Eds Edn, eds R. K. Rattan, J. C. Katyal, B. S. Dwivedi, A. K. Sarkar, T. Bhattacharya, J. C. Tarafdar, et al. (New Delhi: Indian Society of Soil Science), 352–384.

Collins, M., and Fritz, J. (2003). "Forage establishment," in *Forages: An introduction to grassland agriculture*, Eds Edn, eds R. F. Barnes, C. J. Nelson, M. Collins, and K. J. Moore (Ames, IA: Blackwell Publishing), 363–384.

Cuevas, J., Daliakopoulos, I. N., del Moral, F., Hueso, J. J., and Tsanis, I. K. (2019). A review of soil-improving cropping systems for soil salinization. *Agronomy* 9:295.

Dagar, J. C. (2005). Ecology, management and utilization of Halophytes. *Bull. Nat. Ins. Ecol.* 15, 81–97.

Dagar, J. C. (2018). Utilization of degraded saline habitats and poor-quality waters for livelihood security. *Scho. J. Food Nutr.* 1, 1–19. doi: 10.32474/sjfn.2018.01.000115

Farissi, M., Faghire, M., Bargaz, A., Bouizgaren, A., Makoudi, B., Sentenac, H., et al. (2014). Growth, nutrient concentrations, and enzymes involved in plants nutrition of alfalfa populations under saline conditions. *J. Agric. Sci. Technol* 16, 301–314.

Fita, A., Rodriguz-Burrezo, A., Boscaiu, M., Prohens, J., and Vicente, O. (2015). Breeding and domesticating crops adapted to drought and salinity: a new paradigm for increasing food production. *Front. Plant Sci.* 6:978. doi: 10.3389/fpls.2015.00978

Gabriel, J. L., Almendros, P., Hontoria, C., and Quemada, M. (2012). The role of cover crops in irrigated systems: Soil salinity and salt leaching. *Agric. Ecosyt. Environ.* 158, 200–207. doi: 10.1016/j.agee.2012.06.012

Gelaye, K. K., Zehetner, F., Loiskandl, W., and Klik, A. (2019). Comparison of growth of annual crops used for salinity bioremediation in the semi-arid irrigation area. *Plant Soil Env.* 65, 165–171. doi: 10.17221/499/2018-PSE

Ghaffarian, M. R., Nasab, A. D. M., Salehi, M., and Dehnavi, M. M. (2021). Forage yield and quality evaluation in intercropping kochia, ssebania and guar under saline irrigation. *J. Agric. Sci. Technol.* 23, 149–165.

Gill, S. S., and Tuteja, N. (2010). Reactive oxygen species and antioxidant machinery in abiotic stress tolerance in crop plants. *Plant Physiol. Biochem* 48, 909–930. doi: 10.1016/j.plaphy.2010.08.016

Grattan, S. R., and Grieve, C. M. (1999). Salinity-mineral nutrient relations in horticultural crops. *Sci. Hortic.* 78, 127–157. doi: 10.1016/S0304-4238(98)00192-7

Guo, Q., Meng, L., Mao, P., and Tian, X. (2014). Salt tolerance in two tall wheatgrass species is associated with selective capacity for $K^+$ over $Na^+$. *Acta Physio. Plant* 37:1708. doi: 10.1007/s11738-014-1708-4

Hamilton, E. W., McNaughton, S. J., and Coleman, J. S. (2001). Molecular, physiological and growth responses to sodium stress in C4 grasses from a soil salinity gradient in the Serengeti ecosystem. *Am. J. Bot.* 88, 1258–1265. doi: 10.2307/3558337

Hanson, B., Grattan, A., and Fulton, A. (2006). *Agricultural Salinity and Drainage*. Available online at https://lawr.ucdavis.edu/cooperative-extension/irrigation/manuals/agricultural-salinity-and-drainage (Accessed December 8, 2021).

Hasanuzzaman, M., Bhuyan, M. H. M., Nahar, K., Hossain, M. S., Al Mahmud, J., and Hossen, M. S. (2018). Potassium: a vital regulator of plant response and tolerance to abiotic stress. *Agronomy* 8:31. doi: 10.3390/agronomy8030031

Hedayati-Firoozabadi, A., Kazemeni, S. A., Pirasteh-Anosheh, H., Ghadari, H., and Pessarakli, M. (2020). Forage yield and quality as affected by salt stress in different ratios of sorghum bicolor-bassia indica intercropping. *J. Plant Nutr.* 43, 2579–2589. doi: 10.1080/01904167.2020.1783301

Hossain, S. (2019). Present scenario of global salt affected soils its management and importance of salinity research. *Int. Res. J. Biol. Sci.* 1, 1–3. doi: 10.1007/978-3-030-78435-5_1

Hussain, S., Shaukat, M., Ashraf, M., Zhu, C., Jin, Q., and Zhang, J. (2020). "Salinity stress in Arid and Semi-Arid Climates: Effects and Management in Field Crops," in *Climate Change and Agriculture*, Ed Edn, ed. S. Husein (Landon UK: Intechopen), 26.

Islam, M.A., and Ashilenje, D.S., (2018). Diversified Forage Cropping Systems and Their Implications on Resilience and Productivity. *Sustainability* 10:3920. doi: 10.3390/su113920

Jaikumar, N. S., Snapp, S. S., and Sharky, T. D. (2016). Older thynopyrum intermedium (Poacea) plants exhibit superior photosynthetic tolerance to cold stress and greater increase in two photosynthetic enzymes under freezing stress compared with young plants. *J. Exp. Bot* 67, 4743–4753. doi: 10.1093/jxb/erw253

Kamran, M., Parveen, A., Ahmar, S., Malik, Z., Hussain, S., Chattha, M. S., et al. (2020). An overview of Hazardous Impacts of Soil Salinity in Crops. Tolerance Mechanisms, and Amelioration through Selenium Supplementation. *Int. J. Mol. Sci.* 21:148. doi: 10.3390/ijms21010148

Kizildag, N., Sagliker, H. A., and Darici, C. (2013). Nitrogen mineralization in some saline soils at eastern mediterranean coasts. *Turkey EurAsian J. Biosci.* 7, 95–100. doi: 10.5053/ejobios.2013.7.0.11

Kumar, A., Kumar, A., Kumar, P., Lata, C., and Kumar, S. (2018). Effect of individual and interactive alkalinity and salinity on physiological, biochemical and nutritional traits of Marvel grass Indian. *J. Exp. Biol.* 56, 573–581.

Lal, R. (2009). Soil degradation as a reason for inadequate human nutrition. *Food Secur.* 1, 45–57. doi: 10.1007/s12571-009-0009-z

Lambers, L., Chapin, F. S., and Pons, T. L. (2008). *Plant physiological ecology*. New York:NY: Springer, 216.

Lodhi, A., Arsad, M., Azam, F., and Sajjad, M. H. (2009). Changes in mineral and mineralizable N of soil incubated at varying salinity, moisture and temperature regimes. *Pak. J. Bot.* 4, 967–980.

Matosic, S., Birkás, M., Vukadinovic, V., Kisic, I., and Bogunovic, I. (2018). Tillage, manure and gypsum use in reclamation od saline-sodic soils. *Agric. Conspec. Sci.* 183, 131–138.

Munns, R., and Gillham, M. (2015). Salinity tolerance of crops– what is the cost? *New Phytol.* 208, 668–673. doi: 10.1111/nph.13519

Munns, R., James, R. A., and Läuchli, A. (2006). Approaches to increasing the salt tolerance of wheat and other cereals. *J. Exp. Bot.* 57, 1025–1043. doi: 10.1093/jxb/erj100

Nabati, J., Kafi, M., Nezami, A., Maghaddam, P. R., Masoumi, A., and Mahrjerdi, M. Z. (2011). Effect of salinity on biomass production and activities of some key enzymatic antioxidants in kochia (*Kochia scoparia*). *Pak. J. Bot.* 43, 539–548.

Pal, D. K., Bhattacharyya, T., Ray, S. K., Chandran, P., Shrivastava, P., Durge, S. L., et al. (2006). Significance of soil modifiers (Ca-zeolite and gypsum) in naturally degraded vertisols of the peninsular India in redefining the sodic soils. *Geoderma* 136, 210–228. doi: 10.1016/j.geoderma.2006.03.020

Patel, N. T., and Pandey, A. N. (2009). Effect of soil salinity on growth water status and nutrient accumulation in seedlings of Sueda nudiflora (chenopodiaceae). *An. Biol.* 31, 61–70.

Patel, P. R., Kajal, S. S., Patel, V. R., Patel, V. J., and Khristi, S. M. (2010). Impact of salt stress on nutrient uptake and growth of cowpea. *Braz. J. Plant Physiol.* 22, 43–48. doi: 10.1590/S1677-04202010000100005

Pedranzani, H., Rodríguez-Rivera, M., Gutíerrez, M., Porcel, R., Hanse, B., and Ruiz-Lozano, J. M. (2016). Arbuscular mycorrhizal symbiosis regulates physiology and performance of digitaria eriantha plants subjected to abiotic stresses by modulating antioxidant and jasmonate levels. *Mycorrhiza* 26, 141–152. doi: 10.1007/s00572-015-0653-4

Qadir, M., Osters, J. D., Schubert, S., Noble, A. D., and Sahrawat, K. L. (2007). Phytoremediation of sodic and saline-sodic soils. *Adv. Agron.* 96, 197–247. doi: 10.1016/S0065-2113(07)96006-X

R Core Team (2019). *R: A Language and Environment for Statistical Computing. Release 3.3.1*. Available online at https://www.r-project.org/ (Accessed June 20, 2021)

Rabhi, M., Ferchichi, S., Jouni, J., Hamrouni, M. H., Koyro, H., Ranieri, A., et al. (2010). Phytodesalinisation of a salt–affected soil with halophyte *Sesuvium portulacastrum* L. to arrange in advance the requirements for the successful growth of a glycophytic crop. *Bioresour. Technol.* 101, 6822–6828. doi: 10.1016/j.biortech.2010.03.097

Rafay, M., Abid, M., Abdullah, M., Malik, Z., Makki, H. A., Ahmed, Z., et al. (2021). Growth parameters and antioxidant enzymes activities in selected halophytic grass species from cholistan rangeland. *Pak. J. Bot.* 53, 805–811. doi: 10.30848/PJB2021-3(22)

Ramadan, T. (2001). Dynamics of salt secretion by *sporobolus spicatus* (Vahl) kunth from sites of differing salinity. *Ann. Bot.* 87, 259–266. doi: 10.1006/anbo.2001.1326

Rejii, M., and Mahdhi, M. (2014). The phenotypic, phylogenetic and symbiotic characterization of rhizobia nodulating Lotus Sp. In tunisian arid soils. *Ann. Microbiol.* 64, 355–362. doi: 10.1007/s13213-013-0670-5

Rietz, D. W., and Haynes, R. J. (2003). Effects of Irrigation induced salinity and sodicity on soil microbial activity. *Soil Biol. Biochem* 35, 845–854. doi: 10.1016/s0038-0717(03)00125-1

Rodriguez, J. P., Beard, T. D., Bennett, E. M., Cumming, G. M., Cork, S. J., Agard, J., et al. (2006). Tradeoffs across space. *Time Ecosystem Serv. Ecol.* 11:28.

Romero-Munar, A., Barasa, E., Gulias, J., and Cabot, C. (2019). Arbuscular mycorrhizal fungi confer salt tolerance in giant reed (*Arundo donax* L.) plants grown under low phosphorus by reducing leaf $na^+$ Concentration and Improving Phosphorus use efficiency. *Front. Plant Sci.* 10:843. doi: 10.3389/fpls.2019.00843

Roy, S., and Chakraborty, U. (2017). Screening of salt-tolerance potential of some native forage grasses from the eastern part of terai-duar grasslands in India. *Trop. Grassl.* 5, 129–142. doi: 10.17138/TGFT(5)129-142

Roy, S., and Chowdhury, N. (2020). "Salt stress in plants and amelioration strategies: A critical review," in *Abiotic Stress in Plants*, Eds Edn, eds S. Fahad, S. Saudy, Y. Chen, C. Wu, and D. Wang (Landon UK: Intechopen). doi: 10.1186/s13054-016-1208-6

Rutherford, M. C., and Powrie, L. W. (2013). Impacts of heavy grazing on plant species richness: a comparison across rangeland biomes of South Africa. *Afr. J. Bot* 87, 146–156. doi: 10.1016/j.sajb.2013.03.020

Shabani, A., Sepaskhah, A. R., and Kamgar-Haghighi, A. A. (2013). Growth and physiologic reponse of rapeseed (*Brassica napus* L.) to deficit irrigation, water salinity and planting method. *Int. J. Plant Prod.* 7, 569–596. doi: 10.22069/ijpp.2013.1119

Sheikh-Mohamadi, M., Etemadi, N., and Nikbakht, A. (2017). Screening and selection of twenty iranian wheatgrass genotypes for tolerance to salinity stress during seed germination and seedling growth stage. *HortScience* 52, 1125–1134. doi: 10.21273/HORTSCI12103-17

Shi-Chu, L., Yong, J., Ma-bo, L., Wen-xu, Z., Nan, X., and Hui-hui, Z. (2019). Improving plant growth and alleviating photosynthetic inhibition from salt stress using AMF in alfalfa seedlings. *J. Plant Interact.* 14, 482–491. doi: 10.1080/17429145.2019.1662101

Shokri, S., and Maadi, B. (2009). Effect of arbuscular mycorrhizal fungus on the mineral nutrition and yield of trifolium alexandrium plants under salinity stress. *J. Agron.* 8, 79–83. doi: 10.3923/ja.2009.79.83

Shrivastava, P., and Kumar, R. (2015). Soil salinity: a serious environmental issue and plant growth promoting bacteria as one of the tools for its elevation. *Saudi J. Biol. Sci.* 22, 123–131. doi: 10.1016/j.sjbs.2014.12.001

Singh, Y. P., Mishra, V. K., Arora, S. J., Dagar, J. C., and Lal, K. (2022). Restoration of degraded sodic soils through silvipastoral systems in the indo-gangetic plains. *Land Degrad. Dev.* 2022, 1–15. doi: 10.1002/Idr.4222

Suyama, H., Benes, S. E., Robinson, P. H., Getachew, G., Grattan, S. R., and Grieve, C. M. (2007). Biomass yield and nutritional quality of forage species under long-term irrigation with saline-sodic drainage water: field evaluation. *Anim. Feed Sci. Technol.* 135, 329–345. doi: 10.1016/j.anifeedsci.2006.08.010

Tabatabaei, S. A., Ranjbar, G. H., and Anagholi, A. (2012). Evaluation of physiological indices of salinity tolerance in forage sorghum (*Sorghum bicolor*) lines. *Int. Res. J. Appl. Basic Sci.* 3, 305–308.

Tawfik, M. M., Thalooth, A. T., and Zaaki, N. M. (2013). "Exploring Saline Land Improvement Through Testing Leptochloa fusca and Sporobolus virginicus in Egypt," in *Developments in Soil Salinity Assessment and Reclamation*, Eds Edn, eds S. A. Shahid, M. A. Abdelfattah, and F. K. Taha (Berlin: Springer), 615–625. doi: 10.1007/978-94-007-5684-7_40

Teakle, N. L., Real, D., and Colmer, T. D. (2006). Growth and ion relations in response to combined salinity and water logging in the perennial forage legumes lotus corniculatus and lotus tenuis. *Plant Soil* 289, 369–383. doi: 10.1007/s11104-006-9146-8

Temel, S., Keskin, B., Simsek, U., and Yilmaz, T. H. (2015). Performance of some forage grass species in halomorphic soil. *Turkish J. Field Crop.* 20, 131–144. doi: 10.17557/tjfc.82860

Toderich, K. N., Ismail, S., Juylova, E. A., Rabbimov, A. A., Beckchanov, B. B., Shyuskaya, E. V., et al. (2008). "New approaches for biosaline agriculture development, management and conservation of sandy desert ecosystems," in *Biosaline Agriculture and High Salinity Tolerance. Switzerland*, Eds Edn, eds C. Abdelly, M. Öztürk, M. Ashraf, and C. Grignon (Basel: Birkhäuser Verlag), 247–264. doi: 10.1007/978-3-7643-8554-5_23

Tokarz, B., Wójtowicz, T., Makowski, W., Jędrzejczyk, R. J., and Tokarz, K. M. (2020). What is the difference between Response of Grass Pea (*Lathyrus sativus* L.) to salinity and drought stress? A Physiological study. *Agronomy* 10:833. doi: 10.3390/agronomy10060833

Wahba, M. M., Labib, F., and Zanhloul, A. (2019). Management of calcarious soils in arid region. *Int. J. Env. Poll. Env. Model.* 2, 248–258.

Waldron, B. L., Sagers, J. K., Peel, M. D., Rigby, C. W., Bugbee, B., and Creech, J. E. (2020). Salinity reduces the forage quality of forage kochia: a halophytic chenopodiaceae shrub. *Rangel. Ecol. Manag.* 73, 384–393. doi: 10.1016/j.rama.2019-12.005

Wang, D., Poss, J. A., Donovan, T. J., Shannon, M. C., and Lesch, S. M. (2002). Biophysical properties and biomass production of elephant grass under saline conditions. *J. Arid Env.* 52, 447–456. doi: 10.1006/jare.2002.1016

William, M. N. V., and Signer, E. R. (1990). Metabolism of tryptophan and tryptophan analogues by rhizobium meliloti. *Plant Physiol.* 92, 1009–1013. doi: 10.1104/pp.92.4.1009

Wong, V. N. L., Green, R. S. B., Dalal, R. C., and Murphy, B. W. (2010). Soil carbon dynamics in saline and sodic soils: a review. *Soil Use Manag.* 26, 2–11. doi: 10.1111/j.1475-2743.2009.00251.x

Worku, A., Mamo, B. N. L., and Bekele, T. (2019). Evaluation of some selected forage grasses for their salt tolerance, ameliorative effect and biomass yield under salt affected soil at Southern Afar Ethiopia. *J. Soil Sci. Env. Manage.* 10, 94–102. doi: 10.5897/JSSEM2018.0733

Xiang, M., Moss, J. Q., Martin, D. L., Su, K., and Dunn, B. L. (2015). Evaluating the salinity tolerance of bermudagrass cultivars and experimental selections. *Hortiscience* 52, 185–191. doi: 10.21273/HORTSCI10773-16

Xu, R., and Fujiyama, H. (2013). Comparison of ionic concentration, organic solute accumulation and osmotic adaptation in kentucky bluegrass and Tall fescue under NaCl stress. *Soil Sci. Plant Nutr.* 59, 168–179. doi: 10.1080/00380768.2012.763215

Yalti, S., and Aksu, H. (2019). Drought analysis of iğdir Turkey. *Turkish JAF Sci. Tech.* 7, 2227–2232. doi: 10.24925/turjaf.v7i12.2227-2232.3004

Yannarell, A. C., and Pearl, H. W. (2007). Effects of salinity and light on organic carbon and nitrogen uptake in a hypersaline microbial mat. *FEMS Microbiol. Ecol* 62, 345–353. doi: 10.1111/j.1574-6941.2007.00384.x

Zahran, H. H. (1999). Rhizobium-legume symbiosis and nitrogen fixation under severe conditions and in arid climate. *Microbiol. Mol. Biology Rev.* 64, 968–989. doi: 10.1128/MMBR.63.4.968-989.1999

Zhou, Q., and Yu, H. (2016). Influence of soil surface sodium ion and soil pH on dispersion of cohesive soil. *Chem. Eng. Trans.* 55, 427–432. doi: 10.3303/CET1655072

**Conflict of Interest:** The authors declare that the research was conducted in the absence of any commercial or financial relationships that could be construed as a potential conflict of interest.

**Publisher's Note:** All claims expressed in this article are solely those of the authors and do not necessarily represent those of their affiliated organizations, or those of the publisher, the editors and the reviewers. Any product that may be evaluated in this article, or claim that may be made by its manufacturer, is not guaranteed or endorsed by the publisher.

frontiers | Frontiers in Plant Science

ORIGINAL RESEARCH
published: 07 July 2022
doi: 10.3389/fpls.2022.918594

# Genome-Wide Analysis of *CqCrRLK1L* and *CqRALF* Gene Families in *Chenopodium quinoa* and Their Roles in Salt Stress Response

*Wei Jiang[1,2†], Chao Li[2†], Leiting Li[2], Yali Li[2,3], Zhihao Wang[2,3], Feiyu Yu[4], Feng Yi[5], Jianhan Zhang[5], Jian-Kang Zhu[2], Heng Zhang[6], Yan Li[1]* and Chunzhao Zhao[2]**

[1] National Key Laboratory of Crop Genetics and Germplasm Enhancement, National Center for Soybean Improvement, Key Laboratory for Biology and Genetic Improvement of Soybean (General, Ministry of Agriculture), Jiangsu Collaborative Innovation Center for Modern Crop Production, Nanjing Agricultural University, Nanjing, China, [2] Shanghai Center for Plant Stress Biology, CAS Center for Excellence in Molecular Plant Sciences, Chinese Academy of Sciences, Shanghai, China, [3] University of the Chinese Academy of Sciences, Beijing, China, [4] The Bright Seed Industry Company, Shanghai, China, [5] Agricultural Technology Center of Bright Rice (Group) Co., Ltd., Shanghai, China, [6] National Key Laboratory of Plant Molecular Genetics, Shanghai Center for Plant Stress Biology, CAS Center for Excellence in Molecular Plant Sciences, Chinese Academy of Sciences, Shanghai, China

OPEN ACCESS

**Edited by:**
*Amr Adel Elkelish,*
*Suez Canal University, Egypt*

**Reviewed by:**
*Shan Tang,*
*Huazhong Agricultural University, China*
*Jeongmin Choi,*
*University of Cambridge, United Kingdom*

***Correspondence:**
*Yan Li*
*yanli1@njau.edu.cn*
*Chunzhao Zhao*
*czzhao@cemps.ac.cn*

*† These authors have contributed equally to this work and share first authorship*

**Specialty section:**
*This article was submitted to Plant Abiotic Stress, a section of the journal Frontiers in Plant Science*

**Received:** *12 April 2022*
**Accepted:** *21 June 2022*
**Published:** *07 July 2022*

**Citation:**
*Jiang W, Li C, Li L, Li Y, Wang Z, Yu F, Yi F, Zhang J, Zhu J-K, Zhang H, Li Y and Zhao C (2022) Genome-Wide Analysis of CqCrRLK1L and CqRALF Gene Families in Chenopodium quinoa and Their Roles in Salt Stress Response. Front. Plant Sci. 13:918594. doi: 10.3389/fpls.2022.918594*

*Chenopodium quinoa* is a halophyte with exceptional nutritional qualities, and therefore it is potentially an ideal crop to grow in saline soils, not only addressing the problem of land salinization, but also providing nutrient food for the health of humans. Currently, the molecular mechanisms underlying salt tolerance in quinoa are still largely unknown. In *Arabidopsis thaliana*, *Catharanthus roseus* receptor-like kinase (*Cr*RLK1Ls) FERONIA (FER) and its ligands rapid alkalinization factors (RALFs) have been reported that participate in the regulation of salt tolerance. Here, we performed a genome-wide analysis and identified 26 *CqCrRLK1L* and 18 *CqRALF* family genes in quinoa genome. Transcriptomic profiling of the leaf, root, stamen, and pistil tissues of quinoa reveals that different *CqCrRLK1L* and *CqRALF* genes exhibit tissue-specific expression patterns, which is consistent with that observed in other plant species. RNA-seq data show that three *CqCrRLK1L* genes are highly up-regulated after salt treatment, suggesting that some *CqCrRLK1L* family genes are transcriptionally responsive to salt stress in quinoa. Biochemical study indicates that CqRALF15, a paralog of Arabidopsis RALF22, is physically associated with *Cr*RLK1L proteins CqFER and AtFER. CqRALF15 and AtRALF22 are functionally conserved in inducing the internalization of AtFER and in triggering root growth inhibition in both quinoa and Arabidopsis. Moreover, overexpression of *CqRALF15* in Arabidopsis results in enhanced leaf bleaching under salt stress, indicating that *CqRALF15* is involved in salt stress response. Together, our study characterizes *CqCrRLK1L* and *CqRALF* family genes in quinoa at genomic, transcriptional, and protein levels, and provides evidence to support their roles in salt stress response.

**Keywords: *Chenopodium quinoa*, *CrRLK1Ls*, RALFs, salt stress, peptides**

## INTRODUCTION

*Catharanthus roseus* receptor-like kinases (*Cr*RLK1Ls) are a family of receptor-like proteins that exist in many different plant species, ranging from charophytes to angiosperms (Zhu et al., 2021). The *Cr*RLK1L family proteins are characterized by two tandemly-linked malectin-like domains that are required for binding to cell wall polymers, such as pectin, and a kinase domain that replays apoplastic signals to intracellular components via a phosphorylation (Feng et al., 2018; Franck and Westermann, 2018; Lin et al., 2022). Because of the critical roles in sensing cell wall integrity, *Cr*RLK1L family proteins are required for the modulation of a wide range of biological processes, including plant growth, root hair elongation, fertility, immunity, and abiotic stress response (Duan et al., 2010; Haruta et al., 2014; Ge et al., 2017; Stegmann et al., 2017; Zhao et al., 2018). In Arabidopsis, there are 17 *Cr*RLK1L family proteins, and among of them the biological functions of FERONIA (FER), THESEUS1 (THE1), HERCULES1 (HERK1), ANXUR1/2 (ANX1/2), and BUDDHA'S PAPER SEAL1/2 (BUPS1/2) have been well studied. AtFER, which is universally expressed in both vegetative and reproductive tissues, is the most extensively studied *Cr*RLK1L family protein in Arabidopsis (Franck and Westermann, 2018). AtTHE1 was initially identified based on a mutant screen for suppressors that can rescue the short hypocotyl phenotype of cellulose-deficient mutant *procuste1-1* (*prc1-1*) (Hématy et al., 2007). It has also been reported that AtTHE1 and AtHERK1 function redundantly in regulating cell elongation (Guo et al., 2009), and AtFER, AtANJEA, and AtHERK1 form a heteromeric receptor complex to control polytubey block in Arabidopsis (Zhong et al., 2022). *AtANX1/2* and *AtBUPS1/2* are preferentially expressed in pollen tubes and participate in the regulation of pollen tube growth during fertilization (Miyazaki et al., 2009; Ge et al., 2017). Although *AtANX1/2* is weakly expressed in vegetative tissues, their roles in plant immunity in leaves have also been reported (Mang et al., 2017).

FER is named after an Etruscan goddess of fertility, because it was initially discovered as a critical regulator of pollen tube-ovule interaction (Huck et al., 2003; Rotman et al., 2003). During the last decade, many progresses have been achieved to decipher the novel functions of FER and the underlying molecular mechanisms. In Arabidopsis, FER regulates cell expansion, polarized cell growth, pathogen defense, and abiotic stress tolerance via the modulation of reactive oxygen species (ROS) balance (Huang et al., 2013) and the homeostasis of multiple phytohormones, such as jasmonic acid (JA), salicylic acid (SA), abscisic acid (ABA), brassinosteroid (BR), and ethylene (Guo et al., 2009, 2018; Deslauriers and Larsen, 2010; Zhao et al., 2021). Many intracellular components that are directly regulated by FER have been discovered, and one of the most well-known pathways is FER-GEFs (guanine exchange factors)-ROPs (Rho-GTPases of plants) signaling pathway. FER controls the activity of ROPs to regulate apoplastic ROS production, polarized cell elongation, and pavement cell morphogenesis (Duan et al., 2010; Huang et al., 2013; Lin et al., 2022; Tang et al., 2022). Recent studies indicate that FER participates in the regulation of salt tolerance, as mutation of *FER* results in enhanced leaf bleaching and short root elongation under high salinity (Feng et al., 2018; Zhao et al., 2018). It was pointed out that FER modulates cell wall integrity under salt stress via a $Ca^{2+}$-mediated signaling pathway (Feng et al., 2018). Similar to *fer* mutation, *herk1* mutation combined with a gain of function allele of *the1* mutation also leads to leaf bleaching phenotype under salt stress (Gigli-Bisceglia et al., 2020). These results suggested that *Cr*RLK1L family proteins are required for salt tolerance in plants.

Based on biochemical, physiological, and genetic studies, it has been well demonstrated that rapid alkalinization factors (RALFs) are the ligands of *Cr*RLK1L family proteins (Haruta et al., 2014; Stegmann et al., 2017; Blackburn et al., 2020). In analogy to *CrRLK1L* family genes, different *RALFs* also exhibit tissue-specific expression patterns (Cao and Shi, 2012; Murphy and De Smet, 2014), which determines the tissue-specific pairs of *Cr*RLK1Ls and RALFs. For example, in Arabidopsis, AtFER recognizes AtRALF1, AtRALF22, and AtRALF23 that are dominantly expressed in leaves and roots (Haruta et al., 2014; Stegmann et al., 2017; Zhao et al., 2018). AtRALF4 and AtRALF19 are specifically expressed in pollen tubes, and thereby physically associate with pollen tube–specific AtANX1/2 and AtBUPS1/2 (Ge et al., 2017). A recent study showed that pollen tube–specific AtRALF6, 7, 16, 36, and 37 are recognized by AtFER, AtANJ, and AtHERK1 that are highly expressed in ovule (Zhong et al., 2022). In vegetative tissues, application of exogenous mature RALFs inhibits root growth in a process that depends on FER, and inhibition is proposed to be caused by the alkalization of apoplastic regions via the regulation of plasma membrane $H^+$-ATPase AHA2 activity (Haruta et al., 2014; Abarca et al., 2021).

*Chenopodium quinoa* is an allotetraploid plant that originates from hybridization between diploid *Chenopodium pallidicaule* and diploid *Chenopodium suecicum* (Jarvis et al., 2017). Quinoa is a halophyte that processes a capacity to tolerate soil salinity, drought and cold stress, and sterile soil (Hinojosa et al., 2018). Due to its high nutritional value and stress tolerance property, quinoa has gained globally increased attention, and growth areas of quinoa have been dramatically increased in many countries during last few years. Whole-genome sequencing reveals that the genome size of quinoa is approximately 1.4 Gb and there are around 54,348 protein-encoding genes (Jarvis et al., 2017; Zou et al., 2017). Recently, quinoa has been selected as a model to study salt-tolerant mechanisms in halophyte (Zou et al., 2017). It is generally considered that epidermal bladder cells (EBCs) on the surface of quinoa are of primary importance for salt tolerance due to its capacity to accumulate high concentration of sodium in vacuoles (Kiani-Pouya et al., 2017; Böhm et al., 2018). However, a recent study reported that $Na^+$ concentration is not substantially increased in the EBCs of salt-treated quinoa (Jaramillo Roman et al., 2020), suggesting that compensation mechanisms are associated with salt tolerance in quinoa. Therefore, identification of components required for salt tolerance would be critical for full understanding of salt-tolerant mechanisms in quinoa. In this study, we performed a genome-wide analysis of *CrRLK1L* and *RALF* family genes in quinoa and investigated the tissue-specific expression patterns of these two gene families and their roles in salt stress response.

# MATERIALS AND METHODS

## Plant Materials and Growth Conditions

*Arabidopsis thaliana* wild-type (WT) was the Columbia (Col-0) ecotype. *fer-4* mutant and *AtFER-GFP* transgenic plants have been described previously (Zhao et al., 2018). The *C. quinoa* variety NL-6 was obtained from Prof. Heng Zhang. Both *Arabidopsis* and *C. quinoa* seeds were sterilized and sown on half Murashige and Skoog (MS) solid medium containing 1% sucrose and kept at 4°C for 2 days. Seeds were geminated in a light incubator at 22°C with a long-day cycle (16 h light/8h dark). For RNA-seq analysis, quinoa seedlings were transferred to soil and grown in a growth chamber at 22°C with a long-day cycle (16 h light/8 h dark).

## Plasmid Construction

For split luciferase complementation assay, the whole CDS sequences of *CqRALF15* and *AtRALF22*, as well as the ectodomain of *AtFER* and *CqFER*, were amplified by using Phanta® Max Super-Fidelity DNA Polymerase (Vazyme, Nanjing, China). PCR products were purified by FastPure Gel DNA Extraction Mini Kit (Vazyme, Nanjing, China) and cloned into pDONR207 ENTRY vector using BP Clonase II Enzyme Mix (Thermo Fisher Scientific). Plasmids were extracted using FastPure Plasmid Mini Kit (Vazyme, Nanjing, China). Finally, all fragments mentioned above were recombined into pCAMBIA-nLUC or pCAMBIA-cLUC vectors using LR Clonase II Enzyme Mix (Thermo Fisher Scientific). For the generation of *CqRALF15* transgenic plants in Arabidopsis, *CqRALF15* was also recombined into the destination vector pEarleyGate 101. Primers used for constructs are listed in **Supplementary Table 11**.

## Mature RALF Peptides Treatment

For mature AtRALF22 and CqRALF15 treatment in Arabidopsis, WT and *fer-4* mutant seeds were geminated on 1/2 MS solid medium and grown for 5 d. Then the seedlings were transferred into 12-well plate. Each well of plate was filled with 4 mL of 1/2 Hoagland nutrient (pH 5.8) supplemented without or with 2 μM AtmRALF22 or CqmRALF15. The plates were gently shaken on a shaker in greenhouse. After treatment for 6 d, the root length of *Arabidopsis* seedlings was measured.

For mature RALF treatment in quinoa, the seeds of NL-6 were geminated on 1/2 MS solid medium for 2 days, and then seedlings were transferred into 5 mL centrifuge tube. Each centrifuge tube was filled with 4 mL of 1/2 Hoagland nutrient (pH 5.8) supplemented without or with 2 μM AtmRALF22 or CqmRALF15. The centrifugal tubes were placed in a light incubator. After treatment for 3 d, the root length of NL-6 seedlings was measured.

## Salt Stress Treatment

To conduct salt stress treatment, the seeds of wild type and *CqRALF15* transgenic plants were sown on 1/2 MS medium supplemented with or without 120 mM NaCl and kept at 4°C for 3 days before they were placed in an incubator at 22°C with long-day lighting conditions (16 h light/8 h dark). After growth for 12 days, the survival rate of seedlings on NaCl media was calculated.

## Identification of *CrRLK1L* and *RALF* Genes in Quinoa

The protein sequences of 17 CrRLK1L and 37 RALF genes in A. thaliana were downloaded from the Arabidopsis Information Resource (TAIR).[1] The genomic databases of two sequenced quinoa varieties QQ74 and NL-6, were obtained from https://www.cbrc.kaust.edu.sa/chenopodiumdb/ and Prof.Heng Zhang, respectively.

To identify CrRLK1L genes in two quinoa genomes, Malectin_like (PF12819) and Pkinase_Tyr (PF07714) domains were downloaded from Pfam 35.0[2](Mistry et al., 2021). To identify CqRALF genes, RALF domain (PF05498) was downloaded. HMMER v3.0 (Finn et al., 2011) was used for searching quinoa sequences with the conserved domains, and SMART[3] (Letunic and Bork, 2018) was used to manually check the domain architectures of candidate proteins. In addition, using the Arabidopsis and quinoa protein sequences as queries, sequence alingment and phylogenetic analysis were performed, and the protein sequences lacking conserved domains or conserved residues were removed.

## Chromosomal Locations, Phylogenetic Analysis of the *CrRLK1L* and *RALF* Genes

The physical locations of *CrRLK1L* genes on chromosomes were analyzed based on QQ74 genome database (Jarvis et al., 2017) and drawn by MG2C[4] (Chao et al., 2021).

*Cr*RLK1L or RALF protein sequences of quinoa and Arabidopsis were aligned using Muscle 3 (Edgar, 2004). The phylogenetic trees were constructed by using IQ-TREE2 with the best-fit model and 1,000 replicates of ultrafast bootstrap (Minh et al., 2020). The resulting tree files were submitted to iTOL (Letunic and Bork, 2021) for modification.

## Protein Domain Structure of Cq*Cr*RLK1Ls and CqRALFs

TBtools (Chen et al., 2020) was used to display Cq*Cr*RLK1L protein domains that were predicted by SMART. Multiple sequence alignments of CqRALFs were subjected to CLC Sequence Viewer 8[5] for visualization and the conserved residues and motifs of CqRALFs were indicated.

## RNA-Seq Analysis

NL-6 variety was used for transcriptomic analysis. For root sample, NL-6 were sown on half MS medium, and roots were

[1]http://www.arabidopsis.org

[2]http://pfam.xfam.org

[3]http://smart.embl-heidelberg.de

[4]http://mg2c.iask.in/mg2c_v2.1/

[5]https://digitalinsights.qiagen.com/products/clc-sequence-viewer-direct-download/

collected after growth under dark conditions for three days. Stamen and pistil samples were collected from newly opened flowers of quinoa after growth on soils for about seven weeks. Vegetative leaves were sampled from 14-day-old seedlings either exposed to 400 mM NaCl for 8 h or under normal conditions. These different tissue samples were immediately frozen in liquid nitrogen and stored at −80°C.

Total RNA extraction, mRNA purification, library preparation, Illumina NovaSeq 6000 paired-end (150 bp) sequencing, transcriptomic assembly and analysis were

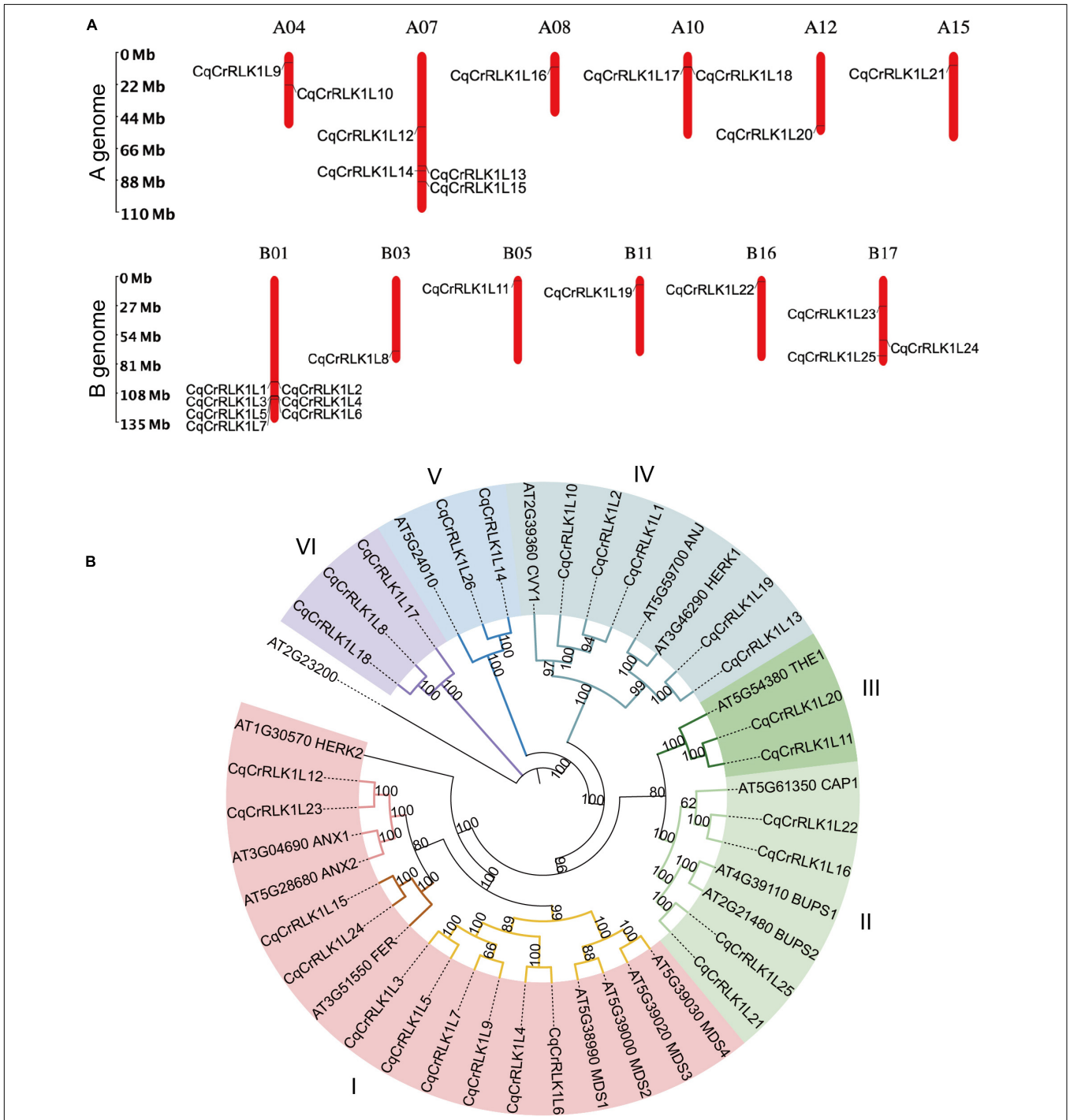


**FIGURE 1 |** Identification and characterization of *CqCrRLK1L* genes in *Chenopodium quinoa*. **(A)** Distribution of *CqCrRLK1L* genes on the chromosomes of quinoa is shown. The chromosomes of A and B genomes are presented separately. **(B)** Phylogenetic analysis of *Cr*RLK1L proteins in quinoa and Arabidopsis. The full-length amino acids of *Cr*RLK1L proteins were aligned and phylogenetic tree was generated by using IQ-TREE2 program.

all performed by Personalbio (Shanghai, China). The clean reads that were filtered from raw reads were aligned to the genome reference of quinoa NL-6 variety using HISAT2 (Kim et al., 2019). The number of read hits for each gene was calculated by HTSeq (Anders et al., 2015), and then converted into FPKM (fragments per kilobase of transcript per million reads mapped). Differential expression analysis was performed using DESeq based on the criteria: $p \leq 0.05$ and $|\log_2(\text{fold change})| \geq 1$. Heatmaps were generated by TBtools based on the row Z-Scores of FPKM values of *CqCrRLK1L* and *CqRALF* genes.

## RNA Extraction and Quantitative RT–PCR

Total RNAs of all samples were extracted by using EastepTM Super Total RNA Extraction Kit (Promega, United States). cDNAs were synthesized using HiScript III RT SuperMix for qPCR (+gDNA wiper) according to the manufacturer's instructions (Vazyme, Nanjing, China). qRT-PCR was performed using ChamQ Universal SYBR qPCR Master Mix (Vazyme, Nanjing, China) and Bio-Rad CFX connect real time detection system (BIO-RAD, United States). Primers used for qRT-PCR are listed in **Supplementary Table 11**.

## Split Luciferase Complementation Assay

*Agrobacterium* (GV3101 strain) harboring different recombinant plasmids were harvested from liquid Lysogeny Broth (LB) by centrifugation. Each strain was suspended in 10 mM $MgCl_2$ with a final concentration of $OD_{600}$ = 0.8–1.0. Then two different strains carrying indicated nLUC- and cLUC-tagged constructs were mixed with an equal volume. The mixed strains were added with 200 μM acetosyringone and 10 mM MES (pH 5.6) and incubated at room temperature for 3 h. The mixed strains were infiltrated into the leaves of *N. benthamiana* using a 1 mL disposable syringe. After 48 h, D-Luciferin was injected into the same tobacco leaves and the fluorescence was visualized by living plant imaging system (LB985 NightSHADE, Germany) after 10 min.

## Confocal Imaging

*AtFER-GFP* transgenic seeds were germinated and grown on 1/2 MS solid medium for 5 days, and then the seedlings were transferred into 1/2 liquid MS medium. After incubation overnight, the seedlings were treated with 2 μM AtmRALF22 or 2 μM CqmRALF22 peptide for 1 h before the roots were subjected to confocal imaging. GFP fluorescence was detected by Leica confocal laser scanning microscope SP8 with 488 nm excitation light and 510–550 nm emission light.

# RESULTS

## Identification and Characterization of *Cr*RLK1L Family Proteins in Quinoa

To identify *Cr*RLK1L family proteins in quinoa, we aligned the sequences of all 17 Arabidopsis *Cr*RLK1Ls proteins against the protein database of quinoa. Because quinoa QQ74 variety genome is currently the most well annotated genome (Jarvis et al., 2017), we explored this genome as a reference in this study. Combining the information of sequence similarity and the canonical malectin and kinase domains of C*r*RLK1L family proteins, totally 26 *Cr*RLK1L-like proteins were identified in quinoa, which were designed as Cq*Cr*RLK1L1 to Cq*Cr*RLK1L26 based on their locations on chromosomes, and these proteins were all predicted to be localized at plasma membrane (**Supplementary Table 1**). Quinoa genome consists of 18 chromosomes, and 25 *CqCrRLK1L* genes have been annotated on these chromosomes, while only *CqCrRLK1L26* has not been mapped yet (**Figure 1A**). Interestingly, *CqCrRLK1L3-CqCrRLK1L6* were tandemly localized on chr1, and protein sequences alignment showed that Cq*Cr*RLK1L3 and Cq*Cr*RLK1L5 share 100% protein identity, while Cq*Cr*RLK1L4 and Cq*Cr*RLK1L6 share an identity of 89.2%, implying a tandem duplication event occurred in this region. Besides, Cq*Cr*RLK1L1 and Cq*Cr*RLK1L2 as well as Cq*Cr*RLK1L17 and Cq*Cr*RLK1L18 are closely located on chr1 and chr10, respectively (**Figure 1A**). *Cr*RLK1L family proteins are characterized by their malectin domain and kinase domain. We performed protein structural analysis and found that all 26 Cq*Cr*RLK1L proteins harbor a canonical extracellular malectin-like domain and a cytosolic kinase domain (**Supplementary Figure 1**).

To understand the evolutionary relationship of these Cq*Cr*RLK1L proteins with their equivalents in Arabidopsis, phylogenetic analysis was performed (**Figure 1B**). The *Cr*RLK1L proteins were classified into six subgroups based on homology between Arabidopsis and quinoa, and for most of *Cr*RLK1L proteins in Arabidopsis, their counterparts were identified in quinoa (**Figure 1B**). In Arabidopsis, several C*r*RLK1L proteins, including AtFER, AtTHE1, AtCAP1, AtANX1/2, AtBUPS1/2, AtHERK1, AtANJ, and AtCVY1, have been well characterized. In quinoa, two copies of CqFER (Cq*Cr*RLK1L15/Cq*Cr*RLK1L24), CqTHE1 (Cq*Cr*RLK1L11/Cq*Cr*RLK1L20), CqCAP1 (Cq*Cr*RLK1L16/Cq*Cr*RLK1L22), CqANX1/2 (Cq*Cr*RLK1L12/Cq*Cr*RLK1L23), CqBUPS1/2 (Cq*Cr*RLK1L21/Cq*Cr*RLK1L25), and CqHERK1/ANJ (Cq*Cr*RLK1L13/Cq*Cr*RLK1L19), and three copies of CqCVY1 (Cq*Cr*RLK1L1/Cq*Cr*RLK1L2/Cq*Cr*RLK1L10) were identified (**Figure 1B**). Notably, for each of these duplicates they were identified on A genome and B genome of quinoa, respectively (**Figure 1A**), suggesting that they originated from the two ancestors of quinoa.

## Tissue-Specific Expression Patterns of *CqCrRLK1L* Genes

In Arabidopsis, *CrRLK1L* genes are expressed in a tissue-specific pattern. For example, *AtFER* is ubiquitously expressed in both vegetative and reproductive tissues, while *AtANX1/2* and *AtBUPS1/2* are dominantly expressed in pollen tubes (Franck and Westermann, 2018). To understand whether *CqCrRLK1Ls* genes in quinoa also exhibit tissue-specific expression patterns, we collected leaf, root, stamen, and pistil tissues of quinoa NL-6 variety, and performed RNA-seq analysis. Three independent replicates were conducted for

each tissue. Based on the criterion that the reads matched to genes should be detected in all three independent replicates, totally 32,368, 35,204, 31,257, and 36,068 genes were expressed in leaves, roots, stamen, and pistil, respectively. Combining all these four samples, totally 40,456 genes were detected in our RNA-seq data (**Supplementary Table 2**), accounting for approximately 69% of predicted genes in quinoa. Among these genes, 462 were specifically expressed in leaf, 1935 were specifically expressed in root, 901 were specifically expressed in stamen, and 1098 were specifically expressed in pistil (**Supplementary Table 3**).

By using these RNA-seq data, we analyzed the expression of all *CqCrRLK1L* genes. For the 26 *CqCrRLK1L* genes in quinoa QQ74 variety, 25 of them were identified in quinoa NL-6 variety (**Supplementary Table 1**). RNA-seq data showed that the expressions of 23 *CqCrRLK1L* genes were detected in all four or specific tissues, while two genes *CqCrRLK1L3* and *CqCrRLK1L9* were not or weakly detected in all four RNA-seq samples (**Supplementary Table 4**). We then analyzed the expression patterns of the 23 *CqCrRLK1L* genes in different tissues. *CqAUX1/2* and *CqBUPS1/2* were dominantly expressed in stamen, while *CqCrRLK1L7*, *CqCrRLK1L17*, and *CqCrRLK1L18* were mainly expressed in pistil. *CqACAP1* was mainly detected in root, and *CqHERK1* and *CqCURVY1* were relatively highly expressed in root and pistil. *CqTHE1*, *CrRLK1L14*, and *CrRLK1L26* were evenly expressed in leaf, root, and pistil. Similar to *AtFER* in Arabidopsis, *CqFER* was ubiquitously expressed in all four tissues (**Figure 2**). Remarkably, two copies of *CqFER*, *CqANX1, CqBUPS1/2*, *CqHERK1*, *CqCAP1*, *CqCVY1*, and *CqTHE1* exhibited very similar expression patterns (**Figure 2**), corroborating that they are the duplicated genes originating from the two ancestors of quinoa. Collectively, these results suggested that *CqCrRLK1L* genes in quinoa also exhibit tissue-specific expression patterns, and the expression patterns are reminiscent of their paralogs in Arabidopsis.

## Transcriptional Analysis of *CqCrRLK1L* Genes in Response to Salt Stress

Studies have shown that AtFER, AtTHE1, and AtHERK1 are involved in the regulation of salt tolerance in Arabidopsis (Zhao et al., 2018; Gigli-Bisceglia et al., 2020). To decipher whether salt stress affects the expression of *CqCrRLK1L* genes in quinoa, we performed RNA-seq analysis for the leaves of quinoa NL-6 variety before and after salt treatment. Totally three independent biological replicates were performed. RNA-seq data revealed that 2,772 genes were significantly up-regulated (fold change $>$ 2, $p$ value $<$ 0.05), while 3096 genes were significantly down-regulated after salt treatment (fold change $>$ 2, $p$ value $<$ 0.05) (**Supplementary Table 5**).

Based on RNA-seq data, we found that the expression of *CqFER*, *CqTHE1*, and *CqHERK1* genes was not significantly changed after NaCl treatment based on the criterion of fold change $>$ 2, (**Figure 3A** and **Supplementary Table 6**), which is consistent with that reported in Arabidopsis (Zhao et al., 2021). These results suggested that the responses of these three *CrRLK1L* genes to salt stress were not regulated at a transcriptional level. Nevertheless, RNA-seq data showed that the expression of 21 *CqCrRLK1L* genes was increased after salt stress, and among of them three *CqCrRLK1L* genes, *CqCrRLK1L5*, *CqCrRLK1L7*, and *CqCrRLK1L9*, were significantly up-regulated after salt treatment (fold change $>$ 2, $p$ value $<$ 0.05). Specifically, *CqCrRLK1L9* was increased more than 30-fold, *CqCrRLK1L7* was increased around 10-old, and *CqCrRLK1L5* was increased 3.7-fold (**Figure 3A** and **Supplementary Table 6**). qRT-PCR analysis verified that the transcript levels of *CqCrRLK1L5*, *CqCrRLK1L7*, and *CqCrRLK1L9* were dramatically increased after salt treatment (**Figure 3B**). Intriguingly, these three genes are grouped in a same cluster in the phylogenetic tree and the close homologs of these genes were not identified in Arabidopsis (**Figure 1B**), implying that these three genes may function redundantly and uniquely in quinoa to regulate salt stress response. Our RNA-seq data showed that, although *CqCrRLK1L21_BUPS1/2* was dominantly expressed in reproductive tissues, its expression was also weekly detected in leaves, and salt stress treatment significantly repressed its expression (fold change $>$ 2, $p$ value $<$ 0.05) (**Figure 3A** and **Supplementary Table 6**). Independent qRT-PCR was also performed to validate the expression of *CqCrRLK1L21_BUPS1/2* gene before and after salt stress, but due to its extremely low expression level, the expression of this gene in leaves could not be effectively detected by using qRT-PCR assay.

## Tissue-Specific Expression Patterns of *CqRALFs* in Quinoa

It has been experimentally demonstrated that RALFs are the ligands of *Cr*RLK1L family proteins, and there are approximately 37 RALFs in Arabidopsis (Abarca et al., 2021). By aligning all these AtRALFs against the database of both quinoa QQ74 and NL-6 varieties, 18 paralogs were identified and these genes were named as *CqRALF1-CqRALF18* based on their locations on chromosomes (**Supplementary Table 7**). Notably, *CqRALF3* and *CqRALF4*, as well as *CqRALF15* and *CqRALF16*, are tandemly arrayed on quinoa chromosomes, and the genomic sequences of all these four genes were identified in the genome of both QQ74 and NL-6 varieties. However, in the latter genome, both *CqRALF3*/*CqRALF4* and *CqRALF15*/*CqRALF16* pairs were annotated as one gene (**Supplementary Table 7**), and they need to be manually corrected in the new version of genome annotation.

In analogy to AtRALFs, the typical features of RRXL motif, YISY motif, and four conserved cysteines were also identified in all 18 CqRALF peptides (**Supplementary Figure 2**), corroborating that these motifs are evolutionarily conserved and are critical for RALFs to conduct their functions. Phylogenetic analysis between quinoa and Arabidopsis showed that the well-studied AtRALF1, AtRALF22, and AtRALF23 peptides in Arabidopsis were closely associated with CqRALF3, CqRALF4, CqRALF15, and CqRALF16, while AtRALF4 and AtRALF19, which are specifically expressed in pollen tubes and participates in the regulation of pollen tube growth in Arabidopsis (Ge et al., 2017), were closely linked to CqRALF2 and CqRALF17 (**Figure 4A**).

Transcriptomic analysis showed that all these *CqRALF* genes were detected in all or either of the four tissues

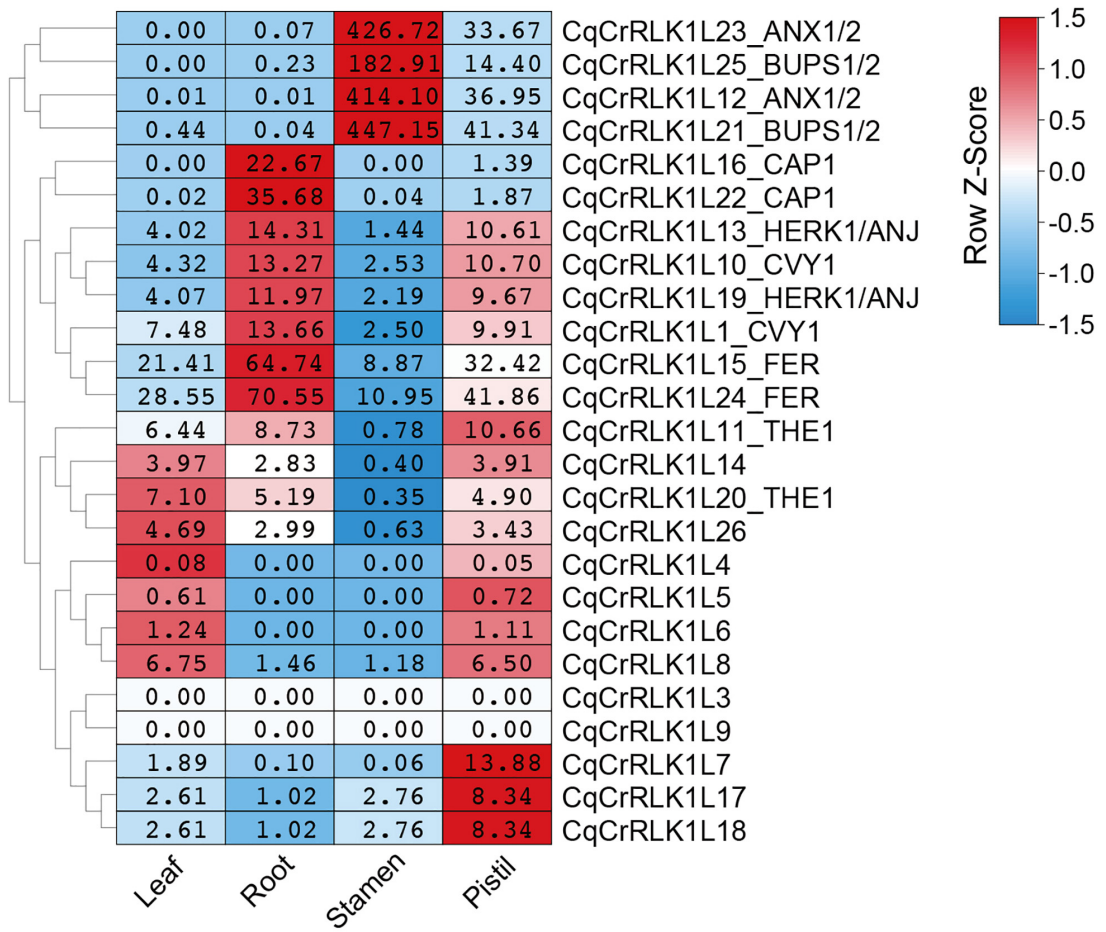


**FIGURE 2 |** Tissue-specific expression pattern of *CqCrRLK1L* genes in quinoa. RNA-seq analysis was performed for the leaf, root, stamen, and pistil tissues of quinoa, and three independent replicates were conducted for each tissue. For each replicate, 8 quinoa roots were collected from three-day-old seedlings grown on half MS medium under dark conditions; more than 80 stamens and 30 pistils were sampled from newly opened flowers after growth on soils for seven weeks; all vegetative leaves were collected from four independent 14-day-old seedlings. The expression of each *CqCrRLK1L* gene in all four tissues was analyzed based on RNA-seq data. For each *CqCrRLK1L* gene, its expression in four tissues was normalized by row scale before plotting. Different colors in the heatmap indicate the relative expression level of each gene in different tissues based on the row Z-scores of the fragments per kilobase of transcript per million reads mapped (FPKM), while the digital numbers presented in the heatmap cells indicate the accurate values of the averaged FPKM of the three independent biological replicates.

(**Supplementary Table 8**). Specifically, *CqRALF2* and *CqRALF17* were extremely highly expressed in stamen, and less expressed in pistil, but their transcripts were not detected at all in leaves and roots (**Figure 4B** and **Supplementary Table 8**). This expression pattern was reminiscent of their paralogs *AtRALF4* and *AtRALF19* in Arabidopsis (Ge et al., 2017), suggesting that these two *CqRALFs* may specifically participate in the regulation of reproduction process. *CqRALF6* and *CqRALF10* were highly expressed in pistil, but not expressed in stamen. *CqRALF8* and *CqRALF12* were dominantly expressed in leaves and roots, and weakly expressed in stamens and pistils (**Figure 4B** and **Supplementary Table 8**). Interestingly, *CqRALF9* and *CqRALF18* were only expressed in roots, but not expressed in other tissues (**Figure 4B** and **Supplementary Table 8**), suggesting that they may play a pivotal role in the regulation of root development. These results indicated that, similar to the *RALFs* in other plant species, *RALFs* in quinoa also exhibited obvious tissue-specific expression patterns. We also analyzed the expression of these *CqRALF* genes in response to salt stress, and none of them were significantly affected after salt treatment (fold change $> 2$, $p$ value $< 0.05$) (**Supplementary Table 9**).

## CqRALF15 Is Physically Associated With CqFER and AtFER

AtRALFs are physically associated with At*Cr*RLK1L proteins in Arabidopsis (Stegmann et al., 2017; Zhao et al., 2018). To test whether this is also the case in quinoa, we chose CqRALF15, a CqRALF with the best hit after aligning AtRALF22 with quinoa genome, and analyze its interaction with CqFER. Split-LUC assay indicated that CqRALF15 interacts with the ectodomain of CqFER (CqFER$^{ecto}$) (**Figure 5A**), which verified the formation of RALF-FER complex in plants. Besides, split-LUC assay indicated that AtRALF22 from Arabidopsis also interacts with CqFER$^{ecto}$,

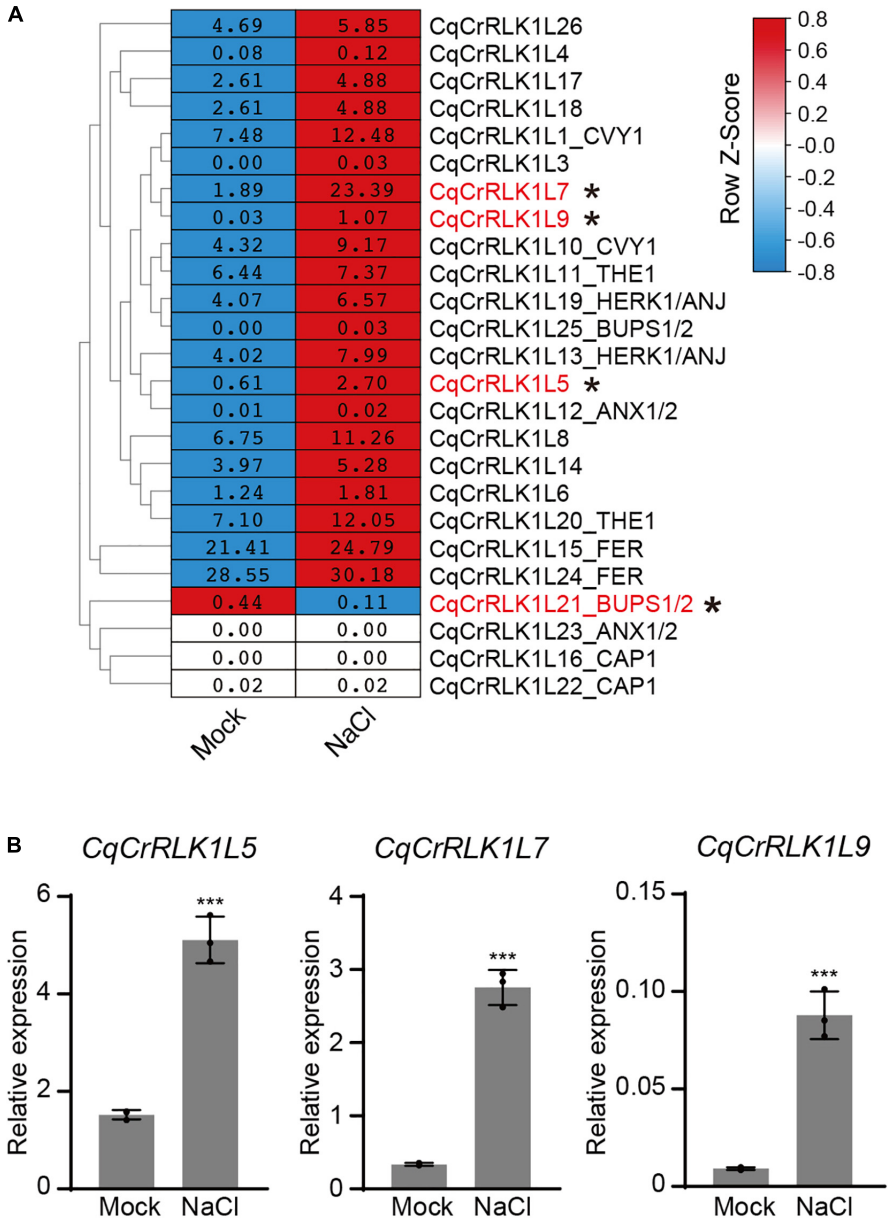


**FIGURE 3 |** Analysis of the expression of *CqCrRLK1L* genes in response to salt stress. **(A)** RNA-seq analysis was performed for the leaves of quinoa before and after NaCl treatment. 14-day-old seedlings were treated with or without 400 mM NaCl for 8 h, and for each replicate all vegetative leaves from four different plants of the same treatment were collected and totally three replicates were conducted. The mean FPKM value of each *CqCrRLK1L* gene was normalized by row scale before plotting. Different colors in the heatmap indicate the relative expression level of each gene before and after NaCl treatment based on the row Z-scores of FPKM, while the digital numbers presented in the heatmap cells represent the averaged FPKM of the three independent biological replicates. Differential expression analysis was performed using DESeq, and the *CqCrRLK1L* genes that were significantly up-regulated or down-regulated ($p \leq 0.05$ and $|\log_2(\text{fold change})| \geq 1$) are marked by asterisks. **(B)** Quantitative real-time (qRT)-PCR analysis of *CqCrRLK1L5*, *CqCrRLK1L7*, and *CqCrRLK1L9* genes before and after NaCl (400 mM) treatment. qRT-qPCR assay was performed using samples independent of RNA-seq samples. *CqEF1a* was used as an internal control. Values are the means ± SD of three biological replicates. Asterisks indicate statistically significant differences (***$p < 0.001$, Student's *t*-test).

and CqRALF15 interacts with AtFER$^{ecto}$ (**Figure 5A**), indicating that RALFs and FER from quinoa and Arabidopsis are conserved in their physical interactions.

Studies have shown that treatment of *AtFER-GFP* transgenic plants with exogenous mature AtRALFs triggers the internalization of AtFER that colocalizes with the endocytic tracer FM4-64 in Arabidopsis (Zhao et al., 2018; Yu et al., 2020). Here, to further clarify the functional conservation of RALFs in Arabidopsis and quinoa, we synthesized mature AtRALF22 (AtmRALF22) and mature CqRALF15 (CqmRALF15) peptides (**Supplementary Table 10**). Under normal conditions, AtFER-GFP fusion protein was dominantly localized at plasma

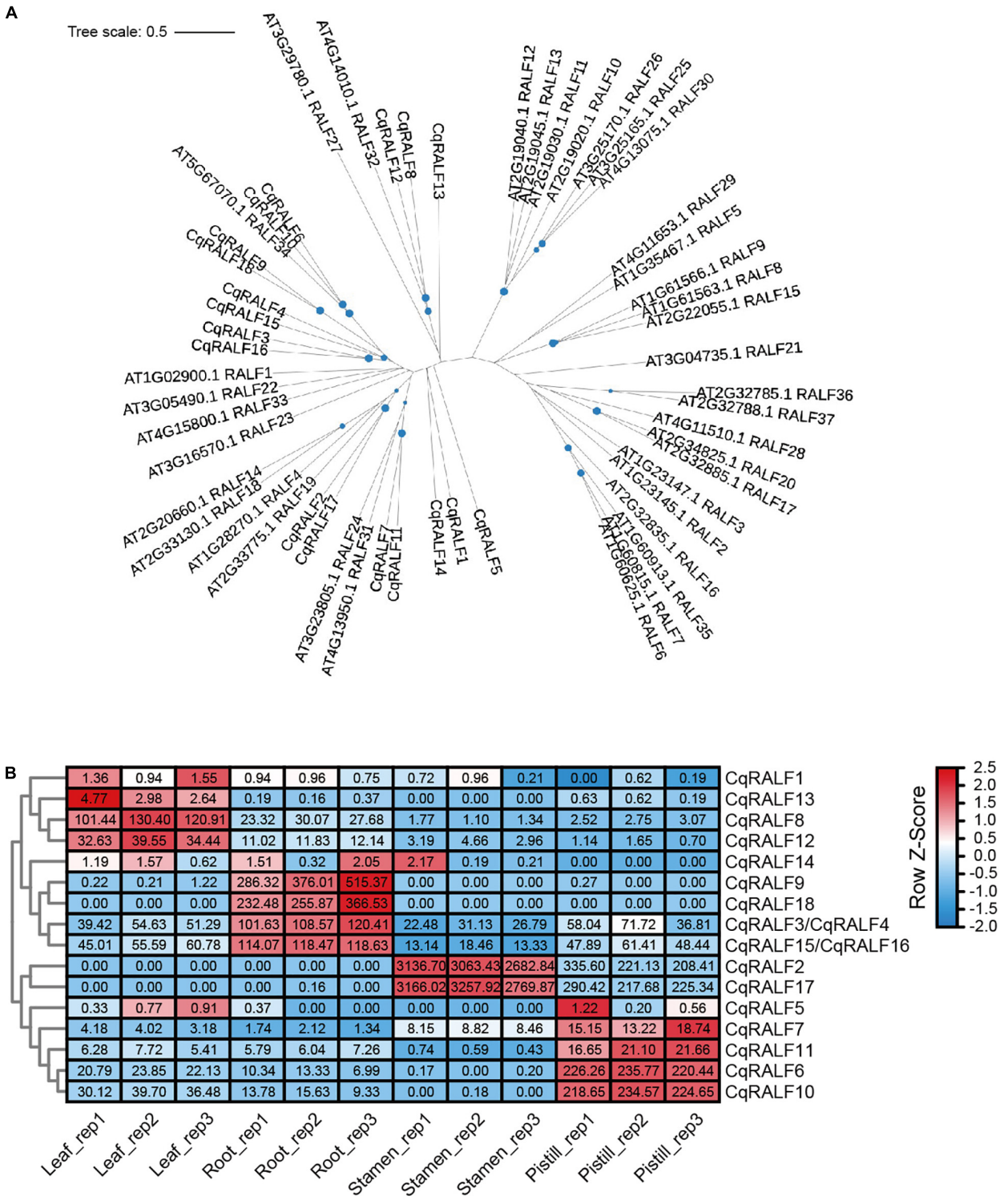


**FIGURE 4 |** Characterization of *CqRALFs* in quinoa. **(A)** Phylogenetic analysis of RALFs in quinoa and Arabidopsis. The full-length amino acids of RALF peptides were used for phylogenetic analysis, and phylogenetic tree was generated by using IQ-TREE2 program. **(B)** Analysis of the tissue-specific expression patterns of *CqRALFs* in leaf, root, stamen, and pistil tissues of quinoa. The RNA-seq data used for gene expression analysis are the same as that described in **Figure 2**. The FPKM values of each *CqRALF* gene in four tissues were normalized by row scale before plotting. Different colors in the heatmap indicate the relative expression level of each gene in different tissues based on the row Z-scores of FPKM, while the digital numbers presented in the heatmap cells represent the accurate FPKM values in three independent biological replicates. Notably, *CqRALF3*/*CqRALF4* and *CqRALF15*/*CqRALF16* pairs were annotated as one gene in the current version of NL-6 genome annotation.

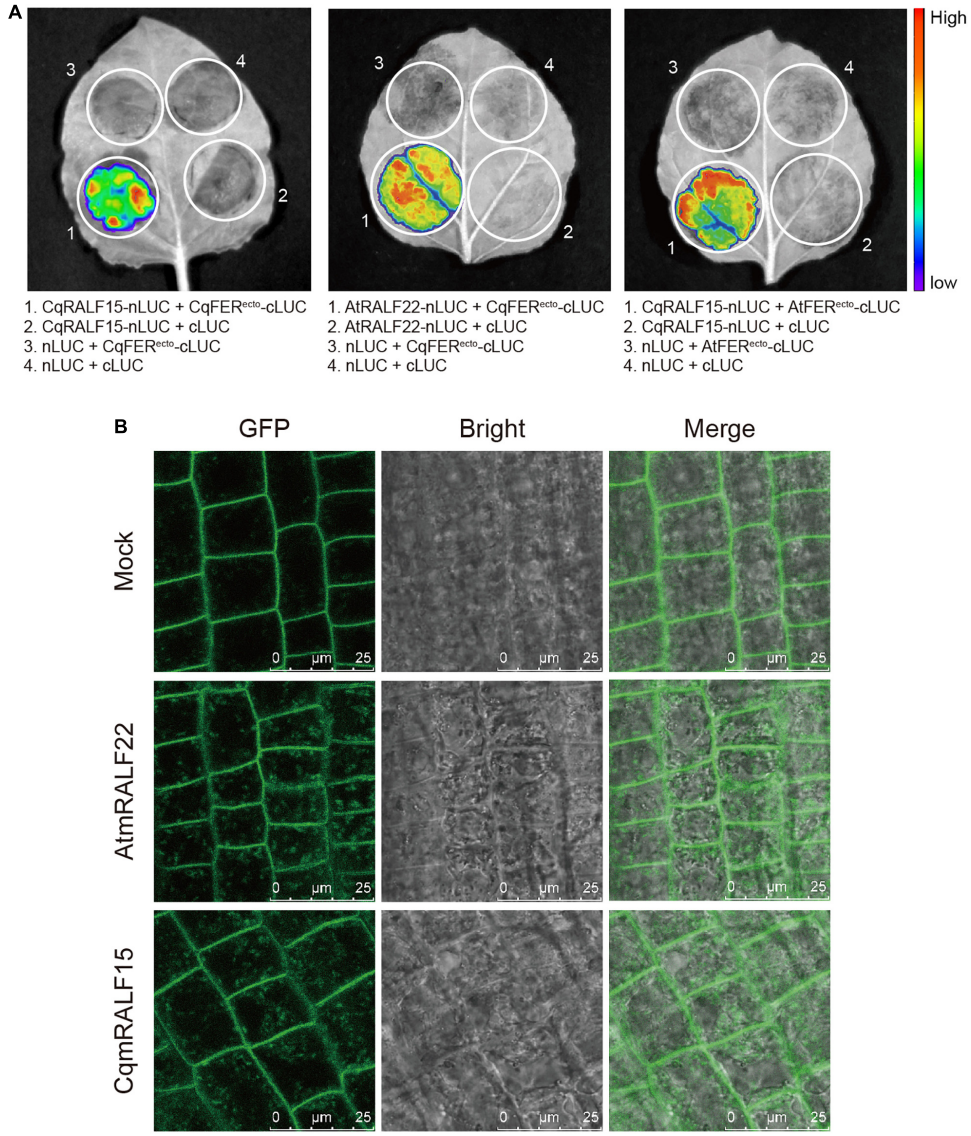


**FIGURE 5 |** CqRALF15 interacts with both CqFER and AtFER. **(A)** Split luciferase complementation assays showing the interactions of CqRALF15 with the ectodomain of CqFER (CqFER$^{ecto}$) and AtFER (AtFER$^{ecto}$), as well as the interaction of AtRALF22 with CqFER$^{ecto}$. Fluorescence was detected at 48 h after infiltration of the indicated constructs. **(B)** Analysis of the internalization of FER-GFP after mature RALF peptides treatment. Six-day-old seedlings were treated without or with 2 μM CqmRALF15 or AtmRALF22 for 1 h. Fluorescence in root cells were detected using confocal laser scanning microscopy. Bar = 25 μm.

membrane. Application of AtmRALF22, however, rapidly triggered the internalization of FER-GFP (**Figure 5B**). Similarly, treatment of seedlings with CqmRALF15 was also able to trigger the internalization of FER-GFP (**Figure 5B**), verifying that AtRALF22 and CqRALF15 are functionally conserved.

## CqmRALF15 and AtmRALF22 Inhibits Root Growth in Both Quinoa and Arabidopsis

RALFs are well characterized by their ability to inhibit root growth (Haruta et al., 2014), so we tested the influence of mature RALF peptides on the root growth of quinoa. Our results showed that both CqmRALF15 and AtmRALF22 inhibited root elongation in quinoa (**Figures 6A,B**). Notably, with a same concentration, CqmRALF15 had a more serious effect than AtmRALF22 on root growth inhibition in quinoa (**Figures 6A,B**). We also treated Arabidopsis seedlings with CqmRALF15 and AtmRALF22, and found that these two mature RALFs exhibited a comparable effect on root growth inhibition in Arabidopsis (**Figures 6C,D**). It is known that AtRALF1-mediated root growth inhibition depends on its receptor AtFER (Haruta et al., 2014). Here both CqmRALF15- and AtmRALF22-triggered root growth inhibition was abolished in *fer-4* mutant (**Figures 6C,D**), indicating that CqmRALF15 and AtmRALF22 exhibit a similar biological function via FER-mediated signaling pathways.

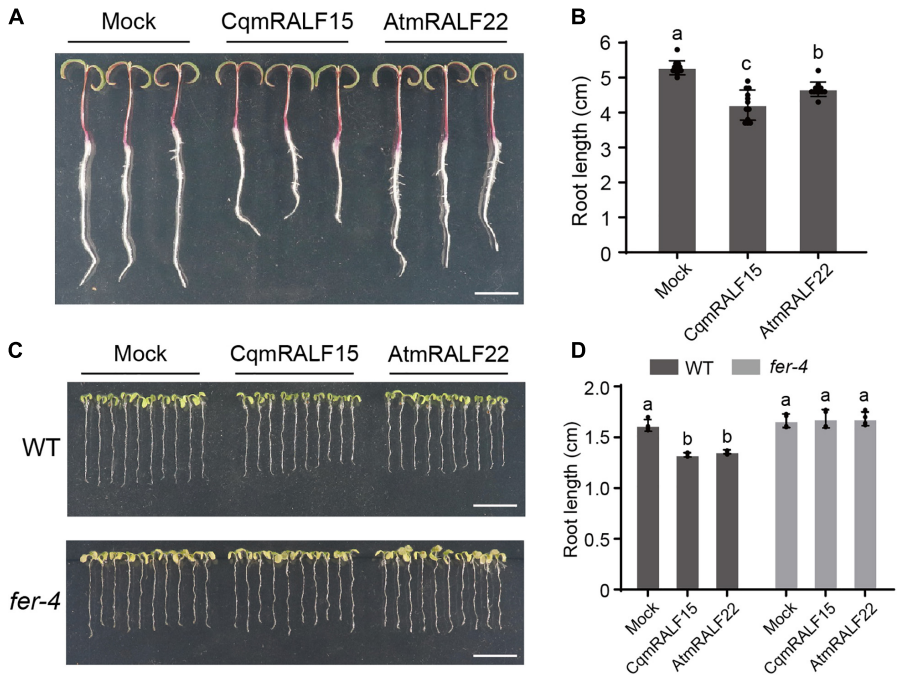


**FIGURE 6 |** CqmRALF15 and AtmRALF22 inhibit the root growth of both quinoa and Arabidopsis. **(A)** Two-day-old seedlings of quinoa NL-6 treated with 2 μM CqmRALF15 or AtmRALF22. The picture was photographed after treatment for 3 days. Bar = 1 cm. **(B)** Measurement of the root length of quinoa seedlings shown in panel **(A)**. Values are the means ± SD ($n$ = 12 seedlings). Different letters indicate statistically significant differences ($p < 0.01$, one-way ANOVA). **(C)** Arabidopsis wild type seedlings treated with CqmRALF15 or AtmRALF22. Five-day-old wild type and *fer-4* seedlings grown in liquid medium overnight were treated with 2 μM CqmRALF15 or AtmRALF22. After treatment for 6 days, the seedlings were placed on solid MS medium for photograph. Bar = 1 cm. **(D)** Quantification of the root length of seedlings shown in panel **(C)**. Values are the means of four independent replicates ± SD (n = 10–15 for each replicate). Different letters indicate statistically significant differences ($p < 0.01$, one-way ANOVA).

## Overexpression of *CqRALF15* in Arabidopsis Leads to Leaf Bleaching Phenotype Under High Salinity

In Arabidopsis, FER was shown to be involved in salt tolerance (Feng et al., 2018; Zhao et al., 2018), so we were interested in elucidating whether CqFER in quinoa is also required for salt tolerance. Because genetic transformation in quinoa is still technically challenging, we attempted to transform *CqFER* construct to *fer-4* mutant in Arabidopsis and test whether *CqFER* can complement the leaf bleaching phenotype of *fer-4* mutant under salt stress. However, we failed to generate *CqFER* transgenic construct, because this construct was unstable in *Escherichia coli* strain DH5α grown under different growth conditions. More than 12 independent strain clones were selected for plasmid isolation and Sanger sequencing, but only *CqFER* constructs with missense/non-sense mutations or truncated fragments were obtained. We speculated that the instability of *CqFER* construct is because of the constitutive kinase activity of CqFER, which may be detrimental to *E. coli*. This assumption was supported by the fact that correct FER construct was successfully obtained when K551, an ATP binding residue that is essential for the kinase activity of CqFER, was substituted with alanine.

Similar to *fer-4* mutant, Arabidopsis plants overexpressing *RALF22* or *RALF23* exhibit leaf bleaching phenotype under salt stress (Zhao et al., 2018). We then generated *CqRALF15* construct driven by 35S promoter and transformed this construct to wild type Arabidopsis plants. qRT-PCR analysis showed that *CqRALF15* was highly expressed in the transgenic plants (**Figure 7A**). Phenotype analysis showed that overexpression of *CqRALF15* in Arabidopsis results in enhanced leaf bleaching phenotype under high salinity (**Figures 7B,C**), indicating that *CqRALF15* in quinoa also participates in the regulation of salt tolerance. In addition, it has been reported that Arabidopsis plants overexpressing *AtRALF22* or *AtRALF23* exhibit dwarf phenotype, which is caused by the over-activation of JA signaling pathway (Guo et al., 2018; Zhao et al., 2021). Here, *CqRALF15*-overexpressing plants exhibited a smaller plant size and higher expression levels of JA-responsive genes, such as *PDF1.2*, *PDF1.3*, and *CYP71A20*, than the wild type plants (**Figures 7D,E**), suggesting that *CqRALF15* is also involved in the regulation of plant growth and JA signaling pathway.

## DISCUSSION

With increasing efforts on the study of *CrRLK1L* and *RALF* family genes, the importance of these genes in the regulation of plant development and stress responses has been highlighted in the past decade. Therefore, identification and characterization of *CrRLK1L* and *RALF* family genes in different plant species will advance our understanding of the roles of *CrRLK1L* and *RALF*

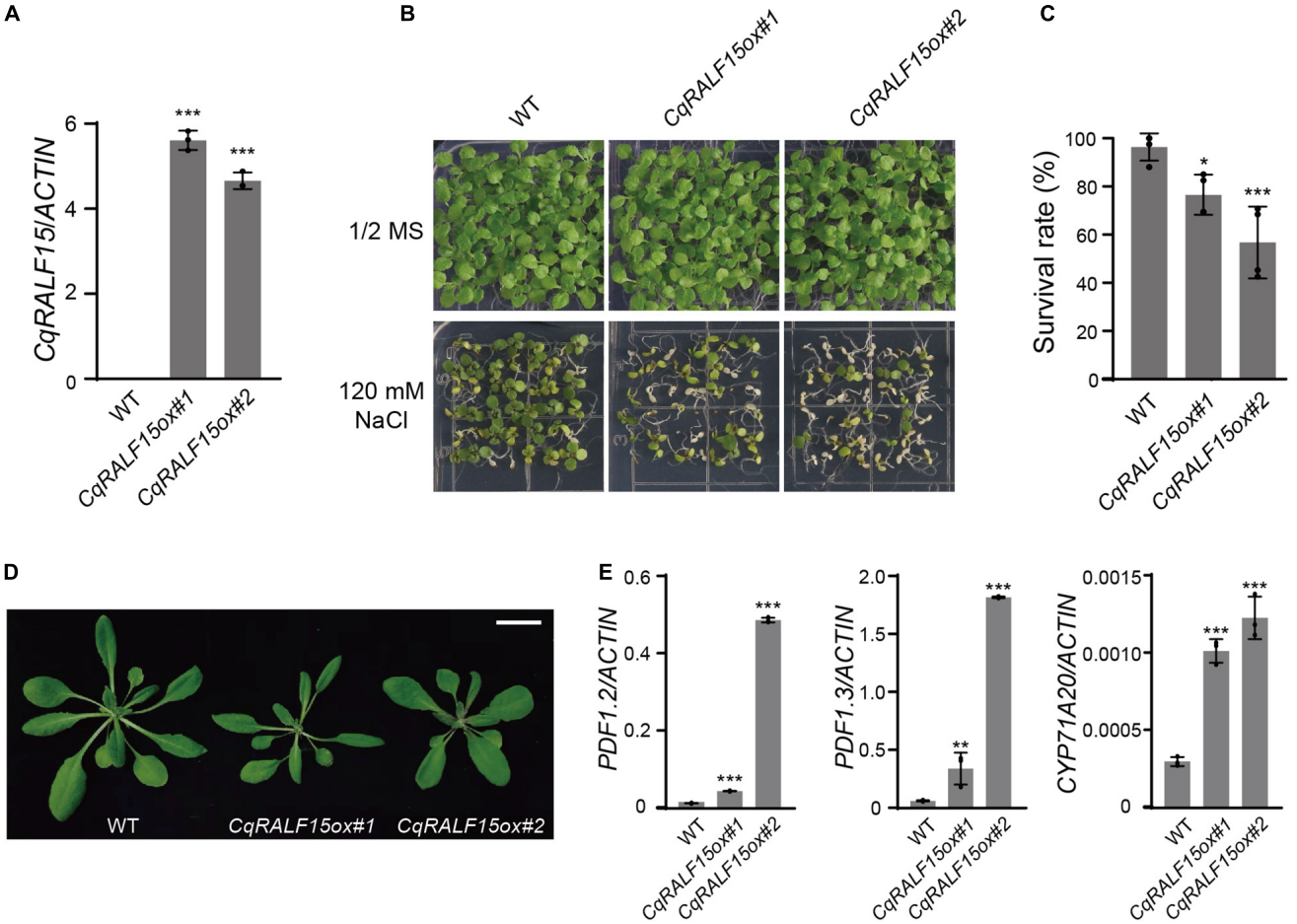


**FIGURE 7 |** Arabidopsis transgenic plants overexpressing *CqRALF22* exhibit enhanced leaf bleaching under salt stress. **(A)** qRT-PCR analysis of *CqRALF22* transcript level in *CqRALF22* transgenic plants in Arabidopsis. *ACTIN* gene was used as an internal control. Values are the means ± SD of three biological replicates. Asterisks indicate statistically significant differences (***p < 0.001, Student's *t*-est). **(B)** Phenotype of 12-day-old seedlings grown on 1/2 MS medium supplemented without or with NaCl (120 mM). **(C)** Survival rate of seedlings grown on NaCl medium (120 mM). The seedlings with full leaf bleaching were considered as dead plants. Values are the means ± SD of four biological replicates ($n$ = 42 seedlings). Asterisks indicate statistically significant differences (*$p < 0.05$, ***$p < 0.001$, Student's *t*-test). **(D)** Phenotype of each genotype grown in soil for 25 days. Bar = 2 cm. **(E)** Analysis of the expression of *PDF1.2*, *PDF1.3*, and *CYP71A20* genes in *CqRALF22*-overexpressing plants. Values are the means ± SD of three biological replicates. Asterisks indicate statistically significant differences (**$p < 0.01$, ***$p < 0.001$, Student's *t*-test).

genes at both evolutionary and plant species-specific levels. In this study, we performed a genome-wide analysis for *CrRLK1L* and *RALF* family genes in quinoa and identified 26 *CqCrRLK1L* and 18 *CqRALF* genes, respectively. The number of *CrRLK1L* genes in quinoa is more than that in Arabidopsis, which is because of the allotetraploid property of quinoa that contains duplicated genes originating from two ancestors. Compared with approximately 37 *RALF* genes in Arabidopsis (Abarca et al., 2021), the amount of *RALF* genes in quinoa is much less, which could be due to evolutionary divergence or different terrestrial habitats. Because current quinoa genome assembly and annotations have not been fully completed yet, we still cannot exclude the possibility that some *CqRALF* genes were missing in our analysis.

*Cr*RLK1L family proteins share similar protein structural domains, but different family members exhibit distinct biological functions, which is to some extent caused by the tissue-specific expression patterns of these *CrRLK1L* genes (Franck and Westermann, 2018). One of the best examples in Arabidopsis is that *AtBUPS1* and *AtBUPS2* are specifically expressed in pollen tube and they are required for pollen tube elongation (Ge et al., 2017). In quinoa, *CqBUPS1/2* was dominantly expressed in stamen, suggesting that *CqBUPS1/2* probably also contribute to the regulation of pollen tube growth in quinoa. Currently, FER is considered as one of the most important *Cr*RLK1L family proteins, because it participates in multiple biological processes, including cell expansion, root hair growth, fertility, plant immunity, and abiotic stress response (Duan et al., 2010; Haruta et al., 2014; Stegmann et al., 2017; Zhao et al., 2018; Huang et al., 2020; Ortiz-Morea et al., 2020; Zhong et al., 2022). These biological functions coincide with the ubiquitous expression of *AtFER* in leaf, primary root, root hair, and ovule

in Arabidopsis (Franck and Westermann, 2018). RNA-seq data showed that *CqFER* was also highly expressed in leaf, root, and pistil in quinoa, indicating that *CqFER* probably exhibits similar biological functions as *AtFER*. Together, these results not only elucidate the tissue-specific expression patterns of *CrRLK1L* family members in quinoa, but also reveal that the expression patterns of *CrRLK1L* genes are conserved in different plant species. Similarly, *RALF* genes in quinoa also exhibited an obvious tissue-specific expression pattern, suggesting that different *CqRALFs* may execute distinct biological functions depending on the tissues they are expressed. For those *CqRALF* genes that are specifically expressed in reproductive tissues or in roots, their roles in fertility and root development merits further investigations. Besides, which Cq*Cr*RLK1Ls and CqRALFs are coupled in quinoa to regulate a specific physiological process requires further exploration.

Transcriptome profiling indicated that the transcript levels of *FER*, *THE1*, and *HERK1*, which are required for salt tolerance in plants (Zhao et al., 2018; Gigli-Bisceglia et al., 2020), are not significantly up-regulated after salt treatment in both quinoa and Arabidopsis (Zhao et al., 2021), suggesting that these three proteins may undergo posttranslational modifications in response to salt stress. It has been reported that ABA, a major phytohormone responsive to abiotic stress, can trigger the phosphorylation of FER (Chen et al., 2016). Therefore, whether these three *Cr*RLK1L proteins undergo phosphorylation modifications upon exposure to salt stress needs to be addressed in future. Interestingly, RNA-seq data revealed that the expression of three phylogenetically clustered *CqCrRLK1L* genes in quinoa was highly up-regulated after salt treatment, indicating that partial *CqCrRLK1L* genes are transcriptionally regulated in response to salt stress. Because the close paralogs of these three *CqCrRLK1L* genes do not exist in Arabidopsis, it will be quite interesting to investigate whether they uniquely evolved in quinoa and confer quinoa to tolerate high concentration of salts.

*RALFs* are identified in a wide range of land plants but not in charophytes, while *CrRLK1Ls* are found in both land plants and charophytes, suggesting that *RALFs* probably emerged later than *CrRLK1Ls* during evolution (Zhu et al., 2021). Evolutionary study indicates that *RALFs* experienced rapid expansion after separation of eudicot and monocot species, and the number of *RALFs* varies greatly among different plant species, implying that *RALFs* appeared accompanied by plant adaptation to different terrestrial habitats (Cao and Shi, 2012). Although the number of *RALFs* in quinoa is less than that in Arabidopsis, *CqRALF15* and its Arabidopsis paralog AtRALF22 exhibited similar functions, as both of them interacted with FER protein and triggered the internalization of AtFER. Besides, in analogy to mature *AtRALF22*, application of mature *CqRALF15* inhibited the root growth of both quinoa and Arabidopsis. These results suggest that RALF paralogs in quinoa and Arabidopsis are functionally conserved. In Arabidopsis, overexpression of *AtRALF22* or *AtRALF23* leads to pronounced leaf bleaching under salt stress (Zhao et al., 2018), and here the Arabidopsis plants overexpressing *CqRALF15* also exhibited enhanced leaf bleaching under salt stress, indicating that *CqRALF15* processes a similar function as *AtRALF22/23* in the regulation of salt tolerance. In future, whether other *CqRALFs* also participate in salt stress response needs to be further studied.

Quinoa is a natural halophyte, and the mechanisms underlying its salt tolerance have gained increasing attention, but to date salt tolerance mechanisms in quinoa still lack molecular insights. Elucidation of the roles of Cq*Cr*RLK1Ls and CqRALFs in the regulation of salt tolerance will guide us to take a close view of the functional specificity of Cq*Cr*RLK1Ls and CqRALFs in quinoa and lay a foundation for mechanical insights of salt tolerance in quinoa. EBCs are the typical feature that confers salt tolerance in quinoa. In future, the expression of *CqCrRLK1Ls* and *CqRALFs* in EBCs after salt treatment needs to be investigated, especially for those genes that are required for the regulation of salt stress response.

## DATA AVAILABILITY STATEMENT

The datasets presented in this study can be found in online repositories. The RNA-seq data have been deposited in the NCBI GEO under accession number: GSE198572.

## AUTHOR CONTRIBUTIONS

WJ, CL, and CZ contributed to conception and design of the study. WJ and CL performed the most of experiments. YLL and ZW assisted the growth of quinoa. LL and HZ conducted genome assembly and annotation of quinoa NL-6. FYu, FYi, and JZ provided quinoa materials. HZ and J-KZ participated in scientific discussions. YL and CZ supervised the research. CZ wrote the manuscript with the contributions of WJ and CL. All authors contributed to the article and approved the submitted version.

## FUNDING

This work was supported by Shanghai Agriculture Applied Technology Development Program, China (Grant No. X20200101).

## SUPPLEMENTARY MATERIAL

The Supplementary Material for this article can be found online at: https://www.frontiersin.org/articles/10.3389/fpls.2022.918594/full#supplementary-material

**Supplementary Figure 1 |** Protein structural analysis of Cq*Cr*RLK1L proteins. Predicted domains in each Cq*Cr*RLK1L protein are shown. Signal peptide, malectin-like domain, transmembrane domain, and kinase domain are marked as dark green, green, yellow, and red, respectively.

**Supplementary Figure 2 |** Protein structural analysis of CqRALF peptides. The full-length amino acids of all 18 CqRALF peptides were aligned, and the motifs RRXL, YISY, and four conserved cysteines are indicated.

## REFERENCES


Abarca, A., Franck, C. M., and Zipfel, C. (2021). Family-wide evaluation of rapid alkalinization factor peptides. *Plant Physiol.* 187, 996–1010. doi: 10.1093/plphys/kiab308

Anders, S., Pyl, P. T., and Huber, W. (2015). HTSeq–a Python framework to work with high-throughput sequencing data. *Bioinformatics* 31, 166–169. doi: 10.1093/bioinformatics/ btu638

Blackburn, M. R., Haruta, M., and Moura, D. S. (2020). Twenty years of progress in physiological and biochemical investigation of RALF peptides. *Plant Physiol.* 182, 1657–1666. doi: 10.1104/pp.19.01310

Böhm, J., Messerer, M., Müller, H. M., Scholz-Starke, J., Gradogna, A., Scherzer, S., et al. (2018). Understanding the molecular basis of salt sequestration in epidermal bladder cells of *Chenopodium quinoa*. *Curr. Biol.* 28, 3075–3085. doi: 10.1016/j.cub.2018.08.004

Cao, J., and Shi, F. (2012). Evolution of the RALF gene family in plants: gene duplication and selection patterns. *Evol. Bioinforma.* 8, 271–292. doi: 10.4137/EBO.S9652

Chao, J., Li, Z., Sun, Y., Aluko, O. O., Wu, X., Wang, Q., et al. (2021). MG2C: a user-friendly online tool for drawing genetic maps. *Mol. Hortic.* 1:16. doi: 10.1186/s43897-021-00020-x

Chen, C., Chen, H., Zhang, Y., Thomas, H. R., Frank, M. H., He, Y., et al. (2020). TBtools: an integrative toolkit developed for interactive analyses of big biological data. *Mol. Plant* 13, 1194–1202. doi: 10.1016/j.molp.2020.06.009

Chen, J., Yu, F., Liu, Y., Du, C., Li, X., Zhu, S., et al. (2016). FERONIA interacts with ABI2-type phosphatases to facilitate signaling cross-talk between abscisic acid and RALF peptide in *Arabidopsis*. *Proc. Natl. Acad. Sci. U.S A.* 113, E5519–E5527. doi: 10.1073/pnas.1608449113

Deslauriers, S. D., and Larsen, P. B. (2010). FERONIA is a key modulator of brassinosteroid and ethylene responsiveness in *Arabidopsis* hypocotyls. *Mol. Plant* 3, 626–640. doi: 10.1093/mp/ssq015

Duan, Q., Kita, D., Li, C., Cheung, A. Y., and Wu, H. M. (2010). FERONIA receptor-like kinase regulates RHO GTPase signaling of root hair development. *Proc. Natl. Acad. Sci. U. S. A.* 107, 17821–17826. doi: 10.1073/pnas.1005366107

Edgar, R. C. (2004). MUSCLE: multiple sequence alignment with high accuracy and high throughput. *Nucleic Acids Res.* 32, 1792–1797. doi: 10.1093/nar/gkh340

Feng, W., Kita, D., Peaucelle, A., Cartwright, H. N., Doan, V., Duan, Q., et al. (2018). The FERONIA receptor kinase maintains cell-wall integrity during salt stress through $Ca^{2+}$ signaling. *Curr. Biol.* 28, 666–675. doi: 10.1016/j.cub.2018.01.023

Finn, R. D., Clements, J., and Eddy, S. R. (2011). HMMER web server: interactive sequence similarity searching. *Nucleic Acids Res.* 39, W29–W37. doi: 10.1093/nar/gkr367

Franck, C. M., and Westermann, J. (2018). Plant malectin-like receptor kinases: from cell wall integrity to immunity and beyond. *Annu. Rev. Plant Biol.* 69, 301–328. doi: 10.1146/annurev-arplant-042817

Ge, Z., Bergonci, T., Zhao, Y., Zou, Y., Du, S., Liu, M.-C., et al. (2017). *Arabidopsis* pollen tube integrity and sperm release are regulated by RALF-mediated signaling. *Science* 358, 1596–1600. doi: 10.1126/science.aao3642

Gigli-Bisceglia, N., van Zelm, E., Huo, W., Lamers, J., and Testerink, C. (2020). *Arabidopsis* root responses to salinity depend on pectin modification and cell wall sensing. *bioRxiv*[Preprint], 1–30. doi: 10.1101/2020.12.18.423458

Guo, H., Li, L., Ye, H., Yu, X., Algreen, A., and Yin, Y. (2009). Three related receptor-like kinases are required for optimal cell elongation in *Arabidopsis thaliana*. *Proc. Natl. Acad. Sci. U.S.A.* 106, 7648–7653.

Guo, H., Nolan, T. M., Song, G., Liu, S., Xie, Z., Chen, J., et al. (2018). FERONIA receptor kinase contributes to plant immunity by suppressing jasmonic acid signaling in *Arabidopsis thaliana*. *Curr. Biol.* 28, 3316–3324. doi: 10.1016/j.cub.2018.07.078

Haruta, M., Sabat, G., Stecker, K., Minkoff, B. B., and Sussman, M. R. (2014). A peptide hormone and its receptor protein kinase regulate plant cell expansion. *Science* 343, 408–411. doi: 10.1126/science.1244454

Hématy, K., Sado, P. E., Van Tuinen, A., Rochange, S., Desnos, T., Balzergue, S., et al. (2007). A receptor-like kinase mediates the response of *Arabidopsis* cells to the inhibition of cellulose synthesis. *Curr. Biol.* 17, 922–931. doi: 10.1016/j.cub.2007.05.018

Hinojosa, L., González, J. A., Barrios-Masias, F. H., Fuentes, F., and Murphy, K. M. (2018). Quinoa abiotic stress responses: a review. *Plants* 7:106. doi: 10.3390/plants7040106

Huang, G. Q., Li, E., Ge, F. R., Li, S., Wang, Q., Zhang, C. Q., et al. (2013). *Arabidopsis* RopGEF4 and RopGEF10 are important for FERONIA-mediated developmental but not environmental regulation of root hair growth. *New Phytol.* 200, 1089–1101. doi: 10.1111/nph.12432

Huang, Y., Yin, C., Liu, J., Feng, B., Ge, D., Kong, L., et al. (2020). A trimeric CrRLK1L-LLG1 complex genetically modulates SUMM2-mediated autoimmunity. *Nat. Commun.* 11:4859. doi: 10.1038/s41467-020-18600-8

Huck, N., Moore, J. M., Federer, M., and Grossniklaus, U. (2003). The *Arabidopsis* mutant feronia disrupts the female gametophytic control of pollen tube receptor. *Development* 130, 2149–2159. doi: 10.1242/dev.00458

Jaramillo Roman, V., den Toom, L. A., Castro Gamiz, C., van der Pijl, N., Visser, R. G. F., van Loo, E. N., et al. (2020). Differential responses to salt stress in ion dynamics, growth and seed yield of European quinoa varieties. *Environ. Exp. Bot.* 177:104146. doi: 10.1016/j.envexpbot.2020.104146

Jarvis, D. E., Ho, Y. S., Lightfoot, D. J., Schmöckel, S. M., Li, B., Borm, T. J. A., et al. (2017). The genome of *Chenopodium quinoa*. *Nature* 542, 307–312. doi: 10.1038/nature21370

Kiani-Pouya, A., Roessner, U., Jayasinghe, N. S., Lutz, A., Rupasinghe, T., Bazihizina, N., et al. (2017). Epidermal bladder cells confer salinity stress tolerance in the halophyte quinoa and *Atriplex* species. *Plant Cell Environ.* 40, 1900–1915. doi: 10.1111/pce.12995

Kim, D., Paggi, J. M., Park, C., Bennett, C., and Salzberg, S. L. (2019). Graph-based genome alignment and genotyping with HISAT2 and HISAT-genotype. *Nat. Biotechnol.* 37, 907–915. doi: 10.1038/s41587-019-0201-4

Letunic, I., and Bork, P. (2018). 20 years of the SMART protein domain annotation resource. *Nucleic Acids Res.* 46, D493–D496. doi: 10.1093/nar/gkx922

Letunic, I., and Bork, P. (2021). Interactive Tree Of Life (iTOL) v5: an online tool for phylogenetic tree display and annotation. *Nucleic Acids Res.* 49, W293–W296. doi: 10.1093/nar/gkab301

Lin, W., Tang, W., Pan, X., Huang, A., Gao, X., Anderson, C. T., et al. (2022). *Arabidopsis* pavement cell morphogenesis requires FERONIA binding to pectin for activation of ROP GTPase signaling. *Curr. Biol.* 32, 497–507. doi: 10.1016/j.cub.2021.11.030

Mang, H., Feng, B., Hu, Z., Boisson-Dernier, A., Franck, C. M., Meng, X., et al. (2017). Differential regulation of two-tiered plant immunity and sexual reproduction by ANXUR receptor-like kinases. *Plant Cell* 29, 3140–3156. doi: 10.1105/tpc.17.00464

Minh, B. Q., Schmidt, H. A., Chernomor, O., Schrempf, D., Woodhams, M. D., von Haeseler, A., et al. (2020). IQ-TREE 2: new models and efficient methods for phylogenetic inference in the genomic era. *Mol. Biol. Evol.* 37, 1530–1534. doi: 10.1093/molbev/ msaa015

Mistry, J., Chuguransky, S., Williams, L., Qureshi, M., Salazar, G. A., Sonnhammer, E. L. L., et al. (2021). Pfam: the protein families database in 2021. *Nucleic Acids Res.* 49, D412–D419. doi: 10.1093/nar/gkaa913

Miyazaki, S., Murata, T., Sakurai-Ozato, N., Kubo, M., Demura, T., Fukuda, H., et al. (2009). ANXUR1 and 2, sister genes to FERONIA/SIRENE, are male factors for coordinated fertilization. *Curr. Biol.* 19, 1327–1331. doi: 10.1016/j.cub.2009.06.064

Murphy, E., and De Smet, I. (2014). Understanding the RALF family: a tale of many species. *Trends Plant Sci.* 19, 664–671. doi: 10.1016/j.tplants.2014.06.005

Ortiz-Morea, F. A., He, P., Shan, L., and Russinova, E. (2020). It takes two to tango – molecular links between plant immunity and brassinosteroid signalling. *J. Cell Sci.* 133:jcs246728. doi: 10.1242/jcs.246728

Rotman, N., Rozier, F., Boavida, L., Dumas, C., Berger, F., and Faure, J. E. (2003). Female control of male gamete delivery during fertilization in *Arabidopsis thaliana*. *Curr. Biol.* 13, 432–436. doi: 10.1016/S0960-9822(03)00093-9

Stegmann, M., Monaghan, J., Smakowska-Luzan, E., Rovenich, H., Lehner, A., Holton, N., et al. (2017). The receptor kinase FER is a RALF-regulated scaffold controlling plant immune signaling. *Science* 355, 287–289. doi: 10.1126/science.aal2541

Tang, W., Lin, W., Zhou, X., Guo, J., Dang, X., Li, B., et al. (2022). Mechano-transduction via the pectin-FERONIA complex activates ROP6 GTPase signaling in *Arabidopsis* pavement cell morphogenesis. *Curr. Biol.* 32, 508–517. doi: 10.1016/j.cub.2021.11.031

Yu, M., Li, R., Cui, Y., Chen, W., Li, B., Zhang, X., et al. (2020). The RALF1-FERONIA interaction modulates endocytosis to mediate control of root growth in *Arabidopsis*. *Development.* 147:dev189902. doi: 10.1242/dev.189902

Zhao, C., Jiang, W., Zayed, O., Liu, X., Tang, K., Nie, W., et al. (2021). The LRXs-RALFs-FER module controls plant growth and salt stress responses by modulating multiple plant hormones. *Natl. Sci. Rev*. 8:nwaa149. doi: 10.1093/nsr/nwaa149

Zhao, C., Zayed, O., Yu, Z., Jiang, W., Zhu, P., Hsu, C. C., et al. (2018). Leucine-rich repeat extensin proteins regulate plant salt tolerance in *Arabidopsis*. *Proc. Natl. Acad. Sci. U.S.A.* 115, 13123–13128. doi: 10.1073/pnas.1816991115

Zhong, S., Li, L., Wang, Z., Ge, Z., Li, Q., Bleckmann, A., et al. (2022). RALF peptide signaling controls the polytubey block in *Arabidopsis*. *Science* 375, 290–296. doi: 10.1126/science.abl4683

Zhu, S., Fu, Q., Xu, F., Zheng, H., and Yu, F. (2021). New paradigms in cell adaptation: decades of discoveries on the CrRLK1L receptor kinase signalling network. *New Phytol.* 232, 1168–1183. doi: 10.1111/nph.17683

Zou, C., Chen, A., Xiao, L., Muller, H. M., Ache, P., Haberer, G., et al. (2017). A high-quality genome assembly of quinoa provides insights into the molecular basis of salt bladder-based salinity tolerance and the exceptional nutritional value. *Cell Res.* 27, 1327–1340. doi: 10.1038/cr.2017.124

**Conflict of Interest:** FYu was employed by Agricultural Technology Center of Bright Rice (group) Co., Ltd., Shanghai, China and FYi and JZ were employed by The Bright Seed Industry Company, Shanghai, China.

The remaining authors declare that the research was conducted in the absence of any commercial or financial relationships that could be construed as a potential conflict of interest.

**Publisher's Note:** All claims expressed in this article are solely those of the authors and do not necessarily represent those of their affiliated organizations, or those of the publisher, the editors and the reviewers. Any product that may be evaluated in this article, or claim that may be made by its manufacturer, is not guaranteed or endorsed by the publisher.

frontiers | Frontiers in Plant Science

ORIGINAL RESEARCH
published: 15 July 2022
doi: 10.3389/fpls.2022.882884

# Physiological Measurements and Transcriptome Survey Reveal How Semi-mangrove *Clerodendrum inerme* Tolerates Saline Adversity

*Minting Liang[1†], Feng Hu[2†], Dongsheng Xie[1], Zhibin Chen[2], Qingzhi Zheng[2], Qiyun Xie[2], Feng Zheng[1], Dongming Liu[1], Shuguang Jian[1], Hongfeng Chen[1], Xuncheng Liu[1]* and Faguo Wang[1]**

[1] Key Laboratory of South China Agricultural Plant Molecular Analysis and Genetic Improvement and Guangdong Provincial Key Laboratory of Applied Botany, South China Botanical Garden, Chinese Academy of Sciences, Guangzhou, China, [2] Department of Landscape and Tourism Planning and Design, Guangzhou Urban Planning and Design Survey Research Institute, Guangzhou, China

OPEN ACCESS

**Edited by:**
Esmaeil Bakhshandeh,
Sari Agricultural Sciences and Natural Resources University, Iran

**Reviewed by:**
Kourosh Vahdati,
University of Tehran, Iran
Vadim Volkov,
London Metropolitan University, United Kingdom

***Correspondence:**
Xuncheng Liu
xunchengliu@scbg.ac.cn
Faguo Wang
wangfg@scbg.ac.cn

[†] These authors have contributed equally to this work

**Specialty section:**
This article was submitted to Plant Abiotic Stress, a section of the journal Frontiers in Plant Science

**Received:** 24 February 2022
**Accepted:** 20 June 2022
**Published:** 15 July 2022

**Citation:**
Liang M, Hu F, Xie D, Chen Z, Zheng Q, Xie Q, Zheng F, Liu D, Jian S, Chen H, Liu X and Wang F (2022) Physiological Measurements and Transcriptome Survey Reveal How Semi-mangrove Clerodendrum inerme Tolerates Saline Adversity. Front. Plant Sci. 13:882884. doi: 10.3389/fpls.2022.882884

Salinity adversity has been a major environmental stressor for plant growth and reproduction worldwide. Semi-mangrove *Clerodendrum inerme*, a naturally salt-tolerant plant, can be studied as a successful example to understand the biological mechanism of saline resistance. Since it is a sophisticated and all-round scale process for plants to react to stress, our greenhouse study interpreted the response of *C. inerme* to salt challenge in the following aspects: morphology, osmotic protectants, ROS production and scavenging, ion homeostasis, photosynthetic efficiency, and transcriptome reprogramming. The results drew an overview picture to illustrate the tolerant performance of *C. inerme* from salt acclimatization (till medium NaCl level, 0.3 mol/L) to salinity stress (high NaCl level, 0.5 mol/L). The overall evaluation leads to a conclusion that the main survival strategy of *C. inerme* is globally reshaping metabolic and ion profiles to adapt to saline adversity. These findings uncover the defense mechanism by which *C. inerme* moderates its development rate to resist the short- and long-term salt adversity, along with rebalancing the energy allocation between growth and stress tolerance.

**Keywords: salt tolerance, halophyte, *Clerodendrum inerme*, physiological response, transcriptome reprogramming**

## INTRODUCTION

Among various abiotic stresses, salinity is one of the major environmental factors affecting the geographical distribution of plants and reducing the productivity of crops (Zhu, 2016). Approximately 7% of the world's land is affected by either salinity or sodium toxicity, and the production of over 30% of irrigated crops is limited by salinity stress (Schroeder et al., 2013). Halophytes, also known as salinity tolerant plants, representing only 2% of terrestrial plant species, have evolved diverse strategies to survive in salinity (Glenn et al., 1999). Understanding the adaptive strategies of halophytes to salt stress will be extremely important for us to cultivate salt-tolerant plants.

The salt sodium chloride (NaCl) is the main cause of salt stress in plants. The high concentration of $Na^+$ causes consecutively adverse impacts on plants. First, the accumulation of $Na^+$ limits water uptake and nutrient absorption, which induces primary stresses including osmotic stress and ionic stress. Second, the primary stresses lead to oxidative stress, which is defined as excess production of reactive oxygen species (ROS). Over-accumulated ROS causes a series of secondary stresses in plant cells such as reducing cell division, inhibiting photosynthesis, and damaging cellular components, which eventually impedes plant growth (Zhu, 2002, 2016).

As sessile organisms, plants have evolved diverse physiological strategies to defend saline environments and adjust growth under high salt conditions. Plants can scavenge excessive ROS for detoxification by the antioxidant systems including superoxide dismutase (SOD), peroxidase (POD), ascorbate peroxidase (APX), catalase (CAT), glutathione peroxidase (GPX), and peroxiredoxin (PrxR). Plants also advantageously use ROS as an important messenger in response to high salinity (Takahashi and Asada, 1988; Mittler et al., 2004; Dietz et al., 2006; Zhu, 2016). Maintenance of the intracellular $K^+$ and $Na^+$ homeostasis is important for the activities of many cytosolic enzymes. Plants restore ion homeostasis by removing $Na^+$ from the cytoplasm *via* $Na^+/H^+$ antiporters, which confers better salinity tolerance (Zhu, 2003; James et al., 2006; Park et al., 2016; Bose et al., 2017). Moreover, abundant osmolytes like proline, glycine-betaine, trehalose, and sugar alcohols were produced by plants in salinity. These compounds adjust the osmotic pressure of the cytosolic compartment to alleviate salt-induced water deficiency (Flowers et al., 2015; Munns and Gilliham, 2015).

In recent years, extensive investigations of salt stress responses using transcriptomic approaches have been characterized for various halophytes. It was demonstrated that transcripts related to membrane transport, osmoprotection, redox metabolism, or protein synthesis expressed differentially in *Beta vulgaris* subsp. *maritima* to saline adversity (Skorupa et al., 2016). In *Glehnia littoralis*, genes encoding transcription factors or involved in multiple signaling pathways, such as plant hormone, calcium, and phospholipase, were responsive to salinity conditions (Li et al., 2018). Besides, expression pattern cluster analysis revealed that genes related to secondary metabolic pathway and transcription were enriched significantly in sweet sorghum RIO during salt imposition (Chen et al., 2022). Moreover, in Guar *Cyamopsis tetragonoloba* (L.) Taub., genes associated with stress-signaling pathways, transporters, chromatin remodeling, microRNA biogenesis, and translational machinery play primary roles to tolerate salt stress (Acharya et al., 2022).

*Clerodendrum inerme*, a halophyte in the family Lamiaceae, usually grows on coastal beaches as an important semi-mangrove plant. In Pakistan, it has been scheduled as a hydro-halophyte used in saline agriculture while in China it was listed as a medicinal halophyte for many diseases (http://www.grhc.sdnu.edu.cn/) (Khan and Qaiser, 2006). Although the salt tolerance mechanisms of *C. inerme* are unclear, it is an ideal salt-tolerant material to study its great agricultural and scientific values. In this study, we quantified and interpreted the physiological and biochemical responses of *C. inerme* to different salt concentrations, such as growth inhibition, developmental changes, metabolic adaptations, photosynthetic acclimation, and ionic homeostasis. We also investigated the rapid and long-term transcriptomic changes of *C. inerme* to salt exposure. Our findings evaluate an overall defense and tolerance strategy of *C. inerme* overcoming salt adversity, which will be helpful to guide salinity-tolerant plant engineering in the future.

# RESULTS

## Plant Growth in Response to Saline Stress

The growth state of the *C. inerme* plant visibly reflects tolerance to salt stress. Low (0.1 M), medium (0.3 M), and high (0.5 M) concentrations of NaCl were set for saline stress treatment, according to the saline concentration of seawater in plant habitat and the maximum salt content range that *C. inerme* can bear (Lotfi et al., 2010; Rad et al., 2021). Inhibition of plant height was not observed on day 14 in the presence of NaCl at different experimental concentrations, yet more yellow leaves appeared and premature defoliation was observed with the increase in salt level (**Figures 1A,B**; **Supplementary Figure 1A**). Although *C. inerme* exhibited more yellow sagged leaves at low NaCl concentrations compared to mock control, the yellow leaves barely fell off. However, leaves turned yellow, softened, deformed, and shed rapidly under medium and high salt concentrations, leaving only fewer leaves at the base of the plant. The growth response to saline stress was also detected *via* biomass accumulation. The fresh and dry weights of root, stem, and leaf decreased gradually with the aggravation of NaCl adversity (**Figures 1C,D**). Under high salt stress, the fresh and dry weights of root were 63.73 and 62.68% lower than the control, respectively. Accordingly, fresh and dry weights of stem were 68.33% and 63.95% lower than those of control, respectively. A similar reduction was also observed in leaf. The remarkable decrease in biomass was likely due to arrested development. Consistent with the general stress response, under medium and high concentration salt adversity, *C. inerme* distributes more biomass to roots to utilize more metabolites and energy to resist the stress environment around the root with an increased root-to-shoot ratio by dry weight (**Supplementary Figure 1B**).

## Alleviation of Intracellular Oxidative Stress Caused by Salinity

Plants rapidly accumulate ROS to activate defense response to environmental stress and MDA is also produced to aggravate the lesion of the membrane system, which is an important index to detect the degree of damage in plant cells (Meloni et al., 2003). The MDA level gradually increased in accordance with the concentration of NaCl treatment. Under low, medium, and high salt treatment, the MDA content in plants were 16.6, 43.7, and 68.3% higher than the control group, respectively (**Figure 2A**).

Proline (Pro) is ubiquitous in plants and acts as a regulator to maintain the osmotic homeostasis across the cell membrane. Content of Pro increased with the aggravation of salt stress, and a higher level of Pro showed stronger osmotic regulation. Accumulation of Pro content in *C. inerme* leaves boosted with the concentration of the saline solution. The Pro levels were

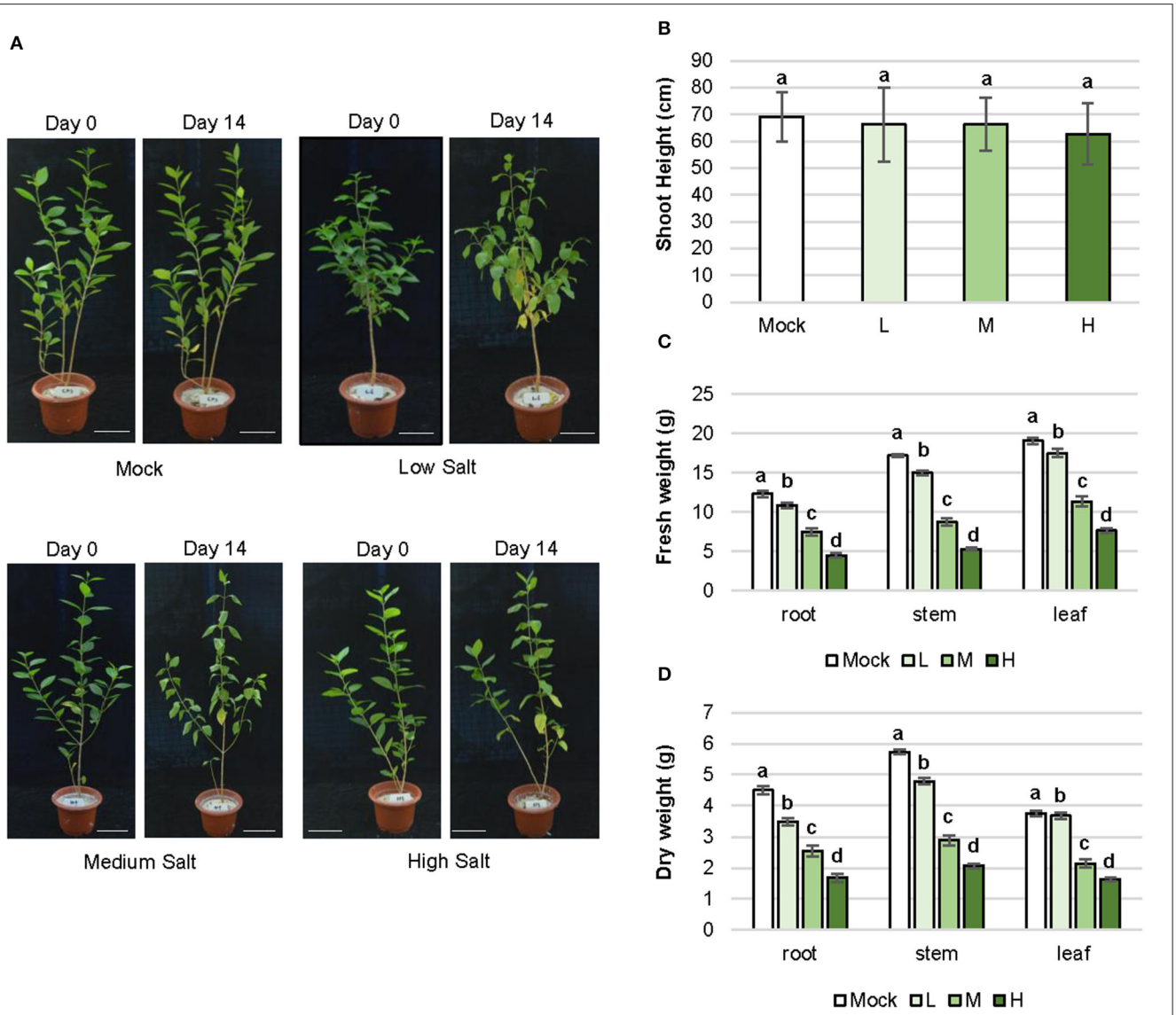


**FIGURE 1 |** Morphogenesis and biomass alteration of *C. inerme* in response to salinity stress. **(A)** Plant architecture of *C. inerme* on day 0 and day 14 after corresponding salt treatment. Shoot height **(B)**, fresh weight **(C)** and dry weight **(D)** of root, stem and leaf respectively on day 14 under NaCl stress. Different letters indicate significant differences among plant groups ($p < 0.05$, Mann Whitneytest). Mock, no salt control; L, low salt stress; M, medium salt stress; H, high salt stress.

500.6 mg/g and 658.6 mg/g under medium and high salt treatments, that is, 2,895.2 and 3,840.4% higher than the mock control (**Figure 2B**). To sum up, osmotic stress occurred under low salt stress, but Pro began to increase dramatically under medium salt stress, suggesting the strong Pro regulation ability of *C. inerme*.

Glutathione (GSH) is a kind of γ-tripeptide consisting of glutamate, cysteine, and glycine with amide bonds and thiol groups, namely the most widely distributed non-protein sulfhydryl antioxidant in cells. The GSH content of *C. inerme* was maintained from 85.31 to 116.71 μg/g, showing no significant difference under various levels of saline stress, indicating the increase of ROS in the *C. inerme* plant caused by NaCl unlikely affecting the biosynthesis of GSH (**Figure 2C**).

The low molecular secondary metabolite flavonoids not only regulate the growth of plants but also reflect strong antioxidant properties. The accumulation of flavonoids improves stress resistance and reduces oxidative damage. Content of total flavonoids in *C. inerme* decreased gradually with the aggravation of saline stress. Under high salt stress, total flavonoids were left to 4.24 mg/g, which decreased by 28.57% compared with that in the control treatment (**Figure 2D**). The result suggests that the flavonoids of *C. inerme* were greatly affected by the salt imposition.

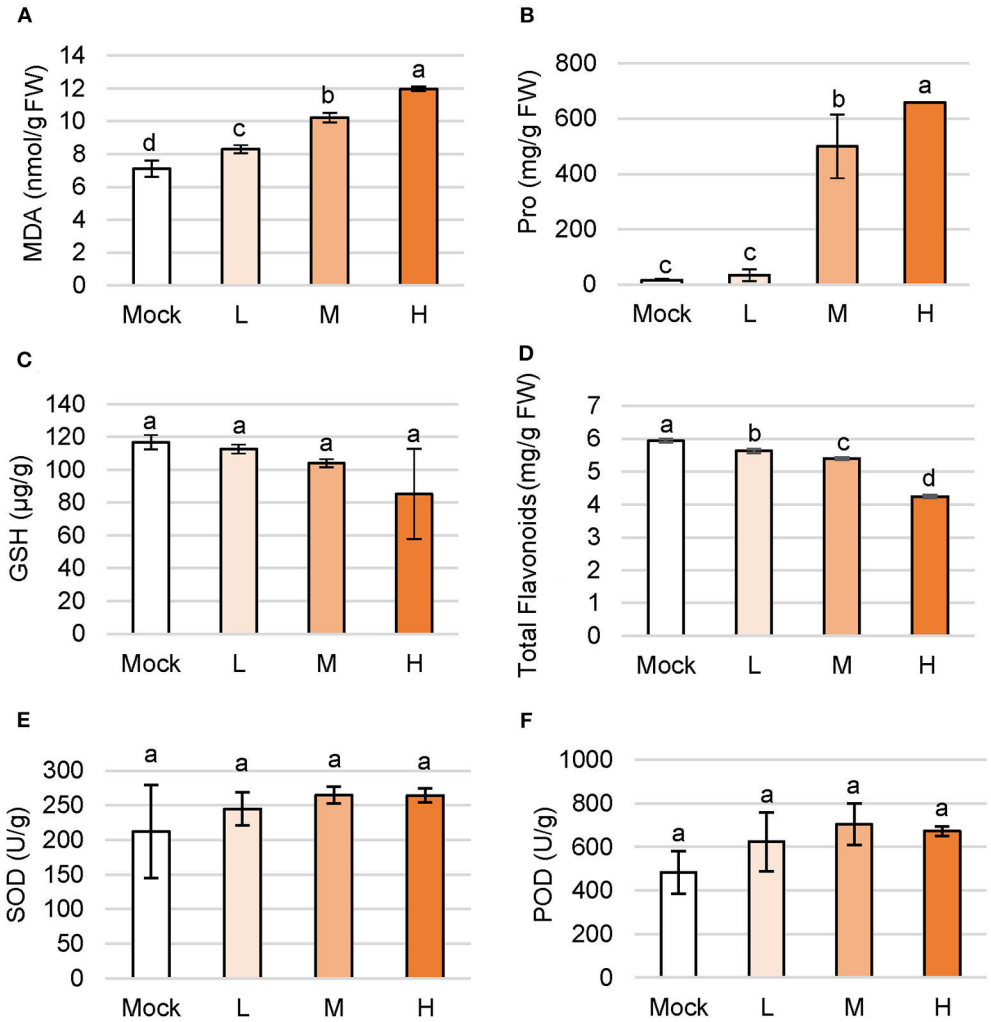


**FIGURE 2 |** Changes of primary and secondary metabolites in *C. inerme* under salinity stress. Content of MDA **(A)**, proline **(B)**, GSH **(C)**, total flavonoids **(D)**, SOD **(E)** and POD **(F)** in plant leaves on day 14 under salt adversity. Different letters indicate significant differences among plant groups ($p < 0.05$, Mann Whitney test). Mock, no salt control; L, low salt stress; M, medium salt stress; H, high salt stress.

SOD is the first defense line of ROS scavenging in the antioxidant enzyme system, which disproportionates $O^{2-}$ to $H_2O_2$. SOD scavenges ROS and peroxides together with POD and CAT. SOD activity of *C. inerme* maintained between 212.45 and 264.58 U/g among groups (**Figure 2E**), indicating that these concentrations of saline solution influenced little on SOD activity in this halophyte. Correlatively, no significant effect on POD activity was observed under indicated salt treatment (**Figure 2F**), which together suggests that the strength of saline adversity was below the sensitivity of the antioxidant enzyme system in the long-term salinity aggression, or was already adapted by this salt-tolerant plant.

## Photosynthetic Performance to the Salt Stress

Chlorophyll is the key pigment for photosynthesis, directly determining the photosynthetic rate and the ability of assimilation in plants. Salt-sensitive plants decompose chlorophyll under salt stress whereas salt-tolerant ones continue to maintain the biosynthesis of chlorophyll or even tend to enhance this process. *C. inerme* showed a decreasing chlorophyll level under low salt adversity with a reduction of 11.89% compared with no salt control (**Figure 3A**). However, the chlorophyll content climbed and saturated to 1.36 mg/g when treated with the medium and high saline conditions, increasing by 28.02% compared with no salt treatment, in agreement with its halophyte properties.

The intercellular $CO_2$ content indicates $CO_2$ storage in plant cells. It directly affects the stock of substrates for photosynthesis, and yet the absorption against the environmental $CO_2$ through guard cells. The $CO_2$ content gradually declined with the increase in salt concentration (**Figure 3B**). The net photosynthetic rate directly reflects the $CO_2$ assimilation capacity of the unit leaf area in the plant. Low and medium salt adversity lead to a subtle decrease, whereas high salt treatment caused a significant

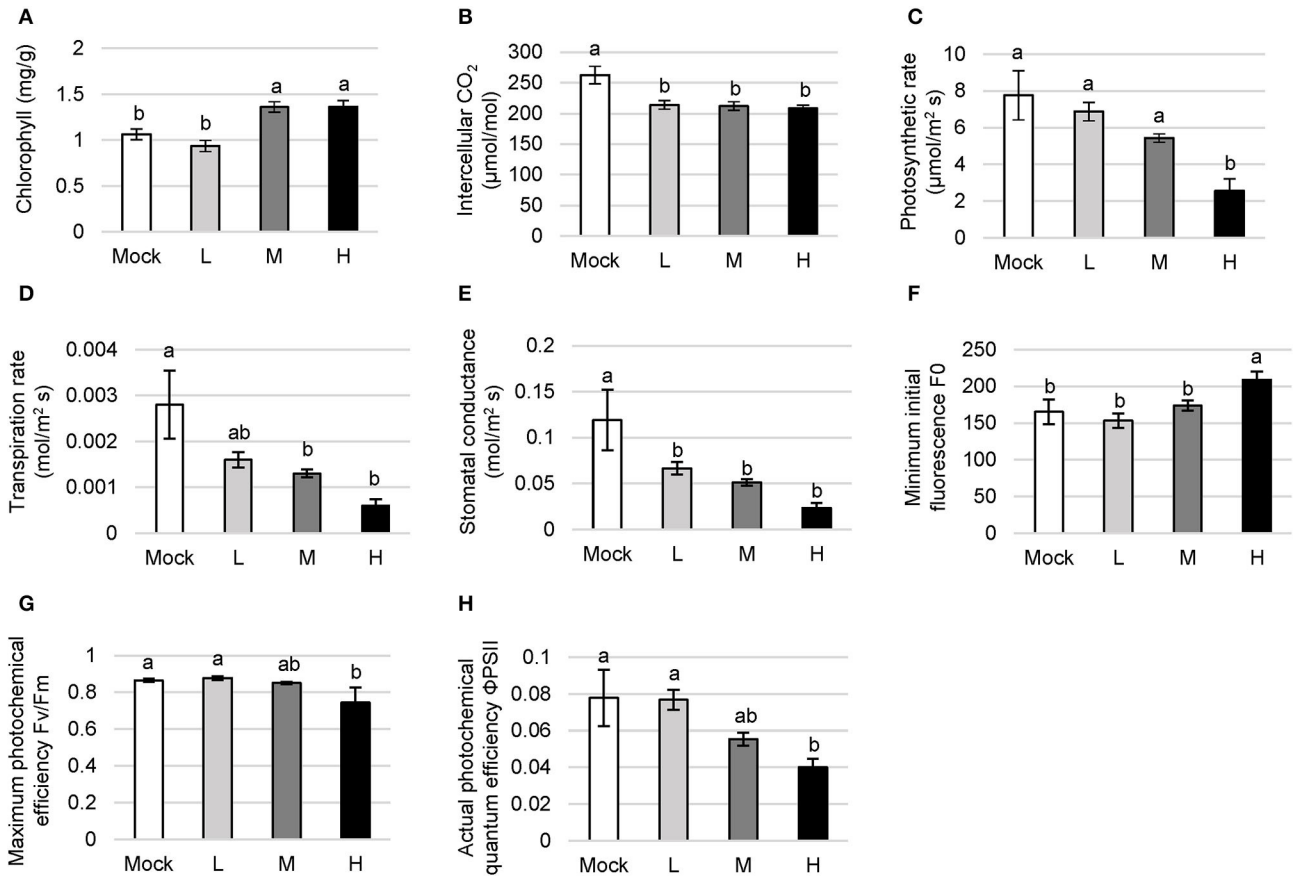


**FIGURE 3 |** Photosynthetic function in *C. inerme* to the saline adversity. Content of chlorophyll **(A)**, photosynthetic rate **(B)**, transpiration rate **(C)**, intercellular $CO_2$ level **(D)**, stomatal conductance **(E)**, F0 **(F)**, Fv/Fm **(G)** and ΦPSII **(H)** of *C. inerme* leaves were determined on day 14 to different levels of NaCl stress. Different letters indicate significant differences among plant groups ($p < 0.05$, Mann Whitney test). Mock, no salt control; L, low salt stress; M, medium salt stress; H, high salt stress.

reduction in the photosynthetic rate of *C. inerme* compared with the mock control. The photosynthetic rate was down to 2.56 mol/m$^2$s under high NaCl, reduced by 67.04% compared with mock treatment (**Figure 3C**).

The usage and transportation of water by the plant can be indicated *via* transpiration rate. The transpiration rate in *C. inerme* decreased with the increase of salt concentration, and dropped to 0.0006 mol/m$^2$s under high salinity, counting for 78.57% lower than control. The highest transpiration rate was 0.0028 mol/m$^2$s without NaCl but showed no significant difference compared with that under low salinity conditions (**Figure 3D**). The degree of stomata opening was reflected by stomatal conductance, and directly affects the photosynthesis, respiration, and transpiration in the plant. Correlatively, the stomatal conductance of *C. inerme* peaked to 0.1190 mol/m$^2$ s under no salinity while dropped to 0.0233 mol/m$^2$ s when treated with the highest level of NaCl, which was 80.42% lower than no salt control (**Figure 3E**).

Photosystem II (PSII) is an important component of the thylakoid membrane and its destruction under adversity directly affects the photosynthetic rate. F0 represents the intensity of chlorophyll fluorescence emission and reflects the heat dissipation protection mechanism of PSII. The *C. inerme* showed similar F0 under no, low, or medium salt conditions, except in the presence of high salinity F0 peaked to 208.93, which was 26.48% higher than that of no NaCl control (**Figure 3F**). The result suggests that PSII was lightly destroyed under high salinity stress and its potential activity was inhibited.

Fv/Fm reflects the maximum photochemical efficiency of PSII to use light energy and electron transfer. Under low and medium salinity, Fv/Fm showed no difference compared to control (**Figure 3G**). Fv/Fm under high NaCl treatments was 0.74, which was 13.98% lower than the mock control. Besides, *Φ*PSII represents the actual photochemical quantum efficiency of PSII in plants under the light. It shows the ratio of excitation energy used for photochemical pathways to the total excitation energy entering PSII, which is an important indicator for plant photosynthetic capacity. *Φ*PSII in *C. inerme* decreased gradually with the increase of salt concentration (**Figure 3H**). Like Fv/Fm, there was no significantly different *Φ*PSII among no, low, or medium salinity stress. However, the *Φ*PSII value decreased remarkably under high salt treatment, which was 48.59% lower than control, suggesting the inhibition of photosynthetic rate as well as certain

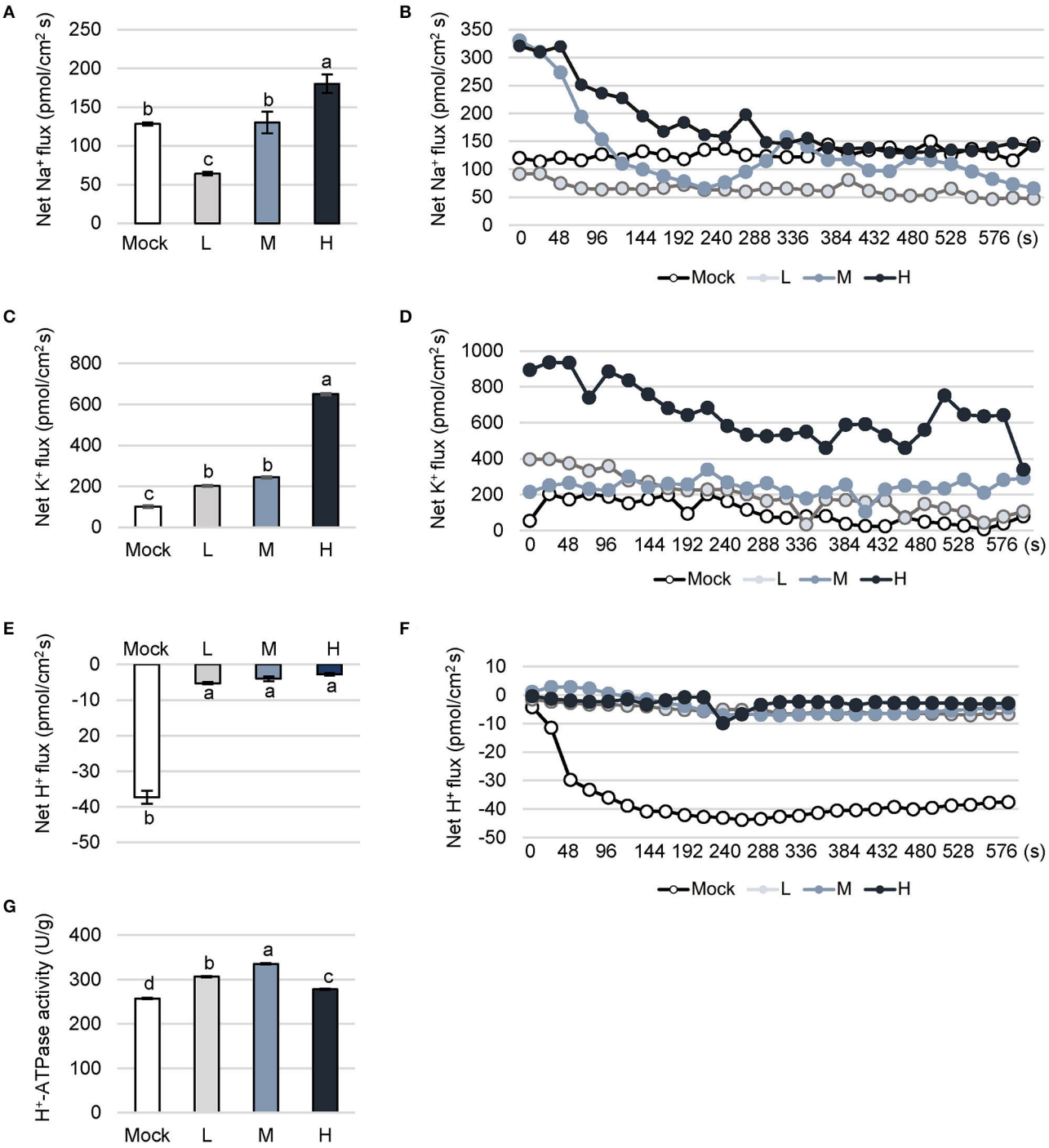


**FIGURE 4 |** Dynamic fluctuation of cation flow under different levels of salt stress. $Na^+$ **(A,B)**, $K^+$ **(C,D)** and $H^+$ **(E,F)** flux and activity of $H^+$-ATPase **(G)** in *C. inerme* leaves were detected on day 14 under different saline stress. Different letters indicate significant differences among plant groups ($p < 0.05$, Mann Whitney test). Mock, no salt control; L, low salt stress; M, medium salt stress; H, high salt stress.

damage to the photosynthetic apparatus. Collectively, these data reveal that the photosynthetic system of *C. inerme* was damaged to some extent by the salinity, especially under high salinity stress.

## Dynamic Change of Cations Flow Under NaCl Adversity

Plant cells accumulate $Na^+$ in response to salt stress. Excessive $Na^+$ triggers peroxidation on plasma membranes, and seriously

affects cellular transport. Terrestrial plants have evolved a complex mechanism to reduce the entry of $Na^+$ by the selective absorption of $K^+$. Redundant $Na^+$ is then pumped out of the cytoplasm through the $Na^+/H^+$ antiporter on the tonoplast and isolated in the vacuole. In this study, the measurement is equally divided into 26 time points with 10 min. Beyond this time range, the value is unreliable due to serious plant tissue damage. The column chart showed the average of the values at 26 time points. The ions outflow when the value is above zero and ions flow into cells when the value is below zero. $Na^+$ flux was significantly decreased in *C. inerme* plants under a low level of saline compared to mock plants (**Figures 4A,B**). However, no difference was detected between medium saline treatment and control. Whereas, $Na^+$ flux increased to 180.18 pmol/cm$^2$s under high NaCl, counting for 1.4 times of mock control.

$K^+$ plays a vital role in the osmotic adjustment of plant resistance to stress. $K^+$ competes with $Na^+$ to bind some sites on the plasma membrane. Moreover, $Na^+$ accumulation stimulates $K^+$ influx to the cell, and in turn, the influx of $K^+$ promotes the efflux of $Na^+$ under salt stress. In *C. inerme,* $K^+$ flux climbed to 201.78 pmol/cm$^2$s and 243.37 pmol/cm$^2$s in the presence of low or medium salt stress, which were significantly higher than no salt control (**Figures 4C,D**). Under high salinity stress, $K^+$ flux increased to 650.67 pmol/cm$^2$s, which was 6.4 times that of control. It is speculated that the ion channels of the plasma membrane in the presence of high salt levels are significantly activated.

Dynamic change of $H^+$ is related to the efflux of $Na^+$ for plant stress resistance. The $H^+$-ATPase on the plasma membrane and tonoplast provides energy for the reverse transport of $Na^+/H^+$. The $H^+$ influx of *C. inerme* under control increased gradually and finally saturated (**Figures 4E,F**). Under different levels of salinity, $H^+$ showed an influx much lower than control, basically maintaining between 2.73 and 5.24 pmol/cm$^2$s. Besides, $H^+$-ATPase locates on the plasma membrane and plays an important role in ion homeostasis. $H^+$-ATPase provides the energy for the $Na^+/H^+$ antiporter on the membrane, pumping $H^+$ out of the cytoplasm to form an $H^+$ electrochemical potential gradient to facilitate the efflux of $Na^+$. Increased $H^+$-ATPase activity is a sign to reflect the plant salt tolerance and decreased one shows irreversible damage to the plasma membrane. The results showed the decrease in $H^+$ influx and the increase in outflow reflects the enhancement of $Na^+/H^+$ antiporter and $H^+$-ATPase. The activity of $H^+$-ATPase in *C. inerme* under low and medium salt stress were 306.5 and 335.74 U/g, which were 19.15and 30.51% higher than control, separately (**Figure 4G**). Under high NaCl stress, the activity of $H^+$-ATPase dropped to the level between low and no salt treatment, suggesting slightly decreased activity of this enzyme in response to high adversity.

## Transcriptional Reprofiling in the Short- and Long-Term Response to Salt

To further explore the mechanism underlying the transcriptional response of *C. inerme* under short- and long-term salt stress, we performed RNA-sequencing (RNA-seq) to analyze the transcriptomes of *C. inerme* treated with the salt of different levels for 3 h (short-term) or 7 d plus 3 h (long-term). Although the physiological index was recorded on day 14 under the NaCl treatment, the transcriptome should be detected much earlier. It takes a certain time from transcriptional reprofiling, proteome remodeling, metabolic alterations, physiological changes, and cell differentiation for final morphological transformation. The commonly regulated salt-responsive genes were selected based on the following criteria: genes are up- or downregulated ($|\log2| \geq 1$, adjusted $P < 0.05$) by salinity application compared to no salt control. Under short-term exposure, the transcripts of 10,505, 3,276, and 5,022 genes were altered by low, medium, and high salinity, respectively (**Figure 5A**, **Supplementary Table S3**). In contrast, under long-term stress, there were 5,112, 10,528, and 16,202 genes differentially regulated by low, medium, and high salinity, respectively (**Figure 5A**; **Supplementary Table S4**). Only 1,075 and 2,142 genes were coregulated by different levels of NaCl treatment for short-term and long-term, respectively (**Figures 5B**, **6A,B**). The above data revealed that *C. inerme* may reprogram divergent transcriptional machineries in adaption to distinct salinity conditions.

For the short-term salt treatment, KEGG enrichment analysis revealed that salinity-induced genes were mainly involved in the metabolism of carbohydrates and secondary metabolites, such as phenylpropanoid, amino acids, starch and sucrose, cyanoamina acid, proline, and glycerolipid (**Figure 5C**). Phenylpropanoid is an important secondary metabolite and plays a crucial role in response to stimuli and stresses (Ignat et al., 2011). Starch and sugar provide energy to support plant growth under stress and function as osmoprotectants to mitigate the negative effect of the stress (Dong and Beckles, 2019). Elevated expression of phenylpropanoid, proline, starch, and sugar metabolism-related genes suggested that *C. inerme* produces abundant secondary metabolites and increases energy supply in defense of early salt injury. In contrast, salinity-repressed genes were mainly related to transporters, organismal systems, nucleotide metabolism, and plant hormone signal transduction (**Figure 5D**), indicating *C. inerme* rapidly slows down its growth at the early salt stress stage.

For the long-term salinity acclimation, the genes involved in the metabolism of amino acids, proteins, and carbohydrates, as well as organismal systems and environmental adaption were upregulated (**Figure 5E**), suggesting that *C. inerme* promotes comprehensive cellular processes in adaption to continuous salt stress. In contrast, the genes related to cellular processes, such as DNA replication, DNA repair, protein processing, folding, sorting, and degradation were downregulated (**Figure 5F**), revealed that *C. inerme* reduces its cellular energy consumption under continuous salt conditions.

To confirm the changes in expression of salt-induced genes, we conducted qRT-PCR with *C. inerme* young leaves under a simple time course of salinity treatment. As expected, genes involved in the environmental response, metabolism, and ion exchange were upregulated after NaCl application for 1 day, yet finally decreased after 7 days under high level of salt (**Figures 7A–F**). While, other metabolite-related genes were downregulated in general at all levels of NaCl for these indicated days (**Figures 7G–I**). In summary, the results suggested that *C. inerme* shifts from salt acclimation

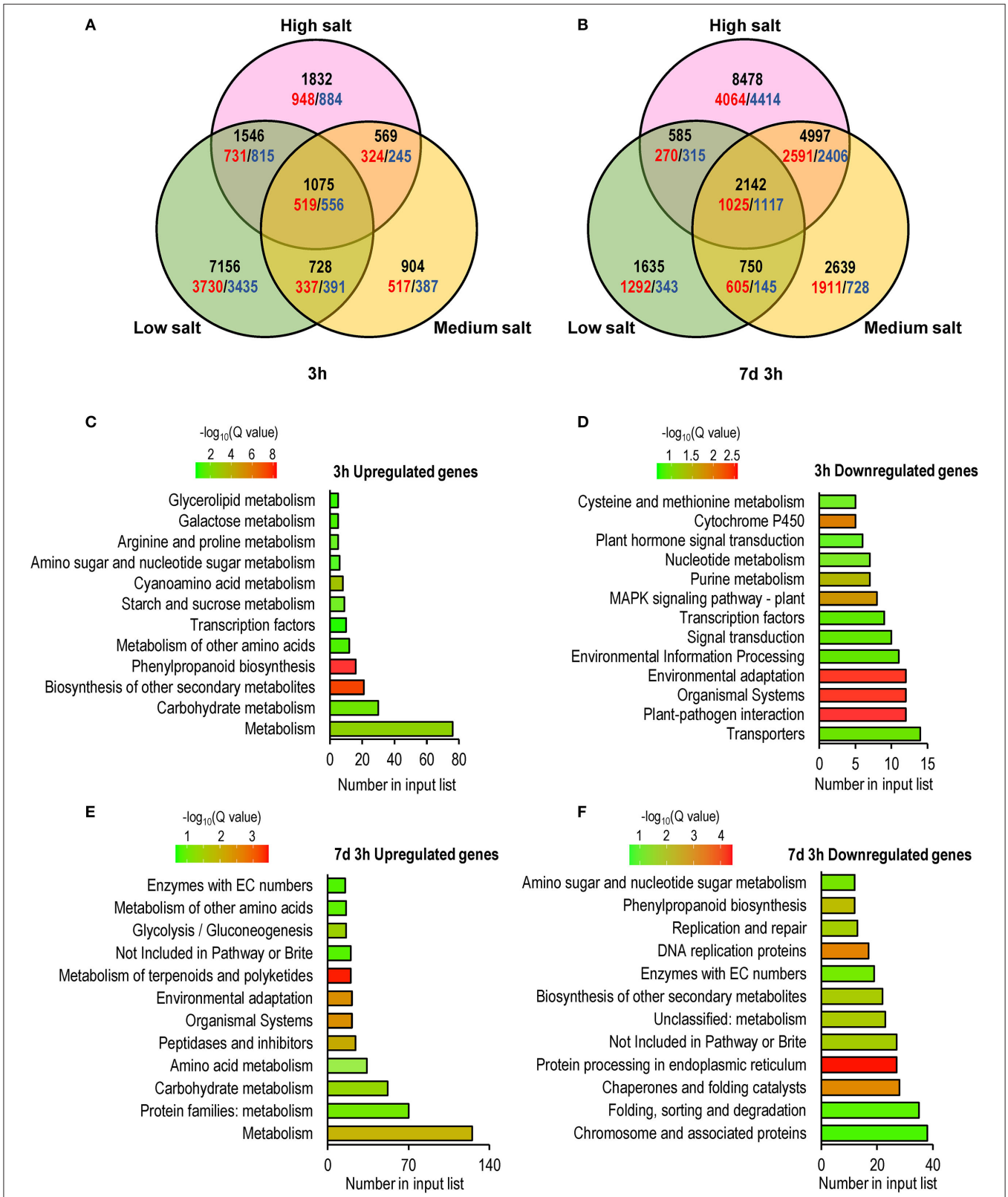


**FIGURE 5 |** Global comparison of transcriptome profiling identified early and long-term salt response genes. **(A)** Venn diagrams indicating the numbers of early (3 h) and long-term (7 days and 3 h) salt-related genes compared to no salt control. The unregulated genes were colored red while downregulated genes were colored blue, and the total numbers were black. KEGG enrichment analysis of salt-response genes commonly regulated after 3h **(C,D)** or 7 days and 3h **(E,F)** treated in salt of all levels.

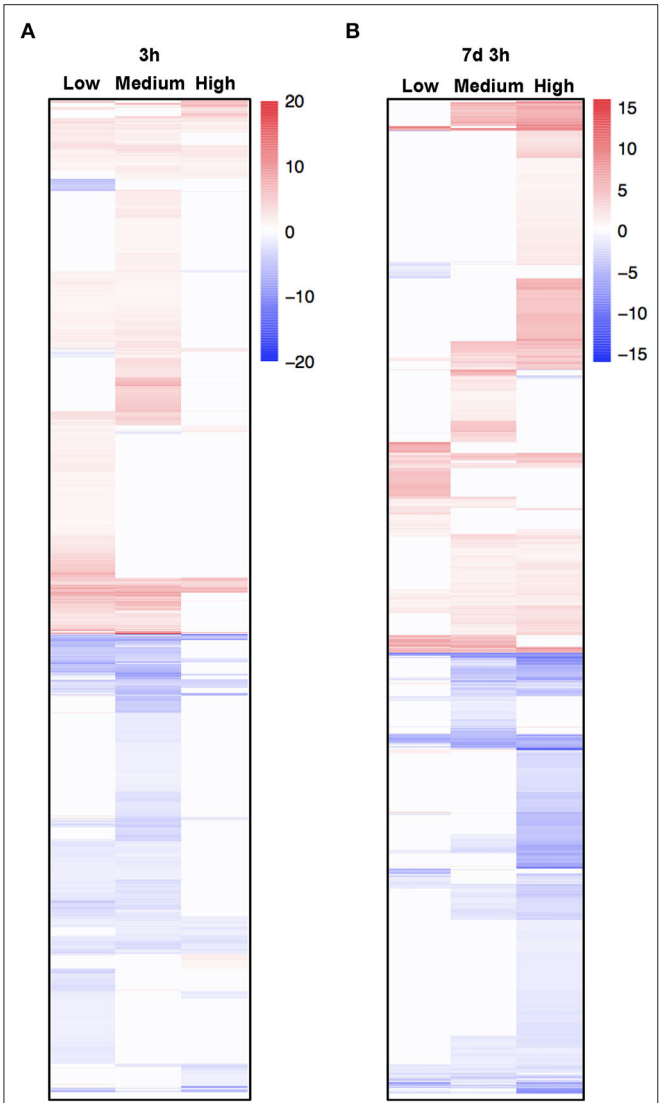


**FIGURE 6 |** Heatmap of coregulated genes in response to different salt concentrations. **(A,B)** Heat map of differentially expressed genes (DEGs) commonly regulated under salt stress of all levels. The color scale in the heat map indicates the log-ratio of the normalized gene expression value in each sample to that in mock control.

to salt tolerance by metabolic readjustment *via* the analysis of transcriptional profile.

## DISCUSSION

The woody shrub *C. inerme* belongs to the Lamiaceae family, whose natural habitats are coast, beach, and tide with salt-tolerant ability. However, how *C. inerme* displays its developmental plasticity to adjust the salinized soils remains unclear. In this study, we provide evidence showing that *C. inerme* trim its growth at different levels to adapt to the saline environment although suffered from salt stress. First, phenotypic analyses revealed that premature senescence and biomass reduction are results from resources redirected to improve the tolerance to saline adversity. Secondly, that the increase of MDA and the decrease of GSH indicates the damage was gradually serious, yet the boosting of Pro under medium and high salt treatment demonstrated that *C. inerme* relocates energy for produced osmotic-resistant metabolite to survive. Third, ROS scavenging enzymes climbed gradually from no salt to medium salt treatment but declined significantly under high salt, which explains that the saline tolerance system is robust under the medium level of salt stress yet overloads when faced with high salt adversity. Fourth, enhanced chlorophyll and ionic fluxes content increases photosynthesis, whereas declined photosynthesis efficiency reflects the tolerance mechanism, in which *C. inerme* tries to increase photosynthesis to produce energy for resistance and make up for the damage caused by the elevated salt environment. Finally, global transcriptional profiling revealed that *C. inerme* switched on osmoprotection mainly to modulate the expression of genes related to metabolism to maintain cellular osmotic homeostasis and retard growth under salt stress. These findings thus uncover how *C. inerme* survive and strive in the salinized circumstance with salt-tolerant ability.

The plant actively retards the growth rate in response to salt stress, leading to increased survival. Thus, a positive relationship between reduced biomass and elevated NaCl concentration has been observed in this long-term salt stress experiment (1∼2 weeks here), although the chlorophyll content increased yet photosynthetic efficiency declined (**Figures 1C,D**, **2**). Salt stress activates ethylene biosynthesis and signaling, which reduced photosynthesis in young leaves while accelerating plant senescence (Ceusters and Van de Poel, 2018). Likewise, the etiolation and crease of leaves were more and more obvious with the increase of salt (**Figure 1A**). These results agree with the general observation that after being stressed, photosynthetic efficiency will rapidly decrease, whether it is salt-sensitive or salt-tolerant plants.

Dramatic accumulation of Pro is a conventional physiological response of plants in the face of various abiotic stresses. Pro effectively maintains cell turgor, promotes water flow into the cytoplasm, stabilizes the active conformation of enzyme proteins, preserves cell pH value, and eliminates free radicals and redox potential (Kaur and Asthir, 2015). There is a general consensus that the increase of proline content following stress is beneficial for the plant (Verbruggen and Hermans, 2008). In particular, Pro indirectly protects the photochemical efficiency of PSII as well as directly scavenges ROS during drought (Molinari et al., 2007). Here, we found that Pro stayed at a low level in the presence of no or low salt treatment, but rocketed under medium and high saline stress (**Figure 2B**). Accordingly, the actual photochemical quantum efficiency ΦPSII decreased gently with the increase of salt concentration (**Figure 3H**). These results agree with the previous discovery that Pro protects the PSII reaction center from damage, although PSII is somehow destroyed and its potential activity is inhibited under high salt stress.

It is generally believed that salt stress can increase the production of ROS such as singlet oxygen ($^1O^2$), superoxide radical ($O^{2-}$), hydrogen peroxide ($H_2O_2$), and hydroxyl radical

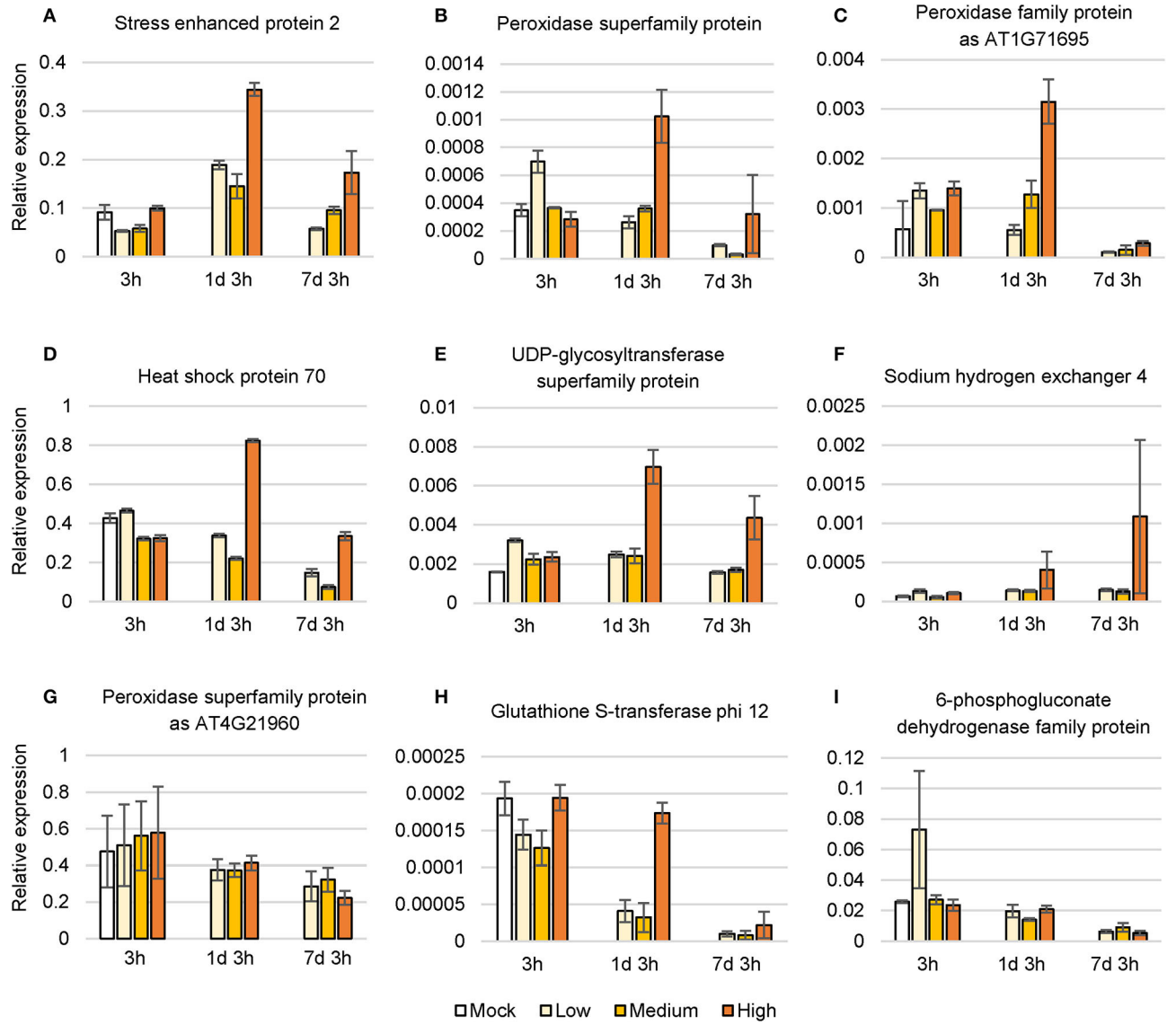


**FIGURE 7 |** Relative expression level of nine salt response genes under NaCl stress. **(A–I)** Differentially expressed genes under different saline concentration for the indicated time. $H_3$ was used as a normalization control. Data are the means of three technical replicates ± SD. Mock, no salt control; Low, low salt stress; Medium, medium salt stress; High, high salt stress.

($OH^-$), which seriously disrupt normal metabolism in the plant through oxidation of membrane lipids, proteins, and nucleic acids (Smirnoff, 1993; Hernandez et al., 2001). On the other hand, plants evolve a resistance system including antioxidant enzymes such as SOD, CAT, and POD to protect their cells against ROS. Some studies suggest that salt stress leads to an increase in SOD activity in salt-tolerant plants but a decrease in salt-sensitive ones (Rout and Shaw, 2001). Meanwhile, POD and CAT can catalyze $H_2O_2$ into $H_2O$ and $O_2$ to prevent the continuous accumulation of ROS and decelerate the senescence of the plant. In this study, no significant changes in SOD and POD were observed, probably due to the 2-week long-term stress condition when the intracellular homeostasis already reached before then (**Figures 2E,F**). Little change was also detected in GSH content, which participates in the elimination of $H_2O_2$ through the catalysis of NADPH-dependent glutathione reductase and can be used as an antioxidant (**Figure 2C**).

Various indicators of photosynthesis showed that the photosynthetic rate of *C. inerme* decreased significantly under medium and high salt treatment (**Figures 3B–H**), but the chlorophyll content was higher than that at no or low salt concentration (**Figure 3A**). It can be explained that *C. inerme* attempts to synthesize more chlorophyll through the metabolic pathway to improve photosynthetic efficiency and produce energy to make up for the energy loss to resist salt stress. However, mainly due to the damage to chloroplast structure

or the destruction of enzymes required for photosynthesis, the overall photosynthetic efficiency in *C. inerme* was decreased under medium and high salinity, which reflects the destructive effect of the salt environment.

Various experimental results support the notion that $Na^+/H^+$ antiporters in the plasma membrane mediate $Na^+$ effluxes (Qiu et al., 2002, 2003; Xiong et al., 2002), whose proton motive force is offered by P-type $H^+$-ATPases (Schachtman and Liu, 1999). In this study, the outflow of $Na^+$ and $K^+$ increased significantly from mesophyll cells to balance the passive absorption of excess $Na^+$ by the plant under high NaCl concentration (**Figures 4A–D**). However, the influx of $H^+$ stagnated as more $H^+$ participated in the function of $H^+$-ATPase and flew out (**Figures 4E,F**). Finally, the activity of $H^+$-ATPase was increased (**Figure 4G**), which is in agreement with other studies mentioned. The results suggested that *C. inerme* copes with the absorption of excessive $Na^+$ caused by salt stress by increasing the outflow of cations by the motive force from $H^+$-ATPase.

High throughput and transcriptome analysis are important for salt-stress-related gene screening and effective approaches for studying the molecular regulation of salt tolerance in the plant (Song et al., 2020). Results of this study showed that *C. inerme* adapted to salinity stress by adjusting the metabolism of nucleotides, amino acids, carbohydrates, and enzymes along with transcriptional factors and plant hormones at the early stage (**Figures 5–7**). These findings are in agreement with and include the discovery shown in the previous RNA-Seq study on *C. inerme*, which demonstrated that genes related to plant hormone signaling were crucial to the saline response of *C. inerme* (Xiong et al., 2019). However, decreased expression of genes in the cellular process and increased expression of genes related to metabolism were detected, indicating the survival strategy of *C. inerme* by constitutively modulating metabolism to meet the challenges of ion disorders and the toxic effect caused by NaCl adversity.

# MATERIALS AND METHODS

## Plant Materials and Growth Conditions

Seedlings of *C. inerme* were planted in the local red soil in a greenhouse in South China Botanical Garden, Chinese Academy of Sciences in Guangzhou City, Guangdong Province. The 30-day-old *C. inerme* seedlings were transferred to the coral sand which was collected from Paracel Islands. Before transplanting, the coral sands were pre-washed five times to a final pH at 9.35, electrical conductivity at 0.170 ms/cm, and mass fraction of salt at 0.319. After transplanting, seedlings were irrigated with deionized water supplemented with 1 g/L water-soluble fertilizer Huawuque containing 20% N, 20% P, and 20% K, every 3 days. Then, 7 days after acclimation, the seedlings were treated with 0.1, 0.3, and 0.5 M NaCl solution, respectively. To avoid the adverse effects of rapid change in soil salt content, NaCl was gradually added to the final concentration on the 7th day (**Supplementary Table S1**). The control group was irrigated with deionized water. Five replicates were set for each treatment. After treatment, the 3rd and 4th newly grown leaves were harvested for physiology and gene expression analysis. All enzyme extract procedures were conducted at 4°C.

## Phenotyping and Biomass Analysis

Forteen days after salt treatment, the plant height, fresh weight, and dry weight of the seedlings were measured. The fresh weight was determined after the root, stem, and leaf of the seedlings were fully washed. For dry weight analysis, clean seedlings were placed at 105°C for 30 min, then dried to constant weight at 80°C.

## MDA Analysis

The 0.5 g leaves were ground and homogenized in 10% cold TCA buffer. After centrifuging for 10 min, the supernatant was collected and 0.5% TBA was added. After being boiled for 20 min, the supernatant was collected and the OD values were tested at 450, 532, and 600 nm, respectively.

$$\mathrm{MDA}(\mu\mathrm{mol/g}) = \frac{[6.45(OD_{532} - OD_{600}) - 0.56OD_{450}]^{*}V}{W}$$

$OD_{450}$, $OD_{532}$, and $OD_{600}$, absorbance values at 450, 532, and 600 nm, respectively; V, volume of the supernatant (ml); W, fresh weight of the plant tissue (g).

## Proline Analysis

The 0.3 g leaves were ground and homogenized in 2 mL 80% ethanol, and then placed in 80°C water bath for 20 min. After filtering, 2 mL glacial acetic acid and 2 mL ninhydrin were added to 2 mL homogenate. After boiling for 15 min, the mixture was cooled to room temperature and the OD value at 520 nm was measured. A standard curve was established with pure proline as reference.

$$\mathrm{Pro}(\mathrm{mg/g}) = \frac{C^{*}V}{1000M}$$

V, volume of the homogenate (mL); C, proline content analysis using standard curve as reference (g/mL); M, fresh weight of the leaf sample (g).

## GSH Analysis

The 0.5 g tissue was ground and homogenized in 5 mL 5% trichloroacetic acid. After centrifuging at 15,000 rpm for 10 min, 0.25 mL supernatant was added with 2.6 mL 150 mM PBS (pH7.7) and 0.15 mL DTNB (75.3 mg DTNB dissolved in 30 mL 100 mM PBS pH6.8). The OD value was determined at 412 nm and the content of GSH was calculated according to the standard curve made with pure GSH.

## Total Flavonoids Analysis

The 0.5 g leaves were ground and homogenized in 5 mL 70% ethanol. The homogenate was shattered by ultrasonic for 30 min and rotated for 12 h at room temperature. After centrifuging at 12,000 rpm for 10 min, 300 μL supernatant was added with 7 mL 70% ethanol, 500 μL 5% $NaNO_2$ solution, and stayed at room temperature for 6 min. The 500 μL of 10% Al $(NO_3)_3$ was then added and placed at room temperature for 6 min. Finally, 4 mL 4% NaOH and 2 mL 70% ethanol were added and stayed still for 15 min. The OD value at 510 nm was determined and the content

of total flavonoids was calculated according to the standard curve. The standard curve was established by diluting pure rutin with a 70% ethanol solution.

## SOD Activity Analysis

About 0.5 g of leaves were ground and homogenized with 5 mL cold PBS buffer. The homogenate was centrifuged at 10,000 rpm for 15 min. 50 μL supernatant was mixed with the reaction solution including 0.05 M PBS, 220 mM Met, 1.25 mM NBT, and 33.5 mM riboflavin, and placed under light for 20 min. The mixture of PBS buffer and reaction solution without plant homogenate which was kept in the dark was used as a control group. The OD value of the reaction was measured at 560 nm.

$$\text{SODactivity(U/g)} = \frac{(A_{CK} - A_E) * V}{A_{CK} * 0.5 * W * V}$$

$A_{CK}$, OD value of the control group; $A_E$, OD value of the sample; V, volume of enzymic reaction mixture; $V_t$, sample volume added to reaction solution; W, fresh weight of plant leaves (g).

## POD Activity Analysis

About 0.2 g of leaves were added with five times the volume of PBS pH 7.0 by mass concentration in a precooled 5-ml tube and ground in the 60 Hz grinder for 2 min. The homogenate was centrifuged at 15,000 rpm for 15 min at 4°C. And 50 μl supernatant was mixed with 1 mL 0.3% $H_2O_2$, 0.95 mL guaiacol, and 1 mL PBS pH7. The OD value at 470 nm was then measured every 10 s for 1 min. The 0.01 increase of OD value per minute was defined as one enzyme activity unit.

## Chlorophyll Content Analysis

About 0.4 g of leaves were cut into pieces and extracted with the extraction buffer containing acetone, anhydrous ethanol, and deionized water in a ratio of 4.5:4.5:1. The extract stayed at 4°C for 24 h. OD value of the mixture was taken at 645 nm and 663 nm, and the chlorophyll content of plant leaves was then calculated according to the formula below.

$$\text{Chla(mg/g)} = \frac{12.7OD_{663} - 2.69OD_{645} * V}{1000W}$$

$$\text{Chlb(mg/g)} = \frac{-22.9OD_{645} - 4.68OD_{663} * V}{1000W}$$

Total chlorophyll (mg/g) = Chla + Chlb

V, final volume of the extract (mL); W, fresh weight of leaves (g).

## Determination of Photosynthetic Index

The net photosynthetic rate, transpiration rate, stomatal conductance, and intercellular $CO_2$ concentration from the 3rd and 4th leaves of plants were measured *via* portable photosynthetic instrument Li-6800 (LI-COR, USA) under cloudless sunny weather with unfolded greenhouse canopy as well as avoiding the morning and evening time with strong and weak sunlight.

## Determination of Chlorophyll Fluorescence

The plants were placed in dark for more than 3 h. The maximum photochemical efficiency (Fv/Fm), initial fluorescence (F0), and photochemical quantum efficiency of (ΦPSII) from the 3rd and 4th leaves of plants were then measured by portable photosynthetic instrument Li-6800 (LI-COR, USA).

## Concentration, Direction, and Velocity of $K^+$, $H^+$, and $Na^+$ Flow in Mesophyll Cells

A 0.5-mm diameter disc dissected from the 3rd and 4th newly grown leaves after 14 days of salinity treatment were harvested and placed on buffer (100 mM KCl for $K^+$; 15 mM NaCl, 40 mM $KH_2PO_4$ pH 7.0 for $H^+$; 250 mM NaCl for $Na^+$) in the petri dish. A pair of needle tip-like microsensors controlled by the software were inserted into both sides of the mesophyll cell membrane under a microscope. Voltage signals were captured to reflect the ionic fluxes between the cytoplasm and the intercellular space. The concentration, direction, and velocity of $K^+$, $H^+$, and $Na^+$ ion flow were then detected *via* selective microsensors. This micro measurement technology was provided by Xuyue (Beijing) Scientific Technology Company and the technical service center of Jiangsu Normal University (BIO-IM Series, Younger USA LLC, Amherst, Ma 01002).

## $H^+$-ATP Synthase Activity

The activity of $H^+$-ATP synthase was determined by the ELISA kit (CUSABIO BIOTECH Co., Ltd., Wuhan, China) according to the manufacturer's instructions. In brief, 0.2 g leaves were added with nine times the volume of PBS pH 7.4 by mass concentration in a precooled 5-ml tube and ground in the 60 Hz grinder for 2 min. The homogenate was centrifuged at 15,000 rpm for 15 min at 4°C. About 10 μL reference standard or 40 μL supernatant sample was added into the well plate with the micropores pre-coated with plant hydrogen ATPase ($H^+$-ATP) antibody. HRP labeled antibody was successively added and washed thoroughly. The substrate TMB used for color development was added to convert into blue under the catalysis of peroxidase and finally into yellow by the presence of acid. The color depth was positively correlated with the synthase activity in the sample. OD value of the sample was taken at 450 nm and the activity was calculated.

## RNA-Seq Analysis

The total RNA was extracted using Column Plant RNAout2.0 (Tiandz Inc., Beijing, China) according to the manufacturer's protocol. Extracted RNA was treated with DNase (Tiandz Inc., Beijing, China) to remove genomic DNA. The sequencing libraries with an average insert length of 240 bp were generated using the NEBNextR UltraTM Directional RNA Library Prep Kit for IlluminaR (NEB, USA) and sequenced on the Illumina HiSeq4000 platform (Illumina Inc., USA) by Bio&Data Biotechnology Co., Ltd (Guangzhou, China) following manufacturer's recommendations. The reads were assembled into unigenes which were aligned with the *Arabidopsis thaliana* genome by BLASTN for functional annotation since the genomic information of *Clerodendrum*

*inerme* was not yet available. Differentially expressed genes were defined based on the following criteria: a DESeq2 adjusted $P < 0.05$ and fold change $> 2$ compared with the control samples. The hypergeometric Fisher exact test ($P < 0.01$) and Benjamini (FDR $< 0.05$) were performed to detect statistically significant enrichment of the KEGG pathway. All sequence data were uploaded into the BioProject database hosted by the National Center for Biotechnology Information (NCBI) under the BioProject PRJNA817709. Three independent replicates were performed in this experiment.

### RNA Extraction and qRT-PCR

Total RNA was extracted by a HiPure Plant RNA Mini Kit (Magen, China). The cDNA was synthesized by HiScript® III All-in-one RT SuperMix Perfect for qPCR (Vazyme, China). The qRT-PCR reaction was performed in a 384-well block using a ChamQ Universal SYBR qPCR Master Mix (Vazyme, China). The values for each set of primers were normalized relative to the *H3* gene. All qRT-PCR reactions were performed in triplicates. The specific primers used in this study are listed in **Supplementary Table S2**.

## CONCLUSION AND FUTURE PERSPECTIVES

The response of *C. inerme* to salt stress begins to show under a low level of salt stress. Membrane lipid peroxidation is manifested in the early stage, and it responds to saline stress through antioxidant enzymes, osmotic regulators, and antioxidants, which is consistent with the finding of transcriptional global profiling. The photosynthetic rate of *C. inerme* was also affected; PSII can maintain a certain efficiency under low and medium salt stress, but it is aggrieved under high salt stress. In the face of NaCl stress, the outflow of $Na^+$ tends to decrease and the influx of $H^+$ decreases at low and medium saline levels, which may be due to the induction of the $Na^+/H^+$ antiporter of the tonoplast membrane by $H^+$-ATPase to store $Na^+$ store in vacuoles. Thus the accumulation of $Na^+$ reduces in the cytoplasm. All these biochemical and physiological results show that *C. inerme* suffers ion toxicity under high salt stress. Moreover, efforts should be made in the future to investigate the roles of salt tolerance of *C. inerme* through a multi-omics approach. Together, the findings can provide a rich resource for breeding salt-tolerant cultivars through biotechnological measures of the time.

## DATA AVAILABILITY STATEMENT

The datasets presented in this study can be found in online repositories. The names of the repository/repositories and accession number(s) can be found below: National Center for Biotechnology Information (NCBI) BioProject database under accession number PRJNA817709.

## AUTHOR CONTRIBUTIONS

XL and FW designed the research. ML, FH, DX, ZC, QZ, QX, FZ, and DL performed the experiments. ML, DX, SJ, and HC analyzed the data. ML and XL wrote the manuscript. All authors contributed to the article and approved the submitted version.

## FUNDING

This work was supported by the National Natural Science Foundation of China (32070551), the Science and Technology Planning Project of Guangdong Province (2021B1212110004), the Strategic Priority Research Program of the Chinese Academy of Sciences (XDA13020603), and the Urban Forestry Plan of Guangzhou (2021-120).

## SUPPLEMENTARY MATERIAL

The Supplementary Material for this article can be found online at: https://www.frontiersin.org/articles/10.3389/fpls.2022.882884/full#supplementary-material

**Supplementary Figure 1 |** Morphogenesis of *C. inerme* before salinity stress. **(A)** Shoot height was measured on day 0 under NaCl stress. **(B)** Root-to-shoot ratio by dry weight after 14 days under different saline condition. Different letters indicate significant differences among plant groups ($p < 0.05$, Mann Whitney test). Mock, no salt control; L, low salt stress; M, medium salt stress; H, high salt stress.

**Supplementary Table S1 |** NaCl concentration for salinity stress.

**Supplementary Table S2 |** Primers used for qRT-PCR.

**Supplementary Table S3 |** Alternatively expressed transcripts under short-term salt exposure.

**Supplementary Table S4 |** Alternatively expressed transcripts under long-term salt exposure.

## REFERENCES

Acharya, B. R., Sandhu, D., Duenas, C., Ferreira, J. F. S., and Grover, K. K. (2022). Deciphering molecular mechanisms involved in salinity tolerance in Guar (*Cyamopsis tetragonoloba* (L.) Taub.) using transcriptome analyses. *Plants (Basel)* 11, 291. doi: 10.3390/plants11030291

Bose, J., Munns, R., Shabala, S., Gilliham, M., Pogson, B., and Tyerman, S. D. (2017). Chloroplast function and ion regulation in plants growing on saline soils: lessons from halophytes. *J. Exp. Bot.* 68, 3129–3143. doi: 10.1093/jxb/erx142

Ceusters, J., and Van de Poel, B. (2018). Ethylene exerts species-specific and age-dependent control of photosynthesis. *Plant Physiol.* 176, 2601–2612. doi: 10.1104/pp.17.01706

Chen, C. X., Shang, X. L., Sun, M. Y., Tang, S. Y., Khan, A., Zhang, D., et al. (2022). Comparative transcriptome analysis of two sweet sorghum genotypes with different salt tolerance abilities to reveal the mechanism of salt tolerance. *Int. J. Mol. Sci.* 23, 2272. doi: 10.3390/ijms23042272

Dietz, K. J., Jacob, S., Oelze, M. L., Laxa, M., Tognetti, V., de Miranda, S. M., et al. (2006). The function of peroxiredoxins in plant organelle redox metabolism. *J. Exp. Bot.* 57, 1697–1709. doi: 10.1093/jxb/erj160

Dong, S. Y., and Beckles, D. M. (2019). Dynamic changes in the starch-sugar interconversion within plant source and sink tissues promote a better abiotic stress response. *Plant Physiol.* 234, 80–93. doi: 10.1016/j.jplph.2019.01.007

Flowers, T. J., Munns, R., and Colmer, T. D. (2015). Sodium chloride toxicity and the cellular basis of salt tolerance in halophytes. *Ann. Bot.* 115, 419–431. doi: 10.1093/aob/mcu217

Glenn, E. P., Brown, J. J., and Blumwald, E. (1999). Salt tolerance and crop potential of halophytes. *Crit. Rev. Plant Sci.* 18, 227–255. doi: 10.1080/07352689991309207

Hernandez, J. A., Ferrer, M. A., Jimenez, A., Barcelo, A. R., and Sevilla, F. (2001). Antioxidant systems and $O^{-2(\cdot,-)}/H_2O_2$ production in the apoplast of pea leaves. Its relation with salt-induced necrotic lesions in minor veins. *Plant Physiol.* 127, 817–831. doi: 10.1104/pp.010188

Ignat, I., Volf, I., and Popa, V. I. (2011). A critical review of methods for characterisation of polyphenolic compounds in fruits and vegetables. *Food Chem.* 126, 1821–1835. doi: 10.1016/j.foodchem.2010.12.026

James, R. A., Davenport, R. J., and Munns, R. (2006). Physiological characterization of two genes for $Na^+$ exclusion in durum wheat, *Nax1* and *Nax2*. *Plant Physiol.* 142, 1537–1547. doi: 10.1104/pp.106.086538

Kaur, G., and Asthir, B. (2015). Proline: a key player in plant abiotic stress tolerance. *Biol. Plantarum* 59, 609–619. doi: 10.1007/s10535-015-0549-3

Khan, M. A., and Qaiser, M. (2006). *"Halophytes of Pakistan: characteristics, distribution and potential economic usages," in Sabkha Ecosystems. Tasks for Vegetation Science, Vol.* 42, eds M. A. Khan, B. Böer, G. S. Kust, and H. J. Barth (Dordrecht: Springer). doi: 10.1007/978-1-4020-5072-5_11

Li, L., Li, M. M., Qi, X. W., Tang, X. L., and Zhou, Y. F. (2018). *De novo* transcriptome sequencing and analysis of genes related to salt stress response in *Glehnia littoralis*. *PeerJ* 6, e5681. doi: 10.7717/peerj.5681

Lotfi, N., Vahdati, K., Amiri, R., and Kholdebarin, B. (2010). Drought-induced accumulation of sugars and proline in radicle and plumule of tolerant walnut varieties during germination phase. *Acta. Hortic.* 861, 289–295. doi: 10.17660/ActaHortic.2010.861.39

Meloni, D. A., Oliva, M. A., Martinez, C. A., and Cambraia, J. (2003). Photosynthesis and activity of superoxide dismutase, peroxidase and glutathione reductase in cotton under salt stress. *Environ. Exp. Bot.* 49, 69–76. doi: 10.1016/S0098-8472(02)00058-8

Mittler, R., Vanderauwera, S., Gollery, M., and Van Breusegem, F. (2004). Reactive oxygen gene network of plants. *Trends. Plant Sci.* 9, 490–498. doi: 10.1016/j.tplants.2004.08.009

Molinari, H. B. C., Marur, C. J., Daros, E., de Campos, M. K. F., de Carvalho, J. F. R. P., Bespalhok, J. C., et al. (2007). Evaluation of the stress-inducible production of proline in transgenic sugarcane (*Saccharum* spp.): osmotic adjustment, chlorophyll fluorescence and oxidative stress. *Physiol. Plantarum* 130, 218–229. doi: 10.1111/j.1399-3054.2007.00909.x

Munns, R., and Gilliham, M. (2015). Salinity tolerance of crops - what is the cost? *New Phytol.* 208, 668–673. doi: 10.1111/nph.13519

Park, H. J., Kim, W. Y., and Yun, D. J. (2016). A new insight of salt stress signaling in plant. *Mol. Cells* 39, 447–459. doi: 10.14348/molcells.2016.0083

Qiu, Q. S., Barkla, B. J., Vera-Estrella, R., Zhu, J. K., and Schumaker, K. S. (2003). Na+/H+ exchange activity in the plasma membrane of Arabidopsis. *Plant Physiol.* 132, 1041–1052. doi: 10.1104/pp.102.010421

Qiu, Q. S., Guo, Y., Dietrich, M. A., Schumaker, K. S., and Zhu, J. K. (2002). Regulation of SOS1, a plasma membrane Na+/H+ exchanger in Arabidopsis thaliana, by SOS2 and SOS3. *Proc. Natl. Acad. Sci. U. S. A* 99, 8436–8441. doi: 10.1073/pnas.122224699

Rad, P. B., Roozban, M. R., Karimi, S., Ghahremani, R., and Vahdati, K. (2021). Osmolyte Accumulation and Sodium Compartmentation Has a Key Role in Salinity Tolerance of Pistachios Rootstocks. *Agriculture* 11, 708. doi: 10.3390/agriculture11080708

Rout, N. P., and Shaw, B. P. (2001). Salt tolerance in aquatic macrophytes: possible involvement of the antioxidative enzymes. *Plant Sci.* 160, 415–423. doi: 10.1016/S0168-9452(00)00406-4

Schachtman, D., and Liu, W. (1999). Molecular pieces to the puzzle of the interaction between potassium and sodium uptake in plants. *Trends. Plant Sci.* 4, 281–287. doi: 10.1016/S1360-1385(99)01428-4

Schroeder, J. I., Delhaize, E., Frommer, W. B., Guerinot, M. L., Harrison, M. J., Herrera-Estrella, L., et al. (2013). Using membrane transporters to improve crops for sustainable food production. *Nature* 497, 60–66. doi: 10.1038/nature11909

Skorupa, M., Golebiewski, M., Domagalski, K., Kurnik, K., Abu Nahia, K., Zloch, M., et al. (2016). Transcriptomic profiling of the salt stress response in excised leaves of the halophyte Beta vulgaris ssp maritima. *Plant Sci.* 243, 56–70. doi: 10.1016/j.plantsci.2015.11.007

Smirnoff, N. (1993). Tansley review. 52. The role of active oxygen in the response of plants to water-deficit and desiccation. *New Phytol.* 125, 27–58. doi: 10.1111/j.1469-8137.1993.tb03863.x

Song, Q. S., Joshi, M., and Joshi, V. (2020). Transcriptomic analysis of short-term salt stress response in watermelon seedlings. *Int. J. Mol. Sci.* 21, 6036. doi: 10.3390/ijms21176036

Takahashi, M., and Asada, K. (1988). Superoxide production in aprotic interior of chloroplast thylakoids. *Arch. Biochem. Biophys.* 267, 714–722. doi: 10.1016/0003-9861(88)90080-X

Verbruggen, N., and Hermans, C. (2008). Proline accumulation in plants: a review. *Amino Acids* 35, 753–759. doi: 10.1007/s00726-008-0061-6

Xiong, L. M., Schumaker, K. S., and Zhu, J. K. (2002). Cell signaling during cold, drought, and salt stress. *Plant Cell* 14, S165–S183. doi: 10.1105/tpc.000596

Xiong, Y. P., Yan, H. F., Liang, H. Z., Zhang, Y. Y., Guo, B. Y., Niu, M. Y., et al. (2019). RNA-Seq analysis of *Clerodendrum inerme* (L.) roots in response to salt stress. *BMC Genomics* 20, 724. doi: 10.1186/s12864-019-6098-y

Zhu, J. K. (2002). Salt and drought stress signal transduction in plants. *Annu. Rev. Plant. Biol.* 53, 247–273. doi: 10.1146/annurev.arplant.53.091401.143329

Zhu, J. K. (2003). Regulation of ion homeostasis under salt stress. *Curr. Opin. Plant Biol.* 6, 441–445. doi: 10.1016/S1369-5266(03)00085-2

Zhu, J. K. (2016). Abiotic stress signaling and responses in plants. *Cell* 167, 313–324. doi: 10.1016/j.cell.2016.08.029

**Conflict of Interest:** The authors declare that the research was conducted in the absence of any commercial or financial relationships that could be construed as a potential conflict of interest.

frontiers | Frontiers in Plant Science

ORIGINAL RESEARCH
published: 22 July 2022
doi: 10.3389/fpls.2022.887091

# Impact of Folic Acid in Modulating Antioxidant Activity, Osmoprotectants, Anatomical Responses, and Photosynthetic Efficiency of *Plectranthus amboinicus* Under Salinity Conditions

*Omar A. A. I. Al-Elwany[1], Khaulood A. Hemida[2], Mohamed A. Abdel-Razek[3], Taia A. Abd El-Mageed[3], Mohamed T. El-Saadony[4], Synan F. AbuQamar[5]*, Khaled A. El-Tarabily[5,6,7]* and Ragab S. Taha[8]*

[1] Horticulture Department, Faculty of Agriculture, Fayoum University, Fayoum, Egypt, [2] Botany Department, Faculty of Science, Fayoum University, Fayoum, Egypt, [3] Soil and Water Department, Faculty of Agriculture, Fayoum University, Fayoum, Egypt, [4] Department of Agricultural Microbiology, Faculty of Agriculture, Zagazig University, Zagazig, Egypt, [5] Department of Biology, College of Science, United Arab Emirates University, Al-Ain, United Arab Emirates, [6] Khalifa Center for Genetic Engineering and Biotechnology, United Arab Emirates University, Al-Ain, United Arab Emirates, [7] Harry Butler Institute, Murdoch University, Murdoch, WA, Australia, [8] Botany Department, Faculty of Agriculture, Beni-Suef University, Beni-Suef, Egypt

OPEN ACCESS

**Edited by:**
*Amr Adel Elkelish,*
*Suez Canal University, Egypt*

**Reviewed by:**
*Mohamed Farag Mohamed Ibrahim,*
*Ain Shams University, Egypt*
*Khalil Saad-Allah,*
*Tanta University, Egypt*

***Correspondence:**
*Khaled A. El-Tarabily*
*ktarabily@uaeu.ac.ae*
*Synan F. AbuQamar*
*sabuqamar@uaeu.ac.ae*

**Specialty section:**
*This article was submitted to Plant Abiotic Stress, a section of the journal Frontiers in Plant Science*

**Received:** *01 March 2022*
**Accepted:** *02 May 2022*
**Published:** *22 July 2022*

**Citation:**
*Al-Elwany OAAI, Hemida KA, Abdel-Razek MA, Abd El-Mageed TA, El-Saadony MT, AbuQamar SF, El-Tarabily KA and Taha RS (2022) Impact of Folic Acid in Modulating Antioxidant Activity, Osmoprotectants, Anatomical Responses, and Photosynthetic Efficiency of Plectranthus amboinicus Under Salinity Conditions. Front. Plant Sci. 13:887091. doi: 10.3389/fpls.2022.887091*

Salinity is a major threat to the sustainability of agricultural production systems. Salt stress has unfavorable implications on various plant physio-morphological and biochemical reactions, causing osmotic and ionic stress. Exogenously applied folic acid (FA) may at least provide one mechanism to evade the injurious stress effects of saline irrigation water on *Plectranthus amboinicus*. In this regard, two pot trials were performed during the 2018–2019 and 2019–2020 seasons in an open greenhouse of an experimental farm (29°17'N; 30°53'E) in Fayoum, Egypt. We tested four levels of saline irrigation water (SW): 34, 68, and 102 mM NaCl, plus tap water as the control = 0), combined with FA at three concentrations (25 and 50 μM, plus spray with distilled water as the control = 0). The growth parameters, biochemistry, physiology, elemental leaf status, essential oil content, and anatomical responses were assessed. Salt markedly reduced photosynthetic productivity [Fv/Fm and performance index (PI)], total chlorophyll [soil plant analysis development (SPAD)], and leaf osmoprotectant compounds, i.e., total soluble sugars (TSS), free amino acids, proline, and total phenolics, thus hampering *P. amboinicus* growth and essential oil yield. However, the addition of FA as a foliar spray to *P. amboinicus* irrigated with saline water induced increases in Fv/Fm, SPAD, and PI. These were linked with enriched stem anatomical structures, leaf osmoprotectant compounds, and enhanced leaf enzymatic activity, e.g., superoxide dismutase, catalase, ascorbate peroxidase, glutathione reductase, glutathione, ascorbic acid, and antioxidant content. Under salt stress, supplementation of 25 and 50 μM FA increased the growth and production of essential oil by 27.8 and 55.6%, respectively, compared with no applied FA. The highest growth characteristics and elemental leaf contents were obtained

when *P. amboinicus* was irrigated with 0 mM saline water and treated foliarly with 50 μM of FA compared with non-treated plants. Overall, these data showed that foliar spraying with FA reduces the impact of salt stress on *P. amboinicus* irrigated with saline water.

**Keywords: folic acid, leaf osmoprotectant growth, oil yield, photosynthetic productivity, saline water**

## INTRODUCTION

*Plectranthus* is a large genus of the family Lamiaceae, including around 300 species of *Plectranthus* native to tropical Africa, Asia, and Australia (Lukhoba et al., 2006). Globally, *Plectranthus* spp. are well known and are extensively used in traditional medicine. Many species of *Plectranthus* are used to treat digestive system disturbance, including vomiting, diarrhea, mouth and throat infections, stomach pain, and nausea (Lukhoba et al., 2006). Some species are also employed as purgatives, carminatives, and anthelmintic remedies (Githinji and Kokwaro, 1993). *P. amboinicus* is the most commonly-used species for treating burns, injuries, sores, insect bites, and sensitivities (Chifundera, 2001). Common names of *P. amboinicus* in English include Indian borage, country borage, French thyme, Indian mint, Mexican mint, Cuban oregano, soup mint, Spanish thyme (Bañuelos-Hernández et al., 2020). The leaf extract is used to make a forskolin-like chemical utilized in hair coloring (Kanne et al., 2015). Furthermore, it yields an essential oil with anti-allergenic properties *via* passive cutaneous anaphylaxis suppression (Bañuelos-Hernández et al., 2020). *Plectranthus* spp. are reported to have cytotoxic and anti-tumor properties and can be used to treat cancer (Lukhoba et al., 2006).

Salinity is distinctive environmental stress faced by plants in arid and semi-arid environments. Yield restriction resulting from salinity in soil or irrigation water has led to the desertification of about one-third of the irrigated land worldwide (Shaaban et al., 2022). In response to salt stress, morphological and biochemical changes are imposed (Ali et al., 2013) due to a reduction in the water supply to leaf tissues (Abd El-Mageed et al., 2019). Consequently, plant root length and mass are reduced (Shannon and Grieve, 1998). A reduction in leaf area could be ascribed to a decrease in turgor due to changes in cell elongation and division or a reduction in photosynthetic degree (Abd El-Mageed et al., 2019). In salt-stressed plants, reactive oxygen species (ROS), such as superoxide ($O_2^{\bullet-}$), hydrogen peroxide ($H_2O_2$), and hydroxyl ($OH^{\bullet}$) radicals, are overproduced from chloroplasts during photosynthesis (Abdou et al., 2021), leading to lipid and protein destruction and dysfunctional DNA (Yasar et al., 2006). As well, chlorophyll degradation and membrane lipid peroxidation occurs (Yildirim et al., 2008). The rapid removal of the harmful impacts of ROSs is an effective stress-defense mechanism. Antioxidant defense systems play an important role in this regard (Abd El-Mageed et al., 2018).

Salinity causes both osmotic and oxidative stress in higher plants; therefore, they have evolved complicated coping systems. These mechanisms are accomplished by either external uptake of organic compounds or by synthesizing favorable solutes, such as amino acids, sugars, and vitamins that act as osmolytes (Rady et al., 2021a). These activate protein configuration and membrane stabilization against denaturation (Munns, 2002); furthermore, they prevent water loss and maintain cell turgor under salt stress (Rady et al., 2021b). The oxidative stress mechanism occurs when ROS production represses the antioxidant system capacity (Semida et al., 2021). For these reasons, plants evolved multi-antioxidant defense mechanisms, including the antioxidants glutathione, ascorbate, β-carotene, and α-tocopherol; besides, enzymes like superoxide dismutase (SOD), catalase (CAT), ascorbate peroxidase (APX), phenol peroxidase (GPX), and glutathione reductase (GR) substitute as ROS scavengers (Semida et al., 2015b).

Folic acid (FA, folates), also called vitamin B9, is an important constituent of metabolism in all living organisms (Bekaert et al., 2008) and is a donor/acceptor for one-carbon transfer reactions taking place in the formation of many significant biomolecules, such as amino acid metabolism and nucleic acid synthesis (Gorelova et al., 2017), which enables plants to synthesize proteins (Poudineh et al., 2015). In the methyl cycle, reactions catalyzed by FA through providing methyl groups are indispensable in regulating gene expression but are also prerequisites for the synthesis of lipids, proteins, chlorophyll, and lignin (Gorelova et al., 2017).

During the past decades, *P. amboinicus* has been subjected to many agronomical and environmental studies. However, no available studies have evaluated the role of FA in the adaptation of plants under saline water (SW) irrigation.

Consequently, the current study aimed to determine the strategies through which *P. amboinicus* seedlings withstand salinity. In this investigation, the growth attributes, leaf osmoprotectant compounds, essential oil yield, leaf enzymatic activity and antioxidants, and stem and leaf anatomical structures of *P. amboinicus* plants increased when FA was imposed under SW irrigation. This was assessed by investigating the physio-morphological changes induced by salinity stress, and using FA to enhance essential oil yield and salt tolerance in *P. amboinicus* seedlings exposed to different saline irrigation water levels.

## MATERIALS AND METHODS

### Trial Site, Climatic Conditions, and Growing Media

Two pot experiments were performed in an open greenhouse of the experimental farm (southeast Fayoum; 29°17'N; 30°53'E), of the Faculty of Agriculture, Fayoum University, Fayoum, Egypt, throughout the seasons of 2018 and 2019. The average climatic conditions throughout the two experimental periods (March 6–May 26) were the average one-day and night temperatures of 32 ± 3°C and 18 ± 2°C, respectively. Relative humidity was 65 ± 4%,

and daylight interval averaged 13 h. Natural sunlight conditions were suitable throughout the experiment for all plant growth periods. Pots (40 cm in diameter and 35 cm deep) were filled with homogenized peat moss, vermiculite, and sand (2:1:1 v/v) as substrates for the growing media.

## Plant Material, Trial Design, and Cultural Practices

*P. amboinicus* cuttings were rooted on a plastic box (10 cm in diameter) in the growth chamber next to the greenhouse in February 2018 and 2019. After 2 weeks, when seedlings had an intact and healthy root, they were resettled into black plastic pots on 6 March of the two respective seasons. *P. amboinicus* seedlings were allowed to establish for 21 days after transplantation (DAT) before irrigation with SW on 27 March. During this period, the developed shoots were pinched over the 3$^{rd}$ leaf for branching. Before transplantation, all pots of all treatments were set in a completely randomized form in a factorial scheme in an open greenhouse.

Regardless of the irrigation with SW levels as an experimental factor, standard agronomic practices were performed according to need, including fertilization and pest and disease control. Before transplantation, the growing media in each pot (1.4 L) was supplemented with 1.5 g of Nutri-Leaf NPK fertilizer (20, 20, and 20% of N, $P_2O_5$, and $K_2O$, respectively) (Agro-Consult Co., Corniche El-Neil, Cairo, Egypt). After transplantation, the fertilizer was regularly applied once a week for all plants of all treatments as a foliar spray of 1 g $l^{-1}$ of Kristalon (20, 5, 10, and 2% of N, $P_2O_5$, $K_2O$, and Mg, respectively) (YARA Agri, Staré Město, Czech Republic) starting from 20 DAT and through the end of the flowering stage.

## Treatments and Other Practices

For both seasons, we started saline irrigation treatments [SW: 34, 68, and 102 mM NaCl, and control (0; tap water)] after 21 days of transplantation (27 March) to the end of the experiment (May 26). The *P. amboinicus* plants were irrigated twice a week. Seedlings of each salinized-water stress level were regularly sprayed with foliar FA at concentrations of 0, 25, and 50 μM (0 = control = spray with distilled water). Sixty pots were allocated for each SW treatment. The pots for each water treatment were divided into three groups, each with 20 pots occupied by three levels of FA. Therefore, 12 treatments (4 SW × 3 FA) were applied with three replicates under greenhouse conditions. FA as the foliar spray was applied three times during the experiment (21, 28, and 35 DAT, respectively).

## Plant Sampling

At 45 DAT, five plants were randomly selected from every treatment and cut to ground level for anatomical study. For the agronomical study, at 90 DAT, five *P. amboinicus* plants and their whole root systems were carefully removed from each experimental plot. In addition, five plants from each treatment were chosen at random for dry matter and physio-biochemical evaluations.

## Growth Characteristics

Plants were immersed in a bucket of water and shaken gently to eliminate any adhering growing media, and the length of roots and shoots (cm) were assessed by a meter scale. The number of shoots and leaves on each plant were counted. The stem diameter (mm) was assessed by a Sealy So707-Digital Electronic Vernier Caliper (0–150 mm/0–6″) above the soil surface by 5 cm. The shoot/root systems were weighed to determine their fresh weight (g plant$^{-1}$), then placed in an over at 80°C for 72 h. The dry shoot and dry root weights were recorded (g plant$^{-1}$).

## Determination of Total Chlorophyll, Chlorophyll Fluorescence, and PI of Photosynthesis

Total chlorophyll [soil plant analysis development (SPAD)] was assessed using a Konica Minolta chlorophyll meter [SPAD 502 model (Konica Minolta Optics, Osaka, Japan)] on the third developed leaf from the lateral shoot. Chlorophyll fluorescence ($F_v/F_m$) and the performance index (PI) were assessed on two different sunny days by a portable fluorometer (Handy PEA, Hansatech Instruments Ltd., Kings Lynn, United Kingdom) as previously reported (Clark et al., 2000; Maxwell and Johnson, 2000).

## Determination of Leaf Osmoprotectant Compounds

Total soluble sugars (TSS) were extracted and measured at 625 nm by a Bausch and Lomb-2000 Spectronic Spectrophotometer (Bausch and Lomb analytical systems divisions, Rochester, New York, USA) (Irigoyen et al., 1992). The colorimetric approach described by Bates et al. (1973) was used to identify proline concentration (mg 100 g DW$^{-1}$). Using the methanolic extract of the same leaf material, the total phenolics (mg g DW$^{-1}$) were assessed by the Folin–Ciocalteu colorimetric technique reported by Singleton and Rossi (1965). We used the formula [phenol content (mg catechin g$^{-1}$ DW) = ($A_s/A_c$) × R × 250] of Hashemi et al. (2011) to compute the phenolic contents, where $A_s$ and $A_c$ represent the absorbance readings of the sample and the catechin, respectively. The percentage of extraction yield was denoted by R. Soluble proteins were extracted according to the method described by Hassanein (1977). Then, the extractable was identified according to the method adopted by Bradford (1976). Free amino acids were extracted and determined according to the methods by Yemm et al. (1955) and Vartanian et al. (1992).

## Extraction of Essential Oil

The essential oil was assessed by the hydro-distillation method wherein the aerial parts of dried plants (100 g) in a modified Clevenger apparatus for 3 h of extraction (Esquível et al., 1999). Subsequently, distillation was stopped, so the essential oil percentage was measured using the dry weight of the aerial parts (biomass yield) of *P. amboinicus* plants.

**TABLE 1 |** The effect of SW irrigation and FA spraying on growth characteristics of *Plectranthus amboinicus* plants grown under greenhouse conditions.

| Treatment | Shoot length (cm) | Number of shoots plant$^{-1}$ | Number of leaves plant$^{-1}$ | Stem diameter (mm) | Root length (cm) | Shoot weight (g plant$^{-1}$) | |
|---|---|---|---|---|---|---|---|
| | | | | | | FW | DW |
| SW (mM) | * | * | * | * | * | * | * |
| 0 (Control) | 145.8 ± 5.8a | 13.3 ± 0.9a | 26.5 ± 1.4a | 16.3 ± 1.6a | 19.7 ± 0.9a | 679.3 ± 42.2a | 306.4 ± 14.0a |
| 34 | 135.2 ± 5.5b | 11.7 ± 0.6b | 21.8 ± 1.1b | 14.2 ± 0.9b | 16.7 ± 0.9b | 526.9 ± 35.0b | 260.1 ± 14.7b |
| 68 | 120.5 ± 5.7c | 9.1 ± 0.7c | 16.7 ± 0.9c | 12.4 ± 1.5c | 14.5 ± 0.6c | 434.7 ± 35.1c | 199.4 ± 15.2c |
| 102 | 106.5 ± 4.3d | 7.0 ± 0.4d | 13.0 ± 1.1d | 10.4 ± 0.7d | 11.6 ± 0.3d | 351.3 ± 37.0d | 137.1 ± 15.2d |
| FA (μM) | * | * | * | * | * | * | * |
| 0 (Control) | 117.6 ± 4.9c | 8.1 ± 0.5c | 15.0 ± 1.0c | 11.6 ± 1.2c | 13.5 ± 0.6c | 438.7 ± 40.3c | 201.0 ± 15.5c |
| 25 | 127.6 ± 5.0b | 10.2 ± 0.6b | 19.2 ± 0.7b | 13.5 ± 1.4b | 15.6 ± 0.4b | 503.3 ± 39.1b | 226.4 ± 14.5b |
| 50 | 135.9 ± 6.0a | 12.4 ± 0.8a | 24.3 ± 1.8a | 14.9 ± 1.0a | 17.7 ± 1.0a | 552.2 ± 32.7a | 249.9 ± 14.4a |
| SW×FA | * | * | * | * | * | * | * |

*Indicates significant differences at $P \leq 0.05$ probability level.
According to the least-significant difference test, means ± SE followed by different letters in each column are significantly different at $P \leq 0.05$.
SW, saline water; FA, folic acid; FW, fresh weight; DW, dry weight.

## Determination of the Enzymatic and Non-Enzymatic Antioxidant Compounds

Fresh *P. amboinicus* leaf (1 g) samples were homogenized in liquid $N_2$ with 0.05 M phosphate buffer (pH 7.0) containing 0.1 M EDTA and 1% PVP at 4°C by a mortar and pestle, followed by centrifugation at 4°C in a Beckman Coulter refrigerated centrifuge (Brea, California, USA) at 15,000 × g for 15 min (Garratt et al., 2002). Then, the concentration of SOD, APX, CAT, and GR was assessed according to the methods of Beauchamp and Fridovich (1971), Nakano and Asada (1981), Thomas et al. (1982) and Aebi (1984). The performance of non-enzymatic, e.g., ascorbic acid (AsA) and glutathione (GSH), was determined according to Jablonski and Anderson (1978) and Kampfenkel et al. (1995).

## Determination of Mineral Content of Leaves

Using the same leaf material, the N content (%) was assessed (Donald and Robert, 1998). The P content (mg g$^{-1}$ DW) was quantitatively measured using the molybdenum-reduced molybdophosphoric blue color method (Jackson, 1973) in sulfuric acid, and using diluted sulfomolybdic acid and sodium bisulphite-$H_2SO_4$ solutions as reagents. The contents of $K^+$ and $Na^+$ (mg g$^{-1}$ DW) were measured using a Perkin-Elmer Model 52-A Flame Photometer (PerkinElmer, Inc., Waltham, Massachusetts, USA) (Wilde et al., 1985). The leaf $Cl^-$ content (mg g$^{-1}$ DW) was measured using a Perkin-Elmer Atomic Absorption Spectrophotometer (PerkinElmer, Inc.) (Higinbotham et al., 1967).

## Anatomical Study

For the anatomical measurement, leaf and stem samples were taken at 50 DAT. Measurements of stem diameter, cortex thickness, phloem thickness, xylem thickness, vessel diameter, and pith thickness were measured with the AnalySIS®3.2 software program for image analysis. The fragments were detected and recognized according to Sass (1961) using an upright light microscope (AxioPlan, Zeiss, Jena, Germany).

## Statistical Analysis

All data were displayed as means ± standard errors. Combined analysis for the two study periods was conducted according to the homogeneity of experimental error variance. Duncan's Multiple Range Test was used to identify the significant differences among means, which were compared at $p \leq 0.05$ by INFOSTAT computer software (v.2019 statistical package, Córdoba University, Córdoba, Argentina).

# RESULTS

## Growth Parameters

Different sodium chloride (NaCl) concentrations of SW-irrigated *P. amboinicus* plants significantly decreased growth parameters in terms of shoot length (cm), number of shoots plant$^{-1}$, number of leaves plant$^{-1}$, stem diameter (mm), root length (cm), and fresh and dry weight (g) of shoots compared with the unstressed control (tap water; **Table 1**). It is worth noting that plants irrigated with 102 mM NaCl reflected the lowest shoot length (cm) by 26.9%, number of shoots plant$^{-1}$, by 47.4%, number of leaves plant$^{-1}$, by 51.0%, stem diameter (mm) by 36.2%, root length (cm) by 41.1%, shoot fresh weight (g plant$^{-1}$) by 48.3%, and shoot dry weight (g plant$^{-1}$) by 55.3% compared with those of the unstressed control ($SW_0$). About the FA impact, the abovementioned parameters of *P. amboinicus* increased significantly with foliar FA spray at any concentration (i.e., 25 or 50 μM) compared with those of the control (**Table 1**).

Plants supplemented with FA at 25 or 50 μM increased shoot length (cm) by 8.5 and 15.6%, number of shoots plant$^{-1}$, by 25.9 and 53.1%, number of leaves plant$^{-1}$, by 28.0 and 62.0%, stem diameter (mm) by 16.4 and 28.4%, root length (cm) by 15.6 and 31.1%, shoot fresh weight (g plant$^{-1}$) by 14.7 and 25.9%, and shoot dry weight (g plant$^{-1}$) by 12.6 and 24.3%, respectively, compared with the control. The interaction effect between SW and FA applications was significant for *P. amboinicus* growth parameters (**Table 1**). In general, the highest growth parameters were obtained from the interactive treatment of non-saline water of $SW_0$ (tap water) × FA at 50 μM, followed by irrigation with

**TABLE 2 |** The effect of SW irrigation and FA spraying on SPAD, Fv/Fm, and PI of *Plectranthus amboinicus* plants grown under greenhouse conditions.

| Treatment | SPAD | Fv/Fm | PI |
|---|---|---|---|
| SW (mM) | * | * | * |
| 0 (Control) | 32.99 ± 0.4a | 0.86 ± 0.0a | 7.30 ± 0.2a |
| 34 | 29.40 ± 0.3b | 0.84 ± 0.0b | 6.30 ± 0.4b |
| 68 | 26.69 ± 0.7c | 0.82 ± 0.0c | 5.09 ± 0.3c |
| 102 | 23.71 ± 0.6d | 0.77 ± 0.0d | 3.35 ± 0.2d |
| FA (μM) | * | * | * |
| 0 (Control) | 23.84 ± 0.4c | 0.79 ± 0.0c | 4.33 ± 0.3c |
| 25 | 28.38 ± 0.5b | 0.83 ± 0.0b | 5.43 ± 0.2b |
| 50 | 32.38 ± 0.6a | 0.84 ± 0.0a | 6.78 ± 0.3a |
| SW×FA | * | * | * |

**Indicates significant differences at $P \leq 0.05$ probability level.*
*According to the least-significant difference test, means ± SE followed by different letters in each column are significantly different at $P \leq 0.05$.*
*SW, saline water; FA, folic acid; SPAD, total chlorophyll (soil plant analysis development); Fv/Fm, chlorophyll fluorescence; PI, performance index.*

SW of 34 mM NaCl × FA at 50 μM, then irrigation with SW of 68 mM NaCl × FA at 50 μM, and finally, the lowest irrigation with SW of 102 mM NaCl × FA at 50 μM. Conversely, the lowest growth parameters were obtained from the interactive treatments of the irrigation with SW of 102 mM NaCl × FA at 0.0 μM (distilled water).

## Total Chlorophyll (SPAD), Fv/Fm, and PI

Applied SW at different concentrations (i.e., 34, 68, and 102 mM of NaCl) significantly decreased phytochemical constituents in fresh leaves of *P. amboinicus* plants, including total chlorophyll (SPAD), chlorophyll florescence (Fv/Fm), and PI of photosynthesis compared to the control (tap water) (**Table 2**). For instance, irrigating plants with SW at 102 mM NaCl decreased SPAD by 28.1%, chlorophyll florescence (Fv/Fm) by 10.5%, and PI of photosynthesis by 54.1% compared with the control ($SW_0$). Foliar FA treatment significantly increased the aforementioned phytochemical constituents of *P. amboinicus* using a solution of 25 μM FA by 19.0, 5.1, and 25.4%, respectively. Using a solution of 50 μM FA, the SPAD, Fv/Fm, and PI further increased by 35.8, 6.3, and 56.6%, respectively, compared with the control (**Table 2**).

The interactive effect between SW treatments and FA applications was significant for the phytochemical constituents in fresh leaves of *P. amboinicus* (**Figure 1**). Generally, the highest phytochemical constituents were recorded from the interactive treatment of non-saline water of SW0 (tap water) × FA at 50 μM, followed by irrigation with SW of 34 mM NaCl × FA at 50 μM, then irrigation with SW of 68 mM NaCl × FA at 50 μM, and finally, the lowest SW irrigation of 102 mM NaCl × FA at 50 μM. The lowest phytochemical constituents were obtained from the interactive treatments of the irrigation with SW of 102 mM NaCl × FA at 0.0 μM (distilled water).

## Leaf Osmoprotectant Compounds and Essential Oil Yield (%)

When the NaCl concentration reached 34 mM, the leaf osmoprotectant compounds of *P. amboinicus* plants, i.e., TSS, free amino acids, proline, and phenolic content (mg $g^{-1}$ DW) increased significantly by 23.8, 29.4, 21.4, and 19.2%, respectively. At 68 mM NaCl, they further increased by 47.6, 70.6, 42.9, and 50.0%, respectively. Conversely, they significantly decreased when the NaCl concentration was elevated to 102 mM, compared with the control (tap water) (**Table 3**). Protein content (mg $g^{-1}$ DW) and essential oil yield (%) significantly decreased with higher NaCl concentration compared with the control plants. Therefore, the SW treatment of 102 mM NaCl resulted in the lowest protein content (0.13 mg $g^{-1}$ DW) and essential oil yield (0.14%) compared with the control plants (**Table 3**). The abovementioned leaf osmoprotectant compounds increased significantly with the application of a 25 μM FA foliar spray. They further increased with 50 μM FA application compared with the control (**Table 3**). FA foliar treatment at 25 and 50 μM increased TSS content by 27.8 and 61.1%, protein content by 29.4 and 70.6%, free amino acids by 35.7 and 85.7%, proline by 20.0 and 44.0%, total phenolics by 30.4 and 47.8%, and essential oil yield by 27.7 and 55.6%, respectively, compared with the control. The effect of treatment with SW and FA was significant for the leaf osmoprotectant compounds of *P. amboinicus* (**Table 3**).

In general, the highest leaf TSS, free amino acids, proline, and phenolic content were recorded under the interactive treatment SW68 + FA50, followed by SW34 + FA 50. Conversely, the lowest TSS, free amino acids, and proline content were obtained from the interactive treatments SW102 + FA0, followed by SW0 + FA0. Concerning leaf protein content and essential oil yield, the highest mean values were recorded from the interactive treatment of SW0 + FA50, followed by SW34 + FA50, then SW68 +FA50, and finally, SW102 + FA50. However, the lowest leaf protein content and essential oil yield were recorded from the interactive treatments of SW102 + FA0 (**Table 3**).

## Leaf Enzymatic Activity and Some Antioxidants Content

Enzymatic and non-enzymatic systems (SOD, CAT, APX, GR, GSH, and AsA) of *P. amboinicus* increased significantly with increasing salinity levels (i.e., 34 and 68 mM NaCl). However, their levels decreased significantly under a salinity level of 102 mM NaCl compared with the control (tap water) (**Table 4**). SW treatments of 34 and 68 mM NaCl increased SOD by 20 and 39.2%, CAT by 9.6 and 30.3%, APX by 15.3 and 31.2%, GR by 21.9 and 42.2%, GSH by 16.7 and 40.5%, and AsA by 45.9 and 73.8%, respectively. Notably, the lowest levels of enzymatic and non-enzymatic antioxidants were obtained when the salinity level reached 102 mM NaCl compared with the control. As for FA foliar treatments, treatment of 25 or 50 μM markedly enhanced the content of enzymatic and non-enzymatic components of *P. amboinicus* compared with the control (**Table 4**).

FA applied in foliar sprays at 25 and 50 μM increased SOD by 15.0 and 30.0%, CAT by 12.6 and 23.4%, APX by 14.0 and 28.0%, GR by 16.9 and 31.5%, GSH by 18.0 and 39.5%, and

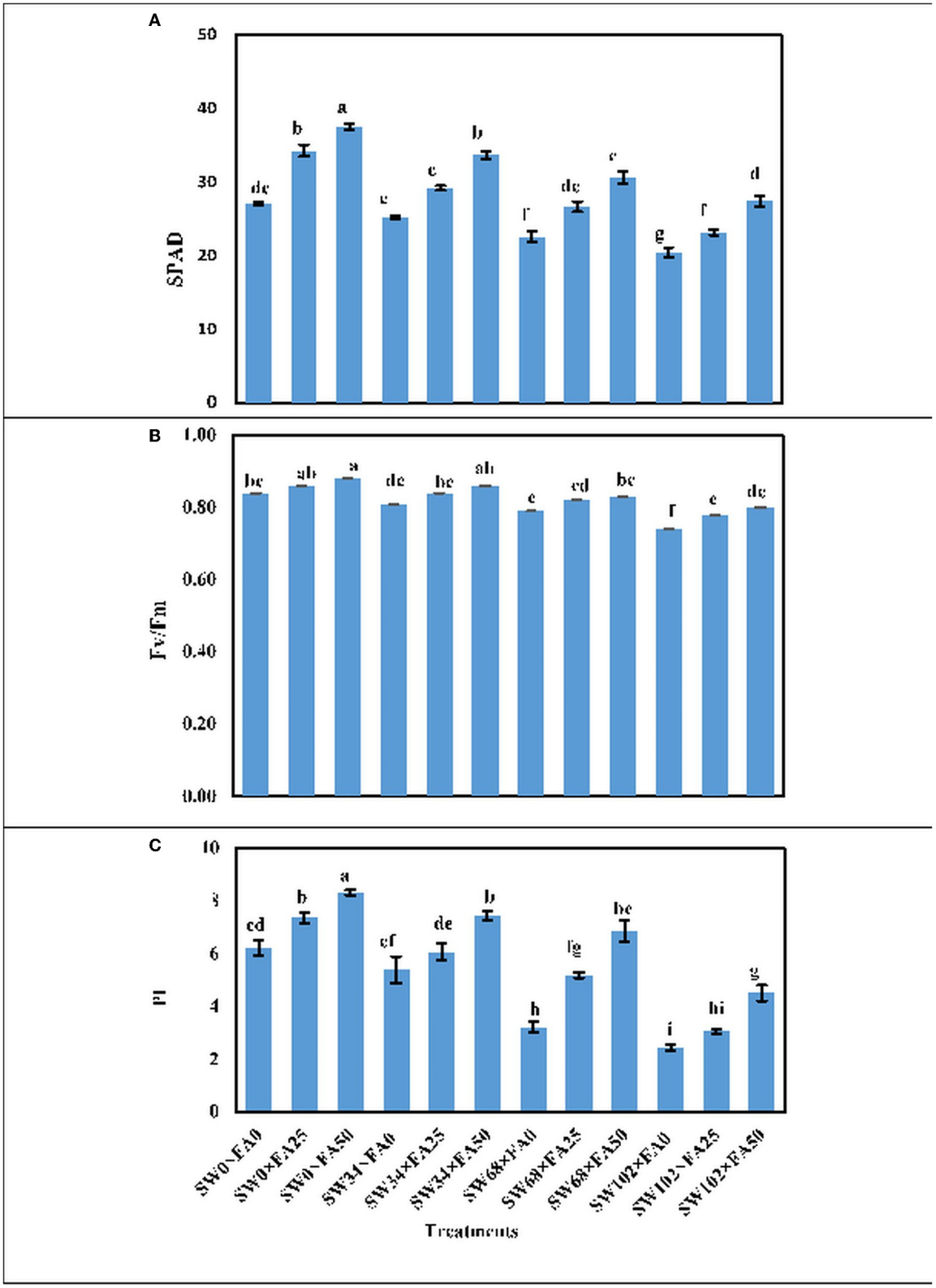


**FIGURE 1 |** The interactive effect of folic acid (FA) and saline water (SW) on photosynthetic productivity of *Plectranthus amboinicus*. **(A)** SPAD; **(B)** Fv/Fm; and **(C)** PI of *P. amboinicus* measured in the two seasons of 2018/2019 and 2019/2020. Different letters on the bars refers to significant differences among means based on Fisher's least-significant difference test at $p < 0.05$. SPAD, total chlorophyll (soil plant analysis development); *Fv/Fm*, chlorophyll fluorescence; *PI*, performance index; SW0, 0 mM NaCl; SW34, 34 mM NaCl; SW68, 68 mM NaCl; SW102, 102 mM NaCl; FA0, 0 μM FA; FA 25, 25 μM FA; FA50, 50 μM FA.

**TABLE 3 |** The effect of SW irrigation and FA spraying on leaf osmoprotectant compounds and essential oil yield of *Plectranthus amboinicus* plants grown under greenhouse conditions.

| Treatment | TSS | Proteins | Amino acids | Proline | Phenolic | Essential oil yield (%) |
|---|---|---|---|---|---|---|
| | mg g$^{-1}$ DW | | | | | |
| SW (mM) | * | * | * | * | * | * |
| 0 (Control) | 0.21 ± 0.02c | 0.32 ± 0.03a | 0.17 ± 0.02c | 0.28 ± 0.02c | 0.26 ± 0.01c | 0.32 ± 0.02a |
| 34 | 0.26 ± 0.03b | 0.26 ± 0.03b | 0.22 ± 0.02b | 0.34 ± 0.00b | 0.31 ± 0.02b | 0.27 ± 0.02b |
| 68 | 0.31 ± 0.04a | 0.19 ± 0.02c | 0.29 ± 0.03a | 0.40 ± 0.03a | 0.39 ± 0.02a | 0.19 ± 0.01c |
| 102 | 0.16 ± 0.01d | 0.13 ± 0.01d | 0.11 ± 0.01d | 0.19 ± 0.01d | 0.20 ± 0.01d | 0.14 ± 0.01d |
| FA (μM) | * | * | * | * | * | * |
| 0 (Control) | 0.18 ± 0.02c | 0.17 ± 0.02c | 0.14 ± 0.01c | 0.25 ± 0.02c | 0.23 ± 0.01c | 0.18 ± 0.01c |
| 25 | 0.23 ± 0.02b | 0.22 ± 0.01b | 0.19 ± 0.02b | 0.30 ± 0.02b | 0.30 ± 0.03b | 0.23 ± 0.01b |
| 50 | 0.29 ± 0.01a | 0.29 ± 0.03a | 0.26 ± 0.03a | 0.36 ± 0.03a | 0.34 ± 0.01a | 0.28 ± 0.01a |
| SW×FA | * | * | * | * | * | * |

** Indicates significant differences at $P \leq 0.05$ probability level.*
*According to the least-significant difference test, means ± SE followed by different letters in each column are significantly different at $P \leq 0.05$.*
*SW, saline water; FA, folic acid; TSS, total soluble sugars; DW, dry weight.*

**TABLE 4 |** The effect of SW irrigation and FA spraying on leaf enzymatic activity and some antioxidant contents of *Plectranthus amboinicus* plants grown under greenhouse conditions.

| Treatment | SOD | CAT | APX | GR | GSH | AsA |
|---|---|---|---|---|---|---|
| | μmol g$^{-1}$ FW | | | | | |
| SW (mM) | * | * | * | * | * | * |
| 0 (Control) | 0.125 ± 0.01c | 0.178 ± 0.01c | 0.157 ± 0.01c | 0.128 ± 0.01c | 0.227 ± 0.02c | 0.183 ± 0.02c |
| 34 | 0.150 ± 0.01b | 0.195 ± 0.02b | 0.181 ± 0.01b | 0.156 ± 0.02b | 0.265 ± 0.01b | 0.267 ± 0.01b |
| 68 | 0.174 ± 0.02a | 0.232 ± 0.4a | 0.206 ± 0.02a | 0.182 ± 0.02a | 0.319 ± 0.01a | 0.318 ± 0.02a |
| 102 | 0.102 ± 0.1d | 0.144 ± 0.2d | 0.139 ± 0.03d | 0.109 ± 0.03d | 0.166 ± 0.03d | 0.140 ± 0.01d |
| FA (μM) | * | * | * | * | * | * |
| 0 (Control) | 0.120 ± 0.01c | 0.167 ± 0.02c | 0.150 ± 0.03c | 0.124 ± 0.01c | 0.205 ± 0.01c | 0.185 ± 0.01c |
| 25 | 0.138 ± 0.01b | 0.188 ± 0.02b | 0.171 ± 0.1b | 0.145 ± 0.01b | 0.242 ± 0.02b | 0.224 ± 0.03b |
| 50 | 0.156 ± 0.01a | 0.206 ± 0.01a | 0.192 ± 0.1a | 0.163 ± 0.02a | 0.286 ± 0.01a | 0.272 ± 0.03a |
| SW×FA | * | * | * | * | * | * |

** Indicates significant differences at $P \leq 0.05$ probability level.*
*According to the least-significant difference test, means ± SE followed by different letters in each column are significantly different at $P \leq 0.05$.*
*SW, saline water; FA, folic acid; SOD, superoxide dismutase; CAT, catalase; APX, ascorbate peroxidase; GR, glutathione reductase; GSH, glutathione; AsA, ascorbic acid; FW, fresh weight.*

AsA by 35.7 and 47.0%, respectively, compared with the control. Treatment with SW and FA significantly affected the enzymatic and non-enzymatic antioxidants in *P. amboinicus* (**Figure 2**). Sequential FA application at any rate (i.e., 25 or 50 μM) under different salinity levels significantly increased enzymatic and non-enzymatic systems in comparison with untreated plants (control). In this regard, the most noticeable increments of the abovementioned antioxidants were observed with a salinity level of 34 mM NaCl × FA at 50 μM, and a further salinity level of 68 mM NaCl × FA at 50 μM.

## Mineral Content of Leaves

The salinity levels of 34, 68, and 102 mM NaCl markedly decreased the elemental leaf contents (i.e., N, P, $K^+$, and the leaf $K^+/Na^+$ ratio), but positively increased the leaf contents of $Na^+$ and $Cl^-$, compared with the control (tap water) (**Table 5**). SW applied at a concentration of 102 mM NaCl decreased leaf content of N by 55.3%, P by 48.1%, $K^+$ by 39.7%, and the leaf $K^+/Na^+$ ratio by 61.8%, whereas the leaf $Na^+$ and $Cl^-$ content increased by 52.9 and 89.6%, respectively, compared with the SW0 treatment. FA foliar treatments resulted in significant increases in the contents of leaf N, P, $K^+$, and the leaf $K^+/Na^+$ ratio. However, the leaf $Na^+$ and $Cl^-$ content significantly decreased with foliar spray of 25 or 50 μM FA compared with the control treatment (SW0) (**Table 5**). FA foliar spray applied at 25 and 50 μM increased the content of N by 30.7 and 72.3%, P by 17.6 and 41.2%, $K^+$ by 13.9 and 29.2%, and increased the leaf $K^+/Na^+$ ratio by 50.2 and 96.4%, respectively. The leaf $Na^+$ content decreased by 12.0 and 28.0%, and $Cl^-$ content decreased by 16.7 and 32.8%, respectively, compared with the control. The interaction effect between SW treatments and FA applications was significant for leaf macro- and micro-nutrient content of

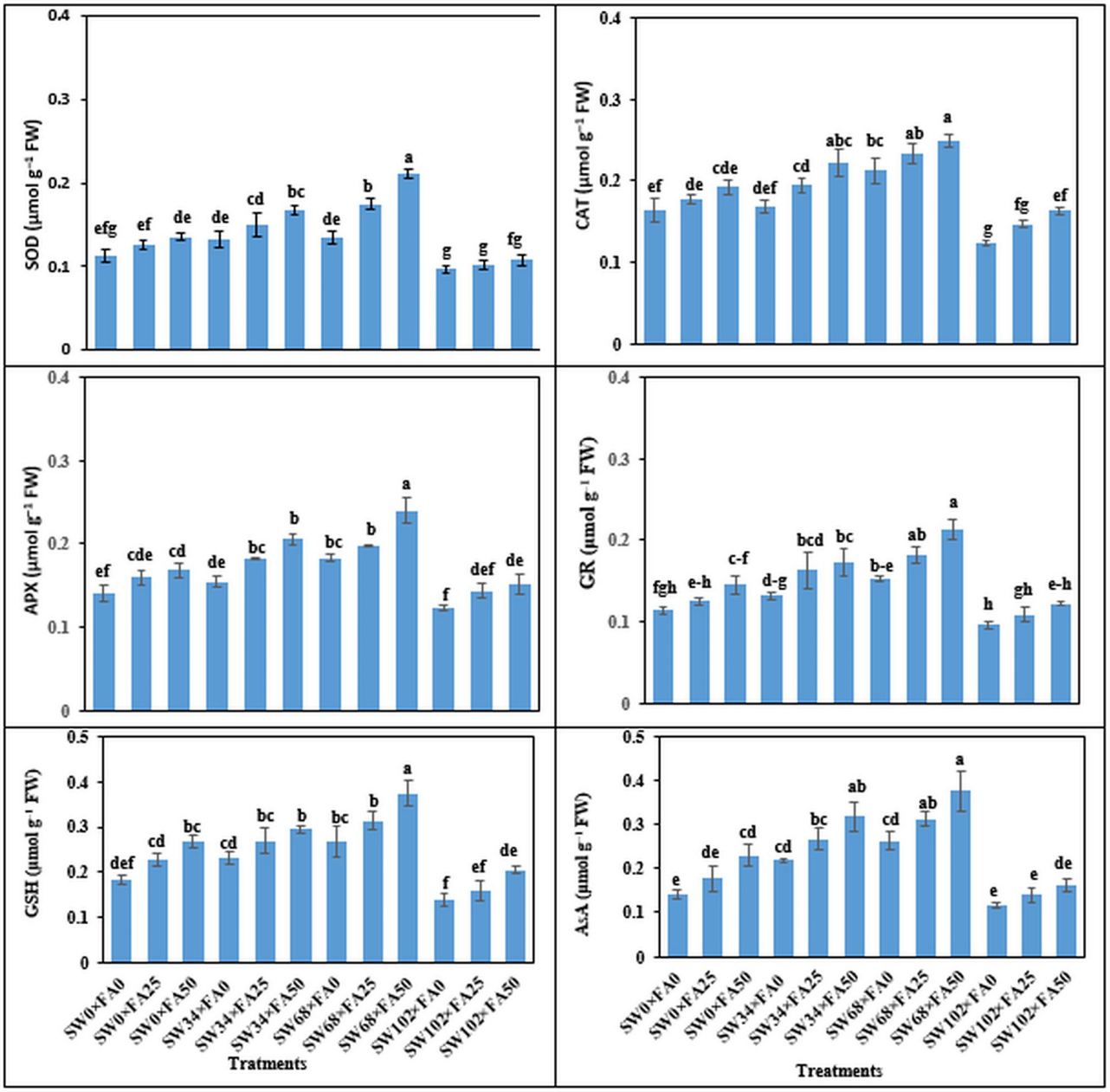


**FIGURE 2 |** The interactive effect of folic acid (FA) and saline water (SW) on enzymatic antioxidant activity of *Plectranthus amboinicus*. **(A)** SOD; **(B)** CAT; **(C)** APX; **(D)** GR; **(E)** GSH; and **(F)** AsA activity of *P. amboinicus* the two seasons of 2018/2019 and 2019/2020. Different letters on the bars refer to significant differences among means based on Fisher's least-significant difference test at $p < 0.05$. SOD, superoxide dismutase; CAT, catalase; APX, ascorbate peroxidase; GR, glutathione reductase; GSH, glutathione; AsA, ascorbic acid; SW0, 0 mM NaCl; SW34, 34 mM NaCl; SW68, 68 mM NaCl; SW102, 102 mM NaCl; FA0, 0 µM FA; FA 25, 25 µM FA; FA50, 50 µM FA.

*P. amboinicus* (**Table 5**). Generally, the highest leaf N, P, $K^+$ contents, and leaf $K^+/Na^+$ ratio, or the lowest leaf $Na^+$ and $Cl^-$ content, were obtained from the interactive treatment of non-saline water 0 mM NaCl × FA at 50 µM, followed by SW 34 mM NaCl × FA at 50 µM, then SW 68 mM NaCl × FA at 50 µM, and finally, the lowest was obtained for the treatment of SW 102 mM NaCl × FA at 50 µM. The lowest leaf contents of N, P, and $K^+$ and lowest leaf $K^+/Na^+$ ratio, or the highest leaf $Na^+$ and $Cl^-$ content, were obtained from the interactive treatments of SW 102 mM NaCl × FA at 0 mM.

## Anatomical Stem Structure

The impact of FA on the morphological characteristics of *P. amboinicus* watered with saline water was also assessed

**TABLE 5 |** The effect of SW irrigation and FA spraying on leaf elemental status of *Plectranthus amboinicus* plants grown under greenhouse conditions.

| Treatment | N% | P | $K^+$ | $Na^+$ | $Cl^-$ | $K^+/Na^+$ |
|---|---|---|---|---|---|---|
| | | mg $g^{-1}$ DW | | | | |
| SW (mM) | * | * | * | * | * | * |
| 0 (Control) | 25.3 ± 0.71a | 0.27 ± 0.02a | 41.6 ± 1.5a | 0.17 ± 0.01d | 1.15 ± 0.1d | 55.5 ± 2.1a |
| 34 | 20.6 ± 0.81b | 0.22 ± 0.02b | 36.6 ± 1.5b | 0.20 ± 0.02c | 1.47 ± 0.1c | 41.9 ± 2.4b |
| 68 | 16.4 ± 0.65c | 0.18 ± 0.01c | 31.6 ± 1.5c | 0.23 ± 0.02b | 1.81 ± 0.2b | 32.0 ± 2.1c |
| 102 | 11.3 ± 0.48d | 0.14 ± 0.01d | 25.1 ± 1.3d | 0.26 ± 0.02a | 2.18 ± 0.2a | 21.2 ± 2.0d |
| FA (μM) | * | * | * | * | * | * |
| 0 (Control) | 13.7 ± 0.56c | 0.17 ± 0.01c | 29.5 ± 1.6c | 0.25 ± 0.01a | 1.98 ± 0.2a | 25.3 ± 1.8c |
| 25 | 17.9 ± 0.78b | 0.20 ± 0.01b | 33.6 ± 1.3b | 0.22 ± 0.02b | 1.65 ± 0.2b | 38.0 ± 2.6b |
| 50 | 23.6 ± 0.65a | 0.24 ± 0.02a | 38.1 ± 1.4a | 0.18 ± 0.02c | 1.33 ± 0.2c | 49.7 ± 2.0a |
| SW×FA | * | * | * | * | * | * |

**Indicates significant differences at $P \leq 0.05$ probability level.*
*According to the least-significant difference test, means ± SE followed by different letters in each column are significantly different at $P \leq 0.05$.*
*SW, saline water; FA, folic acid; DW, dry weight.*

**TABLE 6 |** The effect of SW irrigation and FA spraying on the anatomical stem structures of *Plectranthus amboinicus* plants grown under greenhouse conditions.

| Treatment | Stem diameter (μm) | Cortex thickness (μm) | Phloem thickness (μm) | Xylem thickness (μm) | Vessel diameter (μm) | Pith thickness (μm) |
|---|---|---|---|---|---|---|
| SW (mM) | * | * | * | * | * | * |
| 0 (Control) | 4312.0 ± 7.0a | 375.0 ± 2.7a | 186.7 ± 2.2a | 230.0 ± 2.6a | 58.3 ± 1.6a | 2762.0 ± 5.8a |
| 34 | 4008.0 ± 6.3b | 362.3 ± 3.4b | 170.0 ± 2.5b | 226.7 ± 2.6b | 51.8 ± 1.5b | 2399.7 ± 4.2b |
| 68 | 3845.7 ± 6.5c | 320.3 ± 2.6c | 135.0 ± 2.4c | 160.0 ± 2.4c | 47.1 ± 1.4c | 2249.7 ± 3.9c |
| 102 | 2487.3 ± 5.8d | 266.7 ± 3.1d | 111.7 ± 2.2d | 160.0 ± 2.2c | 44.0 ± 1.6d | 2170.7 ± 3.3d |
| FA (μM) | * | * | * | * | * | * |
| 0 (Control) | 3278.0 ± 6.8c | 303.0 ± 2.9c | 136.3 ± 2.2c | 173.8 ± 2.6c | 45.5 ± 1.4c | 2159.0 ± 4.3c |
| 25 | 3509.0 ± 6.4b | 334.3 ± 3.0b | 157.5 ± 2.2b | 191.3 ± 2.4b | 50.7 ± 1.6b | 2456.0 ± 4.8b |
| 50 | 4203.8 ± 6.1a | 356.0 ± 3.0a | 158.8 ± 2.5a | 217.5 ± 2.3a | 54.8 ± 1.5a | 2571.5 ± 3.8a |
| SW×FA | * | * | * | * | * | * |

**Indicates significant differences at $P \leq 0.05$ probability level.*
*According to the least-significant difference test, means ± SE followed by different letters in each column are significantly different at $P \leq 0.05$.*
*SW, saline water; FA, folic acid.*

(**Table 6**, **Figure 3**). At all levels of salt stress, the application of FA had a stimulating effect on stem structure. All anatomical attributes dropped dramatically with increased salinity irrigation level. Overall, in the absence of salinity stress, FA application resulted in a significant increase in stem diameter, especially at high doses. However, exogenous FA alleviated the inhibitory effect of salt stress. The highest stem diameter was observed in plants treated with distilled water and 50 μM FA (an increase of 22.27% compared with control). This increase in stem diameter led to increases in cortex thickness, pith thickness, phloem tissue thickness, xylem tissue thickness, and xylem vessel diameter by 14.29, 34.5, 19.35, 15.0, and 30.0%, respectively, compared to control plants. It is noteworthy that the decrease in stem diameter due to the increase in SW irrigation from 34 to 102 mM NaCl was compensated by FA application, and a significant stem diameter decrease was recorded for the high level of salt stress. Application of FA 50 μM resulted in stem diameter increases by 10.18, 9.66, and 119.25%, in plants irrigated with SW at concentrations 102, 68, 34, and 0 mM, respectively, and resulted from increases in cortex thickness by 0, 26.77, and 33.33 %, respectively. FA spray of 50 μM in plants irrigated with SW at concentrations 34, 68, and 102 mM resulted in increases in phloem thickness by 12.5, 11.11, and 26.32%, xylem thickness by 10, 6.67, and 6.9%, xylem vessel diameter by 10, 12.5, and 10%, pith thickness by 9.14, 16.15, and 14%, respectively, compared with the control.

## DISCUSSION

Plant morphological and physiochemical attributes are significantly affected by salinity. One of the earliest reactions of crops to salinity is the reduction in leaf development rate (Franco et al., 1997); the excess salt surrounding the roots causes osmotic pressure, which reduces the supply of water to leaf cells. Root growth can be inhibited by high external salt absorption (Krzymińska and Ulczycka-Walorska, 2015), resulting in reduced root length (Shannon and Grieve, 1998) and

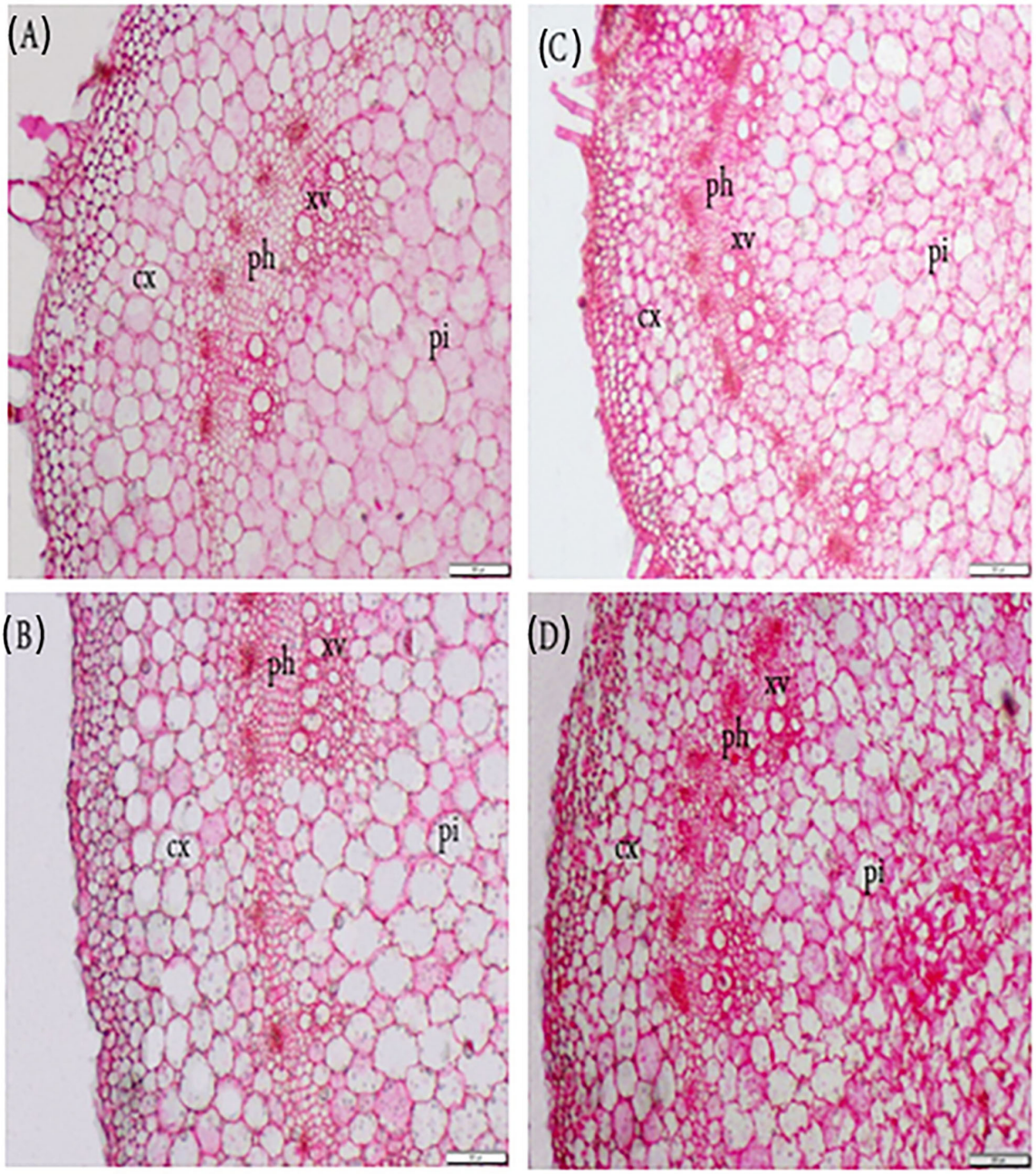


**FIGURE 3 |** Exogenous application of folic acid (FA) and saline water (SW) on the stem anatomical structure of *Plectranthus amboinicus*. **(A)** $FA_0$ $SW_0$; **(B)** $FA_{50}$ $SW_0$; **(C)** $FA_0$ $SW_{102}$; and **(D)** $FA_{25}SW_{102}$. Cx, cortex; ph, phloem; xv, xylem vessels; pi, pith; SW0, 0 mM NaCl; SW102, 102 mM NaCl; FA0, 0 μM FA; FA 25, 25 μM FA; FA50, 50 μM FA.

function. Cell elongation and leaf division are reduced, causing a reduction in leaf area (Munns and Tester, 2008).

A decrease in turgor in the leaves as a result of changes in cell wall characteristics or a fall in photosynthetic rate could induce a decrease in leaf area (Franco et al., 1997). The remarkable reduction of morphological characteristics of *P. amboinicus* are attributed to different levels of salt in irrigation water. Such consequences have been observed in several plant species including *Plectranthus forsteri* (Krzymińska and Ulczycka-Walorska, 2015), *P. amboinicus* (Karimian et al., 2019), and lavender (*Salvia splendens*) (Paraskevopoulou et al., 2020). On the other hand, significant increases in the abovementioned growth

parameters of *P. amboinicus* compared with the control (spray with water) were observed when FA was applied as a foliar spray at concentrations of 25 or 50 μM.

One of the most important cellular functions of FA is that it serves as a co-factor for crucial enzymes for RNA and DNA synthesis, and has a stimulating effect on plant growth and development (Scott et al., 2000). In addition, FA deficiency slows down nucleic acid synthesis and interrupts cell division (Kim et al., 2009). FA also plays a critical role in maintaining genome stability and protecting the metabolism and DNA of plants (Fenech, 2001). It has been long known that FA increases mitotic division, thereby increasing plant growth and development (Hillis et al., 2011). Emam et al. (2011) showed that foliar application of vitamins including FA (B9) markedly increased the growth parameters of flax (*Linum usitatissimum*) plants compared with the control. A similar trend was reported by Farouk and El-Saidy (2013) and Heo et al. (2019) on sunflower and snapdragons (*Antirrhinum majus*) plants, respectively. Folic acid-treated plants had a stronger stimulatory impact, possibly because of its effect on protein and nucleic acid biosynthesis regulation (Andrew et al., 2000).

Salt stress suppresses photosynthesis by reducing leaf photosynthetic pigments (SPAD index), chlorophyll fluorescence, and its performance (i.e., Fv/Fm and PI). Furthermore, salt stress causes stomatal closure, which reduces $CO_2$ availability in the leaves and prevents carbon fixation. Salt stress also exposes chloroplasts to high excitation energy, which increases the production of ROS like $O_2\bullet$-, $H_2O_2$, OH•, and singlet oxygen atoms ($1O_2$) (Parvaiz and Satyawati, 2008; Abd El-Mageed et al., 2021b). Accumulating dangerous ions ($Na^+$ and/or $Cl^-$) under salt stress conditions may hinder photosynthesis and protein production, deactivate enzymes and destroy chloroplasts and other organelles (Taiz and Zeiger, 2002). The reduction in chlorophyll capacity and photosynthetic rates under salt stress are described in several studies (Semida et al., 2014, 2015a).

In the present study, a positive increase was observed in the phytochemical constituents of *P. amboinicus* with a FA foliar spray compared with the control plants. This observation was supported by the study demonstrating a reduction in whole folate abundance and chlorophyll level in pea leaves upon application of the anti-folate drug MTX (Van Wilder et al., 2009). Also, Stakhova et al. (2000) found that FA had a favorable effect on plant growth. Pretreating barley plants with FA significantly boosted their photosynthetic apparatus and reduced the negative effects of salt stress (Kiliç and Aca, 2016). The increase of TSS, amino acids, proline, total phenolic content, and decrease in crude protein content observed in *P. amboinicus* with increasing salinity levels proves this plant's tolerance to salt stress. The sugars act as respiratory substrates or as osmolytes to confer salinity stress tolerance (Kotagiri and Kolluru, 2017).

Osmoprotectants are neutral compounds that protect proteins and membranes from salt denaturation (Munns, 2002). Furthermore, plant cells modify their osmotic potential to avoid water loss and preserve cell turgor when exposed to salinity (Naidoo and Naidoo, 2001). The increased content of soluble sugars and proline under salinity environments was described by Ramezani et al. (2011). Proline accumulation may occur either due to protein degradation or inhibition of proline conversion under salinity (Singh et al., 1973). Proline has also been recommended as a ROS scavenger and molecular chaperone (Verbruggen and Hermans, 2008). Its accumulation can improve the structure of membranes and proteins to reduce cell destruction under salinity. It has been proved that increasing amino acid content may be due to free-radical scavenging, osmotic adjustment, and protein and membrane integrity (Keutgen and Pawelzik, 2008). These findings are consistent with those of Semida et al. (2019).

Osmoprotectants are substances that can intercept and neutralize the harmful effects of oxygen-free radicals generated during normal cellular metabolism (Benzie, 2003). As seen in **Table 3**, osmotic adjustment substances (i.e., TSS, proteins, amino acids, proline, and phenolics) increased significantly with foliar application of FA treatments compared with the control. Application of vitamins like FA enhances alpha-ketoglutaric acid biosynthesis, which combines with $NH_3$ to form amino acids and proteins, thereby promoting the creation of natural hormones such as IAA, cytokinins, and gibberellins. These, in turn, encourage cell division, accumulation of pigments and enzymes, and plant metabolism (Samiullah et al., 1988). The increase in vegetative growth characteristics caused by FA may be attributed to enhancing the accumulation of leaf osmoprotectants. For example, phenolics play a significant role in regulating plant metabolic processes and overall plant growth, as well as lignin synthesis (Lewis and Yamamoto, 1990). Enhancement of plant growth responses by FA under salt stress is closely linked to phenolic stimulation that occurred via the pentose phosphate pathway. Such stimulation resulted in overexpression of phenolic contents and GPX activity for the structural development and extra phenolics in late free-radical scavenging-linked antioxidant activity (Burguieres et al., 2007).

Additionally, the application of FA increased proline content under salinity stress, developing plant resistance against stress (Burguieres et al., 2007). Our results are consistent with those obtained by El-Metwally and Dawood (2017), who found that the percentages of TSS and phenolic compounds in fava bean were appreciably influenced by FA. Ionic effects of salinity bring accumulation or reduction of specific secondary metabolites (Mahajan and Tuteja, 2005) such as phenols, which are known to increase under stressful conditions and help plants bring osmotic balance. In this study, there was an increase in phenolic content by 30.0, 55.0, and 95.0% at salinity levels of 34, 68, and 102 mM NaCl, respectively, compared with the control. Hussein and Alva (2014) indicated that the concentration of total phenols in pepper (*Capsicum annuum* L.) leaves significantly increased with an increase in irrigation water salinity. These results are consistent with those obtained by Ali et al. (2013). The decrease in growth was linked to a lower osmotic potential in the soil, which resulted in decreased water intake, reduced transpiration, and stomatal closure (Ben-Asher et al., 2006). A similar study by Abdelrazik et al. (2016) reported that the essential oil yield significantly decreased when irrigation water salinity was increased to the highest level.

Salinity causes oxidative stress in plants (Rout and Shaw, 2001). ROS, created during metabolism, are the source of oxidative damage (Hasanuzzaman et al., 2020). ROS can harm membrane lipids, proteins, and nucleic acids (Noctor and Foyer, 1998). To minimize the effect of oxidative stress caused by salinity, a plant cell has developed an antioxidant system that includes compounds such as GSH and AsA, in addition to antioxidant enzymes such as SOD, CAT, APX, and GR, which scavenges ROS (Apel and Hirt, 2004). The increase of antioxidant enzyme activity as a response to salinity stress could indicate increasing ROS and the development of a defensive mechanism to mitigate the oxidative damage caused by salt stress (Chaparzadeh et al., 2004). Our results indicated a significant increase in enzymatic and non-enzymatic antioxidants (SOD, CAT, APX, GR, GSH, and AsA) of *P. amboinicus* leaves with increasing salinity levels up to 68 mM NaCl. The levels subsequently declined significantly when exposed to the highest salinity level of 102 mM NaCl compared with the control plants (tap water). The high levels of SOD are necessary to convert the superoxide radical $O_2^-$ to $H_2O_2$, which is scavenged by CAT, APX, and GPX, protecting plants from the negative effects of ROS (Badawi et al., 2004). Elevated SOD activity without scavenging $H_2O_2$, can result in cytotoxicity by virulent OH● generated from $H_2O_2$ (Gossett et al., 1994).

Furthermore, plants sprayed with FA showed a significant improvement in the scavenging activity of $H_2O_2$, as evidenced by a steady rise in CAT and APX activities up to moderate salinity levels, resulting in decreased $H_2O_2$ content. Currently, foliar-feeding with FA in *P. amboinicus* can ameliorate the oxidative stress induced by salinity; moreover FA application at 50 μM markedly enhanced levels of enzymatic and non-enzymatic antioxidants under SW irrigation levels of 34 or 68 mM NaCl. Marked increases in ascorbate and glutathione were observed in salinized *P. amboinicus* plants treated with FA. Glutathione plays a significant role in the defense against oxidative stress. The AsA/GSH cycle is complex and adapts the protein thiol-disulfide redox status of plants in response to abiotic and biotic stresses (Mullineaux and Rausch, 2005). Decreases in ascorbate and glutathione in response to salinity were observed by Emam et al. (2011). Furthermore, the enhancement in SOD and GR activities was followed by increased levels of polyphenols and ascorbate content. Increasing salinity in irrigation water from 34 to 102 mM NaCl caused significant increases in $Na^+$ and $Cl^-$ accumulation in the dry leaves of *P. amboinicus*. Meanwhile, the levels of N, P, $K^+$, and the $K^+/Na^+$ ratio significantly decreased compared with control plants.

Salinity severely affected crop performance, especially nutritional disorders, in which the relationships between salinity and mineral nutrition in crops are complex (Maas and Grattan, 1999). The increase of salts in the cell apoplast causes ionic toxicity, imbalance, and hyperosmotic activities because the increase of $Na^+$ and $Cl^-$ inhibits the processes of cytosol and organelles (Zhu et al., 1998).

Several studies indicated that salinity reduces the absorption and accumulation of nutrients in the plant (Hu and Schmidhalter, 2005). Nitrogen absorption is reduced due to the competition between sodium and ammonium or chloride with nitrates, which reduces the growth and productivity of crops (Rozeff, 1995). In addition, nitrate absorption decreases due to chloride competition or low water absorption under saline conditions (Lea-Cox and Syvertsen, 1993; Bar et al., 1997). Furthermore, phosphorous availability decreases in saline soils because salts reduce phosphate activity. Since sodium competes with potassium for absorption sites in the roots or transport in the xylem, increasing sodium in the soil reduces the absorption of potassium and calcium (Abd El-Mageed et al., 2021b; Qadir et al., 2021). Additionally, an increase in sodium chloride leads to potassium disturbance, which causes defects in cell membranes, photosynthesis, and other vital processes, the generation of ROS, and cell death (Chakraborty et al., 2016).

Potassium is a vital plant nutrient, but sodium competes with it for absorption in cells, especially when its concentration is higher than potassium (Rodriguez-Navarro, 2000). These results are consistent with the results from Abd El-Mageed et al. (2021a). Our results reflect the functional role of FA as a foliar spray in enhancing nutrient uptake; FA application yielded the highest values of N, P, and $K^+$ as well as leaf $K^+/Na^+$ ratio, in contrast to decreased leaf $Na^+$ and $Cl^-$ contents when compared with the control (sprayed with water). The positive effects of B-vitamins on the growth and development of *P. amboinicus* might be due to their crucial role in protecting plant cells from aging and several disorders, as well as enhancing cell division, natural hormone biosynthesis, and uptake of nutrients and water (Samiullah et al., 1988). Emam et al. (2011) clarified that under salinity stress, $Na^+$ noticeably accumulated in salinized flax seedlings, while $K^+$ concentration and the $K^+/Na^+$ ratio significantly decreased as salinity levels increased.

FA increases growth traits through increased absorption of essential elements by binding to them, which increases cell division and differentiation (Poudineh et al., 2015). All anatomical attributes decreased with increased levels of salinity irrigation; these decreases could be attributed to the negative effect of salt stress to decrease the measured characteristics (i.e., stem diameter, thicknesses of the cortex, phloem, and xylem; xylem vessel diameter, and pith thickness) (Abd El-Mageed et al., 2018). In contrast, FA application improved all anatomical attributes; this amelioration resulted from increases in the thicknesses of plant cortex, phloem, xylem, and xylem vessel diameter and pith thickness. These increases may be due to the regulatory role that FA may have in DNA function, thereby increasing cell division (Kiliç and Aca, 2016). All improved characteristics resulting from foliar application of FA were accompanied by an ameliorated stem anatomy (**Table 6**), giving the plants a chance for sufficiently healthy cell metabolic processes. FA foliar application has a positive effect on *P. amboinicus* growth and yield under conditions of saline water irrigation.

## CONCLUSION

The results of this study clearly showed that the application of FA reduces the inhibitory effects of saline water stress on *P. amboinicus*. In addition, FA can boost the antioxidant activity (AsA, SOD, GSH, GR, APX, and CAT) and osmolytes accumulation (proline, free amino acids, TSS, $K^+/Na^+$, and $K^+$) as well as increase the phenolic and protein contents. Application of FA increases SPAD, Fv/Fm, PI, nutrient acquisition, and oil yield, consequently promoting growth and productivity of salt-stressed *P. amboinicus*. Thus, future applications of the biostimulant, FA, can be used to improve plant performance under salt stress conditions.

## DATA AVAILABILITY STATEMENT

The original contributions presented in the study are included in the article/supplementary material, further inquiries can be directed to the corresponding authors.

## AUTHOR CONTRIBUTIONS

OA-E, TAE-M, ME-S, SA, and KE-T conceived and designed the research. OA-E, KH, MA-R, TAE-M, ME-S, SA, KE-T, and RT supervised the study. OA-E, KH, MA-R, TAE-M, ME-S, and RT performed greenhouse experiments. OA-E, KH, TAE-M, and RT performed the microscopic experiments. OA-E, MA-R, TAE-M, ME-S, SA, KE-T, and RT analyzed the data. SA and KE-T assisted with experiments and/or data evaluation. TAE-M, ME-S, SA, KE-T, and RT wrote the manuscript. All authors critically revised the manuscript and approved the final version.

## FUNDING

This project was funded by the Khalifa Center for Biotechnology and Genetic Engineering-UAEU (Grant #: 31R286) to SA and the Abu Dhabi Award for Research Excellence-Department of Education and Knowledge (Grant #: 21S105) to KE-T.

## REFERENCES

Abd El-Mageed, T. A., Abdelkhalik, A., Abd El-Mageed, S. A., and Semida, W. M. (2021a). Co-composted poultry litter biochar enhanced soil quality and eggplant productivity under different irrigation regimes. *J. Soil Sci. Plant Nutr.* 21, 1917–1933. doi: 10.1007/s42729-021-00490-4

Abd El-Mageed, T. A., El-sherif, A. M. A., Abd El-Mageed, S. A., and Abdou, N. M. (2019). A novel compost alleviate drought stress for sugar beet production grown in Cd-contaminated saline soil. *Agric. Water Manag.* 226:105831. doi: 10.1016/j.agwat.2019.105831

Abd El-Mageed, T. A., Rady, M. O. A., Semida, W. M., Shaaban, A., and Mekdad, A. A. (2021b). Exogenous micronutrients modulate morpho-physiological attributes, yield, and sugar quality in two salt-stressed sugar beet cultivars. *J. Soil Sci. Plant Nutr.* 21, 1421–1436. doi: 10.1007/s42729-021-00450-y

Abd El-Mageed, T. A., Semida, W. M., Taha, R. S., and Rady, M. M. (2018). Effect of summer-fall deficit irrigation on morpho-physiological, anatomical responses, fruit yield and water use efficiency of cucumber under salt affected soil. *Sci. Hortic.* 237, 148–155. doi: 10.1016/j.scienta.2018.04.014

Abdelrazik, T. M., Sabra, A. S., Astatkie, T., Hegazy, M. H., Grulova, D., Hah, S., et al. (2016). Response of growth, essential oil content and its constituent's of *Plectranthus amboinicus* to iron and/or urea foliar application under saline irrigation. *Int. J. Pharm. Pharm. Sci.* 8, 223–231.

Abdou, N. M., Abdel-razek, M. A., El-mageed, S. A. A., Semida, W. M., Leilah, A. A. A., Abd El-Mageed, T. A., et al. (2021). High nitrogen fertilization modulates morpho-physiological responses, yield, and water productivity of lowland rice under deficit irrigation. *Agronomy* 11, 1291. doi: 10.3390/agronomy11071291

Aebi, H. (1984). Catalase *in vitro*. *Methods Enzymol.* 105, 121–126. doi: 10.1016/S0076-6879(84)05016-3

Ali, Z., Khan, D., and Ahmed, N. (2013). Physiological parameters of salt tolerance in three cultivars of *Sorghum bicolor* (L.) moench at seedling stage under single salt (NaCl) salinity. *Int. J. Biol. Biotech.* 10, 125–142.

Andrew, W. J., Youngkoo, C., Chen, X., and Pandalai, S. G. (2000). Vicissitudes of a vitamin. *Recent Res. Dev. Phytochem.* 4, 89–98.

Apel, K., and Hirt, H. (2004). Reactive oxygen species: Metabolism, oxidative stress, and signal transduction. *Annu. Rev. Plant Biol.* 55, 373–399. doi: 10.1146/annurev.arplant.55.031903.141701

Badawi, G. H., Yamauchi, Y., Shimada, E., Sasaki, R., Kawano, N., Tanaka, K., et al. (2004). Enhanced tolerance to salt stress and water deficit by overexpressing superoxide dismutase in tobacco (*Nicotiana tabacum*) chloroplasts. *Plant Sci.* 166, 919–928. doi: 10.1016/j.plantsci.2003.12.007

Bañuelos-Hernández, A. E., Azadniya, E., Moreno, E. R., and Morlock, G. E. (2020). Bioprofiling of Mexican *Plectranthus amboinicus* (Lour.) essential oil *via* planar chromatography–effect-directed analysis combined with direct analysis in real time high-resolution mass spectrometry. *J. Liq. Chromatogr. Relat. Technol.* 43, 344–350. doi: 10.1080/10826076.2020.1737542

Bar, Y., Apelbaum, A., Kafkafi, U., and Goren, R. (1997). Relationship between chloride and nitrate and its effect on growth and mineral composition of avocado and citrus plants. *J. Plant Nutr.* 20, 715–731. doi: 10.1080/01904169709365288

Bates, L. S., Waldren, R. P., and Teare, I. D. (1973). Rapid determination of free proline for water-stress studies. *Plant Soil* 39, 205–207. doi: 10.1007/BF00018060

Beauchamp, C., and Fridovich, I. (1971). Superoxide dismutase: improved assays and an assay applicable to acrylamide gels. *Anal. Biochem.* 44, 276–287. doi: 10.1016/0003-2697(71)90370-8

Bekaert, S., Storozhenko, S., Mehrshahi, P., Bennett, M. J., Lambert, W., Gregory, J. F., et al. (2008). Folate biofortification in food plants. *Trends Plant Sci.* 13, 28–35. doi: 10.1016/j.tplants.2007.11.001

Ben-Asher, J., Tsuyuki, I., Bravdo, B. A., and Sagih, M. (2006). Irrigation of grapevines with saline water: I. Leaf area index, stomatal conductance, transpiration and photosynthesis. *Agric. Water Manag.* 83, 13–21. doi: 10.1016/j.agwat.2006.01.002

Benzie, I. F. F. (2003). Evolution of dietary antioxidants. *Comp. Biochem. Physiol. A Mol. Integr. Physiol.* 136, 113–126. doi: 10.1016/S1095-6433(02)00368-9

Bradford, M. M. (1976). A rapid and sensitive method for the quantitation of microgram quantities of protein utilizing the principle of protein-dye binding. *Anal. Biochem.* 72, 248–254. doi: 10.1016/0003-2697(76)90527-3

Burguieres, E., McCue, P., Kwon, Y. I., and Shetty, K. (2007). Effect of vitamin C and folic acid on seed vigour response and phenolic-linked antioxidant activity. *Bioresour. Technol.* 98, 1393–1404. doi: 10.1016/j.biortech.2006.05.046

Chakraborty, K., Bhaduri, D., Meena, H. N., and Kalariya, K. (2016). External potassium ($K^+$) application improves salinity tolerance by promoting $Na^+$-exclusion, $K^+$-accumulation and osmotic adjustment in contrasting peanut cultivars. *Plant Physiol. Biochem.* 103, 143–153. doi: 10.1016/j.plaphy.2016.02.039

Chaparzadeh, N., D'Amico, M. L., Khavari-Nejad, R. A., Izzo, R., and Navari-Izzo, F. (2004). Antioxidative responses of *Calendula officinalis* under salinity conditions. *Plant Physiol. Biochem.* 42, 695–701. doi: 10.1016/j.plaphy.2004.07.001

Chifundera, K. (2001). Contribution to the inventory of medicinal plants from the Bushi area, South Kivu Province, Democratic Republic of Congo. *Fitoterapia* 72, 351–368. doi: 10.1016/S0367-326X(00)00294-X

Clark, A. J., Landolt, W., Bucher, J. B., and Strasser, R. J. (2000). Beech (*Fagus sylvatica*) response to ozone exposure assessed with a chlorophyll *a* fluorescence performance index. *Environ. Pollut.* 109, 501–507. doi: 10.1016/S0269-7491(00)00053-1

Donald, A. H., and Robert, O. (1998). "Determination of total nitrogen in plant tissue" in *Handbook and Reference Methods for Plant Analysis*, eds Y. P. *Kalra, (Boca Raton, FL: CRC Press),* 75–84.

El-Metwally, I. M., and Dawood, M. G. (2017). Weed management, folic acid and seaweed extract effects on faba bean plants and associated weeds under sandy soil conditions. *Agric. Eng. Int. CIGR J.* 2017, 27–34.

Emam, M. M., El-Sweify, A. H., and Helal, N. M. (2011). Efficiencies of some vitamins in improving yield and quality of flax plant. *African J. Agric. Res.* 6, 4362–4369.

Esquível, M. M., Ribeiro, M. A., and Bernardo-Gil, M. G. (1999). Supercritical extraction of savory oil: study of antioxidant activity and extract characterization. *J. Supercrit. Fluids.* 14, 129–138. doi: 10.1016/S0896-8446(98)00115-6

Farouk, S., and El-Saidy, E. A. (2013). Seed invigoration techniques to improve germination and early growth of sunflower cultivars. *J. Renew. Agric.* 1, 33–38. doi: 10.12966/jra.06.02.2013

Fenech, M. (2001). The role of folic acid and Vitamin B12 in genomic stability of human cells. *Mutat Res.* 475, 57–67. doi: 10.1016/S0027-5107(01)00079-3

Franco, J. A., Fernández, J. A., Bañón, S., and González, A. (1997). Relationship between the effects of salinity on seedling leaf area and fruit yield of six muskmelon cultivars. *HortScience* 32, 642–644. doi: 10.21273/HORTSCI.32.4.642

Garratt, L. C., Janagoudar, B. S., Lowe, K. C., Anthony, P., Power, J. B., and Davey, M. R. (2002). Salinity tolerance and antioxidant status in cotton cultures. *Free Radic. Biol. Med.* 33, 502–511. doi: 10.1016/S0891-5849(02)00838-9

Githinji, C. W., and Kokwaro, J. O. (1993). Ethnomedicinal study of major species in the family Labiatae from Kenya. *J. Ethnopharmacol.* 39, 197–203. doi: 10.1016/0378-8741(93)90036-5

Gorelova, V., Ambach, L., Rébeill,é, F., Stove, C., and Van Der Straeten, D. (2017). Folates in plants: research advances and progress in crop biofortification. *Front. Chem.* 5:21. doi: 10.3389/fchem.2017.00021

Gossett, D. R., Millhollon, E. P., and Lucas, M. C. (1994). Antioxidant response to NaCl stress in salt-tolerant and salt-sensitive cultivars of cotton. *Crop Sci.* 34, 706–714. doi: 10.2135/cropsci1994.0011183X003400030020x

Hasanuzzaman, M., Bhuyan, M. H. M. B., Zulfiqar, F., Raza, A., Mohsin, S. M., Al Mahmud, J., et al. (2020). Reactive oxygen species and antioxidant defense in plants under abiotic stress: revisiting the crucial role of a universal defense regulator. *Antioxidants* 9, 1–52. doi: 10.3390/antiox9080681

Hashemi, M. B., Niakousari, M., and Saharkhiz, M. J. (2011). Antioxidant activity of *Satureja bachtiarica* Bunge essential oil in rapeseed oil irradiated with UV rays. *Eur. J. Lipid Sci. Technol.* 113, 1132–1137. doi: 10.1002/ejlt.201000547

Hassanein, R. A. (1977). *Effect of certain growth regulators on plant growth and development* (Ph.D dissertation). Ain-Shams University, Cairo, Egypt.

Heo, K., Gibson, G., and Evans, R. (2019). Effects of bisphenol-A and folic acid on growth, reproductive development, and DNA methylation in snapdragons (*Antirrhinum majus*). *Botany* 97, 149–160. doi: 10.1139/cjb-2018-0116

Higinbotham, N., Etherton, B., and Foster, R. J. (1967). Mineral ion contents and cell transmembrane electropotentials of pea and oat seedling tissue. *Plant Physiol.* 42, 37–46. doi: 10.1104/pp.42.1.37

Hillis, D. G., Fletcher, J., Solomon, K. R., and Sibley, P. K. (2011). Effects of ten antibiotics on seed germination and root elongation in three plant species. *Arch. Environ. Contam. Toxicol.* 60, 220–232. doi: 10.1007/s00244-010-9624-0

Hu, Y., and Schmidhalter, U. (2005). Drought and salinity: a comparison of their effects on mineral nutrition of plants. *J. Plant Nutr. Soil Sci.* 168, 541–549. doi: 10.1002/jpln.200420516

Hussein, M. M., and Alva, A. K. (2014). Growth, yield and water use effeciency of forage sorghum as affected by NPK fertilizer and deficit irrigation. *Am. J. Plant Sci.* 5, 2134–2140. doi: 10.4236/ajps.2014.513225

Irigoyen, J. J., Einerich, D. W., and Sánchez-Díaz, M. (1992). Water stress induced changes in concentrations of proline and total soluble sugars in nodulated alfalfa (*Medicago sativa*) plants. *Physiol. Plant.* 84, 55–60. doi: 10.1111/j.1399-3054.1992.tb08764.x

Jablonski, P. P., and Anderson, J. W. (1978). Light-dependent reduction of oxidized glutathione by ruptured chloroplasts. *Plant Physiol.* 61, 221–225. doi: 10.1104/pp.61.2.221

Jackson, M. L. (1973). *Soil chemical Analysis*. Prentice Hall of India Pvt. Ltd., New Delhi, p. 498.

Kampfenkel, K., Van Montagu, M., and Inz,é, D. (1995). Extraction and determination of ascorbate and dehydroascorbate from plant tissue. *Anal. Biochem.* 225, 165–167. doi: 10.1006/abio.1995.1127

Kanne, H., Burte, N. P., Prasanna, V., and Gujjula, R. (2015). Extraction and elemental analysis of *Coleus forskohlii* extract. *Pharmacogn. Res.* 7, 237–241. doi: 10.4103/0974-8490.157966

Karimian, Z., Samiei, L., and Nabati, J. (2019). Alleviating the salt stress effects in *Salvia splendens* by humic acid application. *Acta Sci. Pol. Hortorum Cultus* 18, 73–82. doi: 10.24326/asphc.2019.5.7

Keutgen, A. J., and Pawelzik, E. (2008). Contribution of amino acids to strawberry fruit quality and their relevance as stress indicators under NaCl salinity. *Food Chem.* 111, 642–647. doi: 10.1016/j.foodchem.2008.04.032

Kiliç, S., and Aca, H. (2016). Role of exogenous folic acid in alleviation of morphological and anatomical inhibition on salinity-induced stress in barley. *Ital. J. Agron.* 11, 246–251. doi: 10.4081/ija.2016.777

Kim, H. N., Kim, Y. K., Lee, I. K., Yang, D. H., Lee, J. J., Shin, M. H., et al. (2009). Association between polymorphisms of folate-metabolizing enzymes and hematological malignancies. *Leuk. Res.* 33, 82–87. doi: 10.1016/j.leukres.2008.07.026

Kotagiri, D., and Kolluru, V. C. (2017). Effect of salinity stress on the morphology and physiology of five different *Coleus* species. *Biomed. Pharmacol. J.* 10, 1639–1649. doi: 10.13005/bpj/1275

Krzymińska, A., and Ulczycka-Walorska, M. (2015). The effect of sodium chloride on growth and quality of *Plectranthus forsteri* Benth. "Nico". *J. Hortic. Res.* 23, 17–20. doi: 10.2478/johr-2015-0003

Lea-Cox, J. D., and Syvertsen, J. P. (1993). Salinity reduces water use and nitrate-N use efficiency of citrus. *Ann. Bot.* 72, 47–54. doi: 10.1006/anbo.1993.1079

Lewis, N. G., and Yamamoto, E. (1990). Lignin: occurrence, biogenesis and biodegradation. *Annu. Rev. Plant Biol.* 41, 455–496. doi: 10.1146/annurev.pp.41.060190.002323

Lukhoba, C. W., Simmonds, M. S. J., and Paton, A. J. (2006). *Plectranthus*: a review of ethnobotanical uses. *J. Ethnopharmacol.* 103, 1–24. doi: 10.1016/j.jep.2005.09.011

Maas, E. V., and Grattan, S. R. (1999). "Crop Yields as Affected by Salinity", in *Agricultural Drainage*, eds Skaggs, R.W., and van Schilfgaarde, J. (USA: American Society of Agronomy), pp. 55–108. doi: 10.2134/agronmonogr38.c3

Mahajan, S., and Tuteja, N. (2005). Cold, salinity and drought stresses: an overview. *Arch. Biochem. Biophys.* 444, 139–158. doi: 10.1016/j.abb.2005.10.018

Maxwell, K., and Johnson, G. N. (2000). Chlorophyll fluorescence - a practical guide. *J. Exp. Bot.* 51, 659–668. doi: 10.1093/jexbot/51.345.659

Mullineaux, P. M., and Rausch, T. (2005). Glutathione, photosynthesis and the redox regulation of stress responsive gene expression. *Photosynth. Res.* 47, 459–474. doi: 10.1007/s11120-005-8811-8

Munns, R. (2002). Comparative physiology of salt and water stress. *Plant Cell Environ.* 25, 239–250. doi: 10.1046/j.0016-8025.2001.00808.x

Munns, R., and Tester, M. (2008). Mechanisms of salinity tolerance. *Annu. Rev. Plant Biol.* 59, 651–681. doi: 10.1146/annurev.arplant.59.032607.092911

Naidoo, G., and Naidoo, Y. (2001). Effects of salinity and nitrogen on growth, ion relations and proline accumulation in *Triglochin bulbosa*. *Wetl. Ecol. Manag.* 9, 491–497. doi: 10.1023/A:1012284712636

Nakano, Y., and Asada, K. (1981). Hydrogen peroxide is scavenged by ascorbate-specific peroxidase in spinach chloroplasts. *Plant Cell Physiol.* 22, 867–880.

Noctor, G., and Foyer, C. H. (1998). Ascorbate and glutathione: keeping active oxygen under control. *Annu. Rev. Plant Biol.* 49, 249–279. doi: 10.1146/annurev.arplant.49.1.249

Paraskevopoulou, A. T., Karantzi, A. K., Liakopoulos, G., Londra, P. A., and Bertsouklis, K. (2020). The effect of salinity on the growth of lavender species. *Water* 12, 618. doi: 10.3390/w12030618

Parvaiz, A., and Satyawati, S. (2008). Salt stress and phyto-biochemical responses of plants – a review. *Plant Soil Environ.* 54, 89–99. doi: 10.17221/2774-PSE

Poudineh, Z., Moghadam, Z. G., and Mirshekari, S. (2015). Effects of humic acid and folic acid on sunflower under drought stress. *Biol. Forum* 7, 451–454.

Qadir, M., Sposito, G., Smith, C. J., and Oster, J. D. (2021). Reassessing irrigation water quality guidelines for sodicity hazard. *Agric. Water Manag.* 255:107054. doi: 10.1016/j.agwat.2021.107054

Rady, M. M., Boriek, S. H. K., El-Mageed, T. A. A., El-Yazal, M. A. S., Ali, E. F., Hassan, F. A. S., et al. (2021a). Exogenous gibberellic acid or dilute bee honey boosts drought stress tolerance in *Vicia faba* by rebalancing osmoprotectants, antioxidants, nutrients, and phytohormones. *Plants* 10, 748. doi: 10.3390/plants10040748

Rady, M. O. A., Semida, W. M., Howladar, S. M., and Abd El-Mageed, T. A. (2021b). Raised beds modulate physiological responses, yield and water use efficiency of wheat (*Triticum aestivum* L.) under deficit irrigation. *Agric. Water Manag.* 245:106629. doi: 10.1016/j.agwat.2020.106629

Ramezani, E., Sepanlou, M. G., and Badi, H. A. N. (2011). The effect of salinity on the growth, morphology and physiology of *Echium amoenum* Fisch. and Mey. *Afr. J. Biotechnol.* 10, 8765–8773. doi: 10.5897/AJB10.2301

Rodriguez-Navarro, A. (2000). Potassium transport in fungi and plants. *Biochim. Biophys. Acta.* 1469, 1–30. doi: 10.1016/S0304-4157(99)00013-1

Rout, N. P., and Shaw, B. P. (2001). Salt tolerance in aquatic macrophytes: possible involvement of the antioxidative enzymes. *Plant Sci.* 160, 415–423. doi: 10.1016/S0168-9452(00)00406-4

Rozeff, N. (1995). Sugarcane and salinity - a review paper. *Sugarcane.* 5, 8–19.

Samiullah, S. A., Ansori, M. M., and Afridi, R. K. (1988). B- Vitamins in relation to crop productivity. *Indian Rev. Life Sci.* 8, 51–74.

Sass, J. E. (1961). *Botanical Microtechnique*. Iowa, USA: Ames, Iowa State College Press, p. 240.

Scott, J., Rébeillé, F., and Fletcher, J. (2000). Folic acid and folates: the feasibility for nutritional enhancement in plant foods. *J. Sci. Food Agric.* 80, 795–824. doi: 10.1002/(SICI)1097-0010(20000515)80:7<795::AID-JSFA599>3.0.CO;2-K

Semida, W. M., Abd El-Mageed, T. A., Hemida, K., and Rady, M. M. (2019). Natural bee-honey based biostimulants confer salt tolerance in onion *via* modulation of the antioxidant defence system. *J. Hortic. Sci. Biotechnol.* 94, 632–642 doi: 10.1080/14620316.2019.1592711

Semida, W. M., Abd El-Mageed, T. A., and Howladar, S. M. (2014). A novel organo-mineral fertilizer can alleviate negative effects of salinity stress for eggplant production on reclaimed saline calcareous soil. *Acta Hort.* 1034, 493–499. doi: 10.17660/ActaHortic.2014.1034.61

Semida, W. M., Abd El-Mageed, T. A., Howladar, S. M., Mohamed, G. F., and Rady, M. M. (2015a). Response of *Solanum melongena* L. seedlings grown under saline calcareous soil conditions to a new organo-mineral fertilizer. *J. Anim. Plant Sci.* 25, 485–493.

Semida, W. M., Abdelkhalik, A., Mohamed, G., Abd El-Mageed, T., A., Abd El-Mageed, S. A., et al. (2021). Foliar application of zinc oxide nanoparticles promotes drought stress tolerance in eggplant (*Solanum melongena* L.). *Plants* 10, 421. doi: 10.3390/plants10020421

Semida, W. M., Rady, M. M., Abd El-Mageed, T. A., Howladar, S. M., and Abdelhamid, M. T. (2015b). Alleviation of cadmium toxicity in common bean (*Phaseolus vulgaris* L.) plants by the exogenous application of salicylic acid. *J. Hortic. Sci. Biotechnol.* 90, 83–91. doi: 10.1080/14620316.2015.11513156

Shaaban, A., Al-Elwany, O. A. A. I., Abdou, N. M., Hemida, K. A., El-Sherif, A. M. A., Abdel-Razek, M. A., et al. (2022). Filter mud enhanced yield and soil properties of water-stressed *Lupinus termis* L. in saline calcareous soil. *J. Soil Sci. Plant Nutr.* 22, 1572–1588. doi: 10.1007/s42729-021-00755-y

Shannon, M. C., and Grieve, C. M. (1998). Tolerance of vegetable crops to salinity. *Sci. Hortic.* 78, 5–38. doi: 10.1016/S0304-4238(98)00189-7

Singh, T. N., Aspinall, D., Paleg, L. G., and Boggess, S. F. (1973). Stress metabolism II. Changes in proline concentration in excised plant tissues. *Aust. J. Biol. Sci.* 26, 57–63. doi: 10.1071/BI9730057

Singleton, V. L., and Rossi, J. A. (1965). Colorimetry of total phenolics with phosphomolybdic-phosphotungstic acid reagents. *Am. J. Enol. Vitic.* 16, 144–158.

Stakhova, L. N., Stakhov, L. F., and Ladygin, V. G. (2000). Effects of exogenous folic acid on the yield and amino acid content of the seed of *Pisum sativum* L. and *Hordeum vulgare* L. *Prikl. Biokhimiya Mikrobiol.* 36, 98–103. doi: 10.1007/BF02738142

Taiz, L., and Zeiger, E. (2002). *Plant Physiology*. Sunderland, UK: Sinauer Associates, pp. 690.

Thomas, R. L., Jen, J. J., and Morr, C. V. (1982). Changes in soluble and bound peroxidase—IAA oxidase during tomato fruit development. *J. Food Sci.* 47, 158–161. doi: 10.1111/j.1365-2621.1982.tb11048.x

Van Wilder, V., De Brouwer, V., Loizeau, K., Gambonnet, B., Albrieux, C., Van Der Straeten, D., et al. (2009). C1 metabolism and chlorophyll synthesis: the Mg-protoporphyrin IX methyltransferase activity is dependent on the folate status. *New Phytol.* 182, 137–145. doi: 10.1111/j.1469-8137.2008.02707.x

Vartanian, N., Hervochon, P., Marcotte, L., and Larher, F. (1992). Proline accumulation during drought rhizogenesis in *Brassica napus* var. *oleifera*. *J. Plant Physiol.* 140, 623–628. doi: 10.1016/S0176-1617(11)80799-6

Verbruggen, N., and Hermans, C. (2008). Proline accumulation in plants: A review. *Amino Acids* 35, 753–759. doi: 10.1007/s00726-008-0061-6

Wilde, S. A., Corey, R. B., Lyer, J. G., and Voigt, G. K. (1985). *Soil and Plant Analysis for Tree Culture*. New Delhi, India: Oxford and IBM Publishers, pp. 93–106.

Yasar, F., Kusvuran, S., and Ellialtioglu, S. (2006). Determination of anti-oxidant activities in some melon (*Cucumis melo* L.) varieties and cultivars under salt stress. *J. Hortic. Sci. Biotechnol.* 81, 627–630. doi: 10.1080/14620316.2006.11512115

Yemm, E. W., Cocking, E. C., and Ricketts, R. E. (1955). The determination of amino-acids with ninhydrin. *Analyst* 80, 209–214. doi: 10.1039/an9558000209

Yildirim, B., Yaser, F., Ozpay, T., Turkozu, D., Terziodlu, O., and Tamkoc, A. (2008). Variations in response to salt stress among field pea genotypes (*Pisum sativum* sp. *arvense* L.). *J. Anim. Vet. Adv.* 7, 907–910.

Zhu, J. K., Liu, J., and Xiong, L. (1998). Genetic analysis of salt tolerance in *Arabidopsis*: Evidence for a critical role of potassium nutrition. *Plant Cell* 10, 1181–1191. doi: 10.1105/tpc.10.7.1181

**Conflict of Interest:** The authors declare that the research was conducted in the absence of any commercial or financial relationships that could be construed as a potential conflict of interest.

**Publisher's Note:** All claims expressed in this article are solely those of the authors and do not necessarily represent those of their affiliated organizations, or those of the publisher, the editors and the reviewers. Any product that may be evaluated in this article, or claim that may be made by its manufacturer, is not guaranteed or endorsed by the publisher.

frontiers | Frontiers in Plant Science

TYPE Original Research
PUBLISHED 16 August 2022
DOI 10.3389/fpls.2022.886862



OPEN ACCESS

EDITED BY
Alvaro Sanz-Saez,
Auburn University, United States

REVIEWED BY
Iker Aranjuelo,
Institute of Agrobiotechnology (CSIC), Spain
Maite Lacuesta,
University of the Basque Country, Spain

*CORRESPONDENCE
Haiying Lu
luhaiying@njfu.edu.cn
Khaled A. El-Tarabily
ktarabily@uaeu.ac.ae
Synan F. AbuQamar
sabuqamar@uaeu.ac.ae

†These authors have contributed equally to this work

SPECIALTY SECTION
This article was submitted to Plant Abiotic Stress, a section of the journal Frontiers in Plant Science

RECEIVED 01 March 2022
ACCEPTED 04 July 2022
PUBLISHED 16 August 2022

CITATION
Sheteiwy MS, Ulhassan Z, Qi W, Lu H, AbdElgawad H, Minkina T, Sushkova S, Rajput VD, El-Keblawy A, Jośko I, Sulieman S, El-Esawi MA, El-Tarabily KA, AbuQamar SF, Yang H and Dawood M (2022) Association of jasmonic acid priming with multiple defense mechanisms in wheat plants under high salt stress. *Front. Plant Sci.* 13:886862. doi: 10.3389/fpls.2022.886862



# Association of jasmonic acid priming with multiple defense mechanisms in wheat plants under high salt stress

Mohamed S. Sheteiwy[1,2,3†], Zaid Ulhassan[4], Weicong Qi[5], Haiying Lu[1,6*], Hamada AbdElgawad[7†], Tatiana Minkina[3], Svetlana Sushkova[3], Vishnu D. Rajput[3], Ali El-Keblawy[8], Izabela Jośko[9], Saad Sulieman[10], Mohamed A. El-Esawi[11], Khaled A. El-Tarabily[12,13,14*], Synan F. AbuQamar[12*], Haishui Yang[15] and Mona Dawood[16†]

[1]College of Biology and the Environment, Nanjing Forestry University, Nanjing, China, [2]Department of Agronomy, Faculty of Agriculture, Mansoura University, Mansoura, Egypt, [3]Southern Federal University, Academy of Biology and Biotechnology, Rostov-on-Don, Russia, [4]Institute of Crop Science and Zhejiang Key Laboratory of Crop Germplasm, Zhejiang University, Hangzhou, China, [5]Institute of Agriculture Resources and Environment, Jiangsu Academy of Agricultural Sciences (JAAS), Nanjing, China, [6]Co-innovation Center for the Sustainable Forestry in Southern China, Nanjing Forestry University, Nanjing, China, [7]Department of Botany, Faculty of Science, University of Beni-Suef, Beni-Suef, Egypt, [8]Department of Applied Biology, Faculty of Science, University of Sharjah, Sharjah, United Arab Emirates, [9]Faculty of Agrobioengineering, Institute of Plant Genetics, Breeding and Biotechnology, University of Life Sciences, Lublin, Poland, [10]Department of Agronomy, Faculty of Agriculture, University of Khartoum, Khartoum North, Sudan, [11]Department of Botany, Faculty of Science, Tanta University, Tanta, Egypt, [12]Department of Biology, College of Science, United Arab Emirates University, Al-Ain, United Arab Emirates, [13]Khalifa Center for Genetic Engineering and Biotechnology, United Arab Emirates University, Al-Ain, United Arab Emirates, [14]Harry Butler Institute, Murdoch University, Murdoch, WA, Australia, [15]College of Agriculture, Nanjing Agricultural University, Nanjing, China, [16]Department of Botany and Microbiology, Faculty of Science, Assiut University, Assiut, Egypt

Salinity is a global conundrum that negatively affects various biometrics of agricultural crops. Jasmonic acid (JA) is a phytohormone that reinforces multilayered defense strategies against abiotic stress, including salinity. This study investigated the effect of JA (60 μM) on two wheat cultivars, namely ZM9 and YM25, exposed to NaCl (14.50 $dSm^{-1}$) during two consecutive growing seasons. Morphologically, plants primed with JA enhanced the vegetative growth and yield components. The improvement of growth by JA priming is associated with increased photosynthetic pigments, stomatal conductance, intercellular $CO_2$, maximal photosystem II efficiency, and transpiration rate of the stressed plants. Furthermore, wheat cultivars primed with JA showed a reduction in the swelling of the chloroplast, recovery of the disintegrated thylakoids grana, and increased plastoglobuli numbers compared to saline-treated plants. JA prevented dehydration of leaves by increasing relative water content and water use efficiency via reducing water and osmotic potential using proline as an osmoticum. There was a reduction in sodium ($Na^+$) and increased potassium ($K^+$) contents, indicating a significant role of JA priming in ionic homeostasis, which was associated with induction of the transporters, *viz.*, *SOS1*, *NHX2*, and *HVP1*. Exogenously applied JA mitigated the

inhibitory effect of salt stress in plants by increasing the endogenous levels of cytokinins and indole acetic acid, and reducing the abscisic acid (ABA) contents. In addition, the oxidative stress caused by increasing hydrogen peroxide in salt-stressed plants was restrained by JA, which was associated with increased α-tocopherol, phenolics, and flavonoids levels and triggered the activities of superoxide dismutase and ascorbate peroxidase activity. This increase in phenolics and flavonoids could be explained by the induction of phenylalanine ammonia-lyase activity. The results suggest that JA plays a key role at the morphological, biochemical, and genetic levels of stressed and non-stressed wheat plants which is reflected in yield attributes. Hierarchical cluster analysis and principal component analyses showed that salt sensitivity was associated with the increments of $Na^+$, hydrogen peroxide, and ABA contents. The regulatory role of JA under salinity stress was interlinked with increased JA level which consequentially improved ion transporting, osmoregulation, and antioxidant defense.

KEYWORDS

**jasmonic acid, $Na^+$ transporter-related gene expression, nutrient homeostasis, salinity, wheat**

## Introduction

Wheat (*Triticum aestivum* L.) is an important cereal crop widely consumed globally as a valuable food. With a dramatically increasing in the human population worldwide and to meet the food demands, wheat production should increase by more than 60% to feed the 9.6 billion world population by 2050 (Tadesse et al., 2019). The major constraints in wheat productivity are abiotic stress such as water stress, heat, and salinity. Although wheat is reported as a moderately salt-tolerant crop, the grain yield could be reduced when the salinity is higher than 10 $dSm^{-1}$ (Munns et al., 2006). Therefore, enhancing wheat yield is the ultimate goal of coping with the food security challenges under changing climate conditions and limited resources.

Salt stress is one of the major environmental issues encountered by plants. It has been determined that about 20% (50 million hectares) of agricultural land is affected by salt stress (Shrivastava and Kumar, 2015). Salt stress impacts the plants' osmotic potential that affects the hydraulic conductivity through reducting water uptake or affecting solute potential (Munns and Tester, 2008). The prolonged exposure and high concentrations of salt ions by plants disturb the $Na^+/K^+/Ca^{++}$ homeostasis, increase the release of reactive oxygen species (ROS), and the oxidation of membrane lipids (Ahanger et al., 2017; Sehar et al., 2019). This could cause injuries to the cellular structure of chloroplast and mitochondria, ionic imbalance, and impairment in water relations and photosynthesis, thereby inhibiting plant growth and causing cell death (Sheteiwy et al., 2018; Sehar et al., 2019).

To handle the excessive accumulation of ROS and induced oxidative damages, plant cells intricately synthesize enzymatic antioxidants such as superoxide dismutase (SOD), catalase (CAT), and ascorbate peroxidase (APX) to scavenge ROS (He et al., 2017; Ulhassan et al., 2019; Sheteiwy et al., 2021b). The increased concentration of non-enzymatic antioxidants such as osmoprotectants including proline (Ahmad et al., 2016), non-enzymatic antioxidants (tocopherols), secondary metabolites such as total phenols and flavonoids (Mir et al., 2018), and modulation of phytohormones such as abscisic acid (ABA) and ethylene (Garcia de la Garma et al., 2015) also contribute to alleviating salt stress. At the cellular level, tolerant genotypes use different mechanisms to adapt to salt stress by reducing $Na^+$ accumulation in the cytoplasm and restricting its entry into the cell via mediating $Na^+$ extrusion using *SOS1* (salt overly sensitive1) and $Na^+$ compartmentalization in the vacuole (Shi et al., 2003).

However, tissue tolerance via $Na^+$ sequestration in shoots is considered one of the essential mechanisms of salt stress tolerance (Munns et al., 2016). Another salt tolerance mechanism is $Na^+$ exclusion from the cytosol by mediating $Na^+$ uptake and movement in different organs and/or by $Na^+$ compartmentation into the vacuole. Many transporters, such as the high-affinity $K^+$ transporters (*HKT1*), plasma membrane $Na^+/H^+$ exchanger (*SOS1*, *SOS2*, and *SOS3*), $H^+$-pyrophosphatase (*HVP*), and tonoplast $Na^+/H^+$ antiporters (*NHX*) have been reported to have an important role in $Na^+$ uptake mechanisms and transport pathway (Tuteja, 2007;

Shavrukov, 2014). Hence, it is greatly essential to find a practical approach to increase wheat tolerance against stress conditions.

Seed priming is being used to enhance seed germination and crop yield under different environmental stresses (Sheteiwy et al., 2018, 2019; Gao et al., 2020b; Dawood et al., 2021a, 2022; Basit et al., 2022). During seed priming, seed metabolism activation is controlled by the hydration level of seeds, resulting in carbohydrates hydrolysis to be easily taken by the embryo. Seed germination can improve the metabolic process (pre-germinated) to stimulate radicle protrusion (Paparella et al., 2015). During imbibition, seed priming limits the endosperm resistance, nurtures the immature embryos, and repairs membranes (Balestrazzi et al., 2011). In this way, priming can enhance abiotic stress tolerance during dehydration or soaking steps. Seed priming with phytohormones such as jasmonic acid (JA) has been widely utilized to mitigate abiotic stress effects and regulate physio-biochemical processes in plants (Sheteiwy et al., 2018, 2021a).

Earlier studies have reported that seed priming with low concentrations of JA can alleviate salt stress by improving water potential (*via* increased synthesis of osmoregulators), reducing $Na^+$ accumulation in tissues, and promoting photosynthesis, growth, and yield of several crops (Sheteiwy et al., 2018, 2021a). For example, it has been reported that seed priming with JA can improve the germination rate, seed vigor, photosynthetic machinery, water use efficiency (WUE), relative water contents (RWC), and metabolites accumulation in soybean (Sheteiwy et al., 2021a), and rice cultivars (Sheteiwy et al., 2018). Similarly, Al-harthi et al. (2021) have found that seed priming with JA can alleviate salt stress in summer squash (*Cucurbita pepo* L.) by upregulating the antioxidant (enzymatic and non-enzymatic) defense system, ionic homeostasis, and pigmentation resulted in higher biomass accumulation.

Hence, the purpose of the current study is to investigate the potential roles of seed priming with JA in adapting the physiological, cellular, and molecular mechanisms of wheat plants exposed to high salt stress. We hypothesize that the primed JA may modulate the osmoregulators, induce the nutrients balance, produce endogenous phytohormones, accumulate secondary metabolites, and stimulate antioxidant defense machinery or stress-related transcripts of wheat plants to improve growth, biomass accumulation, and photosynthetic apparatus. Thus, seeds primed with JA may minimize the effect of salt stress by scavenging the ROS accumulation and improving wheat growth in saline stress conditions.

## Materials and methods

### Experimental design, plant growth, and stress treatment

Field experiments were performed during the 2018/2019 and 2019/2020 growing seasons from November to June at the experimental farm of the Academy of Agricultural Science (JAAS), Nanjing, Jiangsu, China (35.31°N 113.87 °E). The seeds of two cultivars of spring wheat i.e. Zheng Mai9 (ZM9, salt-sensitive) and Yang Mai25 (YM25, salt-tolerant), were brought from the Seed Center of Nanjing, Jiangsu, China (JAAS).

Both cultivars selected in the current experiment were widely cultivated in the delta of the Yangtz river of China, based on their excellent traits, e.g., ZM9 with more resistance to wheat diseases such as *Fusarium* head blight and powdery mildew, YM25 with stronger resistance to lodging, and both showing higher yield and better grain quality. The area has a humid subtropical climate, and the mean temperature and humidity of both growing seasons are shown in Supplementary Table S1. The soil's main properties were as follows: 24.9% clay; 55.6% silt; 19.5% sand. The soil chemical properties from 0 to 30 cm of the experimental site were represented in Supplementary Table S2. The plots' size used in this study was 13 $m^2$ (3.25 × 4 m), with a distance between each ridge of 45 cm. The experiments were performed using a complete randomized block design (CRBD, factorial), with three biological replications and eight treatments. The experiment field differs in salinity levels. The plots with 4.6 $dSm^{-1}$ were served as a control, and plots with 14.50 $dSm^{-1}$ were used as salinity stress. This salinity was designed as high salt stress for wheat plants as it was comparable to saline-alkaline lands in the coastal areas of Jiangsu Province, China (Ju et al., 2021). Salt soil plots were established by mixing normal soil with salt (1:100). In order to confine the lateral diffusion of salt with water movement among plots, a plastic membrane was mulched on the ridges of each plot.

For the priming treatments, two levels of JA (0 and 60 μM) were used. Prior to seed priming, diluted sodium hypochlorite was used as a sanitizer solution of wheat grains for 15 min and then washed several times to remove any debrides of the disinfectant. Then, the grains were divided into two sets, a group soaked in distilled water representing the control, and the second group was soaked in JA with a concentration of 60 μM at 15 °C in darkness for 24 h (Sheteiwy et al., 2021a). The time and the selected dose of JA were preliminarily tested and optimized. The seeds were left to dry, and the sowing was performed in the second week of November during the seasons (2018 and 2019).

The seeds were sown in rows at depth of 4 cm and 20 cm space between rows. The recommended amount of essential fertilizers such as N (388 kg $h^{-1}$), P (87.75 kg $h^{-1}$), and K (120 kg $h^{-1}$) was applied according to the soil fertility status. The entire P and K fertilizers were provided before planting as basal doses; however, the doses of N were completely applied at the stem elongation and node formation stages (after 50 days from sowing). The water requirement was supplied to soils based on the wheat growth stages, in which 15, 25, 30, and 25% were supplied to the soil at the initial stage, vegetative growth, reproductive stage, grain filling stage, respectively of the total water requirements. In comparison, the soil was naturally dried during maturation (5%). Irrigation water was supplied and pumped to the plots from a pond through pipes. The irrigation

system has pipes buried in the soil at a specific depth and water is pumped to enter these pipes for irrigation. This system was equipped with a water meter to control the water flow to the plots at the different growth stages. Other agricultural practices for wheat production were similar to those applied by farmers' practices in the Jiangsu region of China.

In order to determine the physiological, morphological, and yield, 20 wheat plants with the same vigor were selected, tagged in each plot, and used for the different analyses. The morphological and physiological parameters were recorded after 60 days after sowing. Plant heights were measured from the base to the tip of the plant shoot. The fresh weight (FW) and dry weight (DW; dried in an oven at 80 °C for 24 h) of treated plants were recorded. After the maturity of plants and spikes, the spike/$m^2$, grains/ spike, and weight of 100 grains were estimated and it was determined during only the first growing season (2018/2019).

## Determination of photosynthetic pigments, photosynthesis efficiency, and transpiration

The leaf physiological traits such as stomatal conductance ($g_s$), transpiration rate ($T_r$), net photosynthetic rate ($P_n$), and intercellular $CO_2$ ($C_i$) were determined using a portable photosynthesis system (LI-6400; Lincoln, NE, USA) after 2 h of acclimation in the growth cabinet at 27 °C, 70% relative humidity, the light intensity of 1000 μ mol $m^{-2}$ $s^{-1}$, and $CO_2$ of 380 μ mol $mol^{-1}$ (Sheteiwy et al., 2021a). The chlorophyll contents were measured spectrophotometrically using the method described previously by Sheteiwy et al. (2018). Briefly, the fresh leaf samples (0.2 g) were ground in 3 mL ethanol (95%, v/v). The homogenate was centrifuged at 5,000 x*g* for 10 min and the supernatant was extracted. The mixture was then determined by monitoring the absorbance at the wavelengths 665, 649, and 470 nm using a spectrophotometer (UV-2101/3101 PC; Shimadzu Corporation, Analytical Instruments Division, Kyoto, Japan). The chlorophyll fluorescence (CF) was measured by the chlorophyll fluorometer (IMAG-MAXI, Heinz Walz, Effeltrich, Germany) in the expanded leaves after dark adaptation for 15 min according to the methodology of Ali et al. (2015).

## Ultrastructural changes in wheat leaves

To deeply observe the changes in the cellular structures of the plant cell and major structural organelles in terms of chloroplast, cell wall, and starch grain and their functions in response to salt stress and JA priming, the leaf ultrastructural changes were investigated using a protocol reported by Yang et al. (2021) with slight modifications. Segments (6–8 per treatment) were randomly selected from wheat plants and overnight immersed in glutaraldehyde (2.5%, v/v) and washed four times with.1 M of phosphate-buffered saline (PBS), with 10-min intervals between each washing. Then, at 15–20 min intervals, the samples were dehydrated in a graded series of ethanol (50%, 60%, 70%, 80%, 90%, 95%, and 100%) and then washed with absolute acetone for 20 min. The samples were then assembled and fixed on copper grids to be scanned using the transmission electron microscope (JEOL TEM-1230 EX), as described by Yang et al. (2021).

## Determination of $Na^+$ accumulation and $k^+$ uptake in the different tissues of wheat

The $Na^+$ and $K^+$ contents of the blade, sheath, stem, and roots of both wheat cultivars were recorded using the method described by Zhao et al. (2014). The tissues were washed with distilled water and then dried at 50 °C for 4 d. After that, the dried samples were ground into a fine powder by liquid nitrogen and digested in nitric acid (5 mL) overnight. Then, $Na^+$ and $K^+$ contents of different tissues were monitored using a flame photometer following the methodology of Zhao et al. (2014).

## Determination of water-relation parameters

The water relation parameters such as water potential and osmotic potential were measured following the protocol reported by Ahmed et al. (2013). Briefly, the segments of the fully expanded leafy sample were macerated in a mortar. After extract filtration, the sap was centrifuged at 10,000 x g for 10 min at 4 °C, then the supernatant was used to estimate osmolality (c) using a vapor pressure osmometer (Wescor Inc., Logan, UT, USA). WUE was measured as the ratio between $P_n$ and $T_r$ as described by Jones (2013). Briefly, fresh eight of the leaf sample, and the dry weight (for 48 h in an oven at 75 °C) were recorded and used for the RWC determination. The leaf was then soaked for 24 h in distilled $H_2O$. The leaves were then dried using tissue paper prior to turgid weight calculation and the RWC was measured. The RWC was quantified in tissues using the equations of Barr and Weatherley (1962) as follows:

$$RWC\,(\%) = \frac{Fresh\ weight - Dry\ weight}{Turgid\ weight - Dry\ weight} \times 100$$

## Determination of $H_2O_2$, proline, phenolic metabolism, and antioxidants profile

The hydrogen peroxide ($H_2O_2$) content was measured in the root and shoot according to Halliwell et al. (1987). Briefly, the

root and shoot samples (0.5 g) were macerated in trichloroacetic acid (5.0 mL of 0.1%), and the supernatant was mixed with 1 mL of 1 mM KI, and the absorbance at the wavelengths 390 nm by using spectrophotometer was monitored. Proline was determined in the root and shoot samples according to Sheteiwy et al. (2021b). The leaf samples (100 mg) were homogenized in 3% sulfosalicylic acid (5 mL) and centrifuged at 5,000 x*g* for 10 min. The supernatant was mixed with acid-ninhydrin and acetic acid and boiled for 1 h at 100 °C followed by incubation in an ice bath. The absorbance of chromophore-containing toluene was monitored at 520 nm. Tocopherol in root and shoot samples was recorded at 520 nm following Backer et al. (1980). The flavonoid content in root and shoot samples was determined according to Zhishen et al. (1999). Total phenolic content in root and shoot were quantified and calculated using gallic acid (Sigma-Aldrich Chemie GmbH, Taufkirchen, Germany) as a standard (Shohag et al., 2012).

The antioxidant enzyme activities, such as APX, SOD, and Phenylalanine ammonia-lyase (PAL) were determined in the leaf and root tissues spectrophotometrically at 290 nm by the method of Sheteiwy et al. (2021a). Briefly, fresh leaf and root samples (0.5 g) were homogenized in liquid nitrogen and then macerated in K-phosphate buffer (8 mL, 50 mmol $L^{-1}$, pH 7.8) in ice-cold conditions. The extract was then centrifuged at 10,000 x *g* for 20 min at 4 °C where the supernatant was utilized for the aforementioned enzyme activity measurements.

APX activity was determined following the methodology of Nakano and Asada (1981). The reaction mixture was composed of 1.4 mL PBS (25 mmol $L^{-1}$ pH 7.0 + 2 mmol $L^{-1}$ ethylene diamine tetra acetic acid (EDTA), 300 mmol $L^{-1}$ $H_2O_2$, 7.5 mmol $L^{-1}$ ascorbic acid 100 μL, and 100 μL enzyme extract in a total volume of 1.7 mL. APX enzyme was measured by noticing the reduction percentage of the absorbance of ascorbic acid at 290 nm for 2 min. SOD activity was measured according to the method of Giannopolitis and Ries (1977). The reaction mixture contained 3 mL 50 mmol $L^{-1}$ phosphate buffer (pH 7.8), 13 mmol $L^{-1}$ methionine, 1.22 mmol $L^{-1}$ riboflavin, 78.2 μmol $L^{-1}$ EDTA, 56 μmol $L^{-1}$ of Nitro blue tetrazolium (NBT) and 100 μL extract. The mixture was illuminated and the reaction was used to measure the inhibition of the photochemical reduction of NBT at 560 nm. One unit of SOD was defined as the amount required to inhibit the photoreduction of NBT by 50%. SOD activity was expressed as $mg^{-1}$ protein as reported earlier by Zhu et al. (2015).

## Determination of hormones profile

The concentrations of cytokinins (CKs) were determined according to the method of Rauf and Sadaqat (2007). The indole acetic acid (IAA) was measured following the methodology of Sheteiwy et al. (2021c). Abscisic acid (ABA) was quantified in shoot and root tissues following the methodology of Gao et al. (2020a). For JA determination, frozen root and shoot samples (200 mg) were ground into fine powder using liquid nitrogen. The extracts were then centrifuged at 12000 x *g* for 10 min at 4 °C, and then JA was quantified using liquid chromatography-mass spectrometry (Waters, Milford, Massachusetts, USA) as described by Tsukahara et al. (2015).

## Determination of relative gene expression level

The transcript levels of $Na^+$ uptake and transport genes such as *SOS1-NHX2- HVP1* were analyzed in leaf blade-, leaf sheath, stem, and root tissues. The total RNA isolation was performed using an RNA isolation (Takara Bio Inc., Shiga, Japan). cDNA was synthesized using Primer Script RT reagent Kit (Takara Bio Inc.) from 1 μ g of total RNA in a 20 μ L reaction, and diluted 4-fold with water. SYBR premix EX Taq (Takara Bio Inc.) was used to perform the quantitative real-time (qRT-PCR) analysis. The frozen tissues (100 mg) were homogenized in liquid nitrogen and qRT-PCR was performed following the methodology of Gao et al. (2020b) using primers used previously by Darko et al. (2017). ACT1 was used as a control to determine the transcription level of the other studied genes. The PCR program was the same as followed by Salah et al. (2015).

## Statistical analysis

Two-way analysis of variance (ANOVA) was applied to determine differences among treatments. The results were described as the means of three replicates ± SD. The data were analyzed using the statistical package (IBM-SPSS, 19, USA). Mean values were compared by applying Duncan's multiple range test at the.05 level of significance. Asterisks indicate significant differences: $^*P < 0.05$, $^{**}P<0.001$, $^{***}P<0.0001$. The Hierarchical Cluster Analysis (HCA) and Principle Component Analysis (PCA) were performed through the SPSS program on $\log_{10}$ of the obtained data.

# Results

## Effect of JA priming on wheat growth under salt stress

Results revealed that salt stress caused a significant ($P \leq 0.05$) reduction in growth and numbers of tillers in wheat seedlings compared to the control seedlings (Table 1). The reduction of shoot length, FW, and DW in response to salinity reached 23, 40, and 44% in the ZM9 cultivar and 22, 45, and 44% in cultivar YM25, respectively, compared with the control. Priming with JA resulted in improved plant height, FW, and

TABLE 1 Effects of JA priming on plant height, FW, DW, number of tillers/plants, $T_r$ and $P_n$ of two wheat cultivars Mai9 (ZM9, salt-sensitive) and Yang Mai25 (YM25, salt-tolerant) under control and salinity stress conditions during two consecutive growing seasons 2019 and 2020.

| | Treatments | Plant height (cm) | FW (g) | DW (g) | Number of tillers plants$^{-1}$ | $T_r$ (mmol $H_2O$ $m^{-2}$ $s^{-1}$) | $P_n$ (μmol $CO_2$ $m^{-2}$ $s^{-1}$) |
|---|---|---|---|---|---|---|---|
| **2019** | | | | | | | |
| ZM9 | Ck | 80.43 ± 2.0c | 2.53 ± 0.15b | 0.624 ± 0.03b | 6.33 ± 0.5b | 6.29 ± 0.34bc | 3.31 ± 0.38b |
| | 60 μM JA | 91.50 ± 3.4b | 3.36 ± 0.15a | 0.831 ± 0.04a | 7.33 ± 0.5a | 8.32 ± 0.13a | 5.14 ± 0.5a |
| | S1 | 62.73 ± 2.4e | 1.50 ± 0.10c | 0.356 ± 0.03c | 4.33 ± 0.5c | 3.41 ± 0.20fg | 2.20 ± 0.10c |
| | S1+60 μM JA | 71.23 ± 1.3d | 2.16 ± 0.15b | 0.540 ± 0.03b | 5.66 ± 0.5b | 5.49 ± 0.31de | 3.08 ± 0.12b |
| YM25 | Ck | 80.83 ± 1.3c | 2.59 ± 0.14b | 0.634 ± 0.02b | 6.00 ± 0.1b | 5.61 ± 0.51c-e | 3.43 ± 0.19b |
| | 60 μM JA | 96.33 ± 1.7a | 3.63 ± 0.15a | 0.901 ± 0.03a | 7.33 ± 0.5a | 7.87 ± 0.32a | 5.30 ± 0.39a |
| | S1 | 63.83 ± 1.4e | 1.43 ± 0.15c | 0.348 ± 0.04c | 4.00 ± 0.10c | 3.60 ± 0.49fg | 1.92 ± 0.06c |
| | S1+60 μM JA | 73.73 ± 1.1d | 2.20 ± 0.17b | 0.533 ± 0.05b | 6.00 ± 0.3b | 5.73 ± 0.32c-e | 3.25 ± 0.17b |
| **2020** | | | | | | | |
| ZM9 | Ck | 79.53 ± 1.7c | 2.56 ± 0.3b | 0.628 ± 0.08b | 6.00 ± 0.3b | 6.44 ± 0.5b | 3.25 ± 0.17b |
| | 60 μM JA | 96.66 ± 2.2a | 3.23 ± 0.1a | 0.798 ± 0.03a | 7.66 ± 0.5a | 7.63 ± 0.4a | 5.34 ± 0.5a |
| | S1 | 63.46 ± 3.0e | 1.50 ± 0.10c | 0.367 ± 0.02c | 4.66 ± 0.5c | 3.28 ± 0.24g | 2.38 ± 0.6**c** |
| | S1+60 μM JA | 72.36 ± 2.2d | 2.20 ± 0.10b | 0.526 ± 0.03b | 6.00 ± 0.3b | 5.10 ± 0.21e | 3.21 ± 0.11b |
| YM25 | Ck | 80.53 ± 0.9c | 2.56 ± 0.15b | 0.627 ± 0.02b | 6.33 ± 0.5b | 5.41 ± 0.50de | 3.57 ± 0.16b |
| | 60 μM JA | 95.06 ± 1.5ab | 3.36 ± 0.68a | 0.833 ± 0.16a | 7.66 ± 0.5a | 7.92 ± 0.30a | 5.76 ± 0.9a |
| | S1 | 61.36 ± 3.5e | 1.53 ± 0.15c | 0.377 ± 0.04c | 4.33 ± 0.5c | 4.07 ± 0.17f | 2.06 ± 0.07c |
| | S1+60 μM JA | 73.16 ± 2.9d | 2.30 ± 0.10b | 0.570 ± 0.01b | 6.33 ± 0.5b | 5.92 ± 0.5b-d | 3.23 ± 0.15b |
| Year (Y) | | Ns | Ns | ns | ns | *** | *** |
| Cultivars (C) | | ** | Ns | ns | ns | ** | *** |
| Treat. (T) | | *** | *** | *** | *** | *** | *** |
| Y×C | | *** | Ns | ns | ns | *** | *** |
| Y×T | | ** | Ns | ns | ns | *** | *** |
| C×T | | * | Ns | ns | ns | *** | *** |
| Y×C×T | | ** | Ns | ns | ns | *** | *** |

Means sharing the same letters, for a parameter during a year, do not differ significantly at $P \leq 0.05$ among the studied factors after the Student–Newman–Keul test.
*P <0.05; **P <0.001; ***P <0.0001.
FW/DW, fresh/dry weight; $T_r$, transpiration rate; $P_n$, net photosynthetic rate; Ck, control; S, salt treatment; JA, jasmonic acid.





10.3389/fpls.2022.886862

DW as well as tiller numbers in both wheat cultivars during both growing seasons, compared to unprimed plants (Table 1).

Comparing both cultivars, the highest DW and FW values were observed in the YM25 cultivar primed with JA in both seasons. On the other hand, JA-primed plants of YM25 in 2019 and ZM9 in 2020 attained taller plants than the corresponding non-primed plants. We noticed that both cultivars showed a similar pattern of growth upon the treatment with 60 μM JA (Table 1). Plant height, FW, DW, and the numbers of tillers were significantly ($P \leq 0.05$) enhanced by JA priming under salt stress compared to the salt-stressed plants of both cultivars during the two growing seasons.

## Effect of JA priming on photosynthetic pigment, photosynthesis efficiency, and transpiration rate under salt stress

As presented in Table 1, and compared with the control, $P_n$ and $T_r$ were enhanced in the salt-stressed primed with JA compared to salt-stressed non-primed plants, which had reductions in both traits. The primed plants of the cultivar ZM9 showed the highest value of Tr in 2019, while the cultivar YM25 produced the highest value of Tr in 2020 growing season (Table 1). A significant decrease was observed in $C_i$, $g_s$, chlorophyll a (Chl *a*), Chl *b*, total chlorophyll, and Chlorophyll fluorescence (FC) in the salt-stressed plants compared to the control plants (Table 2). Interestingly, $C_i$, $g_s$, Chl *a*, Chl *b*, carotenoids, and CF [represented by maximal PSII photochemical efficiency (Fv/Fm)] were increased in the JA-primed control compared to the non-primed seedlings (Table 2). This could potentially mitigate the damaging effect of salinity stress in both wheat cultivars; yet, still lower than the control plants in both growing seasons.

## JA priming reduced $Na^+$ accumulation and improved $K^+$ uptake in wheat tissues

In comparison to the control plants (no salinity stress), there were considerable increases in $Na^+$ concentrations in different tissues of wheat (blade, sheath, stem, and roots) of the two wheat cultivars in both growing seasons in response to salt stress (Table 3). These cultivars showed the highest accumulation of $Na^+$ content in the sheath but the lowest in stems. In salt-stressed plants, $Na^+$ accumulation was higher in the blades, followed by sheath, roots, and finally, stem in both cultivars during the two experimental years. On average, the increments of $Na^+$ content in blade, sheath, root, and stem, were 184.0, 268.0, 227, and 201% in ZM9 and 172, 172, 96, and 133% in YM25, respectively, compared with their corresponding controls.

Interestingly, JA priming significantly ($P \leq 0.05$) restricted the uptake of $Na^+$, which resulted in reductions of $Na^+$ in the tissues of the tested wheat cultivars during the two growing seasons (Table 3). In contrast, $K^+$ content was highly retarded by salinity, mainly in blades (Table 3). Thus, the reduction of $K^+$ reached 49, 40, 39, and 45% in the blade, sheath, stem, and root tissues, respectively, in the ZM9 cultivar salt-stressed plants compared to control plants of the same genotype. In the YM25 cultivar, $K^+$ was reduced by 50, 30, 41, and 47% in the blade, sheath, root, and stem tissues, respectively, compared to the non-stressed control plants. JA retarded the reduction of $K^+$ in different organs partially for more affected organs (blade and sheath) and enhanced its content to be higher than the control plants, especially for root (Table 3).

## Effect of JA priming on water-relation, water, and osmotic potential of wheat under salinity stress

Plants exposed to salinity stress exhibited significant ($P \leq 0.05$) reductions in the water and osmotic potential of the studied wheat cultivars during the two growing seasons compared with that in non-salinized control plants (Figures 1A,B). On the other hand, JA priming significantly ($P \leq 0.05$) increased the water and osmotic potential under saline or non-saline conditions relative to their control. Salinization of soil drastically decreased the RWC of both wheat cultivars comparably throughout the two studied years (Figure 1C). Although WUE was enhanced by salinity, priming in JA profoundly alleviated the damaging impact of salinity on RWC to be statistically highly significant relative to control. These results suggest that JA plays a vital role in alleviating the damage effects of salinity in wheat cultivars through regulating water status and the osmoregulation process.

## Influence of JA priming on $H_2O_2$, proline, secondary metabolites, and antioxidants profile in wheat tissues under salinity stress

The $H_2O_2$ significantly ($P \leq 0.05$) increased in response to salinity in the shoots and roots of both cultivars (Figures 2A,B). JA treatment lowered the content of $H_2O_2$ in roots of salt-stressed plants effectively to be comparable to the control plants. In contrast, the effect of JA on the reduction of shoots' $H_2O_2$ was comparable to saline plants which were generally higher than the control (Figure 2A). The specific activities of antioxidant enzymes viz., SOD (Figures 2C,D), and APX (Figures 2E,F) of both wheat cultivars increased by salinity stress in the different tissues in both wheat cultivars. JA profoundly exacerbated the

TABLE 2 Effects of JA priming on $C_i$, $g_s$, Chl a and b, carotenoids, and CF (FV/Fm) of two wheat cultivars Mai9 (ZM9, salt-sensitive) and Yang Mai25 (YM25, salt-tolerant) under control and salinity stress conditions during two consecutive growing seasons 2019 and 2020.

| | Treatments | $C_i$ (μmol $CO_2$ $mol^{-1}$) | $g_s$ (mol $H_2O$ $m^{-2}$ $s^{-1}$) | Chl a (mg $g^{-1}$ DW) | Chl b (mg $g^{-1}$ DW) | Carotenoids (mg $g^{-1}$ DW) | CF (FV $Fm^{-1}$) |
|---|---|---|---|---|---|---|---|
| **2019** | Ck | 541.0 ± 18cd | 0.820 ± 0.03c | 0.176 ± 0.04cd | 0.151 ± 0.07b | 0.131 ± 0.04e-g | 0.793 ± 0.05c-e |
| ZM9 | | | | | | | |
| | 60 μM JA | 627.33 ± 16ab | 1.19 ± 0.04a | 0.250 ± 0.20a | 0.180 ± 0.02a | 0.200 ± 0.01b | 0.926 ± 0.02ab |
| | S1 | 243.67 ± 13f | 0.363 ± 0.05ef | 0.143 ± 0.15f | 0.120 ± 0.09d | 0.114 ± 0.05gh | 0.406 ± 0.05gh |
| | S1+60 μM JA | 397.67 ± 47e | 0.520 ± 0.11d | 0.160 ± 0.01d-f | 0.148 ± 0.07bc | 0.159 ± 0.06cd | 0.756 ± 0.03e |
| YM25 | Control | 576.00 ± 70b-d | 0.773 ± 0.08c | 0.183 ± 0.02cd | 0.146 ± 0.08bc | 0.144 ± 0.04de | 0.833 ± 0.02 b-e |
| | 60 μM JA | 618.33 ± 25ab | 1.20 ± 0.11a | 0.253 ± 0.03a | 0.172 ± 0.01a | 0.220 ± 0.01a | 0.953 ± 0.02 a |
| | S1 | 224.33 ± 50f | 0.390 ± 0.07d-f | 0.150 ± 0.01ef | 0.111 ± 0.01d | 0.123 ± 0.05f-h | 0.476 ± 0.07 fg |
| | S1+60 μM JA | 387.67 ± 11e | 0.510 ± 0.02d | 0.178 ± 0.07cd | 0.138 ± 0.02c | 0.165 ± 0.05c | 0.816 ± 0.15 b-e |
| **2020** | Ck | 520.67 ± 9d | 0.720 ± 0.06c | 0.170 ± 0.09c-e | 0.149 ± 0.07bc | 0.130 ± 0.01e-g | 0.776 ± 0.15 de |
| ZM9 | | | | | | | |
| | 60 μM JA | 608.33 ± 24a-c | 1.07 ± 0.08ab | 0.220 ± 0.01b | 0.176 ± 0.05a | 0.203 ± 0.02ab | 0.896 ± 0.01 a-c |
| | S1 | 218.33 ± 11f | 0.333 ± 0.05f | 0.144 ± 0.05f | 0.112 ± 0.02d | 0.110 ± 0.01h | 0.343 ± 0.07 h |
| | S1+60 μM JA | 405.00 ± 18e | 0.500 ± 0.10de | 0.173 ± 0.05cd | 0.154 ± 0.07b | 0.160 ± 0.01cd | 0.770 ± 0.02 e |
| YM25 | Ck | 541.33 ± 71cd | 0.713 ± 0.06c | 0.188 ± 0.02c | 0.143 ± 0.08bc | 0.141 ± 0.01d-f | 0.886 ± 0.07 a-d |
| | 60 μM JA | 661.67 ± 52a | 0.980 ± 0.10b | 0.240 ± 0.01ab | 0.167 ± 0.09a | 0.220 ± 0.02a | 0.970 ± 0.01 a |
| | S1 | 212.67 ± 17f | 0.346 ± 0.07f | 0.148 ± 0.08ef | 0.111 ± 0.01d | 0.123 ± 0.05f-h | 0.510 ± 0.06f |
| | S1+60 μM JA | 369.67 ± 54e | 0.456 ± d-f | 0.177 ± 0.06cd | 0.141 ± 0.07bc | 0.170 ± 0.01c | 0.836 ± 0.02b-e |
| Year (Y) | | *** | *** | * | ns | ns | * |
| Cultivars (C) | | *** | Ns | *** | *** | ns | *** |
| Treat. (T) | | *** | *** | *** | *** | *** | *** |
| Y×C | | *** | Ns | ns | ns | ns | *** |
| Y×T | | *** | *** | *** | * | ns | *** |
| C×T | | *** | Ns | ns | ns | ns | *** |
| Y×C×T | | *** | * | * | ns | ns | *** |

Means sharing the same letters, for a parameter during a year, do not differ significantly at $P \leq 0.05$ among the studied factors after Student—Newman—Keul test.
*$P < 0.05$; **$P < 0.001$; ***$P < 0.0001$.
$C_i$, intercellular $CO_2$; $g_s$, stomatal conductance; Chl, chlorophyll; CF, chlorophyll fluorescence; Ck, control; S, salt treatment; JA, jasmonic acid.





10.3389/fpls.2022.886862

TABLE 3 Effects of JA priming on $Na^+$ concentration and $K^+$ concentration in the leaf blade and sheath, stem, and root of two wheat cultivars Mai9 (ZM9, salt-sensitive) and Yang Mai25 (YM25, salt-tolerant) under control and salinity stress conditions during two consecutive growing seasons 2019 and 2020.

| | Treatments | $Na^+$ Concentration (mg $g^{-1}$ DW) | | | | $K^+$ Concentration (mg $g^{-1}$ DW) | | | |
|---|---|---|---|---|---|---|---|---|---|
| | | Blade | Sheath | Stem | Roots | Blade | Sheath | Stem | Roots |
| **2019** | | | | | | | | | |
| ZM9 | Ck | 3.79 ± 0.01f | 3.20 ± 0.05c | 3.75 ± 0.05e | 5.65 ± 0.14d-f | 23.12 ± 0.67b | 19.88 ± 0.57bc | 25.31 ± 0.93c | 18.89 ± 0.57e |
| | 60 μM JA | 2.31 ± 0.03g | 1.98 ± 0.10d | 1.51 ± 0.07g | 3.41 ± 0.08g | 27.12 ± 1.0a | 26.01 ± 0.47a | 34.38 ± 1.20ab | 23.01 ± 0.58a |
| | S1 | 10.24 ± 0.3ab | 8.58 ± 0.21a | 7.57 ± 0.09a | 12.84 ± 0.57a | 11.90 ± 0.58d | 12.00 ± 0.39d | 15.68 ± 0.57g | 10.49 ± 0.60h |
| | S1+60 μM JA | 4.79 ± 0.03d | 3.36 ± 0.06bc | 4.02 ± 0.07cd | 6.16 ± 0.12d | 19.21 ± 0.94c | 18.25 ± 0.05c | 23.32 ± 0.69c-f | 20.64 ± 0.55bc |
| YM25 | Ck | 3.65 ± 0.07f | 3.21 ± 0.10bc | 3.84 ± 0.10de | 5.48 ± 0.12ef | 22.78 ± 0.38b | 19.44 ± 0.59bc | 24.69 ± 0.57cd | 19.61 ± 0.33de |
| | 60 μM JA | 2.21 ± 0.11g | 1.95 ± 0.21d | 1.68 ± 0.07fg | 3.53 ± 0.08g | 26.68 ± 1.0a | 26.35 ± 0.96a | 35.05 ± 2.09ab | 23.01 ± 0.22a |
| | S1 | 9.96 ± 0.23bc | 8.73 ± 0.25a | 7.53 ± 0.37a | 12.82 ± 0.6a | 11.58 ± 0.56d | 13.68 ± 0.50d | 15.65 ± 1.57g | 11.66 ± 0.51h |
| | S1+60 μM JA | 4.45 ± 0.19e | 3.41 ± 0.07bc | 4.04 ± 0.09cd | 6.17 ± 0.04d | 18.96 ± 1.2c | 18.96 ± 1.15bc | 21.34 ± 1.06f | 19.96 ± 0.64cd |
| **2020** | | | | | | | | | |
| ZM9 | Ck | 3.70 ± 0.04f | 3.19 ± 0.01c | 3.85 ± 0.09c-e | 5.19 ± 0.25f | 21.76 ± 1.4b | 21.34 ± 0.20b | 24.32 ± 1.05c-e | 18.33 ± 0.51g |
| | 60 μM JA | 2.33 ± 0.04g | 2.04 ± 0.21d | 1.69 ± 0.09fg | 3.36 ± 0.20g | 26.72 ± 2.34a | 27.03 ± 0.39a | 36.02 ± 0.35a | 22.78 ± 0.67a |
| | S1 | 10.33 ± 0.16a | 8.56 ± 0.29a | 7.65 ± 0.23a | 12.08 ± 0.7b | 12.42 ± 0.89d | 13.03 ± 0.67d | 13.61 ± 0.53gh | 11.19 ± 0.28h |
| | S1+60 μM JA | 4.53 ± 0.24de | 3.38 ± 0.06bc | 4.10 ± 0.11c | 6.09 ± 0.11de | 18.53 ± 0.67c | 18.55 ± 1.27c | 22.65 ± 2.18d-f | 18.70 ± 0.46fg |
| YM25 | Ck | 3.51 ± 0.13f | 3.22 ± 0.12bc | 3.72 ± 0.12e | 5.12 ± 0.23f | 21.68 ± 1.35b | 20.39 ± 0.87bc | 23.58 ± 1.23c-f | 19.52 ± 0.54d-f |
| | 60 μM JA | 2.17 ± 0.05g | 2.08 ± 0.21d | 1.79 ± 0.09f | 3.29 ± 0.21g | 27.10 ± 0.49a | 25.41 ± 0.46a | 33.31 ± 0.91b | 23.22 ± 0.34a |
| | S1 | 9.85 ± 0.30b | 8.55 ± 0.18a | 7.23 ± 0.11b | 11.49 ± 0.3c | 12.64 ± 0.56d | 11.49 ± 0.76d | 13.16 ± 1.13h | 11.57 ± 0.20h |
| | S1+60 μM JA | 4.39 ± 0.21e | 3.52 ± 0.11b | 3.92 ± 0.08c-e | 5.73 ± 0.45d-f | 17.84 ± 0.85c | 19.60 ± 0.55bc | 22.05 ± 2.97ef | 21.12 ± 0.65b |
| Year (Y) | | ns | *** | Ns | *** | ns | *** | *** | *** |
| Cultivars (C) | | ns | *** | *** | *** | * | *** | *** | *** |
| Treat. (T) | | ns | *** | *** | *** | *** | *** | *** | *** |
| Y×C | | ns | ns | *** | *** | ns | *** | *** | *** |
| Y×T | | ns | *** | *** | *** | *** | *** | *** | *** |
| C×T | | ns | *** | *** | *** | ns | *** | *** | *** |
| Y×C×T | | ns | *** | *** | *** | ns | *** | *** | *** |

Means sharing the same letters, for a parameter during a year, do not differ significantly at $P \leq 0.05$ among the studied factors after Student—Newman—Keul test.
$^{*}P < 0.05$; $^{**}P < 0.001$; $^{***}P < 0.0001$.
$Na^+$, sodium; $K^+$, potassium; Ck, control; S, salt treatment; JA, jasmonic acid.



10.3389/fpls.2022.886862

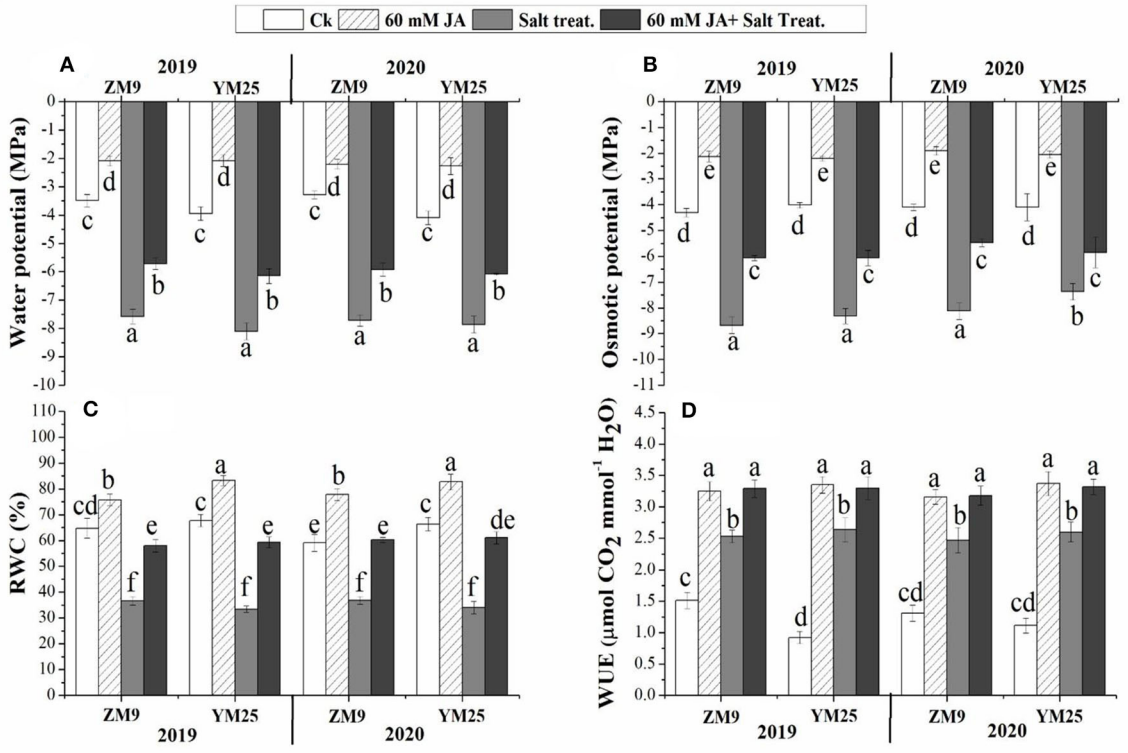


FIGURE 1
Effects of JA priming on water potential **(A)**, osmotic potential **(B)**, relative water content [RWC, **(C)**], water use effciency [WUE, **(D)**] of two wheat cultivars Mai9 (ZM9, salt-sensitive) and Yang Mai25 (YM25, salt-tolerant) under control and salinity stress conditions during two consecutive growing seasons 2019 and 2020. Means sharing the same letters, for a parameter during a year, do not differ significantly at $P \leq 0.05$ among the studied factors. Ck, control; S, salt treatment; JA, jasmonic acid.

activities of the enzymes in the root and shoot higher than their control.

In non-salinized and salinized plants, JA priming notably enhanced SOD and APX activities compared to the non-JA treated plants in root and shoot tissues of both cultivars (Figures 2E,F). The stimulation power of JA on SOD and APX activities was higher in the salinized plants than in non-salinized ones. PAL activity was also enhanced in response to salinity stress reaching ≥ 6-fold in shoots or roots of the two wheat cultivars throughout the two studied seasons. Further increment of PAL activity was denoted for saline and non-saline plants in plants receiving JA compared to their corresponding control (Figures 2G,H).

The contents of proline (an important cell osmolyte) and tocopherols (a non-enzymatic antioxidant) were progressively boosted by salinity stress in the shoots and roots of the two cultivars (Figures 3A–H). The study also included the effect of salinity stress and priming with JA on secondary metabolites of wheat plants. In this regard, flavonoids (Figures 3A,B) and total phenols (Figures 3C,D) accumulated in response to salinity stress in the shoots and roots of both wheat cultivars. JA application had a regulatory role on higher biosynthesis of both metabolites compared to their corresponding control; the highest content was denoted for the non-salinized plants primed with JA. Likely, the antioxidant molecule, tocopherol, was stimulated by soil salinization, and higher exacerbation of tocopherol biosynthesis was also denoted by JA application (Figures 3E,F). Further accumulation of proline could be attributed to the priming of wheat plants with JA. For example, the salinized plants primed with JA demonstrated the highest accumulation capacity of proline in tissues (Figures 3G,H).

## Influence of JA priming on hormonal profile in wheat tissues under salinity stress

The application of JA to wheat seeds caused significant positive changes in hormonal homeostasis (Figure 4). In this regard, the contents of CKs were dramatically ($P \leq 0.05$) reduced (by 31.9–66.7%) in salt-stressed plants, especially in the shoots, for both cultivars during both growing seasons (Figures 4A,B). However, JA increased the content of CKs in shoots and roots of non-stressed plants compared to the control plants. The JA not

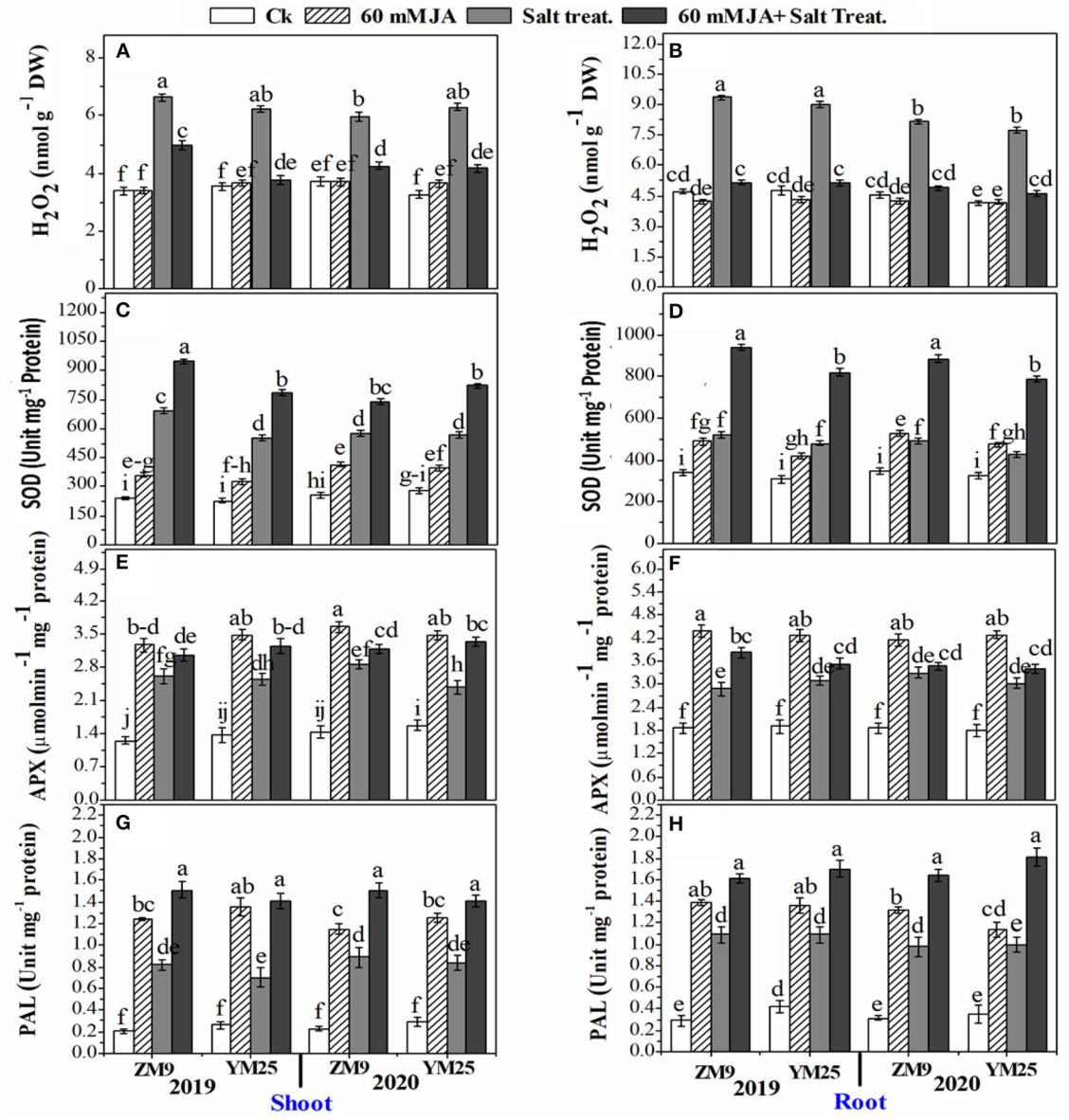


FIGURE 2
Effects of JA priming on the production of reactive oxygen species ($H_2O_2$) in the shoot **(A)** and root **(B)**; SOD in the shoot **(C)** and root **(D)**; APX in the shoot **(E)** and root **(F)**; PAL in the shoot **(G)** and root **(H)** of two wheat cultivars Mai9 (ZM9, salt-sensitive) and Yang Mai25 (YM25, salt-tolerant) under control and salinity stress conditions during two consecutive growing seasons 2019 and 2020. Means sharing the same letters, for a parameter during a year, do not differ significantly at $P \leq 0.05$ among the studied factors. SOD, superoxide dismutase; APX, ascorbate peroxidase; PAL, phenylalanine ammonia-lyase; Ck, control; S, salt treatment; JA, jasmonic acid.

only retrieved the contents of CKs in stressed plants higher than their corresponding stressed plants in those not treated with JA but also increased it to higher levels than in the non-stressed plants (Figures 4A,B). Moreover, IAA was highly attenuated in salt-stressed plants with approximately the same effect on both tissues as well as the two tested cultivars during the two seasons with a percent reduction of ~ 23% compared with non-salinized plants (Figures 4C,D).

JA curtailed the reduction of IAA contents in shoots and roots to be higher than in control plants as well as stimulated IAA contents of non-stressed plants, which is recommended for both cultivars, tissues, and studied growing seasons (Figures 4C,D). Except for the stressed shoots of YM25, endogenous JA contents in shoots and roots were not affected by salinity stress shoots and roots (Figures 4E,F). Furthermore, the exogenous application

10.3389/fpls.2022.886862

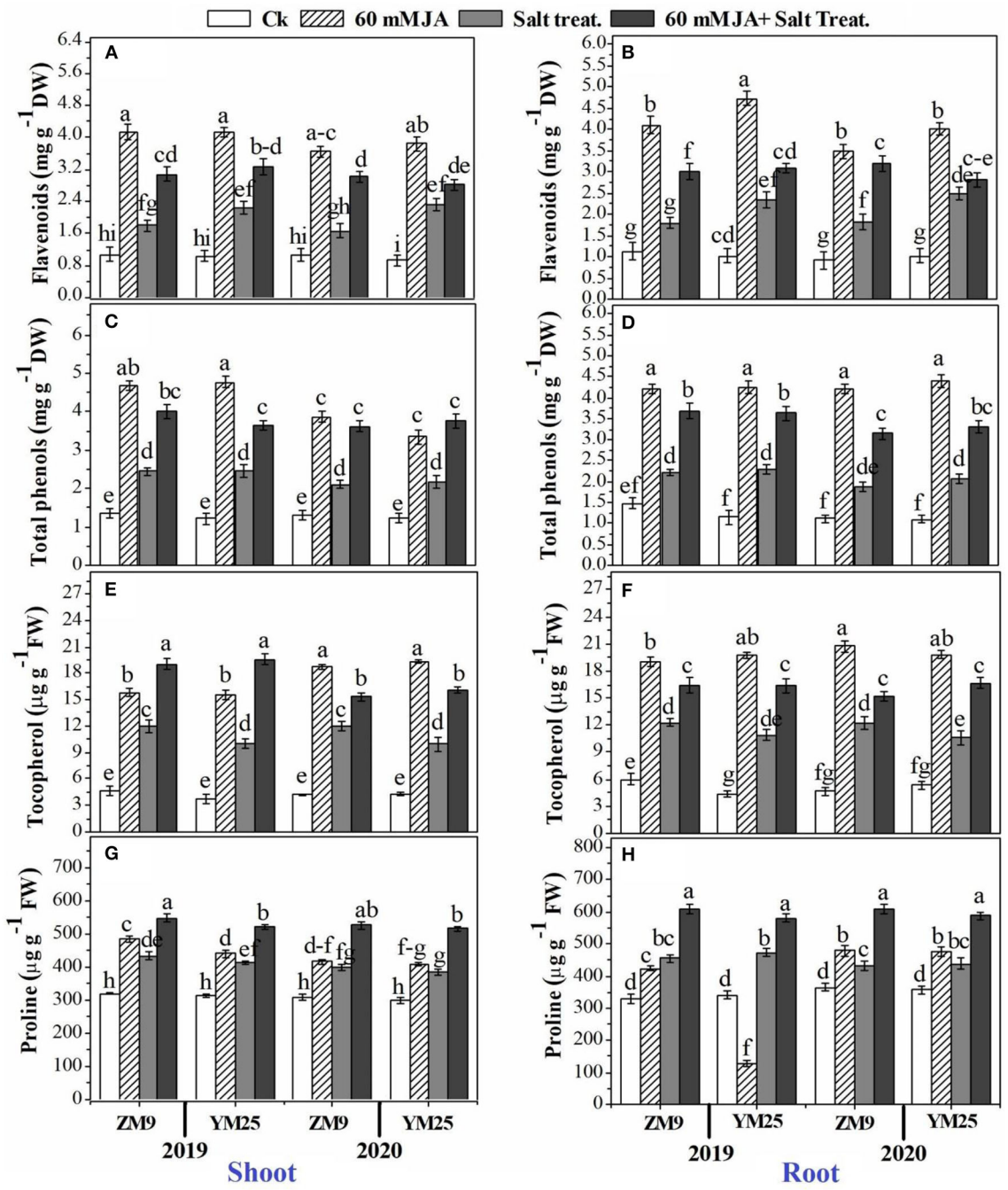


FIGURE 3
Effects of JA priming on flavonoids in the shoot **(A)** and root **(B)**; total phenols in the shoot **(C)** and root **(D)**; tocopherol in the shoot **(E)** and root **(F)**; proline in the shoot **(G)** and root **(H)** of two wheat cultivars Mai9 (ZM9, salt-sensitive) and Yang Mai25 (YM25, salt-tolerant) under control and salinity stress conditions during two consecutive growing seasons 2019 and 2020. Means sharing the same letters, for a parameter during a year, do not differ significantly at $P \leq 0.05$ among the studied factors. Ck, control; S, salt treatment; JA, jasmonic acid.

of JA significantly ($P \leq 0.05$) boosted the JA endogenous content in stressed and non-stressed plants to higher levels than the control treatment (non-primed seeds). It is worth mentioning that the highest endogenous JA contents were noted in JA-primed plants exposed to the high salt concentration.

ABA was differentially affected by salinity stress; the effect depended on the examined tissue and growing season

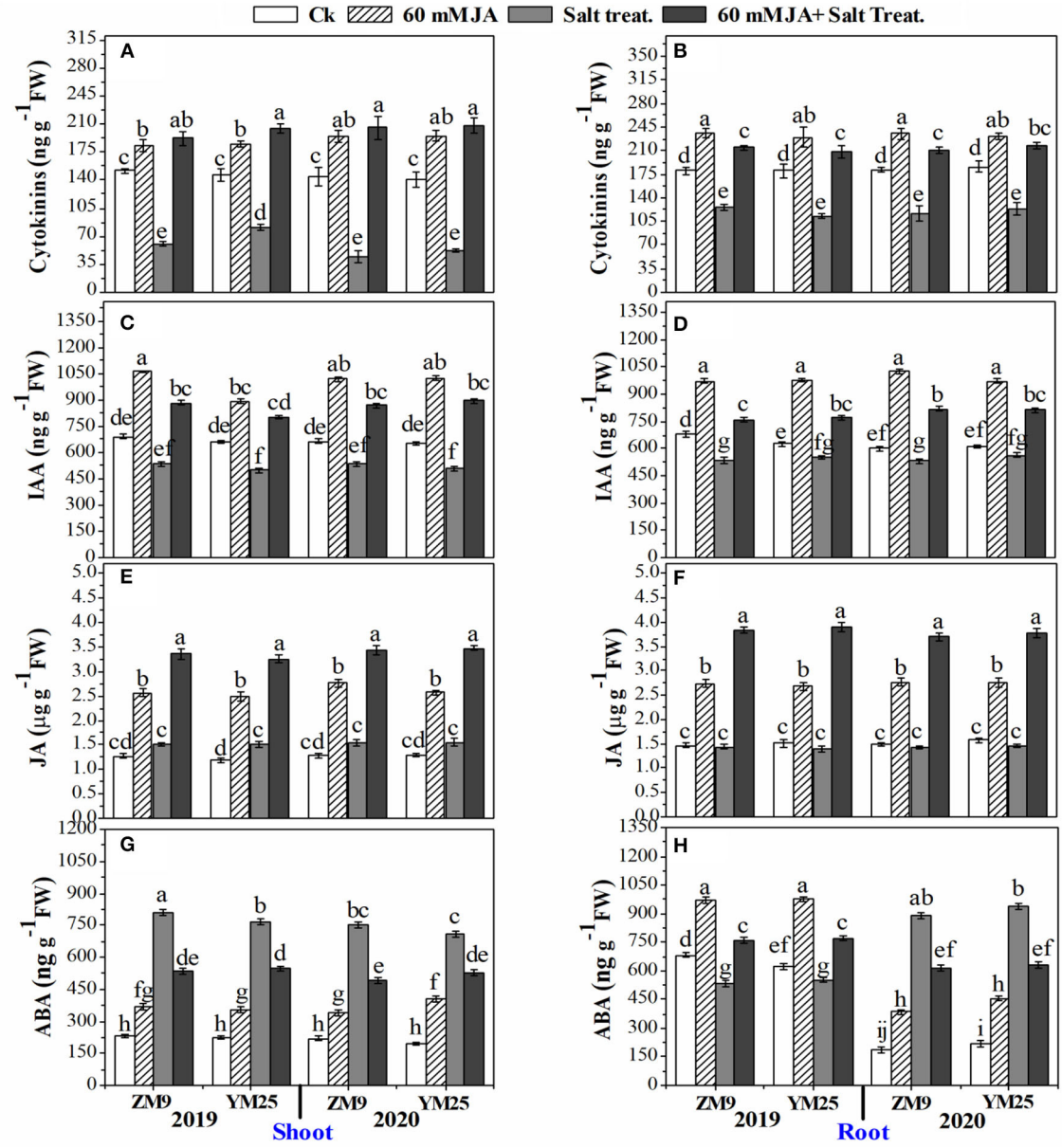


FIGURE 4
Effects of JA priming on cytokinins in the shoot **(A)** and root **(B)**; IAA in the shoot **(C)** and root **(D)**; JA in the shoot **(E)** and root **(F)**; ABA in the shoot **(G)** and root **(H)** of two wheat cultivars Mai9 (ZM9, salt-sensitive) and Yang Mai25 (YM25, salt-tolerant) under control and salinity stress conditions during two consecutive growing seasons 2019 and 2020. Means sharing the same letters, for a parameter during a year, do not differ significantly at $P \leq 0.05$ among the studied factors. IAA, indole acetic acid; JA, jasmonic acid; ABA, abscisic acid; Ck, control; S, salt treatment.

(Figures 4G,H). The shoots of the two cultivars attained significantly ($P \leq 0.05$) higher levels of ABA under salinity stress regardless of the tested season. However, in the roots, salinity stress reduced ABA contents in 2019 but increased it in 2020 for both cultivars. JA increased ABA contents of shoot tissues in non-stressed plants compared to the corresponding treatment. The levels of ABA in shoots of salinized plants treated with JA were lower than in stressed plants but still higher than in non-stressed plants. ABA contents were significantly ($P \leq 0.05$) enhanced in the roots of the non-stressed plant primed with JA in the two growing seasons (Figure 4H). On the other hand, JA treatment restrained the reduction of ABA levels in roots in 2019. During the growing season of 2020, the increased levels of ABA were highly ($P \leq 0.05$) attenuated by salinity stress in response to JA priming, yet the levels were higher than in control plants (Figures 4G,H).

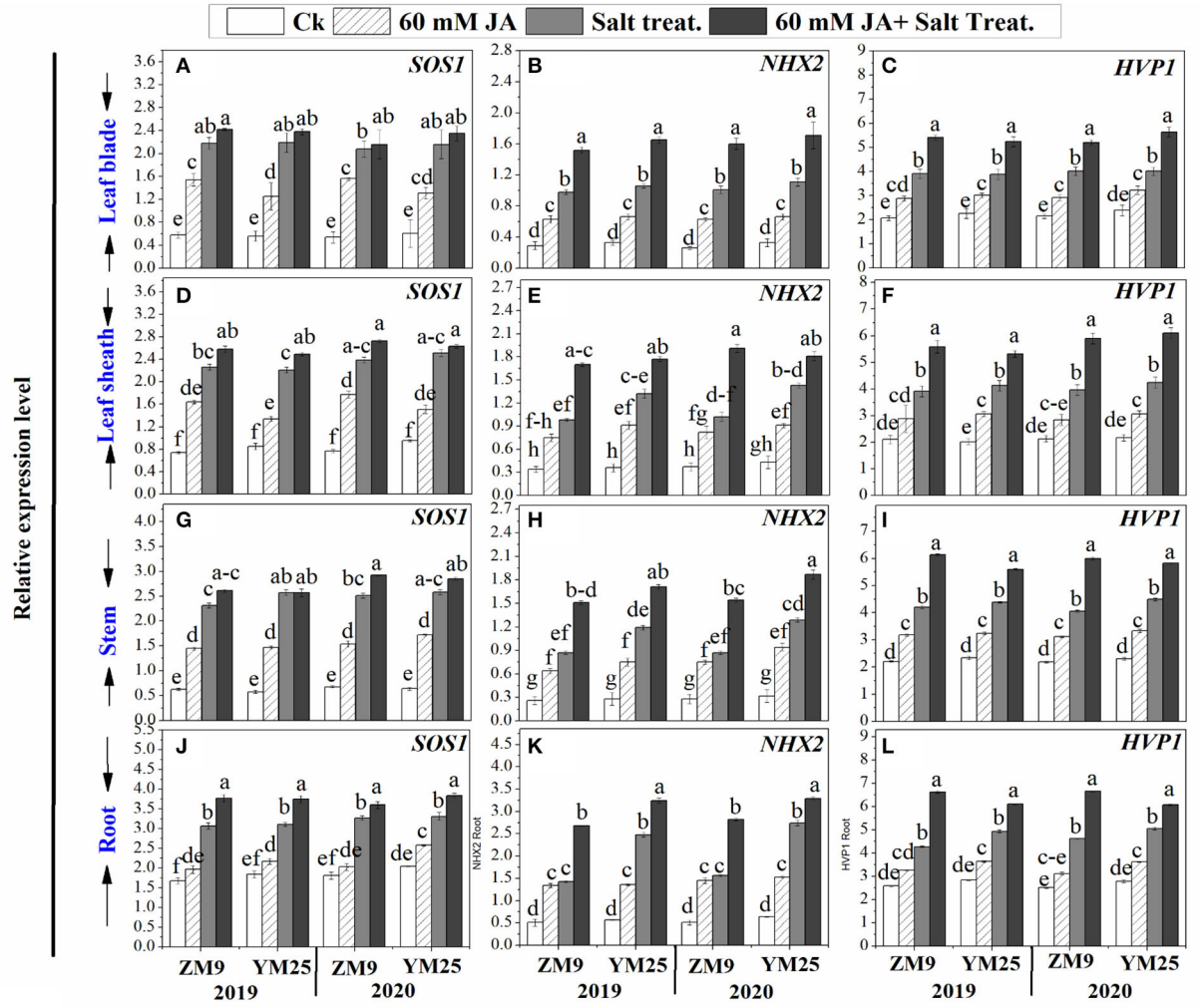


FIGURE 5
Effects of JA priming on the relative expression of *SOS1*, *NHX2*, and *HVP1* in leaf blade [**(A–C)** respectively], in leaf sheath [**(D–F)** respectively], in stem [**(G–I)** respectively], and in the root [**(J–L)** respectively] of two wheat cultivars Mai9 (ZM9, salt-sensitive) and Yang Mai25 (YM25, salt-tolerant) under control and salinity stress conditions during two consecutive growing seasons 2019 and 2020. Means sharing the same letters, for a parameter during a year, do not differ significantly at $P \leq 0.05$ among the studied factors. Ck, control; S, salt treatment; JA, jasmonic acid.

## Effects of JA priming on the relative expression of *SOS1*, *NHX2*, and *HVP1* in wheat tissues under salinity stress

Salinity stress differentially induced the expression levels of *SOS1* based on the organ tested (Figure 5). Upon exposure to high salt, the transcript levels of *SOS1* were significantly ($P \leq 0.05$) increased by 2-, 1.5-, 3.1-, and 4.2-fold in roots, stem, leaf sheaths, and blades, respectively compared to the same tissues of non-stressed plants (Figures 5A,D,G,J). Salinity stress induced the expression level of *NHX2* progressively by 5.8-, 3.3-, 3-, and 3-fold and *HVP1* by 1.6-, 1.92, 1.84-, and 1.92-fold for roots, stems, and leaf sheaths, and blades, respectively compared to non-stressed plants. Priming of JA exhibited stimulatory effects on the expression of *SOS1*, *NHX2*, and *HVP1* genes in wheat plants under saline and non-saline conditions (Figure 5).

## JA upregulated the ultrastructural changes of chloroplast under salinity stress

Salinity dramatically affected the ultra-structural configurations of the cell, where the disintegration of plastid compactness in salinized wheat cultivars was the resultant (Figure 6). Due to salinity stress, starch grains

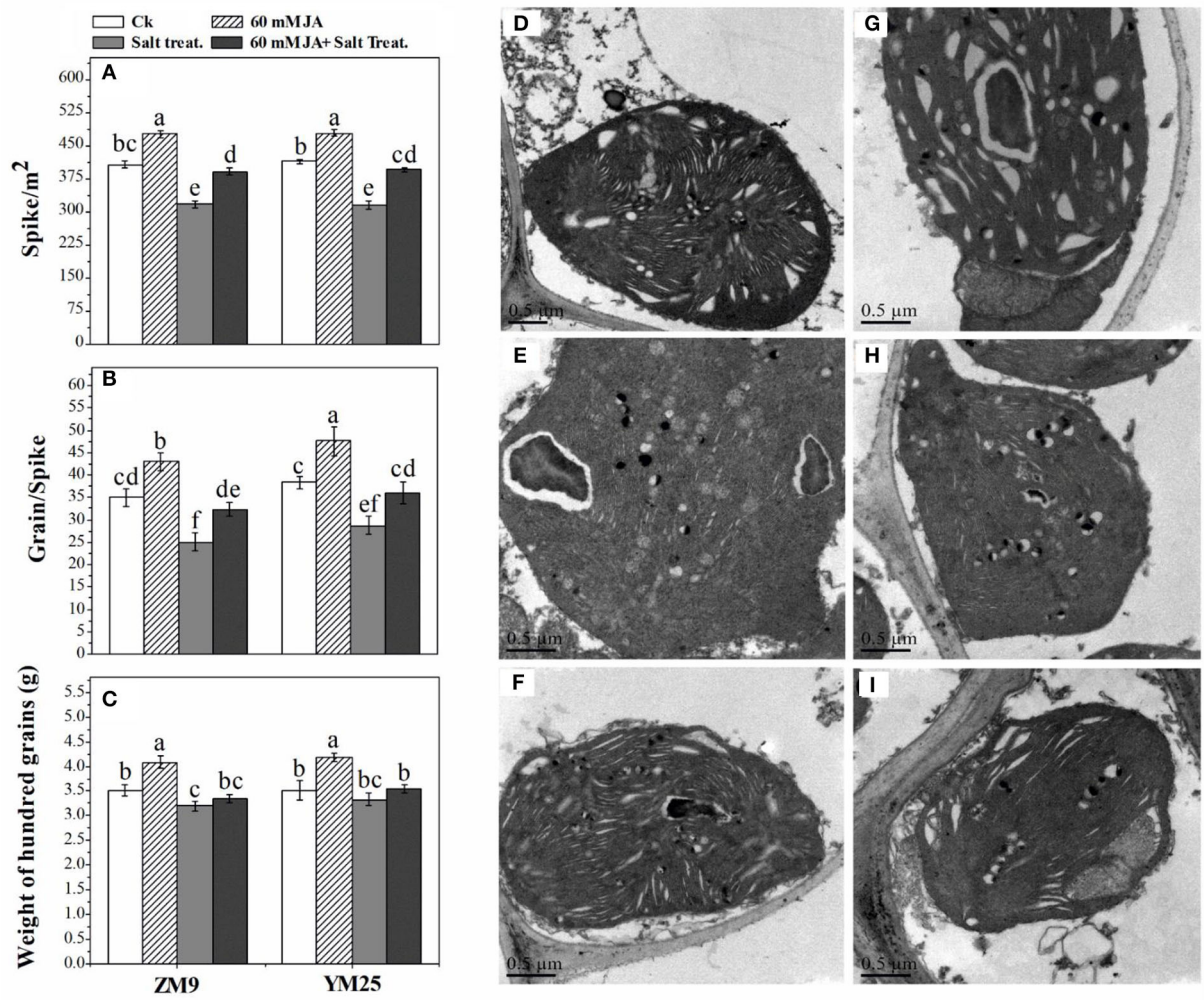


FIGURE 6
Effect of JA priming on Spike /m$^2$ **(A)**, grains/spike **(B)**, and weight of 100 grains [g **(C)**]; the ultrastructure of the leaf of two wheat cultivars Mai9 (ZM9, salt-sensitive) and Yang Mai25 (YM25, salt-tolerant) under salinity stress, CK [without priming under normal conditions in YM25 **(D)** and ZM9 **(G)**]; S1 [exposed to salinity without JA priming in YM25 **(E)** and ZM9 **(H)**]; JA priming+S1 [exposed to salinity with JA priming in YM25 **(F)** and ZM9 **(I)**].

and plastoglobuli particles were reduced alongside the loss of the integrity of grana. Interestingly, the cultivar ZM9 exhibited swollen chloroplasts with non-well-developed and sometimes, unrecognizable granum structures compared to its corresponding control or the other wheat cultivar. By combining JA priming and increased NaCl application on plants, the chloroplasts were oval shaped, more consistent with the regular configuration. In addition, several numbers of starch grains and higher plastoglobuli particles relative to deteriorated chloroplasts' of saline treatments were only found in the JA-treated plants (Figure 6).

## Influence of JA priming on yield of wheat cultivars under salinity stress

The number of spike/m$^2$ and grains/spikes were dramatically ($P \leq 0.05$) reduced by 25 and 21%, respectively, in response to salinity stress compared with their relative control (Figures 6A,B). The weight of 100 grains was slightly affected by salinity stress with an 8% reduction in the cultivar ZM9 (Figure 6C). On the other hand, the same stress in the YM25 cultivar did not affect the weight. Intriguingly, JA significantly ($P \leq 0.05$) increased the yield of non-stressed plants. Salinized-wheat plants treated with JA highly mitigated the detrimental

effects of salinity on wheat yield as compared with the unprimed stressed plants.

## Heat map and PCA analyses of traits related to different treatments

All mean values of the morphological and biochemical parameters were subjected to hierarchical clustering as a heat map of five 5 clusters: Group (A) included ABA and $H_2O_2$ (in shoot and root), and $Na^+$ content (in the root, stem, blade, and sheath); Group (B) included IAA and CKs (in shoot and root), and $K^+$ (root, shoot, blade, and sheath); Group (C) included JA, PAL and proline (in shoot and root), and SOD activity (in roots); Group (D) included the expression of genes *HVP1*, *NHX2*, and *SOS1* (in the stem, root, and leaf sheath and blade) and SOD activity (in the shoot); while Group (E) included APX activity, tocopherol, flavonoids and total phenol (in shoot and root) (Figure 7).

PCA analysis presented in Figure 8 indicated that the variables of group A strongly connected with stressed plants without JA priming, especially ABA. The group–B variables were relatively strongly delineated with JA-primed non-stressed plants (Figure 8) especially Ci, IAA, and cytokinin. On the other hand, the group –C, and –D variables were relatively strongly delineated with JA-primed salinity stressed plants especially proline and SOD (shoot and root).

# Discussion

Many studies found that the endogenous content of JA was boosted under environmental stress. For instance, an enhanced level of endogenous JA due to exposure to salinity stress was demonstrated in many species (Kutik et al., 2004; Zbierzak et al., 2010; Shanmugabalaji et al., 2013; Lohscheider and Bartulos, 2016; Mazur et al., 2020). Thus, higher levels of JA may function as a protection signal against salinity stress in plants (Wang et al., 2020). In the present study, the exogenous application of JA induced multilayered defense mechanisms under salinity stress throughout the two growing seasons. The application of JA significantly increased growth and yields in response to salinity stress, resulting in values close to the control plants without salinity. In general, we found significant differences among treatments (T) for all growth criteria. Except for the plant height, the effect of the year (Y) was not significant, suggesting stability in plant response to JA and/or salinity regardless of the cultivar (C) tested. Similar responses to enhancing growth parameters by JA under salinity stress were previously reported in several species (Yuan et al., 2018; Ali et al., 2019; Liu et al., 2019; Al-harthi et al., 2021; Sheteiwy et al., 2021a).

Notwithstanding, JA stimulated tolerance mechanisms in salt-stressed plants by minimizing $Na^+$ absorption and translocation to foliar organs to a level comparable to non-stressed plants. Thus, JA induced the exclusion mechanism for rendering $Na^+$ at a lower level under the salinity stress of both wheat cultivars. Reduction of ion toxicity by exogenous JA application could be the main regulatory role for several biochemical pathways in the two wheat cultivars. Shahzad et al. (2015) recorded $Na^+$ exclusion by JA in the root by decreasing $Na^+$ uptake, mediating salt tolerance in maize genotypes. $Na^+$ accumulation detected in different organs of salt-stressed plants is usually associated with a high reduction of $K^+$ content, reflecting the antagonistic effect of $Na^+$ to $K^+$, which is a common metabolic feature under salinity stress (Javed et al., 2021). Thus, the metabolic processes associated with $K^+$, such as $g_s$, WUE, and photosynthetic efficiency, are retarded in saline environments (Al-harthi et al., 2021). In the current study, there were significant differences in the acquisition of $Na^+$ or $K^+$ in plant organs, except for blades, among cultivars, treatments, or their interaction. The highly significant Y × C × T interaction indicates the varying responses of genotypes to JA and salinity in each season. The exogenous application of JA on salt-stressed plants mainly retained $Na^+$ and $K^+$ homeostasis, diminishing ion toxicity, and its consequences. In conformity, the foliar application of JA to the seedlings of strawberries and summer squash plants increased $K^+$ content under salt stress (Faghih et al., 2017; Al-harthi et al., 2021).

Plants instigate complex ion transporters to cope with salt stress. In this work, the relative expression levels of genes involved in $Na^+$ uptake, transport, and sequestration (*SOS1*, *NHX2*, and *HVP1*) were upregulated in the blade, sheath, shoot, and roots of the two wheat cultivars under salt treatment. Salt stress caused the transcript level of *SOS1* to increase to its highest in blades and the lowest in roots, and there was a reverse trend in the case of *NHX2*. Such response was accompanied by the highest increase in the percentage of $Na^+$ ions in the blade and the lowest increment of $Na^+$ in roots, suggesting that sequestration of $Na^+$ into vacuoles may be an important component trait for the salt tolerance mechanism in wheat. This response could be interpreted by the enhanced levels of ABA, which reduce $Na^+$ exclusion in roots and activate its translocation and accumulation in leaves as was reported by Cabot et al. (2009). Similarly, Yu et al. (2007) stated that ABA stimulates the expression of salt-tolerant genes, *HVP1* and *HVP10*, for $Na^+/H^+$ antiporter and vacuolar $H^+$-pyrophosphatases.

The key role of the *NHX2* gene seems to be $Na^+$ sequestration to the vacuole. This suggests that $Na^+$ accumulation in the vacuoles in the different organs of salinized plants cannot protect the cytosol against excess $Na^+$ as has been reviewed by Darko et al. (2017). The higher level of *HVP1* reported in the salinized plants; herein, could be linked to higher WUE observed in salt-stressed plants (Haq et al., 2019). It has been demonstrated that *HVP1* acts as an influential pump that activates the sequestration of toxic salts to the vacuoles.

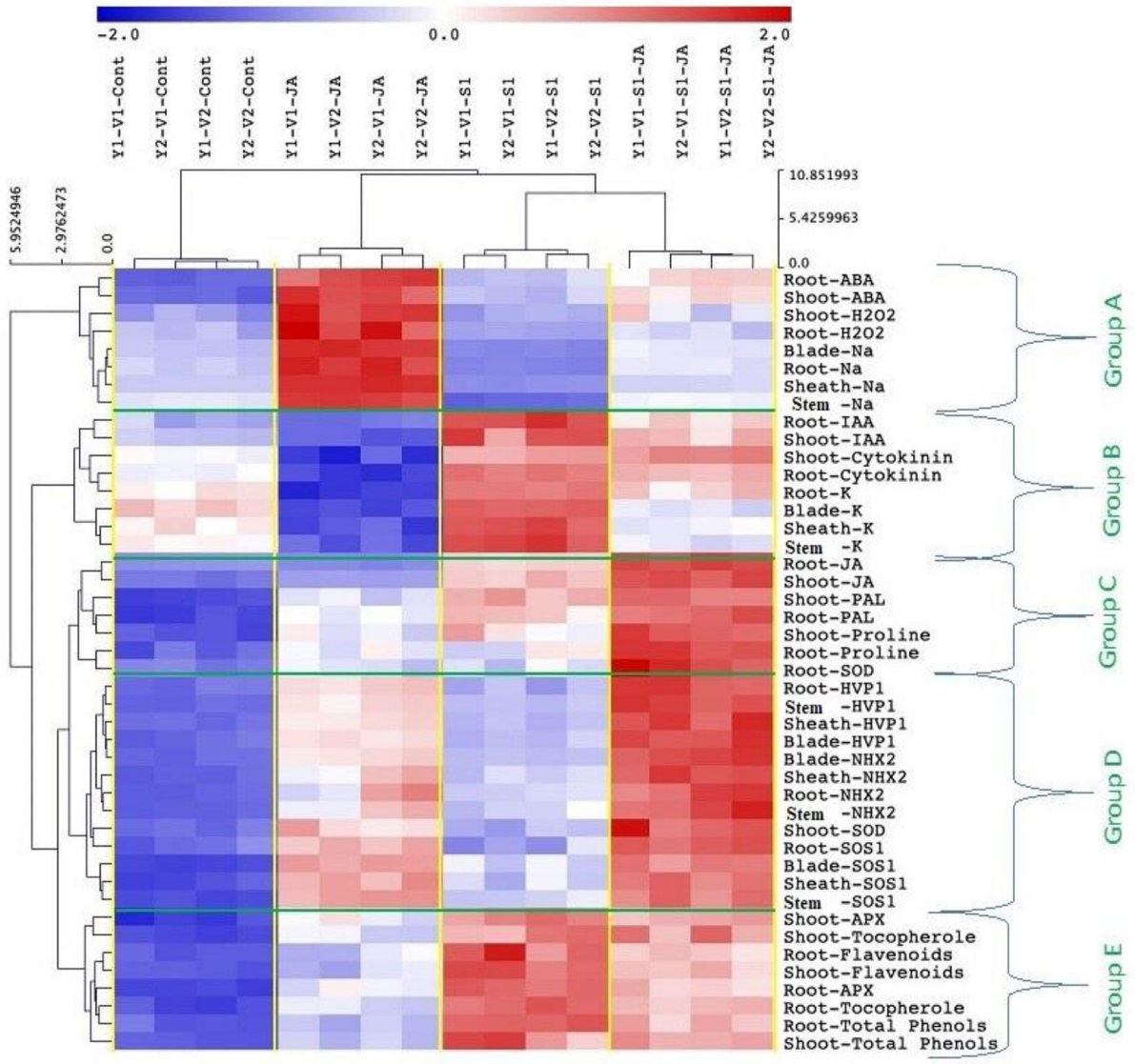


FIGURE 7
Cluster analysis showing data correlation clustered the metabolic activities to five clusters; Group A) included ABA (shoot and root), $H_2O_2$ (shoot and root), $Na^+$ content (root, shoot, blade, and sheath), Group B) included IAA (shoot and root), cytokinins (shoot and root), and K+ (root, stem, blade, and sheath), Group C) included JA (shoot and root), PAL (shoot and root), proline (shoot and root), and SOD activity of roots, Group D) included the expression of genes *HVP1*, *NHX2*, and *SOS1* of stem, root, leaf sheath, and leaf blade, as well as the SOD activity in the shoot, and Group E) included APX activity (shoot and root), tocopherol (shoot and root), flavonoids (shoot and root), and total phenol (shoot and root). ABA, abscisic acid; IAA, indole acetic acid; JA, jasmonic acid; PAL, phenylalanine ammonia-lyase; SOD, superoxide dismutase; APX, ascorbate peroxidase.

Interestingly, a plant supplemented with JA exhibited a further increase in *SOS1*, *HVP1*, and *NHX2* expression levels. These observations indicate that $Na^+$ exclusion components are highly activated in salt-stressed plants by JA application. It has been reported that JA can increase salinity tolerance through activating $Na^+$ efflux and $K^+$ influx in tissues where exclusion of $Na^+$ was sufficiently documented (Khan et al., 2020). In harmony, the heatmap and PCA analyses highly recommended the role of JA in a synergistic increase in the expression of *SOS1*, *NHX2*, and *HVP1* in plant organs in response to salinity. Higher salinity levels increase $Na^+$ content in plant tissues, which activates K-uptake via enhanced $Na^+$ exclusion. In this regard, Malakar and Chattopadhyay (2021) have reported that when the concentration of salt increases, NHX mediates $Na^+$ influx into the cytoplasm, affecting membrane depolarization and triggering $K^+$ efflux from the cytoplasm.

On the other hand, JA priming can restrain $Na^+$ accumulation, which activates vacuolar $K^+$ influx without

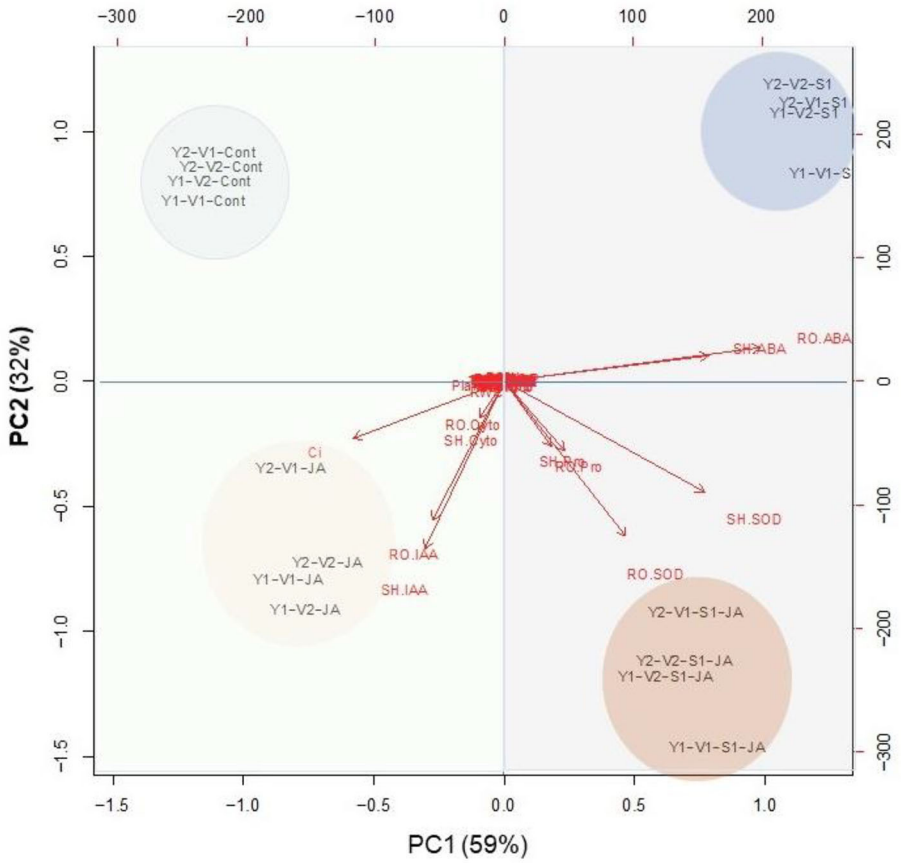


FIGURE 8
A principal component analysis (PCA) determines the degree of association within the treatments and variables of two wheat cultivars Mai9 (ZM9, salt-sensitive) and Yang Mai25 (YM25, salt-tolerant) primed with jasmonic acid (JA) and grown under salinity stress.

moving $Na^+$. In this context, we suggest the priming role of JA to be through upregulating the NHXs that mediate $Na^+$ localization in vacuoles, which in turn modulate $Na^+$ toxicity *via* using it as a cheap vacuolar osmoticum aid in osmotic adjustment during salt stress (Shabala, 2013). Malakar and Chattopadhyay (2021) have reported that *NHX1* and *NHX2* genes instigate salinity tolerance through enhancing $K^+$ level, $K^+$ to $Na^+$ ratio, and reducing oxidative damage. In addition, Andrés et al. (2014) have referred to ion exchangers, *NHX1* and *NHX2* mediate $K^+$ uptake into vacuoles to regulate cell turgor and stomatal function for higher transpiration rates.

Our results showed salinity-induced damage to the chloroplast, grana lamellar organization, and chloroplast swelling. Such damage was more pronounced in the wheat salt-sensitive cultivar, ZM9. Several studies have reported similar modifications in the lamellar organization (Papadakis et al., 2007), swelling of chloroplast lamellae, and undefined grana structure (Štefanic et al., 2013; Hameed et al., 2021). Furthermore, wheat cultivar YM25 exhibited increases in the numbers of plastoglobuli under salinity stress. Similar to our results, salt stress induction enhanced the numbers of plastoglobuli and the disordering of the chloroplast envelope of cucumber leaves (Shu et al., 2012). The enlargement of plastoglobules reported in our study was associated with a disintegration of the thylakoid structure. Bejaoui et al. (2016) attributed the increase in the number and size of plastoglobuli in salt-treated plants of *Sulla carnosa* to a disturbance of the thylakoid membrane. Thus, salinity stress can prevent the formation of thylakoid lamellae from plastoglobules which reflects great damage to chloroplast and their membranes, resulting in low efficiency of the photosynthetic moiety, and thereby, retarding the growth of wheat plants. However, our results indicated that wheat cultivars primed with JA showed a reduction in the swelling of the chloroplast stroma and recovery of the thylakoids grana compared to only saline-treated plants.

Ali et al. (2018) reported a similar recovery of chloroplast ultrastructure in rapeseed by JA application under cadmium stress. It is worth mentioning that the production of JA is linked to plastoglobules which are recruited with JA precursors and four enzymes involved in its production in chloroplasts (Lundquist et al., 2012, 2013; Van Wijk and Kessler, 2017). Under salinity stress, endogenous JA increments, however, are

stimulated parallel to the enrichment of the salinized plants' chloroplast with high plastoglobules number, while further stimulation of endogenous JA under the interactive effect of JA and salinity ascribed more efficient chloroplast ultrastructure with a higher number of plastoglobules. It is worth noting that the enhancement of endogenous JA in salinized plants combined with JA application is the main regulatory defense strategy of JA against salinity stress. Likely, the data of the current study exhibited a reduction in shoots' and roots' CKs, but much more so for shoots, accounting for early senescence, reduced pigment content, and may be affected in plastids ultrastructure.

Thus, the observed changes in the endogenous CK contents clearly indicated the involvement of these hormones in plant stress responses. JA adjusted the CKs biosynthesis in different organs under salinity stress to be higher than control plants parallel to better leaves status and higher photosynthetic machinery. Also, high levels of IAA parallel to improvement of growth in response to JA application of stressed and non-stressed plants could be associated with the regulatory role of JA on hormonal homeostasis and induction of plant growth. So, JA interacts with different kinds of hormones to regulate the growth and development of plants such as auxin, cytokinin, and ABA. These interactions may help to optimize the growth and development of plants under abiotic stress conditions. Salinity inhibited photosynthesis by reducing photosynthetic pigments content, the maximal PSII photochemical efficiency (Fv/Fm), $P_n$, $g_s$, and $C_i$. On the other hand, there was an increase in the photosynthetic efficiency with JA priming correlated with the regulation of $g_s$, photosynthetic rate, $CO_2$ transport rates, and Chl biosynthesis. The photosynthetic-related traits, particularly Fv/Fm, $P_n$, and $C_i$ were also affected by Y, T, C, or their corresponding interactions. In general, increasing $g_s$ and $C_i$ by JA indicates a pivotal feature in fulfilling the requirements of photosynthesis by increasing the photosynthetic rate that ensures a high level of photoassimilates for the growing tissues, enhancing salinity tolerance. Besides, the increased Fv/Fm ratio by JA priming also measures the maximum efficiency of photosystem II (PSII, the quantum efficiency), reflecting enough energy for higher photosynthetic efficiency of wheat cultivars under salinity stress (Maxwell and Johnson, 2000).

Similarly, Ghassemi-Golezani and Hosseinzadeh-Mahootchi (2015) reported enhancements in Chl a and b, and PSII (Fv/Fm) of safflower under the interactive effect of JA combined with saline stress. We argue that the enhancement of Chl *a*, Chl *b*, and carotenoids by JA under salinity stress can also be denoted. Thus, this effect was recommended according to the significant variation among treatments recorded without any effect of Y × C or C × T on the studied parameters.

It has also been proposed that plastoglobules actively cope with abiotic stress via the regulation of plastid development and metabolic processes (Rottet et al., 2015). Our data demonstrated that JA further increased α-tocopherol content in response to salinity stress. This confirms that the pre-treatment of JA plays an important role in preventing chloroplast degradation by enhancing the production of protective antioxidant compounds (e.g., α-tocopherols) which tend to conserve membrane against ROS (Bashandy et al., 2020; Younes et al., 2020) and hinder photoinactivation of PSII (Havaux et al., 2005). In this regard, plastoglobules are a sink of lipophilic antioxidants such as α-tocopherol where main enzymes have been present in their membranes (Wójtowicz et al., 2021). The data of current work found that α-tocopherol content elevated parallel to a higher number of plastoglobules as was reported by Wójtowicz et al. (2021). Thus, JA instigates cellular signaling under salinity stress through mediating α-tocopherol content.

The accumulation of $Na^+$ in cells affects the water status and osmotic potential of stressed plants, causing osmotic stress. In this study, the negative impact of salinity on water status was coined from a high reduction of RWC, but not WUE. Salinity stress reduces $g_s$ and $T_r$ which ultimately decreases WC (Pooja et al., 2019). The salinized wheat cultivars exhibited a reduction in osmotic potential, revealing plants cannot take up enough water as the cells have low turgor, as reported by Soni et al. (2021). Interestingly, the enhancement of WUE under salinity stress in both cultivars could be associated with the reduction of $g_s$, $C_i$, and $T_r$, as illustrated by Sandhu et al. (2019). However, JA priming improved RWC, osmotic potential, and WUE in wheat plants treated with salinity, a trend observed in several other studies (e.g., Yosefi et al., 2018; Taheri et al., 2020; Sheteiwy et al., 2021a; Soni et al., 2021).

Nevertheless, JA treatment was not efficient enough to return the osmotic and water potential of the salinized plants to the level of the control plants. The maintenance of turgor under the interactive effect of salinity and JA could be linked with proline accumulation which acts as osmotica co-opted in salinity stress tolerance (El-Sayed et al., 2014; Salimi et al., 2016; Taheri et al., 2020). Thus, we can conclude that JA induces osmotic adjustment, which reduces the osmotic potential by increasing proline content that increases external osmolality, maintaining water absorption, and various physiological processes associated with water availability, which reduce osmotic stress.

ROS are generally accumulated in plant cells under stress and are commonly documented for salinity. In that sense, salinity stimulates electron flows to molecular oxygen (Dawood et al., 2021b; Sofy et al., 2021), causing the enhancement of different forms of ROS. For example, $H_2O_2$ content is enhanced under salinity stress as a secondary stress factor that negatively affects wheat cultivars, causing an oxidative burst. On the other hand, exogenous JA coupled with NaCl treatment significantly reduced the level of $H_2O_2$ in wheat seedlings. This positive effect can be attributed to the potential ability of JA to enhance antioxidant metabolites (e.g., tocopherols and phenolics) and enzyme activities (SOD and APX). Similarly, previous studies have shown that the application of JA effectively suppressed the toxic effects of oxidative burst by enhancing the ROS-scavenging potential of the antioxidant defense system in stressed plants (Sirhindi et al., 2015; Ahmad et al., 2018; Najafi kakavand et al., 2019; Bali et al., 2020; Lang et al.,

2020; Kamran et al., 2021). In addition, the activity of PAL was upregulated in response to salinity stress alone or in combination with JA, resulting in increased phenolic and flavonoid contents, ultimately leading to enhanced tolerance to salinity stress.

The heat map analysis clustered the metabolic activities of wheat plants under the combined effects of salinity and JA into five clusters (Figure 7), indicating that JA modulates the salinity effect in wheat plants through different pathways. For example, JA-treated plants retained $Na^+$ and $K^+$ homeostasis that reduces ion toxicity, which damages cell membranes, and other cellular compartments. On the other hand, $K^+$ is required for several physiological and biochemical processes. Besides, JA helps $Na^+$ uptake, transport, and compartmentalize in vacuoles to minimize its adverse effects on the biochemical processes in the cytosol. This was facilitated by the accumulation of ABA and the upregulations of genes such as *SOS1* and *NHX2* that help sequester $Na^+$ from roots to the leaf vacuoles. Furthermore, JA priming helps the recovery of chloroplast ultrastructure, increasing the photosynthesis efficiency in salt-treated plants more than in non-primed plants. Moreover, JA priming might increase the efficiency of the photosynthesis process through the regulation of $g_s$, $CO_2$ transport rates, and Chl biosynthesis. This was evident in the enhanced Fv/Fm ratio and the increased growth and yields of wheat plants treated with both JA and salts. Still, JA stimulates antioxidant defense machinery (e.g., tocopherols, phenolics, SOD, and APX) that scavengers the ROS accumulation, improving wheat growth in the saline stress environment.

## Conclusions

The current study demonstrated that JA priming significantly improved all plant growth parameters and yield traits of two wheat cultivars under control and saline conditions. Moroever, co-stressors (tissue dehydration, osmotic stress, and oxidative stress) encountered by plants under salinity stress were also alleviated by JA treatment. This mitigation effect can be explained by JA's ability to enhance the structural stability and functional activity of PSII, which was reflected by the performance indices ($g_s$, $C_i$, and $T_r$). JA also increased $Na^+$ exclusion and transportation in various organs by upregulating several key genes potentially involved in $Na^+$ uptake, transport and sequestration *i.e. SOS1*, *NHX2*, and *HVP1*. The restriction of $Na^+$ accumulation in organs under salt stress was correlated with salt stress tolerance in wheat. Therefore, upon subsequent exposure to salinity stress, seed priming with JA can effectively mitigate stress-responsive criteria and enhance plant tolerance to salinity stress in an eco-friendly way. In this regard, the adoption of better agricultural practices such as on-farm hormone seeds priming by agricultural sectors could significantly have a potential for environmental stress mitigation. Development of these sustainable practices will also ensure that high crop yield and quality are available to meet total demand from agriculture.

## Data availability statement

The raw data supporting the conclusions of this article will be made available by the authors, without undue reservation.

## Author contributions

MS, AE-K, KE-T, and SA: conceptualization, methodology, writing—reviewing and editing, and supervision. MS, WQ, HL, and MD: data curation, writing—original draft preparation, software, and investigation. ZU, HA, TM, SSus, VR, AE-K, IJ, SSul, ME-E, KE-T, and SA: data curation, writing—original draft preparation, methodology, visualization, and investigation. HA and HY: software and validation. All authors contributed to the article and approved the submitted version.

## Funding

This research was supported by the Strategic Academic Leadership Program of the Southern Federal University (Priority 2030). This work was also funded by Abu Dhabi Research Award (AARE2019) for Research Excellence-Department of Education and Knowledge (ADEK-007; Grant #: 21S105) to KE-T and Khalifa Center for Biotechnology and Genetic Engineering-UAEU (Grant #: 12R028) to SA. This work was also supported by the Nature Science Foundation for Excellent Young Scholars of Jiangsu Province (BK20200057) to HL.

## Conflict of interest

The authors declare that the research was conducted in the absence of any commercial or financial relationships that could be construed as a potential conflict of interest.

## Publisher's note



## Supplementary material

The Supplementary Material for this article can be found online at: https://www.frontiersin.org/articles/10.3389/fpls.2022.886862/full#supplementary-material

# References


Ahanger, M. A., Tomar, N. S., Tittal, M., Argal, S., and Agarwal, R. M. (2017). Plant growth under water/salt stress: ROS production; antioxidants and significance of added potassium under such conditions. *Physiol. Mol. Biol. Plants* 23, 731–744. doi: 10.1007/s12298-017-0462-7

Ahmad, P., Abd Allah, E. F., Alyemeni, M. N., Wijaya, L., Alam, P., Bhardwaj, R., et al. (2018). Exogenous application of calcium to 24-epibrassinosteroid pre-treated tomato seedlings mitigates NaCl toxicity by modifying ascorbate–glutathione cycle nd secondary metabolites. *Sci. Rep.* 8, 13515. doi: 10.1038/s41598-018-31917-1

Ahmad, P., Abdel Latef, A. A., Hashem, A., Abd Allah, E. F., Gucel, S., and Tran, L. S. P. (2016). Nitric oxide mitigates salt stress by regulating levels of osmolytes and antioxidant enzymes in chickpea. *Front. Plant Sci.* 7, 347. doi: 10.3389/fpls.2016.00347

Ahmed, I. M., Dai, H., Zheng, W., Cao, F., Zhang, G., and Sun, D. (2013). Genotypic differences in physiological characteristics in the tolerance to drought and salinity combined stress between Tibetan wild and cultivated barley. *Plant Physiol. Biochem.* 63, 49–60. doi: 10.1016/j.plaphy.2012.11.004

Al-harthi, M. M., Bafeel, S. O., and El-Zohri, M. (2021). Gibberellic acid and jasmonic acid improve salt tolerance in summer squash by modulating some physiological parameters symptomatic for oxidative stress and mineral nutrition. *Plants* 10, 2768. doi: 10.3390/plants10122768

Ali, A. Y. A., Ibrahim, M. E. H., Zhou, G., Nimir, N. E. A., Jiao, X., Zhu, G., et al. (2019). Ameliorative effects of jasmonic acid and humic acid on antioxidant enzymes and salt tolerance of forage sorghum under salinity conditions. *Agron. J.* 111, 3099–3108. doi: 10.2134/agronj2019.05.0347

Ali, B., Gill, R. A., Yang, S., Gill, M. B., Farooq, M. A., Liu, D., et al. (2015). Regulation of cadmium-induced proteomic and metabolic changes by 5-aminolevulinic acid in leaves of *Brassica napus* L. *PLoS One.* 10, e0123328. doi: 10.1371/journal.pone.0123328

Ali, E., Hussain, N., Shamsi, I. H., Jabeen, Z., Siddiqui, M. H., and Jiang, L. X. (2018). Role of jasmonic acid in improving tolerance of rapeseed (*Brassica napus* L.) to Cd toxicity. *J. Zhejiang Univ. Sci. B.* 19, 130–146. doi: 10.1631/jzus.B1700191

Andrés, Z., Pérez-Hormaechea, J., Leidia, E. O., Schlückingb, K., Steinhorstb, L., McLachlanc, D. H., et al. (2014). Control of vacuolar dynamics and regulation of stomatal aperture by tonoplast potassium uptake. *Proc. Natl. Acad. Sci. USA* 111, E1806–E1814. doi: 10.1073/pnas.1320421111

Backer, H., Frank, O., de Angells, B., and Feingold, S. (1980). Plasma tocopherol in man at various times after ingesting free or ocetylaned tocopherol. *Nutr. Rep. Int.* 21, 531–536.

Balestrazzi, A., Confalonieri, M., Macovei, A., and Carbonera, D. (2011). Seed imbibition in *Medicago truncatula* Gaertn. Expression profiles of DNA repair genes in relation to PEG-mediated stress. *J. Plant Physiol.* 168,706–713. doi: 10.1016/j.jplph.2010.10.008

Bali, S., Kaur, P., Jamwal, V. L., Gandhi, S. G., Sharma, A., Ohri, P., et al. (2020). Seed priming with jasmonic acid counteracts root knot nematode infection in tomato by modulating the activity and expression of antioxidative enzymes. *Biomolecules.* 10, 98. doi: 10.3390/biom10010098

Barr, H. D., and Weatherley, P. E. (1962). A re-examination of the relative turgidity technique for estimating water deficit in leaves. *Aust. J. Biol. Sci.* 15, 413–428. doi: 10.1071/BI9620413

Bashandy, S. R., Abd-Alla, M. H., and Dawood, M. F. (2020). Alleviation of the toxicity of oily wastewater to canola plants by the N2-fixing, aromatic hydrocarbon biodegrading bacterium *Stenotrophomonas maltophilia*-SR1. *Appl. Soil Ecol.* 154, 103654. doi: 10.1016/j.apsoil.2020.103654

Basit, F., Ulhassan, Z., Mou, Q., Nazir, M. M., Hu, J., Hu, W., et al. (2022). Seed priming with nitric oxide and/or spermine mitigate the chromium toxicity in rice (*Oryza sativa*) seedlings by improving the carbon-assimilation and minimizing the oxidative damages. *Func. Plant Biol.* doi: 10.1071/FP21268

Bejaoui, F., Salas, J., Nouairi, I., Smaoui, A., Abdelly C., Martínez-Force, E., et al. (2016). Changes in chloroplast lipid contents and chloroplast ultrastructure in *Sulla carnosa and Sulla coronaria* leaves under salt stress. *J. Plant Physiol.* 198, 32–38 doi: 10.1016/j.jplph.2016.03.018

Cabot, C., Sibole, J. V., Barcelo, J., and Poschenrieder, C. (2009). Abscisic acid decreases leaf $Na^+$ exclusion in salt-treated *Phaseolus vulgaris* L. *J. Plant Growth Regul.* 28, 187–192. doi: 10.1007/s00344-009-9088-5

Darko, E., Gierczik, K., Hudak, O., Forgo, P., Pal, M., Turkosi, E., et al. (2017). Differing metabolic responses to salt stress in wheat-barley addition lines containing different 7H chromosomal fragments. *PLoS One.* 12, e0174170. doi: 10.1371/journal.pone.0174170

Dawood, M. F., Sohag, A. A. M., Tahjib-Ul-Arif, M., and Latef, A. A. H. A. (2021b). Hydrogen sulfide priming can enhance the tolerance of artichoke seedlings to individual and combined saline-alkaline and aniline stresses. *Plant Physiol. Biochem.*, 159: 347–362. doi: 10.1016/j.plaphy.2020.12.034

Dawood, M. F. A., Tahjib-Ul-Arif, M., Abdullah Al Mamun Sohag, A. A., and Latef, A. A. H. A. (2022). Fluoride mitigates aluminum-toxicity in barley: morpho-physiological responses and biochemical mechanisms. *BMC Plant Biol.* 22, 287 doi: 10.1186/s12870-022-03610-z

Dawood, M. F. A., Zaid, A., and Latef, A. A. H. A. (2021a). Salicylic acid spraying-induced resilience strategies against the damaging impacts of drought and/or salinity stress in two varieties of *Vicia faba* L. seedlings. *J. Plant Growth Regul.* 41, 1919–1942. doi: 10.1007/s00344-021-10381-8

El-Sayed, O. M., El-Gammal, O. H. M., and Salama, A. S. M. (2014). Effect of ascorbic acid, proline and jasmonic acid foliar spraying on fruit set and yield of Manzanillo olive trees under salt stress. *Sci. Hort.* 176, 32–37. doi: 10.1016/j.scienta.2014.05.031

Faghih, S., Ghobadi, C., and Zarei, A. (2017). Response of strawberry plant cv. 'camarosa' to salicylic acid and methyl jasmonate application under salt stress condition. *J. Plant Growth Regul.* 36, 651–659. doi: 10.1007/s00344-017-9666-x

Gao, C., El-Sawah, A. M., Ali, D. F. I., Hamoud, Y. A., Shaghaleh, H., and Sheteiwy, M. S. (2020a). The integration of bio and organic fertilizers improve plant growth, grain yield, quality and metabolism of hybrid maize (*Zea mays* L.). *Agronomy.* 10, 319. doi: 10.3390/agronomy10030319

Gao, C., Sheteiwy, M. S., Han, J., Dong, Z., Pan, R., and Guan, Y., et. al. (2020b). Polyamine biosynthetic pathways and their relation with the cold tolerance of maize (*Zea mays*, L.) seedlings. *Plant Sign. Behav.* 15, 1807722. doi: 10.1080/15592324.2020.1807722

Garcia de la Garma, J., Fernandez-Garcia, N., Bardisi, E., Pallol, B., Asensio-Rubio, J. S., Bru, R., et al. (2015). New insights into plant salt acclimation: the roles of vesicle trafficking and reactive oxygen species signaling in mitochondria and the endomembrane system. *New Phytol.* 205, 216–239. doi: 10.1111/nph.12997

Ghassemi-Golezani, K., and Hosseinzadeh-Mahootchi, A. (2015). Improving physiological performance of safflower under salt stress by application of salicylic acid and jasmonic acid. *WALIA J.* 31, 104–109.

Giannopolitis, C. N., and Ries, S. K. (1977). Superoxide dismutases I. Occurrence in higher plants. *Plant Physiol.* 59, 309–314. doi: 10.1104/pp.59.2.309

Halliwell, B., Gutteridge, J. M., and Aruoma, O. I. (1987). The deoxyribose method, a simple 'test tube' assay for determination of rate constants for reactions of hydroxyl radicals. *Anal Biochem.* 165, 215–219. doi: 10.1016/0003-2697(87)90222-3

Hameed, A., Ahmed, M. Z., Hussain, T., Aziz, I., Ahmad, N., Gul, B., and Nielsen, B. L. (2021). Effects of salinity stress on chloroplast structure and function. *Cells.* 10, 2023. doi: 10.3390/cells10082023

Haq, R. F. U., Saeed, N. A., Ahmed, M., Arshad, Z., Mansoor, S., Habib, I., et al. (2019). Barley vacuolar pyrophosphatase (HVP1) gene confers salinity tolerance in locally adapted wheat (*Triticum aestivum*). *Int. J. Agric. Biol.* 22, 1338–1346. doi: 10.17957/IJAB/15.1206

Havaux, M., Eymery, F., Porfirova, S., Rey, P., and Dormann, P. (2005). Vitamin E protects against photoinhibition and photooxidative stress in *Arabidopsis thaliana*. *Plant Cell.* 17, 3451–3469. doi: 10.1105/tpc.105.037036

He, F., Shen, H., Lin, C., Fu, H., Sheteiwy, M. S., Guan, Y., et al. (2017). Transcriptome analysis of chilling-imbibed embryo revealed membrane recovery related genes in maize. *Front. Plant Sci.* 7, 1978. doi: 10.3389/fpls.2016.01978

Javed, S. A., Shahzad, S. M., Ashraf, M., Kausar, R., Arif, M. S., Albasher, G., et al. (2021). Interactive effect of different salinity sources and their formulations on plant growth, ionic homeostasis and seed quality of maize. *Chemosphere.* 132678. doi: 10.1016/j.chemosphere.2021.132678

Jones, H. G. (2013). *Plants and Microclimate: A Quantitative Approach to Environmental Plant Physiology.* Cambridge: Cambridge University Press. doi: 10.1017/CBO9780511845727

Ju, F., Pang, J., Huo, Y., Zhu, J., Yu, K., Sun, L., et al. (2021). Potassium application alleviates the negative effects of salt stress on cotton (*Gossypium hirsutum* L.) yield by improving the ionic homeostasis, photosynthetic capacity and carbohydrate metabolism of the leaf subtending the cotton boll. *Field Crops Res.* 272, 108288. doi: 10.1016/j.fcr.2021.108288

Kamran, M., Wang, D., Alhaithloul, H. A. S., Alghanem, S. M., Aftab, T., Xie, K., et al. (2021). Jasmonic acid-mediated enhanced regulation of oxidative, glyoxalase defense system and reduced chromium uptake contributes to alleviation

of chromium (VI) toxicity in choysum (*Brassica parachinensis* L.). *Ecotoxic. Environ. Saf.* 208, 111758. doi: 10.1016/j.ecoenv.2020.111758

Khan, W. U. D., Tanveer, M., Shaukat, R., Ali, M., and Pirdad, F. (2020). "An overview of salinity tolerance mechanism in plants" in *Salt and Drought Stress Tolerance in Plants. Signaling and Communication in Plants,* Hasanuzzaman, M., and Tanveer, M. (eds). (Cham: Springer) p. 1–16. doi: 10.1007/978-3-030-40277-8_1

Kutik, J., Hola, D., Kocova, M., Rothova, O., Haisel, D., Wilhelmova, N., et al. (2004). Ultrastructure and dimensions of chloroplasts in leaves of three maize (*Zea mays* L.) inbred lines and their F-1 hybrids grown under moderate chilling stress. *Photosynthetica.* 42, 447–455. doi: 10.1023/B:PHOT.0000046165.15048.a4

Lang, D., Yu, X., Jia, X., Li, Z., and Zhang, X. (2020). Methyl jasmonate improves metabolism and growth of NaCl-stressed *Glycyrrhiza uralensis* seedlings. *Sci. Hortic.* 266, 109287. doi: 10.1016/j.scienta.2020.109287

Liu, S., Zhang, P., Li, C., and Xia, G. (2019). The moss jasmonate ZIM-domain protein PnJAZ1 confers salinity tolerance via crosstalk with the abscisic acid signaling pathway. *Plant Sci.* 280, 1–11. doi: 10.1016/j.plantsci.2018.11.004

Lohscheider, J. N., and Bartulos, C. R. (2016). Plastoglobules in algae: A comprehensive comparative study of the presence of major structural and functional components in complex plastids. *Mar. Genom.* 28, 127–136. doi: 10.1016/j.margen.2016.06.005

Lundquist, P. K., Poliakov, A., Bhuiyan, N. H., Zybailov, B., Sun, Q., and van, Wijk, K. J. (2012). The functional network of the *Arabidopsis* plastoglobule proteome based on quantitative proteomics and genome-wide coexpression analysis. *Plant Physiol.* 158, 1172–1192. doi: 10.1104/pp.111.193144

Lundquist, P. K., Poliakov, A., Giacomelli, L., Friso, G., Appel, M., McQuinn, R. P., et al. (2013). Loss of plastoglobule kinases ABC1K1 and ABC1K3 causes conditional degreening, modified prenyl-lipids, and recruitment of the jasmonic acid pathway. *Plant. Cell.* 25, 1818–1839. doi: 10.1105/tpc.113.111120

Malakar, P., and Chattopadhyay, D. (2021). Adaptation of plants to salt stress: the role of the ion transporters. *J. Plant Bioch. Biotech.* 30, 668–683. doi: 10.1007/s13562-021-00741-6

Maxwell, K., and Johnson, G. N. (2000). Chlorophyll fluorescence—a practical guide. *J. Exp Bot.* 51, 659–668. doi: 10.1093/jexbot/51.345.659

Mazur, R., Gieczewska, K., Kowalewska, L., Kuta, A., Proboszcz, M., Gruszecki, W. I., et al. (2020). Specific composition of lipid phases allows retaining an optimal thylakoid membrane fluidity in plant response to low-temperature treatment. *Front. Plant Sci.* 11, 723. doi: 10.3389/fpls.2020.00723

Mir, M. A., Sirhindi, G., Alyemeni, M. N., Alam, P., and Ahmad, P. (2018). Jasmonic acid improves growth performance of soybean under nickel toxicity by regulating nickel uptake, redox balance, and oxidative stress metabolism. *J. Plant Growth Regul.* 37, 1195–1209. doi: 10.1007/s00344-018-9814-y

Munns, R., James, R. A., Gilliham, M., Flowers, T. J., and Colmer, T. D. (2016). Tissue tolerance: an essetial but elusive trait for salt-tolerant crops. *Funct. Plant Biol.* 43, 1103–1113. doi: 10.1071/FP16187

Munns, R., James, R. A., and Lauchli, A. (2006). Approaches to increasing the salt tolerance of wheat and other cereals. *J. Exp. Bot.* 57, 1025–1043. doi: 10.1093/jxb/erj100

Munns, R., and Tester, M. (2008). Mechanisms of salinity tolerance. *Annu. Rev. Plant Biol.* 59, 651–681. doi: 10.1146/annurev.arplant.59.032607.092911

Najafi kakavand, S., Karimi, N., and Ghasempour, H. R. (2019). Salicylic acid and jasmonic acid restrains nickel toxicity by ameliorating antioxidant defense system in shoots of metallicolous and non-metallicolous *Alyssum inflatum* Nayr. *Populations. Plant Physiol. Biochem.* 135, 450–459. doi: 10.1016/j.plaphy.2018.11.015

Nakano, Y., and Asada, K. (1981). Hydrogen peroxide is scavenged by ascorbate specific peroxidase in spinach chloroplasts. *Plant Cell Physiol.* 22, 867–880.

Papadakis, I. E., Giannakoula, A., Therios, I. N., Bosabalidis, A. M., Moustakas, M., and Nastou, A. (2007). Mn-induced changes in leaf structure and chloroplast ultrastructure of *Citrus volkameriana* (L.) plants. *J. Plant Physiol.* 164, 100–103. doi: 10.1016/j.jplph.2006.04.011

Paparella, S., Araújo, S. S., Rossi, G., Wijayasinghe, M., Carbonera, D., and Balestrazzi, A. (2015). Seed priming: state of the art and new perspectives. *Plant Cell Rep.* 34, 1281–1293. doi: 10.1007/s00299-015-1784-y

Pooja., Nandwal, A. S., Chand, M., Singh, K., Mishra, A. K., Kumar, A., et al. (2019). Varietal variation in physiological and biochemical attributes of sugarcane varieties under different soil moisture regimes. *Ind. J. Exp. Biol.* 57, 721–732.

Rauf, S., and Sadaqat, H. A. (2007). Effects of varied water regimes on root length, dry matter partitioning and endogenous plant growth regulators in sunflower (*Helianthus annuus* L.). *J. Plant Interact.* 2, 41–51. doi: 10.1080/17429140701422512

Rottet, S., Besagni, C., and Kessler, F. (2015). The role of plastoglobules in thylakoid lipid remodeling during plant development. *Bioch. Biophys. Acta.* 1847, 889–899. doi: 10.1016/j.bbabio.2015.02.002

Salah, M. S., Guan, Y., Cao, D., Li, J., Nawaz, A., Hu, Q., et al. (2015). Seed priming with polyethylene glycol regulating the physiological and molecular mechanism in rice (*Oryza sativa* L.) under nano-ZnO stress. *Sci. Rep.* 5, 14278. doi: 10.1038/srep14278

Salimi, F., Shekari, F., and Hamzei, J. (2016). Methyl jasmonate improves salinity resistance in German chamomile (*Matricaria chamomilla* L.) by increasing activity of antioxidant enzymes. *Acta Physiol. Plant* 38, 1. doi: 10.1007/s11738-015-2023-4

Sandhu, D., Pudussery, M. V., Ferreira, J. F. S., Liu, X., Pallete, A., Grover, K. K., et al. (2019). Variable salinity responses and comparative gene expression in woodland strawberry genotypes. *Sci. Horticul.* 254, 61–69. doi: 10.1016/j.scienta.2019.04.071

Sehar, Z., Masood, A., and Khan, N. A. (2019). Nitric oxide reverses glucose-mediated photosynthetic repression in wheat (*Triticum aestivum* L.) under salt stress. *Environ. Exp. Bot.* 161, 277–289. doi: 10.1016/j.envexpbot.2019.01.010

Shabala, S. (2013). Learning from halophytes: physiological basis and strategies to improve abiotic stress tolerance in crops. *Ann. Bot.* 112, 1209–1221. doi: 10.1093/aob/mct205

Shahzad,. A. N., Pitann, B., Ali, H., Qayyum, M. F., Fatima, A., and Bakhat, H. F. (2015). Maize genotypes differing in salt resistance vary in jasmonic acid accumulation during the first phase of salt stress. *J. Agron. Crop Sci.* 201, 443–451. doi: 10.1111/jac.12134

Shanmugabalaji, V., Besagni, C., Piller, L. E., Douet, V., Ruf, S., Bock, R., et al. (2013). Dual targeting of a mature plastoglobulin/fibrillin fusion protein to chloroplast plastoglobules and thylakoids in transplastomic tobacco plants. *Plant Mol. Biol.* 81, 13–25. doi: 10.1007/s11103-012-9977-z

Shavrukov, Y. (2014). "Vacuolar $H^+$-PPase (HVP) genes in barley: Chromosome location, sequence and gene expression relating to $Na^+$ exclusion and salinity tolerance," in *Barley: Physical Properties, Genetic Factors and Environmental Impacts on Growth*, Hasunuma, K. (ed). (New York: Nova Science Publishers), pp. 125–142.

Sheteiwy, M. S., Abd Elgawad, H., Xiong, Y. C., Macovei, A., Brestic, M., Skalicky, M., et al. (2021c). Inoculation with *Bacillus amyloliquefaciens* and mycorrhiza confers tolerance to drought stress and improve seed yield and quality of soybean plant. *Physiol. Plant.* 172, 2153–2169.

Sheteiwy, M. S., Ali, D. F. I., Xiong, Y. C., Brestic, M., Skalicky, M., Hamoud, Y. A., et al. (2021b). Physiological and biochemical responses of soybean plants inoculated with Arbuscular mycorrhizal fungi and *Bradyrhizobium* under drought stress. *BMC Plant Biol.* 21, 195. doi: 10.1186/s12870-021-02949-z

Sheteiwy, M. S., An, J., Yin, M., Jia, X., Guan, Y., He, F., et al. (2019). Cold plasma treatment and exogenous salicylic acid priming enhances salinity tolerance of *Oryza sativa* seedlings. *Protoplasma.* 256, 79–99. doi: 10.1007/s00709-018-1279-0

Sheteiwy, M. S., Gong, D., Gao, Y., Pan, R., Hu, J., and Guan, Y. (2018). Priming with methyl jasmonate alleviates polyethylene glycol-induced osmotic stress in rice seeds by regulating the seed metabolic profile. *Environ. Exp. Bot.* 153, 236–248. doi: 10.1016/j.envexpbot.2018.06.001

Sheteiwy, M. S., Shao, H., Qi, W., Daly, P., Sharma, A., et al. (2021a). Seed priming and foliar application with jasmonic acid enhance salinity stress tolerance of soybean (*Glycine max* L.) seedlings. *J. Sci. Food Agric.* 101, 2027–2041. doi: 10.1002/jsfa.10822

Shi, H., Lee, B. H., Wu, S. J., and Zhu, J. K. (2003). Overexpression of a plasma membrane $Na^+$ /$H^+$ antiporter gene improves salt tolerance in *Arabidopsis thaliana*. *Nat. Biotech.* 21, 81–85. doi: 10.1038/nbt766

Shohag, M. J. I., Wei, Y., and Yang, X. (2012). Changes of folate and potential other health promoting phytochemicals in legume seeds as affected by germination. *J. Agric. Food Chem.* 60, 9137–9143. doi: 10.1021/jf302403t

Shrivastava, P., and Kumar, R. (2015). Soil salinity: a serious environmental issue and plant growth promoting bacteria as one of the tools for its alleviation. *Saudi J. Biol. Sci.* 22, 123–131. doi: 10.1016/j.sjbs.2014.12.001

Shu, S., Guo, S. R., Sun, J., and Yuan, L. Y. (2012). Effects of salt stress on the structure and function of the photosynthetic apparatus in *Cucumis sativus* and its protection by exogenous putrescine. *Physiol. Plant.* 146, 285–296. doi: 10.1111/j.1399-3054.2012.01623.x

Sirhindi, G., Mir, M. A., Sharma, P., Gill, S. S., Kaur, H., and Mushtaq, R. (2015). Modulatory role of jasmonic acid on photosynthetic pigments, antioxidants and stress markers of *Glycine max* L. under nickel stress. *Physiol. Mol. Biol. Plants* 21, 559–565. doi: 10.1007/s12298-015-0320-4

Sofy, M., Mohamed, H., Dawood, M., Abu-Elsaoud, A., and Soliman, M. (2021). Integrated usage of *Trichoderma harzianum* and biochar to ameliorate salt stress on spinach plants. *Arch Agron Soil Sci* 1–22. doi: 10.1080/03650340.2021.1949709

Soni, S., Kumar, A., Sehrawat, N., Kumar, A., Kumar, N., Lata, C., et al. (2021). Effect of saline irrigation on plant water traits, photosynthesis and ionic balance in durum wheat genotypes. *Saudi J. Biol. Sci.* 28, 2510–2517. doi: 10.1016/j.sjbs.2021.01.052

Štefanic, P. P., Koffler, T., Adler, G., and Bar-Zvi, D. (2013). Chloroplasts of salt-grown *Arabidopsis* seedlings are impaired in structure, genome copy number and transcript levels. *PLoS One.* 8, e82548. doi: 10.1371/journal.pone.0082548

Tadesse, W., Sanchez-Garcia, M., Assefa, S. G., Amri, A., Bishaw, Z., Ogbonnaya, F. C., et al. (2019). Genetic gains in wheat breeding and its role in feeding the world. *Crop Breed. Genet. Genom.* 1, e190005. doi: 10.20900/cbgg20190005

Taheri, Z., Vatankhah, E., and Jafarian, V. (2020). Methyl jasmonate improves physiological and biochemical responses of *Anchusa italica* under salinity stress. *S. African J. Bot.* 130: 375–382. doi: 10.1016/j.sajb.2020.01.026

Tsukahara, K., Sawada, H., Kohno, Y., Matsuura, T., Mori, I. C., Terao, T., et al. (2015). Ozone-induced rice grain yield loss is triggered via a change in panicle morphology that is controlled by ABERRANT PANICLE ORGANIZA-TION 1 gene. *PLoS One.* 10, e0123308. doi: 10.1371/journal.pone.0123308

Tuteja, N. (2007). Mechanisms of high salinity tolerance in plants. *Methods Enzymol.* 428, 419–438. doi: 10.1016/S0076-6879(07)28024-3

Ulhassan, Z., Gill, R. A., Huang, H., Ali, S., Mwamba, T. M., Ali, B., et al. (2019). Selenium mitigates the chromium toxicity in *Brassicca napus* L. by ameliorating nutrients uptake, amino acids metabolism and antioxidant defense system. *Plant Physiol. Bioch.* 145, 142–152. doi: 10.1016/j.plaphy.2019.10.035

Van Wijk, K. J., and Kessler, F. (2017). Plastoglobuli: plastid microcompartments with integrated functions in metabolism, plastid developmental transitions, and environmental adaptation. *Annu. Rev. Plant Biol.* 68, 253–289. doi: 10.1146/annurev-arplant-043015-111737

Wang, J., Song, L., Gong, X., Xu, J., and Li, M. (2020). Functions of jasmonic acid in plant regulation and response to abiotic stress. *Int. J. Mol. Sci.* 21, 1446. doi: 10.3390/ijms21041446

Wójtowicz, J., Grzyb, J., Szach, J., Mazur, R., Gieczewska, K. B. (2021). Bean and Pea plastoglobules change in response to chilling stress. *Int. J. Mol. Sci*. 22, 11895. doi: 10.3390/ijms222111895

Yang, S., Ulhassan, Z., Shah, A. M., Khan, A. R., Azhar, W., Hamid, Y., et al. (2021). Salicylic acid underpins silicon in ameliorating chromium toxicity in rice by modulating antioxidant defense, ion homeostasis and cellular ultrastructure. *Plant Physiol. Bioch.* 166: 1001–1013. doi: 10.1016/j.plaphy.2021.07.013

Yosefi, M., Sharafzadeh, S., Bazrafshan, F., Zare, M., and Amiri, A. (2018). Application of jasmonic acid can mitigate water deficit stress in cotton through yield-related physiological properties. *Acta Agrobot*. 71, 1741. doi: 10.5586/aa.1741

Younes, N. A., Dawood, M. F., and Wardany, A. A. (2020). The phyto-impact of fluazinam fungicide on cellular structure, agro-physiological, and yield traits of pepper and eggplant crops. *Environ. Sci. Pollut. Res.* 27, 18064–18078. doi: 10.1007/s11356-020-08289-z

Yu, J. N., Huang, J., Wang, Z. N., Zhang, J. S., and Chen, S. Y. (2007). An $Na^+/H^+$ antiporter gene from wheat plays an important role in stress tolerance. *J. Biosci.* 32, 1153–1161. doi: 10.1007/s12038-007-0117-x

Yuan, F., Liang, X., Li, Y., Yin, S., and Wang, B. (2018). Methyl jasmonate improves tolerance to high salt stress in the recretohalophyte *Limonium bicolor*. *Fun. Plant Biol.* 46, 82–92. doi: 10.1071/FP18120

Zbierzak, A. M., Kanwischer, M., Wille, C., Vidi, P. A., Giavalisco, P., Lohmann, A., et al. (2010). Intersection of the tocopherol and plastoquinol metabolic pathways at the plastoglobule. *Biochem. J.* 425, 389–399. doi: 10.1042/BJ20090704

Zhao, X., Wang, W., Zhang, F., Deng, J., Li, Z., and Fu, B. (2014). Comparative metabolite profiling of two rice genotypes with contrasting salt stress tolerance at the seedling stage. *PLoS One.* 9, e108020. doi: 10.1371/journal.pone.0108020

Zhishen, J., Mengcheng, T., and Jianming, W. (1999). The determination of flavonoid contents in mulberry and their scavenging effects on superoxide radicals. *Food Chem.* 64, 555–559. doi: 10.1016/S0308-8146(98)00102-2

Zhu, L. W., Cao, D. D., Hu, Q. J., Guan, Y. J., Hu, W. M., Nawaz, A., et al. (2015). Physiological changes and sHSPs genes relative transcription in relation to the acquisition of seed germination during maturation of hybrid rice seed. *J. Sci. Food Agric.* 96, 1764–1771. doi: 10.1002/jsfa.7283

frontiers | Frontiers in Plant Science

TYPE Original Research
PUBLISHED 17 August 2022
DOI 10.3389/fpls.2022.923872



OPEN ACCESS

EDITED BY
Fayçal Boughalleb,
Institut des Régions Arides,
Tunisia

REVIEWED BY
Jose Ramon Acosta Motos,
Catholic University San Antonio of Murcia,
Spain
Muhammad Kamran,
Lanzhou University,
China

*CORRESPONDENCE
Khaled A. El-Tarabily
ktarabily@uaeu.ac.ae
Synan F. AbuQamar
sabuqamar@uaeu.ac.ae

SPECIALTY SECTION
This article was submitted to
Plant Abiotic Stress,
a section of the journal
Frontiers in Plant Science

RECEIVED 19 April 2022
ACCEPTED 20 June 2022
PUBLISHED 17 August 2022

CITATION
Selim DA-FH, Zayed M, Ali MME, Eldesouky HS, Bonfill M, El-Tahan AM, Ibrahim OM, El-Saadony MT, El-Tarabily KA, AbuQamar SF and Elokkiah S (2022) Germination, physio-anatomical behavior, and productivity of wheat plants irrigated with magnetically treated seawater. *Front. Plant Sci.* 13:923872. doi: 10.3389/fpls.2022.923872



# Germination, physio-anatomical behavior, and productivity of wheat plants irrigated with magnetically treated seawater

Dalia Abdel-Fattah H. Selim[1], Muhammad Zayed[2], Maha M. E. Ali[3], Heba S. Eldesouky[4], Mercedes Bonfill[5], Amira M. El-Tahan[6], Omar M. Ibrahim[6], Mohamed T. El-Saadony[7], Khaled A. El-Tarabily[8,9,10]*, Synan F. AbuQamar[8]* and Samira Elokkiah[11]

[1]Department of Agricultural Botany, Faculty of Agricultural, Menoufia University, Shibin El-Kom, Egypt, [2]Department of Botany and Microbiology, Menoufa University, Shebin El-Kom, Egypt, [3]Department of Soils and Water, Faculty of Agriculture, Benha University, Toukh, Egypt, [4]Department of Botany, Faculty of Agriculture, Benha University, Toukh, Egypt, [5]Department of Plant Physiology, Faculty of Pharmacy, University of Barcelona, Barcelona, Spain, [6]Department of Plant Production, Arid Lands Cultivation Research Institute, The City of Scientific Research and Technological Applications, SRTA-City, Alexandria, Egypt, [7]Department of Agricultural Microbiology, Faculty of Agriculture, Zagazig University, Zagazig, Egypt, [8]Department of Biology, College of Science, United Arab Emirates University, Al-Ain, United Arab Emirates, [9]Khalifa Center for Genetic Engineering and Biotechnology, United Arab Emirates University, Al-Ain, United Arab Emirates, [10]Harry Butler Institute, Murdoch University, Murdoch, WA, Australia, [11]Department of Agricultural Botany, Faculty of Agriculture, Kafrelsheikh University, Kafrelsheikh, Egypt

Salinity is an abiotic stress that reduces the seed germination and productivity of wheat. The objective of this study was to assess the impact of irrigation with magnetically treated seawater on the germination, growth, certain physiological and anatomical parameters, and production attributes of wheat (*Triticum aestivum* L.) cv. Sakha 93 plants. Experiments were conducted in the Experimental Farm of the Faculty of Agriculture, Menoufia University, Egypt, during two consecutive winter seasons. Pot experiments involved ten treatments with non-magnetized and magnetized water with various degrees of salinity. Plant samples were taken 95 days after sowing. Irrigation with magnetically treated seawater was found to have beneficial effects on plant growth, water relations, biochemical characteristics, and yield components compared with untreated plants. The germination of wheat seeds increased 13% when treated with magnetic seawater. On the yield scale, the spike length was increased by 40% in season one, and 82% in season two when compared to the control, while the weight of 100 grains increased by 148% and 171%, in each season, respectively, when treated with magnetic water. The anatomical leaf and stem parameters of the plants were markedly improved by watering with magnetically treated seawater at 10 dS $m^{-1}$ compared to the control. However, the leaf water deficit, transpiration rate, and abscisic acid content in the plant shoots decreased significantly ($p$ <0.05). The use of magnetically treated seawater of up to 7.5 dS $m^{-1}$, instead of tap water, is recommended due to benefits to germination and seedling parameters, growth, yield, and physiological, chemical, and anatomical characteristics. In conclusion,

magnetic treatment of seawater improved germination performance, growth, and yield of wheat under saline conditions.

KEYWORDS

chemical constituents, growth, leaf blade and stem structure, magnetic field, seawater, water relations

# Introduction

Wheat (*Triticum aestivum* L.) is the most important strategic crop in Egypt, and its cultivation area reached 3.8 million acres during the winter growing season of 2018–19, with an entire national output of approximately 9 million tons (FAOSTAT, 2018). Wheat grain has high protein and carbohydrate content, and wheat straw is used as animal feed (Selim et al., 2019).

Water scarcity and drought are increasingly significant environmental challenges impacting both plant growth and human uses. Alternative water sources, such as recycled water, brackish water, seawater, and storm water, have been used for irrigation in various parts of the world and for a variety of purposes, including irrigating agricultural crops (Tyagi et al., 2005). In recent decades, salinity has received more attention, especially in arid and semi-arid areas where there is a serious problem of water shortages allocated for agricultural irrigation (Nerd and Pasternak, 1992). Consequently, to deal with the problem of water scarcity, food and feed crops have been irrigated with saline water. Unfortunately, salt can cause reactive oxygen species (ROS) to form, which can harm membranes and macro molecules (Parvanova et al., 2004).

Plants are harmed by salinity primarily as a result of the osmotic impact and specific ion toxicity (Ferrante et al., 2011). Additionally, salt stress decreases total dry matter (DM) and relative water content (RWC) while increasing proline (Pro) accumulation, enzyme activity, and electrolyte leakage (Tuna et al., 2008). To counteract the damaging effects of salt, plants produce Pro, carbohydrates, and hormones; as well as attracting ions which help the plant's cells to regulate their osmotic balance and conserve water (Munns, 2002).

Magnetized fields have been found to change the properties of tap water, increasing solubility, pH, viscosity, electrical conductivity (EC), and refractive index, while lowering surface tensions and salt levels in the soil (Takatshinko, 1997). These changes occur by increasing the number of hydrogen bonds through the destruction of larger clusters and the generation of smaller clusters, which allows them to pass through plasma membranes more easily (Wang et al., 2013). Under normal and saline conditions, magnetic water treatments have been demonstrated to enhance germination rates, growth rates, leaf areas, water content, chloroplast levels, enzyme activity, nutrient absorption rates, chemical content, anatomical measurements, and overall yields of plants (Selim et al., 2019).

Seawater has the potential to be used as an alternative source for irrigation of crop plants in order to address water scarcity and overpopulation. Furthermore, effective technologies, such as the use of magnetic fields, should be utilized to overcome the adverse effects of salinity on plant growth. However, to date, studies on using magnetic fields to reduce the negative effects of seawater are scarce. Therefore, the aim of the current study was to evaluate the impact of irrigation with magnetically treated seawater on germination, growth, and certain physiological, anatomical, and yield components of wheat plants.

# Materials and methods

## Experimental procedures

*In vitro* and pots experiments were conducted to investigate physiological and anatomical changes as well as the germination parameters of wheat cultivar, Sakha 93 irrigated with seawater of varying salinity levels and exposures to magnetic fields. The wheat grains were obtained from different resources, Ministry of Egyptian Agriculture and Land Reclamation, Giza, Egypt, and Field Crops Research Institute, Agricultural Research Center, Giza, Egypt. Sakha 93 is a stripe rust-resistant Egyptian cultivar that was introduced in 1990 (Shehab-El-Din et al., 1999).

Water was pumped *via* a magnetron device with conditions, a magnetic tube model U.T.I, one-inch diameter, production 4–6 $m^3$ $h^{-1}$ (Magnetic Technologies L.C.C., Dubai, United Arab Emirates).

The laboratory and pot trails were conducted as the following:

### *In vitro* experiments

These experiments were carried out to study the germination parameters. Ten grains with five replicates were put in Petri plates containing moisturized Whatman No.1 filter paper.

### *In vivo* experiments

Pot experiment was carried out in a greenhouse at the Faculty of Agriculture's experimental farm in Shebin El-Kom, Egypt. This

trial was carried out during two successive winter seasons (2018–19 and 2019–20), from ten November to 3 May; Supplementary Table S1 shows the chemical and physical parameters of the clay loam soil that was utilized in this study. Polyethylene pots (30 cm diameter × 30 cm depth) were packed with 8 kg of made soil. The experiment involved ten treatments with four replicates of each treatment. Fifteen grains of wheat without visible defect were sown in each pot. Plant samples (one plant sample from each replicate) were obtained on day 95 post-sowing at 7:00 AM for chemical and physiological assessments. The soil was amended with N, P, and K, based on the recommendation of the Ministry of Egyptian Agriculture and Land Reclamation, Giza, Egypt.

## Treatments

The experimental treatments were described as the following:

1. Irrigation using tap water with an EC of 0.40 dS $m^{-1}$ (control) and various levels of diluted seawater (EC at 5.0, 7.5, 10.0, and 12.5 dS $m^{-1}$) without magnetic treatment.
2. Irrigation with the same above-mentioned treatments but treated with exposure to a magnetic field by passing the water through a magnetron.

Irrigation was carried out with seawater with different levels of salinity (EC at 5.0, 7.5, 10.0, and 12.5 dS $m^{-1}$) prepared from 100% synthetic seawater following the method of Lunin et al. (1961). The water was composed of NaCl, $MgCl_2.6H_2O$, $CaSO_4$ and $K_2SO4$ with the volume of 473:102:20:12 mEq.$l^{-1}$, respectively. Irrigation was carried out manually, based on the field capability, by supplying the needed amount of prepared water.

## Studied traits

### Germination parameters

Germination (%): the number of normal seedlings was counted 15 days after sowing (DAS), according to the following formula:

$$\text{Germination}(\%) = \text{Number of germinated seeds/Total number of seeds} \times 100\%.$$

Mean germination time (MGT) was calculated according to the equation of Ellis and Roberts (1981), as follows:

$$MGT = \sum Dn / \sum n$$

where $n$ is the number of seeds germinated on day $D$ and $D$ is the number of days counted from the beginning of germination.

Germination index (GI) or germination sprouting was determined according to the equation of Scott et al. (1984), as follows:

$$GI = \left(\sum T_i\, N_i\right) / \left(S\right)$$

where $T_i$ = Number of DAS; $N_i$ = Number of germinated seeds on day $i$; $S$, the total number of seeds.

Coefficient of velocity (CV) was estimated according to Scott et al. (1984) as follows:

$$CV = [(\sum Ni)/(\sum NiTi)] \times 100$$

where $N_i$, number of germinated seeds on day i; $T_i$, number of DAS.

Seedling growth characteristics, such fresh weight (FW; g 10 seedlings$^{-1}$), and dry weight (DW; g 10 seedlings$^{-1}$), radicle length (RL; cm), and plumule length (PL; cm), were also determined.

Vigor index (VI) was calculated using the formula according to Abdul-Baki and Anderson (1973):

$$VI = Germination\left(\%\right) \times Total\ seedling\ length\left(cm\right)$$

### Physiological and productive parameters

#### Growth measurements

Root length (RL; cm), plant height (PH; cm), number of leaves plant$^{-1}$, shoot DW (g), root DW (g), and the entire plant DW (g), shoot/root ratio, leaf area (cm$^2$ plant$^{-1}$) were determined following the according to the procedure of disk and leaf area indices measured by Simane et al. (1993).

Flag leaf width, length and flag leaf area (cm$^2$) were also measured according to the formula provided by Gardner et al. (2017):

$$Flag\ leaf\ area\left(cm^2\right) = Flag\ leaf\ length \times Flag\ leaf\ width \times 0.75$$

#### Water relations parameters

The total water content (TWC) in leaves was estimated as previously described (Gossev, 1960).

The RWC and leaf water deficit (LWD) were calculated using the formula of Kalapos (1994):

$$\text{RWC}\ (\%) = (\text{Turgid weight} - \text{FW/Turgid weight} - \text{DW} \times 100$$

$$\text{LWD}\ (\%) = 100 - \text{RWC}$$

The osmotic pressure (atm) was obtained by using special tables following the method of Gossev (1960).

The transpiration rate (TR; mg $cm^{-2}$ $h^{-1}$) was estimated by the following formula (Kreeb, 1990):

$$TR = \left[\frac{FW - \text{Plant weight after 1 hour}}{\text{Plant area in } cm^2}\right] \times 1000$$

The absorption of solute leakage crossways the cell membranes of tissues was evaluated at the 273 nm UV wavelength using a spectrophotometer (UV-2101/3101 PC; Shimadzu Corporation, Analytical Instruments Division, Kyoto, Japan) to determine the membrane integrity (MI; Leopold et al., 1981).

### Chemical parameters

Photosynthetic pigments, such as chlorophyll (Chl) *a* and *b* and carotenoids (Car), were determined using a spectrophotometer (Fadeel, 1962).

UV-absorbing substances (UVAS) were determined in the leaves according to Lichtenthaler (1987), as follows: leaf samples (1.0 g) were boiled in 100 ml of water. After discarding the leaves, the residue was resolved in 10 ml of methanol. The absorbance of extracts was measured at 300 nm using a UV spectrophotometer and the concentration of UVAS was expressed as E300 nm g $FW^{-1}$.

Total soluble sugars (TSS; mg g $DW^{-1}$) and total free amino acids (FAA) in the fine dry leaf powder were separated with chloroform: methanol (3:7, v/v) on ice for 30 min according to the method of Lohaus et al. (2000).

To determine the content of Pro (μmol g $FW^{-1}$), 3% sulphosalicylic acid was recovered from fresh wheat leaves (Bates et al., 1973).

Phenoloxidase (EC 1.14.18.1) and peroxidase (EC 1.11.1.7) activities were determined according to the previous methods (Kar and Mishra, 1976) as the following: Ten grams of fresh leaves from each treatment was separately homogenized in liquid nitrogen and ground with 10 ml phosphate buffer (pH 7.0). Extracts were then centrifuged at 12,000 x *g*, for 15 min at less than 4°C. The terminal volume of the supernatant was adjusted to 10 ml by supplying distilled water and this final solution was considered as the source of the enzymes. The color intensity was measured at 430 nm, and enzyme activity was calculated as a modification in optical density g $FW^{-1}$ $h^{-1}$.

For the mineral elements, 0.2 g of dried powdered leaves was digested in concentrated $H_2SO_4$ and $H_2O_2$ (5:1) for chemical analyses of nitrogen (N), phosphorus (P), potassium (K), iron (Fe), and chloride (Cl; AOAC, 1995); while sodium (Na) was assessed using a flame photometer (Model: 400 FP).

### Concentration of phytohormones

The endogenous phytohormone levels in the leaves of the wheat plants were determined 65 DAS and hormone concentrations were estimated using high-pressure liquid chromatography (HPLC; Crozier and Moritz, 1999).

### Components of yield at harvest

The yield components, spike length (SpL; cm), spike weight (SpW; g $plant^{-1}$), grains number.$spike^{-1}$ (GNSp), grains weight (g $plant^{-1}$), 100 grains weight (GI; g), and straw yield (g $plant^{-1}$) were also estimated.

### Anatomical characteristics

Flag leaves and the fourth upper internode of stem samples were collected at 85 DAS during the second growing season (2019/2020). In FAA, specimens were fixed in fixation solution (5 ml glacial acetic acid, 10 ml formaldehyde, and 85 ml of ethanol 70%) for 2 days. The fixed specimens were cleaned in 50% ethanol, dehydrated in a series of butanol concentrations, embedded in melted paraffin wax at 56°C, segmented to a 20 μm thickness, then stained in safranin-light green, and destained in xylene and mounted in Canada balsam based method (Nassar and El-Sahhar, 1998). Pieces were photomicrographic and examined using Olympus BH-2 (Olympus Optical Co. Ltd, Tokyo, Japan) light microscope equipped with a digital camera and software (Jenoptik ProgRes Camera, C12plus, Frankfurt, Germany).

## Statistical analysis

The data means were analyzed by analysis of variance (ANOVA) using SAS software, v 9.2 (SAS, 2014). The ANOVA examined the differences among the means of interaction among the two main factors (magnetic water treatments at two levels; magnetic and non-magnetic water) and seawater levels (five levels: control, 5.0, 7.5, 10.0, and 12.5 dS $m^{-1}$). The significant differences between means were adopted *via* Duncan's New Multiple Range Test at 5% significance degree.

# Results

## Germination and seedling characteristics

Germination and seedling parameters of Sakha 93 wheat seeds irrigated with different seawater levels and exposed to magnetic treatment are shown in Table 1. As salinity stress increased, the germination and seedling parameters decreased significantly ($p < 0.05$). Examining seawater at 12.5 dS $m^{-1}$, the largest drop in germination % and DW of seedlings was observed at 15% and 20%, respectively, when compared to their controls.

## Growth characteristics

Growth characteristics of wheat plants as affected by different levels of magnetically treated seawater are shown in Table 2. During both seasons, the growth parameters reduced significantly ($p < 0.05$) as seawater level increased. With a seawater level of 12.5 dS $m^{-1}$, the DM deficit in whole plants was 33% and 49% in the first and second seasons, respectively, compared to the control. With a seawater level of 7.5 dS $m^{-1}$, significant increases of 36% and 69% in leaf area index and flag leaf area of wheat plants were

TABLE 1 Effect of seawater stress levels, magnetic treatments on germination, and seedling characters of wheat grains.

| Magnetic treatment | (dS m$^{-1}$) | Germination (%) | MGT (days) | GI | CV | (FW g 10 seedlings$^{-1}$) | (DW; g 10 seedlings$^{-1}$) | RL (cm) | PL (cm) | VI |
|---|---|---|---|---|---|---|---|---|---|---|
| No magnetic | Control | 90.00$^{bc}$ | 4.38$^{a}$ | 16.84$^{ab}$ | 54.11$^{c}$ | 2.82$^{ab}$ | 0.284$^{a}$ | 12.91$^{bc}$ | 14.19$^{ab}$ | 24.42$^{c}$ |
| | 5 | 83.33$^{de}$ | 4.64$^{a}$ | 12.44$^{d}$ | 34.72$^{e}$ | 2.78$^{ab}$ | 0.248$^{a}$ | 11.35$^{cd}$ | 14.64$^{a}$ | 21.50$^{d}$ |
| | 7.5 | 80.00$^{bc}$ | 4.56$^{a}$ | 12.15$^{d}$ | 32.44$^{ef}$ | 2.55$^{ab}$ | 0.283$^{a}$ | 9.57$^{de}$ | 12.92$^{abc}$ | 17.99$^{ef}$ |
| | 10 | 80.00$^{ef}$ | 4.64$^{a}$ | 12.08$^{d}$ | 33.11$^{ef}$ | 2.59$^{ab}$ | 0.281$^{a}$ | 7.83$^{ef}$ | 13.62$^{abc}$ | 17.15$^{f}$ |
| | 12.5 | 76.67$^{f}$ | 4.59$^{a}$ | 11.93$^{d}$ | 30.72$^{f}$ | 1.78$^{b}$ | 0.226$^{a}$ | 6.89$^{f}$ | 11.71$^{c}$ | 14.30$^{g}$ |
| Magnetic water | Control | 96.67$^{a}$ | 4.29$^{a}$ | 19.03$^{a}$ | 65.72$^{a}$ | 3.07$^{a}$ | 0.304$^{a}$ | 15.43$^{a}$ | 14.30$^{ab}$ | 28.63$^{a}$ |
| | 5 | 90.00$^{bc}$ | 4.26$^{a}$ | 18.24$^{a}$ | 59.00$^{b}$ | 2.84$^{ab}$ | 0.287$^{a}$ | 14.67$^{ab}$ | 14.88$^{a}$ | 26.60$^{b}$ |
| | 7.5 | 93.33$^{ab}$ | 4.31$^{a}$ | 18.11$^{a}$ | 59.72$^{b}$ | 2.88$^{a}$ | 0.286$^{a}$ | 11.03$^{cd}$ | 14.20$^{ab}$ | 23.52$^{c}$ |
| | 10 | 83.33$^{de}$ | 4.42$^{a}$ | 15.22$^{bc}$ | 45.03$^{d}$ | 2.68$^{ab}$ | 0.288$^{a}$ | 9.10d$^{ef}$ | 13.82$^{abc}$ | 19.07$^{e}$ |
| | 12.5 | 86.67$^{cd}$ | 4.47$^{a}$ | 14.57$^{c}$ | 43.79$^{d}$ | 2.08$^{ab}$ | 0.238$^{a}$ | 7.49$^{ef}$ | 11.98$^{bc}$ | 16.88$^{f}$ |

Values followed by different letters within a column are significantly different ($p < 0.05$) according to Duncan's new multiple range test. MGT, mean germination time; GI, germination index; CV, coefficient of velocity; FW, fresh weight; DW, dry weight; RL, radicle length; PL, plumule length; and VI, vigor index.

obtained utilizing magnetically treated seawater compared to the non-magnetic treatment in the first growing season. In this respect, the results of both seasons are similar.

## Water relations

During both seasons, increased seawater levels resulted in a significant decrease in water relations values (Table 3). The RWC (%) shortfall was 12% and 33% in the first and second seasons, respectively, as compared to the control, at a seawater level of 12.5 dS m$^{-1}$.

## Chemical characteristics

### Photosynthetic pigments

When seawater stress increased, the photosynthetic pigment content in the wheat plants reduced dramatically compared to the control (Supplementary Table S2). With a seawater level of 12.5 dS m$^{-1}$, the decrease in total chlorophyll ($a + b$) was 31% and 27% lower in the first and second seasons, respectively, compared to the control. These changes boost photosynthetic efficiency. Additionally, magnetic treatments increased the synthesis of ultraviolet absorbing compounds in the leaves, making them more resistant to harmful UV-B radiation.

### TSS, FAA, and Pro concentrations

Table 4 shows that the entire soluble sugar concentration in wheat plant leaves decreased by approximately 36% when non-magnetic seawater level was increased to 12.5 dS m$^{-1}$ compared to the control during the second season. In the second season, FAA and Pro were enhanced in wheat plant leaves by approximately 11% and 250%, respectively, under a stress level of 12.5 dS m$^{-1}$, compared to the control. The same trend in grains was observed (Table 4). In the second season, however, TSS concentration in leaves treated with magnetic water increased by approximately 45% and 65% under seawater levels of 10 and 12.5 dS m$^{-1}$, respectively, when compared to plants treated with non-magnetically treated water. In the second season, as compared to untreated plants, the application of magnetically treated water elevated whole FAA and Pro concentration in leaves by approximately 10 and 80%, respectively, at a seawater level of 12.5 dS m$^{-1}$.

### Phenoloxidase and peroxidase enzymes activity

The activity of phenoloxidase enzymes decreased as seawater levels increased, whereas the activity of peroxidase enzymes increased significantly in wheat plant leaves (Table 4). With a seawater level of 10 dS m$^{-1}$, the reduction in phenoloxidase activity was approximately 9%, and the increase in peroxidase activity was approximately 11%, respectively, compared to the control.

TABLE 2 Effect of seawater stress levels, magnetic treatment on some vegetative growth characters of wheat plants during the first and second growing seasons.

| Characteristic magnetic treatment | | RL (cm) | PH (cm) | Number of leaves plant$^{-1}$ | DW (g plant$^{-1}$) | | | S/R ratio | LA (cm$^2$ plant$^{-1}$) | LAI | FLL (cm) | FLW (cm) | FLFW (g plant$^{-1}$) | FLDW (g plant$^{-1}$) | FLA (cm$^2$) |
|---|---|---|---|---|---|---|---|---|---|---|---|---|---|---|---|
| **Treatment** | **dS m$^{-1}$** | | | | **R** | **S** | **W** | | | | | | | | |
| First season | | | | | | | | | | | | | | | |
| No magnetic | Control | 4.83$^{b}$ | 49.00$^{a}$ | 7.00$^{ab}$ | 0.020$^{cd}$ | 0.472$^{de}$ | 0.492$^{de}$ | 23.18$^{ab}$ | 153.17$^{ef}$ | 1.219$^{de}$ | 12.67$^{cd}$ | 0.900$^{ef}$ | 0.253$^{abc}$ | 0.080$^{cd}$ | 8.30$^{d}$ |
| | 5 | 5.67$^{b}$ | 48.17$^{ab}$ | 6.00$^{bc}$ | 0.020$^{cd}$ | 0.435$^{de}$ | 0.455$^{de}$ | 21.75$^{abc}$ | 148.96$^{f}$ | 1.186$^{def}$ | 12.33$^{d}$ | 1.033$^{cd}$ | 0.207$^{bcd}$ | 0.070$^{cd}$ | 9.58$^{c}$ |
| | 7.5 | 5.00$^{b}$ | 43.50$^{c}$ | 6.00$^{bc}$ | 0.017$^{d}$ | 0.377$^{ef}$ | 0.393$^{ef}$ | 22.89$^{ab}$ | 141.95$^{g}$ | 1.130$^{efg}$ | 12.33$^{d}$ | 0.833$^{f}$ | 0.180$^{cd}$ | 0.078$^{cd}$ | 7.30$^{d}$ |
| | 10 | 3.83$^{c}$ | 43.00$^{c}$ | 5.67$^{c}$ | 0.014$^{d}$ | 0.337$^{f}$ | 0.351$^{f}$ | 24.06$^{ab}$ | 137.10$^{gh}$ | 1.092$^{fg}$ | 11.67$^{d}$ | 0.833$^{f}$ | 0.217$^{bc}$ | 0.063$^{d}$ | 7.93$^{d}$ |
| | 12.5 | 3.67$^{c}$ | 32.67$^{e}$ | 5.33$^{c}$ | 0.015$^{d}$ | 0.317$^{f}$ | 0.331$^{f}$ | 22.50$^{a}$ | 134.91$^{h}$ | 1.074$^{g}$ | 8.67$^{e}$ | 0.700$^{g}$ | 0.105$^{d}$ | 0.055$^{e}$ | 4.60$^{e}$ |
| Magnetic water | Control | 6.83$^{a}$ | 49.17$^{a}$ | 7.33$^{a}$ | 0.047$^{a}$ | 1.040$^{a}$ | 1.087$^{a}$ | 22.03$^{abc}$ | 220.83$^{a}$ | 1.758$^{a}$ | 15.33$^{a}$ | 1.167$^{ab}$ | 0.303$^{ab}$ | 0.142$^{a}$ | 12.30$^{b}$ |
| | 5 | 7.00$^{a}$ | 48.33$^{ab}$ | 7.33$^{a}$ | 0.040$^{ab}$ | 0.868$^{b}$ | 0.908$^{b}$ | 22.51$^{abc}$ | 200.48$^{b}$ | 1.596$^{b}$ | 15.67$^{a}$ | 1.233$^{a}$ | 0.338$^{a}$ | 0.152$^{a}$ | 14.38$^{a}$ |
| | 7.5 | 5.83$^{b}$ | 45.67$^{ab}$ | 7.67$^{a}$ | 0.037$^{b}$ | 0.800$^{b}$ | 0.836$^{b}$ | 22.49$^{abc}$ | 192.30$^{c}$ | 1.531$^{b}$ | 14.00$^{b}$ | 1.167$^{ab}$ | 0.267$^{abc}$ | 0.127$^{b}$ | 12.35$^{b}$ |
| | 10 | 5.17$^{b}$ | 44.00$^{bc}$ | 6.00$^{bc}$ | 0.029$^{c}$ | 0.610$^{c}$ | 0.639$^{c}$ | 21.33$^{bc}$ | 169.87$^{d}$ | 1.352$^{c}$ | 14.00$^{b}$ | 0.967$^{de}$ | 0.207$^{bcd}$ | 0.078$^{c}$ | 11.08$^{b}$ |
| | 12.5 | 5.33$^{b}$ | 38.67$^{d}$ | 6.00$^{bc}$ | 0.025$^{cd}$ | 0.487$^{d}$ | 0.511$^{d}$ | 20.19$^{c}$ | 155.36$^{e}$ | 1.237$^{d}$ | 13.67$^{bc}$ | 1.100$^{bc}$ | 0.203$^{bcd}$ | 0.072$^{cd}$ | 11.35$^{b}$ |
| Second season | | | | | | | | | | | | | | | |
| No magnetic | Control | 4.50$^{cd}$ | 48.83$^{a}$ | 7.33$^{ab}$ | 0.020$^{c}$ | 0.515$^{e}$ | 0.535$^{f}$ | 25.35$^{a}$ | 158.09$^{f}$ | 1.259$^{f}$ | 14.33$^{ab}$ | 0.933$^{bc}$ | 0.253$^{abc}$ | 0.080$^{b}$ | 9.98$^{c}$ |
| | 5 | 5.00$^{bc}$d | 47.33$^{a}$ | 6.00$^{c}$ | 0.019$^{c}$ | 0.472$^{e}$ | 0.491$^{f}$ | 24.38$^{ab}$ | 153.05$^{g}$ | 1.219$^{f}$ | 12.00$^{def}$ | 0.933$^{bc}$ | 0.207$^{bcd}$ | 0.077$^{bc}$ | 8.43$^{de}$ |
| | 7.5 | 5.00$^{bcd}$ | 43.67$^{b}$ | 6.33$^{bc}$ | 0.018$^{c}$ | 0.437$^{e}$ | 0.455$^{f}$ | 24.72$^{ab}$ | 148.92$^{h}$ | 1.186$^{f}$ | 11.67$^{ef}$ | 0.833$^{cd}$ | 0.180$^{cd}$ | 0.070$^{cd}$ | 7.30$^{ef}$ |
| | 10 | 4.00$^{d}$ | 43.00$^{b}$ | 6.33$^{bc}$ | 0.015$^{c}$ | 0.315$^{f}$ | 0.330$^{g}$ | 22.53$^{cd}$ | 134.76$^{i}$ | 1.073$^{g}$ | 11.00$^{f}$ | 0.800$^{d}$ | 0.163$^{cd}$ | 0.067$^{cd}$ | 6.63$^{cd}$ |
| | 12.5 | 4.00$^{d}$ | 34.00$^{d}$ | 5.33$^{c}$ | 0.013$^{c}$ | 0.262$^{f}$ | 0.274$^{g}$ | 20.88$^{de}$ | 128.43$^{j}$ | 1.023$^{g}$ | 8.67$^{g}$ | 0.700$^{e}$ | 0.105$^{d}$ | 0.047$^{e}$ | 4.60$^{cd}$ |
| Magnetic water | Control | 6.67$^{a}$ | 49.33$^{a}$ | 7.67$^{a}$ | 0.043$^{b}$ | 1.093$^{a}$ | 1.136$^{a}$ | 25.51$^{a}$ | 226.39$^{a}$ | 1.803$^{a}$ | 15.00$^{a}$ | 1.167$^{a}$ | 0.320$^{a}$ | 0.113$^{a}$ | 13.18$^{ab}$ |
| | 5 | 7.00$^{a}$ | 49.00$^{a}$ | 7.33$^{ab}$ | 0.065$^{a}$ | 0.960$^{b}$ | 1.024$^{b}$ | 25.67$^{a}$ | 213.65$^{b}$ | 1.701$^{b}$ | 15.00$^{a}$ | 1.233$^{a}$ | 0.319$^{ab}$ | 0.112$^{a}$ | 13.78$^{a}$ |
| | 7.5 | 5.33$^{bc}$ | 46.33$^{ab}$ | 8.00$^{a}$ | 0.045$^{b}$ | 0.875$^{b}$ | 0.920$^{c}$ | 23.12$^{bc}$ | 201.77$^{c}$ | 1.606$^{c}$ | 13.67$^{bc}$ | 1.167$^{a}$ | 0.267$^{abc}$ | 0.098$^{a}$ | 12.05$^{b}$ |
| | 10 | 5.33$^{bc}$ | 43.33$^{b}$ | 6.00$^{c}$ | 0.037$^{b}$ | 0.727$^{c}$ | 0.764$^{d}$ | 20.49$^{e}$ | 184.04$^{d}$ | 1.465$^{d}$ | 13.00$^{cd}$ | 0.967$^{b}$ | 0.207$^{bcd}$ | 0.065$^{d}$ | 9.45$^{cd}$ |
| | 12.5 | 6.00$^{ab}$ | 39.00$^{c}$ | 6.00$^{c}$ | 0.034$^{b}$ | 0.617$^{d}$ | 0.651$^{e}$ | 18.13$^{f}$ | 171.24$^{e}$ | 1.363$^{e}$ | 12.67$^{cde}$ | 0.933$^{bc}$ | 0.203$^{cd}$ | 0.063$^{d}$ | 8.85$^{cd}$ |

Values followed by different letters within a column are significantly different ($p < 0.05$) according to Duncan's new multiple range test. RL, root length; PH, plant height; DW, dry weight; R, root; S, shoot; W, whole; LA, leaf area; LAI, leaf area index; FLL, flag leaf length; FLW, flag leaf width; FLFW, flag leaf fresh weight; FLDW, flag leaf dry weight; and FLA, flag leaf area.





10.3389/fpls.2022.923872

TABLE 3 Effect of seawater stress levels, magnetic treatment on water relation in leaves of wheat plants during the first and second growing seasons.

| Characters treatments | | TWC (%) | RWC (%) | LWD (%) | Osmotic pressure (atm) | TR (mg cm$^{-2}$ h$^{-1}$) | MI (%) |
|---|---|---|---|---|---|---|---|
| Magnetic treatments | dS m$^{-1}$ | | | | | | |
| First season | | | | | | | |
| No magnetic | Control | 71.56$^{bc}$ | 49.78$^{c}$ | 50.22$^{e}$ | 7.71$^{a}$ | 1.139$^{a}$ | 22.06$^{g}$ |
| | 5 | 71.41$^{bc}$ | 35.72$^{f}$ | 64.28$^{b}$ | 7.89$^{a}$ | 1.044$^{a}$ | 26.19$^{ef}$ |
| | 7.5 | 68.53$^{cd}$ | 44.66$^{d}$ | 55.34$^{d}$ | 8.00$^{a}$ | 0.893$^{b}$ | 27.90$^{b}$ |
| | 10 | 69.11$^{cd}$ | 33.89$^{fg}$ | 66.11$^{ab}$ | 8.15$^{a}$ | 0.870$^{b}$ | 39.58$^{b}$ |
| | 12.5 | 66.51$^{d}$ | 31.43$^{g}$ | 68.57$^{a}$ | 8.26$^{a}$ | 0.834$^{bc}$ | 41.30$^{b}$ |
| Magnetic water | Control | 76.44$^{a}$ | 54.55$^{ab}$ | 45.45$^{fg}$ | 7.89$^{a}$ | 0.903$^{b}$ | 25.43$^{f}$ |
| | 5 | 72.88$^{b}$ | 56.64$^{a}$ | 43.36$^{g}$ | 8.11$^{a}$ | 0.879$^{b}$ | 30.34$^{d}$ |
| | 7.5 | 69.06$^{d}$ | 52.23$^{bc}$ | 47.77$^{ef}$ | 8.33$^{a}$ | 0.858$^{b}$ | 35.16$^{c}$ |
| | 10 | 69.98$^{cd}$ | 34.72$^{f}$ | 65.28$^{b}$ | 8.44$^{a}$ | 0.752$^{c}$ | 40.00$^{b}$ |
| | 12.5 | 68.50$^{cd}$ | 39.03$^{e}$ | 60.97$^{c}$ | 8.55$^{a}$ | 0.750$^{c}$ | 43.72$^{a}$ |
| Second season | | | | | | | |
| No magnetic | Control | 79.37$^{a}$ | 59.46$^{c}$ | 40.54$^{e}$ | 7.60$^{a}$ | 1.122$^{a}$ | 15.54$^{g}$ |
| | 5 | 77.38$^{ab}$ | 41.27$^{e}$ | 58.73$^{c}$ | 7.64$^{a}$ | 1.054$^{ab}$ | 23.12$^{e}$ |
| | 7.5 | 73.08$^{c}$ | 59.42$^{c}$ | 40.59$^{e}$ | 7.86$^{a}$ | 0.932$^{cd}$ | 26.89$^{d}$ |
| | 10 | 68.90$^{d}$ | 35.51$^{f}$ | 64.49$^{b}$ | 7.89$^{a}$ | 0.882$^{d}$ | 34.01$^{c}$ |
| | 12.5 | 60.00$^{e}$ | 21.34$^{g}$ | 78.66$^{a}$ | 8.07$^{a}$ | 0.782$^{e}$ | 34.78$^{c}$ |
| Magnetic water | Control | 81.42$^{a}$ | 59.86$^{c}$ | 40.15$^{e}$ | 6.49$^{b}$ | 0.991$^{bc}$ | 20.90$^{f}$ |
| | 5 | 78.53$^{a}$ | 65.83$^{b}$ | 34.17$^{f}$ | 7.89$^{a}$ | 0.909$^{cd}$ | 32.84$^{c}$ |
| | 7.5 | 78.01$^{a}$ | 89.40$^{a}$ | 30.60$^{g}$ | 8.04$^{a}$ | 0.890$^{cd}$ | 45.48$^{a}$ |
| | 10 | 73.70$^{bc}$ | 43.17$^{e}$ | 56.83$^{c}$ | 8.11$^{a}$ | 0.743$^{ef}$ | 44.54$^{a}$ |
| | 12.5 | 71.29$^{cd}$ | 46.76$^{d}$ | 53.24$^{d}$ | 8.18$^{a}$ | 0.646$^{f}$ | 39.26$^{b}$ |

Values followed by different letters within a column are significantly different ($p < 0.05$) according to Duncan's new multiple range test. TWC, total water content; RWC, relative water content; LWD, leaf water deficit; TR, transpiration rate; and MI, membrane integrity.

## Mineral concentrations

Table 5 shows that as seawater levels rose, macro and micro minerals in wheat plants and grains declined with the exception of Na and Cl, which increased. With a 12.5 dS m$^{-1}$ seawater level, the concentrations of the elements N, P, K, and Fe in the wheat plant shoots declined by approximately 19%, 27%, 13%, and 69%, respectively, compared to the control. When examining all seawater levels, the magnetic treatment caused significant increases in concentration of all the minerals, except Na and Cl, in all areas of wheat plants. In comparison to the non-magnetic treatment, the N, P, and K concentrations in grains increased by roughly 50%, 24% and 25%, respectively, while the Na and Cl concentrations in the shoot decreased by approximately 20% and 25%, at a seawater level of 12.5 dS m$^{-1}$.

## Concentration of phytohormones

The concentrations of indole-3-acetic acid (IAA), cytokinins (CKs) and gibberellic acid ($GA_3$) decreased by approximately 28%, 19%, and 14%, respectively, with increasing seawater levels; while the concentration of abscisic acid (ABA) increased by about 90% at a 10 dS m$^{-1}$ seawater level compared to the control (Table 6). The influence of the magnetic field resulted in an increase in growth phytohormone levels and had positive effects on the mineral uptake, Chl synthesis and plant growth.

## Yield attributes

Table 7 shows that all yield features of wheat plants [SpL (cm), SpW (g plant$^{-1}$), GNSp, grain weight (g plant$^{-1}$), weight of 100 grains (g), and straw yield (g plant$^{-1}$)] dropped significantly with increasing seawater levels during both seasons. In the first and second seasons, the reduction in grain weight was 91% and 68%, respectively, at the elevated seawater of 12.5 dS m$^{-1}$ in contrast to the control. The irrigation with magnetic water; however, increased the previous yield attributes by roughly 16%, 30%, 58%, 688%, 37%, and 11%, respectively, at a seawater stress level of 10 dS m$^{-1}$ in the first season, compared to controls. The second season followed the same pattern.

## Anatomical structure of leaf blade and stem

The magnetic technology utilized in this study had a strong positive effect and reduced the negative impacts of seawater

TABLE 4 Effect of seawater stress levels, magnetic treatment on some chemical constituents in shoot and grains of wheat plants during the second growing season.

| Characters treatments | | Shoot | | | | | | Grains | | |
|---|---|---|---|---|---|---|---|---|---|---|
| | | TSS | FAA | Pro | Enzymes activity | | TSS | FAA | Pro |
| | | | | | Phenoloxidase | Peroxidase | | | |
| Magnetic treatments | dS m$^{-1}$ | mg g DW$^{-1}$ | | µmol g FW$^{-1}$ | OD g FW$^{-1}$ | | mg g DW$^{-1}$ | µmol g FW$^{-1}$ | |
| No magnetic | Control | 242.19$^{f}$ | 97.20$^{d}$ | 1.45$^{f}$ | 0.65$^{cde}$ | 0.45$^{f}$ | 369.12$^{c}$ | 88.78$^{f}$ | 0.36$^{h}$ |
| | 5 | 234.38$^{g}$ | 97.20$^{d}$ | 2.91$^{de}$ | 0.74$^{c}$ | 0.68$^{e}$ | 334.38$^{e}$ | 102.20$^{e}$ | 1.02$^{f}$ |
| | 7.5 | 203.13$^{h}$ | 113.40$^{bc}$ | 3.34$^{de}$ | 0.61$^{de}$ | 0.54$^{f}$ | 318.11$^{f}$ | 103.40$^{e}$ | 1.23$^{e}$ |
| | 10 | 187.5$^{i}$ | 102.60$^{d}$ | 3.78$^{d}$ | 0.59$^{de}$ | 0.50$^{f}$ | 251.10$^{i}$ | 112.60$^{d}$ | 1.45$^{d}$ |
| | 12.5 | 156.25$^{j}$ | 108.00$^{c}$ | 5.08$^{c}$ | 0.58$^{e}$ | 0.90$^{d}$ | 236.29$^{j}$ | 110.09$^{d}$ | 2.25$^{c}$ |
| Magnetic water | Control | 390.63$^{a}$ | 113.40$^{bc}$ | 2.62$^{e}$ | 0.68$^{cd}$ | 0.95$^{d}$ | 412.73$^{a}$ | 153.40$^{a}$ | 0.80$^{g}$ |
| | 5 | 312.50$^{b}$ | 113.40$^{bc}$ | 3.63$^{d}$ | 1.01$^{a}$ | 1.71$^{a}$ | 400.50$^{b}$ | 141.40$^{c}$ | 1.45$^{d}$ |
| | 7.5 | 281.25$^{c}$ | 118.80$^{ab}$ | 5.23$^{c}$ | 0.86$^{b}$ | 1.26$^{b}$ | 351.25$^{d}$ | 146.50$^{b}$ | 2.18$^{c}$ |
| | 10 | 272.42$^{d}$ | 124.20$^{a}$ | 7.70$^{b}$ | 0.72$^{c}$ | 0.99$^{d}$ | 293.49$^{h}$ | 138.40$^{c}$ | 3.12$^{b}$ |
| | 12.5 | 256.94$^{e}$ | 118.80$^{ab}$ | 9.15$^{a}$ | 0.72$^{c}$ | 1.13$^{c}$ | 302.81$^{g}$ | 148.80$^{b}$ | 3.63$^{a}$ |

Values followed by different letters within a column are significantly different ($p < 0.05$) according to Duncan's new multiple range test. TSS, total soluble sugars; FAA, free amino acids; Pro, proline; DW, dry weight; and FW, fresh weight.

irrigation on all the previously described characteristics of Sakha 93 wheat plants. In addition, the internal composition of the flag leaf and stem of wheat plants developed underneath seawater stress subjected to a magnetic field should be studied. In comparison with the control, wheat plants treated with magnetic technology and seawater at 10 dS m$^{-1}$ exhibited histological features of flag leaf formation and stems (Table 8; Figures 1, 2). In the second season, at a seawater level of 10 dS m$^{-1}$ the deficits in lamina thickness (µm), midvein bundle dimensions (µm), stem diameter (mm), and vascular bundle thickness (µm) were approximately 29%, 11%, 40%, and 12%, respectively, as contrasted to the control.

Magnetic water treatment raised the lamina and midrib thickness (µm) of the flag leaf by approximately 17% and 40%, respectively, at the 10 dS m$^{-1}$ level when compared to the control. Magnetic seawater of 10 dS m$^{-1}$ increased the midvein bundle and metaxylem vessel diameter (µm) by 8% and 100%, respectively, as compared to the control. In comparison to untreated plants, the application of magnetically treated water increased stem diameter (mm) and stem cavity diameter (mm) by approximately 17% and 32%, respectively, at seawater levels of 10 dS m$^{-1}$. The magnetic seawater at level 10 dS m$^{-1}$ increased the number of vascular bundle cross sections, thickness, and metaxylem vessel diameter (µm) of the stem by 29%, 39%, and 73%, respectively compared to the non-magnetic treatment.

## Path analysis

Path analysis (Tabachnick and Fidell, 1996) was accomplished using R statistical software version 4.1.0, 2021 using the package (lavaan) and the function (sem), which is the abbreviation of structural equation modeling. Path diagram was generated by using the function (semPaths) in the same package. Path analysis results are shown on the path diagrams in Figure 3. Three types of arrows are shown on the path diagram. The first type is representing the path; it is a single-headed arrow and is representing the causal relationships between the two variables, independent and dependent, the independent locates at the tail of the arrow while the dependent variable locates at the head of the arrow. The second type is representing the covariance between two variables; it is a double-headed arrow. The third type is representing the variance between two variables, it is a double-headed; however, the arrow is pointed at the same variable. Path diagram (Figure 3) included three direct effects and two indirect effects.

Concerning the direct effects, the first is the direct effect of plant leaf area (PLA), Chl *a* and *b* on GI where $R^2$ value was 0.708. The second, is the direct effect of GI and GNSp where $R^2$ value was 0.933.

The third, is the direct effect of SpW, Chl *a* and Chl *b* on grain weight plant$^{-1}$ (GWP) where $R^2$ value was 0.950. On the other hand, the indirect effects were two effects, the first is the indirect effect of plant leaf area (PLA), Chl *a* and Chl *b* on SpW, *via* GI. The second is the indirect effect of GI and GNSp on GWP *via* SpW. All

10.3389/fpls.2022.923872

TABLE 5 Effect of seawater stress levels, magnetic treatment on the concentrations of some elements in different organs of wheat plants during the second growing season.

| Characters treatments | | Root | | | | | | Shoot | | | | | | Grains | | | | | |
|---|---|---|---|---|---|---|---|---|---|---|---|---|---|---|---|---|---|---|---|
| Magnetic treatments | dS m$^{-1}$ | N (%) | P (%) | K (%) | Cl (ppm) | Na (ppm) | Fe (ppm) | N (%) | P (%) | K (%) | Cl (ppm) | Na (ppm) | Fe (ppm) | N (%) | P (%) | K (%) | Cl (ppm) | Na (ppm) |
| No magnetic | Control | 2.312$^{b}$ | 0.163$^{a}$ | 2.653$^{abcd}$ | 3.053$^{f}$ | 1.418$^{g}$ | 310.20$^{b}$ | 2.604$^{ab}$ | 0.250$^{ab}$ | 3.511$^{b}$ | 2.272$^{de}$ | 0.409$^{bc}$ | 351.00$^{c}$ | 2.520$^{e}$ | 0.483$^{b}$ | 0.729$^{bc}$ | 0.639$^{cd}$ | 0.172$^{a}$ |
| | 5 | 2.100$^{b}$ | 0.154$^{a}$ | 2.229$^{bcd}$ | 3.408$^{e}$ | 1.518$^{f}$ | 284.80$^{d}$ | 2.436$^{b}$ | 0.218$^{ab}$ | 3.301$^{cd}$ | 2.769$^{cde}$ | 0.377$^{cd}$ | 321.00$^{e}$ | 2.520$^{e}$ | 0.455$^{bc}$ | 0.733$^{bc}$ | 0.675$^{c}$ | 0.183$^{a}$ |
| | 7.5 | 1.977$^{b}$ | 0.150$^{a}$ | 1.786$^{cd}$ | 3.692$^{d}$ | 2.130$^{c}$ | 230.80$^{g}$ | 2.294$^{b}$ | 0.213$^{ab}$ | 3.200$^{d}$ | 3.053$^{bcd}$ | 0.583$^{a}$ | 274.20$^{g}$ | 2.272$^{f}$ | 0.429$^{bc}$ | 0.694$^{c}$ | 0.710$^{c}$ | 0.192$^{a}$ |
| | 10 | 2.040$^{b}$ | 0.148$^{a}$ | 1.707$^{d}$ | 4.402$^{b}$ | 2.283$^{b}$ | 185.34$^{i}$ | 2.152$^{b}$ | 0.199$^{ab}$ | 3.057$^{e}$ | 3.692$^{bc}$ | 0.583$^{a}$ | 207.20$^{h}$ | 2.040$^{g}$ | 0.378$^{c}$ | 0.686$^{c}$ | 0.852$^{b}$ | 0.197$^{a}$ |
| | 12.5 | 1.004$^{c}$ | 0.141$^{a}$ | 1.662$^{d}$ | 5.183$^{a}$ | 2.507$^{a}$ | 170.00$^{j}$ | 2.100$^{b}$ | 0.182$^{b}$ | 3.043$^{e}$ | 5.112$^{a}$ | 0.583$^{a}$ | 108.40$^{j}$ | 1.904$^{h}$ | 0.356$^{c}$ | 0.562$^{d}$ | 0.994$^{a}$ | 0.200$^{a}$ |
| Magnetic water | Control | 3.876$^{a}$ | 0.221$^{a}$ | 3.391$^{a}$ | 2.272$^{i}$ | 1.076$^{h}$ | 365.22$^{a}$ | 3.528$^{a}$ | 0.304$^{a}$ | 3.692$^{a}$ | 1.988$^{e}$ | 0.216$^{e}$ | 376.80$^{a}$ | 3.024$^{b}$ | 0.611$^{a}$ | 0.822$^{a}$ | 0.497$^{e}$ | 0.115$^{a}$ |
| | 5 | 2.407$^{b}$ | 0.193$^{a}$ | 3.043$^{ab}$ | 2.485$^{h}$ | 1.352$^{g}$ | 291.02$^{c}$ | 2.688$^{ab}$ | 0.228$^{ab}$ | 3.482$^{b}$ | 2.272$^{de}$ | 0.309$^{d}$ | 361.00$^{b}$ | 3.192$^{a}$ | 0.497$^{b}$ | 0.793$^{ab}$ | 0.568$^{de}$ | 0.133$^{a}$ |
| | 7.5 | 2.342$^{b}$ | 0.184$^{a}$ | 2.818$^{abc}$ | 2.840$^{g}$ | 1.536$^{f}$ | 266.82$^{e}$ | 2.468$^{b}$ | 0.241$^{ab}$ | 3.300$^{c}$ | 2.698$^{cde}$ | 0.425$^{bc}$ | 342.20$^{d}$ | 2.772$^{d}$ | 0.606$^{a}$ | 0.772$^{abc}$ | 0.639$^{cd}$ | 0.138$^{a}$ |
| | 10 | 2.309$^{b}$ | 0.180$^{a}$ | 2.385$^{abcd}$ | 3.621$^{d}$ | 1.783$^{e}$ | 239.02$^{f}$ | 2.352$^{b}$ | 0.233$^{ab}$ | 3.271$^{cd}$ | 3.053$^{bcd}$ | 0.471$^{b}$ | 321.60$^{e}$ | 2.940$^{bc}$ | 0.530$^{ab}$ | 0.762$^{abc}$ | 0.710$^{c}$ | 0.152$^{a}$ |
| | 12.5 | 2.105$^{b}$ | 0.188$^{a}$ | 2.026$^{bcd}$ | 4.189$^{c}$ | 1.907$^{d}$ | 211.22$^{h}$ | 2.290$^{b}$ | 0.221$^{ab}$ | 3.229$^{cd}$ | 3.834$^{b}$ | 0.469$^{b}$ | 300.20$^{f}$ | 2.856$^{cd}$ | 0.442$^{bc}$ | 0.702$^{bc}$ | 0.923$^{ab}$ | 0.157$^{a}$ |

Values followed by different letters within a column are significantly different ($p < 0.05$) according to Duncan's new multiple range test.

the direct effects were significant ($p < 0.05$) except for GI on SpW. All the indirect effects were insignificant except for the indirect effect of GNSp on GWP *via* SpW. The total direct effects (0.533) were almost equal to the total indirect effects (0.514). In conclusion, GWP was affected directly and indirectly through interrelationships among yield components.

Heatmap in Figure 4A showed the relationship between the treatments and the studied traits (TSS, FAA, and Pro in shoot and grains). The relationship was constructed based on standardized data using color scale. As the data were measured in different scales, they were standardized by subtracting the mean from each value and dividing by standard deviation. In the heatmap, cells with red color represents high values, while cells with blue color represents low values of the traits.

From the heatmap in Figure 4A, it was clear that high values of Pro (red color) in shoot and grains were found in the treatment with magnetic seawater 12.5 dS m$^{-1}$ while the low values (blue color) were found in the treatment of no magnetic tap water. The highest values of TSS in shoot and grains were found in the treatment with magnetic tap water, while the lowest values were found in the treatment of no magnetic seawater 12.5 dS m$^{-1}$. The lowest values of FAA were in no magnetic tap water, while the highest were in the treatment of magnetic seawater 10 dS m$^{-1}$ for shoot and the treatment of magnetic tap water for grains. It seems that magnetizing seawater increased the Pro in both shoot and grains; however, wheat grain yield was more associated with TSS than FAA and Pro.

Heatmap in Figure 4B shows the relationship between the treatments and GWP, N, P, K, Na, and Cl in shoot, root, and grains as well as Fe in shoot and root. It is clear that GWP was inversely associated with Na and Cl in shoot, root, and grains; however, GWP was positively associated with N, P, and K in shoot, root, and grains as well as Fe in shoot and root.

In conclusion, magnetization was more effective under 5 and 7.5 dS m$^{-1}$ than 10 and 12.5 dS m$^{-1}$ where Na and Cl in shoot and root were decreased and consequently N, P, and K in both shoot and root were increased. These results may be due to the decreasing in water surface tension and viscosity which resulted in an improvement in water uptake (Takatshinko, 1997). Similarly, Elhindi et al. (2020) reported that the magnetizing water in pot marigold plant decreased Na and Cl, but increased N, P, and K.

## Discussion

Water scarcity and drought are increasingly significant environmental challenges impacting both plant growth and human uses. Furthermore, alternative water sources, such as recycled water, brackish water, seawater, and storm water, have been used for irrigation in various parts of the world and for a variety of purposes, including irrigating agricultural crops. Such examples from the current and previous studies showed the challenges associated with higher salinity water irrigation in general, and those which negatively affect wheat crops in particular (Qin and Horvath, 2020; Dolan et al., 2021).

TABLE 6 Effect of seawater stress levels, magnetic treatment on concentration of plant phytohormones in the shoot of wheat plants during the second growing season.

| Characters treatments | | IAA | CK | $GA_3$ | ABA | Activators/ inhibitors ratio |
|---|---|---|---|---|---|---|
| Magnetic treatments | dS $m^{-1}$ | (μg 100 g $FW^{-1}$) | | (mg 100 g $FW^{-1}$) | | |
| No magnetic | Control | 897.38$^{a}$ | 338.7$^{b}$ | 29.68$^{c}$ | 2.55$^{b}$ | 12.124$^{c}$ |
| | 10 | 643.39$^{b}$ | 272.99$^{b}$ | 25.53$^{c}$ | 4.85$^{a}$ | 5.453$^{d}$ |
| Magnetic water | Control | 958.2$^{a}$ | 443.56$^{a}$ | 64.78$^{a}$ | 1.20$^{c}$ | 55.151$^{a}$ |
| | 10 | 683.31$^{b}$ | 442.59$^{a}$ | 54.51$^{b}$ | 1.50$^{bc}$ | 37.091$^{b}$ |

Values followed by different letters within a column are significantly different ($p < 0.05$) according to Duncan's new multiple range test. IAA, indole acetic acid; CKs, cytokinins; $GA_3$, gibberellic acid; ABA, abscisic acid; and FW, fresh weight.

TABLE 7 Effect of seawater stress levels, magnetic treatment, and their interactions on yield attributes of wheat plants during the first and second growing seasons.

| Characters treatments | | SpL (cm) | SpW (g $plant^{-1}$) | GNSp | Grains weight (g $plant^{-1}$) | GI (g) | Straw weight (g $plant^{-1}$) |
|---|---|---|---|---|---|---|---|
| Magnetic treatments | dS $m^{-1}$ | | | | | | |
| First season | | | | | | | |
| No magnetic | Control | 6.40$^{ab}$ | 0.320$^{cd}$ | 8.75$^{cd}$ | 0.352$^{c}$ | 2.500$^{b}$ | 0.409$^{b}$ |
| | 5 | 5.80$^{ab}$ | 0.290$^{d}$ | 6.25$^{ef}$ | 0.180$^{g}$ | 1.500$^{c}$ | 0.335$^{d}$ |
| | 7.5 | 5.80$^{ab}$ | 0.270$^{d}$ | 5.00$^{f}$ | 0.053$^{h}$ | 1.100$^{d}$ | 0.336$^{d}$ |
| | 10 | 5.70$^{ab}$ | 0.270$^{d}$ | 4.75$^{f}$ | 0.040$^{i}$ | 0.750$^{f}$ | 0.323$^{d}$ |
| | 12.5 | 4.00$^{c}$ | 0.130$^{e}$ | 3.00$^{g}$ | 0.031$^{j}$ | 0.375$^{g}$ | 0.271$^{f}$ |
| Magnetic water | Control | 7.00$^{a}$ | 0.460$^{a}$ | 12.25$^{a}$ | 0.560$^{a}$ | 3.500$^{a}$ | 0.471$^{a}$ |
| | 5 | 6.80$^{ab}$ | 0.430$^{ab}$ | 10.75$^{ab}$ | 0.398$^{b}$ | 2.500$^{b}$ | 0.365$^{c}$ |
| | 7.5 | 6.90$^{ab}$ | 0.380$^{abc}$ | 9.75$^{bc}$ | 0.340$^{d}$ | 1.500$^{c}$ | 0.361$^{c}$ |
| | 10 | 6.60$^{ab}$ | 0.350$^{bcd}$ | 7.50$^{ed}$ | 0.315$^{e}$ | 1.025$^{d}$ | 0.357$^{c}$ |
| | 12.5 | 5.60$^{b}$ | 0.290$^{d}$ | 5.50$^{f}$ | 0.300$^{f}$ | 0.925$^{e}$ | 0.307$^{e}$ |
| Second season | | | | | | | |
| No magnetic | Control | 10.50$^{bc}$ | 0.384$^{cd}$ | 13.40$^{c}$ | 0.285$^{de}$ | 2.132$^{bc}$ | 1.307$^{cd}$ |
| | 5 | 10.70$^{bc}$ | 0.341$^{ef}$ | 10.80$^{d}$ | 0.221$^{ef}$ | 2.070$^{bc}$ | 1.016$^{ef}$ |
| | 7.5 | 10.30$^{c}$ | 0.381$^{fg}$ | 11.60$^{d}$ | 0.201$^{f}$ | 1.975$^{c}$ | 0.819$^{fg}$ |
| | 10 | 9.10$^{d}$ | 0.323$^{h}$ | 8.40$^{e}$ | 0.151$^{fg}$ | 1.962$^{c}$ | 0.444$^{h}$ |
| | 12.5 | 9.00$^{d}$ | 0.168$^{g}$ | 4.80$^{g}$ | 0.090$^{g}$ | 1.923$^{c}$ | 0.714$^{g}$ |
| Magnetic water | Control | 13.60$^{a}$ | 1.207$^{a}$ | 27.00$^{a}$ | 1.013$^{a}$ | 3.018$^{a}$ | 2.900$^{a}$ |
| | 5 | 11.50$^{b}$ | 0.710$^{b}$ | 19.60$^{b}$ | 0.683$^{b}$ | 2.856$^{a}$ | 2.061$^{b}$ |
| | 7.5 | 10.70$^{bc}$ | 0.772$^{c}$ | 18.80$^{b}$ | 0.518$^{c}$ | 2.792$^{a}$ | 1.495$^{c}$ |
| | 10 | 10.50$^{bc}$ | 0.579$^{de}$ | 13.20$^{c}$ | 0.366$^{d}$ | 2.713$^{ab}$ | 1.100$^{de}$ |
| | 12.5 | 10.20$^{c}$ | 0.256$^{de}$ | 6.40$^{f}$ | 0.164$^{fg}$ | 2.531$^{abc}$ | 1.140$^{de}$ |

Values followed by different letters within a column are significantly different ($p < 0.05$) according to Duncan's new multiple range test. SpL, spike length; SpW, spike weight; GNSp, grains number $spike^{-1}$; and GW, 100 grains weight.

The magnetic technology examined in this study was found to have a strong positive effect and alleviated the adverse effects of seawater irrigation on all the previously examined characteristics of wheat plant Sakha 93. In addition, the endogenous composition of the flag leaf and stem of wheat plants developed below seawater stress subjected to a magnetic field should be evaluated in comparison to the control.

Previous studies have found that irrigation with salt water considerably lowered the FW and DW of wheat and rice seedlings (Jasim et al., 2017). This negative effect of saline water on germination could be attributed to a decrease in leaf water potential, photosynthesis, and cell membrane degradation (Table 3; Supplementary Table S2). According to Parvanova et al. (2004), salt stress induces the formation of ROS, which causes oxidative damage to membrane lipids, proteins, and nucleic acids when available at high concentrations. This study found that at all seawater salinity levels, irrigation with magnetically treated seawater resulted in dramatic increases in all germination parameters compared with those in non-magnetic treatments.

TABLE 8 Effect of seawater stress levels, magnetic treatment on some anatomical parameters in flag leaf and stem of wheat plants during the second growing season.

| Treatments characters | | 0.40 dS $m^{-1}$ (Control) | | | 10 dS $m^{-1}$ | | | | |
|---|---|---|---|---|---|---|---|---|---|
| | | No magnetic | Magnetic water | ±% to control | No magnetic | ±% to control | Magnetic water | ±% to control | ±% to (10 dS $m^{-1}$) |
| Flag leaf | Lamina thickness (μm) | 170$^{ab}$ | 200$^{a}$ | +18 | 120$^{c}$ | −29 | 140$^{bc}$ | −18 | +17 |
| | Midrib thickness (μm) | 340$^{b}$ | 420$^{a}$ | +24 | 200$^{d}$ | −41 | 280$^{c}$ | −18 | +40 |
| | Midvein bundle dimensions (μm) | 120.7$^{b}$ | 154.5$^{a}$ | +28 | 107.9$^{b}$ | −11 | 116.2$^{b}$ | −4 | +8 |
| | Metaxylem vessel diameter (μm) | 29.6$^{b}$ | 47.4$^{a}$ | +60 | 16.6$^{c}$ | −44 | 33.2$^{b}$ | +12 | +100 |
| Stem | Stem diameter (mm) | 2.80$^{ab}$ | 3.22$^{a}$ | +15 | 1.68$^{b}$ | −39 | 1.96$^{b}$ | −30 | +15 |
| | Stem cavity diameter (mm) | 149$^{a}$ | 2.48$^{b}$ | +66 | 0.94$^{b}$ | −40 | 1.24$^{b}$ | −17 | +38 |
| | Number of vascular bundle cross section$^{-1}$ | 56$^{ab}$ | 69$^{a}$ | +23 | 38$^{b}$ | −32 | 49$^{b}$ | −13 | +29 |
| | Vascular bundle thickness (μm) | 100.2$^{c}$ | 175.8$^{a}$ | +75 | 88.0$^{c}$ | −12 | 122.2$^{b}$ | +22 | +39 |
| | Metaxylem vessel diameter (μm) | 23.5$^{c}$ | 45.6$^{a}$ | +94 | 18.5$^{c}$ | −21 | 32.0$^{b}$ | +36 | +73 |

Values followed by different letters within a column are significantly different ($p < 0.05$) according to Duncan's new multiple range test.

Utilizing magnetically treated seawater increased the germination index and VI by approximately 49% and 31%, respectively, compared to untreated seeds under 7.5 dS $m^{-1}$ salinity stress. Similar findings in Neva (poplar trees) where the irrigation with magnetically treated salt water boosted relative growth rate and leaf area of seedlings compared to non-magnetically treated salt water irrigation (Liu et al., 2019). This could be attributed to the effects of magnetic energy, which raise TWC and nutrient absorption (N, P, K, and Fe) through increases in the pH and reductions in the EC (Takatshinko, 1997; Tables 3 and 5). This effect resulted in improvements in the photosynthesis process and increases in products transfer in seedlings.

Turhan et al. (2014) have also reported similar results, demonstrating a substantial decrease in lettuce growth and DM when salt concentrations increased in irrigation water. When comparing low and high seawater levels, it was found that diluted seawater promoted *Conocarpus erectus* growth (El-Mahrouk et al., 2010). This finding may result from the fact that salinity inhibits photosynthesis, respiration, and protein synthesis, as well as causing higher osmotic pressure, lack of absorbed water, and harmful salt and chloride accumulation (Ferrante et al., 2011). Thus, all growth characteristics of wheat plants irrigated with magnetic seawater increased significantly.

Surendran et al. (2016) have observed that magnetic treatment of normal and saline water improved cow pea growth parameters. The positive effect of magnetism on plant growth characteristics may be attributed to the lower water surface tension and solubility (Takatshinko, 1997), and faster enzyme and hormone synthesis during the growth process (Selim et al., 2019). Thus, this may result in improved nutrient mobilization and transportation, and enhancing cell enlargement and vegetative growth.

Our results in Table 3 were consistent with those of Tuna et al. (2008), who previously reported that RWC was decreased when salinity levels increased in maize plants. The deleterious effect of seawater on the water relations and membrane integrity in wheat plants could possibly be due to the accumulation of toxic ions in leaves to harmful levels; thus, resulting in a significant reduction in water uptake which then leads to slower growth (Munns, 2002). Under salt stress, closing stomata, thickening of the leaf blade and epidermal cell diameters, increasing leaf mass per unit area, and rolling leaves, all reduce water transpiration and intracellular $CO_2$

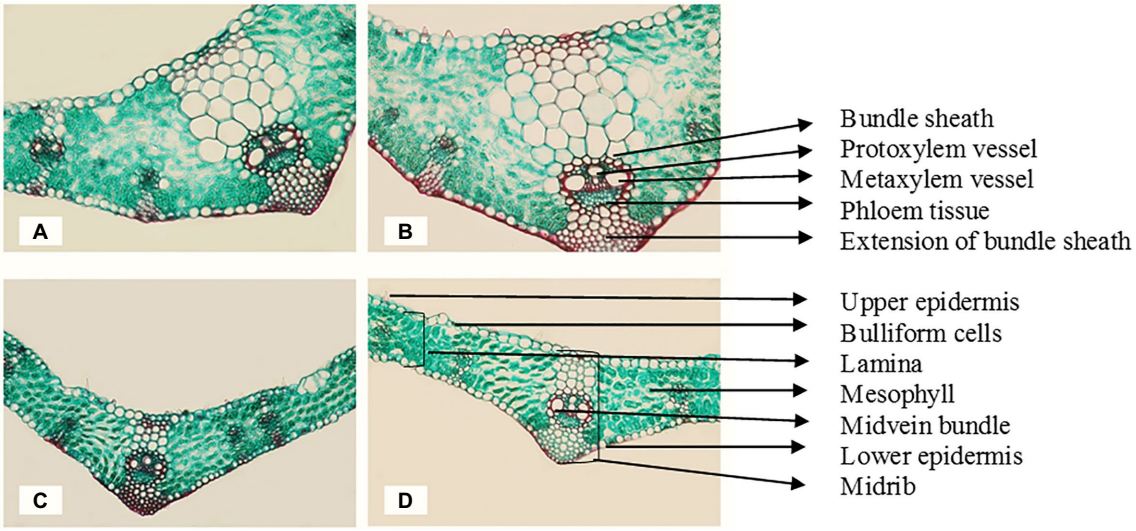


FIGURE 1
Transverse cross sections of the marginal part of the flag leaf blade at the main stem of wheat cv. Sakha 93 at the heading stage (X 300). **(A)** Control (from plants irrigated with normal tap water); **(B)** magnetic treatment (from plants irrigated with magnetized water); **(C)** seawater treatment (from plants irrigated with seawater at 10 dS $m^{-1}$ level); **(D)** magnetic seawater treatment (from plants irrigated with magnetized seawater at 10 dS $m^{-1}$ level).

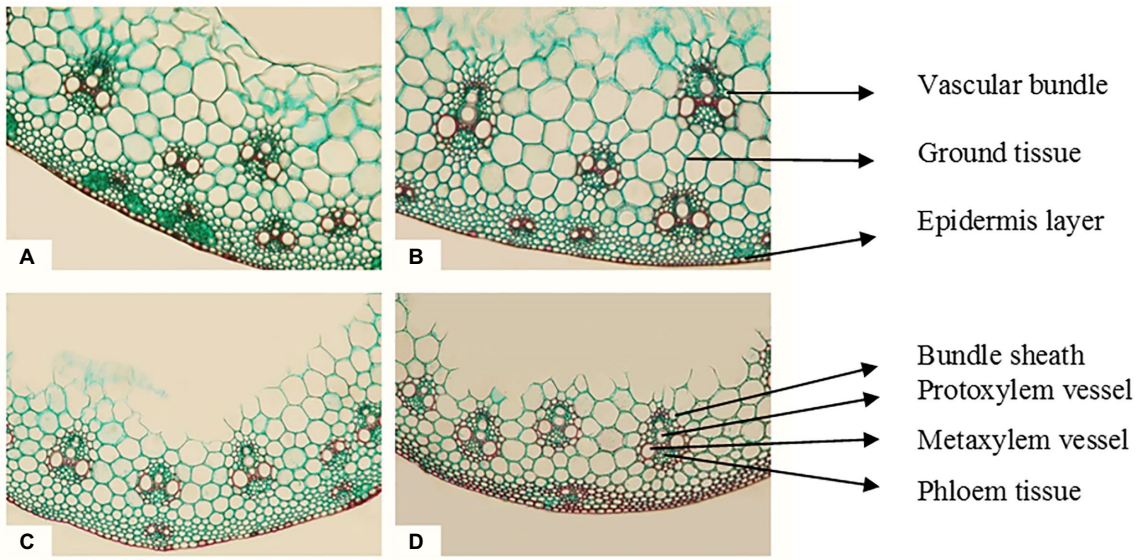


FIGURE 2
Transverse cross sections of the main stem of wheat cv. Sakha 93 at the heading stage (X 300). **(A)** Control (from plants irrigated with normal tap water); **(B)** magnetic treatment (from plants irrigated with magnetized water); **(C)** seawater treatment (from plants irrigated with seawater at 10 dS $m^{-1}$ level); **(D)** magnetic seawater treatment (from plants irrigated with magnetized seawater at 10 dS $m^{-1}$ level).

levels (Koundouras et al., 2008). The magnetic water irrigation in the second season of the current study; however, resulted in a substantial increase ($p < 0.05$) in TWC, osmotic pressure and MI; while LWD and TR were both reduced by approximately 12% and 16%, respectively, when irrigated with 10 dS $m^{-1}$ seawater. According to our data, the obtained results in both seasons were almost similar in this study. These findings were in-line with Liu et al. (2019) of which magnetically treated water and magnetically treated saline water reduced TR when compared to controls. Lower surface tension, higher permeability, and lower hydrogen ions (Takatshinko, 1997), as well as an increase in the number and thickness of vessels in plant leaves and stems, might explain the observed improvements in water relations under seawater stress when utilizing magnetically treated water (Selim et al., 2019).

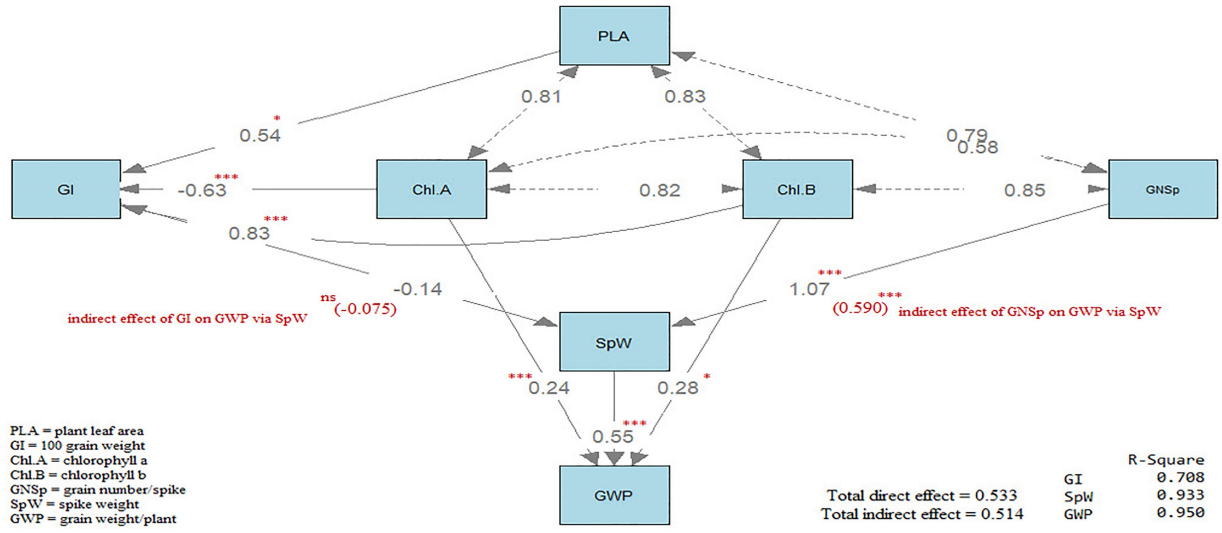


FIGURE 3
Path diagram showing the direct and indirect effects on wheat grain yield.

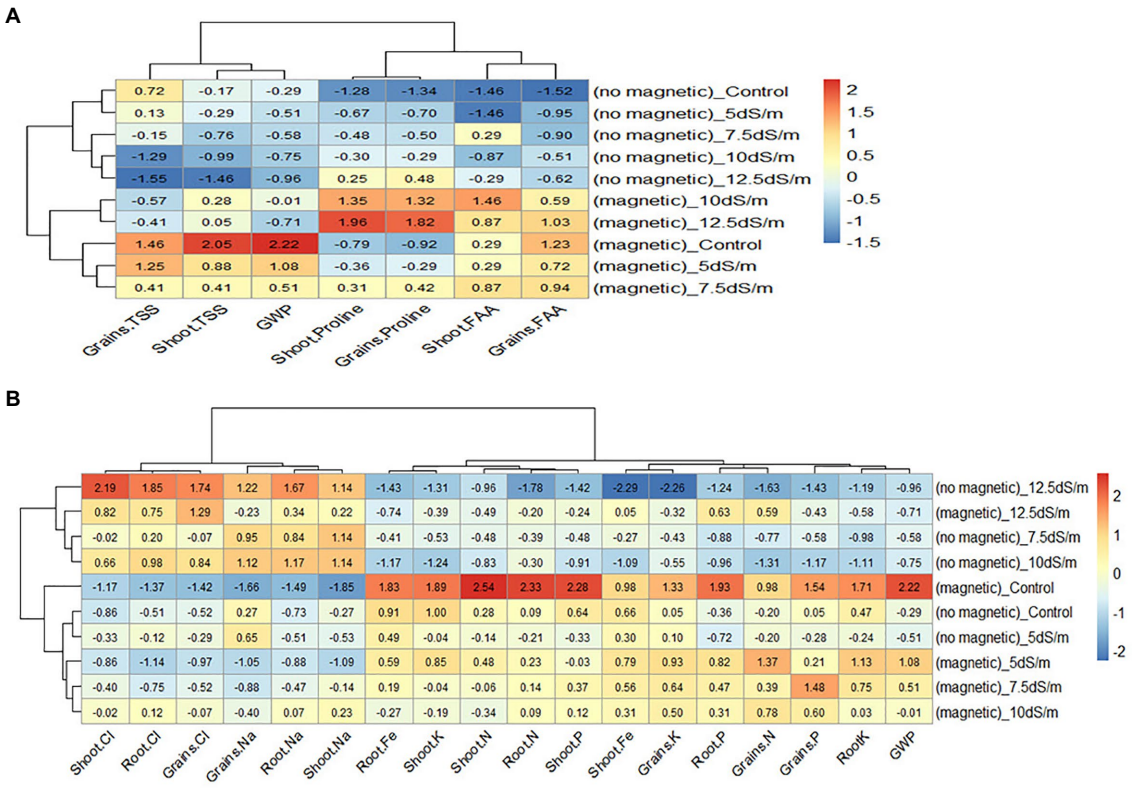


FIGURE 4
Heatmap of the relationship between the treatments and related parameters. The relationship between the treatments and the studied **(A)** traits and **(B)** nutrients. TSS, total soluble sugars; GWP, grain yield/plant; FAA, free amino acids.

Salt stress reduced the Chl content of maize plants (Tuna et al., 2008); thus, it was consistent with our findings in the present study (Supplementary Table S1). The concentration of $Na^+$ in seawater can damage the membrane system, decrease cell osmotic potential, stomatal conductance, gas exchange, and the absorption of iron ions. This is involved in Chl-protein production; and therefore, this

resulted in a decrease in the photosynthetic rate (Tuna et al., 2008; Supplementary Table S2; Table 5). The use of magnetically treated seawater, on the other hand, resulted in a considerable increase in photosynthetic pigments in wheat plant leaves. In magnetically treated seawater of 12.5 dS $m^{-1}$, the increase in total Chl *a* + *b*, Car, and UVAS was approximately 25%, 38%, and 33%, respectively, compared to the controls in the first season. The same trend was also observed during the second season. Liu et al. (2019) have shown that both magnetic tap water and saline water can improve the net photosynthetic rate of Neva plants when compared to the control. The enhancing effects of magnetically treated water could be due to the increases in protein production, enzyme activity, $K^+$ levels and $GA_3$ concentrations (Selim et al., 2009).

Our findings illustrated in Table 4 on wheat match those of Amuthavalli et al. (2012) when NaCl treatment can reduce the total sugar concentration in cotton (*Gossypium*). In their study, it was found that cotton plants synthesized Pro, aspartic acids, stress-related proteins, and enzyme levels using N ions when were under salinity stress. The patterns of grain measurements were similar to those examined in this study. These findings were consistent with those of Selim et al. (2019), claiming that the soluble sugar, total free amino acids, and Pro levels of wheat plants improved after magnetic treatments. Because soluble sugars and Pro accumulation can operate as osmoregulators, which stabilize cellular membranes and sustain turgor in response to increased salt levels, such increases could be a defense mechanism resulting in elevated osmotic pressure.

Tuna et al. (2008) have found that salt stress increased the antioxidant enzyme activity of peroxidase and polyphenol in maize plants, which normally protects them from the detrimental effects of activated oxygen species and salinity stress. Magnetic water at 12.5 dS $m^{-1}$ was found to boost phenoloxidase and peroxidase enzyme activity in wheat plant leaves by approximately 24% and 26%, respectively, compared to the controls. Similarly, magnetic treatments increased the activity of the enzymes phenoloxidase and peroxidase in potato plants (Selim, 2019). When seawater levels elevated, macro- and micro-minerals in wheat plants and grains declined. Similarly, the treatment of high seawater levels decreased N, P, K, and Fe contents in spinach compared to that of low seawater levels (Turhan et al., 2014). On the other hand, irrigation with seawater caused a significant increase in Na content, resulting in an increase in the Na/K ratio in spinach plants. Irrigation with magnetically treated water enhanced the mineral contents of N, P, K, Fe, Zn, and Cu, but decreased $Na^+$ and $Cl^-$ levels in *Calendula officinalis* leaves (Elhindi et al., 2020). The reduction in the surface tension and viscosity of water, which increases the absorption of water and nutrients, as well as affecting many biosynthetic processes, could be related to the favorable effects of magnetically treated water (Takatshinko, 1997).

Salt stress has been shown to reduce plant hormones involved in cellular division, which has a negative impact on plant growth (Munns, 2002). Using magnetic technology, on the other hand, resulted in a considerable increase in the plant phytohormone concentrations in wheat plant shoots. Under seawater levels of 10 dS $m^{-1}$, the concentrations of IAA, CKs and $GA_3$ increased by approximately 6%, 62%, and 114%, respectively; whereas ABA decreased by 69%. These findings were aligned with those of Mousa et al. (2013) in wheat plants cultivated under salt soil stress, when magnetic treatments increased the concentrations of IAA, kinetin (CK) and $GA_3$ but decreased the concentration of ABA in the shoot. Similarly, Turhan et al. (2014) have demonstrated that irrigation with seawater may result in reduced yield in lettuce. This could be attributed to the role of seawater in reducing water absorption, necessary nutrients and photosynthetic processes associated with high osmotic pressure of saline water (Tuna et al., 2008) as well as the inhibition of growth hormones (Table 6). Thus, this could have an effect on suppressing the vegetative growth and yield in wheat plant.

Our results were also consistent with what was found previously in potato (Mostafa, 2020) and cow pea (Surendran et al., 2016) plants, when the electromagnetic treatment of saline water has led to lessen the detrimental effects of salt while simultaneously increasing yield. This might be due to the fact of the involvement of magnetic water under seawater stress in enhancing photosynthetic pigments, water intake, nutrient availability, osmoregulatory chemicals, enzyme activity, and growth regulators. The physical and chemical features of magnetically treated water, including factors such as surface tension, polarity, hydrogen bonding, conductivity, salt solubility and pH, may be responsible for the observed improvements in physiological, growth, and yield factors (Takatshinko, 1997).

It has been reported that diluted saltwater up to 30% enhanced most stem and leaf structural parameters (El-Mahrouk et al., 2010). Similar results were also observed in the current study. Furthermore, seawater has been shown to inhibit plant hormone regulation of cellular division, which has a negative impact on plant growth (Munns, 2002). Moreover, the decrease in DNA content and CKs has led to the inhibition of cambial cell activity; consequently, reduced cell division and expansion as well as reduced leaf and stem diameters (Matsumoto-Kitano et al., 2008). Aligned with the magnetic approach used, Mousa et al. (2013) have revealed increased thickness of stems, leaves, metaxylem arteries, and vascular bundles in plants exposed to salt soil stress. Magnetic water increased the plant phytohormones (IAA, CKs, and $GA_3$; Table 6), water uptake (Table 3), and elements absorption (Table 5), which enhanced the photoassimilate translocation and improved anatomical parameters (Aloni, 1995).

## Conclusion

The germination, growth, physiological, biochemical, and morphological features of the wheat cultivar (Sakha 93) were all negatively affected by irrigation with normal (non-magnetic) seawater. Magnetic technology, on the other hand, alleviated the negative effects of seawater stress on all the characteristics evaluated. Consequently, the GWP of wheat plants increased by approximately three-fold compared to the controls after applying a magnetic field. Therefore, the use of magnetically treated

seawater of up to a level of 7.5 dS $m^{-1}$ for wheat irrigation is recommended to replace the fresh tap water irrigation.

## Data availability statement

The original contributions presented in the study are included in the article/Supplementary material, and further inquiries can be directed to the corresponding authors.

## Author contributions

DS, MZ, KE-T, SA, and SE conceived and designed the research. ME-S, KE-T, SA, and SE supervised the study. DS, MA, HE, AE-T, and OI performed field experiments. DS, MZ, MA, ME-S, AE-T, and OI developed the biochemical and physiological analyses. DS, MB, KE-T, SA, and SE analyzed the data. MB and ME-S assisted with experiments and/or data evaluation. DS, KE-T, and SA wrote the manuscript. All authors contributed to the article and approved the submitted version.

## Funding

This project was funded by the Abu Dhabi Research Award (AARE2019) for Research Excellence-Department of Education and Knowledge (ADEK; grant number 21S105) to KE-T and Khalifa Center for Biotechnology and Genetic Engineering-UAEU (grant number 31R286) to SA.

## Acknowledgments

KE-T would like to thank the library at Murdoch University, Australia, for the valuable online resources and comprehensive databases.

## Conflict of interest

The authors declare that the research was conducted in the absence of any commercial or financial relationships that could be construed as a potential conflict of interest.

## Publisher's note

All claims expressed in this article are solely those of the authors and do not necessarily represent those of their affiliated organizations, or those of the publisher, the editors and the reviewers. Any product that may be evaluated in this article, or claim that may be made by its manufacturer, is not guaranteed or endorsed by the publisher.

## Supplementary material

The Supplementary materials for this article can be found online at: https://www.frontiersin.org/articles/10.3389/fpls.2022.923872/full#supplementary-material

## References

Abdul-Baki, A. A., and Anderson, J. D. (1973). Vigor determination in soybean seed by multiple criteria. *Crop. Sci.* 13, 630–633. doi: 10.2135/cropsci1973.0011183X001300060013x

Aloni, R. (1995). "The induction of vascular tissues by auxin," in *Plant Hormones: Physiology, Biochemistry and Molecular Biology. 3rd Edn.* P. J. Davies. (Dordrecht: Kluwer Academic Publishers), 471–492.

Amuthavalli, P., Anbu, D., and Sivasankatamoorthy, S. (2012). Effect of calcium chloride on growth and biochemical constituents of cotton (*Gossypium hirsutum* L.) under salt stress. *Int. J. Res. Bot.* 2, 9–12.

AOAC (1995). *Official Methods of Analysis, 16*th. Arlington, VA, United States of America: Association of Official Analytical Chemists.

Bates, L. S., Waldren, R. P., and Teare, I. D. (1973). Rapid determination of free proline for water-stress studies. *Plant Soil* 39, 205–207. doi: 10.1007/BF00018060

Crozier, A., and Moritz, T. (1999). "Physico-chemical methods of plant hormone analysis," in *Biochemistry and Molecular Biology of Plant Hormones*. eds. P. J. J. Hooykaas, M. A. Hall and K. R. Libbenga (Amsterdam: Elsevier), 23–60.

Dolan, F., Lamontagne, J., Link, R., Hejazi, M., Reed, P., and Edmonds, J. (2021). Evaluating the economic impact of water scarcity in a changing world. *Nat. Commun.* 12:1915. doi: 10.1038/s41467-021-22194-0

Elhindi, K. M., Al-Mana, F. A., Algahtani, A. M., and Alotaibi, M. A. (2020). Effect of irrigation with saline magnetized water and different soil amendments on growth and flower production of *Calendula officinalis* L. plants. *Saudi J. Biol. Sci.* 27, 3072–3078. doi: 10.1016/j.sjbs.2020.09.015

Ellis, R. H., and Roberts, E. H. (1981). The quantification of ageing and survival in orthodox seeds. *Seed Sci. Technol.* 9, 373–409.

El-Mahrouk, M. E., El-Nady, M. F., and Hegazi, M. A. (2010). Effect of diluted seawater irrigation and exogenous proline treatments on growth, chemical composition and anatomical characteristics of (*Conocarpus erectus* L.). *J. Agric. Res. Kafrelsheikh Uni.* 36, 420–446.

Fadeel, A. A. (1962). Location and properties of chloroplasts and pigment determination in roots. *Physiol. Plant.* 15, 130–146. doi: 10.1111/j.1399-3054.1962.tb07994.x

FAOSTAT (2018). Food and agriculture data. Available at: http://digital.library.wisc.edu/1711.web/faostat (Accessed April 12, 2022).

Ferrante, A., Trivellini, A., Malorgio, F., Carmassi, G., Vernieri, P., and Serra, G. (2011). Effect of seawater aerosol on leaves of six plant species potentially useful for ornamental purposes in coastal areas. *Sci. Hortic.* 128, 332–341. doi: 10.1016/j.scienta.2011.01.008

Gardner, F. P., Pearce, R. B., and Mitchell, R. L. (2017). *Physiology of Crop Plants*. Rajasthan: Scientific Publishers. New Delhi, India. 327 pp.

Gossev, N. A. (1960). *Some Methods in Studying Plant Water Relations*. Leningrad Acad. Sci. USSR.

Jasim, A. H., Al-taee, Y. I., Atab, H. A., and Abdulhusain, M. A. (2017). Effect of saline water magnetization on growth and development of wheat and rice seedlings. *Euphrates J. Agri. Sci.* 9, 1–12.

Kalapos, T. (1994). Leaf water potential-leaf water deficit relationship for ten species of semiarid grassland community. *Plant Soil* 160, 105–112. doi: 10.1007/BF00150351

Kar, M., and Mishra, D. (1976). Catalase, peroxidase, and polyphenoloxidase activities during rice leaf senescence. *Plant Physiol.* 57, 315–319. doi: 10.1104/pp.57.2.315

Koundouras, S., Tsialtas, I. T., Zioziou, E., and Nikolaou, N. (2008). Rootstock effects on the adaptive strategies of grapevine (*Vitis vinifera* L. cv. Cabernet-sauvignon) under contrasting water status: leaf physiological and structural responses. *Agric. Ecosyst. Environ.* 128, 86–96. doi: 10.1016/j.agee.2008.05.006

Kreeb, K. H. (1990). *Methoden zur Pflanzenökologie und Bioindikation*. New York: Gustav Fischer Verlag.

Leopold, A. C., Musgrave, M. E., and Williams, K. M. (1981). Solute leakage resulting from leaf desiccation. *Plant Physiol.* 68, 1222–1225. doi: 10.1104/pp.68.6.1222

Lichtenthaler, H. K. (1987). Chlorophylls and carotenoids: pigments of photosynthetic biomembranes. *Methods Enzymol.* 148, 350–382. doi: 10.1016/0076-6879(87)48036-1

Liu, X., Zhu, H., Meng, S., Bi, S., Zhang, Y., Wang, H., et al. (2019). The effects of magnetic treatment of irrigation water on seedling growth, photosynthetic capacity and nutrient contents of *Populus* × *euramericana* 'Neva' under NaCl stress. *Acta Physiol. Plant.* 41:11. doi: 10.1007/s11738-018-2798-1

Lohaus, G., Hussmann, M., Pennewiss, K., Schneider, H., Zhu, J. J., and Sattelmacher, B. (2000). Solute balance of a maize (*Zea mays* L.) source leaf as affected by salt treatment with special emphasis on phloem retranslocation and ion leaching. *J. Exp. Bot.* 51, 1721–1732. doi: 10.1093/jexbot/51.351.1721

Lunin, J., Gallatin, M. H., and Batchelder, A. R. (1961). Effect of stage of growth at time of salinization on the growth and chemical composition of beans: II. Salinization in one irrigation compared with gradual salinization. *Soil Sci.* 92, 194–201. doi: 10.1097/00010694-196109000-00009

Matsumoto-Kitano, M., Kusumoto, T., Tarkowski, P., Kinoshita-Tsujimura, K., Václavíková, K., Miyawaki, K., et al. (2008). Cytokinins are central regulators of cambial activity. *Proc. Natl. Acad. Sci. USA.* 105, 20027–20031. doi: 10.1073/pnas.0805619105

Mostafa, H. (2020). Influence of magnetised irrigation water on the fertigation process and potato productivity. *Res. Agric. Eng.* 66, 43–51. doi: 10.17221/1/2020-RAE

Mousa, E. M., Gendy, A. A., Maria, A. M., and Selim, D. A. (2013). Physio-anatomical responses of salinity stressed wheat plants to magnetic field. *Minufiya J. Agric. Res.* 38, 31–41.

Munns, R. (2002). "Salinity, growth and phytohormones," in *Salinity: Environment-Plants-Molecules*. eds. A. Läuchli and U. Lüttge (Dordrecht: Springer), 271–290.

Nassar, M. A., and El-Sahhar, K. F. (1998). *Botanical Preparations and Microscopy (Microtechnique)*. Giza: Acad. Bookshop.

Nerd, A., and Pasternak, D. (1992). Growth, ion accumulation, and nitrogen fractioning in *Atriplex barclayana* grown at various salinities. *J. Range Manage.* 45, 164–166. doi: 10.2307/4002776

Parvanova, D., Ivanov, S., Konstantinova, T., Karanov, E., Atanassov, A., Tsvetkov, T., et al. (2004). Transgenic tobacco plants accumulating osmolytes show reduced oxidative damage under freezing stress. *Plant Physiol. Biochem.* 42, 57–63. doi: 10.1016/j.plaphy.2003.10.007

Qin, Y., and Horvath, A. (2020). Use of alternative water sources in irrigation: potential scales, costs, and environmental impacts in California. *Environ. Res. Commun.* 2:05500. doi: 10.1088/2515-7620/ab915e

SAS (2014). *SAS User's Guide: Basics*. North Carolina: Institute Statistical Analysis System.

Scott, S. J., Jones, R. A., and Williams, W. A. (1984). Review of data analysis methods for seed germination. *Crop. Sci.* 24, 1192–1199. doi: 10.2135/cropsci1984.0011183X002400060043x

Selim, D. A. F. H. (2019). Physiological response and productivity of potato plant (*Solanum tuberosum* L.) to irrigation with magnetized water and application of different levels of NPK fertilizers. *Middle East J. Agric. Res.* 8, 237–254.

Selim, D. A., Gendy, A. A., Maria, A. M., and Mousa, E. M. (2009). "Response of pepper plants (*Capasicum annuum* L.) to magnetic technologies," in *Proceedings of the First Nile Delta Conference on Export Crops (Improvement and Protection of the Egyptian Export Crops)* (Al Minufya: Menufiya University), 89–104.

Selim, D. A. F. H., Nassar, R. M. A., Boghdady, M. S., and Bonfill, M. (2019). Physiological and anatomical studies of two wheat cultivars irrigated with magnetic water under drought stress conditions. *Plant Physiol. Biochem.* 135, 480–488. doi: 10.1016/j.plaphy.2018.11.012

Shehab-El-Din, T., Mitkees, R. A., and El-Shami, M. A. (1999). Sakha 93 and Giza 168: two new high yielding and rust diseases resistant bread wheat cultivars. *Mansoura Univ. J. Agric. Sci.* 24, 2157–2168.

Simane, B., Peacock, J. M., and Struik, P. C. (1993). Differences in developmental plasticity and growth rate among drought-resistant and susceptible cultivars of durum wheat (*Triticum turgidum* L. var. durum). *Plant Soil* 157, 155–166. doi: 10.1007/BF00011044

Surendran, U., Sandeep, O., and Joseph, E. J. (2016). The impacts of magnetic treatment of irrigation water on plant, water and soil characteristics. *Agric. Water Manag.* 178, 21–29. doi: 10.1016/j.agwat.2016.08.016

Tabachnick, B. G., and Fidell, L. S. (1996). *Using Multivariate Statistics*. New York: HarperCollins College Publishers.

Takatshinko, Y. (1997). "Hydromagnetic systems and their role in creating micro climate," in *Proceedings of the International Symposium on Sustainable Management of Salt Affected Soils in the Arid Ecosystem*, ed. A.M. Elgala (Cairo: ISSS-ESSS). 28.

Tuna, A. L., Kaya, C., Dikilitas, M., and Higgs, D. (2008). The combined effects of gibberellic acid and salinity on some antioxidant enzyme activities, plant growth parameters and nutritional status in maize plants. *Environ. Exp. Bot.* 62, 1–9. doi: 10.1016/j.envexpbot.2007.06.007

Turhan, A., Kuscu, H., Ozmen, N., Serbeci, M. S., and Demir, A. O. (2014). Effect of different concentrations of diluted seawater on yield and quality of lettuce. *Chil. J. Agric. Res.* 74, 111–116. doi: 10.4067/S0718-58392014000100017

Tyagi, N. K., Agrowal, A., Sakthivadel, R., and Ambrest, S. K. (2005). Water management decisions on small farms under scarce canal water supply. A case study from NW India. *Agric. Water Manag.* 77, 180–195. doi: 10.1016/j.agwat.2004.09.031

Wang, Y., Zhang, B., Gong, Z., Gao, K., Ou, Y., and Zhang, J. (2013). The effect of a static magnetic field on the hydrogen bonding in water using frictional experiments. *J. Mol. Struct.* 1052, 102–104. doi: 10.1016/j.molstruc.2013.08.021

frontiers | Frontiers in Plant Science

TYPE Original Research
PUBLISHED 23 September 2022
DOI 10.3389/fpls.2022.973419



OPEN ACCESS

EDITED BY
Amr Adel Elkelish,
Suez Canal University,
Egypt

REVIEWED BY
Ganesh Chandrakant Nikalje,
R. K. Talreja College of Arts, Science and Commerce, India
Bhaskar Gupta,
Government General Degree College, Singur, India

*CORRESPONDENCE
Jianjun Chen
jjchen@ufl.edu
Xiangying Wei
xiangyingwei@mju.edu.cn

†These authors have contributed equally to this work

SPECIALTY SECTION
This article was submitted to Plant Abiotic Stress, a section of the journal Frontiers in Plant Science

RECEIVED 20 June 2022
ACCEPTED 23 August 2022
PUBLISHED 23 September 2022

CITATION
Wang D, Yang N, Zhang C, He W, Ye G, Chen J and Wei X (2022) Transcriptome analysis reveals molecular mechanisms underlying salt tolerance in halophyte *Sesuvium portulacastrum*. *Front. Plant Sci.* 13:973419. doi: 10.3389/fpls.2022.973419



# Transcriptome analysis reveals molecular mechanisms underlying salt tolerance in halophyte *Sesuvium portulacastrum*

Dan Wang[1,2†], Nan Yang[1,2†], Chaoyue Zhang[1,2], Weihong He[1,2], Guiping Ye[1,2], Jianjun Chen[3*] and Xiangying Wei[1,2*]

[1]Institute of Oceanography, College of Geography and Oceanography, Minjiang University, Fuzhou, China, [2]Fuzhou Institute of Oceanography, Fuzhou, China, [3]Department of Environmental Horticulture, Mid-Florida Research and Education Center, Institute of Food and Agricultural Sciences, University of Florida, Apopka, FL, United States

Soil salinity is an important environmental problem that seriously affects plant growth and crop productivity. Phytoremediation is a cost-effective solution for reducing soil salinity and potentially converting the soils for crop production. *Sesuvium portulacastrum* is a typical halophyte which can grow at high salt concentrations. In order to explore the salt tolerance mechanism of *S. portulacastrum*, rooted cuttings were grown in a hydroponic culture containing ½ Hoagland solution with or without addition of 400 mM Na for 21 days. Root and leaf samples were taken 1 h and 21 days after Na treatment, and RNA-Seq was used to analyze transcript differences in roots and leaves of the Na-treated and control plants. A large number of differentially expressed genes (DEGs) were identified in the roots and leaves of plants grown under salt stress. Several key pathways related to salt tolerance were identified through KEGG analysis. Combined with physiological data and expression analysis, it appeared that cyclic nucleotide gated channels (CNGCs) were implicated in Na uptake and $Na^+/H^+$ exchangers (NHXs) were responsible for the extrusion and sequestration of Na, which facilitated a balance between $Na^+$ and $K^+$ in *S. portulacastrum* under salt stress. Soluble sugar and proline were identified as important osmoprotectant in salt-stressed *S. portulacastrum* plants. Glutathione metabolism played an important role in scavenging reactive oxygen species. Results from this study show that *S. portulacastrum* as a halophytic species possesses a suite of mechanisms for accumulating and tolerating a high level of Na; thus, it could be a valuable plant species used for phytoremediation of saline soils.

KEYWORDS

**salt tolerance, *Sesuvium portulacastrum*, transcriptomic analysis, differentially expressed genes, ion transport**

## Introduction

Soil salinization is a soil degradation process and considered as one of the most important global issues (Zelm et al., 2020). Excessive salt, mainly sodium (Na) can affect the decomposition of soil aggregates, deplete soil nutrients, and lead to deteriorate soil structure and soil quality, thereby threatening crop production and the environment (Qadir et al., 2001). Globally, about 831 million hectares of land were affected by salinization (Butcher et al., 2016), of which 23.35% is located in Asia (FAO, 2015). Currently, soil salinization takes up to 1.5 million hectares of farmland per year out of crop production (FAO, 2015). Land restoration under the influence of severe salinization is the key to land resource management and sustainable development. Among the strategies, phytoremediation is regarded as an important strategy for the restoration of saline soils because of its cost-effective and environmentally friendly characteristics (Ashraf et al., 2010; Imadi et al., 2016). Halophytes are naturally salt-tolerant plants and have been used in the reclamation of saline-alkali land based on the characteristics of salt accumulation in their leaves and stems (Ayyappan and Ravindran, 2014; Hasanuzzaman et al., 2014; Hayat et al., 2020). Exploring salt tolerance mechanisms of halophytes could assist in our effort on the use of this group of plants for remediation of saline soils.

Halophytes usually live in intertidal zone or inland saline soil. Unlike glycophytes, halophytes can complete their life cycle when grown in seawater or high-salt soils (Chen et al., 2016). Salt stress generally causes excessive accumulation of $Na^+$ in plants, resulting in osmotic stress and ion toxicity and inhibiting plant growth (Hasegawa et al., 2000; Rana and Mark, 2008). To adapt to the high-salt environments, while sharing the salt tolerance mechanism with glycophytes, halophytes have evolved special features. For example, osmotic protection is a general response to salt that maintains cell osmotic pressure and turgor pressure through osmotic regulation or ion membrane transport (Singh et al., 2015). Primary and secondary metabolites, including proline and soluble sugars, play an osmotic adjustment function under salt stress (Chen and Jiang, 2010). On the other hand, to deal with ionic toxicity and maintain $Na^+/K^+$ homeostasis in the cell, plants develop mechanisms by limiting the excessive accumulation of $Na^+$ in the cytoplasm, including the restriction of the entry of $Na^+$ into cells, removal of $Na^+$ from the cells, and storing excess $Na^+$ into the vacuole (Zhao et al., 2020). Some important ion transporters include SOS1, HKT1, and NHXs, are involved in the removal of $Na^+$ from the cytoplasm, the transport of $Na^+$ from root cells to xylem, and ion isolation in vacuoles (Shi et al., 2000; Davenport et al., 2010; Apse et al., 2019). Compared with glycophytes, most halophytes can accumulate more $Na^+$ in the aerial portion under salt stress and can maintain a better $Na^+/K^+$ ratio (Orsini et al., 2010; Flowers et al., 2015).

*Sesuvium portulacastrum*, as a mangrove companion plant, is a typical halophyte in the family *Aizoaceae* and usually grows on wet sand, such as beaches (Lonard and Judd, 1997; He et al., 2022; Zhang et al., 2022). *Sesuvium portulacastrum* plants are tolerant to salt, drought, and heavy metal stresses and widely used in phytoremediation projects including salt-alkali soil restoration in coastal areas and coastal sand fixation (Lokhande et al., 2013). Early studies have shown that *S. portulacastrum* is a facultative halophyte and salt accumulator, suggesting that *S. portulacastrum* plants can grow well in not only non-saline but also saline soils. Appropriate saline levels could even increase the photosynthetic rate of *S. portulacastrum* plants and promote their growth (Peng et al., 2018). A high salt concentration (200 mM NaCl) significantly alleviated Cd toxicity symptoms in *S. portulacastrum* by both limiting Cd uptake and compartmenting Cd inside plant tissues (Mariem et al., 2014). *Sesuvium portulacastrum* plants are able to sustain their growth by isolating salt ions into the vacuole to maintain the osmotic balance between the vacuole and the cytoplasm (Ramani et al., 2006). A quantitative proteomic analysis identified 96 salt-responsive proteins implicated in salt stress in *S. portulacastrum*, and these proteins are highly involved in ion binding, proton transport, photosynthesis, and ATP synthesis. Under high salinity conditions, the expression of $Na^+/H^+$ antiporter and ATP synthase subunits was activated (Yi et al., 2014). Enzymatic analyses showed that NaCl could induce *S. portulacastrum* P-ATPase and V-ATPase activities, but V-PPase activity was inhibited (Ding et al., 2022). Several genes in *S. portulacastrum* have been demonstrated to promote salt tolerance in plants. For example, an aquaporin gene *SpAQP1* from *S. portulacastrum*, increased salt tolerance in transgenic tobacco (Chang et al., 2016). Heterologous overexpression of *SpSOS1* and *SpAHA1* genes improved salt tolerance in yeast and *Arabidopsis* (Zhou et al., 2015, 2018). With the increasing recognition of *S. portulacastrum* as an important species for phytoremediation of saline soils and water body, there is a need to further study of this species in tolerance to saline environments. Understanding its tolerance to salinity at the molecular level would enable us to better utilize this and other halophytic plants for remediation of saline soils.

The objectives of this study were to (1) evaluate morphological responses of *S. portulacastrum* plants to different concentrations of Na in a hydroponic culture, (2) analyze transcript changes of the plants after exposure to a high level of Na in contrast with those without Na treatment through RNA-Seq, (3) identify important genes involved in the tolerance of high Na concentration, (4) outline the major strategies of the plants in adaptation to saline conditions and maintenance of plant growth. It was anticipated that this effort could provide a global view of the transcript changes in and major routes for *S. portulacastrum* to adapt to saline environments, and such information could assist in our effort on improving crop tolerance of salt stress.

# Materials and methods

## Plant growth and salt treatments

The shoots of *S. portulacastrum* were initially collected from Putian, a coastal city in Fujian Province, China. They were potted in containers filled with a substrate composed of 40% peat, 20% pine bark, 20% perlite, and 20% sand based on volume (Zhonghe Agriculture, Huaian, China) and grown in a greenhouse at the Minjiang University, Fuzhou, Fujian, China. Tip cuttings with four nodes and about 10 leaves were made. After removing leaves from the lowest node, they were rooted in ½ Hoagland solution (Hoagland and Synder, 1933). Uniform rooted cuttings were selected, and four cuttings were planted in each 3-L container filled with 2 L ½ Hoagland solution supplemented with NaCl resulting in Na concentrations at 0, 100, 200, 300, 400, 500, and 600 mM, respectively. The plants were grown in a growth room with a constant temperature of 24°C under a light intensity about 400 μmol/m$^2$/s and a photoperiod of 16 h. The experiment was arranged as a completely randomized design with three replications. Plant growth was monitored every 3 days for 21 days by taking each plant out of the solution culture and carefully blotting with paper towel, and fresh weight and root numbers were recorded (Supplementary Table 1). Plant growth photos were taken on days 0, 12, and 21, and growth curves based on root numbers and fresh weight produced under different concentrations of Na were drawn at the end of experiment.

## RNA extraction and sequencing

Based on the results of above experiment, 400 mM Na was selected for the second solution culture experiment to determine transcript changes in *S. portulacastrum* plants. Rooted cuttings were grown in the same containers filled with ½ Hoagland solution devoid of Na or containing 400 mM Na. The experiment was set as a completely randomized experiment with three replications. Root and leaf samples were taken 1 h and 21 days after the initiation of the experiment. The samples were taken from three containers per treatment, respectively, and frozen immediately in liquid nitrogen. Thus, there were three biological replications for each treatment. After 21 days, entire plants were removed from each container, washed with deionized water three times, blotted with paper towel. Leaves and roots were separated, placed in paper bags, and dried at 105°C for 2 h, and then dried at 80°C for 48 h. Dry weight of each sample was weighed, which were used for analysis of $Na^+$ and $K^+$ contents.

A portion of the frozen leaf and root samples were sent to Novogene Co. (Beijing, China) for RNA extraction and sequencing. RNA was isolated from roots and leaves, respectively, and they were sequenced separately. There were three biological replicates for each sample. The RNA integrity and total concentrations were analyzed using Agilent 2100 BioAnalyzer (Agilent Technologies, Palo Alto, CA, United States). 1 μg of RNA from each sample was taken for library construction. Agilent 2100 BioAnalyzer was used to determine the insert size of the library. The qRT-PCR was used to accurately quantify the library effective concentration to ensure the quality of the library. The prepared libraries were sequenced by the Illumina HiSeq 2000 sequencing system (Novogene Co., Beijing, China) to generate 150 bp paired end readings. To obtain the clean data, reads with adapter, reads containing N and low-quality reads (reads with a Qphred <=20 base number) were removed from the raw data. The sequence data was submitted to the National Center for Biotechnology Information (NCBI) with an accession number of PRJNA848266.

## Differential expression analysis

Trinity (v2.5.1; Grabherr et al., 2011) was used for transcriptome assembly. Clean reads were mapped on the transcriptome to obtain the read count of each gene using the RSEM software (Dewey and Li, 2011). The read count of genes was converted to FPKM (fragments per kilobase of transcript per million fragments mapped). Differential expression analysis of the two treatments (0.0 mM vs. 400.0 mM at each sampling time) was performed using DESeq2 R package (*v1.20.0*) based on padj <0.05 and | log2FoldChange | > 1 (Love et al., 2014). KEGG pathway enrichment analysis of the differential expression genes was conducted using KOBAS software (version 3.0; http://kobas.cbi.pku.edu.cn/). Gene functional annotation was performed using the following five databases: Non-Redundant Protein Sequence Database (Nr), Nucleotide Sequence Database (Nt), Protein family (Pfam), Clusters of Orthologous Groups of proteins (KOG/COG), Swiss-Prot, Kyoto Encyclopedia of Genes and Genomes (KEGG), and Gene Ontology (GO). Furthermore, the top 5,000 differentially expressed genes of FPKM were selected for WGCNA analysis. The WGCNA R package was used for co-expression network analysis (Langfelder and Horvath, 2009).

## qRT-PCR analysis

To verify the expression of identified genes, RNA was extracted from roots and leaves of *S. portulacastrum* grown in 0 or 400 mM Na (A portion of the remaining frozen samples mentioned above) using an Omega plant RNA kit (Omega, Bio-Tek Inc. Norcross, GA, United States). After analysis of the quality of RNA, the first strand of cDNA was synthesized with a FastKing RT Kit (Tiangen, Beijing, China) using 1 μg RNA. For qRT-PCR analysis, the cDNA was diluted fivefold with water. The reaction solution for qRT-PCR included 0.8 μl forward primer and 0.8 μl reverse primer, 1 μl cDNA, 10 μl of 2 × SYBR Premix Ex Taq (Takara, Japan) and 7.4 μl deionized water. The

reaction program was composed of 95°C for 3 min, then 95°C for 10 s, 60°C for 15 s, and 72°C for 20 s with a total of 45 cycles. qRT-PCR was carried out on an iCycler iQ5 thermal cycler (Bio-Rad, Hercules, CA, United States). The *S. portulacastrum SpGAPDH* was used as internal control (Zhou et al., 2015). Three biological replicates were performed for each sample. Gene relative expression levels were calculated using the $2^{-\Delta\Delta Ct}$ method (Livak and Schmittgen, 2002). Primers used for the study are listed in Supplementary Table 2.

## Analysis of reduced glutathione, soluble sugar, proline, K, and Na

The contents of reduced glutathione (GSH), soluble sugar, and proline in leaves and roots of *S. portulacastrum* were measured according to the instructions of the commercial kits (Nanjing Jiancheng Bioengineering Institute, Nanjing, China). Fresh plant samples were ground with liquid nitrogen. Precisely weighted each sample was added to PBS buffer with a ratio of 1:9 (g:ml) and vortexed. The solution was centrifuged for 10 min (2,500 rpm), and resultant supernatant was used for testing. Reagents were added according to the manufacturer instructions. The contents of GSH, soluble sugar, and proline were analyzed by a microplate reader with the absorbance at 405, 620, and 520 nm, respectively.

For analysis of $Na^+$ and $K^+$, the aforementioned dried leaf and root samples harvested at the end of the experiment were digested using the method described by Haynes (1980). The inductively coupled plasma (ICP)-atomic emission spectrometry (Perkin Elmer Instruments, Shelton, CT, United States) was used to measure $Na^+$ and $K^+$ content (Plank, 1992). Three biological replicates were analyzed per treatment.

# Results

## Plant growth responses to different concentrations of Na

Rooted cuttings of *S. portulacastrum* were able to sustain their growth over a 21-day period regardless of Na concentrations (Figure 1A). Fresh weights of plants exposed to Na at a concentration ranging from 100 to 500 mM were either comparable to or higher than those of the control plants (Figure 1B). The highest fresh weights were produced when plants were exposed to 100 mM Na. However, when exposed to 600 mM Na, the magnitude of fresh weight increase over the time was significantly lower than the other treatments, indicating growth suppression. Root numbers of plants grown at 0 and 100 mM Na were the highest, followed by plants grown with Na at 200–400 mM (Figure 1C). Root numbers of plants grown at 500 mM Na were significantly lower than those grown in the other treatments except for plants grown at 600 mM that had the lowest number of roots.

## Global transcriptome analysis of *S. portulacastrum* under salt stress

Since the fresh weights and root numbers were similar between plants grown at 0 mM and 400 mM Na (Figure 1), leaf and root samples of plants grown at the two levels of Na were analyzed using RNA-Seq. We obtained 152.28 Gb of filtered sequence data, of which 90.76% of the data quality reached Q30 or higher (Supplementary Table 3). Because the genome of *S. portulacastrum* has not been released yet, the reads were mapped to the transcriptome assembled with Trinity (*v2.5.1*). The BUSCO software was used to evaluate the quality of "cluster.fasta" file obtained by assembling. The comparison rate of complete transcripts (single copy and duplicated copies) reached 55.2% (Supplementary Table 4). All the genes were clustered according to the correlation coefficient ($r^2$). Genes from roots and leaves were separately clustered, and three biological replicates of the same treatment were clustered together (Figure 2A). The results showed that replicate samples were highly correlated. In order to identify differentially expressed salt-responsive genes in roots and leaves, respectively, we compared the expression levels between the following pairs: R_S_1h vs. R_M_1h (R_S_1h represented roots treated with Na for 1 h, and R_M_1h was roots without exposure to Na for 1 h); R_S_21d vs. R_M_21d (R_S_21d, roots treated with Na for 21 days, and R_M_21d, roots without Na treatment for 21 days); L_S_1h vs. L_M_1h (L_S_1h, leaves of plants treated with Na for 1 h, and L_M_1h, leaves of plants without Na treatment); and L_S_21d vs. L_M_21d (L_S_21d, leaves of plants treated with Na for 21 days, and L_M_21d, leaves of plants without Na treatment for 21 days). Compared with the control, a total of 13,013 differentially expressed genes (DEGs) were identified in the roots, of which 8,135 were up-regulated and 4,878 were down-regulated. Whereas 1652 DEGs were identified in leaves, of which 929 were up-regulated, and 723 were down-regulated after 1 h of salt treatment. For plants exposed to 400 mM for 21 days, 18,282 DEGs were identified in the roots (7,584 up-regulated and 10,698 down-regulated) and 3,318 DEGs were identified in leaves (624 were up-regulated, and 2,694 were down-regulated; Figure 2B). These results indicated that the expression of salt-responsive genes varied significantly between roots and leaves, and the expression levels were affected by the duration of the treatments.

## Stress-responsive genes of *S. portulacastrum* enriched under salt stress

To further explore the changes in gene expression in *S. portulacastrum* under salt stress, GO enrichment analysis was performed with DEGs by pair comparisons: R_S_1h vs. R_M_1h; R_S_21d vs. R_M_21d; L_S_1h vs. L_M_1h; and L_S_21d vs. L_M_21d (Figures 3A–D). Several GO terms related to stress responses were identified in both roots and leaves, such as response to stimulus, response to stress, and response to oxidative

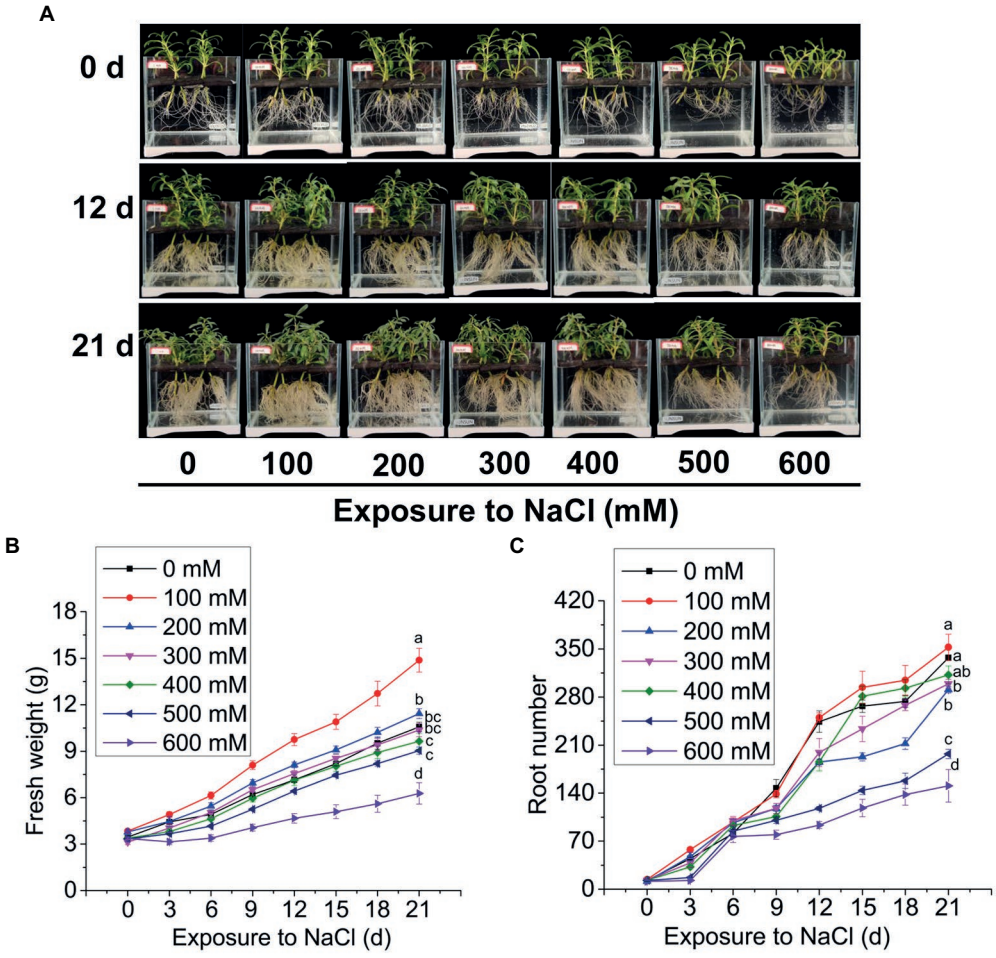


FIGURE 1
The growth of *Sesuvium portulacastrum* in a hydroponic culture. The phenotype of *S. portulacastrum* plants grown in different concentrations of NaCl over 0, 12, and 21days **(A)**, fresh weight **(B)**, and root numbers **(C)** of plants over 21 days of growth. Data were means of three replications. Different letters at the end of lines indicate significant differences among treatments based on Tukey HSD test at $p<0.05$ level.

stress. But some GO terms were not identified in leaves after salt treatment for 1-h and 21-day, such as response to reactive oxygen species and cellular response to oxidative stress (Figure 3). More DEGs were identified in roots (Figures 3A,B) than leaves (Figures 3C,D), indicating the numbers of stress-responsive genes in roots were significantly higher than those in leaves.

## Genes related to ion transport in *S. portulacastrum*

A large number of DEGs related to ion transporters were identified (Table 1), which included four $Na^+/K^+$ transporters (*HKTs*), 10 shaker-type $K^+$ channels (*AKT1s*), two high affinity potassium (*HAKs*), 12 cyclic nucleotide gated channels (*CNGCs*), 47 aquaporins, and nine glutamate receptors (*GLRs*). At the same time, multiple DEGs involved in $Na^+$ extrusion and sequestration were identified, including four $Na^+/H^+$ exchangers (*NHXs*) and 71 $H^+$-ATPases. In addition, multiple cation channel genes were detected, including five $K^+$ efflux antiporters (*KEAs*), three $K^+$ uptake permeases (*KUPs*), two pore potassium channels (*TPKs*), two $Ca^{2+}/H^+$ antiporters, and nine cation/$H^+$ antiporters (Supplementary Table 5). In general, the expression of DEGs involved in $Na^+$ extrusion and sequestration increased after being exposed to Na stress.

The analysis of $Na^+$ and $K^+$ contents in roots and leaves showed that the $Na^+$ content increased significantly in roots and leaves after salt treatment. $Na^+$ contents in roots and leaves reached 58.11 and 152.05 mg/g, respectively, after 21 days of salt treatment. Compared with the control samples at the same period, the Na content in the roots and leaves increased by 42.9 folds and 2.1 folds, respectively (Figure 4A). The $K^+$ contents in *S. portulacastrum* decreased after 21 days of salt treatment, and the contents in roots and leaves were 17.60 and 27.37 mg/g, respectively. Compared with the control samples at the same period, the K content in the roots and leaves was reduced by 0.5 and 0.43 folds, respectively (Figure 4B). We further used qRT-PCR to analyze the expression levels of ion transport related genes in roots. The expression level of *CNGC*

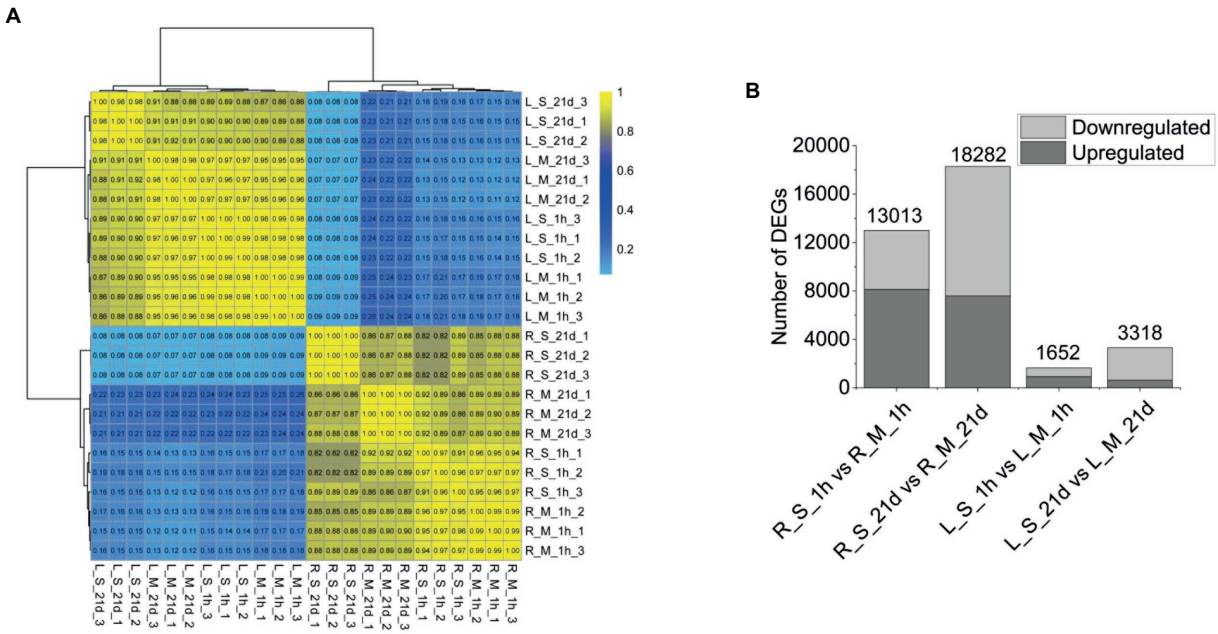


FIGURE 2
RNA-Seq data and DEGs resulted from *S. portulacastrum* plants treated and untreated with 400mM NaCl. **(A)** Hierarchical clustering of 24 samples based on the correlation coefficient ($r^2$), where R_M_1h and R_M_21d were samples of roots (1h and 21days) without NaCl treatment; L_M_1h and L_M_21d were samples of leaves (1h and 21days) without NaCl treatment; R_S_1h and R_S_21d were samples of roots (1h and 21days) with NaCl treatment; and L_S_1h and L_S_21d were samples of leaves (1h and 21days) with NaCl treatment. **(B)** Statistics of DEGs numbers in roots and leaves.

increased significantly after 1 h of salt stress, and decreased after 21-day. The expression level of NHX was significantly increased relative to the control after salt treatment for 1-h and 21-day (Figure 4C). In addition, the expression of $K^+$ transport related genes *AKT* and *HTK1*, was inhibited under salt stress (Figure 4C). The quantitative expression trends of these genes were consistent with the trends in RNA-Seq (Figure 4D).

## Metabolic pathways related to salt stress in *S. portulacastrum*

In order to explore metabolic pathways involved in salt stress, a pathway enrich analysis was conducted using KEGG. We analyzed DEGs in roots of *S. portulacastrum* under salt stress and found that 20 pathways were significantly enriched, including photosynthesis – antenna proteins, alpha-linolenic acid metabolism, lysine biosynthesis, and GSH metabolism (Figures 5A,B). Among them, GSH metabolism was among the most enriched pathways. As a result, the expression levels of genes involved in GSH metabolism were analyzed. Results showed that after 1-h salt treatment, a large number of glutathione S-transferase (GST) genes were highly up-regulated in roots. In addition, genes involved in catalyzing the production of oxidized glutathione (GSSG) from GSH, such as isocitrate dehydrogenase (IDH), 6-phosphogluconate dehydrogenase (PGD), glucose-6-phosphate 1-dehydrogenase (G6PD), and glutathione peroxidase (GPX) were mostly up-regulated (Figure 5C). However, after 21-day salt treatment, the expression of these DEGs in roots were largely down-regulated compared to those after 1-h salt treatment (Figure 5C). We further analyzed the GSH content and found that salt treatment led to a reduction of the GSH content in the *S. portulacastrum* roots (Figure 5D).

The KEGG pathway enrichment was also used for analysis of DEGs in leaves, and 20 significantly enriched pathways were identified, including plant hormone signal transduction, phenylpropanoid biosynthesis, starch and sucrose metabolism, and GSH metabolism (Figures 6A,B). Considering the importance of plant hormones in abiotic stress, we analyzed the expression changes of DEGs involved in the plant hormone signal transduction. After 1-h salt treatment, DEGs related to signaling network of auxin: auxin influx carrier (AUX), auxin-responsive protein (IAA), gibberellin (gibberellin receptor, GID1), abscisic acid (protein phosphatase 2C, PP2C), and ABA responsive element binding factor (ABF) were highly up-regulated. While DEGs involved in ethylene (ethylene-responsive transcription factor 1, ERF1), brassinosteroid (BR-signaling kinase, BSK), and xyloglucosyl transferase (TCH) were down-regulated. On the other hand, the numbers of DEGs involved in plant hormone signal transduction were lower after 21-day salt treatment than those after 1-h salt treatment (Figure 6C). Soluble sugars play an important role in the osmotic adjustment of plant salt tolerance. Soluble sugar in leaves of *S. portulacastrum* increased 1.5 fold after 1 h of salt treatment but decreased 0.72 fold after 21 days of salt treatment (Figure 6E). These results were consistent with the

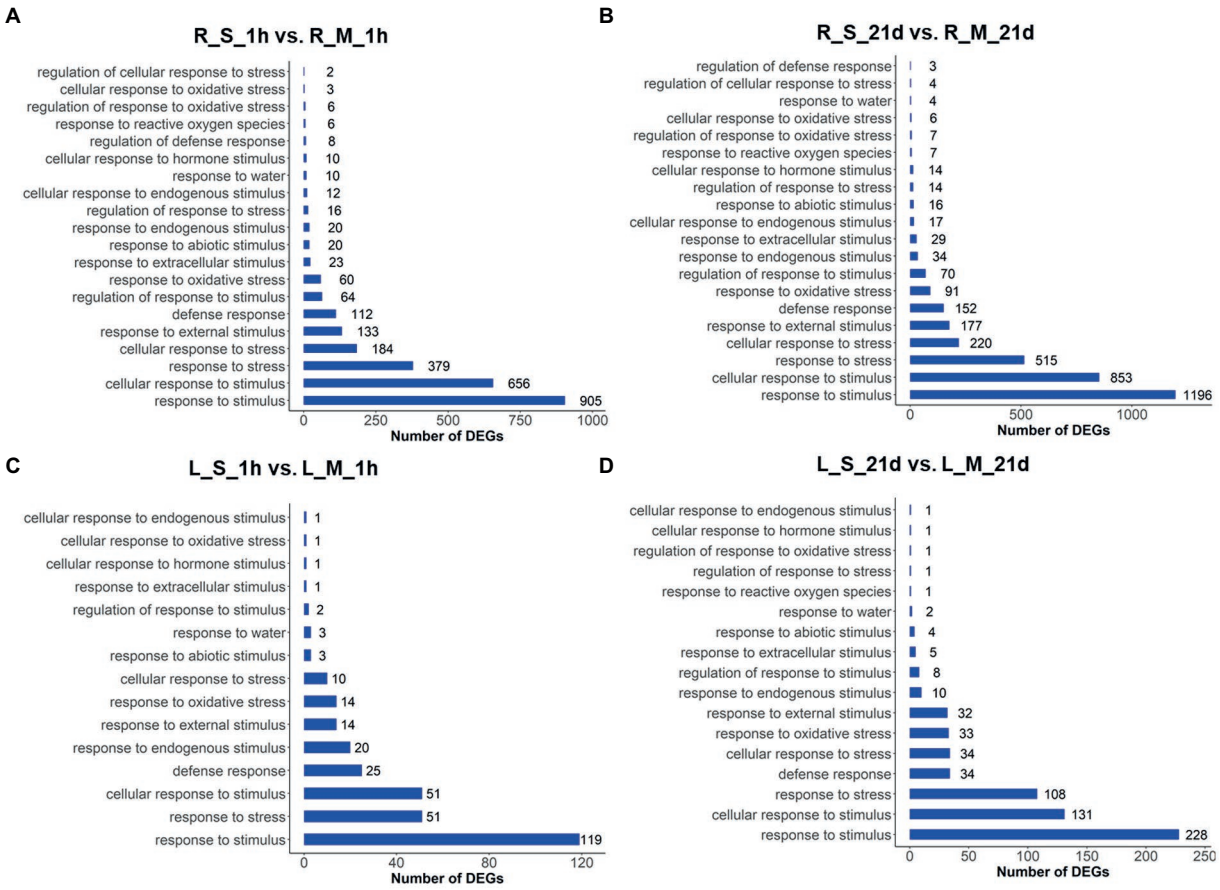


FIGURE 3
GO analysis of DEGs in roots and leaves of plants treated and untreated with 400mM Na. The GO terms were identified based on DEGs of different comparisons: R_S_1h vs. R_M_1h **(A)**; R_S_21d vs. R_M_21d **(B)**; L_S_1h vs. L_M_1h **(C)**; L_S_21d vs. L_M_21d **(D)**. The bars represent the number of DEGs in each GO term.

expression trend of genes related to starch and sucrose metabolism in the transcriptome (Figure 6D).

Our results showed that genes involved in proline metabolism were differentially expressed (Figures 7A,B) and proline content in *S. portulacastrum* significantly increased after 21-day salt stress (Figure 7C). Proline is an important osmolyte in higher plants, which is synthesized from glutamic acid and ornithine. Δ-1pyrroline-5-carboxylate synthetase (P5CS) and 1-pyrroline-5-carboxylate reductase (P5CR) catalyze the biosynthesis of proline from glutamic acid (Székely et al., 2008). In catabolism, proline dehydrogenase (PDH) degrades proline as pyrroline-5-carboxylate (P5C; Peng et al., 1996). In roots, the increased content of proline was mainly due to the up-regulated expression of *P5CS*, *P5CR* and ornithine-oxo-acid transaminase (*rocD*), which catalyzed the production of proline from ornithine. At the same time, the down-regulated expression of *PDH* might inhibit the degradation of proline (Figure 7A). The increase in proline content in leaves could be due to the inhibition of *PDH* expression (Figure 7B). Additionally, genes in regulation of polyamine metabolism were also differentially expressed (Figures 7D,E).

## Differential expression of transcription factors under salt stress

A large number of transcription factors (TFs) were differentially expressed after the exposure to Na. In roots of *S. portulacastrum*, 367 TFs and 452 TFs were differentially expressed 1-h and 21-day after salt treatment, respectively (Supplementary Table 6). The top five most differentially expressed transcription factors were genes in MYB, C2H2, AP2/ERF, WRKY, and bZIP families (Figure 8A). Compared with roots, the number of differentially expressed TFs in *S. portulacastrum* leaves was significantly lower than in roots. There were 367 and 452 DEGs in roots compared to 77 and 111 in leaves after 1 h and 21 days, respectively. The top five abundant TF families in leaves were AP2/ERF, MYB, WRKY, NAC, and bHLH (Figure 8A). The analysis of differentially expressed TFs showed that more TFs in the roots than leaves of *S. portulacastrum* after 1-h salt treatment, and their expressions were mostly up-regulated (Figure 8B). However, after 21 days of salt treatment, the number of down-regulated TFs increased significantly (Figure 8C).

TABLE 1 Differentially expressed ion transporters in roots and leaves under salt stress.

| Cluster ID | Database description | $log_2$ (Fold change) | | | |
|---|---|---|---|---|---|
| | | Root_1h | Root_21d | Leaf_1h | Leaf_21d |
| $Na^+$ uptake | | | | | |
| Cluster-51977.13165 | Glutamate receptor (GLR) | −1.5703 | 1.3975 | – | – |
| Cluster-51977.5676 | Glutamate receptor (GLR) | −3.1902 | −9.2789 | – | – |
| Cluster-51977.32649 | Glutamate receptor (GLR) | – | 1.7076 | – | – |
| Cluster-51977.87644 | Glutamate receptor (GLR) | 1.3652 | – | – | – |
| Cluster-51977.137910 | Glutamate receptor (GLR) | – | 1.8601 | – | – |
| Cluster-51977.81862 | Cyclic nucleotide-gated ion channel (CNGC) | 1.0804 | – | – | 1.0344 |
| Cluster-51977.81878 | Cyclic nucleotide-gated ion channel (CNGC) | 1.9346 | −1.1817 | – | – |
| Cluster-51977.100764 | Cyclic nucleotide-gated ion channel (CNGC) | – | −1.0047 | – | – |
| Cluster-51977.51402 | Cyclic nucleotide-gated ion channel (CNGC) | 1.6637 | – | – | – |
| Cluster-51977.51403 | Cyclic nucleotide-gated ion channel (CNGC) | 1.4292 | – | – | – |
| Cluster-51977.131278 | $Na^+/K^+$ transporter (HKT) | – | −4.1136 | – | – |
| Cluster-51977.72258 | $Na^+/K^+$ transporter (HKT) | – | −3.2744 | – | – |
| Cluster-51977.70693 | $Na^+/K^+$ transporter (HKT) | – | −3.1004 | – | – |
| Cluster-51977.12531 | $Na^+/K^+$ transporter (HKT) | – | −4.6243 | – | – |
| Cluster-51977.102438 | Shaker-type $K^+$ channels AKT1 | – | −1.6052 | – | – |
| Cluster-51977.93455 | Shaker-type $K^+$ channels AKT1 | −1.135 | 1.5776 | – | – |
| Cluster-51977.102439 | Shaker-type $K^+$ channels AKT1 | – | −1.7222 | – | – |
| Cluster-51977.87709 | Shaker-type $K^+$ channels AKT1 | −1.2702 | 1.5352 | – | – |
| Cluster-51977.24379 | Shaker-type $K^+$ channels AKT1 | – | – | – | −1.0309 |
| Cluster-51977.68836 | High affinity potassium (HAK) | – | 1.306 | – | – |
| Cluster-51977.83444 | High affinity potassium (HAK) | – | 1.3255 | – | – |
| Cluster-51977.100439 | Aquaporin TIP | −1.3463 | – | – | – |
| Cluster-51977.44303 | Aquaporin PIP | −1.2535 | – | – | – |
| Cluster-51977.65599 | Aquaporin PIP | – | – | 1.0919 | – |
| Cluster-51977.70411 | Aquaporin TIP | −1.47 | – | – | −1.1722 |
| Cluster-51977.53002 | Aquaporin PIP | – | −2.0825 | – | – |
| $Na^+$ extrusion and $Na^+$ sequestration | | | | | |
| Cluster-51977.50507 | $Na^+/H^+$ exchanger (NHX) | 1.1936 | – | 1.2854 | – |
| Cluster-51977.37461 | $Na^+/H^+$ exchanger (NHX) | 1.219 | – | 1.0589 | – |
| Cluster-51977.50509 | $Na^+/H^+$ exchanger (NHX) | 2.4805 | – | 1.6241 | – |
| Cluster-69520.0 | $Na^+/H^+$ exchanger (NHX) | – | 5.7103 | – | – |
| Cluster-51977.72274 | Plasma membrane $H^+$-ATPase | – | 1.1546 | – | – |
| Cluster-51977.106274 | Plasma membrane $H^+$-ATPase | – | 1.6041 | – | – |
| Cluster-51977.72273 | Plasma membrane $H^+$-ATPase | – | 1.4131 | – | – |
| Cluster-51977.150164 | Plasma membrane $H^+$-ATPase | – | 9.8178 | – | – |
| Cluster-41429.0 | Plasma membrane $H^+$-ATPase | −2.9645 | – | −2.9645 | – |
| $K^+$ channel | | | | | |
| Cluster-51977.78847 | $K^+$ efflux antiporter (KEA) | – | – | – | −1.2637 |
| Cluster-51977.73195 | $K^+$ efflux antiporter (KEA) | – | −1.059 | – | – |
| Cluster-51977.78854 | $K^+$ efflux antiporter (KEA) | – | – | – | −1.4937 |
| Cluster-51977.128334 | $K^+$ efflux antiporter (KEA) | – | 1.687 | – | – |

*(Continued)*

TABLE 1 Continued

| Cluster ID | Database description | $log_2$ (Fold change) | | | |
|---|---|---|---|---|---|
| | | Root_1h | Root_21d | Leaf_1h | Leaf_21d |
| Cluster-36451.0 | $K^+$ efflux antiporter (KEA) | −3.8638 | – | – | – |
| Cluster-51977.9496 | $K^+$ uptake permease (KUP) | −1.4907 | −5.7325 | – | – |
| Cluster-51977.5805 | $K^+$ uptake permease (KUP) | −4.4418 | −2.8311 | – | – |
| Cluster-51977.65788 | $K^+$ uptake permease (KUP) | – | 1.4587 | – | – |
| Cluster-51977.32311 | Two pore potassium channel (TPK) | – | −1.5353 | – | −1.0312 |
| Cluster-51977.32312 | Two pore potassium channel (TPK) | – | −2.003 | – | – |
| Other cation channels | | | | | |
| Cluster-29290.0 | $Ca2^+/H^+$ antiporter | −2.9047 | – | – | – |
| Cluster-51977.27292 | $Ca2^+/H^+$ antiporter | – | −1.0955 | – | – |
| Cluster-51977.101674 | Cation/$H^+$ antiporter | 1.0254 | – | 1.1723 | – |
| Cluster-51977.61674 | Cation/$H^+$ antiporter | −2.0507 | −3.4027 | – | −4.1648 |
| Cluster-51977.111068 | Cation/$H^+$ antiporter | – | 2.6856 | – | 1.5372 |
| Cluster-51977.24139 | Cation/$H^+$ antiporter | 2.2506 | – | – | – |
| Cluster-51977.109616 | Cation/$H^+$ antiporter | 1.2815 | 2.4522 | – | – |

The data is from RNA-seq. "–" means the gene is not expressed.

## Identification of coexpression modules related to salt tolerance

In order to gain a better understanding of the relationships among different genes implicated in *S. portulacastrum* responses to salt stress, the WGCNA analysis was carried out. The top 5000 DEGs with the average FPKM were divided into 15 modules, which were presented in the cluster dendrogram (Figure 9A). Each module was marked with a different color. Further correlation analysis between the modules and the samples was carried out (Figure 9B). The results showed that the yellow module, with 431 identified genes, was highly associated with the R_S_1h sample (Supplementary Table 7). The brown module (438 genes) was highly associated with R_S_21d sample. The purple module, representing 144 genes, was highly correlated with L_S_1h sample. The cyan module, containing 45 genes, was highly related to the L_S_21d sample.

The WGCNA was also be used to screen the hub genes in the module based on the KME (eigengene connectivity) value. The hub gene means a high degree of connection with the genes in the module, which may play an important role in the salt tolerance of *S. portulacastrum*. Heatmap showed that the yellow module-specific genes were over-expressed in R_S_1h (Figure 9C). Cytochrome P450 71A1, UDP-glycosyltransferase 88B1, cellulose synthase-like protein G2, chitin elicitor receptor kinase 1, and chitin synthase were identified as candidate hub genes in this module. The brown module genes were over-expressed in R_S_21d (Figure 9C). Genes encoding peroxidase 12, cysteine-rich receptor-like protein kinase, clathrin interactor 1, CO (2)-response secreted protease, and CNGC15b were identified as candidate hub genes for this module. The purple module genes were over-expressed in L_S_1h (Figure 9C). Glutaredoxin-C6, fructose-bisphosphate aldolase 1, ultraviolet-B receptor UVR8, heat shock factor protein HSF30, and cytochrome P450 4d2 were identified as candidate hub genes in this module. The cyan module genes were over-expressed in L_S_21d (Figure 9C). Genes encoding bifunctional purple acid phosphatase 26, vesicle transport v-SNARE 12, telomere capping C-terminal wHTH, translation factor SUI1 homolog, and beta-3 tubulin were identified as candidate hub genes for this module.

# Discussion

Land salinization is one of the most important environmental problems in the world. It was estimated that about 10% of the land surface and 50% of irrigated land have been affected by salinization (Ruan et al., 2010). Annual losses due to salt-affected land in agricultural production are more than US$12 billion and rising (Flowers et al., 2010). Salinity is now a key restraint to crop productivity (Shahzad et al., 2019). On the other hand, world food production is projected to increase between 50% and 70% by 2050 to match the estimated growth of population (Shabala et al., 2013). It is certain that the current arable land is far less sufficient for crop production. A solution to expand crop production is to use halophytic plants to remediate soil salinity and convert the soils to cultivable land (Karakas et al., 2020; Munir et al., 2022). Thus, an in-depth understanding of halophytic plant tolerance to salt stress would enable us to better use this group of plants for remediation of saline soils. *Sesuvium portulacastrum* is a typical halophyte, but its salt tolerance mechanisms remain largely unclear. Our study showed that *S. portulacastrum* plants when exposed to 400 mM Na were able to produce shoot fresh weight and root numbers

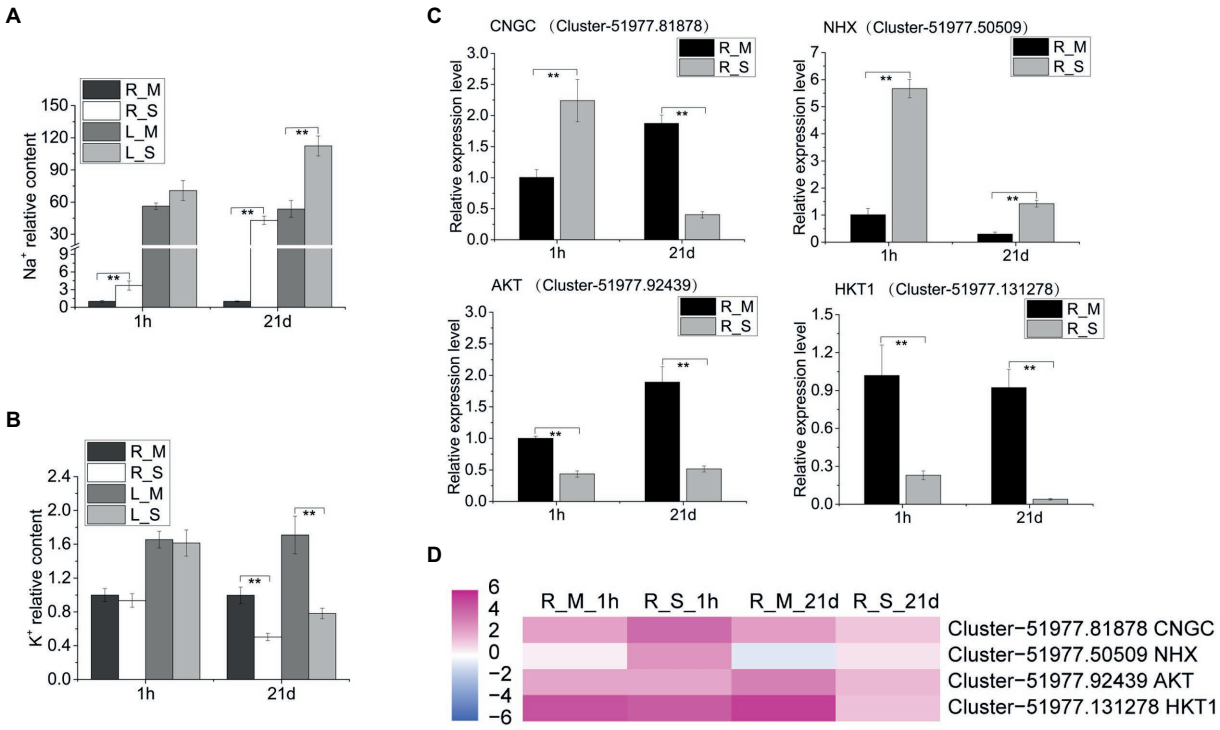


FIGURE 4
Tissue concentrations of Na and K and qRT-PCR analysis of relevant gene expression. **(A,B)** The relative content of Na and K in roots and leaves of plants after 1h and 21days of growth with 400mM Na compared to the R_M sample. R_M and L_M mean roots and leaves of plants unexposed to Na. R_S and L_S mean roots and leaves of plants exposed to 400mM Na. **(C)** qRT-PCR analysis of the expression of $Na^+$ and $K^+$ transport related genes. The error bars were calculated from three biological replicates. Mean differences were analyzed based on Tukey's HSD test at $p<0.01$ (**) levels. **(D)** The expression of genes (CNGC, NHX, AKT, and HKT1) in roots of plants treated with or without 400mM Na. The data represent $\log_2$ FPKM values based on RNA-Seq analysis.

comparable to those of control plants (Figure 1). The ability of *S. portulacastrum* to thrive in such a higher concentration of Na was elucidated through RNA-Seq and qRT-PCR analyses. Our results showed that *S. portulacastrum* has developed multiple strategies to cope with saline growth conditions.

## Regulation of cellular $Na^+/K^+$ homeostasis

Maintaining a proper intracellular $K^+/Na^+$ ratio is critical for plants to tolerate salt stress. *Sesuvium portulacastrum* is able to deliberately control $K^+$ and $Na^+$ levels when grown under high salt stress. Compared with the control samples, higher content of $Na^+$ was detected in the leaves and roots of *S. portulacastrum* after 21 days of salt treatment. At the same time, the $K^+$ content in the samples of the treatment group was significantly reduced (Figures 4A,B). Like other halophytes, *S. portulacastrum* can maintain a higher $Na^+/K^+$ ratio in roots and leaves. This is likely due to the expression of ion transport related genes. We have identified a large number of ion transport related genes that were differentially expressed in *S. portulacastrum* under salt stress. The expression of *CNGC* genes in roots after 1 h of Na treatment was up-regulated (Table 1). This suggests that *CNGC* gene was involved in Na uptake in the early stage of salt stress. After 21 days of salt treatment, the expression of *CNGC* was down-regulated, which could inhibit Na uptake at the later stage of salt stress (Figure 4C). Recent studies have shown that increased transcript levels of a few *AtCNGCs* in *Arabidopsis* roots or shoots after exposed to high levels of NaCl (Duszyn et al., 2019). For example, *AtCNGC20* was up-regulated in roots after exposure to Na; *AtCNGC5* and *AtCNGC17* were reported to be implicated in salt tolerance (Guo et al., 2008; Mian et al., 2011; Ladwig et al., 2015; Massange-Sánchez et al., 2016; Vadim, 2018). Our speculation is that ion transporter, such as CNGCs regulate Na absorption, while NHXs may play an important role in control of Na accumulation. From our result, NHX and $H^+$-ATPase genes were up-regulated in *S. portulacastrum* root under salt stress (1 h and 21 days). NHX is one of the important families participating in $Na^+$ extrusion and sequestration. NHXs located on the plasma membrane of the cell, such as NHX7/SOS1 can exclude $Na^+$ from the root system (Ji et al., 2013). In addition, NHX1 and NHX2 located on the vacuole membrane may participate in the compartmentalization of $Na^+$ in the vacuole and the $K^+$ balance in the vacuole (Jiang et al., 2010). At the same time, proton pump ($H^+$-ATPase)

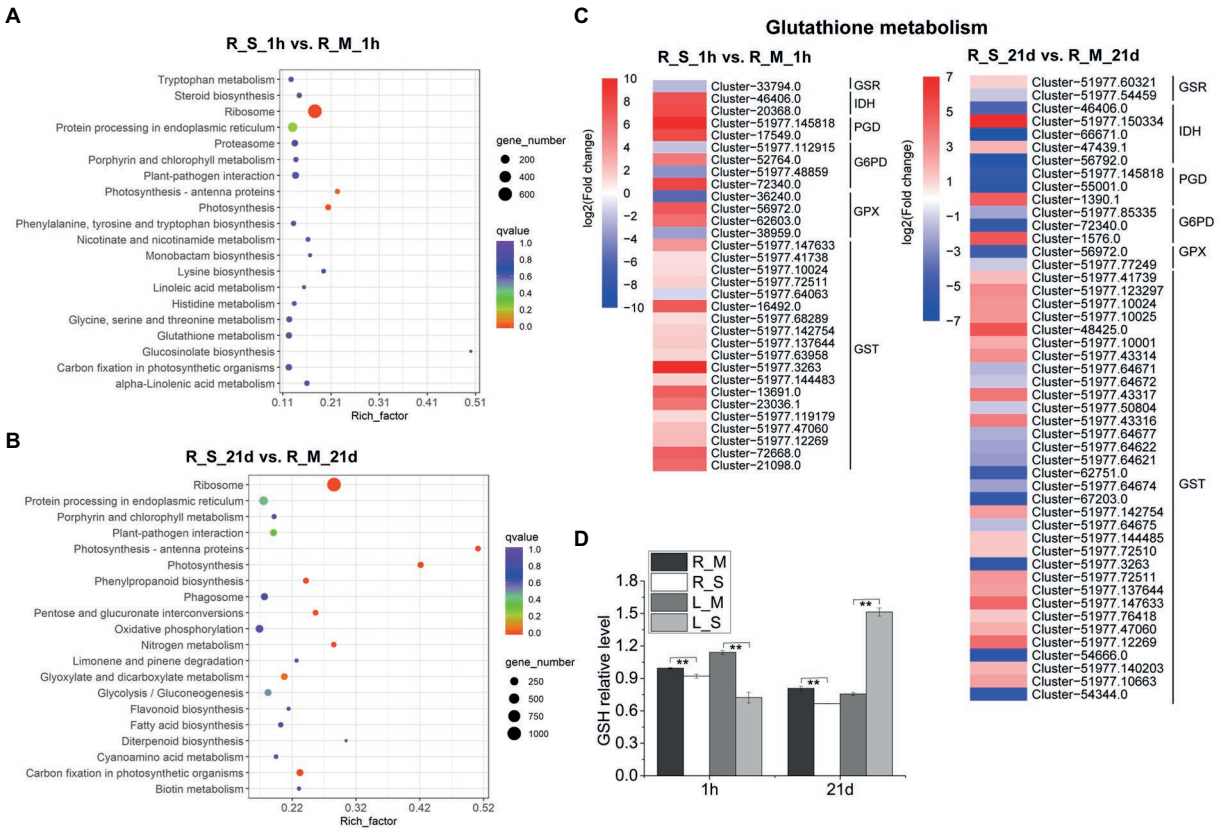


FIGURE 5
KEGG analysis of DEGs in roots and expression analysis of DEGs involved in "glutathione (GSH) metabolism." **(A)** The top 20 pathways that were significantly enriched in roots after 1h of salt treatment (400mM Na). **(B)** The top 20 pathways that were significantly enriched in roots after 21days of salt treatment. **(C)** Expression analysis of DEGs in roots involved in "Glutathione metabolism" after 1h and 21days of salt treatment. **(D)** The relative content of GSH in roots and leaves compared to the R_M sample. R_M and L_M mean roots and leaves of plants untreated with Na. R_S and L_S mean roots and leaves of plants treated with 400mM Na. The error bars were calculated from three biological replicates. Mean separation was based on Tukey HSD test at $p<0.01$ (**) levels.

located on the plasma membrane of the cell provided power for $Na^+$ extrusion and sequestration (Gaxiola et al., 2007). In addition, several ion transport related genes in *S. portulacastrum* had been reported. Previous studies found that heterologous overexpression of *SpSOS1* and *SpAHA1* genes improved salt tolerance in yeast and *Arabidopsis* (Zhou et al., 2015, 2018). These genes were also identified in our study (Supplementary Table 5). In addition, more ion transport related genes were identified in our study, such as *AKT* and *HKT*. The expression of *AKT* and *HKT* in roots of *S. portulacastrum* was down-regulated after salt stress. But in halophytic turf grass, *SvHKT1;1* gene was up-regulated in response to high concentrations of NaCl (500 mM), (Kawakami et al., 2020). This is in contrast to the results in the *S. portulacastrum*. We think that *CNGCs* and *NHXs* are important gene families implicated in the regulation of $Na^+$ uptake, extrusion, and sequestration, and their coordinate actions could maintain $Na^+/K^+$ at appropriate ratios and lead to Na tolerance in *S. portulacastrum*. Further research is warranted to confirm these propositions.

## Changes in osmolytes

The loss of water due to the decrease in osmotic pressure is one of the great constraints faced by plants growing in saline soils. Accumulation of compatible osmolytes is an important strategy for plants to cope with osmotic stress (Apse and Blumwald, 2002). Different species have different osmolyte profiles under salt stress. Halophytes usually accumulate one or more than one compatible osmolytes, such as proline, glycine betaine, and sorbitol. Previous studies showed that under salt and drought conditions, the proline content in the callus and axillary buds of *S. portulacastrum* significantly increased (Lokhande et al., 2010). Our study also found that, compared with the control samples, the proline content in *S. portulacastrum* roots and leaves significantly increased under short-term (1-h) and long-term (21-day) salt treatments (Figure 7C). According to transcriptome data, we found that the accumulation of proline in roots depends on the up-regulated expression of genes related to proline synthesis (P5CS, P5CR, rocD) on the one hand, and on the other hand from the down-regulated expression of genes related to degradation

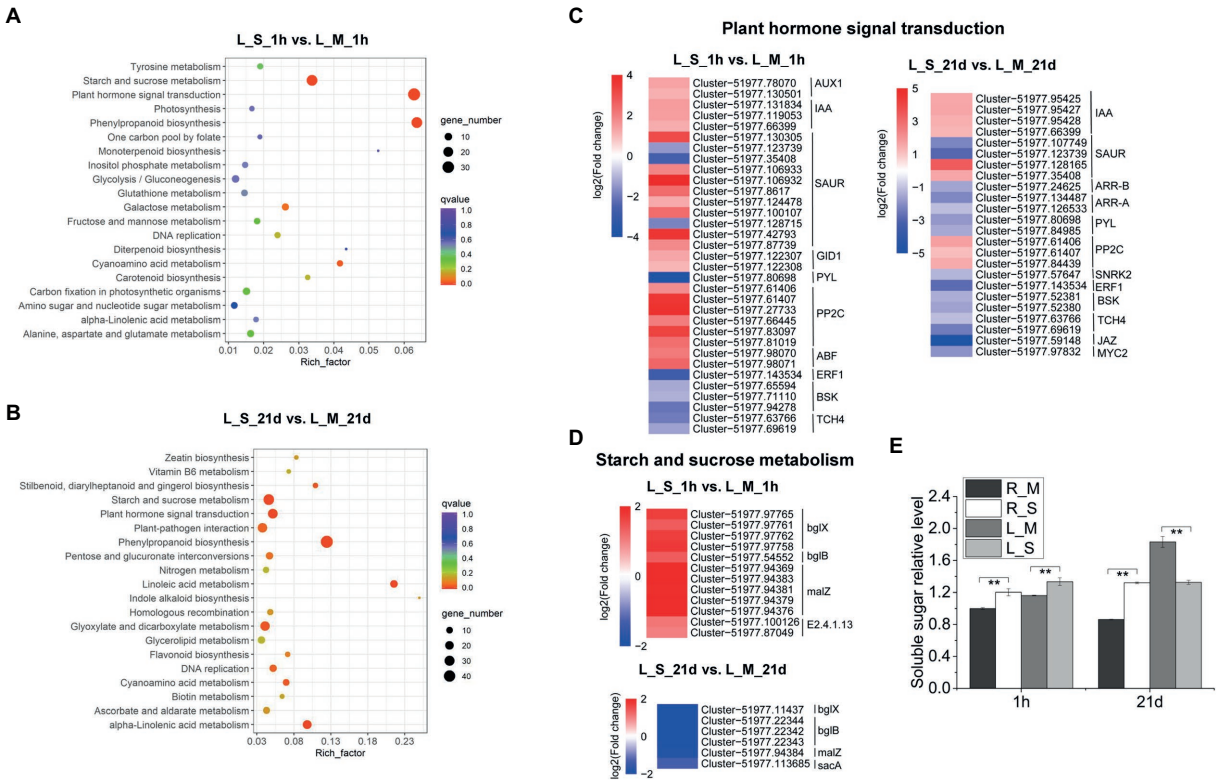


FIGURE 6
KEGG analysis of DEGs in leaves and expression analysis of DEGs involved in "plant hormone signal transduction" and "starch and sucrose metabolism." **(A)** The top 20 pathways that were significantly enriched in leaves of plants after 1h of salt treatment (400mM Na). **(B)** The top 20 pathways that were significantly enriched in leaves after 21days of salt treatment. **(C,D)** Expression analysis of DEGs in leaves involved in "plant hormone signal transduction" and "starch and sucrose metabolism" after 1h and 21days of salt treatment. **(E)** The relative content of soluble sugar content in roots and leaves compared to the R_M sample. R_M and L_M mean roots and leaves of plants untreated with Na. R_S and L_S mean roots and leaves of plants treated with 400mM Na. The error bars were calculated from three biological replicates. Mean separation was based on Tukey HSD test at $p<0.01$ (**) levels.

(PDH; Figure 7A). However, the accumulation of proline in leaves is more dependent on the inhibition of degradation-related genes (Figure 7B). Soluble sugar is another important osmolyte under salt stress, which can protect specific macromolecules or sustain membrane stability (Bartels and Sunkar, 2005). Other studies have demonstrated that halophyte *Thellungiella* under salt treatment accumulated high content of soluble sugars (Wang et al., 2013). From the result of KEGG analysis, the pathway of starch and sucrose metabolism was enriched in leaves of *S. portulacastrum* under salt stress (Figures 6A,B). Further study showed that the soluble sugar content in leaves of *S. portulacastrum* increased after 1 h of salt stress but decreased after 21d of salt stress (Figure 6E). Thus, proline and soluble sugar may play an important role in maintaining the osmotic balance of *S. portulacastrum* in a high-salt environment.

Polyamines play significant roles in regulating plant defense responses to various environmental stresses, including salt stress, metal toxicity, and oxidative stress (Zhong et al., 2020). Exogenous application of putrescine (Put) improved plant salt tolerance (Chattopadhayay et al., 2002; Gill and Tuteja, 2010). In plants, the first rate-limiting reaction of Put synthesis is either arginine catalyzed by arginine decarboxylase (ADC) or ornithine catalyzed by ornithine decarboxylase (ODC). In this study, after 1 h of salt stress, the expression of several *ODC* genes in the root of *S. portulacastrum* increased, which catalyzed the biosynthesis of putrescine from ornithine. The expression of polyamine oxidase 4 (*PAO4*) was up-regulated (Figure 7D). After 1 h of salt stress, the polyamine oxidase gene *MAPO* was up-regulated in leaves of *S. portulacastrum* (Figure 7E). *PAO4* is able to catalyze the biosynthesis of putrescine from spermine and spermidine (Alcázar et al., 2011). After 21 days of salt stress, the expression of spermidine synthase genes (*speEs*) in *S. portulacastrum* was up-regulated, which catalyzes putrescine to spermine and spermidine (Figure 7D). This suggests that the balance of polyamines plays a role in the salt tolerance of the *S. portulacastrum*.

## ROS homeostasis

Salt stress can induce excessive ROS accumulation in plants which leads to cell damage and cell death. The tolerance of halophytes to high salinity depends to a certain extent on their ability to maintain ROS homeostasis (Jayakumar et al., 2014).

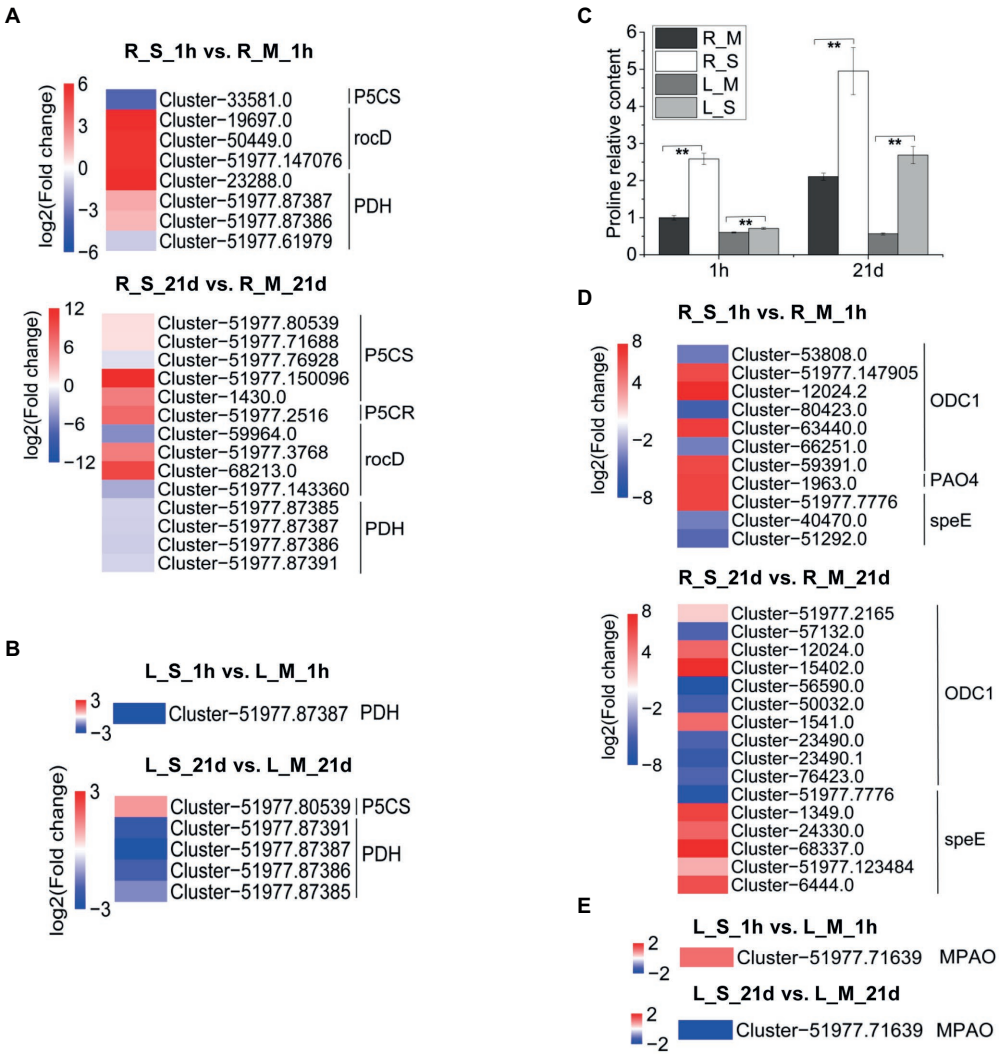


FIGURE 7
Expression analysis of DEGs involved in proline metabolism. **(A)** Expression analysis of DEGs in *S. portulacastrum* roots involved in proline metabolism after 1h (R_S_1h vs. R_M_1h) and 21days (R_S_21d vs. R_M_21d) of salt treatment (400mM Na). **(B)** Expression analysis of DEGs in *S. portulacastrum* leaves involved in proline metabolism after 1h (L_S_1h vs. L_M_1h) and 21days (L_S_21d vs. L_M_21d) of salt treatment. **(C)** The relative content of proline in roots and leaves compared to the R_M sample. R_M and L_M mean roots and leaves under control condition. R_S and L_S mean roots and leaves under salt stress. The error bars were calculated from three biological replicates. Mean separation was based on Tukey HSD test at $p$ <0.01 (**) levels. **(D,E)** Expression analysis of DEGs in *S. portulacastrum* roots and leaves respectively involved in polyamines metabolism after 1h and 21days of salt treatment.

Synthesis of antioxidant metabolites is an important strategy for plants to eliminate excess ROS under high salt stress. Ascorbate and GSH are important antioxidant metabolites in plants. Halophytes are found to have a more efficient ascorbate-glutathione cycle. For example, the ascorbate and GSH content of halophyte *Lycopersicon pennellii* was significantly higher than that of glycophyte relative *L. esculentum* (Shalata et al., 2001). However, the content of GSH in *S. portulacastrum* decreased after 1-h of salt treatment (Figure 5D). This may be due to the oxidation of GSH to GSSG. RNA-Seq data also showed that the expression of genes involved in catalyzing the oxidation of GSH into GSSG was significantly up-regulated (Figure 5C). Another important way to scavenge ROS in halophytes is through enzymatic agents, such as SOD (Grene et al., 2002), CAT (Willekens et al., 2014), APX (Shigeru et al., 2002), and POX (Fagerstedt et al., 2010). From the WGCNA analysis of this study, POX was identified as one of the hub genes in the salt-stressed modules in roots (Figure 9C). POXs are isoenzyme that removes $H_2O_2$ in the outer plastid space (Fagerstedt et al., 2010). Previous studies showed that increased activity of POXs was found in halophytes, such as *Cakile maritima* and *Hordeum marinum* (Seckin et al., 2010; Ellouzi et al., 2011). Our results also indicated that the expression of POX genes was up-regulated in roots of *S. portulacastrum* under salt stress (Figure 9C). Therefore, we believe that the GSH/GSSH cycle and POX play an important role in the scavenging ROS induced by salt in *S. portulacastrum*.

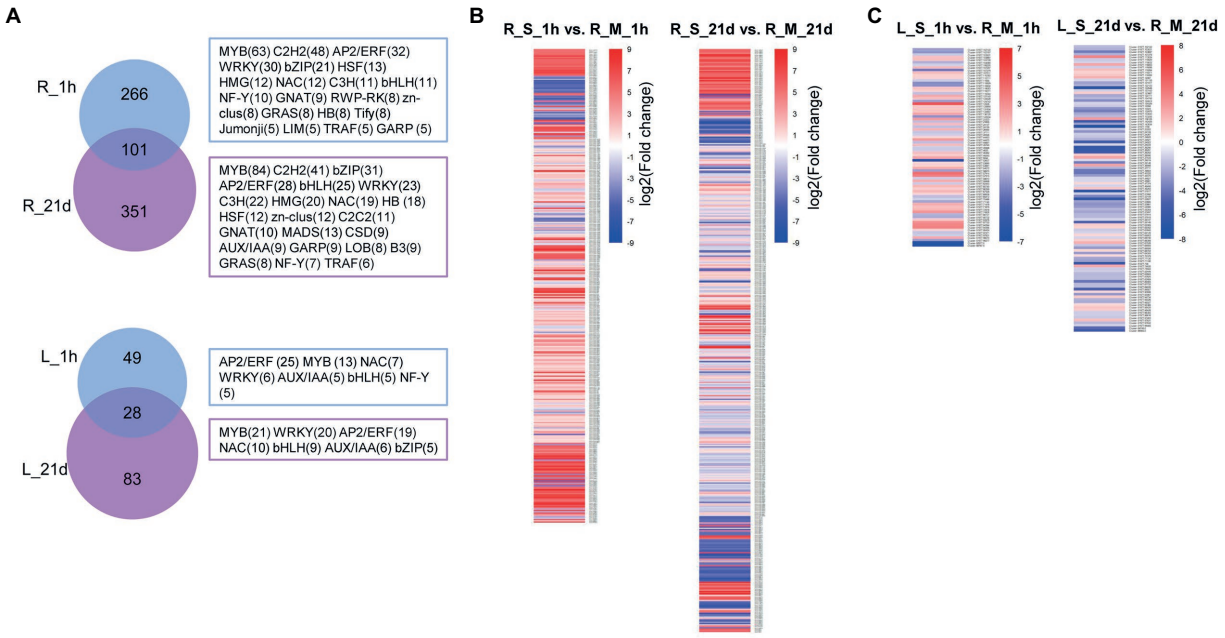


FIGURE 8
Analysis of differentially expressed TFs in roots and leaves of *S. portulacastrum*. **(A)** Venn diagrams for salt-induced TFs in roots and leaves of *S. portulacastrum*. R_1h and R_21d means differentially expressed TFs in roots after salt treatment (400mM Na) for 1h and 21days. L_1h and L_21d means differentially expressed TFs in leaves after salt treatment after 1h and 21days. The TF families and gene numbers ($n$>4) were shown in the right. **(B)** Expression analysis of the TFs in each comparison.

## Changes in tissue-special gene modules

Another finding in this study is tissue-special gene modules identified by WGCNA analysis (Figure 9). WGCNA analysis aimed to identify co-expressed gene modules and to explore the core genes in the modules, through which a hierarchical clustering tree was constructed by calculating the correlation coefficient between any two genes. Different branches of the clustering tree represent different gene modules, and different colors represent different module. Based on the weighted correlation coefficients of genes, genes were classified according to their expression patterns, and genes with similar patterns were grouped into one module. The identification of hub genes in relation to modules provided a new and important perspective for understanding the salt tolerance mechanism in *S. portulacastrum*. In roots of *S. portulacastrum*, the expression of genes related to lignin synthesis in the phenylpropane metabolic pathway (cytochrome P450 71A1-like), cellulose synthesis (cellulose synthase-like protein G2), endocytosis (clathrin interactor 1-like), and perceive $CO_2$ concentration to regulate the pathway of stomatal development $CO_2$-response secreted protease-like) were up-regulated. An important adaptation of plants to salt stress is differential regulation of growth, accompanied by dynamic changes and rearrangement of plant cell walls, and cellulose and lignin were the structural composition of cell walls (Cosgrove, 2015; Tenhaken, 2015; Yan et al., 2021). This may indicate that the strong cell wall regulation ability of *S. portulacastrum* enhances its salt tolerance. In leaves of *S. portulacastrum*, the expression level of vesicle transport related genes (vesicle transport v-SNARE 12) and tubulin (beta-3 tubulin) were up-regulated under salt stress. Vesicle transport and tubulin play important roles in plant salt tolerance. Under high salinity conditions, regulating the reorganization of cortical microtubules is the key to the survival of plant cells (Endler et al., 2015). In *Arabidopsis*, ethylene signal promotes the reorganization of cortical microtubules induced by salt stress (Dou et al., 2018). This inspired us to think what role does tubulin play in promoting salt tolerance in halophytes? These questions will be part of our follow-up research.

The mechanisms of salt tolerance in halophytes have been continuously studied over the years. Most studies focus on osmotic protection and ion homeostasis. Some halophytes maintain $Na^+/K^+$ balance through salt secretion. For example, in halophyte quinoa, salts are deposited in epidermal bladder cells (EBCs; Kiani-Pouya et al., 2017). In *S. portulacastrum*, the maintenance of $Na^+/K^+$ balance is mainly dependent on the storage of the excess Na in the vacuole. Halophytes maintain a better Na/K ratio by removing Na from the cytoplasm, transporting Na from root cells to the xylem, and sequestrating Na in the vacuole in which *SOS1*, *HKT1*, and *NHXs* ion transporters play important roles (Flowers et al., 2015). In this study, more ion transport related genes (*GLRs*, *CNGCs*, *AKTs*, *HAKs*, *KEAs*, *KUPs* and *TPKs*) were identified in response to salt stress. In addition, the results of WGCNA analysis suggest that cell wall formation, vesicle transport and tubulin may play significant roles in salt tolerance in *S. portulacastrum*.

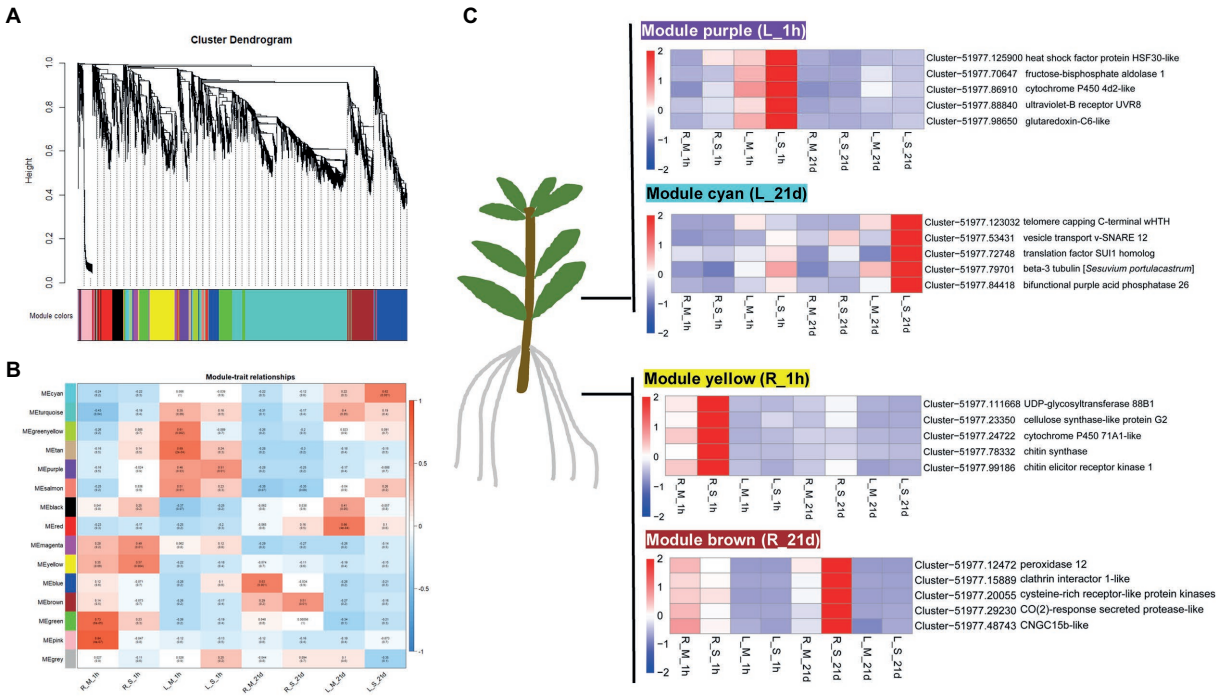


FIGURE 9
WGCNA analysis of genes in roots and leaves of *S. portulacastrum*. **(A)** Hierarchical cluster tree showing co-expression modules identified by WGCNA. Each leaf in the tree represents one gene. The major tree branches constitute 15 modules, labeled with different colors. **(B)** Module–sample association. Each row corresponds to a module, labeled with a color as in **(A)**. The numbers in each cell at the row-column intersection indicates the correlation coefficient between the module and the sample. **(C)** Heatmaps showing the selected hub genes in each module.

## Conclusion

*Sesuvium portulacastrum* is a halophytic species and has been considered a valuable plant to be used for phytoremediation of saline soils. After 400 mM Na treatment, Na contents in roots and leaves were much higher than K contents in *S. portulacastrum*. A large number of DEGs were detected from RNA-Seq data. A variety of ion transport related genes (*CNGCs, NHXs, AKTs, HKTs*) are implicated in Na uptake and accumulation, of which *CNGCs* could be involved in Na uptake, and *NHXs* could be responsible for controlling Na extrusion and sequestration. Their coordinated action could maintain $Na^+$/ $K^+$ homeostasis in the *S. portulacastrum*. Soluble sugar and proline play an important role in the osmotic regulation of *S. portulacastrum* under salt stress. Glutathione metabolism and POX participated in scavenging reactive oxygen species under salt stress. Additionally, transcription factors and plant hormones including auxin, gibberellin, abscisic acid, and ethylene are involved in regulating the salt tolerance of *S. portulacastrum*. Our study shows that *S. portulacastrum* has developed a suite of mechanisms for accumulation and tolerance of Na, suggesting that it could be an important species to be used for remediation of saline soils (Figure 10).

## Data availability statement

The datasets presented in this study were deposited in the NCBI repository with an accession number of PRJNA848266, available at: https://www.ncbi.nlm.nih.gov/bioproject/PRJNA848266.

## Author contributions

DW: conceptualization, data curation, formal analysis, investigation, methodology, and writing–original draft. NY: data curation, methodology, software, and visualization. CZ: methodology. WH: methodology. GY: methodology and software. JC: conceptualization and writing–review and editing. XW: conceptualization, funding acquisition, project administration, resources, supervision, and writing–review and editing. All authors contributed to the article and approved the submitted version.

## Funding

The authors are thankful to the National Natural Science Foundation of China (32102331), the Natural Science Foundation of Fujian Province (2022J011141 and 2020J01867) and

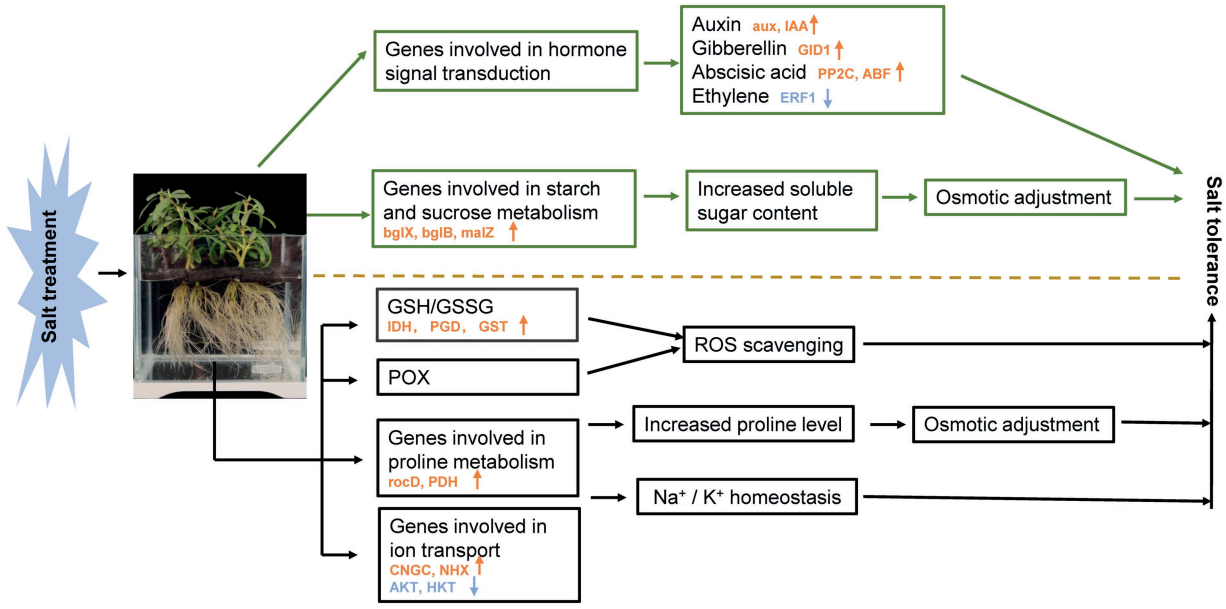


FIGURE 10
Schematic presentation of the potential mechanism of salt stress tolerance in *S. portulacastrum*. The yellow arrows in the figure represent the increased expression of related genes. Blue arrows represent decreased gene expression. The mentioned genes were selected from plants after 1h of Na treatment.

Department of Education, Fujian Province (JAT200426) for providing the financial support.

## Acknowledgments

We are grateful to all the members of our team for helpful discussion on this project.

## Conflict of interest

The authors declare that the research was conducted in the absence of any commercial or financial relationships that could be construed as a potential conflict of interest.

## Publisher's note



## Supplementary material

The Supplementary material for this article can be found online at: https://www.frontiersin.org/articles/10.3389/fpls.2022.973419/full#supplementary-material

## References

Alcázar, R., Bitrián, M., Bartels, D., Koncz, C., Altabella, T., and Tiburcio, A. F. (2011). Polyamine metabolic canalization in response to drought stress in Arabidopsis and the resurrection plant *Craterostigma plantagineum*. *Plant Signal. Behav.* 6, 243–250. doi: 10.4161/psb.6.2.14317

Apse, M. P., and Blumwald, E. (2002). Engineering salt tolerance. *Cur. Opin. Biotech.* 13, 146–150. doi: 10.1016/S0958-1669(02)00298-7

Apse, M. P., Aharon, G. S., Snedden, W. A., and Blumwald, E. (2019). Salt tolerance conferred by overexpression of a vacuolar $Na^+/H^+$ antiport in *Arabidopsis*. *Science* 285, 1256–1258. doi: 10.1126/science.285.5431.1256

Ashraf, M. Y., Ashraf, M., Mahmood, K., Akhter, J., Hussain, F., and Arshad, M. (2010). "Phytoremediation of saline soils for sustainable agricultural productivity," in *Plant Adaptation and Phytoremediation*. eds. M. Ashraf, M. Ozturk and M. Ahmad (Dordrecht: Springer Netherlands), 335–355.

Ayyappan, D., and Ravindran, K. C. (2014). Potentiality of *suaeda monoica* forsk. A salt marsh halophyte on bioaccumulation of heavy metals from tannery effluent. *Int. J. Modn. Res. Revs.* 2, 267–274. doi: 10.5829/idosi.wasj.2013.28.12.2136

Bartels, D., and Sunkar, R. (2005). Drought and Salt Tolerance in Plants. *Crit. Rev. Plant Sci.* 24, 23–58. doi: 10.1080/07352680590910410

Butcher, K., Wick, A. F., DeSutter, T., Chatterjee, A., and Harmon, J. (2016). Soil salinity: a threat to global food security. *Agron. J.* 108, 2189–2200.

Chang, W., Liu, X., Zhu, J., Fan, W., and Zhang, Z. (2016). An aquaporin gene from halophyte *Sesuvium portulacastrum*, SpAQP1, increases salt tolerance in transgenic tobacco. *Plant Cell Rep.* 35, 385–395. doi: 10.1007/s00299-015-1891-9

Chattopadhayay, M. K., Tiwari, B. S., Chattopadhyay, G., Bose, A., Sengupta, D. N., and Ghosh, B. (2002). Protective role of exogenous polyamines on salinity-stressed

rice (*Oryza sativa*) plants. *Physiol. Plant.* 116, 192–199. doi: 10.1034/j.1399-3054.2002.1160208.x

Chen, H., and Jiang, J. G. (2010). Osmotic adjustment and plant adaptation to environmental changes related to drought and salinity. *Environ. Rev.* 18, 309–319. doi: 10.1139/A10-014

Chen, T., Yuan, F., Song, J., and Wang, B. (2016). Nitric oxide participates in waterlogging tolerance through enhanced adventitious root formation in the euhalophyte *Suaeda salsa*. *Funct. Plant Biol.* 43, 244–253. doi: 10.1071/FP15120

Cosgrove, D. J. (2015). Plant expansins: diversity and interactions with plant cell walls. *Curr. Opin. Plant Biol.* 25, 162–172. doi: 10.1016/j.pbi.2015.05.014

Davenport, R. J., Muoz-Mayor, A., Jha, D., Essah, P. A., Rus, A., and Tester, M. (2010). The $Na^+$ transporter AtHKT1;1 controls retrieval of $Na^+$ from the xylem in *Arabidopsis*. *Plant Cell Environ.* 30, 497–507. doi: 10.1111/j.1365-3040.2007.01637.x

Dewey, C. N., and Li, B. (2011). RSEM: accurate transcript quantification from RNA-Seq data with or without a reference genome. *BMC Bioinf.* 12:323. doi: 10.1186/1471-2105-12-323

Ding, G., Yang, Q., Ruan, X., Si, T., Yuan, B., Zheng, W., et al. (2022). Proteomics analysis of the effects for different salt ions in leaves of true halophyte *Sesuvium portulacastrum*. *Plant Physiol. Biochem.* 170, 234–248. doi: 10.1016/j.plaphy.2021.12.009

Dou, L., He, K. K., Higaki, T., Wang, X., and Mao, T. (2018). Ethylene signaling modulates cortical microtubule reassembly in response to salt stress. *Plant Physiol.* 176, 2071–2081. doi: 10.1104/pp.17.01124

Duszyn, M., Świeżawska, B., Szmidt-Jaworska, A., and Jaworski, K. (2019). Cyclic nucleotide gated channels (CNGCs) in plant signaling: current knowledge and perspectives. *J. Plant Physiol.* 241:153035. doi: 10.1016/j.jplph.2019.153035

Ellouzi, H., Hamed, K. B., Cela, J., Munné-Bosch, S., and Abdelly, C. (2011). Early effects of salt stress on the physiological and oxidative status of *Cakile maritima* (halophyte) and *Arabidopsis thaliana* (glycophyte). *Physiol. Plant.* 142, 128–143. doi: 10.1111/j.1399-3054.2011.01450.x

Endler, A., Kesten, C., Schneider, R., Zhang, Y., Ivakov, A., Froehlich, A., et al. (2015). A mechanism for sustained cellulose synthesis during salt stress. *Cells* 162, 1353–1364. doi: 10.1016/j.cell.2015.08.028

Fagerstedt, K. V., Kukkola, E. M., Koistinen, V., Takahashi, J., and Marjamaa, K. (2010). Cell wall lignin is polymerised by class III secretable plant peroxidases in Norway spruce. *J. Integr. Plant Biol.* 52, 186–194. doi: 10.1111/j.1744-7909.2010.00928.x

Flowers, T. J., Galal, H. K., and Bromham, L. (2010). Evolution of halophytes: multiple origins of salt tolerance in land plants. *Funct. Plant Biol.* 37, 604–612. doi: 10.1038/79602

Flowers, T. J., Rana, M., and Colmer, T. D. (2015). Sodium chloride toxicity and the cellular basis of salt tolerance in halophytes. *Ann Bot.* 3, 419–431. doi: 10.1093/aob/mcu217

Food and Agricultural Organization (FAO) (2015). *Status of the World's Soil Resources*. FAO, Rome.

Gaxiola, R. A., Palmgren, M. G., and Schumacher, K. (2007). Plant proton pumps. *FEBS Lett.* 581, 2204–2214. doi: 10.1016/j.febslet.2007.03.050

Gill, S. S., and Tuteja, N. (2010). Polyamines and abiotic stress tolerance in plants. *Plant Signal. Behav.* 5, 26–33. doi: 10.4161/psb.5.1.10291

Grabherr, M. G., Haas, B. J., Yasssour, M., Levin, J. Z., Thompson, D. A., Ido, A., et al. (2011). Full-length transcriptome assembly from RNA-Seq data without a reference genome. *Nat. Biotechnol.* 29, 644–652. doi: 10.1038/nbt.1883

Grene, A. R., Neval, E., and Heath, L. S. (2002). Role of superoxide dismutases (SODs) in controlling oxidative stress in plants. *J. Exp. Bot.* 53, 1331–1341. doi: 10.1093/jexbot/53.372.1331

Guo, K. M., Babourina, O., Christopher, D. A., Borsics, T., and Rengel, Z. (2008). The cyclic nucleotide-gated channel, AtCNGC10, influences salt tolerance in *Arabidopsis*. *Physiol. Plant.* 134, 499–507. doi: 10.1111/j.1399-3054.2008.01157.x

Hasanuzzaman, M., Nahar, K., Alam, M. M., Bhowmik, P. C., and Fujita, M. (2014). Potential use of halophytes to remediate saline soils. *J. Biomed. Biotechnol.* 2014:589341. doi: 10.1155/2014/589341

Hasegawa, P. M., Bressan, R. A., Zhu, J. K., and Bohnert, H. J. (2000). Plant cellular and molecular responses to high salinity. *Annu. Rev. Plant Physiol. Plant Mol. Biol.* 51, 463–499. doi: 10.1146/annurev.arplant.51.1.463

Hayat, K., Bundschuh, J., Jan, F., Menhas, S., Hayat, S., Haq, F., et al. (2020). Combating soil salinity with combining saline agriculture and phytomanagement with salt-accumulating plants. *Crit. Rev. Env. Sci. Tec.* 50, 1085–1115. doi: 10.1080/10643389.2019.1646087

Haynes, R. (1980). A comparison of two modified Kjeldahl digestion techniques for multi-element plant analysis with conventional wet and dry ashing methods. *Commun. Soil Sci. Plant Anal.* 11, 459–467. doi: 10.1080/00103628009367053

He, W., Wang, D., Yang, N., Cao, D., Chen, X., Chen, J., et al. (2022). In vitro shoot culture of *Sesuvium portulacastrum*: an important plant for phytoremediation. *Agriculture* 12:47. doi: 10.3390/agriculture12010047

Hoagland, D. R., and Synder, W. C. (1933). Nutrition of strawberry plants under controlled conditions. *Proc. Am. Soc. Hortic. Sci.* 30, 288–294.

Imadi, S. R., Shah, S. W., Kazi, A. G., Azooz, M., and Ahmad, P. (2016). "Phytoremediation of saline soils for sustainable agricultural productivity," in *Plant Metal Interaction*. ed. P. Ahmad (New York, NY: Elsevier), 455–468.

Jayakumar, B., Ana, R. M., and Sergey, S. (2014). ROS homeostasis in halophytes in the context of salinity stress tolerance. *J. Exp. Bot.* 65, 1241–1257. doi: 10.1093/jxb/ert430

Jiang, X., Leidi, E. O., and Pardo, J. M. (2010). How do vacuolar NHX exchangers function in plant salt tolerance? *Plant Signal. Behav.* 5, 792–795. doi: 10.4161/psb.5.7.11767

Ji, H., Pardo, J. M., Batelli, G., Van, O. M. J., Bressan, R. A., and Li, X. (2013). The salt overly sensitive (SOS) pathway: established and emerging roles. *Mol. Plant* 6, 275–86. doi: 10.1093/mp/sst017

Karakas, S., Dikilitas, M., and Tıpırdamaz, R. (2020). "Phytoremediation of salt-affected soils using halophytes," in *Handbook of Halophytes*. ed. M. N. Grigore (Cham: Springer).

Kawakami, Y., Imran, S., Katsuhara, M., and Tada, Y. (2020). $Na^+$ transporter svhkt 1;1 from a halophytic turf grass is specifically upregulated by high $Na^+$ concentration and regulates shoot $Na^+$ concentration. *Int. J. Mol. Sci.* 21:6100. doi: 10.3390/ijms21176100

Kiani-Pouya, A., Roessner, U., Jayasinghe, N. S., Lutz, A., Rupasinghe, T., Bazihizina, N., et al. (2017). Epidermal bladder cells confer salinity stress tolerance in the halophyte quinoa and Atriplex species. *Plant Cell Environ.* 40, 1900–1915. doi: 10.1111/pce.12995

Ladwig, F., Dahlke, R. I., Stuhrwohldt, N., Hartmann, J., Harter, K., and Sauter, M. (2015). Phytosulfokine regulates growth in *Arabidopsis* through a response module at the plasma membrane that includes CYCLIC NUCLEOTIDE-GATED CHANNEL17, $H^+$-ATPase, and BAK1. *Plant Cell* 27, 1718–1729. doi: 10.1105/tpc.15.00306

Langfelder, P., and Horvath, S. (2009). WGCNA: an R package for weighted correlation network analysis. *BMC Bioinf.* 9:559. doi: 10.1186/1471-2105-9-559

Livak, K. J., and Schmittgen, T. D. (2002). Analysis of relative gene expression data using real-time quantitative PCR. *Methods* 25, 402–408. doi: 10.1006/meth.2001.1262

Lokhande, V. H., Gor, B. K., Desai, N. S., Nikam, T. D., and Suprasanna, P. (2013). *Sesuvium portulacastrum*, a plant for drought, salt stress, sand fixation, food and phytoremediation. A review. *Agron. Sustain. Dev.* 33, 329–348. doi: 10.1007/s13593-012-0113-x

Lokhande, V. H., Nikam, T. D., and Penna, S. (2010). Differential osmotic adjustment to iso-osmotic NaCl and PEG stress in the in vitro cultures of *Sesuvium portulacastrum* (L.). *J. Crop Sci. Biotech.* 13, 251–256. doi: 10.1007/s12892-010-0008-9

Lonard, R. I., and Judd, F. W. (1997). The biological flora of coastal dunes and wetlands. *Sesuvium portulacastrum* (L.) L. *J. Coastal Res.* 13, 96–104. doi: 10.2307/4298595

Love, M. I., Huber, W., and Anders, S. (2014). Moderated estimation of fold change and dispersion for RNA-seq data with DESeq2. *Genome Bio.* 15:550. doi: 10.1186/s13059-014-0550-8

Mariem, W., Kilani, B. R., Benet, G., Abdelbasset, L., Stanley, L., Charlotte, P., et al. (2014). How does NaCl improve tolerance to cadmium in the halophyte *Sesuvium portulacastrum*? *Chemosphere* 117, 243–250. doi: 10.1016/j.chemosphere.2014.07.041

Massange-Sánchez, J. A., Palmeros-Suárez, P. A., Espitia-Rangel, E., Rodríguez-Arévalo, I., Sánchez-Segura, L., Martínez-Gallardo, N. A., et al. (2016). Overexpression of grain amaranth (*Amaranthus hypochondriacus*) AhERF or AhDOF transcription factors in *Arabidopsis thaliana* increases water deficit- and salt-stress tolerance, respectively, via contrasting stress-amelioration mechanisms. *PLoS One* 11:e0164280. doi: 10.1371/journal.pone.0164280

Mian, A., Oomen, R., Isayenkov, S., Sentenac, H., Maathuis, F., and Véry, A. (2011). Over-expression of an $Na^+$-and $K^+$-permeable HKT transporter in barley improves salt tolerance. *Plant J.* 68, 468–479. doi: 10.1111/j.1365-313X.2011.04701.x

Munir, N., Hasnaina, M., Roessnerb, U., and Abideen, Z. (2022). Strategies in improving plant salinity resistance and use of salinity resistant plants for economic sustainability. *Crit. Rev. Environ. Sci. Technol.* 52, 2150–2196. doi: 10.1080/10643389.2021.1877033

Orsini, F., DUrzo, M. P., Inan, G., Serra, S., Oh, D. H., Mickelbart, M. V., et al. (2010). A comparative study of salt tolerance parameters in 11 wild relatives of *Arabidopsis thaliana*. *J. Exp. Bot.* 61, 3787–3798. doi: 10.1093/jxb/erq188

Peng, C., Chang, L., Yang, Q., Tong, Z., Wang, D., Tan, Y., et al. (2018). Comparative physiological and proteomic analyses of the chloroplasts in halophyte

*Sesuvium portulacastrum* under differential salt conditions. *J. Plant Physiol.* 232, 141–150. doi: 10.1016/j.jplph.2018.10.028

Peng, Z., Lu, Q., and Verma, D. (1996). Reciprocal regulation of delta 1-pyrroline-5-carboxylate synthetase and proline dehydrogenase genes controls proline levels during and after osmotic stress in plants. *Mol. Gen. Genet.* 253, 334–341. doi: 10.1007/pl00008600

Plank, C. O. (1992). Plant analysis reference procedures for the southern region of the United States. *South. Coop. Ser. Bull.* 368:9. Athens, GA: The Georgia Agricultural of Experiment Stations.

Qadir, M., Ghafoor, A., and Murtaza, G. (2001). Amelioration strategies for saline soils: a review. *Land Degrad. Dev.* 12, 357–386. doi: 10.1002/1099-145X(200011/12)11:63.0.CO;2-S

Ramani, B., Reeck, T., Debez, A., Stelzer, R., Huchzermeyer, B., Schmidt, A., et al. (2006). *Aster tripolium* L. and *Sesuvium portulacastrum* L.: two halophytes, two strategies to survive in saline habitats. *Plant Physiol. Biochem.* 44, 395–408. doi: 10.1016/j.plaphy.2006.06.007

Rana, M., and Mark, T. (2008). Mechanisms of salinity tolerance. *Annu. Rev. Plant Biol.* 59, 651–681. doi: 10.1146/annurev.arplant.59.032607.092911

Ruan, C. J., da Silva, J. A. T., Mopper, S., Qin, P., and Lutts, S. (2010). Halophyte improvement for a salinized world. *Crit. Res. Plant Sci.* 29, 329–359. doi: 10.1080/07352689.2010.524517

Seckin, B., Turkan, I., Sekmen, A. H., and Ozfidan, C. (2010). The role of antioxidant defense systems at differential salt tolerance of *Hordeum marinum* Huds. (sea barleygrass) and *Hordeum vulgare* L. (cultivated barley). *Environ. Exp. Bot.* 69, 76–85. doi: 10.1016/j.envexpbot.2010.02.013

Shabala, S., Hariadi, Y., and Jacobsen, S. E. (2013). Genotypic difference in salinity tolerance in quinoa is determined by differential control of xylem $Na^+$ loading and stomatal density. *J. Plant Physiol.* 170, 906–914. doi: 10.1016/j.jplph.2013.01.014

Shahzad, B., Fahad, S., Tanveer, M., Saud, S., and Khan, I. A. (2019). "Plant responses and tolerance to salt stress," in *Approaches for Enhancing Abiotic Stress Tolerance in Plants*. eds. M. Hasanuzzaman, K. Nahar, M. Fujita, H. Oku and M. T. Islam (Boca Raton, Florida, USA: CRC press,Taylor & Francis), 61–77.

Shalata, A., Mittova, V., Volokita, M., Guy, M., and Tal, M. (2001). Response of the cultivated tomato and its wild salt-tolerant relative *Lycopersicon pennellii* to salt-dependent oxidative stress: the root antioxidative system. *Physiol. Plant.* 112, 487–494. doi: 10.1080/10715760290006402

Shi, H., Ishitani, M., Kim, C., and Zhu, J. K. (2000). The *Arabidopsis thaliana* salt tolerance gene *SOS1* encodes a putative $Na^+/H^+$ antiporter. *Proc. Natl. Acad. Sci. U. S. A.* 97, 6896–6901. doi: 10.1073/pnas.120170197

Shigeru, S., Takahiro, I., Masahiro, T., Yoshiko, M., Toru, T., Yukinori, Y., et al. (2002). Regulation and function of ascorbate peroxidase isoenzymes. *J. Exp. Bot.* 53, 1305–1319. doi: 10.1093/jexbot/53.372.1305

Singh, M., Kumar, J., Singh, S., Singh, V. P., and Prasad, S. M. (2015). Roles of osmoprotectants in improving salinity and drought tolerance in plants: a review. *Rev. Environ. Sci. Biotechnol.* 14, 407–426. doi: 10.1007/s11157-015-9372-8

Székely, G., Brahám, E., Csépl, G., Rigó, G., Zsigmond, L., Csiszár, J., et al. (2008). Duplicated P5CS genes of *Arabidopsis* play distinct roles in stress regulation and developmental control of proline biosynthesis. *Plant J.* 53, 11–28. doi: 10.1111/j.1365-313X.2007.03318.x

Tenhaken, R. (2015). Cell wall remodeling under abiotic stress. *Front. Plant Sci.* 5:771. doi: 10.3389/fpls.2014.00771

Vadim, D. (2018). ROS-activated ion channels in plants: biophysical characteristics, physiological functions and molecular nature. *Int. J. Mol. Sci.* 19:1263. doi: 10.3390/ijms19041263

Wang, X., Chang, L., Wang, B., Wang, D., Li, P., Wang, L., et al. (2013). Comparative proteomics of *Thellungiella halophila* leaves under different salinity revealed chloroplast starch and soluble sugar accumulation played important roles in halophyte salt tolerance. *Mol. Cell. Proteomics* 12, 2174–2195. doi: 10.1074/mcp.M112.022475

Willekens, H., Chamnongpol, S., Davey, M., Schraudner, M., Langebartels, C., Montagu, M. V., et al. (2014). Catalase is a sink for $H_2O_2$ and is indispensable for stress defence in C3 plants. *EMBO J.* 16, 4806–4816. doi: 10.1093/emboj/16.16.4806

Yan, J., Liu, Y., Yang, L., He, H., Huang, Y., Fang, L., et al. (2021). Cell wall β-1, 4-galactan regulated by BPC1/BPC2-GALS1 module aggravates salt sensitivity in *Arabidopsis thaliana*. *Mol. Plant* 14, 411–425. doi: 10.1016/j.molp.2020.11.023

Yi, X., Sun, Y., Yang, Q., Guo, A., Chang, L., Wang, D., et al. (2014). Quantitative proteomics of *Sesuvium portulacastrum* leaves revealed that ion transportation by V-ATPase and sugar accumulation in chloroplast played crucial roles in halophyte salt tolerance. *J. Proteome* 99, 84–100. doi: 10.1016/j.jprot.2014.01.017

Zelm, E., Zhang, Y., and Testerink, C. (2020). Salt tolerance mechanisms of plants. *Annu. Rev. Plant Biol.* 71, 403–433. doi: 10.1146/annurev-arplant-050718-100005

Zhang, C., Wang, D., He, W., Liu, H., Chen, J., Wei, X., et al. (2022). *Sesuvium portulacastrum*-mediated removal of nitrogen and phosphorus affected by sulfadiazine in aquaculture wastewater. *Antibiotics* 11:68. doi: 10.3390/antibiotics11010068

Zhao, C., Zhang, H., Song, C., Zhu, J. K., and Shabala, S. (2020). Mechanisms of plant responses and adaptation to soil salinity. *Innovation (N Y)* 1:100017. doi: 10.1016/j.xinn.2020.100017

Zhong, M., Song, R., Wang, Y., Shu, S., and Guo, S. (2020). TGase regulates salt stress tolerance through enhancing bound polyamines-mediated antioxidant enzymes activity in tomato. *Environ. Exp. Bot.* 179:104191. doi: 10.1016/j.envexpbot.2020.104191

Zhou, Y., Yin, X., Duan, R., Hao, G., Guo, J., Jiang, X., et al. (2015). SpAHA1 and SpSOS1 coordinate in transgenic yeast to improve salt tolerance. *PLoS One* 10:e0137447. doi: 10.1371/journal.pone.0137447

Zhou, Y., Yin, X., Wan, S., Hu, Y., Xie, Q., Li, R., et al. (2018). The *Sesuvium portulacastrum* plasma membrane $Na^+/H^+$ antiporter SpSOS1 complemented the salt sensitivity of transgenic *Arabidopsis* sos 1 mutant plants. *Plant Mol. Bio. Rep.* 36, 553–563. doi: 10.1007/s11105-018-1099-6

frontiers | Frontiers in Plant Science

TYPE Original Research
PUBLISHED 17 January 2023
DOI 10.3389/fpls.2022.1040520



OPEN ACCESS

EDITED BY
Amr Adel Elkelish,
Suez Canal University, Egypt

REVIEWED BY
Sheikh Adil Edrisi,
Thapar Institute of Engineering &Technology, India
Roberta Calone,
Council for Agricultural and Economics Research (CREA), Italy
Dennis Shibonje Ashilenje,
Mohammed VI Polytechnic University, Morocco

*CORRESPONDENCE
Zhenyong Zhao
zhaozhy@ms.xjb.ac.cn

SPECIALTY SECTION
This article was submitted to Plant Abiotic Stress, a section of the journal Frontiers in Plant Science

RECEIVED 09 September 2022
ACCEPTED 22 December 2022
PUBLISHED 17 January 2023

CITATION
Wang N, Zhao Z, Zhang X, Liu S, Zhang K and Hu M (2023) Plant growth, salt removal capacity, and forage nutritive value of the annual euhalophyte *Suaeda salsa* irrigated with saline water.
*Front. Plant Sci.* 13:1040520.
doi: 10.3389/fpls.2022.1040520



# Plant growth, salt removal capacity, and forage nutritive value of the annual euhalophyte *Suaeda salsa* irrigated with saline water

Ning Wang[1,2], Zhenyong Zhao[2]*, Xinyi Zhang[1,2], Sihai Liu[1,2], Ke Zhang[2] and Mingfang Hu[2]

[1]College of Resources and Environment, University of Chinese Academy of Sciences, Beijing, China, [2]Xinjiang Institute of Ecology and Geography, Chinese Academy of Sciences, Urumqi, China

Sustainable agricultural development in semiarid and arid regions is severely restricted by soil and water salinization. Cultivation of the representative halophyte *Suaeda salsa*, which can be irrigated with saline water and cultivated on saline soils, is considered to be a potential solution to the issues of freshwater scarcity, soil salinization, and fodder shortage. However, the salt removal capacity and differences in the forage nutritive value of *S. salsa* under different saline water treatments remain unknown. Using the methods of field trials and randomized blocks design, we quantified salt accumulation in the aboveground biomass, and the biochemical and nutritive value of field-cultivated *S. salsa* in arid northwestern China under irrigation with water of different salinities [i.e., freshwater or water containing10, 20, 30, or 40 g/L NaCl). The fresh and dry weights of *S. salsa* increased, then decreased, with increase in salinity. The salt content of the plant's aboveground biomass increased to a constant range and, thus, the salt extraction of *S. salsa* was relatively stable under different salinities of irrigation water. Under the experimental conditions, the crude protein content significantly increased to 9.45% dry weight (DW) and then decreased to 6.85% DW, with an increase in salinity ($p < 0.05$). The neutral detergent fiber (42.93%–50.00% DW) and acid detergent fiber (34.76%–39.70% DW) contents were suitable for forage. The contents of trace elements, such as copper and zinc, were significantly increased after irrigation with saline water ($p < 0.05$). The forage of *S. salsa* is of high nutritive value for livestock, and contains low concentrations of anti-nutrients. Therefore, *S. salsa* can be considered for cultivation in saline soils irrigated with saline water. In addition, it provides a viable additional source of fodder in arid regions, where the availability of freshwater and non-saline arable land is limited.

KEYWORDS

**halophyte, *Suaeda salsa*, brine irrigation, revegetation, saline–alkali soil, forage nutritive value**

# 1 Introduction

Global livestock production has rapidly expanded in recent years, with much of the increase occurring in China. In this context, the demand for forage grain is increasing (Zhou et al., 2008). The rising global food demand will be difficult to meet with existing agricultural systems because an equivalent increase in agricultural land area is not possible (Al-Azzawi and Flowers, 2022). Water scarcity and salt stress are crucial factors that contribute to the scarcity of pasture resources in arid and semiarid areas of the world (Agudelo et al., 2021). Reported potential yield losses are estimated to be 17% and 20% under drought and salinity, respectively (Hedayati-Firoozabadi et al., 2020). In arid and semiarid climates, including low-rainfall saline regions of Australia, the USA, many Asian countries, and the Mediterranean region, the combination of high levels of water evaporation, low rainfall, irrigation with low-quality water, and other irrational anthropogenic activities results in soil salinization and good-quality forage for livestock being in short supply (Hessini et al., 2020). However, these areas are important for agricultural development and the ecological environment, especially in developing countries. For example, many of the saline–alkali areas in China have a small human population and underdeveloped industrialization, thus making them highly suitable for large-scale animal husbandry (Liu and Wang, 2021). However, conventional forage grows slowly or cannot survive in saline–alkali soil. Therefore, the integration of salt-affected soils and saline water resources to enable sustainable agricultural production with constrained resources is an important problem requiring urgent resolution.

Halophytes, which constitute 1% of the global flora (Flowers and Colmer, 2008), can produce relatively high quantities of consumable biomass in saline areas where non-halophytic species cannot grow or produce only low dry-matter yields (El Shaer, 2010). In addition, in general, the forage produced from saline land has higher forage nutritive values and can improve the quality, nutritional composition, and weight of meat from cattle and sheep (Sun et al., 2015; Ali et al., 2016). Hence, the use of naturally salt-tolerant species to provide forage resources in arid and saline environments is an emerging agricultural strategy (Hessini et al., 2020). This approach has been applied worldwide. For example, Australia is classified as the world's driest continent and is challenged by soil salinization (Ben Salem and Morand-Fehr, 2010). In this context, various halophytes are now widely accepted as forage plants. There are some relatively successful examples of the integration of halophytes and salt-tolerant forage into small-ruminant production systems (Norman et al., 2010). In low-rainfall saline regions of the USA, Mexico, and many Asian countries, water for agricultural use is extremely limited. Therefore, local agriculture largely depends on the use of marginal water sources, such as saline water and seawater, and drives the cultivation of plants that can tolerate salt water for a variety of uses (Ali et al., 2016; Ozturk et al., 2018; Garza-Torres et al., 2020; Hedayati-Firoozabadi et al., 2020). Salinity and aridity are also encountered in Mediterranean countries. There are many halophytes that grow naturally in almost all estuarine, lagoon, and coastal ecosystems; some of these species have been cultivated as alternative vegetable crops and forage for animal consumption (e.g., 20% and 9% of Iberian halophytes, respectively) (Duarte and Cacador, 2021).

However, achieving grazing value from saline systems is not straightforward (Norman et al., 2013). Different species respond to salinity in different ways because salt tolerance varies greatly among halophytes (Fita et al., 2015; Kumari et al., 2015; Himabindu et al., 2016). It is reported that chenopods are generally more salt tolerant than other halophytic grasses and legumes, and have high crude protein and mineral contents, which are important for ruminant production (Norman et al., 2013). Therefore, chenopods are suitable for use as a forage reserve during drought, or as a supplementary feed source in arid and semiarid environments.

*Suaeda salsa*, an annual euhalophytic herb, and a member of the Chenopodiaceae family, is widely distributed in the intertidal zone and inland saline sites in China (Zhao et al., 2018; Wang and Song, 2019). The succulence and salt absorption capacities of halophytic plants allow them to thrive in high-salinity habitats and to be pioneer plants in saline–alkali lands (Wu et al., 2012; Xu et al., 2013; Song and Wang, 2015). Hence, *S. salsa* is considered to be a promising model plant to enable us to understand salt tolerance and to develop saline agriculture with halophytes (Song and Wang, 2015). *Suaeda salsa* can provide high-quality forage (Li et al., 2017). Wei (2016) reported that the inclusion of an appropriate proportion of *S. salsa* forage can improve pig fattening performance, provide economic benefits, and help to improve immunity. Zhang et al. (2018) reported that *S. salsa* can increase the daily gain of Altay sheep, reduce the feed conversion ratio, increase the net meat yield, and reduce the carcass fat percentage. In addition, *S. salsa* is of high ecological value and is widely suitable as a pioneer species for saline–alkali vegetation restoration. Harvesting of the aboveground biomass of *S. salsa* can significantly decrease the salt content of saline soils. *S. salsa* has also been proposed to be a biomaterial useful in the removal of heavy metals from heavy metal-contaminated soils, especially contaminated saline soils (Wang and Song, 2019; Shang et al., 2020).

Given these attributes, we consider that *S. salsa* may be suitable as a halophytic forage and as an aid to the process of revegetation. However, forage mass and survival alone do not adequately describe its grazing potential on saline rangelands (Waldron et al., 2020). Environmental factors affect plant growth rate and forage nutritive value and production by altering the physiological processes of plants (Etesami and Beattie, 2018). Considering the unique physiological characteristics of halophytes, the effect of salt ions and certain secondary compounds on forage nutritive values should also be taken into account (Masters et al., 2007; Munns and Tester, 2008). Under severe salt stress, halophytes can absorb and synthesize ions and solutes to maintain osmotic pressure, and protein and fiber synthesis may be affected (Muchate et al., 2016). In addition, antioxidants synthesized by halophytes to detoxify reactive oxygen species are critical to forage nutritive values (Norman et al., 2013; Wang et al., 2020). Therefore, whether or not *S. salsa* can be used as forage and how its forage nutritive value changes under irrigation with high-salinity water are unclear. Further evaluation of the effect of salinity on its forage nutritive value is needed.

Hence, a field study was conducted to determine the yield, forage nutritive value indicators [including the contents of ash, crude protein, crude fat, minerals, neutral detergent fiber (NDF), and acid detergent fiber (ADF)], and selected secondary metabolites of *S. salsa*. This research aimed to address the following questions: (i) From an economic perspective, under irrigation with highly saline water, can *S.*

*salsa* survive and produce adequate biomass, and how is its forage nutritive value affected? (ii) With regard to the rehabilitation and improvement of natural ecosystems, does the salt removal capacity of *S. salsa* vary with different degrees of salinity? The results will enrich knowledge of the utilization of saline land and water resources, and provide a scientific basis to promote the development of local animal husbandry in saline environments.

# 2 Materials and methods

## 2.1 Study location

The study was conducted in saline wasteland in the Agricultural Comprehensive Development Zone of Karamay, Xinjiang, China, from June to November 2021. The development zone is located on the lacustrine plain 10 km southeast of Karamay, and has a temperate desert climate. In the summer, this area is extremely hot, with a maximum average temperature of 49.1°C, and in winter it is cold, with a minimum average temperature of –42.0°C (Qiao et al., 2011). The average annual precipitation is 108.9 mm, and the average annual evaporation is 3,008.9 mm. Irrigation water in the experimental area was obtained from a reservoir in the western suburb of Karamay; the water quality properties are summarized in Table 1. The physicochemical attributes of the soil in the experimental field before the study are listed in Table 2.

## 2.2 Plant irrigation and soil salinity

The experiment consisted of five treatments according to different saline contents of irrigation water, consisting of CK and water containing 10, 20, 30, and 40 g/L NaCl. All treatments were replicated four times, and 20 experimental plots were arranged in a randomized block design to reduce the influence of one-way soil difference on the experiment (Figure 1D). Freshwater was drawn from the local drip irrigation system and mixed with different amounts of NaCl to achieve the required salinity. Each treatment was equipped with an independent gravity drip irrigation system, consisting of a water tank (2 m above the ground), polyvinyl chloride pipes, ball valves, water meters, and capillaries (Figure 1B).

Each plot was 5 m long and 6 m wide (Figure 1C). The distance between adjacent capillary belts was 60 cm. The *S. salsa* seeds, fine sand, and water were mixed into loose grains and sown at a depth of 20 cm on both sides of the capillary to form a 40-cm seeding belt (Figure 1A). The seeding belts were irrigated immediately after sowing. Thereafter, irrigation was carried out every 2 d. At the seedling stage, irrigation was carried out based on the soil condition. Irrigation was carried out until overlap was attained in the humidification ranges between adjacent capillary belts. All plots were irrigated using the same irrigation interval and irrigation volumes.

## 2.3 Plant material, sampling, and growth measurements

A 0.6 m × 0.6 m quadrat was randomly selected in each plot, reflecting the distance between adjacent capillary belts. A previous report indicates that the maximum forage nutritive value of *S. salsa* is reached during its initial flowering stage (Li et al., 2017). Therefore, sampling determined for forage nutritive value was performed at this stage. The fresh weight (FW) was determined using a balance. The plant was then placed in an oven for fixation at 105 ± 2°C for 30 min and dried at 60 ± 2°C until constant weight, and weighed again to determine the dry weight (DW). The yield per hectare, including FW and DW, was estimated in proportion to the sampled area. The fixation process can rapidly inactivate biologically active enzymes by way of thermochemical reactions. Thus, fixation is widely used as the primary processing method for using plants. Fixation before dying can reduce the loss of active component content. The plant height (cm) was measured from the soil surface to the highest shoot tip. Succulence was calculated as the FW to DW ratio.

The ash content was measured based on Chinese national standard GB/T 64382007. The crude protein (CP) content was determined based on national standard GB/T 6432-2018 using the Kjeldahl method. The van Soest method was used to determine the NDF and ADF content (Van Soest, 1963). In accordance with

TABLE 1 Chemical characteristics of irrigation water (g/L).

| pH | $K^+$ | $Na^+$ | $Ca^{2+}$ | $Mg^{2+}$ | $Cl^-$ | $SO_4^{2-}$ | $HCO_3^-$ | $CO_3^{2-}$ |
|---|---|---|---|---|---|---|---|---|
| 7.07 | 0.004 | 0.020 | 0.034 | 0.006 | 0.022 | 0.070 | 0.083 | 0.000 |

TABLE 2 Initial salt content and ion composition of soil.

| Depth (cm) | Salinity (g/kg) | Moisture (%) | $Na^+$ (g/kg) | $K^+$ (g/kg) | $Ca^{2+}$ (g/kg) | $Mg^{2+}$ (g/kg) | $Cl^-$(g/kg) | $SO_4^{2-}$(g/kg) | $HCO_3^-$(g/kg) |
|---|---|---|---|---|---|---|---|---|---|
| 0–20 | 3.62 | 13.00 | 0.68 | 0.03 | 0.28 | 0.17 | 0.59 | 1.56 | 0.27 |
| 20–40 | 8.77 | 19.14 | 1.89 | 0.04 | 0.69 | 0.28 | 2.48 | 2.55 | 0.23 |
| 40–60 | 7.46 | 21.38 | 1.49 | 0.04 | 0.72 | 0.21 | 2.18 | 2.15 | 0.24 |
| 60–80 | 5.01 | 23.63 | 1.07 | 0.03 | 0.35 | 0.15 | 1.17 | 1.69 | 0.26 |
| 80–100 | 4.96 | 23.12 | 0.69 | 0.03 | 0.59 | 0.18 | 1.30 | 1.45 | 0.24 |

TABLE 3 Mineral and heavy metal contents of *S. salsa* under irrigation with water of different salinities.

| Ion | CK | 10 g/L | 20 g/L | 30 g/L | 40 g/L |
|---|---|---|---|---|---|
| $K^+$ | 10.39 ± 0.55c | 12.03 ± 0.42bc | 13.7 ± 0.98b | 16.8 ± 0.70a | 16.49 ± 0.49a |
| $Ca^{2+}$ | 7.94 ± 0.25b | 7.40 ± 0.18b | 7.16 ± 0.36b | 9.66 ± 0.61a | 9.74 ± 0.34a |
| $Na^+$ | 29.32 ± 5.44b | 46.96 ± 1.55ab | 42.43 ± 0.38ab | 59.27 ± 7.18a | 54.97 ± 8.96a |
| $Mg^{2+}$ | 13.40 ± 0.22b | 11.04 ± 0.42b | 12.63 ± 0.82b | 15.86 ± 0.52a | 17.61 ± 0.86a |
| $Cl^-$ | 77.67 ± 11.74b | 95.88 ± 2.17ab | 92.33 ± 4.86ab | 119.63 ± 17.20a | 126.82 ± 3.65a |
| $S^+$ | 4.97 ± 0.10c | 4.99 ± 0.19c | 5.70 ± 0.33bc | 6.42 ± 0.46ab | 7.20 ± 0.14a |
| P | 734.85 ± 59.56c | 817.31 ± 132.10c | 1227.93 ± 71.04b | 1223.71 ± 37.88b | 1689.25 ± 105.43a |
| $Fe^{2+}$ | 131.08 ± 10.24a | 129.09 ± 3.67a | 145.17 ± 1.74a | 150.75 ± 26.06a | 134.75 ± 7.65a |
| $Cu^{2+}$ | 23.07 ± 9.75a | 36.91 ± 19.82a | 82.75 ± 46.51a | 135.39 ± 88.69a | 145.55 ± 58.02a |
| $Zn^{2+}$ | 35.23 ± 1.28d | 58.60 ± 3.76cd | 65.62 ± 11.41bc | 86.07 ± 7.47b | 111.11 ± 1.89a |
| Mo | 0.96 ± 0.02b | 1.01 ± 0.02b | 1.02 ± 0.03b | 1.14 ± 0.10ab | 1.48 ± 0.18a |
| $Ni^{2+}$ | 2.22 ± 0.27a | 0.20 ± 0.20a | 0.33 ± 0.33a | 0.74 ± 0.74a | 1.17 ± 0.70a |
| $Cr^{2-}$ | 1.01 ± 0.27a | 1.06 ± 0.25a | 1.38 ± 0.36a | 1.33 ± 0.50a | 2.42 ± 0.65a |
| $Cd^{2+}$ | 0.18 ± 0.04b | 0.24 ± 0.02ab | 0.32 ± 0.04ab | 0.31 ± 0.04ab | 0.35 ± 0.04a |
| $As^{3+}$ | 0.18 ± 0.04ab | 0.06 ± 0.01b | 0.2 ± 0.09ab | 0.13 ± 0.00b | 0.35 ± 0.04a |
| $Pb^{2+}$ | 1.09 ± 0.30a | 1.06 ± 0.62a | 2.75 ± 1.83a | 4.63 ± 3.41a | 4.40 ± 2.45a |
| $Hg^{2+}$ | 0.02 ± 0.00a | 0.02 ± 0.00a | 0.02 ± 0.00a | 0.03 ± 0.00a | 0.02 ± 0.00a |

The data are the mean ± SE. Different lowercase letters within a row indicate a significant difference ($p < 0.05$). The unit for $K^+$, $Ca^{2+}$, $Na^+$, $Mg^{2+}$, and $Cl^-$ is g/kg DW. The unit for the other ions is mg/kg DM. CK, freshwater; DM, dry matter; DW, dry weight.

TABLE 4 Ash content and concentration of *S. salsa* under irrigation with water of different salinities.

| Treatment | Bud stage | | Flower bud stage | | Fruit stage | |
|---|---|---|---|---|---|---|
| | Ash content (% DW) | Ash accumulation (kg/hm$^2$) | Ash content (% DW) | Ash accumulation (kg/hm$^2$) | Ash content (% DW) | Ash accumulation (kg/hm$^2$) |
| CK | 25.25 ± 0.88c | 1181.21 ± 49.70b | 20.61 ± 0.35c | 1666.62 ± 25.51d | 17.67 ± 0.09b | 3539.76 ± 155.42b |
| 10 g/L | 33.95 ± 0.45b | 1484.12 ± 37.79a | 24.47 ± 0.20b | 2627.76 ± 111.75b | 21.90 ± 0.44a | 5316.86 ± 389.90a |
| 20 g/L | 37.30 ± 0.22a | 1394.55 ± 92.54a | 28.99 ± 0.70a | 3307.99 ± 27.57a | 22.47 ± 0.69a | 5671.03 ± 269.02a |
| 30 g/L | 36.93 ± 1.49ab | 898.75 ± 24.54c | 28.54 ± 0.31a | 2065.14 ± 74.08c | 21.87 ± 0.32a | 5657.56 ± 299.24a |
| 40 g/L | 36.35 ± 0.3ab | 784.18 ± 60.29c | 29.24 ± 0.44a | 1816.70 ± 113.45cd | 22.81 ± 0.50a | 5607.76 ± 458.41a |

The data are the mean ± SE. Different lowercase letters within a column indicate a significant difference ($p < 0.05$). CK, freshwater; DM, dry matter; DW, dry weight.

national standard GB 5009.268-2016, the contents of K, Ca, Na, Mg, and P were determined by inductively coupled plasma emission spectrometry (ICP-OES). The contents of Fe, Zn, Cu, Mo, Ni, Cr, Cd, As, Pb, and Hg were determined by inductively coupled plasma mass spectrometry (ICP-MS). The contents of Cl and oxalate were determined by ion chromatography using the following specific equipment and conditions: AS-LH-AC-3 chromatographic column (250mm * 4.6 mm); column temperature 35°C; mobile phase 2 mmol/L $Na_2CO_3$ and 10 mmol/L $NaHCO_3$; and flow rate 1.5 mL/min.

The content of S was determined using an elemental analyzer (Vario MICRO Cube, Germany). We followed the operating conditions and instructions recommended by the manufacturer, which are as follows: oxidation tube temperature 1,150°C; reduction tube temperature 850°C; helium pressure 1,200 mbar; helium flow rate 230 mL/min; oxygen flow rate 45 mL/min; the absorption and release temperature of the $CO_2$ absorption column were 40°C and 60°C, respectively; the absorption and release temperature of the water absorption column were 40°C and 140°C, respectively; and the absorption and release temperature of the $SO_2$ absorption column were 40°C and 240°C, respectively.

The betaine concentration was determined using ion chromatography in accordance with national standard GB/T 23710-2009. The tannin content was determined using UV–Vis spectrophotometry (8453, Agilent). Samples of about 2–5 g were weighed, then washed in a 100-mL volumetric flask with 80 mL of water. We then placed the extract in a boiling water bath for 30 min, and completed to 100 mL measuring flask by deionized water. A 2-mL sample extract was absorbed, then centrifuged at 8,000 rev/min for

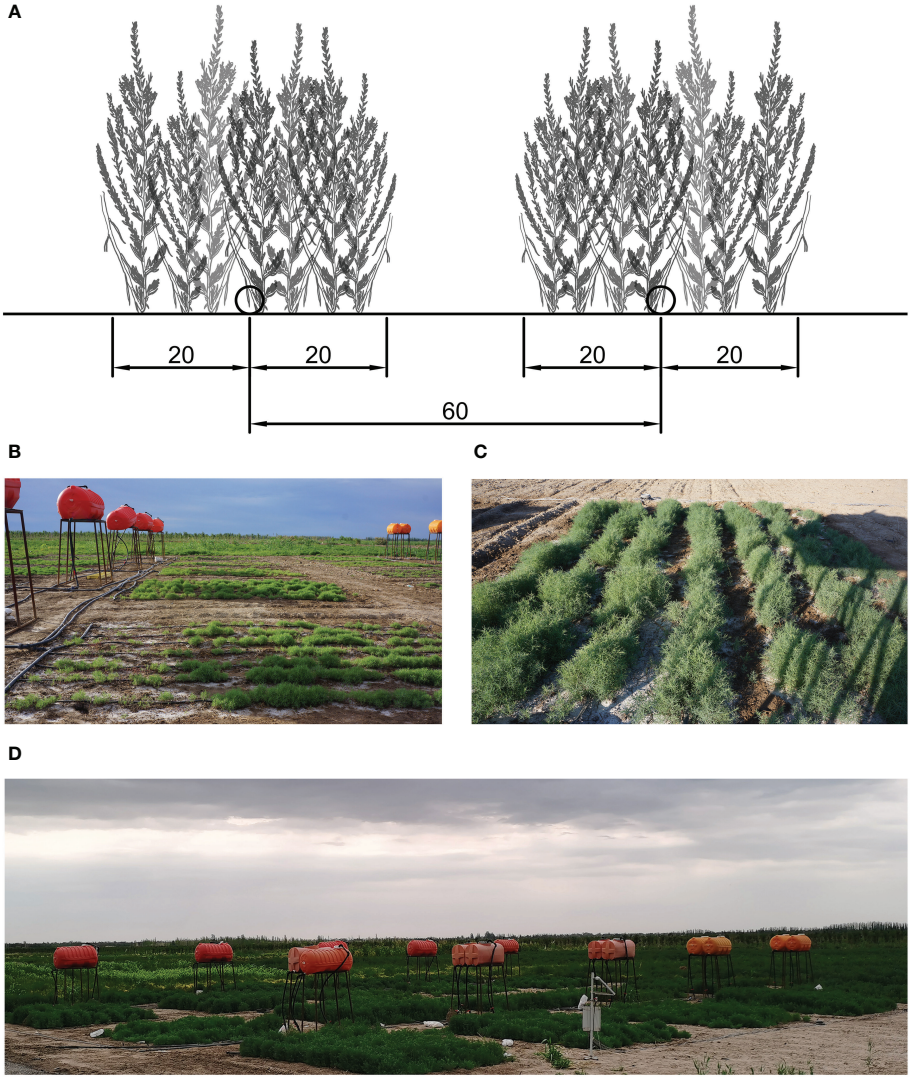


FIGURE 1
**(A)** Planting design used in the study. The distance between adjacent capillary belts was 60 cm and the planting belt was 40 cm in length. **(B)** Irrigation system consisting of water tanks, polyvinyl chloride pipes, ball valves, water meters, and capillaries. **(C)** View of one experimental plot. **(D)** View of the overall experimental area.

5 min at room temperature. The supernatant was removed and stored. The following was added to 1 mL of clear supernatant: 5.0 mL of water, 1.0 mL of a sodium tungstate–sodium molybdate mixed solution, and 3.0 mL of a sodium carbonate solution. After being set aside for 2 hours, the absorbance of the sample solution was determined at 765 nm, with the standard 0.00 mg/L used as a blank. The tannin concentration of the sample solution was calculated and expressed as mg/L gallic acid equivalent from the standard curve.

Soil column samples of 0–40 cm were taken with a soil drill. We allowed the air-dried soil samples to pass through screens with an opening size of 2 mm. We then weighed a 5.0-g soil sample, put it in a 250-mL flask and added 50 mL of $NH_4OAc$ solution. After shaking for 30 min, samples were filtered through dry qualitative filter paper. The Na concentration in the filtrate was determined using a flame photometer.

The ash accumulation was calculated as the product of ash content and aboveground biomass. *Suaeda salsa* can absorb salt from the rhizosphere and salt also accumulates in its aboveground plant tissues. Thus, this portion of the salt is removed from the soil when the aboveground biomass is harvested, and the ash accumulation represents its salt removal capacity.

In accordance with Antisari et al. (2020), the salt bioaccumulation factor (BCF) was calculated as the ratio of the Na content of aboveground biomass to the Na concentration in the rhizosphere.

## 2.4 Statistical analysis

Figures were prepared using Microsoft Excel 2016. Statistical analyses were conducted using SPSS 24.0 software. All data were analyzed by one-way analysis of variance (ANOVA), with the salinity of irrigation water as the independent variable. The response variables for these ANOVAs were growth, composition, ion content, and secondary metabolites concentration. Tukey's honestly significant difference test was used for a comparison of means. The

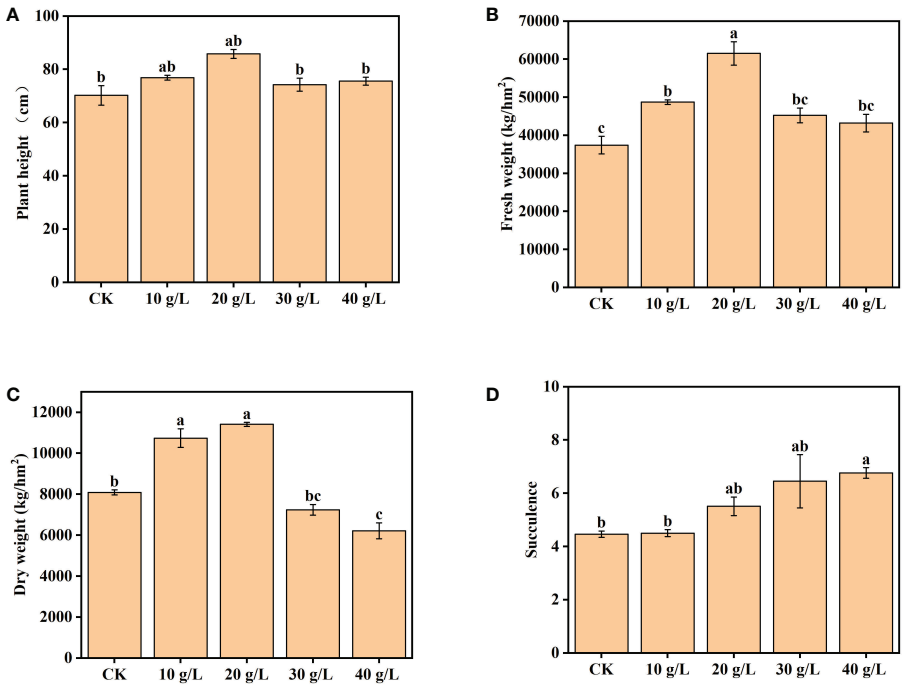


FIGURE 2
Effects of irrigation water salinity on **(A)** plant height, **(B)** fresh weight, **(C)** dry weight, and **(D)** succulence of *Suaeda salsa*. Bars and error bars indicate the mean ± SE ($n$ = 4). Different lowercase letters indicate a significant difference ($p < 0.05$).

significance was determined at the 5% significance level. All results are presented as means plus or minus the standard error (SE). Histograms were drawn using OriginPro 2021 software.

# 3 Results

## 3.1 Growth of *S. salsa*

The growth of *S. salsa* was significantly promoted by low-salinity irrigation water ($p < 0.05$). Plant height and aboveground biomass (both FW and DW) initially increased and then decreased with the increase in irrigation water salinity, and the maximum was attained at 20 g/L (Figure 2). In the 20 g/L treatment, the plant height, FW, and DW aboveground biomass of *S. salsa* were higher than those of the control by 22.23%, 64.53%, and 41.11%, respectively. In the treatment with irrigation water of 30 g/L or 40 g/L salinity, the plant height, and FW and DW aboveground biomass decreased compared with lower-salinity irrigation water, but were still higher than those of the control. The degree of succulence of *S. salsa* increased significantly with the increase in irrigation water salinity ($p < 0.05$), as evident in the succulence of the leaves.

## 3.2 Forage nutritive value of *S. salsa*

### 3.2.1 Composition

The content of ash increased from 20.6% dry matter (DM) to 29.2% DM with increased salinity of the irrigation water from freshwater (CK) to high salinity (40 g/L) (Figure 3A). The CP content increased initially, then decreased, with increase in irrigation water salinity (Figure 3B). The maximum CP content was observed under moderate salinity (20 g/L). The content of NDF was 42.93%–50.00% DW and decreased significantly under irrigation with water of a salinity of 20 g/L and higher (Figure 3C). The ADF content ranged from 35.62% DW to 39.70% DW and was not significantly affected by the salinity of the irrigation water (Figure 3D).

### 3.2.2 Mineral and heavy metal composition of *S. salsa*

Halophytes, which grow naturally in saline environments, generally have higher mineral contents than other plants. Irrigation with brine had a significant effect on the ion content of *S. salsa* ($p < 0.05$) (Table 3).

The concentration of macro elements, including Na, K, Ca, Mg, P, and Cl, increased with the increase in irrigation water salinity. The cation and anion with the highest concentrations were $Na^+$ (2.93%–5.50% DW) and $Cl^-$ (7.77%–11.60% DW), and the highest concentrations were, respectively, 2.02 times and 1.63 times higher than in the control.

Salinity promoted the absorption and accumulation of Cu and Zn. Compared with the control, the Cu and Zn contents increased by 5.9 times and 3.9 times, respectively. The content of Fe (129.09– 150.75 mg/kg DW) did not respond to an increase in irrigation water salinity.

The content of heavy metals increased with the increase in irrigation water salinity. However, with reference to the national standard "Hygienical Standard for Feeds" (GB13078-2017), the concentrations were below the maximum permitted limit and did not pose a risk to human health.

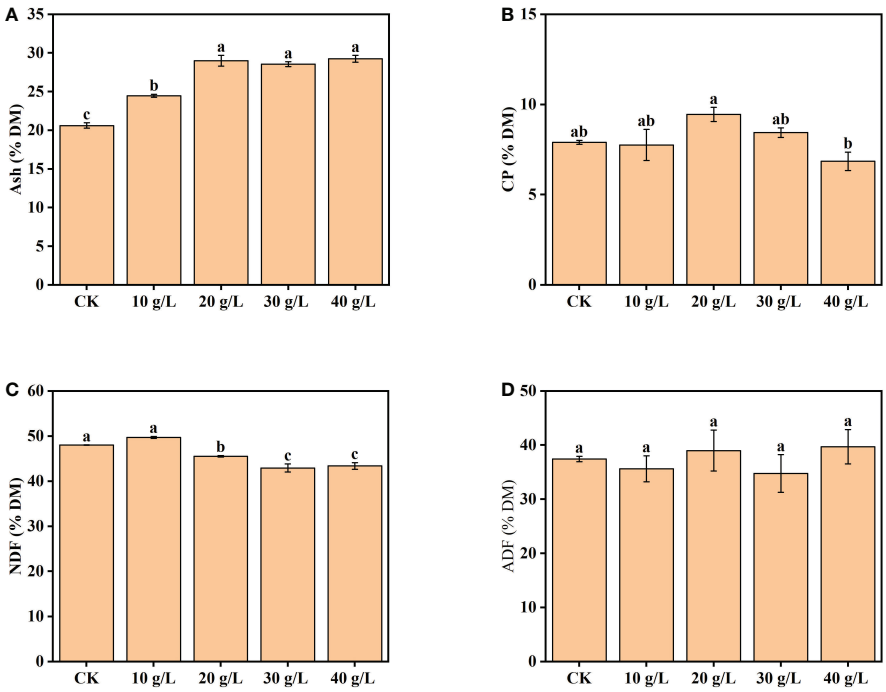


FIGURE 3
Effects of irrigation water salinity on the contents of **(A)** ash, **(B)** crude protein (CP), **(C)** neutral detergent fiber (NDF), and **(D)** acid detergent fiber (ADF) of *Suaeda salsa*. Bars and error bars are the mean ± SE ($n$ = 4). Different lowercase letters indicate a significant difference ($p < 0.05$).

### 3.2.3 Secondary metabolites

The betaine content increased from 7.13% DW to 19.44% DW with increased salinity of the irrigation water. Compared with the control, the betaine content of plants irrigated with 40 g/L saline increased 2.73 times (Figure 4A). The content of tannin first increased and then decreased with increase in irrigation water salinity; the maximum tannin content was observed under moderate salinity (30 g/L) (Figure 4B). Under irrigation with water of 40 g/L salinity, the tannin content decreased, but the content was still higher than that of the control. The oxalate content ranged from 0.87% DW to 1.62% DW, which would not reduce feed intake or pose a risk to human health (Figure 4C).

## 3.3 Salt removal capacity of *S. salsa* at different developmental stages

The effect of saline water irrigation on the ash content of *S. salsa* was consistent at all growth stages (Table 4). The ash content increased significantly with increase in irrigation water salinity from the control (freshwater) to 40 g/L irrigation water concentration. The change in ash content during the entire growth period was consistent under the different treatments. The ash content decreased from the bud stage to the fruit stage.

From the bud stage to the fruit stage, although the ash content decreased, the total accumulation of ash increased because of the gradual accumulation of biomass. The ash accumulation increased first and then decreased at all growth stages, which was similar to the trend observed for accumulation in biomass.

Ash accumulation is mainly affected by biomass, and ash content is significantly affected by environmental salinity. To compare the plant's relative salt removal capacity while subjected to the different treatments, its BCF was calculated to assess its ability to absorb salt from the soil. The mean BCF calculated in the different treatments at the flower bud stage is shown in Figure 5. The BCF significantly decreased with increase in salinity of the irrigation water ($p < 0.05$) and stabilized at the highest salinities (20 g/L and higher).

# 4 Discussion

## 4.1 Intermediate salinity can improve the growth of *S. salsa*

The aboveground biomass is an important factor in the selection of a halophyte as a forage plant, as it affects the salt removal capacity of the plant. From the perspective of forage, it is meaningless to discuss the nutritive value if substantial biomass, generally measured by DW, is not formed. Based on the present data for growth indicators of *S. salsa*, the forage yield first increased and then decreased with increase in irrigation water salinity, and the peak yield was observed at a salinity of 20 g/L. These results conform to a typical "curvilinear" growth response to salt stress in halophytes, with peak growth observed under moderate salinity (Ma et al., 2019). This is because halophytes have evolved mechanisms by which high concentrations of salt in the environment can be used to their benefit (Guo et al., 2006). Appropriate salt concentrations can promote the vegetative growth of halophytes and are conducive to

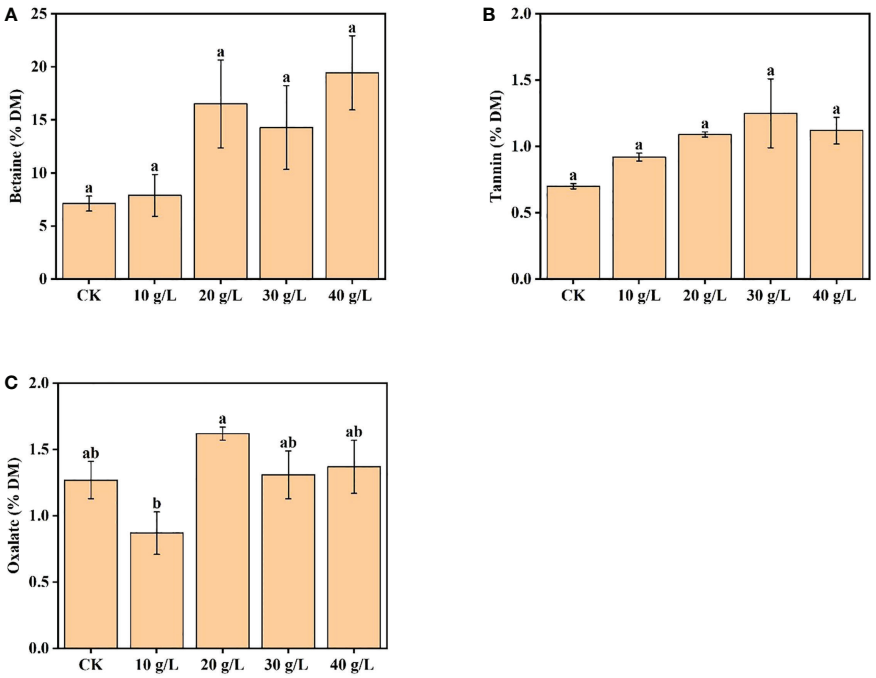


FIGURE 4
Effects of irrigation water salinity on contents of **(A)** betaine, **(B)** tannin, and **(C)** oxalate of *Suaeda salsa*. Bars and errors bars indicate the mean ± SE ($n$ = 4). Different lowercase letters indicate a significant difference ($p$ < 0.05).

the completion of their life cycle (Yuan et al., 2019). Among the five treatments in this study, the 20 g/L irrigation concentration may be the most suitable treatment for the growth of *S. salsa*. Morphologically, halophytes have evolved several specific structures. Leaf succulence, which enables accumulation of excessive salt concentrations and conserves water, is a typically visible characteristic of *S. salsa* under high levels of salinity (Zhao et al., 2020). Succulence in itself is not of importance to ruminants (Norman et al., 2013), but can represent the growth state of plants under complex abiotic stress. Ma et al. (2019) argue that succulence could be caused by changes in cell size as a consequence of improved osmotic adjustment. However, in a saline environment, the photosystem of *S. salsa* can be maintained at its normal state and the concentrations of some ions that accumulate in the leaves can promote photosynthetic capacity, which may be one reason for the increase in its aboveground dry weight under salinity (Li et al., 2022).

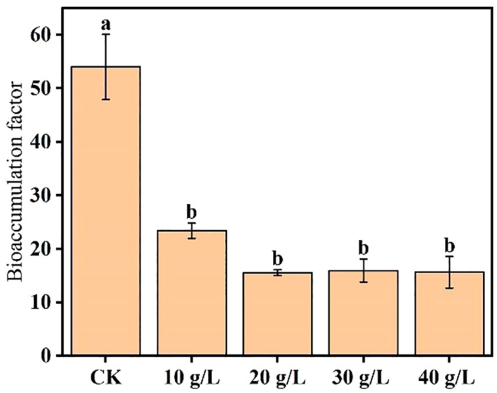


FIGURE 5
Effects of irrigation water salinity on the salt bioaccumulation factor of *Suaeda salsa*. Different lowercase letters indicate a significant difference ($p$ < 0.05).

The annual biomass production of halophytes ranges from 400 to 40,000 kg/hm$^2$ in a saline environment (Norman et al., 2013) because the degree of salt tolerance of forage species varies widely. Chenopods are generally more salt tolerant than halophytic grasses and legumes, and as such are widely recognized to show potential for utilization of saline land and water (Masters et al., 2010; Norman et al., 2013). In the present study, the growth of *S. salsa* was promoted by irrigation water of moderate salinity. The annual biomass production ranged from 6,213.07 to 11,410.79 kg/hm$^2$; thus, *S. salsa* is potentially suitable as a forage resource. Notably, this yield was achieved under deficit irrigation (irrigation quota: 1,760 m$^3$/hm$^2$), and would be expected to increase significantly under appropriate agronomic management, such as the supply of appropriate nitrogen and/or adequate water (X. Wang et al., 2021). These results show that *S. salsa* can produce substantial biomass for use as a potential source of forage. Thus, *S. salsa* can fill the annual feed shortage, and allow farmers to earn income from saline wasteland.

## 4.2 Moderate salinity can improve the forage nutritive value of *S. salsa*

In addition to yield, forage nutritive value, mainly referring to the CP, fiber, and ash content, is an important aspect of forage (Al-Dakheel et al., 2015). For the same species in the same growth period, it is generally believed that the treatment with the highest CP content and lowest fiber content has the highest forage nutritive value (Jungers et al., 2020).

In the present study, the CP content of *S. salsa* first increased to 9.45% DW and then decreased to 6.85% DW with increase in the irrigation water salinity. Abundant salt-responsive proteins, which contribute to diverse functions such as photosynthesis, osmotic and ionic homeostasis, signal transduction, and reactive oxygen species-scavenging systems, have been identified (Kumari et al., 2015). The increase in CP content is an essential feature of salt tolerance (Koyro et al., 2013). Hence, there is a general tendency for the abundance and activity of transporter proteins to increase under hyperosmotic salinity initially; these proteins then decrease as the external salt concentration continues to increase. This decrease in CP content is an indicator of severe stress and leads to the eventual death of the plant (Koyro et al., 2013), which is consistent with the present results. Decreased CP content in a saline environment may be due to the reduction in nutrient uptake from saline soils, which leads to reduced synthesis or enhanced degradation of proteins, low amino acid availability, and the denaturation of enzymes associated with protein synthesis (Hedayati-Firoozabadi et al., 2020). Previous studies have reported the CP content in a range of halophytic plants, ranging from 3.38% DM to 15.1% DM (El Shaer, 2010; Pirasteh-Anosheh et al., 2021). In this study, the CP content of *S. salsa* is higher than that of some halophytic forage considered to provide high-protein forage., There is no unified standard for the CP content of forage, as requirements vary among animals and growth stages, and the protein requirement of ruminants for maintenance, growth, and reproduction is low (Hessini et al., 2020). A plant with a CP content > 7% is considered to be highly suitable as a forage plant, and a plant with a CP content of 5%–7% is considered suitable (Pirasteh-Anosheh et al., 2021). Hence, in the present study, *S. salsa* can be regarded as a high-quality forage or protein supplement for ruminants in arid–saline rangelands. In addition, low CP contents may be improved through agronomic means (Norman et al., 2013).

Halophytes are characterized by having a high content of indigestible fiber (Norman et al., 2013), which generally reduces the forage nutritive value by reducing livestock intake and the digestibility of most nutrients (Harper and McNeill, 2015; Waldron et al., 2020). In the current study, the NDF decreased significantly under irrigation with water of salinity 20 g/L and above, whereas the ADF content was not significantly affected by irrigation water salinity. According to existing research, interactions between the salinity of the environment and the fiber content of grasses are inconsistent. Pasternak et al. (1993) observed no consistent relationship between the fiber content of five halophytic grasses and soil salinity. Robinson et al. (2004) reported that the NDF content of *Cynodon dactylon* increased with salinity, whereas that of *Thinopyrum ponticum* decreased. Hence, the relationship between fiber content and salt stress requires further study. Based on the results of Pirasteh-Anosheh et al. (2021), an ADF content of > 45% is not suitable and 35% < ADF < 45% is suitable, whereas an NDF content > 50% is not suitable and 40% < NDF < 50% is suitable. Accordingly, both the NDF (42.93%–50.00% DM) and ADF (34.76%–39.70% DM) contents of *S. salsa* in the present study were suitable. Trace elements, such as Zn, Cu, and Fe, are involved in most biochemical metabolic processes of the body, as they are the main components of cellular enzymes and transcription factors in animals, and should be given priority when evaluating forage nutritive value (Fang et al., 2013). Xinjiang comprises a vast land area, and mineral elements are widely but unevenly distributed (Li et al., 2017). Herbivorous livestock in Xinjiang are generally deficient in elements such as Cu and Zn, which is a major limiting factor for the development of animal husbandry in the province. Livestock are not commonly fed mineral supplements, either individually or in blocks by way of licks, because of the high cost of such supplements (Gowda et al., 2004). Forage halophytes may be a source of certain mineral elements to meet livestock demands. In the present study, Cu and Zn contents were higher in *S. salsa* plants than in other forage grasses, and were significantly increased after irrigation with saline water. As a result, *S. salsa* forage is an ideal source of mineral supplements for livestock.

## 4.3 Potential feeding risks of *S. salsa* irrigated with saline water

A high ash content can decrease forage nutritive value by affecting palatability, consumption, and nutrient utilization (El Shaer, 2010). A high ash content is a typical characteristic of halophytes. Hence, the ash content can be the main limiting factor for the utilization of halophytes as forage. In this study, the ash content increased with increased salinity of the irrigation water. Similarly, Hessini et al. (2020) reported that species of plants in the Chenopodiaceae family have a much higher ash content in their DW than salt-tolerant grass species, and further suggested that a high ash content is a major factor restricting the forage nutritive value of *S. salsa*.

Ash content reflects a high mineral content, and mineral composition is associated with selective absorption by the plant and the soil properties (Zhang et al., 2012). In the present study, the $Na_{11}$ and Cl contents were highest in *S. salsa*. In general, an increase in Na accumulation corresponds with decreases in K, Mg, and Ca contents (Waldron et al., 2020). However, *S. salsa* is unique in the genus *Suaeda* with respect to K responses; this species has developed high selectivity for K over Na by the roots, and thus can absorb and accumulate large amounts of K in plant tissues to meet the nutrient requirements of the plant (Mori et al., 2011). The K/Na, Mg/Na, and Ca/Na ratios decreased with increased salinity of the irrigation water, which suggests that the increase in K, Mg, and Ca contents of *S. salsa* might be due to an increase in total mineral content.

A high salt concentration (Na and Cl) can reduce the forage nutritive value of *S. salsa* by contributing to a reduction in feed and DM intake and compromising animal health (Hessini et al., 2020; Waldron et al., 2020). In the present study, the salt content accumulated to a level that exceeds the tolerance threshold for livestock (up to 100 g/kg) (Hessini et al., 2020). Thus, *S. salsa*, similar to other halophytic forage, is not suitable for direct use as a staple food source, and should be used in the form of silage or/and mixed with other forage (El Shaer, 2010; Norman et al., 2013). In addition, offering fresh drinking water to animals would reduce the stress of salt intake and enhance halophyte consumption and nutrient utilization (El Shaer, 2010; Runa et al., 2019). This increase may be caused by increased palatability of feed and enhanced digestion owing to the stimulation of microbial activities (Runa et al., 2019). Moreover, salt in the diet can have both positive and negative impacts, depending on the concentration (Hessini et al., 2020). Thus, when administered at an appropriate concentration, *S. salsa* could be used as a natural salt supplement.

Growing in a saline environment, halophytes use organic acids to balance the excessive absorption of anions, and the most abundant of these is oxalate (Masters et al., 2001). Thus, the oxalate content of halophytes, especially that of the chenopodiaceous salt-tolerant shrub, was close to the toxicity threshold (Li et al., 2017). High oxalate concentrations can reduce the availability of mineral nutrients for rumen microflora and the host animal by forming complexes with Ca, Mg, and possibly other minerals, which may lead to calcium deficiency, kidney damage, and, finally, death (El Shaer, 2010; Norman et al., 2013; Hessini et al., 2020). In addition, a more common observation is that a high oxalate concentration can lead to a decrease in feed intake. In this study, the oxalate concentration ranged from 0.87% to 1.62%, and was within the safety threshold (2%).

Tannins, as phenolic plant secondary compounds, represent a "double-edged sword" for forage nutritive value. Condensed tannins (CTs) protect proteins from excessive degradation, but also inhibit the absorption of protected proteins (Waghorn, 2008), depending on their concentration in the feed material. El Shaer (2010) reported that low concentrations of tannins (i.e., 2%–4%) in the diet increase the absorption of essential amino acids in ruminants, whereas higher tannin concentrations (i.e., 4%–10%) decrease forage intake. Zhang et al. (2009) reported that a plant with a tannin concentration of > 3% may limit feed intake and reduce digestibility by ruminants. However, the appropriate concentration and toxicity threshold are dependent on the species and physiological status of ruminants (Waghorn, 2008). For example, the beneficial effects of CTs are observed in the range 2.2%–3.8% DM, and the action of CTs in grazing lactating ewes has been reported to affec milk secretion only in mid and late lactation (Min et al., 2003). In the present study, the tannin content increased with the increase in salinity of the irrigation water, but did not exceed the current safe toxicity threshold.

Therefore, as forage, *S. salsa* poses certain potential risks owing to its excessive ash content, salt accumulation, mineral imbalance, and the presence of anti-nutritional factors. However, these risks should not discourage the use of *S. salsa* in agricultural contexts, as these potential risks might be diminished through the application of specific physical treatments (e.g. chopping, soaking and sun-drying), chemical treatments (e.g. PEG) and biological treatments (e.g. ensiling) (El Shaer, 2010). In conclusion, halophytes such as *S. salsa* have broad prospects as livestock and agronomists should aim to maximize the forage nutritive value.

## 4.4 Ecological significance of planting *S. salsa*

Halophytes occur naturally in high-salinity areas and can absorb salt from the rhizosphere. Salt accumulates to high concentrations in the tissues of halophyte plants, and, thus, halophytes can be used for the remediation of salt-affected land (Congjuan et al., 2018; Shaygan et al., 2018). The accumulation of salt, which is affected by plant aboveground biomass and ion concentration, is an important factor with which to measure the ability of halophytes to improve saline soil (Wang et al., 2022). Based on its salt removal capacity (measured by salt accumulation) and BCF, *S. salsa* is an effective salt absorber in saline soils. *Suaeda salsa* might significantly reduce the soil salinity if harvested at the end of the growing season (Zhao, 1991). In the present study, the aboveground biomass was an important factor affecting salt accumulation. Wu et al. (2012) reported that *S. salsa* grows rapidly in moderate-salinity soil and can survive extreme salinities, which is consistent with our findings in the present study. Salt accumulation ranged from,1666.62 to 3,307.99 kg/hm$^2$ at the flower bud stage and from 3,539.76 to 5,771.03 kg/hm$^2$ at the fruit stage, values that are similar to those reported previously. Liang and Shi (2021) reported that *S. salsa* can remove 3.0–3.8 t/ha of Na, and that its salt extraction potential ranges from 3.75–3.91 t/ha/year. Therefore, these studies, including the present, suggest that *S. salsa* is an ideal species for the artificial revegetation of high-salinity land.

In the present study, to study the growth and forage nutritive value of *S. salsa* under extreme irrigation conditions, we used irrigation water with a salinity as high as 40 g/L. *S. salsa* did not improve the salinity of soil when harvested at the initial flower bud stage. In practical agricultural production, brackish water is often used for irrigation. However, according to the salt balance formula (Zhao et al., 2013), the salt removed from the soil was greater than that introduced by irrigation under the control treatment (freshwater). Therefore, when irrigated with local saline water, *S. salsa* has a huge capacity for improving saline soil, in addition to providing forage for livestock.

Water of high salinity is mainly used for revegetation and ecological restoration in extremely saline–alkali land. In this context, *S. salsa* can be harvested at the fruit stage, once greater biomass has accumulated, to remove greater quantities of salt from the soil. Even if it is not able to reduce the salt content of the soil, it will provide stable vegetation cover. Vegetation cover on the soil surface is a major factor that affects soil moisture content and temperature. *S. salsa* can survive in highly saline environments and replaces soil surface evaporation with its own evapotranspiration. This "mulching effect" of halophytes can inhibit the return of soil salt and transform the environment so that it is more directly conducive to plant growth (Shaygan et al., 2018), and, thereby, improve the ability of the soil to resist saline–alkali damage. In addition, the interspersed roots of salt-tolerant plants improve the physical properties of saline–alkali soil (X. Wang et al., 2021). X. Wang et al. (2021) reported that the absolute water content, total porosity, and capillary porosity were increased after the planting of halophytes. *S. salsa*, having a taproot system, has the potential to act as a tillage tool (Chaudhary et al., 2018). Such biological drilling can stabilize the soil structure by reducing the soil bulk density, thereby improving salt ion leaching from saline–alkali soil by increasing the soil porosity and hydraulic conductivity, and reducing the bulk density (Rahman et al., 2021). In addition, halophytes exert a significant influence on the soil's physical and chemical properties *via* root exudation and litter decay (Mao et al., 2014; Chaudhary et al., 2018; Ping et al., 2018). Mao et al. (2014) reported that the presence of *S. salsa* altered the distribution of soil aggregate size in tidal salt marshes, and increased the concentrations of soil organic C and total N in the salt tidal marshes of the Liaohe Delta. Li et al. (2019) observed that the planting of *S. salsa* in the Tianjin Estuary area, China, increased the soil organic matter content by 43.4% and the total soil N content by 17.8%, and greatly increased the soil microbial amount. In addition, after halophyte planting, the soil microbial species, abundance, microbial activity, and evenness were greatly improved (X. Wang et al., 2021), and the roots of halophytes induced the synthesis of these enzymes (Rathore et al., 2017).

## 5 Conclusion

The present results show that *S. salsa* can tolerate irrigation water with a salinity of 40 g/L. Therefore, based on its salt tolerance, *S. salsa* has strong potential for the development of saline agriculture strategies and to improve the natural ecosystem. Under irrigation with a low concentration of saline water, *S. salsa* can provide high-quality forage and reduce the salt concentration of the soil. The plant's salt removal capacity, as measured by salt accumulation in aboveground tissues, is affected by biomass production and ash content. Therefore, harvesting it at the end of its growth stage, when its biomass is maximal, enables *S. salsa* to reduce the soil salt content to the greatest extent. Under the present experimental conditions, the highest quality forage can be obtained by irrigation with water of 20 g/L salinity. Specifically, at this salinity, the maximum biomass and CP content were attained and minimum fiber content was observed. In addition, trace element contents were improved by irrigation with saline water. However, it cannot be asserted that 20 g/L is the optimal irrigation water salinity for the growth and forage nutritive value of *S. salsa*, because the soil environment is complex and diverse, and plant growth is affected by various factors. Nevertheless, it is certain that this plant's biomass will increase in a suitable saline environment, and salinity can increase its forage nutritive value by increasing the CP content and mineral nutrition, and decreasing the fiber concentration. In addition, high-salinity water can be used for revegetation in a saline wasteland. Even if it is not able to reduce the salt content of the soil, planting with *S. salsa* provides a stable vegetation cover that can transform the environment to improve its physicochemical properties for plant growth. However, the salt tolerance threshold of *S. salsa* and its influence on revegetation need further investigation.

## Data availability statement

The raw data supporting the conclusions of this article will be made available by the authors, without undue reservation.

## Author contributions

NW: conceptualization, investigation, and writing of original draft. ZZ: conceptualization, supervision, and writing (i.e., reviewing and editing). XZ: investigation. SL: investigation and writing of original draft. KZ: investigation and supervision. MH: resources. All authors contributed to the article and approved the submitted version.

## Funding

This work was supported by the National Key Research and Development Program of China (grant numbers No. 2018YFE0207200) and the West Light Talent Program of the Chinese Academy of Sciences (grant numbers 2019-YDYLTD-001).

## Acknowledgments

Sequencing services were provided by Personal Biotechnology CO., Ltd. Shanghai, China and Qing Dao Sci-tech innovation Quality Testing CO., Ltd. Qing Dao, China. We would like to thank Charlesworth (https://www.cwauthors.com.cn) for English language editing.

## Conflict of interest

The authors declare that the research was conducted in the absence of any commercial or financial relationships that could be construed as a potential conflict of interest.

## Publisher's note



## References

Agudelo, A., Carvajal, M., and Martinez-Ballesta, M. C. (2021). Halophytes of the Mediterranean basin–underutilized species with the potential to be nutritious crops in the scenario of the climate change. *Foods* 10, 119. doi: 10.3390/foods10010119

Al-Azzawi, M. J., and Flowers, T. J. (2022). Distribution and potential uses of halophytes within the gulf cooperation council states. *Agronomy-Basel* 12, 1030. doi: 10.3390/agronomy12051030

Al-Dakheel, A. J., Hussain, M. I., and Rahman, A. Q. M. A. (2015). Impact of irrigation water salinity on agronomical and quality attributes of cenchrus ciliaris l. accessions. *Agric. Water Manage.* 159, 148–154. doi: 10.1016/j.agwat.2015.06.014

Ali, H., Gul, B., Adnan, M. Y., Ahmed, M. Z., Ansari, R., and Khan, M. A. (2016). Potential of halophytes as cattle fodder: A case-study in Pakistan. *Pak. J. Agric. Sci.* 53, 719–725. doi: 10.21162/PAKJAS/16.2580

Ben Salem, H., and Morand-Fehr, P. (2010). Foreword. *Small Rumin. Res.* 91, 1–2. doi: 10.1016/j.smallrumres.2010.01.009

Chaudhary, D. R., Kim, J., and Kang, H. (2018). Influences of different halophyte vegetation on soil microbial community at temperate salt marsh. *Microb. Ecol.* 75, 729–738. doi: 10.1007/s00248-017-1083-y

Congjuan, L., Ran, L., Shijie, W., Yongqiang, S., Shengyu, L., Heng, Z., et al. (2018). Growth and sustainability of suaeda salsa in the lop nur, China. *J. Arid Land* 10, 429–440. doi: 10.1007/s40333-018-0002-5

Duarte, B., and Cacador, I. (2021). Iberian Halophytes as agroecological solutions for degraded lands and biosaline agriculture. *Sustainability* 13, 1005. doi: 10.3390/su13021005

El Shaer, H. M. (2010). Halophytes and salt-tolerant plants as potential forage for ruminants in the near East region. *Small Rumin. Res.* 91, 3–12. doi: 10.1016/j.smallrumres.2010.01.010

Etesami, H., and Beattie, G. A. (2018). Mining halophytes for plant growth-promoting halotolerant bacteria to enhance the salinity tolerance of non-halophytic crops. *Front. Microbiol.* 9. doi: 10.3389/fmicb.2018.00148

Fang, R. J., Xiang, Z. F., Yang, Y. S., and Cao, M. H. (2013). Mineral element ideal pattern–from theory to practice. *Chin. J. Anim. Nutr.* 25, 891–898. doi: 10.3969/j.issn.1006-267x.2013.05.001

Fita, A., Rodriguez-Burruezo, A., Boscaiu, M., Prohens, J., and Vicente, O. (2015). Breeding and domesticating crops adapted to drought and salinity: A new paradigm for increasing food production. *Front. Plant Sci.* 6. doi: 10.3389/fpls.2015.00978

Flowers, T. J., and Colmer, T. D. (2008). Salinity tolerance in halophytes. *New Phytol.* 179, 945–963. doi: 10.1111/j.1469-8137.2008.02531.x

Garza-Torres, R., Troyo-Dieguez, E., Nieto-Garibay, A., Lucero-Vega, G., Magallon-Barajas, F. J., Garcia-Galindo, E., et al. (2020). Environmental and management considerations for adopting the halophyte salicornia bigelovii torr. as a sustainable seawater-irrigated crop. *Sustainability* 12, 707. doi: 10.3390/su12020707

Gowda, N. K. S., Ramana, J. V., Prasad, C. S., and Singh, K. (2004). Micronutrient content of certain tropical conventional and unconventional feed resources of southern India. *Trop. Anim. Health Prod.* 36, 77–94. doi: 10.1023/B:TROP.0000009522.30949.1d

Guo, S., Yin, H., Zhang, X., Zhao, F., Li, P., Chen, S., et al. (2006). Molecular cloning and characterization of a vacuolar h+-pyrophosphatase gene, SsVP, from the halophyte suaeda salsa and its overexpression increases salt and drought tolerance of arabidopsis. *Plant Mol. Biol.* 60, 41–50. doi: 10.1007/s11103-005-2417-6

Harper, K. J., and McNeill, D. M. (2015). The role iNDF in the regulation of feed intake and the importance of its assessment in subtropical ruminant systems (the role of iNDF in the regulation of forage intake). *Agriculture-Basel* 5, 778–790. doi: 10.3390/agriculture5030778

Hedayati-Firoozabadi, A., Kazemeini, S. A., Pirasteh-Anosheh, H., Ghadiri, H., and Pessarakli, M. (2020). Forage yield and quality as affected by salt stress in different ratios of sorghum bicolor -bassia indica intercropping. *J. Plant Nutr.* 43, 2579–2589. doi: 10.1080/01904167.2020.1783301

Hessini, K., Jeddi, K., Shaer, H. M. E., Smaoui, A., Salem, H. B., and Siddique, K. H. M. (2020). Potential of herbaceous vegetation as animal feed in semi-arid Mediterranean saline environments: The case for Tunisia. *Agron. J.* 112, 2445–2455. doi: 10.1002/agj2.20196

Himabindu, Y., Chakradhar, T., Reddy, M. C., Kanygin, A., Redding, K. E., and Chandrasekhar, T. (2016). Salt-tolerant genes from halophytes are potential key players of salt tolerance in glycophytes. *Environ. Exp. Bot.* 124, 39–63. doi: 10.1016/j.envexpbot.2015.11.010

Jungers, J., Cherney, J., Martinson, K., Jaqueth, A., and Sheaffer, C. (2020). Forage nutritive value of modern alfalfa cultivars. *Crop Forage Turfgrass Manage.* 6, e20076. doi: 10.1002/cft2.20076

Koyro, H.-W., Zörb, C., Debez, A., and Huchzermeyer, B. (2013). The effect of hyper-osmotic salinity on protein pattern and enzyme activities of halophytes. *Funct. Plant Biol.* 40, 787–804. doi: 10.1071/FP12387

Kumari, A., Das, P., Parida, A. K., and Agarwal, P. K. (2015). Proteomics, metabolomics, and ionomics perspectives of salinity tolerance in halophytes. *Front. Plant Sci.* 6. doi: 10.3389/fpls.2015.00537

Liang, J., and Shi, W. (2021). Cotton/halophytes intercropping decreases salt accumulation and improves soil physicochemical properties and crop productivity in saline-alkali soils under mulched drip irrigation: A three-year field experiment. *Field Crop Res.* 262, 108027. doi: 10.1016/j.fcr.2020.108027

Li, J., Hussain, T., Feng, X., Guo, K., Chen, H., Yang, C., et al. (2019). Comparative study on the resistance of suaeda glauca and suaeda salsa to drought, salt, and alkali stresses. *Ecol. Eng.* 140, 105593. doi: 10.1016/j.ecoleng.2019.105593

Li, Q., Liu, R., Li, Z., Fan, H., and Song, J. (2022). Positive effects of NaCl on the photoreaction and carbon assimilation efficiency in suaeda salsa. *Plant Physiol. Biochem.* 177, 32–37. doi: 10.1016/j.plaphy.2022.02.019

Liu, L., and Wang, B. (2021). Protection of halophytes and their uses for cultivation of saline-alkali soil in China. *Biology-Basel* 10, 353. doi: 10.3390/biology10050353

Li, M.-M., Wu, G.-H., Zhao, Z.-Y., Tu, J.-N., and Tian, C.-Y. (2017). Feed value evaluation of xinjiang five chenopod halophytes. *Pratacult. Sci.* 34, 361–368. doi: 10.11829/j.issn.1001-0629.2016-0245

Ma, F., Barrett-Lennard, E. G., and Tian, C. Y. (2019). Changes in cell size and tissue hydration ('succulence') cause curvilinear growth responses to salinity and watering treatments in euhalophytes. *Environ. Exp. Bot.* 159, 87–94. doi: 10.1016/j.envexpbot.2018.12.003

Mao, R., Zhang, X.-H., and Meng, H.-N. (2014). Effect of suaeda salsa on soil aggregate-associated organic carbon and nitrogen in tidal salt marshes in the liaohe delta, China. *Wetlands* 34, 189–195. doi: 10.1007/s13157-013-0497-7

Masters, D. G., Benes, S. E., and Norman, H. C. (2007). Biosaline agriculture for forage and livestock production. *Agric. Ecosyst. Environ.* 119, 234–248. doi: 10.1016/j.agee.2006.08.003

Masters, D. G., Norman, H. C., and Dynes, R. A. (2001). Opportunities and limitations for animal production from saline land. *Asian Australas. J. Anim. Sci.* 14, 199–211.

Masters, D., Tiong, M., Vercoe, P., and Norman, H. (2010). The nutritive value of river saltbush (Atriplex amnicola) when grown in different concentrations of sodium chloride irrigation solution. *Small Rumin. Res.* 91, 56–62. doi: 10.1016/j.smallrumres.(09.10.019

Min, B. R., Barry, T. N., Attwood, G. T., and McNabb, W. C. (2003). The effect of condensed tannins on the nutrition and health of ruminants fed fresh temperate forages: A review. *Anim. Feed Sci. Technol.* 106, 3–19. doi: 10.1016/S0377-8401(03)00041-5

Mori, S., Suzuki, K., Oda, R., Higuchi, K., Maeda, Y., Yoshiba, M., et al. (2011). Characteristics of na+ and k+ absorption in suaeda salsa (L.). *Pall. Soil Sci. Plant Nutr.* 57, 377–386. doi: 10.1080/00380768.2011.586322

Muchate, N. S., Nikalje, G. C., Rajurkar, N. S., Suprasanna, P., and Nikam, T. D. (2016). Plant salt stress: Adaptive responses, tolerance mechanism and bioengineering for salt tolerance. *Bot. Rev.* 82, 371–406. doi: 10.1007/s12229-016-9173-y

Munns, R., and Tester, M. (2008). Mechanisms of salinity tolerance. *Annu. Rev. Plant Biol.* 59, 651–681. doi: 10.1146/annurev.arplant.59.032607.092911

Norman, H. C., Masters, D. G., and Barrett-Lennard, E. G. (2013). Halophytes as forages in saline landscapes: Interactions between plant genotype and environment change their feeding value to ruminants. *Environ. Exp. Bot.* 92, 96–109. doi: 10.1016/j.envexpbot.2012.07.003

Norman, H. C., Revell, D. K., Mayberry, D. E., Rintoul, A. J., Wilmot, M. G., and Masters, D. G. (2010). Comparison of in vivo organic matter digestion of native Australian shrubs by sheep to in vitro and in sacco predictions. *Small Ruminant Research* 91 (1), 69–80. doi: 10.1016/j.smallrumres.2009.11.019

Ozturk, O. F., Shukla, M. K., Stringam, B., Picchioni, G. A., and Gard, C. (2018). Irrigation with brackish water changes evapotranspiration, growth and ion uptake of halophytes. *Agric. Water Manage.* 195, 142–153. doi: 10.1016/j.agwat.2017.10.012

Pasternak, D., Nerd, A., and De Malach, Y. (1993). Irrigation with brackish-water under desert conditions IX. the salt tolerance of six forage crops. *Agric. Water Manage.* 24, 321–334. doi: 10.1016/0378-3774(93)90010-8

Ping, Y., Cui, L., Pan, X., Li, W., Li, Y., Kang, X., et al. (2018). Decomposition processes in coastal wetlands: The importance of suaeda salsa community for soil cellulose decomposition. *Pol. J. Ecol.* 66, 217–226. doi: 10.3161/15052249PJE2018.66.3.002

Pirasteh-Anosheh, H., Mirhosseini, A., Akram, N. A., and Hasanuzzaman, M. (2021). Forage potential of salsola species in arid-saline rangelands. *Turk. J. Bot.* 45, 203–215. doi: 10.3906/bot-2010-36

Qiao, M., Zhou, S. B., Lu, L., Yan, J. J., and Li, H. P. (2011). Temporal and spatial changes of soil salinization and improved countermeasures of tarim basin irrigation district in recent 25 years. *Arid Land Geogr.* 34, 604–613.

Rahman, M. M., Mostofa, M. G., Keya, S. S., Siddiqui, M. N., Ansary, M. M. U., Das, A. K., et al. (2021). Adaptive mechanisms of halophytes and their potential in improving salinity tolerance in plants. *Int. J. Mol. Sci.* 22, 10733. doi: 10.3390/ijms221910733

Rathore, A. P., Chaudhary, D. R., and Jha, B. (2017). Seasonal patterns of microbial community structure and enzyme activities in coastal saline soils of perennial halophytes. *Land Degrad. Dev.* 28, 1779–1790. doi: 10.1002/ldr.2710

Robinson, P. H., Grattan, S. R., Getachew, G., Grieve, C. M., Poss, J. A., Suarez, D. L., et al. (2004). Biomass accumulation and potential nutritive value of some forages irrigated with saline-sodic drainage water. *Anim. Feed Sci. Technol.* 111, 175–189. doi: 10.1016/S0377-8401(03)00213-X

Runa, R. A., Brinkmann, L., Riek, A., Hummel, J., and Gerken, M. (2019). Reactions to saline drinking water in Boer goats in a free-choice system. *Animal* 13, 98–105. doi: 10.1017/S1751731118000800

Shang, C., Wang, L., Tian, C., and Song, J. (2020). Heavy metal tolerance and potential for remediation of heavy metal-contaminated saline soils for the euhalophyte suaeda salsa. *Plant Signal. Behav.* 15, 1805902. doi: 10.1080/15592324.2020.1805902

Shaygan, M., Mulligan, D., and Baumgartl, T. (2018). The potential of three halophytes (Tecticornia pergranulata, sclerolaena longicuspis, and frankenia serpyllifolia) for the rehabilitation of brine-affected soils. *Land Degrad. Dev.* 29, 2002–2014. doi: 10.1002/ldr.2954

Song, J., and Wang, B. (2015). Using euhalophytes to understand salt tolerance and to develop saline agriculture: Suaeda salsa as a promising model. *Ann. Bot.* 115, 541–553. doi: 10.1093/aob/mcu194

Sun, H. X., Zhong, R. Z., Liu, H. W., Wang, M. L., Sun, J. Y., and Zhou, D. W. (2015). Meat quality, fatty acid composition of tissue and gastrointestinal content, and antioxidant status of lamb fed seed of a halophyte (Suaeda glauca). *Meat Sci.* 100, 10–16. doi: 10.1016/j.meatsci.2014.09.005

Van Soest, P. J. (1963). Use of detergents in the analysis of fibrous feeds. II. a rapid method for the determination of fiber and lignin. *J. Assoc. Off. Agric. Chemists.* 46, 829–835. doi: 10.1093/jaoac/46.5.829

Vittori Antisari, L., Bini, C., Ferronato, C., Gherardi, M., and Vianello, G. (2020). Translocation of potential toxic elements from soil to black cabbage (Brassica oleracea l.) growing in an abandoned mining district area of the apuan Alps (Tuscany, Italy). *Environ. Geochem. Health* 42, 2413–2423. doi: 10.1007/s10653-019-00443-y

Waghorn, G. (2008). Beneficial and detrimental effects of dietary condensed tannins for sustainable sheep and goat production–progress and challenges. *Anim. Feed Sci. Technol.* 147, 116–139. doi: 10.1016/j.anifeedsci.2007.09.013

Waldron, B. L., Sagers, J. K., Peel, M. D., Rigby, C. W., Bugbee, B., and Creech, J. E. (2020). Salinity reduces the forage quality of forage kochia: A halophytic chenopodiaceae shrub. *Rangel. Ecol. Manage.* 73, 384–393. doi: 10.1016/j.rama.2019.12.005

Wang, F., and Song, N. (2019). Salinity-induced alterations in plant growth, antioxidant enzyme activities, and lead transportation and accumulation in suaeda salsa: Implications for phytoremediation. *Ecotoxicology* 28, 520–527. doi: 10.1007/s10646-019-02048-8

Wang, L., Wang, X., Jiang, L., Zhang, K., Tanveer, M., Tian, C., et al. (2021). Reclamation of saline soil by planting annual euhalophyte suaeda salsa with drip irrigation: A three-year field experiment in arid northwestern China. *Ecol. Eng.* 159, 106090. doi: 10.1016/j.ecoleng.2020.106090

Wang, X., Zhang, F., Zhang, B., and Xu, X. (2021). Halophyte planting improves saline-alkali soil and brings changes in physical and chemical properties and soil microbial communities. *Pol. J. Environ. Stud.* 30, 4767–4781. doi: 10.15244/pjoes/134087

Wang, Y., Zhao, Y., Xue, F., Nan, X., Wang, H., Hua, D., et al. (2020). Nutritional value, bioactivity, and application potential of Jerusalem artichoke (Helianthus tuberosus l.) as a neotype feed resource. *Anim. Nutr.* 6, 429–437. doi: 10.1016/j.aninu.2020.09.001

Wang, N., Zhao, Z. Y., Zhang, X. Y., Liu, S. H., Jiang, L., Gong, J. P., et al. (2022). Salt absorption capacity and ecological significance of selected chenopodiaceae halophytes. *J. Plant Nutr. Fertil.* 28, 1104–1112. doi: 10.11674/zwyf.2021509

Wei, M. C. (2016). Experimental study on the effects of suaeda salsa on fattening and blood biochemical indexes of pigs. *Chin. J. Anim. Sci.* 52, 68–70.

Wu, H., Liu, X., You, L., Zhang, L., Zhou, D., Feng, J., et al. (2012). Effects of salinity on metabolic profiles, gene expressions, and antioxidant enzymes in halophyte suaeda salsa. *J. Plant Growth Regul.* 31, 332–341. doi: 10.1007/s00344-011-9244-6

Xu, B., Zhang, M., Xing, C., Mothibe, K. J., and Zhu, C. (2013). Composition, characterisation and analysis of seed oil of suaeda salsa l. *Int. J. Food Sci. Technol.* 48, 879–885. doi: 10.1111/ijfs.12040

Yuan, F., Xu, Y., Leng, B., and Wang, B. (2019). Beneficial effects of salt on halophyte growth: Morphology, cells, and genes. *Open Life Sci.* 14, 191–200. doi: 10.1515/biol-2019-0021

Zhang, F. H., Li, F. M., Cui, S. S., Niu, C. L., Chen, H., and Bao, X. W. (2018). Effect of feeding suaeda salsa on slaughter performance of altay sheep. *China Feed*, 19, 70–73. doi: 10.15906/j.cnki.cn11-2975/s.20181915

Zhang, K., Tian, C. Y., and Li, C. J. (2012). Influence of saline soil and sandy soil on growth and mineral constituents of common annual halophytes in Xinjiang. *Acta Ecologica Sinica*, 32 (10), 3069–76. doi: 10. 5846 /stxb201104230535

Zhang, X. Q., Li, Y., Li, F. D., Wu, Q. J., Ye, D. H., and Hao, Z. L. (2009). Effects Of Tannin Content In Sainfoin (Onobrychis Vici Folia) Hay On Digestibility Of Nutrients And Utilization Of Nitrogen In Sheep Diets. *Acta veterinaria er zootechnica sinica*, 40 (3), 356–62.

Zhao, K. (1991). Desalinization of saline soils by suaeda salsa. *Plant Soil* 135, 303–305. doi: 10.1007/BF00010921

Zhao, Z. Y., Li, Z. S., Zhang, F. H., Zhang, K., Wang, L., and Tian, C. Y. (2013). Impacts of halophytes planting on salt balance in agricultural development region of karamay city. *Bull. Soil Water Conserv.* 33, 211–215.

Zhao, Y., Yang, Y., Song, Y., Li, Q., and Song, J. (2018). Analysis of storage compounds and inorganic ions in dimorphic seeds of euhalophyte suaeda salsa. *Plant Physiol. Biochem.* 130, 511–516. doi: 10.1016/j.plaphy.2018.08.003

Zhao, C., Zhang, H., Song, C., Zhu, J.-K., and Shabala, S. (2020). Mechanisms of plant responses and adaptation to soil salinity. *Innovation-Amsterdam* 1, 100017. doi: 10.1016/j.xinn.2020.100017

Zhou, Z. Y., Tian, W. M., and Malcolm, B. (2008). Supply and demand estimates for feed grains in China. *Agric. Econ.* 39, 111–122. doi: 10.1111/j.1574-0862.2008.00319.x

frontiers | Frontiers in Plant Science

TYPE Original Research
PUBLISHED 31 March 2023
DOI 10.3389/fpls.2023.987514



OPEN ACCESS

EDITED BY
Raoudha Abdellaoui,
Institut des Régions Arides, Tunisia

REVIEWED BY
Muhammad Ishaq Asif Rehmani,
Ghazi University, Pakistan
Sajid Fiaz,
The University of Haripur, Pakistan

*CORRESPONDENCE
Muhammad Awais Farooq
awaisfarooq724@gmail.com
Umer Karamat
umerkaramat23@gmail.com
Amir Shakeel
amirpbg@uaf.edu.pk

†These authors have contributed equally to this work

SPECIALTY SECTION
This article was submitted to Plant Abiotic Stress, a section of the journal Frontiers in Plant Science

RECEIVED 06 July 2022
ACCEPTED 28 February 2023
PUBLISHED 31 March 2023

CITATION
Farooq MA, Chattha WS, Shafique MS, Karamat U, Tabusam J, Zulfiqar S and Shakeel A (2023) Transgenerational impact of climatic changes on cotton production. *Front. Plant Sci.* 14:987514. doi: 10.3389/fpls.2023.987514



# Transgenerational impact of climatic changes on cotton production

Muhammad Awais Farooq[1,2,3*†], Waqas Shafqat Chattha[1†], Muhammad Sohaib Shafique[1,4†], Umer Karamat[1,3*†], Javaria Tabusam[1,3†], Sumer Zulfiqar[1,3†] and Amir Shakeel[1*]

[1]Department of Plant Breeding and Genetics, University of Agriculture, Faisalabad, Pakistan, [2]Molecular Virology Laboratory, National Institute of Biotechnology and Genetic Engineering, Faisalabad, Pakistan, [3]State Key Laboratory of North China Crop Improvement and Regulation, Key Laboratory of Vegetable Germplasm Innovation and Utilization of Hebei, Collaborative Innovation Center of Vegetable Industry in Hebei, College of Horticulture, Hebei Agricultural University, Beijing, China, [4]Institute of Crop Sciences, Chinese Academy of Agricultural Sciences, Beijing, China

Changing climatic conditions are an increasing threat to cotton production worldwide. There is a need to develop multiple stress-tolerant cotton germplasms that can adapt to a wide range of environments. For this purpose, 30 cotton genotypes were evaluated for two years under drought (D), heat (H), and drought + heat stresses (DH) under field conditions. Results indicated that plant height, number of bolls, boll weight, seed cotton yield, fiber fineness, fiber strength, fiber length, $K^+$, $K^+/Na^+$, relative water contents (RWC), chlorophyll a and b, carotenoids, and total soluble proteins got reduced under D and H and were lowest under DH, whereas superoxidase dismutase (SOD), $H_2O_2$, $Na^+$, GOT%, total phenolic contents, ascorbate, and flavonoids got increased for consecutive years. Correlation studies indicated that there was a positive correlation between most of the traits, but a negative correlation with $H_2O_2$ and $Na^+$ ions. PCA and clustering analysis indicated that MNH-786, KAHKSHAN, CEMB-33, MS-71, FH-142, NIAB-820, CRS-2007, and FH-312 consistently performed better than other genotypes for most traits under stress conditions. Identified genotypes can be utilized in the future cotton breeding program to develop high-yielding, climate change-resilient cotton.

KEYWORDS

***Gossypium hirsutum* L. (cotton), climate change, high temperature, drought, antioxidants, reactive oxygen species (ROS)**

**Abbreviations:** D, drought; H, heat; DH, drought + heat stresses; ASA, ascorbic acid; BW, boll weight; Car, carotenoids; CAT, catalase; Chla, chlorophyll a; Chlb, chlorophyll b; FF, fiber fineness; FL, fiber length; FLV, flavonoids; FS, fiber strength; MDA, malondialdehyde; NB, number of bolls; PH, plant height; SCY, seed cotton yield; TPC, total phenolics contents; TSP, total soluble proteins; POD, peroxidase; $K^+$, potassium concentration; $Na^+$, sodium concentrations; SOD, superoxidase dismutase; RWC, relative water contents; $H_2O_2$, hydrogen peroxide; GOT%, ginning out turn percentage; PCA, principal component analysis.

# Introduction

Cotton plays a significant role in the economy of the country. It is the main source of fiber, oil, and feed for the livestock in the country (Salimath et al., 2021). Pakistan ranks fifth among the top cotton-producing countries after India, China, the United States, and Brazil (Fiaz et al., 2021). Due to changing climatic conditions, cotton is facing many abiotic and biotic stresses, which are negatively impacting crop yield. Abiotic stresses, i.e., heat, salt, and drought, are exacerbating a global problem, as these hamper normal plant growth and morphological and physiological development processes that lead to a reduction in crop yield (Abdelraheem et al., 2019).

The search for cotton germplasm resilient to varied abiotic stresses has intensified due to climate change (Ur Rahman et al., 2020). According to the IPCC, the rate of rise in temperature during 2000–2010 has been recorded at 2.2% in comparison to the temperature regime between 1970 and 2000. Moreover, the projected temperature will rise by 2.6–4.8°C from 2016 to 2035 (Jaiswal et al., 2019). Cotton being a C3 plant and a heat-sensitive plant, the yield of cotton is affected by 10%–17%, with the rise of 1°C in temperature (Zafar et al., 2022). High temperatures lead to high evaporation, which results in a high concentration of salts in the rhizosphere that induces salt stress that causes the reduction of water availability to plants (Saleem et al., 2021). Even a short-term water deficit at the boll development stage in cotton can lead to huge yield losses. At the cellular level, drought induces oxidative stress by the overproduction of reactive oxygen species (ROS), which ruptures the cell membrane and stimulates the cascade of oxidative stresses (Jans et al., 2021; Naz et al., 2022). At the plant level, it results in the inhibition of cell division, expansion of leaf surface area, developmental changes, metabolic adaptations, growth of the stem, and proliferation of root cells. In concert, abiotic stresses dramatically reduce the plant's productivity and might lead to the death of the plant upon prolonged exposure (Ullah et al., 2019).

Abiotic stresses affect plant antioxidant activities, leading to decreased cotton seed yield. Oxidative stress induces ROS such as hydrogen peroxide ($H_2O_2$), superoxide radicals ($O_2^-$), singlet oxygen ($^1O_2$), and hydroxyl radicals ($OH^-$) that are produced in high amounts (Miller et al., 2010). The higher production of ROS damages the plant cell organelles such as chloroplasts, peroxisomes, and mitochondria through oxidation (Wang et al., 2019; Munir et al., 2022). To counteract oxidative damage, protect organelles, and maintain the plant's cellular functions, the cell produces antioxidant enzymes. The detoxifying enzymes that are produced in the cell are superoxidase dismutase (SOD), peroxidases (POD), catalase (CAT), and non-enzymatic antioxidants including carotenoids, flavonoids, and ascorbate. Heat and drought stresses are highly detrimental to the cotton plants, so it is the primary objective of the cotton breeders to develop germplasm that can produce a higher yield under changing climatic conditions (Wang et al., 2017).

To combat these abiotic stresses, numerous approaches have been undertaken to develop resilience in cotton plants (Haque et al., 2018). Cotton breeders consider the development of climate change-resistant germplasm to be the only effective, reliable, and long-lasting solution (Ur Rahman et al., 2020). Exploitation of natural variation present in the available germplasm, such as screening of available germplasm based on morphological, physiological, and biochemical traits, can lead to a significant level of tolerance in cotton plants against abiotic stresses. The measurements of the antioxidant enzymes produced as a result of the onset of abiotic stress can be used as an effective strategy to screen the available germplasm that can produce a higher yield under the changing climatic conditions (Abbas, 2020). Accurate knowledge of the correlation of different traits with each other at the onset of multiple stresses can assist in the development of those combinations of traits that actively participate in the enhancement of seed cotton yield (Farooq et al., 2018). Moreover, principal component analysis can efficiently dissect the trait associations, interactions among the traits, and performance of the genotypes (Farooq et al., 2019b).

For this purpose, a study was designed in which cotton genotypes were evaluated under multiple combinations and at different levels of heat and drought stress for two years with the aim of developing changing climate-tuned cultivars. The objective of the present research is (i) to nominate cotton genotypes that can tolerate abiotic stresses and can also be used in cotton breeding programs, and (ii) to develop a selection criterion based on agro-physiological and biochemical traits for the development of climate-resilient cotton cultivars.

# Materials and methods

## Plant material

A set of 30 cotton genotypes with different genetic backgrounds developed by different breeding stations in Pakistan, such as the Central Cotton Research Institute, Multan, the Cotton Research Station Faisalabad, the Cotton Research Station Multan, the Cotton Research Station Vehari, and the Nuclear Institute of Agriculture and Biology, Faisalabad, were collected and grown in a randomized complete block design on ridges in field conditions for two years during June 2020 and June 2021. Row to row distance was 60 cm and plant to plant distance was 45 cm, and all other agronomic practices were followed uniformly throughout the season.

## Experimental treatments

Plants were grown under four treatments: control, drought stress (D), heat stress (H), and drought + heat stress (DH). The imposition of drought stress was carried out by increasing the interval between irrigation times; for normal irrigation, the interval was kept at two weeks, whereas for drought conditions, the irrigation interval was extended to three weeks. At the flowering stage, high temperature stress was imposed for 12 days in September, which increased the temperature by 5–6°C inside the tunnel that was constructed using plastic sheets and bamboo sticks. The plants inside the tunnel were covered during the daytime, while

they remained uncovered during the night. A mercury thermometer was used to measure the temperature inside the tunnel.

## Data collection

### Agronomic traits

Plant height was taken from the first cotyledonary node to the apical bud with a measuring tape when growth halted. Effective mature bolls were counted from all the picks, and their records were maintained for each plant separately. Seed cotton was picked from five plants, and afterwards, their weight was measured on the electronic weighing scale for each genotype. The individual weight of each boll was measured by dividing the total weight of seed cotton picked by the number of bolls picked.

### Fiber quality traits

A single roller ginning machine (Testex, Model: TB510C, USA) was used to gin the representative sample of seed cotton and it was weighed before ginning. The seeds from each genotype were separated from the lint and GOT (ginning out turn) was calculated by dividing the weight of lint in a sample by the seed cotton weight of the sample, which was expressed in percentage. Lint was further processed to take out the parameters of fiber fineness, fiber strength, and fiber length with a high volume instrument (HVI-900, USTER, USA) (Ibrahim et al., 2021).

### Ionic analysis

To calculate concentrations of $Na^+$ and $K^+$ ions, fresh green leaves were harvested from plants at noon, when they reached their state of vegetative maturity. Leaves were dried in a hot air dryer for 72 h and then ground using a pestle and mortar. Leaves were then digested in a sulfuric acid and nitric acid mixture (a molar ratio of 1:2) on a hot plate. On completion of digestion, the material was brought to room temperature by cooling, and analysis was performed on a flame photometer (410 Flame Photometer, Sherwood, UK). The $K^+$ to $Na^+$ ratio was calculated by dividing $K^+$ concentration by $Na^+$ concentration.

### Biochemical traits

For sampling, the top four fully expanded leaf was taken for analyses carried out by the method given by Song et al. (2014). Approximately 0.5 g of cotton samples were taken for enzyme extraction; the leaves were cut with the help of a leaf pincher and then crushed and ground into 1–2 ml of cold potassium phosphate buffer (pH 7.8). The mixture was prepared for 5 min at 1,400 rpm. Residues were discarded, and the supernatant was collected for the determination of biochemical attributes *via* UV spectrophotometers (Evolution One Plus, Thermo Fisher Scientific) at different wavelengths (Sarwar et al., 2017).

### Hydrogen peroxide (μmol/g-FW)

The Velikova protocol was followed for the determination of $H_2O_2$ (Velikova et al., 2000). Fresh leaf tissues (0.5 g) were blended using tichloroacetic acid (TCA). Approximately 5 ml of a 0.1% (w/v) solution) and then centrifuged at 12,000 rpm for 12 min. The supernatant was collected in a volume of 0.5 ml, and then 0.5 ml of phosphate buffer (pH 7.0) and 1 ml of potassium iodide were added. At the 390 nm wavelength of the UV spectrophotometer, the absorbance capacity of each sample was recorded.

### Catalase (U/mg)

Enzyme extract (0.1 ml) was mixed with 3 ml of the reaction mixture, which contained 5.9 mM $H_2O_2$ and 50 mM potassium phosphate bufferat a pH of 7.0. CAT activity was recorded with a spectrophotometer at 240 nm wavelength (Liu et al., 2009).

### Peroxidase (U/mg)

POD solution contained 50 mM phosphate buffer (pH 5), 40 mM $H_2O_2$, 20 mM guaiacol, and 0.1 ml of enzyme extract (Liu et al., 2009). Measurements were taken at 470 nm with an absorbance spectrophotometer.

### Superoxidase dismutase (U/mg)

The reaction mixture consisted of potassium phosphate buffer (pH 5) + 100 μl NBT + 200 μl of Triton X + 200 μl of methionine + enzyme extracts. Approximately 100 μl were dissolved in 800 μl of distilled water and placed for 15 min under ultraviolet light, and then riboflavin in a quantity of 100 μl was added. The absorbance readings were taken at 560 nm using a spectrophotometer.

### Total soluble proteins (mg/g-FW)

For protein content measurements, the Bradford reagent method was used. Approximately 100 μl of aliquots were blended with 5 ml of Bradford reagent, and with a spectrophotometer at 595 nm wavelength, the absorbance was recorded (Bradford, 1976).

### Chlorophyll contents and carotenoids assay

For the determination of carotenoids and chlorophyll a and b, the Arnon method (Arnon, 1949) was followed. Approximately 0.50 g of cotton leaf sample was crushed in 8–10 ml of 80% acetone (v/v). For homogenization, filter paper was used. At 645 and 663 nm, the final solution absorbance value was recorded using a spectrophotometer. The chlorophyll a and b and carotenoids were evaluated as follows.

$$Chl\ a\ (mg\ g^{-1}FW) = [12.7(OD\,663) - 2.69(OD\,645)] \times V/1000 \times W$$

$$Chl\ a\ (mg\ g^{-1}FW) = [22.9(OD\,645) - 2.69(OD\,663)] \times V/1000 \times W$$

$$\text{Carotenoids (mg/g FW)} = A^{car}/\text{Em} \times 100$$

$$A^{car} = \text{O . D } 480 + 0.114\,(\text{O . D } 663) - 0.638\,(\text{O . D } 645)$$

where,

W = weight of leaf sample, V = volume of sample, and Em = 2,500.

### Ascorbic acid (ASA mg $g^{-1}$ FW)

For the determination of ascorbic acid, the 2,6-dichloroindophenol (DCIP) method was adopted, as explained by Davies and Masten (1991). For a concise description, each molecule

of vitamin C converted a DCIP molecule into a DCIPH2 molecule, and the absorbance was recorded at 520 nm.

## Total phenolic contents and flavonoids (mg $g^{-1}$ FW)

Total phenolic contents were measured according to the method of Ainsworth and Gillespie (2007), and flavonoid contents were measured according to the method outlined by Zhishen et al. (1999).

## Leaf relative water contents

Leaf samples for relative water contents were collected at pre-dawn by following the method of Silveira et al. (2009). The RWC% was calculated with a minor modification of Weatherly (1950). The 500-g leaf sample (FW) was immersed overnight in distilled water to get leaf turgidity, then leaves were weighed for turgid weight (TW). To get dry weight (DW), the leaves were oven-dried at 80°C for 24 h. The relative water contents were calculated using the formula given below:

$$\text{RWC\%} = \frac{(\text{FW} - \text{DW})}{(\text{TW} - \text{DW})} \times 100$$

## Malondialdehyde (MDA nmol $g^{-1}$ FW)

To determine the MDA content in cotton leaves, the method of Cakmak and Horst (1991) was adopted. The 500 mg leaf sample was homogenized in 10 ml of a 0.1% trichloroacetic acid (TCA) solution and centrifuged at 14,000×*g* for 5 min. For each ml of extract, 4.5 ml of thiobarbituric acid (0.5%) was used, and the reaction mixture was heated at 95°C for 30 min and then quickly cooled on an ice bath and centrifuged again at 14,000×*g* for 10 min. The absorbance was calculated by:

$$\text{MDA level (nmol)} = \frac{\Delta(\text{A532 nm} - \text{A600 nm})}{156 \times 10^5}$$

A = Absorption coefficient with the value of 156 $mm^{-1}$ $cm^{-1}$.

## Statistical analysis

An analysis of variance (ANOVA) was performed with a two-factor randomized complete block design (Steel et al., 1997). Mean data were analyzed for principal components, heat maps, and correlation analyses using the statistical packages "prcomp," "ggplot2," and "Hmisc" in R 4.1.1 statistical software. Estimates of

TABLE 1 First year mean square values for various agro-physiological, biochemical, and fiber quality traits of 30 cotton genotypes under four treatments.

| SOV / Traits | Genotypes | Treatments | Replication | Treatments * Genotypes | Error |
|---|---|---|---|---|---|
| Degree of freedom | 29 | 3 | 2 | 87 | 238 |
| ASA | 907** | 37,145.4** | 2,094.8 | 13.8 | 59.9 |
| BW | 1.1989** | 12.5525** | 0.5697 | 0.05 | 0.08 |
| CAT | 366.18** | 3,086.05** | 67.21 | 14.79 | 14.16 |
| Car | 0.01632** | 0.06983** | 0.02017 | 0.001 | 0.002 |
| Chla | 0.31028** | 0.63965* | 0.09242 | 0.08 | 0.06 |
| Chlb | 0.04768** | 0.1087** | 0.07183 | 0.000 | 0.002 |
| FF | 2.20056** | 8.39549** | 0.90255 | 0.05 | 0.103 |
| FL | 28.5** | 375.58** | 9.749 | 2.14 | 2.204 |
| FLV | 6,066.61** | 4,685.76** | 7,178.77 | 0.57 | 299.29 |
| FS | 46.499* | 439.118** | 16.15 | 0.87 | 2.20 |
| GOT | 97.952** | 248.643* | 156.093 | 0.52 | 5.02 |
| H202 | 0.04595* | 0.58118** | 0.12092 | 0.002 | 0.005 |
| K | 646.2** | 29,019.1** | 1,291.5 | 139.6* | 76.7 |
| KNA | 3.015* | 101.874** | 4.857 | 0.53** | 0.206 |
| MDA | 0.41053** | 1.27567** | 1.19759 | 0.006 | 0.05 |
| Na | 329.9** | 10,337.3** | 702.3 | 46.1* | 33.2 |
| Nb | 7.928** | 442.121** | 5.278 | 2.87* | 33.2 |
| PH | 148.7** | 38,409** | 859.2 | 4.6 | 12.6 |

*(Continued)*

TABLE 1 Continued

| SOV / Traits | Genotypes | Treatments | Replication | Treatments * Genotypes | Error |
|---|---|---|---|---|---|
| POD | 37.2949* | 54.1865** | 61.4598 | 4.09* | 2.44 |
| RWC | 375.12* | 9,769.94** | 684.3 | 28.82 | 33.28 |
| SCY | 86.01** | 1,267.05** | 19.76 | 3.63 | 6.10 |
| SOD | 35.14** | 1,187.99** | 48.35 | 6.56 | 3.05 |
| TPC | 4.549** | 183.397** | 8.384 | 0.202 | 0.27 |
| TSP | 0.0795** | 0.13087** | 0.01887 | 0.001 | 0.003 |

ASA, ascorbic acid; BW, boll weight; CAR, carotenoids; CAT, catalase; Chla, Chlorophyll a; Chlb, Chlorophyll b; FF, fiber fineness; FL, fiber length; FLV, flavonoids; FS, fiber strength; GOT, ginning out turn percentage; $H_20_2$, Hydrogen per oxide; K+, potassium content; K+/Na+, the potassium over sodium ratio; MDA, malondialdehyde; $Na^+$, the sodium contents; NBP, Number of bolls per plant; PH, plant height; POD, peroxidase; RWC, Relative water content; SCY, seed cotton yield; SOD, superoxide dismutase; TPC, total phenolic content; TSP, total soluble protein. *, Significant at 1% level; **, Significant at 5% level.

TABLE 2 Second year mean square values for various agro-physiological, biochemical, and fiber quality traits of 30 cotton genotypes under four treatments.

| SOV / Traits | Genotypes | Treatments | Replication | Treatments * Genotypes | Error |
|---|---|---|---|---|---|
| DoF | 29 | 3 | 2 | 87 | 238 |
| ASA | 932.9** | 37,950.7** | 3,595.9 | 17 | 59.3 |
| BW | 1.08** | 12.84** | 0.13 | 0.046 | 0.112 |
| CAT | 285.4** | 3,044.44** | 61.77 | 29.99** | 13.61 |
| Car | 0.16** | 0.07** | 0.008 | 0.001 | 0.002 |
| Chla | 0.303** | 0.54* | 0.09 | 0.07 | 0.06 |
| Chlb | 0.04** | 0.10** | 0.03 | 0.000 | 0.002 |
| FF | 2.17** | 7.49** | 4.43 | 0.05 | 0.128 |
| FL | 29.36** | 382.04** | 55.22 | 2.23 | 2.25 |
| FLV | 6,071.0** | 28,511.8** | 9,403.9 | 17.1 | 294.0 |
| FS | 45.55 | 570.3 | 30.85 | 1.15 | 3.82 |
| GOT | 101.19 | 1,247.33 | 145.77 | 0.45 | 6.04 |
| H202 | 0.046 | 0.594 | 0.12 | 0.002 | 0.005 |
| K | 667.0 | 32,020.4 | 2,636.3 | 149.1* | 105.9 |
| KNA | 2.72 | 110.93 | 5.37 | 0.47** | 0.19 |
| MDA | 0.386 | 1.44 | 1.25 | 0.007 | 0.046 |
| Na | 342.9 | 10,888.7 | 740.2 | 48.1* | 35.1 |
| Nb | 13.04 | 549.47 | 84.76 | 3.13 | 3.20 |
| PH | 162.1** | 33,498.6** | 1,637.2 | 4.2 | 25.4 |
| POD | 25.22** | 51.37* | 42.3 | 0.44 | 2.07 |
| RWC | 373.2** | 1,4751.6** | 1,622.7 | 24.3 | 28.3 |
| SCY | 89.07** | 1,230.16** | 29.97 | 3.66 | 3.12 |
| SOD | 36.03** | 1,245.10** | 53.01 | 6.77** | 3.21 |

*(Continued)*

TABLE 2 Continued

| SOV / Traits | Genotypes | Treatments | Replication | Treatments * Genotypes | Error |
|---|---|---|---|---|---|
| TPC | 4.46** | 181.6** | 3.45 | 0.19 | 0.26 |
| TSP | 0.08** | 0.13** | 0.02 | 0.001 | 0.003 |

ASA, ascorbic acid; BW, boll weight; CAR, carotenoids; CAT, catalase; Chla, Chlorophyll a; Chlb, Chlorophyll b; FF, fiber fineness; FL, fiber length; FLV, flavonoids; FS, fiber strength; GOT, ginning out turn percentage; $H_20_2$, Hydrogen peroxide; K+, potassium content; K+/Na+, the potassium over sodium ratio; MDA, malondialdehyde; $Na^+$, the sodium contents; NBP, Number of bolls per plant; PH, plant height; POD, peroxidase; RWC, Relative water content; SCY, seed cotton yield; SOD, superoxide dismutase; TPC, total phenolic content; TSP, total soluble protein. *, Significant at 1% level; **, Significant at 5% level.

heritability analyses were carried out by the protocol outlined by Falconer and Mackay (Falconer, 1996; Racine, 2012).

# Results

## Assessment of variation among cotton genotypes under different treatments

The mean squares from the two-factor analysis of variance showed significant differences for genotypes, treatments, and genotype × treatment interaction for all the agro-physiological, biochemical, and fiber quality traits in both years (Tables 1, 2). As all the traits showed significant differences between genotypes × treatments, the data were analyzed separately for each of the four treatments, i.e., control, D, H, and DH.

## Heat map analysis under different treatments

The heat map analysis for control classified the 30 cotton genotypes into five clusters in the first year and four clusters in the second year based on twenty-four agro-physiological and biochemical traits. In the first year, the six cotton genotypes—Niab-Kiran, MNH-786, IUB-65, FH-312, and CRS-2007—were classified in cluster I. It means that these cotton genotypes attained higher values for $K^+$, $K^+/Na^+$, POD, CAT, TSP, Chla, Chlb, CAR, MDA, TPC, ASA, RWC, FLV, GOT, FS, FL, PH, BW, NBP, and SCY while lower values for $Na^+$, $H_2O_2$, SOD, and FF (Figure 1). In the second year, NIAB-820, FH-142, CIM-598, KAHKSHAN, MS-71, and CEMB-33 were grouped into Cluster I. These genotypes were high performers for FF, BW, FL, SCY, GOT, PH, Nb/p, MDA, FS, CHlb, CHla, ASA, TPC, POD, $K^+/Na^+$, $K^+$, TSP, RWC, and FLV; and they were low performers for $Na^+$, $H_2O_2$, SOD, CAT, and Car (Figure 2).

Under drought stress, the 30 cotton genotypes were grouped into four major clusters in both years. In the first year, the six cotton genotypes, viz., Niab-Kiran, CRS-2007, NIAB-820, MS-71, CEMB-33, and KAHKASHAN, attained the highest values for $K^+$, $K^+/Na^+$, POD, CAT, TSP, Chla, Chlb, CAR, MDA, TPC, ASA, RWC, FLV, GOT, FS, FL, PH, BW, NBP, and SCY, while the lowest values for $Na^+$, $H_2O_2$, SOD, and FF. In the second year, cluster I included seven genotypes, viz., NIAB-820, MS-71, KAHKSHAN, CEMB-33, MNH-786, IUB-65, and CIM-598, which had the highest values for CAT, Car, FS, Chlb, MDA, TPC, PH, POD, TSP, ASA, RWC, BW, FF, Nb/p, SCY, FL, FLV, SOD, $K^+$, and $K^+/Na^+$ and had the lowest values for $Na^+$, $H_2O_2$, and Chla.

In contrast, under heat stress, the heat map analysis classified the 30 cotton genotypes into two major groups in the first year and six clusters in the second year. In the first year, Group-I consisted of cotton genotypes, viz., IUB-65, CIM-598, MNH-786, KAHKSHAN, CEMB-33, MS-71, FH-142, NIAB-820, CRS-2007, FH-312, and NIAB-KIRN. These cotton genotypes attained comparatively higher values for K+, K+/Na+, POD, CAT, TSP, Chla, Chlb, CAR, MDA, TPC, ASA, RWC, FLV, GOT, FS, FL, PH, BW, NBP, and SCY. In contrast, these values for $Na^+$, $H_2O_2$, SOD, and FF are lower. In the second year, NIAB-820, MS-71, KAHKSHAN, and CEMB-33 had high values for all the studied traits except $Na^+$, $H_2O_2$, and Chla.

Under DH, the heat map analysis grouped the cotton genotypes into four clusters in the first year and two clusters in the second year. In the first year, for DH, Clusters I, II, and III possessed the highest values for K+, K+/Na+, POD, CAT, TSP, Chla, Chlb, CAR, MDA, TPC, ASA, RWC, FLV, GOT, FS, FL, PH, BW, NBP, and SCY and the lowest values for Na+, $H_2O_2$, SOD, and FF. The cotton genotypes in these three clusters were IUB-65, CIM-598, MNH-786, KAHKSHAN, CEMB-33, MS-71, FH-142, NIAB-820, CRS-2007, FH-312, and NIAB-KIRN. In the second year, MS-71, CEMB-33, KAHKSHAN, and NIAB-820 were grouped into Cluster I and were high performers for all traits except $Na^+$, $H_2O_2$, and Nb/p.

## Principal component analysis for different treatments

In the first year, under control conditions, the first (PC-1) and second (PC-2) components explained 60.46% and 7.07% of total variation, respectively. PC-1 exhibited positive correlations with $H_2O_2$ and $Na^+$. The lowest values for these two traits were desirable, and there were no single cotton genotypes interacting negatively with these two vectors. The PC-2 exhibited positive correlations with $K^{+/}Na^+$, SOD, POD, CAT, TSP, Chla, Chlb, CAR, MDA, TPC, ASA, RWC, FLV, GOT, FS, FL, PH, NBP, and SCY. There are only four cotton genotypes, viz., NIAN-KIRAN, FH-312, CRS-2007, and CIM-598, that had the highest PC-2 scores and were identified as superior for these traits (Figure 3). In the second year, the first (PC-1) and second (PC-2) components were responsible for more than 65% of the variations. PC-1 was negatively associated with all traits except $H_2O_2$

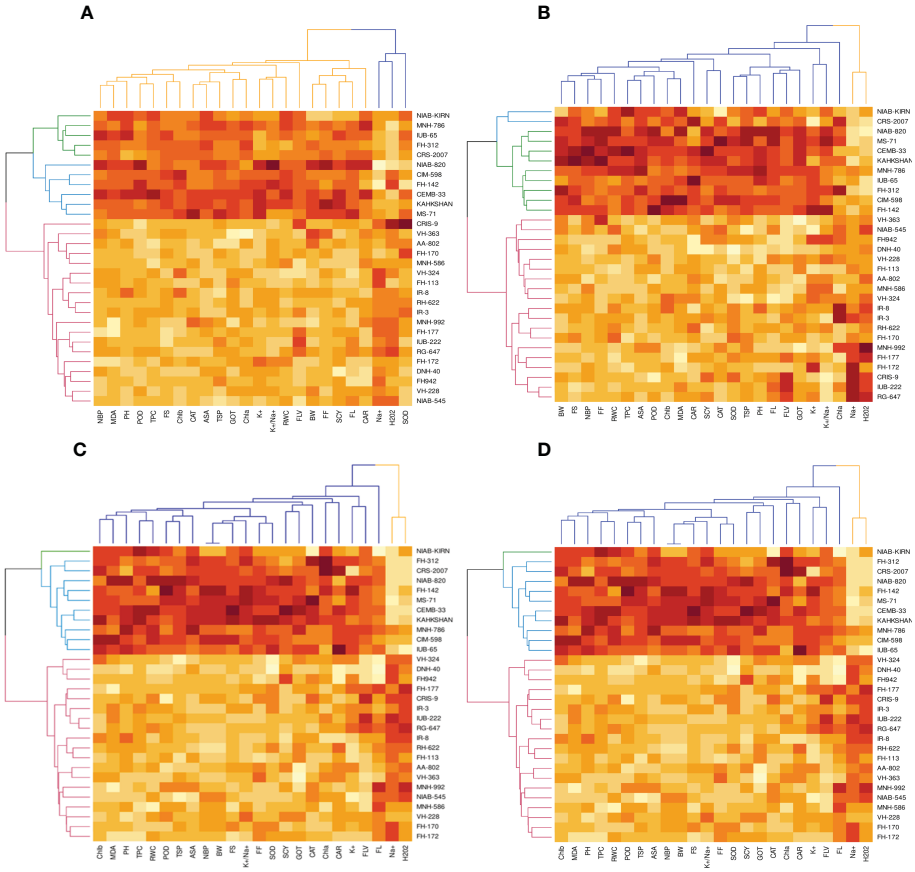


FIGURE 1
First year PCA-Biplot of various agro-physiological, biochemical and fiber quality traits of 30 cotton genotypes. **(A)** control, **(B)** drought stress **(D)**, **(C)** heat stress (H), and **(D)** drought + heat stress (DH). ASA, ascorbic acid; BW, boll weight; CAR, carotenoids; CAT, catalase; Chla, Chlorophyll a; Chlb, Chlorophyll b; FF, fiber fineness; FL, fiber length; FLV, flavonoids; FS, fiber strength; GOT, ginning out turn percentage; H202, Hydrogen peroxide; K+, potassium content; K+/Na+, the potassium over sodium ratio; MDA, malondialdehyde; Na+, the sodium contents; NBP, Number of bolls per plant; PH, plant height; POD, peroxidase; RWC, Relative water content; SCY, seed cotton yield; SOD, superoxide dismutase; TPC, total phenolic content; TSP, total soluble protein.

and $Na^+$. PC-2 was negatively associated with SOD, CAT, FLV, Car, Chla, TPC, ASA, PH, GOT, Chlb, Nb/p, MDA, TSP, and FS, whereas it was positively associated with the rest of the traits (Figure 4).

The PCA for drought stress in the first year revealed that the first component (PC-1) explained 59.81% of the total variation and presented a positive correlation with $H_2O_2$ and $Na^+$. The cotton genotypes CRIS-9, RG-647, IUB-222, and FH-177 exhibited the highest PC-1 scores. PC-2 explained 7.94% of the variation and possessed a positive correlation with SOD, POD, CAT, TSP, Chlb, CAR, MDA, TPC, ASA, RWC, FLV, GOT, FS, FL, PH, NBP, and SCY. The cotton genotypes MNH-786, IUB-65, CIM-598, IUB-65, and FH-142 had a positive correlation with PC-2 and were identified as superior for these traits. In the second year, PC1 and PC2 contributed more than 67% of the total variations. It was found that PC1 was negatively associated with FLV, SOD, SCY, FL, TSP, K, GOT, PH, FF, TPC, and Nb/p and positively correlated with the rest of the traits, whereas PC2 positively correlated with $Na^+$ and $H_2O_2$ and was negatively correlated with the rest of the traits.

Results from the PCA biplot under heat stress in the first year revealed that the first component (PC-1) explained 53.93% of the variation and presented a positive association with $H_2O_2$, $Na^+$, and NBP. The cotton genotypes CRIS-9, RG-647, UB-222, and FH-177 exhibited positive scores for these traits. PC-2 explained 8.58% of the variation and had positive associations with SOD, TSP, Chlb, CAR, MDA, TPC, RWC, FLV, GOT, FS, FL, PH, and SCY. The cotton genotypes IUB-65, MNH-586, and NIAB-KIRN had positive associations with PC-2 and higher values for these traits. In the second year, PC1 and PC2 were responsible for more than 65% of the variations. The PC1 was negatively associated with FLV, Nb/p, SOD, SCY, FL, TSP, FF, PH, CAT, and TPC, whereas the PC2 was positively associated with all the studied traits and was positively associated with $Na^+$ and $H_2O_2$.

For the PCA biplot under drought and heat stress in the first year, the first (PC-1) and second (PC-2) components explained 65.62% and 6.03% of the variation, respectively. PC-1 showed a positive association with $H_2O_2$ and $Na^+$. The cottons VH-228, AA-802, IR-3, IUB-222, and FH-170 had a positive association with PC-1 and attained the highest values for $H_2O_2$ and $Na^+$. Similarly, PC-2 had the positive association with $K^+$, $K^+/Na^+$, SOD, POD, TSP, Chla, Chlb, CAR, MDA, TPC, RWC, GOT, FS, PH, and SCY. The

10.3389/fpls.2023.987514

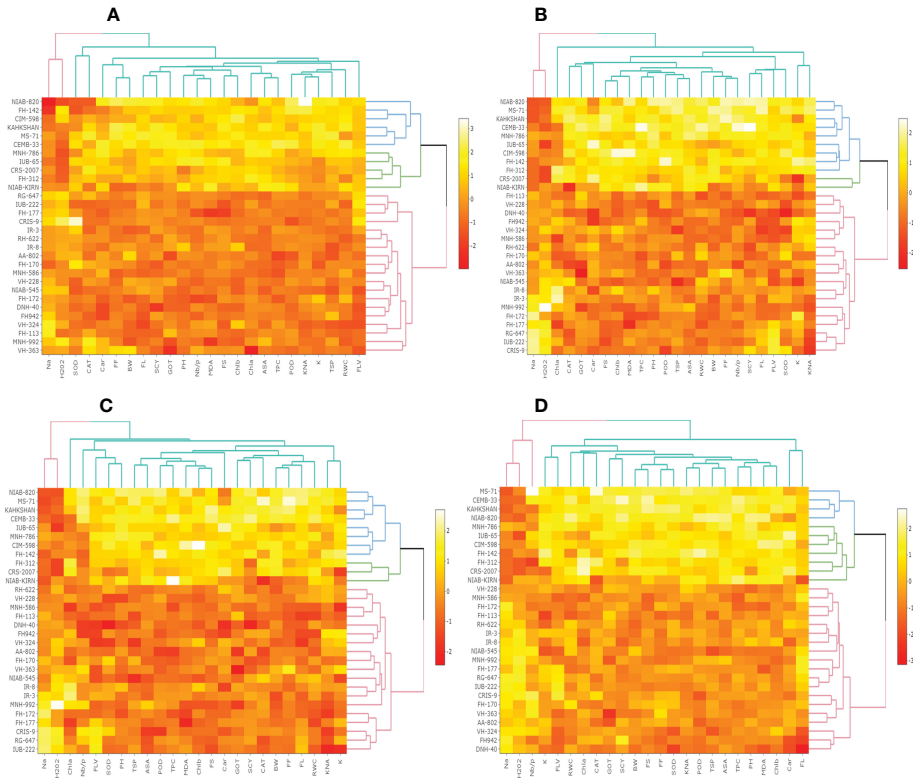


FIGURE 2
Second year PCA-Biplot of various agro-physiological, biochemical, and fiber quality traits of 30 cotton genotypes **(A)** control, **(B)** drought stress **(D)**, **(C)** heat stress (H), and **(D)** drought + heat stress (DH). ASA, ascorbic acid; BW, boll weight; CAR, carotenoids; CAT, catalase; Chla, Chlorophyll a; Chlb, Chlorophyll b; FF, fiber fineness; FL, fiber length; FLV, flavonoids; FS, fiber strength; GOT, ginning out turn percentage; H202, Hydrogen peroxide; K+, potassium content; K+/Na+, the potassium over sodium ratio; MDA, malondialdehyde; Na+, the sodium contents; NBP, Number of bolls per plant; PH, plant height; POD, peroxidase; RWC, Relative water content; SCY, seed cotton yield; SOD, superoxide dismutase; TPC, total phenolic content; TSP, total soluble protein.

cotton genotypes NIAB-KIRN, CIM-598, CRS-2007, FH-312, IUB-65, FH-142, and MNH-786 have the highest values for these traits and interact positively with PC-2. In the second year, PC1 contributed 61.98% and PC2 contributed 6.20% to total variations. PC1 was positively associated with Chla, SCY, Chlb, MDA, ASA, TPC, FS, RWC, and Car, whereas it was negatively associated with the rest of the traits. PC2 was positively associated with $Na^+$, $H_2O_2$, and Nb/p and was negatively associated with the rest of the traits.

## Correlation analysis among 24 agro-physiological, biochemical, and fiber quality traits under different treatments

The correlation among different agro-physiological and biochemical traits is of great importance for selecting the most appropriate genotype in a specific environment. The Pearson correlation coefficients were calculated for two years under each of the four conditions separately, *viz*., control, D, H, and DH.

In the first year, correlation analysis among 24 agro-physiological, biochemical, and fiber quality traits under control revealed that ASA, CAR, and CAT have positive correlations with all the other traits, while $Na^+$ and $H_2O_2$ have negative correlations Figure 5. The fiber quality traits FS, FF, and FL have also a positive correlation with the majority of agro-physiological and biochemical traits except $Na^+$, $H_2O_2$, and SOD, for which there is a negative correlation. Similarly, SCY has a positive but not significant correlation with all agro-physiological and biochemical traits except $Na^+$, $H_2O_2$, and SOD. In the second year, most of the traits were positively correlated with each other but were negatively correlated with $Na^+$, $H_2O_2$, SOD, and CAT (Figure 6).

Under drought stress, in the first year, the ASA, CAR, and CAT have positive correlations with all agro-physiological traits and a negative correlation with $Na^+$ and $H_2O_2$. The $Na^+$ and $H_2O_2$ had negative associations with all other agro-physiological, biochemical traits, and fiber quality traits. The SCY had also a positive but not significant correlation with all agro-physiological, biochemical, and fiber quality traits except $Na^+$, $H_2O_2$, and SOD. In the second year, SCY was positively correlated with $K^+$, SOD, FLV, FL, RWC, BW, Nb/p, MDA, TSP, CAT, GOT, Car, PH, and Chla and Chlb, but it was negatively correlated with $Na^+$ and $H_2O_2$. $Na^+$ and $H_2O_2$ were negatively correlated with all traits.

Under heat stress in the first year, the ASA, CAR, and CAT have positive correlations with all agro-physiological, biochemical, and

10.3389/fpls.2023.987514

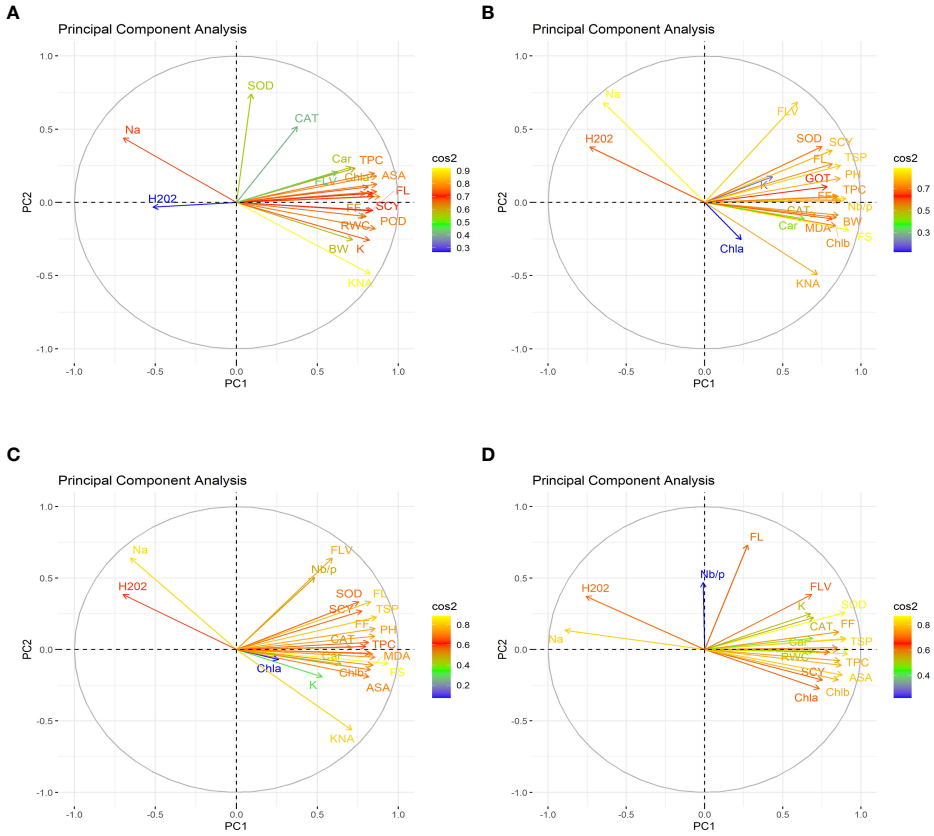


FIGURE 3
First year heat map analysis based on mean values of various agro-physiological, biochemical, and fiber quality traits of 30 cotton genotypes **(A)** control, **(B)** drought stress **(D)**, **(C)** heat stress (H), and **(D)** drought + heat stress (DH). ASA, ascorbic acid; BW, boll weight; CAR, carotenoids; CAT, catalase; Chla, Chlorophyll a; Chlb, Chlorophyll b; FF, fiber fineness; FL, fiber length; FLV, flavonoids; FS, fiber strength; GOT, ginning out turn percentage; H202, Hydrogen peroxide; K+, potassium content; K+/Na+, the potassium over sodium ratio; MDA, malondialdehyde; Na+, the sodium contents; NBP, Number of bolls per plant; PH, plant height; POD, peroxidase; RWC, Relative water content; SCY, seed cotton yield; SOD, superoxide dismutase; TPC, total phenolic content; TSP, total soluble protein.

fiber quality traits, while having a negative correlation with $Na^+$ and $H_2O_2$. The $Na^+$ and $H_2O_2$ had negative associations with all other agro-physiological, biochemical traits, and fiber quality traits. The SCY also had a positive but not significant correlation with all agro-physiological, biochemical, and fiber quality traits except $Na^+$ and $H_2O_2$. In the second year, $Na^+$ and $H_2O_2$ were negatively correlated with all the studied traits, whereas all the other traits were positively correlated with each other.

The correlation analysis under DH during the first year among 24 agro-physiological, biochemical, and fiber quality traits predicted that the ASA, CAR, and CAT would have positive correlations with all agro-physiological, biochemical, and fiber quality traits, while having a negative correlation with $Na^+$ and $H_2O_2$. The SCY also had a positive but not significant correlation with all agro-physiological, biochemical, and fiber quality traits except $Na^+$ and $H_2O_2$. The $Na^+$ and $H_2O_2$ had negative association with all other agro-physiological, biochemical, and fiber quality traits. In the second year, it was observed that Nb/p, $Na^+$, and $H_2O_2$, were negatively associated with the other traits, whereas the other studied traits are positively associated with each other.

## Coefficient of variation and heritability analysis

During the first year, under the control conditions, most of the traits indicated a lower coefficient of variation (CV) except $H_2O_2$, POD, CAT, TSP, Chla and b, Car, MAD, and TPC; however, with the rise of abiotic stresses, the CV of most of the agro-physiological traits increased except, i.e., $K^+$ ions, $Na^+$ ions, POD, Chla, and Car. In the second year, most of the traits indicated a rise in CV with the increase in stress level, especially morphological traits; however, the CV was low under heat stress in comparison to drought stress. For heritability analysis, most of the traits showed moderate to high broad-sense heritability in both years; SCY, BW, and fiber traits indicated high heritability (Tables 3, 4).

# Discussion

Under changing climatic conditions, abiotic stresses are intensifying and are having a negative impact on the cotton crop.

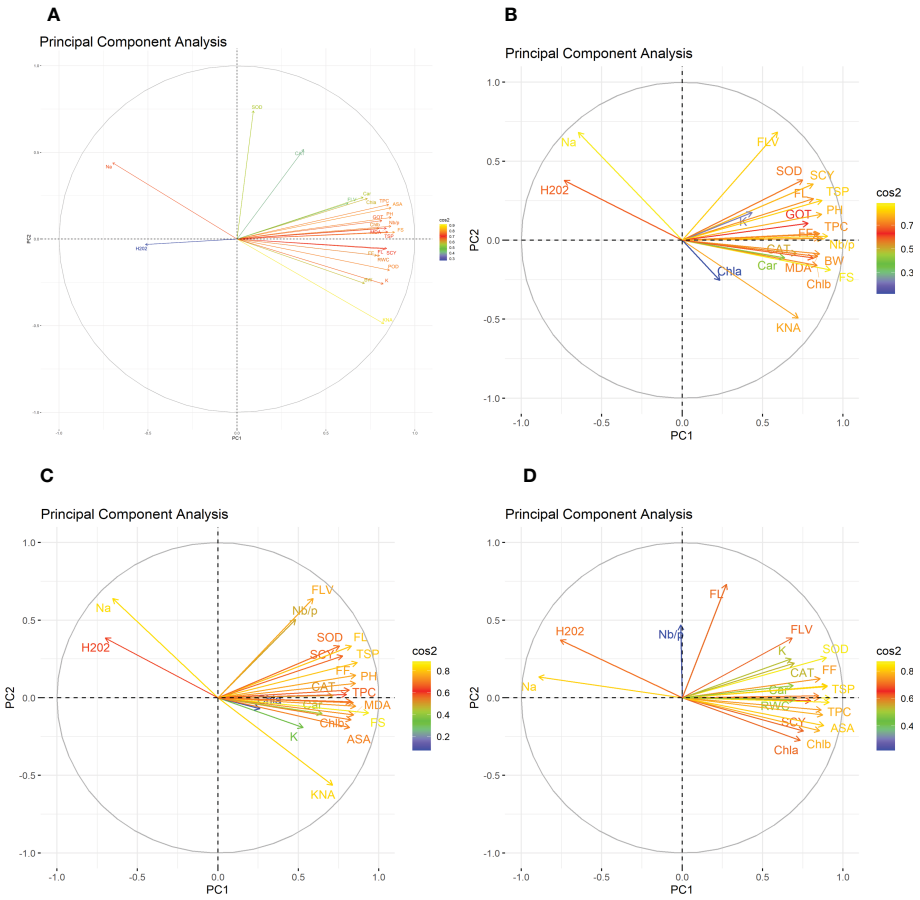


FIGURE 4
Second year heat map analysis based on mean values of various agro-physiological, biochemical, and fiber quality traits of 30 cotton genotypes **(A)** control, **(B)** drought stress **(D)**, **(C)** heat stress (H), and **(D)** drought + heat stress (DH). ASA, ascorbic acid; BW, boll weight; CAR, carotenoids; CAT, catalase; Chla, Chlorophyll a; Chlb, Chlorophyll b; FF, fiber fineness; FL, fiber length; FLV, flavonoids; FS, fiber strength; GOT, ginning out turn percentage; H202, Hydrogen peroxide; K+, potassium content; K+/Na+, the potassium over sodium ratio; MDA, malondialdehyde; Na+, the sodium contents; NBP, Number of bolls per plant; PH, plant height; POD, peroxidase; RWC, Relative water content; SCY, seed cotton yield; SOD, superoxide dismutase; TPC, total phenolic content; TSP, total soluble protein.

These stresses have become a major obstacle to achieving cotton yield potential by disrupting various morphological, physiological, and metabolic processes (Hassan et al., 2020). The development of high yield cultivars tailored according to changing climatic conditions has become inevitable to sustain the high yield of the cotton crop (Wang et al., 2013). To date, efforts have been focused on mostly single abiotic stress; however, under the dynamic climatic circumstances, the situation has ripened such that more than one stress should be applied in a systematic way to the growing cotton plants (Kirungu et al., 2019) so that the climate-resilient cotton genotypes can be identified and can be used in future breeding programs.

Therefore, in the current study, cotton genotypes were subjected to multiple abiotic stresses in different combinations, i.e., drought, heat, and DH, for two consecutive years. Results indicated that under control, all the genotypes performed well, whereas under drought and heat stresses, all the traits showed negative impact. However, the values of all traits were almost similar for all the traits under these two stresses (Singh et al., 2018; Sabagh et al., 2020). However, when DH was applied, it was observed that there was a highly negative impact on all the cotton genotypes. It was observed that, with the changing climatic conditions, there will be a highly negative impact on the cotton genotypes.

Under these abiotic stresses, morphological traits, i.e., plant height, number of bolls, SCY, and boll weight, reduced under the drought and heat stresses, and the reduction in these traits was more pronounced under the DH stress (Singh et al., 2018). At the onset of stress, it is proposed that plants sense osmotic changes first due to drought and heat stress rather than sodium ions, while sodium-specific responses occur much later through the toxic effects of sodium and chloride ions on the leaves (Munns and Tester, 2008). The plant height was decreased due to the reduction in cell wall elasticity due to the absorption of substances that were produced in response to disturbed metabolic processes triggered by the accumulation of toxic ions inside the cell. The absorption of undesirable metabolites decreased cell expansion, and the reduction in cell wall turgidity caused the shoots to remain shorter (Zafar et al., 2020). The reduction in the number of bolls can be attributed

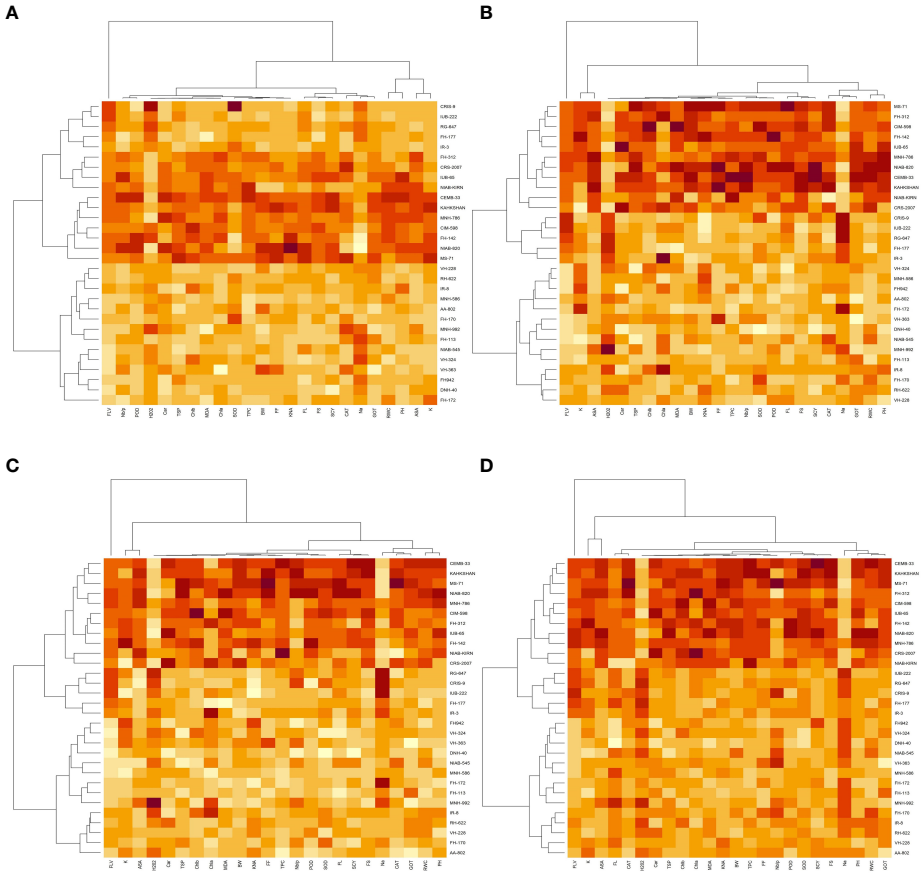


FIGURE 5
First year correlation analysis based on mean values of various agro-physiological, biochemical, and fiber quality traits of 30 cotton genotypes. **(A)** control, **(B)** drought stress **(D)**, **(C)** heat stress (H), and **(D)** drought + heat stress (DH).ASA, ascorbic acid; BW, boll weight; CAR, carotenoids; CAT, catalase; Chla, Chlorophyll a; Chlb, Chlorophyll b; FF, fiber fineness; FL, fiber length; FLV, flavonoids; FS, fiber strength; GOT, ginning out turn percentage; H202, Hydrogen peroxide; K+, potassium content; K+/Na+, the potassium over sodium ratio; MDA, malondialdehyde; Na+, the sodium contents; NBP, Number of bolls per plant; PH, plant height; POD, peroxidase; RWC, Relative water content; SCY, seed cotton yield; SOD, superoxide dismutase; TPC, total phenolic content; TSP, total soluble protein.

to the shrinkage of cell walls, hindrance in the differentiation of the tissues, disturbance of essential ions, and injuries to the growing tissues. Reduced cell division and reduction in the cell size caused the decline in the size of a leaf expansion that ultimately led to the decreased photosynthates generation inside the cell, which resulted in the lesser number of bolls (Yavari, 2020). Similarly, boll weight also got reduced under abiotic stresses due to the disturbance of various metabolic pathways involved in the production of ATP, leading to lesser ATP synthesis than the control (Farooq et al., 2020). The reduction of boll weight and number of bolls on the cotton plant under drought, heat, and DH led to a low SCY. All the fiber quality traits indicated a reduction in values except GOT%, which can be due to the fact that the decrease in the size of the seed resulted in more GOT% (Chaudhary et al., 2020).

When plants lose water due to high temperatures or water deficit conditions, the concentration of salts increases in the rhizosphere, which decreases the osmotic pressure. To maintain the cell volume and turgor, plants undergo osmotic adjustments by producing organic solutes in high amounts, i.e., proline, sugar alcohols, and sorbitol, by utilizing energy resource, which compromises the plant photosynthetic processes (Flowers et al., 2015). The reduction of photosynthesis can be related to the less production of chlorophyll a and b contents in a reduced leaf area, ultimately affecting the yield potential (Sanchez et al., 2008). At the onset of high temperatures and drought stress, stomata close to avoid the loss of water, and this closure also reduces the amount of $CO_2$ available for fixation, although the expected increase in $CO_2$ under climatic changes can only partially recover the photosynthetic rate (Cheeseman, 2013). Moreover, there is also an ionic effect of sodium on photosynthesis; the activity of $CO_2$ fixing enzymes decreases during salt stress, and interestingly, the tolerance of these enzymes for $Na^+$ *in vitro* differs among various genotypes (Bose et al., 2017). Genotypes that accumulated a high concentration of $Na^+$ ions and a low concentration of $K^+$ ions inside the cell were regarded as tolerant. High concentrations of $Na^+$ ions displace $Ca^{++}$ ions in the cell membrane, which reduces the ability of a cell to exclude $Na^+$ ions (Peng et al., 2014). The proton motive force necessary for energy production in chloroplasts depends on the close coordination between PH and electropotential changes over thylakoid membranes. Sodium ions disturb this balance because of their positive change and effect on pH. Overall, drought and heat stresses act in a synergistic fashion and

10.3389/fpls.2023.987514

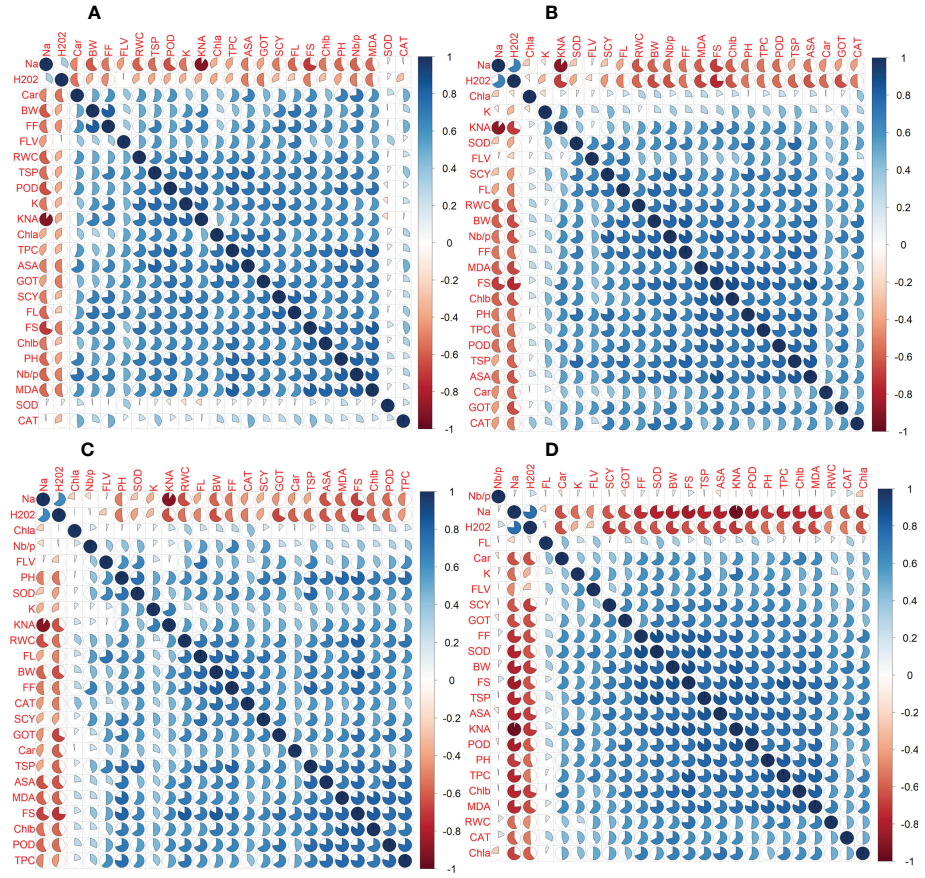


FIGURE 6
Second year correlation analysis based on mean values of various agro-physiological, biochemical, and fiber quality traits of 30 cotton genotypes. **(A)** control, **(B)** drought stress **(D)**, **(C)** heat stress (H), and **(D)** drought + heat stress (DH). ASA, ascorbic acid; BW, boll weight; CAR, carotenoids; CAT, catalase; Chla, Chlorophyll a; Chlb, Chlorophyll b; FF, fiber fineness; FL, fiber length; FLV, flavonoids; FS, fiber strength; GOT, ginning out turn percentage; H202, Hydrogen peroxide; K+, potassium content; K+/Na+, the potassium over sodium ratio; MDA, malondialdehyde; Na+, the sodium contents; NBP, Number of bolls per plant; PH, plant height; POD, peroxidase; RWC, Relative water content; SCY, seed cotton yield; SOD, superoxide dismutase; TPC, total phenolic content; TSP, total soluble protein.

disrupt photosynthesis by disturbing the protein motive force and chloroplast function and by interfering with $CO_2$ enzymes (Bose et al., 2017). The rise of abiotic stress further exacerbates the situation by decreasing the hydraulic conductivity of roots by 70% (Boursiac et al., 2005). Hydraulic conductivity is facilitated to a large extent by aquaporins, which are pores that facilitate water transport over membranes (Javot et al., 2003; Postaire et al., 2010). However, under stress conditions, both the localization and the activities of aquaporins and downstream sodium signals are greatly altered (Li et al., 2014).

Plants respond to ROS by upregulating antioxidant defensive enzyme activities, i.e., peroxidase (POD), catalase (CAT), and superoxidase dismutase (SOD) (Cui et al., 2021). With the increase of abiotic stresses, $H_2O_2$ production increases, against which catalase is synthesized, and it induces its scavenging activity, which greatly reduces the negative implications of $H_2O_2$. SOD is an efficient intercellular enzymatic antioxidant, and its activity increases in high-yielding genotypes, rendering them tolerant. It catalyzes the dismutation of superoxide into molecular oxygen and $H_2O_2$ and acts as a first line of defense against ROS. POD and CAT metabolize $H_2O_2$ into water and oxygen inside the cytosol and chloroplasts, which safeguards the cell from the toxic effects of $H_2O_2$ (Liu et al., 2021). Total soluble proteins got reduced due to the toxic ion accumulation inside the cell that disintegrated the cell membrane. The concentration of carotenoids also increased, as they are important antioxidants for protecting singlet oxygen (Sharma et al., 2019). Heat and drought stress decrease the relative water content (RWC), which ultimately reduces the plant photosynthesis rate as well; therefore, genotypes that had a higher RWC under the stresses were declared as tolerant genotypes. The genotypes that had a high RWC also had a high boll retention rate and a high SCY, which are associated with high tolerance under a multitude of abiotic stresses (Mammadov et al., 2018; Anwar et al., 2022). Total phenolic contents (TPCs) play a significant role in the protection of plant cell components. TPCs are positively correlated with the antioxidant activity. The potential of phenolics to act as antioxidants is mainly due to their ability to act as hydrogen donors, reducing agents, and quenchers of singlet oxygen. TPCs increased in the tolerant genotypes, which indicates the capacity of the plants to cope with the implications of a multitude of stresses (Zafar et al., 2020). Malondialdehyde content estimation can be used to access membrane damage (Hessini et al., 2022). A higher level of observed MDA is an indication of structural damage due to the increasing

TABLE 3 First year components of variability and heritability of various traits under control and stress conditions.

| SOV | Plant Height | | | | | Number of Bolls | | | Seed Cotton Yield | | | | Boll Weight | | | | Fiber Fineness | | | |
|---|---|---|---|---|---|---|---|---|---|---|---|---|---|---|---|---|---|---|---|---|
| | $S_0$ | S1 | S2 | S3 | $S_0$ | S1 | S2 | S3 | $S_0$ | S1 | S2 | S3 | $S_0$ | S1 | S2 | S3 | $S_0$ | S1 | S2 | S3 |
| Mean | 97.76 | 74.78 | 65.57 | 50.6 | 8.6 | 6.27 | 6.5 | 3.2 | 24.01 | 20.48 | 20.08 | 14.9 | 2.9 | 2.5 | 2.5 | 2.01 | 4.02 | 3.82 | 3.78 | 3.3 |
| Max | 113.35 | 82.69 | 76.90 | 57.48 | 12 | 10 | 11 | 6 | 33.37 | 28.65 | 29.76 | 22.32 | 4.2 | 3.434 | 3.4 | 3.13 | 5.2 | 4.94 | 4.94 | 4.28 |
| Min | 90.25 | 67.41 | 60.67 | 45.5 | 6 | 3 | 3 | 1 | 16.32 | 11.65 | 12.89 | 9.63 | 2.27 | 1.82 | 1.9 | 1.12 | 3.1 | 2.65 | 2.62 | 1.54 |
| CV | 4.53 | 4.41 | 4.23 | 4.42 | 11.42 | 14.63 | 13.52 | 24.89 | 12.26 | 13.15 | 10.46 | 15.1 | 9.37 | 11.08 | 11.13 | 14.72 | 9.57 | 10.87 | 11.12 | 12.38 |
| $H^2$ | 47.98 | 49.37 | 49.43 | 49.17 | 47.64 | 31.72 | 22.48 | 34.19 | 58.36 | 66.87 | 38.35 | 57.96 | 44.74 | 57.41 | 59.16 | 48.75 | 68.09 | 71.82 | 72.17 | 47.58 |
| SOV | Fiber Strength | | | | Fiber Length | | | | GOT% | | | | $K^+$ Ion Concentration | | | | $Na^+$ Ion Concentration | | | |
| | $S_0$ | S1 | S2 | S3 | $S_0$ | S1 | S2 | S3 | $S_0$ | S1 | S2 | S3 | $S_0$ | S1 | S2 | S3 | $S_0$ | S1 | S2 | S3 |
| Mean | 22.46 | 19.35 | 19.72 | 17.08 | 27.51 | 24.76 | 24.72 | 22.52 | 38.57 | 42.05 | 41.2 | 44.62 | 149.3 | 128.31 | 128.15 | 105.34 | 33.65 | 43.06 | 43.21 | 59.49 |
| Max | 26.51 | 24.65 | 26.62 | 22.43 | 32.36 | 29.44 | 31.39 | 24.96 | 45.71 | 49.83 | 48.46 | 51.52 | 183.6 | 150.8 | 159.84 | 128.21 | 42.23 | 60.51 | 61.11 | 78.65 |
| Min | 16.65 | 15 | 15.15 | 12.52 | 20.25 | 18.02 | 19.65 | 19.33 | 29.77 | 32.45 | 31.55 | 33.42 | 126.4 | 106.14 | 105.45 | 84.909 | 21.63 | 33.37 | 31.34 | 37.01 |
| CV | 8.39 | 9.46 | 9.5 | 10.85 | 6.55 | 6.55 | 6.5 | 4.18 | 6.17 | 6.17 | 6.172 | 6.1 | 9.16 | 3.6 | 4.05 | 4.72 | 9.76 | 9.2 | 9.6 | 13.95 |
| $H^2$ | 64.88 | 68.22 | 67.7 | 59.56 | 60.18 | 60.3 | 59.02 | 49.06 | 56.09 | 56.06 | 56.25 | 55.91 | 81.41 | 21.66 | 20.94 | 29.33 | 50.08 | 34.63 | 33.31 | 56.16 |
| SOV | $K^+/Na^+$ ratio | | | | Hydrogen Peroxide | | | | Superoxidase dismutase | | | | Peroxidase dismutase | | | | Catalase | | | |
| | $S_0$ | S1 | S2 | S3 | $S_0$ | S1 | S2 | S3 | $S_0$ | S1 | S2 | S3 | $S_0$ | S1 | S2 | S3 | $S_0$ | S1 | S2 | S3 |
| Mean | 4.45 | 3.07 | 3.06 | 1.85 | 0.14 | 0.22 | 0.23 | 0.344 | 6.01 | 9.72 | 10.37 | 14.87 | 11.03 | 9.98 | 9.98 | 9.23 | 42.84 | 36.74 | 36.78 | 28.7 |
| Max | 8.06 | 4.71 | 5.1 | 3.05 | 0.31 | 0.46 | 0.488 | 0.707 | 9.57 | 13.72 | 14.6 | 22.65 | 18.69 | 14.73 | 14.73 | 13.99 | 55.58 | 49.96 | 53.15 | 44.74 |
| Min | 2.8 | 2.05 | 1.99 | 1.11 | 0.01 | 0.05 | 0.05 | 0.07 | 4.15 | 5.57 | 5.91 | 6.69 | 7.24 | 6.22 | 6.23 | 5.48 | 32.32 | 21.32 | 23.04 | 17.26 |
| CV | 21.606 | 10.42 | 11.36 | 18.46 | 22.63 | 22.22 | 20.41 | 20.35 | 9.68 | 12.32 | 12.32 | 22.06 | 18.96 | 16.74 | 16.74 | 17.24 | 12.77 | 14.58 | 15.79 | 14.77 |
| $H^2$ | 80.76 | 30.8 | 31.7 | 56.43 | 32.9 | 36.1 | 31.98 | 33.11 | 29.42 | 31.03 | 31.13 | 69.66 | 61.45 | 61.37 | 61.37 | 60.89 | 67.14 | 70.7 | 73.68 | 57.64 |
| SOV | Total Soluble Proteins | | | | Chlorophyll a | | | | Chlorophyll b | | | | Carotenoids | | | | Malondialdehyde | | | |
| | $S_0$ | S1 | S2 | S3 | $S_0$ | S1 | S2 | S3 | $S_0$ | S1 | S2 | S3 | $S_0$ | S1 | S2 | S3 | $S_0$ | S1 | S2 | S3 |
| Mean | 0.301 | 0.25 | 0.26 | 0.209 | 1.001 | 0.893 | 0.88 | 0.79 | 0.32 | 0.28 | 0.27 | 0.24 | 0.22 | 0.22 | 0.22 | 0.17 | 0.86 | 1.01 | 1.04 | 1.16 |
| Max | 0.53 | 0.47 | 0.48 | 0.41 | 1.83 | 1.58 | 1.56 | 2.006 | 0.66 | 0.6006 | 0.58 | 0.487 | 0.36 | 0.34 | 0.36 | 0.27 | 1.3 | 1.99 | 1.97 | 2.19 |
| Min | 0.11 | 0.01 | 0.02 | 0.017 | 0.136 | 0.24 | 0.24 | 0.199 | 0.14 | 0.129 | 0.12 | 0.11 | 0.101 | 0.103 | 0.10 | 0.07 | 0.12 | 0.54 | 0.53 | 0.63 |
| CV | 23.27 | 30.34 | 30.32 | 34.007 | 22.05 | 16.18 | 16.41 | 16.61 | 17.98 | 18.8 | 19.89 | 24.11 | 18.05 | 12.39 | 12.34 | 12.32 | 11.57 | 12.75 | 12.62 | 13.75 |
| $H^2$ | 59.06 | 56.08 | 56.87 | 63.96 | 47.19 | 27.65 | 28.15 | 21.9 | 49.67 | 50.66 | 54.35 | 70.89 | 41.69 | 23.7 | 22.77 | 22.65 | 22.69 | 25.7 | 26.17 | 31.41 |

*(Continued)*





10.3389/fpls.2023.987514

10.3389/fpls.2023.987514

TABLE 3 Continued

| SOV | Plant Height | | | | Number of Bolls | | | | Seed Cotton Yield | | | | Boll Weight | | | | Fiber Fineness | | | |
|---|---|---|---|---|---|---|---|---|---|---|---|---|---|---|---|---|---|---|---|---|
| | $S_0$ | S1 | S2 | S3 | $S_0$ | S1 | S2 | S3 | $S_0$ | S1 | S2 | S3 | $S_0$ | S1 | S2 | S3 | $S_0$ | S1 | S2 | S3 |
| SOV | Total Phenolic Contents | | | | Ascorbic Acid | | | | Relative Water Contents | | | | Flavonoids | | | | | | | |
| | $S_0$ | S1 | S2 | S3 | $S_0$ | S1 | S2 | S3 | $S_0$ | S1 | S2 | S3 | $S_0$ | S1 | S2 | S3 | $S_0$ | S1 | S2 | S3 |
| Mean | 2.89 | 4.02 | 4.16 | 6.31 | 133.89 | 148.82 | 149.84 | 182.11 | 72.83 | 58.44 | 57.17 | 41.63 | 322.51 | 353.7 | 353.73 | 364.77 | | | | |
| Max | 4.01 | 5.69 | 6.89 | 8.59 | 153 | 167.9 | 182.58 | 206.93 | 89.38 | 74.76 | 72.96 | 59.07 | 375 | 408.307 | 408.01 | 419 | | | | |
| Min | 1.54 | 2.66 | 2.29 | 4.25 | 120.39 | 130.02 | 117.28 | 156.03 | 51.24 | 42.86 | 41.96 | 29.39 | 276 | 307.08 | 307.03 | 318.02 | | | | |
| CV | 12.63 | 11.55 | 14.34 | 12.94 | 4.7 | 4.8 | 5.9 | 4.8 | 5.009 | 11.34 | 10.7 | 9.9 | 5.87 | 5.67 | 5.67 | 5.5 | | | | |
| $H^2$ | 53.98 | 55.01 | 55.13 | 58.1 | 55.25 | 59.37 | 48.82 | 59.52 | 27.73 | 69.46 | 58.07 | 38.39 | 55.47 | 57.26 | 57.26 | 57.26 | | | | |

stress triggered by high ROS production. Ascorbic acid/ascorbate (ASA) is another non-enzymatic antioxidant whose concentration inside the cytosol and chloroplasts increased with the rise of stresses, and it can protect the photosynthetic machinery of the plant under these stresses. In our study, genotypes that had high ASA concentrations were able to produce higher yields and were regarded as tolerant (Kamal et al., 2017). The flavonoid synthesis increased with the increase in stress; its accumulation under the stress conditions indicated that it provided a better antioxidant capacity and played an important role in the reduction of oxidative damage, which improved the plant's tolerance ability against these abiotic stresses (Nix et al., 2017).

To select the best genotypes on the basis of morphological, physiological, and biochemical bases, cluster analysis was carried out and a heatmap was drawn (Hummel et al., 2017). Cluster analysis during the two years under the studied stresses showed that the genotypes MNH-786, KAHKSHAN, CEMB-33, MS-71, FH-142, NIAB-820, and CRS-2007 were present in a single cluster of tolerant genotypes based on 24 agro-physiological and biochemical traits and remained stable. PCA analyses revealed that the first two PCs contributed significantly to the total variation under control and stress conditions for agronomic, fiber-related, morphological, and biochemical traits. These traits affirmed the differences among genotypes regarding the studied traits under control and stress conditions, which can be proved useful for future breeding programs regarding the development of climate-resilient cotton genotypes. $H_2O_2$, $Na^+$, $K^+$, $K^+/Na^+$, SOD, POD, TSP, Chlb, CAR, MDA, TPC, RWC, GOT, FS, PH, and SCY contributed to the first two PCAs under control and stress conditions. In both years, it was observed that $Na^+$ and $H_2O_2$ remained positively correlated with PC2 and negatively correlated with PC1. Moreover, it is also necessary to identify the association of various traits with one another under dynamic climatic conditions; therefore, the correlation matrix was employed to understand the dependency of various traits on each other for better phenotypes and improved yield. During both years, SCY indicated a positive correlation with all traits except $Na^+$ ions and $H_2O_2$. Most of the traits were positively correlated with each other; however, $H_2O_2$ and $Na^+$ were negatively correlated with all other traits. Expected broad-sense heritability was found moderate to high for the studied traits under all levels of stress which indicates that the characters are genetically controlled (Farooq et al., 2019a). CV was low for most of the traits, which indicated that the data was mostly centered around the mean and there was less variation in the data. Heritability estimates did not necessarily increase with the increase in stress; a few traits indicated an increasing trend, while others showed a declining trend. It indicates that there are genes associated with stress that get activated when stress is applied. It can be further argued that hidden genetic variation that was previously unselected could be uncovered when stress is applied (Khokhar et al., 2017).

In a nutshell, genotypes have indicated that under drought and heat stresses, genotypes performed almost in a similar fashion; however, when DH was applied, only the most tolerant genotypes were able to produce yield at the minimum loss. At the onset of abiotic stresses, plant-intrinsic antioxidant defense mechanisms get activated, which try their best to protect the plant's photosynthetic machinery from the damages of ROS. However, there is still a need to study underlying

TABLE 4 Second year components of variability and heritability of various traits under control and stress conditions.

| SOV | Plant Height | | | | | Number of Bolls | | | Seed Cotton Yield | | | | Boll Weight | | | | Fiber Fineness | | | |
|---|---|---|---|---|---|---|---|---|---|---|---|---|---|---|---|---|---|---|---|---|
| | $S_0$ | S1 | S2 | S3 | $S_0$ | S1 | S2 | S3 | $S_0$ | S1 | S2 | S3 | $S_0$ | S1 | S2 | S3 | $S_0$ | S1 | S2 | S3 |
| Mean | 96.49 | 72.87 | 67.42 | 49.74 | 9.97 | 7.56 | 6.48 | 4.02 | 23.98 | 20.39 | 20.07 | 14.99 | 2.91 | 2.37 | 2.49 | 1.99 | 3.96 | 3.71 | 3.70 | 3.27 |
| Max | 115.62 | 85.99 | 79.2 | 58.36 | 13 | 11 | 13 | 8 | 32.7 | 30.25 | 29.03 | 22.23 | 4.36 | 3.32 | 3.51 | 3.16 | 5.4 | 4.98 | 5.13 | 4.19 |
| Min | 87.54 | 63.37 | 59.46 | 41.72 | 7 | 4 | 2 | 1 | 15.9 | 11.42 | 12.63 | 9.34 | 2.27 | 1.67 | 1.84 | 1.07 | 3.06 | 2.49 | 2.59 | 1.5 |
| CV | 4.5 | 4.38 | 4.38 | 4.45 | 9.89 | 12.63 | 24.31 | 17.84 | 12.26 | 13.6 | 10.44 | 15.61 | 9.37 | 11.34 | 11.18 | 14.69 | 9.86 | 10.84 | 11.37 | 12.27 |
| $H^2$ | 47.57 | 49.09 | 49.26 | 49.06 | 47.64 | 34.7 | 39.95 | 29.46 | 58.92 | 64.82 | 37.44 | 58.72 | 44.24 | 56.55 | 58.97 | 48.45 | 69.55 | 72.22 | 71.19 | 47.96 |
| SOV | Fiber Strength | | | | Fiber Length | | | | GOT% | | | | $K^+$ Ion Concentration | | | | $Na^+$ Ion Concentration | | | |
| | $S_0$ | S1 | S2 | S3 | $S_0$ | S1 | S2 | S3 | $S_0$ | S1 | S2 | S3 | $S_0$ | S1 | S2 | S3 | $S_0$ | S1 | S2 | S3 |
| Mean | 22.39 | 18.17 | 20.09 | 16.55 | 27.33 | 24.52 | 24.45 | 22.31 | 37.68 | 45.74 | 41.07 | 44.39 | 152 | 126.12 | 129.43 | 105.95 | 34.55 | 44.57 | 44.37 | 61.08 |
| Max | 26.72 | 25.56 | 26.88 | 23.32 | 32.67 | 29.40 | 31.07 | 25.21 | 44.8 | 53.12 | 47.49 | 53.07 | 187.27 | 149.19 | 169.44 | 135.9 | 43.49 | 62.32 | 62.95 | 81.01 |
| Min | 16.32 | 12.9 | 15.19 | 11.61 | 20.05 | 17.84 | 19.45 | 15.65 | 29.17 | 35.37 | 30.92 | 32.75 | 129.01 | 105.08 | 103.45 | 83.21 | 22.27 | 34.37 | 32.28 | 38.126 |
| CV | 8.39 | 10.38 | 9.39 | 11.05 | 6.55 | 6.55 | 6.8 | 4.84 | 6.5 | 5.9 | 6.16 | 6.09 | 9.26 | 3.65 | 4.05 | 4.96 | 9.7 | 9.16 | 9.54 | 13.78 |
| $H^2$ | 65.09 | 76.31 | 67.02 | 60.33 | 60.18 | 60.26 | 62.92 | 47.4 | 60.68 | 53.88 | 56.59 | 56.33 | 81.73 | 22.04 | 20.15 | 29.92 | 49.97 | 34.37 | 32.95 | 55.52 |
| SOV | $K^+/Na^+$ ratio | | | | Hydrogen Peroxide | | | | Superoxidase dismutase | | | | Peroxidase dismutase | | | | Catalase | | | |
| | $S_0$ | S1 | S2 | S3 | $S_0$ | S1 | S2 | S3 | $S_0$ | S1 | S2 | S3 | $S_0$ | S1 | S2 | S3 | $S_0$ | S1 | S2 | S3 |
| Mean | 4.5 | 2.9 | 3.02 | 1.81 | 0.15 | 0.22 | 0.23 | 0.34 | 6.06 | 9.78 | 10.43 | 15.12 | 11.12 | 10.02 | 10.03 | 9.29 | 42.38 | 36.07 | 36.11 | 28.18 |
| Max | 7.98 | 3.92 | 5.24 | 2.9 | 0.31 | 0.47 | 0.47 | 0.72 | 9.66 | 14.03 | 14.55 | 22.9 | 18.87 | 14.58 | 14.58 | 13.85 | 55.15 | 48.96 | 52.09 | 43.85 |
| Min | 3.12 | 1.97 | 1.89 | 1.06 | 0.01 | 0.05 | 0.05 | 0.07 | 4.15 | 5.8 | 6.02 | 6.75 | 7.31 | 6.34 | 6.36 | 5.59 | 31.64 | 20.89 | 22.58 | 16.92 |
| CV | 20.29 | 9.88 | 11.24 | 18.6 | 24.63 | 21.16 | 31.97 | 19.85 | 9.65 | 12.32 | 12.32 | 22.03 | 18.96 | 17.02 | 16.64 | 17.28 | 13.26 | 14.48 | 15.6 | 14.68 |
| $H^2$ | 83.35 | 32.93 | 30.91 | 56.78 | 41.16 | 33.84 | 20.18 | 31.96 | 29.37 | 30.67 | 31.02 | 69.54 | 61.22 | 61.59 | 59.76 | 62.12 | 67.81 | 70.32 | 73.39 | 57.36 |
| SOV | Total Soluble Proteins | | | | Chlorophyll a | | | | Chlorophyll b | | | | Carotenoids | | | | Malondialdehyde | | | |
| | $S_0$ | S1 | S2 | S3 | $S_0$ | S1 | S2 | S3 | $S_0$ | S1 | S2 | S3 | $S_0$ | S1 | S2 | S3 | $S_0$ | S1 | S2 | S3 |
| Mean | 0.304 | 0.25 | 0.26 | 0.21 | 0.97 | 0.87 | 0.88 | 0.78 | 0.32 | 0.28 | 0.28 | 0.24 | 0.22 | 0.22 | 0.22 | 0.17 | 0.86 | 1.01 | 1.05 | 1.16 |
| Max | 0.54 | 0.48 | 0.49 | 0.41 | 1.81 | 1.55 | 1.57 | 2 | 0.64 | 0.58 | 0.57 | 0.47 | 0.36 | 0.34 | 0.36 | 0.27 | 1.32 | 1.97 | 1.99 | 2.21 |
| Min | 0.11 | 0.02 | 0.02 | 0.01 | 0.13 | 0.24 | 0.25 | 0.19 | 0.14 | 0.13 | 0.13 | 0.01 | 0.09 | 0.1 | 0.1 | 0.07 | 0.11 | 0.53 | 0.54 | 0.62 |
| CV | 23.37 | 29.86 | 30.4 | 34.08 | 22.04 | 14.91 | 16.42 | 16.81 | 17.99 | 18.52 | 19.62 | 23.42 | 18.03 | 12.49 | 11.85 | 12.58 | 11.52 | 12.62 | 12.84 | 14.74 |

*(Continued)*





10.3389/fpls.2023.987514

10.3389/fpls.2023.987514

TABLE 4 Continued

| SOV | Plant Height | | | | Number of Bolls | | | | Seed Cotton Yield | | | | Boll Weight | | | | Fiber Fineness | | | |
|---|---|---|---|---|---|---|---|---|---|---|---|---|---|---|---|---|---|---|---|---|
| | $S_0$ | S1 | S2 | S3 | $S_0$ | S1 | S2 | S3 | $S_0$ | S1 | S2 | S3 | $S_0$ | S1 | S2 | S3 | $S_0$ | S1 | S2 | S3 |
| $H^2$ | 59.28 | 57.36 | 56.98 | 64.07 | 47.06 | 22.39 | 28.51 | 21.69 | 49.88 | 51.2 | 54.03 | 62.85 | 41.6 | 23.69 | 20.8 | 23.61 | 22.57 | 25.86 | 27.18 | 34.22 |
| SOV | Total Phenolic Contents | | | | Ascorbic Acid | | | | Relative Water Contents | | | | Flavonoids | | | | | | | |
| | $S_0$ | S1 | S2 | S3 | $S_0$ | S1 | S2 | S3 | $S_0$ | S1 | S2 | S3 | $S_0$ | S1 | S2 | S3 | $S_0$ | S1 | S2 | S3 |
| Mean | 2.88 | 4.01 | 4.12 | 6.28 | 134.37 | 149.22 | 150.95 | 183.12 | 73.11 | 58.5 | 57.25 | 41.78 | 317.84 | 345.49 | 348.04 | 359.15 | | | | |
| Max | 3.9 | 5.5 | 6.08 | 8.76 | 156.06 | 170.22 | 186.25 | 211.07 | 90.28 | 76.14 | 75.14 | 59.66 | 364 | 398.25 | 398.2 | 408 | | | | |
| Min | 1.57 | 2.7 | 2.3 | 4.21 | 120.54 | 131.32 | 119.63 | 157.59 | 49.7 | 41.58 | 40.7 | 28.69 | 265 | 287 | 294 | 307.02 | | | | |
| CV | 12.67 | 11.58 | 13.92 | 12.99 | 4.77 | 4.88 | 5.97 | 5.03 | 5.01 | 11.52 | 10.44 | 9.89 | 5.9 | 5.91 | 6.2 | 5.4 | | | | |
| $H^2$ | 56.66 | 54.41 | 58.31 | 57.68 | 55.03 | 60.55 | 47.82 | 65.42 | 27.9 | 68.03 | 56.31 | 38.73 | 55.47 | 58.11 | 61.63 | 55.23 | | | | |

synergistic mechanisms under these stresses so that a well-adapted ideotype can be developed under the changing climatic conditions.

## Conclusion

Under the changing climatic conditions, it is imperative to analyze the cotton plants adaptation to various levels of abiotic stresses using agro-physiological and biochemical markers. Resilient germplasm must be developed that has a capacity to tolerate environmental fluctuations without adversely affecting its yield. The current study observed that the cotton genotypes MNH-786, KAHKSHAN, CEMB-33, MS-71, FH-142, NIAB-820, CRS-2007, and FH-312 performed up to 65% better than mean values for studied traits under control and stress conditions during both years and can be efficiently employed in future climate change resilient cotton breeding programs.

## Data availability statement

The original contributions presented in the study are included in the article/supplementary materials. Further inquiries can be directed to the corresponding authors.

## Author contributions

MF: Experimentation, manuscript writing and final editing. WC and MSS: Data collection, manuscript writing, visualization of data, and statistical analysis. UK, SZ. and JT: Formal analysis, data visualization, and validation. AS: Conceptualization, final editing, and approval of the final draft for publication. All authors contributed to the article and approved the submitted version.

## Funding

The study was supported by Higher Education Commission of Pakistan 315-1684-2AV3-007.

## Conflict of interest

The authors declare that the research was conducted in the absence of any commercial or financial relationships that could be construed as a potential conflict of interest.

## Publisher's note

# References


Abbas, S. (2020). Climate change and cotton production: An empirical investigation of Pakistan. *Environ. Sci. pollut. Res. Int.* 27, 29580–29588. doi: 10.1007/s11356-020-09222-0

Abdelraheem, A., Esmaeili, N., O'connell, M., and Zhang, J. F. (2019). Progress and perspective on drought and salt stress tolerance in cotton. *Ind. Crops Products* 130, 118–129. doi: 10.1016/j.indcrop.2018.12.070

Ainsworth, E. A., and Gillespie, K. M. (2007). Estimation of total phenolic content and other oxidation substrates in plant tissues using folin-ciocalteu reagent. *Nat. Protoc.* 2, 875–877. doi: 10.1038/nprot.2007.102

Anwar, M., Saleem, M. A., Dan, M., Malik, W., Ul-Allah, S., Ahmad, M. Q., et al. (2022). Morphological, physiological and molecular assessment of cotton for drought tolerance under field conditions. *Saudi J. Biol. Sci.* 29, 444–452. doi: 10.1016/j.sjbs.2021.09.009

Arnon, D. I. (1949). Copper enzymes in isolated chloroplasts. polyphenoloxidase in beta vulgaris. *Plant Physiol.* 24, 1–15. doi: 10.1104/pp.24.1.1

Bose, J., Munns, R., Shabala, S., Gilliham, M., Pogson, B., and Tyerman, S. D. (2017). Chloroplast function and ion regulation in plants growing on saline soils: Lessons from halophytes. *J. Exp. Bot.* 68, 3129–3143. doi: 10.1093/jxb/erx142

Boursiac, Y., Chen, S., Luu, D. T., Sorieul, M., Van Den Dries, N., and Maurel, C. (2005). Early effects of salinity on water transport in arabidopsis roots. molecular and cellular features of aquaporin expression. *Plant Physiol.* 139, 790–805. doi: 10.1104/pp.105.065029

Bradford, M. M. (1976). A rapid and sensitive method for the quantitation of microgram quantities of protein utilizing the principle of protein-dye binding. *Analytical Biochem.* 72, 248–254. doi: 10.1016/0003-2697(76)90527-3

Cakmak, I., and Horst, W. (1991). Effect of aluminium on lipid peroxidation, superoxide dismutase, catalase, and peroxidase activities in root tips of soybean (Glycine max). *Physiologia Plantarum* 83, 463–468. doi: 10.1111/j.1399-3054.1991.tb00121.x

Chaudhary, M. T., Shakeel, A., Rana, I. A., and Azhar, M. T. (2020). Evaluation of morpho-physiological and biochemical attributes of cotton under salt stress. *Int. J. Agric. Biol.* 24, 1061–1069. doi: 10.17957/IJAB/15.1533

Cheeseman, J. M. (2013). The integration of activity in saline environments: Problems and perspectives. *Funct. Plant Biol.* 40, 759–774. doi: 10.1071/FP12285

Cui, R., Lu, X., Chen, X., Malik, W. A., Wang, D., Wang, J., et al. (2021). A novel raffinose biological pathway is observed by symbionts of cotton≡ verticillium dahliae to improve salt tolerance genetically on cotton. *J. Agron. Crop Sci.* 207, 956–969. doi: 10.1111/jac.12556

Davies, S. H., and Masten, S. J. (1991). Spectrophotometric method for ascorbic acid using dichlorophenolindophenol: Elimination of the interference due to iron. *Analytica Chimica Acta* 248(1), 225–227.

Falconer, D. S. (1996). *Introduction to quantitative genetics* (Harlow, Essex, UK: Pearson Education India).

Farooq, M. A., Shakeel, A., Atif, R. M., and Saleem, M. F. (2018). Genetic variability studies for salinity tolerance in gossypium hirsutum. *Int. J. Of Agric. And Biol.* 20, 2871–2878. doi: 10.17957/IJAB/15.0849

Farooq, M. A., Shakeel, A., Atif, R., and Saleem, M. (2019). Genotypic variations in salinity tolerance among BT cotton. *Pakistan J. Bot.* 51, 1945–1953. doi: 10.30848/PJB2019-6(9)

Farooq, M. A., Shakeel, A., Chattha, W. S., and Tahir, M. (2020). Two-year study on combining ability and heterotic potential in functional traits under salt stress in upland cotton (Gossypium hirsutum). *Plant Breed.* 139, 1221–1243. doi: 10.1111/pbr.12877

Fiaz, S., Wang, X., Younas, A., Alharthi, B., Riaz, A., and Ali, H. (2021). Apomixis and strategies to induce apomixis to preserve hybrid vigor for multiple generations. *GM Crops Food* 12, 57–70. doi: 10.1080/21645698.2020.1808423

Flowers, T. J., Munns, R., and Colmer, T. D. (2015). Sodium chloride toxicity and the cellular basis of salt tolerance in halophytes. *Ann. Bot.* 115, 419–431. doi: 10.1093/aob/mcu217

Haque, E., Taniguchi, H., Hassan, M. M., Bhowmik, P., Karim, M. R., Smiech, M., et al. (2018). Application of CRISPR/Cas9 genome editing technology for the improvement of crops cultivated in tropical climates: Recent progress, prospects, and challenges. *Front. Plant Sci.* 9, 617. doi: 10.3389/fpls.2018.00617

Hassan, A., Ijaz, M., Sattar, A., Sher, A., Rasheed, I., Saleem, M. Z., et al. (2020). Abiotic stress tolerance in cotton. *Adv. Cotton Res*, 25–37. doi: 10.5772/intechopen.89622

Hessini, K., Wasli, H., Al-Yasi, H. M., Ali, E. F., Issa, A. A., Hassan, F. A., et al. (2022). Graded moisture deficit effect on secondary metabolites, antioxidant, and inhibitory enzyme activities in leaf extracts of Rosa damascena mill. var. trigentipetala. *Horticulturae* 8, 177. doi: 10.3390/horticulturae8020177

Hummel, M., Edelmann, D., and Kopp-Schneider, A. (2017). Clustering of samples and variables with mixed-type data. *PLoS One* 12, e0188274. doi: 10.1371/journal.pone.0188274

Ibrahim, I., El Bagoury, M., and Abdel Gaber, S. (2021). An efficiency of standard procedures for moisture analysis tests used in the Egyptian cotton trade. *Egyptian Acad. J. Biol. Sci.* 12, 43–52. doi: 10.21608/eajbsh.2021.150754

Jaiswal, S., Singh, D. K., and Shukla, P. (2019). Gene editing and systems biology tools for pesticide bioremediation: A review. *Front. Microbiol.* 10, 87. doi: 10.3389/fmicb.2019.00087

Jans, Y., Von bloh, W., Schaphoff, S., and Müller, C. (2021). Global cotton production under climate change–implications for yield and water consumption. *J. Hydrology Earth System Sci.* 25, 2027–2044. doi: 10.5194/hess-25-2027-2021

Javot, H., Lauvergeat, V., Santoni, V., Martin-laurent, F., Guclu, J., Vinh, J., et al. (2003). Role of a single aquaporin isoform in root water uptake. *Plant Cell* 15, 509–522. doi: 10.1105/tpc.008888

Kamal, M., Saleem, M., Shahid, M., Awais, M., Khan, H., and Ahmed, K. (2017). Ascorbic acid triggered physiochemical transformations at different phenological stages of heat-stressed bt cotton. *J. Agron. Crop Sci.* 203, 323–331. doi: 10.1111/jac.12211

Khokhar, E. S., Shakeel, A., Maqbool, M. A., Anwar, M. W., Tanveer, Z., and Irfan, M. F. (2017). Genetic study of cotton (Gossypium hirsutum l.) genotypes for different agronomic, yield and quality traits. *Pakistan J. Agric. Res.* 30(4), 363–372. doi: 10.17582/journal.pjar/2017/30.4.363.372

Kirungu, J. N., Magwanga, R. O., Lu, P., Cai, X., Zhou, Z., Wang, X., et al. (2019). Functional characterization of Gh_A08G1120 (GH3. 5) gene reveal their significant role in enhancing drought and salt stress tolerance in cotton. *J. BMC Genet.* 20, 1–17. doi: 10.1186/s12863-019-0756-6

Li, G., Santoni, V., and Maurel, C. (2014). Plant aquaporins: Roles in plant physiology. *Biochim. Biophys. Acta* 1840, 1574–1582. doi: 10.1016/j.bbagen.2013.11.004

Liu, R. N., Jiao, T. Q., Li, J., Wang, A. Y., Li, Y. X., Wu, S. J, et al. (2021). Drought-induced increase in catalase activity improves cotton yield when grown under water-limiting field conditions. *J. Agron. Crop Science* 208(6), 853–867. doi: 10.1111/jac.12533

Liu, H., Weisman, D., Ye, Y.-B., Cui, B., Huang, Y.-H., Colón-Carmona, A., et al. (2009). An oxidative stress response to polycyclic aromatic hydrocarbon exposure is rapid and complex in arabidopsis thaliana. *Plant Sci.* 176, 375–382. doi: 10.1016/j.plantsci.2008.12.002

Mammadov, J., Buyyarapu, R., Guttikonda, S. K., Parliament, K., Abdurakhmonov, I. Y., and Kumpatla, S. P. (2018). Wild relatives of maize, rice, cotton, and soybean: Treasure troves for tolerance to biotic and abiotic stresses. *Front. Plant Sci.* 9, 886. doi: 10.3389/fpls.2018.00886

Miller, G., Suzuki, N., Ciftci-yilmaz, S., and Mittler, R. (2010). Reactive oxygen species homeostasis and signalling during drought and salinity stresses. *Plant Cell Environ.* 33, 453–467. doi: 10.1111/j.1365-3040.2009.02041.x

Munir, N., Hanif, M., Abideen, Z., Sohail, M., El-Keblawy, A., Radicetti, E., et al. (2022). Mechanisms and strategies of plant microbiome interactions to mitigate abiotic stresses. *Agronomy* 12, 2069. doi: 10.3390/agronomy12092069

Munns, R., and Tester, M. (2008). Mechanisms of salinity tolerance. *Annu. Rev. Plant Biol.* 59, 651–681. doi: 10.1146/annurev.arplant.59.032607.092911

Naz, R., Gul, F., Zahoor, S., Nosheen, A., Yasmin, H., Keyani, R., et al. (2022). Interactive effects of hydrogen sulphide and silicon enhance drought and heat tolerance by modulating hormones, antioxidant defence enzymes and redox status in barley (Hordeum vulgare l.). *Plant Bio* 24, 684–696. doi: 10.1111/plb.13374

Nix, A., Paull, C., and Colgrave, M. (2017). Flavonoid profile of the cotton plant, gossypium hirsutum: A review. *Plants (Basel)* 6, 43. doi: 10.3390/plants6040043

Peng, Z., He, S., Gong, W., Sun, J., Pan, Z., Xu, F., et al. (2014). Comprehensive analysis of differentially expressed genes and transcriptional regulation induced by salt stress in two contrasting cotton genotypes. *BMC Genomics* 15, 760. doi: 10.1186/1471-2164-15-760

Postaire, O., Tournaire-Roux, C., Grondin, A., Boursiac, Y., Morillon, R., Schäffner, A. R., et al. (2010). A PIP1 aquaporin contributes to hydrostatic pressure-induced water transport in both the root and rosette of arabidopsis. *J. Plant Physiol.* 152, 1418–1430. doi: 10.1104/pp.109.145326

Racine, J. S. (2012). *RStudio: a platform-independent IDE for r and sweave* (Hamilton Ontario, Canada: JSTOR).

Sabagh, A. E., Hossain, A., Islam, M. S., Barutcular, C., Ratnasekera, D., Gormus, O., et al. (2020). Drought and heat stress in cotton (Gossypium hirsutum l.): Consequences and their possible mitigation strategies. *J. Agronomic Crops* 3, 613–634. doi: 10.1007/978-981-15-0025-1_30

Saleem, M. A., Malik, W., Qayyum, A., Ul-Allah, S., Ahmad, M. Q., Afzal, H., et al. (2021). Impact of heat stress responsive factors on growth and physiology of cotton (Gossypium hirsutum l.). *Mol. Biol. Rep.* 48, 1069–1079. doi: 10.1007/s11033-021-06217-z

Salimath, S. S., Romsdahl, T. B., Konda, A. R., Zhang, W., Cahoon, E. B., Dowd, M. K., et al. (2021). Production of tocotrienols in seeds of cotton (Gossypium hirsutum l.) enhances oxidative stability and offers nutraceutical potential. *Plant Biotechnol. J.* 19 (6), 1268–1282. doi: 10.1111/pbi.13557

Sanchez, D. H., Siahpoosh, M. R., Roessner, U., Udvardi, M., and Kopka, J. (2008). Plant metabolomics reveals conserved and divergent metabolic responses to salinity. *Physiol. Plant* 132, 209–219.

Sarwar, M., Saleem, M., Najeeb, U., Shakeel, A., Ali, S., and Bilal, M. (2017). Hydrogen peroxide reduces heat-induced yield losses in cotton (G ossypium hirsutum

l.) by protecting cellular membrane damage. *J. Agron. Crop Sci.* 203, 429–441. doi: 10.1111/jac.12203

Sharma, P., Jha, A. B., and Dubey, R. S. (2019). "Oxidative stress and antioxidative defense system in plants growing under abiotic stresses," in *Handbook of plant and crop stress, 4th ed.* (London, England: CRC press).

Silveira, J. A. G., Araújo, S. A. M., Lima, J. P. M. S., and Viégas, R. A. (2009). Roots and leaves display contrasting osmotic adjustment mechanisms in response to NaCl-salinity in atriplex nummularia. *J. Environ. Exp. Bot.* 66, 1–8. doi: 10.1016/j.envexpbot.2008.12.015

Singh, K., Wijewardana, C., Gajanayake, B., Lokhande, S., Wallace, T., Jones, D., et al. (2018). Genotypic variability among cotton cultivars for heat and drought tolerance using reproductive and physiological traits. *J. Euphytica* 214, 1–22. doi: 10.1007/s10681-018-2135-1

Song, M., Fan, S., Pang, C., Wei, H., and Yu, S. (2014). Genetic analysis of the antioxidant enzymes, methane dicarboxylic aldehyde (MDA) and chlorophyll content in leaves of the short season cotton (Gossypium hirsutum l.). *J. Euphytica* 198, 153–162. doi: 10.1007/s10681-014-1100-x

Steel, R. G., Torrie, J. H., and Dickey, D. A. (1997). *Principles and procedures of statistics: A biological approach* (New York, USA: McGraw-Hill).

Ullah, A., Akbar, A., Luo, Q., Khan, A. H., Manghwar, H., Shaban, M., et al. (2019). Microbiome diversity in cotton rhizosphere under normal and drought conditions. *Microb. Ecol.* 77, 429–439. doi: 10.1007/s00248-018-1260-7

Ur Rahman, M. H., Ahmad, I., Ghaffar, A., Haider, G., Ahmad, A., Ahmad, B., et al. (2020). Climate resilient cotton production system: A case study in Pakistan. *J. Agronomic Crops* 447, 447–484. doi: 10.1007/978-981-15-1472-2_22

Velikova, V., Yordanov, I., and Edreva, A. J. P. S. (2000). Oxidative stress and some antioxidant systems in acid rain-treated bean plants: Protective role of exogenous polyamines. *J. Plant Sci.* 151, 59–66. doi: 10.1016/S0168-9452(99)00197-1

Wang, H., Chen, Y., Hu, W., Snider, J. L., and Zhou, Z. (2019). Short-term soil-waterlogging contributes to cotton cross tolerance to chronic elevated temperature by regulating ROS metabolism in the subtending leaf. *Plant Physiol. Biochem.* 139, 333–341. doi: 10.1016/j.plaphy.2019.03.038

Wang, N., Qiao, W., Liu, X., Shi, J., Xu, Q., Zhou, H., et al. (2017). Relative contribution of Na+/K+ homeostasis, photochemical efficiency and antioxidant defense system to differential salt tolerance in cotton (Gossypium hirsutum l.) cultivars. *Plant Physiol. Biochem.* 119, 121–131. doi: 10.1016/j.plaphy.2017.08.024

Wang, M., Wang, Q., and Zhang, B. (2013). Evaluation and selection of reliable reference genes for gene expression under abiotic stress in cotton (Gossypium hirsutum l.). *Gene* 530, 44–50. doi: 10.1016/j.gene.2013.07.084

Weatherly, P. (1950). Studies in the water relations of the cotton plant: I. the field measurement of water deficits in leaves. *J. New Phytol.* 49, 81–97. doi: 10.1111/j.1469-8137.1950.tb05146.x

Yavari, N. (2020). *An integrated approach to unravel the physiological and molecular basis of arabidopsis thaliana response to narrow-wavelength light* (Canada: McGill University).

Zafar, M. M., Jia, X., Shakeel, A., Sarfraz, Z., Manan, A., Imran, A., et al. (2022). Unraveling heat tolerance in upland cotton (Gossypium hirsutum l.) using univariate and multivariate analysis. *Front. Plant Sci.* 12, 727835. doi: 10.3389/fpls.2021.727835

Zafar, M. M., Razzaq, A., Farooq, M. A., Rehman, A., Firdous, H., Shakeel, A., et al. (2020). Genetic variation studies of ionic and within boll yield components in cotton (Gossypium hirsutum l.) under salt stress. *J. Natural Fibers* 19 (8), 1–20. doi: 10.1080/15440478.2020.1838996

Zhishen, J., Mengcheng, T., and Jianming, W. (1999). The determination of flavonoid contents in mulberry and their scavenging effects on superoxide radicals. *J. Food Chem.* 64, 555–559. doi: 10.1016/S0308-8146(98)00102-2

frontiers | Frontiers in Plant Science

TYPE Review
PUBLISHED 02 June 2023
DOI 10.3389/fpls.2023.1026063



OPEN ACCESS

EDITED BY
Mirza Hasanuzzaman,
Sher-e-Bangla Agricultural University, Bangladesh

REVIEWED BY
Ewa Joanna Hanus-Fajerska,
University of Agriculture in Krakow, Poland
Md Ahasanur Rahman,
National Cancer Institute at Frederick (NIH), United States

*CORRESPONDENCE
Zainul Abideen
Zuabideen@uok.edu.pk

RECEIVED 23 August 2022
ACCEPTED 20 March 2023
PUBLISHED 02 June 2023

CITATION
Abideen Z, Ansari R, Hasnain M, Flowers TJ, Koyro H-W, El-Keblawy A, Abouleish M and Khan MA (2023) Potential use of saline resources for biofuel production using halophytes and marine algae: prospects and pitfalls.
*Front. Plant Sci.* 14:1026063.
doi: 10.3389/fpls.2023.1026063



# Potential use of saline resources for biofuel production using halophytes and marine algae: prospects and pitfalls

Zainul Abideen[1]*, Raziuddin Ansari[1], Maria Hasnain[2], Timothy J. Flowers[3], Hans-Werner Koyro[4], Ali El-Keblawy[5], Mohamed Abouleish[6] and Muhammed Ajmal Khan[1]

[1]Dr. Muhammad Ajmal Khan Institute of Sustainable Halophyte Utilization, University of Karachi, Karachi, Pakistan, [2]Department of Biotechnology, Lahore College for Women University, Lahore, Pakistan, [3]Department of Evolution Behaviour and Environment, School of Life Sciences, University of Sussex, Brighton, United Kingdom, [4]Institute of Plant Ecology, Research Centre for Bio Systems, Land Use, and Nutrition (IFZ), Justus-Liebig-University Giessen, Giessen, Germany, [5]Department of Applied Biology, College of Sciences, University of Sharjah, Sharjah, United Arab Emirates, [6]Department of Biology, Chemistry and Environmental Sciences, College of Arts and Sciences, American University of Sharjah, Sharjah, United Arab Emirates

There exists a global challenge of feeding the growing human population of the world and supplying its energy needs without exhausting global resources. This challenge includes the competition for biomass between food and fuel production. The aim of this paper is to review to what extent the biomass of plants growing under hostile conditions and on marginal lands could ease that competition. Biomass from salt-tolerant algae and halophytes has shown potential for bioenergy production on salt-affected soils. Halophytes and algae could provide a bio-based source for lignoceelusic biomass and fatty acids or an alternative for edible biomass currently produced using fresh water and agricultural lands. The present paper provides an overview of the opportunities and challenges in the development of alternative fuels from halophytes and algae. Halophytes grown on marginal and degraded lands using saline water offer an additional material for commercial-scale biofuel production, especially bioethanol. At the same time, suitable strains of microalgae cultured under saline conditions can be a particularly good source of biodiesel, although the efficiency of their mass-scale biomass production is still a concern in relation to environmental protection. This review summaries the pitfalls and precautions for producing biomass in a way that limits environmental hazards and harms for coastal ecosystems. Some new algal and halophytic species with great potential as sources of bioenergy are highlighted.

KEYWORDS

**conservation, halophytes, microalgae, non-food biomass, salinity, sustainability**

**Abbreviations:** Mha, Million ha; GHG, Greenhouse gas; PBR, Photo bioreactor; LEDs, Light emitting diodes; MUFAs, Multi-unsaturated fatty acids; PUFA, Poly unsaturated fatty acids; HABs, Harmful algal blooms; EPS, Extracellular polymeric substances; LCA, Life cycle analysis; LCC, Life cycle costing.

10.3389/fpls.2023.1026063

# 1 Introduction

There is a growing demand to feed the expanding human population and to supply its energy needs without exhausting the biological and physical resources of the planet. Besides food security, clean and renewable energy is also central to achieving at least 20% of the world's total energy use with renewable resources by 2020, and 32% by 2030. Field crops like sugarcane, corn, soybean and some cereals have so far been the major source of biofuel production, but their use is in direct conflict with their use as food crops (Wang et al., 2020b). Bioenergy production from unconventional non-edible resources offers significant potential as an alternative, but is not without consequences that need careful consideration from a range of environmental, social and economic perspectives (Hasnain et al., 2021). The consequences of bioenergy production depend on biomass conversion technology, types of lands used for annual crops, forest, grassland, or marginal land, the location and level of production, and how these factors integrate with or displace existing land use (Abideen et al., 2015b). This review is based mostly, but not exclusively, on a global scenario of climatic change, and the advantages and pitfalls of using algae and halophytes as non-food bioenergy crops with potential as sustainable bioenergy resources (Figure 1)

## 1.1 Sustainable alternative bioenergy technologies: advantages and disadvantages

The global population is expected to exceed nine billion by 2050, with the current demographic trends requiring an average annual increase of 44 million tons of food production (Bologna and Aquino, 2020). Achieving this goal is challenging because of the increasing threat of soil salinization and desertification, which are reducing the amount of arable land and crop yields. It is worth mentioning that nearly 98% of earth's water is saline (Li et al., 2020b), ~7-10% of the land surface is estimated as salt-affected (Zhang et al., 2020), and although the scourge of soil salinization is spreading worldwide, the situation is worse in arid and semiarid regions (Edrisi et al., 2020). For instance, India has 7 million ha (Mha) of saline lands, Bangladesh 1 Mha, Pakistan 3-6 Mha, and Australia 2 Mha (Rogers et al., 2020). The current estimate of 3 ha of arable land becoming infertile due to secondary salinization every minute indicates the gravity of the situation and a cause of concern requiring remedial steps (Farooqi et al., 2021). The acuteness of this problem is compounded by changes to the global climate that are expected to increase the frequency and severity of temperature extremes, drought in some places, and floods in other regions (Sharif et al., 2021), with adverse effects on crop production.

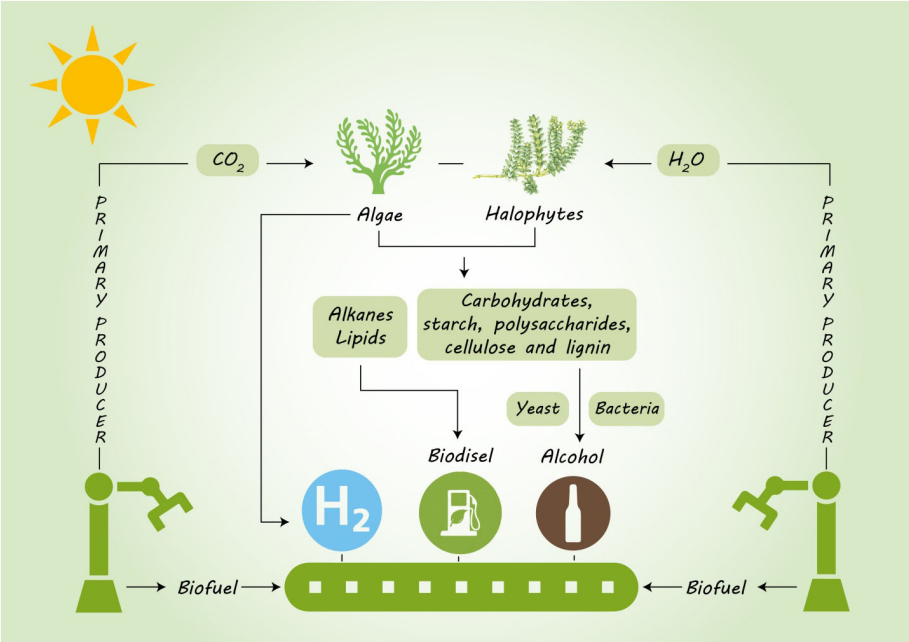


FIGURE 1
Potential of algae and halophytes as a sustainable biofuel feedstock by using saline land and brackish water.

Energy from fossil fuels is important in sustaining human life on earth, but the long-term availability of coal, oil, and natural gas is uncertain and projected to last only until the middle of the next century (Meyer et al., 2017). In order to search for alternative fuels, numerous feedstocks have been identified. Plant-biomass-based feed stocks are consequently gaining momentum with different potential candidates; e.g. edible (first generation), non-edible (second generation) and various saline-irrigated (third generation) feedstocks (Abideen et al., 2014a). Plant-based first-generation biofuel feedstocks such as sugarcane, wheat, corn, rapeseed and soybean have been used extensively for this purpose, but their use faces opposition due to impacts on the human food chain, while second generation crops such as *Miscanthus* and *Jatropha* require land and water that are needed for food crops (Munir et al., 2021). Production of biofuels from biomass of plants that can grow in saline habitats has consequently emerged as an environmentally-friendly, practical and economical alternative (Abideen et al., 2012). Growth rates of halophytes produce similar yield with saline irrigation compared to conventional crops. For instance, using seawater irrigation of plants of *Salicornia bigelovii* yielded 10 to 20 ton/ha of biomass, equivalent to the yield from conventional crops (Christiansen et al., 2021).

Using salt-tolerant species offers an economic opportunity, as well as a possible mechanism to reduce greenhouse gas (GHG) emissions and enhance energy security without encroaching upon resources (arable land, fresh water) needed for crops for human consumption (Abideen et al., 2015b). Increasing the list of environmentally sustainable sources of biofuel by using feedstocks is a proactive soil-security concept necessary for offsetting land degradation and desertification. Similarly, use of algal biomass can enhance the biological and physical resources of the planet, increase the supply of non-crop biomass to produce clean and renewable energy (such as a feedstock for biodiesel) and help to secure food security by reducing the competition on field grown biomass. Algae are largely non-food resources which do not necessarily need arable land and good quality water as many algal strains grow in seawater (Abideen et al., 2020). In addition, algal production offers remarkably high growth rates leading, for example, to a generation of up to 15 times more oil production per ha than palm, rapeseed or *Jatropha*.

Halophytes and algae are alternative resources for biomass and could be used to reduce the food *via* fuel dilemma. While the practicalities of large-scale production are still questionable, solutions may even open the way for a win-win situation by reducing the problems of insufficient bioenergy supply, excessive greenhouse gas (GHG) emission and uncontrolled desertification. The question remains whether biofuel production fed by halophytes and algae can be maintained with long-term stability. This review focuses on the advantages and disadvantages of biofuel production from algae and halophytes. The review highlights the major advancements achieved through biofuel processing technology to enhance bioenergy production. Technical insights that help to maintain optimal operating parameters for successful operation of biofuel processing from algae and halophytes are summarized. The technology must overcome a number of hurdles before it can compete in the fuel market and be broadly deployed. These challenges include strain identification and improvement, both in terms of oil productivity and crop protection, nutrient and resource allocation and use and production of co-products to improve the economics of the entire system. As far as we are aware, there are no studies on a comparison of algae and halophytes as sustainable sources of energy. The mass-scale cultivation of these potential resources for bioenergy production can help to revolutionized world energy production while avoiding competition in land use for food production. In view of the current situation with the energy-water-food nexus and use of plants for bioenergy, the use of new non-food resources, such as halophytes and algae, requires evaluation. Halophytes and algal species are salt-tolerant organism that can prosper in sea or brackish waters and are feedstocks for fuel and food (fuel-food feedstocks) in developing countries. The suitability of these feedstocks is reviewed and recommendations and solution for their cultivation in saline agriculture highlighted. The aim of this article is to incentivize efficient saline agricultural biomass production. We elucidate the major challenges to the economic production of algal and halophytic biofuels at scale, and provide a focus for the scientific community to address the challenges of moving these feedstocks from promise to reality.

## 2 Algal biomass as biofuel feedstock

Algae, ranging from small, single-celled microalgae to multi-cellular macroalgae, occupy a variety of habitats from damp places to bodies of fresh or sea water [36-38] and present a wide range of species that could be cultivated. High oil content; in some cases almost 80% of cell weight, together with the high growth rates with biomass doubling in periods as short as 3.5 h have generated interest in using algae as biofuel feedstock (Jazie et al., 2020). Oil production from algae can exceed that from the oilseed crops such as rapeseed, canola (Petrie et al., 2020), *Jatropha* (Kumar et al., 2017) and karanja (*Pongamia pinnata*) (Tıpırdamaz et al., 2020). Growing algae on a large scale has the benefit of removing greenhouse gases by consuming $CO_2$ for photosynthesis during growth (Gharbia et al., 2019). By utilizing their high photosynthetic ability, algae appear an attractive energy feedstock among renewable resources, for rapid generation of carbohydrates and lipids. There are, in addition, other possible benefits such as use for human food (albeit on a limited scale) or as a source of byproducts of commercial interest (Roostaei et al., 2018). Like other plants, growing algae requires optimizing water, nutrients, light, temperature and pH (Hasnain et al., 2023). The following issues require consideration and further research.

### 2.1 Culturing space

Availability of suitable land is the primary limiting factor for bioenergy development from algal feedstock The largest micro-algal commercial production unit covers 750 ha using an open pond system, but even this facility is insufficient to meet local biofuel demands (Randhir et al., 2020). Although, open ponds are easier to

build and operate than closed systems, a large quantity of water is evaporated. Other constraints that limit algal production are: low light penetration, poor carbon dioxide diffusion from the atmosphere, inefficient stirring causing poor mass transfer, and contamination by microbes and other algal species (Talaei et al., 2020). Proper mixing systems are required if sedimentation is to be avoided and light utilization maximized (Fong-Lee et al., 2020). Closed systems such as photo bioreactors are used to overcome problems of open pond cultivation systems. A photo bioreactor (PBR) is a closed vessel and energy is supplied through electric lights (Zhao et al., 2021). PBRs are classified as flat plate, tubular or columnar on the basis of their illuminated surface and stirred, bubble-column or airlift depending on how mixing is achieved (Sero et al., 2020). So, a PBR should have a highly transparent surface, good uniform illumination, low mutual shading, quick mass transfer of carbon dioxide and oxygen and should attain high growth (Amaral et al., 2020).

## 2.2 Photobioreactor (PBR) design improvements (Data collection and modeling)

Experimental evaluation and consecutive model development are used to predict the behavior of actual and expected algal growth at different culturing conditions, which can be optimized *in situ* (Sheehan et al., 2020).

## 2.3 Light utilization and mixing of algal culture

As light is the source of energy, it needs optimization for biomass productivity (Munir et al., 2022). High productivity of algal culture requires annual average sunshine of 2,500-5,000 lux (its intensity, spectral quality and photoperiod), and temperatures in the range of 18-24°C. Flat plate PBRs are more efficient in utilizing sunlight than other PBRs because of their flat surface area. Light utilization can be optimized using panels of tubes and supplementary light from light emitting diodes (LEDs) using fiber optics (Alzahrani et al., 2020). About 1.5% photosynthetic efficiency has been achieved using the open pond method with 21 ton/ha algal productivity, while with tubular PBRs photosynthetic efficiency was 3% yielding 41 ton/ha algal biomass (Clements et al., 2020). The highest photosynthetic efficiency achieved with flat panel PBRs has been 5% with 64 ton/ha algal productivity (Negi et al., 2020). For naturally illuminated PBRs, the orientation with respect to the sun is highly critical if photosynthetic efficiency is to be maximized. To gain maximum light; at latitudes, above 35° N, an orientation of east/west is preferable over north/south for optimal algal productivity (Sivakaminathan et al., 2020). The effects of self-shading in PBRs are reduced by using thinner algal cultures. Circulation is an important step to maintain proper mixing of algal cells in suspension, remove thermal stratification, optimize the distribution of nutrients, boost gas-liquid mass transfer, and stop oxygen accumulation (El Shenawy et al., 2020). Moving algal cells between the illuminated surfaces and dark regions to induce periodic light/dark cycles, is also very important for maximum growth (Alami et al., 2021). By using circulatory apparatus, with cultures of *Spirulina platensis*, 0.5 g/L/day algal cell productivity was obtained, which was assumed to be a high value by the researchers (Serrà et al., 2020).

Algae are an attractive energy source but important questions still exist about the sustainability of this technology on a large scale. Two particularly important questions concern the method of cultivation and the type of alga to be used. Resurreccion et al. (2012) combined elements of life cycle analysis (LCA) and life cycle costing (LCC) to evaluate open pond systems (OPs) and horizontal tubular photobioreactors for the cultivation of freshwater or brackish-to-saline water algae. According to the LCC, all four systems are currently financially unattractive investments, though OPs are less so than PBRs (Sun et al., 2019). Salt-tolerant species deliver better energy and GHG performance and higher profitability than fresh water species in both OPs and PBRs. Sensitivity analyses suggest that improvements in critical cultivation parameters ($CO_2$ utilization efficiency or algae lipid content), conversion parameters (anaerobic digestion efficiency) and market factors (costs of CO2, electricity, and sale prices for algae biodiesel) could alter these results (Muhammad et al., 2021).

## 2.4 Algal production cost

The overall production cost of algae depends on the selection of algal strain, type of PBR and of biomass production technology; a major cost is that of construction if the installation is large (Ma et al., 2017). The cost of production can be reduced by using flue gases instead of $CO_2$, which is very expensive, and using wastewater instead of adding minerals or nutrients to growth media (Roostaei et al., 2018). More than 150 ton/ha/year algal biomass can be produced with low labor costs, using flue gases as carbon source and wastewater as growth medium (Norsker et al., 2011). By using flat panel tubular PBRs, the production cost can be reduced to €0.70/kg or €0.68/kg as compared to open pounds where the cost cannot be reduced below €1.28/kg (Negi et al., 2020; Oostlander et al., 2020). Using arable land and good quality irrigation water is not advisable, but salt-affected/marginal land, including deserts, together with saline/waste water may be used subject to the availability of suitable strains of algae (Amiri and Ahmadi, 2020).

## 2.5 Growth conditions

Biofuel production depends upon optimizing growth conditions for any species. Good growth in open ponds can be achieved but, generally, not over a whole year, because of short days, low light intensity and temperature during winter, the more so in cold regions (Jacob et al., 2020). However, higher oil production under stressed than optimal conditions has been reported by some researchers (Juneja and Murthy, 2017; Bélanger-Lépine et al., 2018; Tan et al., 2020), but needs assessment. With photo-bioreactors, it is important that mixing is optimized so that algal

cells are transferred between light and dark phases; this has allowed the successful use of very high light intensities (Severes et al., 2017). During photosynthesis, photons are used to synthesize biochemical components in the algae and in different light conditions, a change in photon flux can bring about a noteworthy change in the biochemical compositions of algal cells (Naira et al., 2020). A higher intensity or length of light energy triggers the accumulation of storage lipids (MUFAs) used in biodiesel production, while a lower intensity stimulates the accumulation of structural lipids (PUFA) (Brindhadevi et al., 2021). Carbohydrate content was enhanced from 16.3 to 22.4% in *Scenedesmus obliquus* by the exposure to high light intensity (Ho et al., 2017). Physicochemical properties of algae also change with increasing or decreasing temperature. Table 1 shows the effect of different light intensities and temperature on lipid content and fatty acid profile.

## 2.6 pH effects

Physiological and biochemical functions for optimal growth of most algal species require maintenance of neutral pH in the growth medium (Correa et al., 2020). The relationship between $CO_2$ concentration and pH in algal growing system is complex (Alzahrani et al., 2020). Increasing internal $CO_2$ concentration can lead to higher photosynthetic efficiency but it can also decrease pH; these two factors and their antagonism can alter algal physiology and biomass production. An increase in pH of

TABLE 1 The impact of variable light intensities, change of temperature and pH on lipid accumulation and fatty acid profiles on the basis of % dry weight.

| Algae | Light intensities | Algae response | References |
|---|---|---|---|
| *Chlorella vulgaris* | 2700 lx | lipid 19% | (Azizi et al., 2020) |
| | 3300 lx | lipid 13% | |
| *Chlorella vulgaris* | 24 h photoperiod | Lipid production increased | |
| *Pavlova lutheri* | High light intensities | Lipid production increased | |
| *Isochrysis galbana, Nannochloropsis oculata* | High light intensities | Lipid production increased | |
| *Scenedesmus* sp. | 250–400 μmolm$^2$ s −1 | Lipid production increased | |
| *Isochrysis galbana* | Shorter light/dark regime | PUFA's increased | |
| *Selenastrum capricornutum* | Dark treatment | Increase in 18:3 and decrease in 18:1 | |
| Algae | Temperature (°C) | Response | References |
| *Nannochloropsis oculata* | Shift – 20 to 25 | 15% increase in total lipid | (Wei et al., 2015) |
| *Chaetoceros* sp. | 25 | 16.8% increase in total lipid | |
| *Ochromonas danica* | 15 to 30 | Increase in total lipids | |
| *Nannochloropsis oculata* | > 30 | Polar lipid increased | |
| *Nitzschia laevis* | 15 to 23 | TAG increased | (Touliabah et al., 2020) |
| *Dunaliella salina* | 30 to 12 | UFA's increased | |
| *Synechococcus Lividus* | 55 to 38 | 16:1 and 18:1 increased | |
| *Selenastrum capricornutum* | 25 to 10 | C 18:1 increased | |
| Algae | Optimal pH | Response | References |
| *Chlorella* sp. | 8 | Lipid content 23% | (Qiu et al., 2017) |
| *C. vulgaris* | 7.5 | 53.43 | |
| *Chlorella protothecoides* | 6.5 | 3.75 g/l lipid yield | |
| *Pavlova lutheri* | 8.0 | 35% lipid content | |
| *Nannochloropsis salina* | 8.0–9.0 | 21.8 | |
| *T. suecica* | 9.0 | lipid content increased | |
| *Chlorella vulgaris* | 7.0, 8.0, 9.0, and 10.0. | No change | (Nouri et al., 2021) |
| | 6.0, 7.0, 9.0 | No change | |
| *Chroococcus minor* | 9.0 | 22 | |
| *B. braunii* | 6.5 | 2.2 gm$^{-2}$/d lipid productivity | |

growing media can be favorable for inactivation of harmful pathogens in open-type growth chambers, but can also inhibit growth (Almutairi and Toulibah, 2017). Growth medium pH above 9 generally creates difficulty for the utilization of $HCO_3^-$ and $CO_3^{2}$ for maintaining internal $CO_2$ although there are some resistant species that can survive at pH above 9, but at the cost of metabolic disturbances and compromises in productivity (Alami et al., 2021). In addition to low capacity to absorb internal $CO_2$, elevated pH interferes with the cell's ability to maintain activity of carboxylation *via* Rubisco, which reduces photosynthetic rate (Li et al., 2020a).

High pH may convert ammonium ions to free ammonia which in quantities such as 34 and 51 $gm^3$ (at pH 9.5 and 20-25 C) inhibited the rate of photosynthesis in three micro-algal cultures by 50 and 90%, respectively (Galès et al., 2020). The presence of ammonia also creates problems in sunshine, especially during summer when light intensities may raise pH of the growing medium and ultimately inhibit photosynthesis. Elevated pH can also alter membrane transport processes, metabolic function and uptake of trace metals consequently affecting photosynthesis and growth of algae (Miyauchi et al., 2020). Under elevated pH, flocculation of some microalgal cultures can occur, negatively impacting light absorption, photosynthesis and nutrient uptake. If wastewater is being used for algal culture, pH above 8.3 has been reported to inhibit growth of aerobic bacteria: high pH tolerating algal strains can be used in high pH waste water for cultivation (Vadlamani et al., 2017).

### 2.6.1 Water availability

The production of algal biomass, either in closed photo-bioreactors or open ponds, and its conversion to biofuels, consumes a considerable amount of water (Vu et al., 2020). The availability of fresh water is limited especially in areas where productivity of algae is potentially high - i.e. regions with high year-round solar radiation (Mayer et al., 2020). Algal growth and subsequent processing likely cause substantial water pollution (Rahman et al., 2020). High-value food crops have preference for cultivation with fresh water in arable lands, necessitating exploring the potential of biofuel feedstock from those species that can grow optimally and complete their life cycle in marginal/saline lands irrigated with low quality/brackish water (Fork et al., 2020). Table 2 shows the salt tolerance of algal strains.

Biological desalination is an innovative technology in which salts are absorbed by salt-tolerant organisms. For example, *Scenedesmus obliquus* is a fresh-water alga with a high tolerance of salts and the capacity to remove NaCl from (0.18- 1.4 g/L) when salinity increased from 2.8- 8.8 g/L (El-Katony and El-Adl, 2020). Salinity also enhances hydrocarbon content in algae: *S. obliquus* treated with 8.8 g/L NaCl increased its lipid content (21%) while removing 2.5 g/L NaCl and achieving the highest desalination rate (30%) within 30 min contact time (Wei et al., 2020). The rate of evaporation is another limiting factor in any open pond system and one that will increase when days are long and intensity of light is high in hot regions. The lost volume of water should be made up with fresh water but this might burden supply of this commodity if scarce (Prudkin-Silva et al., 2021). If fresh water is not added, the salinity of the medium may consequently rise to a level too high for growth of even highly salt-resistant strains. A solution may be found in frequent renewal of evaporated water which could, however, pose other problems, as any discharged saline water may still have unused nutrients (Khuram et al., 2019) such as phosphorus and nitrogen creating a disposal challenge downstream, a potential additional cost and raising questions about environmental sustainability. Use of wastewater as a source of water has been advocated to attain a double benefit of biofuel production as well wastewater treatment (Juneja and Murthy, 2017).

## 2.7 Nutrient requirements

The elemental composition of algae with empirical formula $CH_{1.7}O_{0.4}N_{0.15}P_{0.0094}$ will generally fluctuate with environmental conditions and nutrient status of the strains and growth medium.

TABLE 2 Salinity and heat resistance and their interactive effect on growth responses of algae strains.

| Algae species | Salinity levels | Temperature °C | Growth rates | References |
|---|---|---|---|---|
| *Dunaliella tertiolecta* | 33 to 59 g/L | 23 | 1.9696 g/L | (Morales-Sánchez et al., 2020) |
| *Chaetoceros calcitrans* | 3% | 30 | 0.28 µl/d | |
| *Chlorella* sp. | 2.5% | 25 | 0.37 µl/d | (Gour et al., 2020) |
| *Fucus vesiculosus.* | 5 psu | 4-10 | 0.007 g/g.d | (Zamani-Ahmadmahmoodi et al., 2020) |
| | 35 psu | 15–20 | 0.024 g/g.d | |
| *Nannochloropsis oculata* | 15–55 g/L | 26 | 0.078-0.282/d | |
| *Desmodesmus* sp. | 15 g/L | 25 | 5.35 g/L | (Chen et al., 2020) |
| *Ulva prolifera* | 14–32 | 5–32 | 10.6–16.7%/d | (Bews et al., 2021) |
| *Hypnea cervicornis* | 25 | 20–25 | 5.37%/d | (Vo et al., 2020) |
| *Shewanella* sp. | 0–7% | 30 | 0.04 to 0.36 g/L | |
| *Chaetomorpha* sp. | 3.4–90.0 | 20.1–40.9 | 60%/d | |

The essential nutrients (N, P, and in some cases Si) should be provided in adequate amounts for optimal growth (Tan et al., 2020). Approximately 50-80 kg of nitrogen and 5 kg of phosphorus are required to produce one ton of algal biomass. Commercial production of algal biofuels would hence need large quantities of these elements and maybe of other nutrients. For instance, if saline ground water is used, the medium may also require potassium. Algal biomass production under the circumstances can hence be competing with the edible plants for nutrient requirements (El-Katony and El-Adl, 2020). Moreover, production of fertilizers needed for algal growth is at an environmental cost due to use of energy and emission of considerable amounts of the greenhouse gases carbon dioxide, nitrous oxide and methane (Yuasa et al., 2020). It has been reported that ~45% energy input in algal culture is in the form of nitrogenous fertilizer; each kg of this fertilizer produced from natural gas, which is also depleting, generates about 2 kg of $CO_2$.

Phosphorus is not a renewable resource and, at current rates of mining, global phosphate rock reserves are likely to be finished in 50-100 years (Dubey and Dutta, 2020). Taking into consideration the nutrient requirements, which may vary with species, a study found that meeting the demand of algal bioenergy to substitute 5% of the fuel used annually for transportation in the United States would require 44-107% of the total nitrogen and 20-51% of the total phosphorus requirement of the country. In the natural ecosystem, the phosphorus and nitrogen requirements are met to a great extent by dead bodies of animals but in artificial systems these have to be supplemented at a cost to the purchaser. Wastewater can be used as a source of nutrients to attain a double benefit of biofuel production as well as wastewater treatment and pollutant removal (Juneja and Murthy, 2017). *Acutodesmus obliquus* culture consumed 175 mg/g/day nitrogen and 1.5 mg/g/d phosphorus from swine wastewater having 5.2% salinity with 1923 mg/L/d chemical oxygen demand (El-Katony and El-Adl, 2020). At 11 ppt of salinity *Picochlorum atomus* nutrient uptake was four times higher than controls, 34 mg/L/d uptake of nitrogen and 1.3–2.4 mg/L/day uptake of phosphate (Zhang et al., 2018). At 3.2% salinity, *Spirulina platensis* removed 80% nitrogen, 93% phosphate and 90% COD with 15.69, 1.03, and 90.24 mg/L effluent concentration respectively (Koech et al., 2020).

### 2.7.1 Improved growth capacity through increased photosynthetic efficiency

The production of any biofuel is dependent on the efficiency of the metabolic pathways that lead to accumulation of storage compounds, such as lipids and starch, as well as on the ability to produce large amounts of biomass rapidly. Experiments with small- and large-scale microalgal photobioreactors and molecular research in photosynthetic efficiency have revealed several factors that can limit biomass accumulation. One important consideration is the intensity of light at which a given strain of microalga reaches its maximum growth rate, which corresponds to the maximum photosynthetic efficiency and is usually around 200 to 400 μmol photons $m^{-2}$ $s^{-1}$ for most species (Lee et al., 2002). Light intensities above the maximum photosynthetic efficiency actually reduce the growth rate, a phenomenon known as photoinhibition. Photosynthetically active radiation intensities from sunlight can exceed 2,000 μmol photons $m^{-2}$ $s^{-1}$ during midday. Consequently, most microalgae will not grow at maximum efficiency during most of the day.

Microalgae are considered great model organisms to study photosynthetic efficiency, and several attempts have been made to improve the photosynthetic efficiency and/or reduce the effects of photoinhibition on microalgal growth (Melis, 2009). Much of this work has been focused on reducing the size of the chlorophyll antenna or lowering the number of light-harvesting complexes to minimize the absorption of sunlight by individual chloroplasts. This approach may seem counterintuitive, but this strategy may have two positive effects; first, it permits higher light penetration in high-density cultures and second, it can allow a higher maximum rate of photosynthesis due to the fact that the cells are less likely to be subjected to photoinhibition since their light-harvesting complexes absorb less light (Priyadharsini et al., 2022). Earlier, research relied on random mutagenesis strategies to generate mutants with fewer or smaller chlorophyll antennae, but a recent publication used an RNAi-based strategy to knock down efficiently both LHCI and LHCII in *C. reinhardtii* (Mussgnug et al., 2007). This strategy can most likely be applied to many different microalgae more easily than a random mutagenesis approach. It seems clear that manipulation of light-harvesting complexes can lead to increased biomass productivity under high light in controlled laboratory conditions. However, it remains to be seen how well these mutants will perform in larger-scale cultures with more varied conditions and perhaps with competition from wild invasive microalgal species. In one study of algal antenna mutants, no improvement in productivity was observed with outdoor ponds (Mussgnug et al., 2007). However, they also did not observe any improved productivity in laboratory cultures. With more research, it should become clear whether the current approach can be successfully applied to increase biomass production.

## 2.8 Pollution of land and aquatic system

Production of wastewater derived from many anthropogenic activities such as industry, agriculture and domestic use is a major environmental issue and a threat to water security. About half of the global waterbodies such as the lakes, rivers and seas have been contaminated by domestic and industrial wastewaters; it is essential to treat and remediate wastewater so that it could be recycled and reused (Aron et al., 2021). Discharge of residual nutrients from algal cultures could have a negative impact on land and aquatic systems and the natural flora of an area. Ecological consequences that can occur includes decrease in biodiversity, changes in species richness and altered fitness of other living organisms. Toxic discharge and accumulation may create problems for plant agriculture and restoration can be a costly long-term process, depending upon the extent of damage due to effluents (Liu et al., 2017). Introducing production of suitable algal strains that would scavenge harmful excess nutrients could, however, help in reversing the damage. For instance, algal turf scrubber (filtering device) can capture 70-100% of phosphorus runoff and 60-90% of nitrogen from manure

effluents (Aston et al., 2018). Wastewater from municipalities, agriculture and industry could provide cost-effective and sustainable support for the use of algae for biofuels (Tan et al., 2020) In addition, there is also potential for combining wastewater treatment, such as nutrient removal, with biofuel production. The following are three examples; at 35 g/L NaCl, *Potamocorbula laevis*, *A. nodosum* and *F. vesiculosus* accumulated copper from growing medium (Vo et al., 2020); in saline wastewater (2.6% salinity), by bio-assimilation and adsorption *Chlorella* sp. removed 99% of amoxicillin; and under 171 mM NaCl, *S. obliquus* biodegraded 93.4% of levofloxacin (Leng et al., 2020).

### 2.8.1 Environmental aspect of microalgae cultivation

Microalgae introduced into new environments also have the potential to become invasive species. There are an estimated 1–10 million algal species on earth, with the majority being microalgae (ElFar et al., 2022). Microalgae that are native or introduced to an area and become invasive are often referred to as harmful algal blooms (HABs). HABs are species of phytoplankton that cause negative effects on human health (through the production of toxins), impact living marine sources (wild and cultivated fish), impact tourism and recreation of coastal waters (through 'red tides') and damage marine ecosystems by creating anoxic areas that kill marine life (Anton et al., 2019). There are approximately 80 toxic and 200 noxious microalgal species involved in HABs out of a total of 4000 described marine planktonic microalgae (Table 3). Research indicates that the rise in HABs shows the signs of a global epidemic (Zedler and Kercher, 2004). Whether this recognition is the result of an increase of scientific awareness of toxic algal species, utilization of coastal waters for aquaculture, cultural eutrophication of waters, unusual climatalogical conditions or the transport of dinoflagellates by ships ballast water or shellfish stock is unclear. The invasion patterns of microalgae are dependent on human vectors and subsequent adaptation of the algae to their new environment (Gressel et al., 2013). Anthropogenic nutrient enrichment of coastal areas has also been linked to HAB events around the world. Microalgal genera or species proposed for biofuel production that have had HAB incidents include *Amphora*, *Nitzschia*, *Pseudo-nitzschia* and *Prymnesium parvum*. It has been suggested that locating algal biofuel production plants close to seawater will remove the need for fresh water resources and increase their sustainability (Nyström, 2017). However there is little discussion on the ecological impacts resulting from an

TABLE 3 Organisms used for the removal of harmful algal blooms (HABs) from their populations.

| Predatory bacteria | Mode of action | Major host | References |
|---|---|---|---|
| ***Bacillus* sp.** | Cell-to-cell contact mechanism | *Aphanizomenon Flosaquae* | (Jeon et al., 2017) |
| ***Bacillus* sp.** | Production of extracellular product | *M. aeruginosa* | |
| ***Bacillus cereus*** | Secretion of cyanobacteriolytic | *Microcystis aeruginosa* | |
| ***Bacillus* sp.** | Secretion of algalytic substance | *Phaeocystis globosa* | |
| ***Brachybacterium*** | Produce secondary metabolites | *A. catenella* | |
| ***Cytophaga*** | Direct contact | *Microcystis aerugenosa* | |
| ***F. flexilisi, F. sancti*** | Inhibition of glycolate dehydrogenase Electron transport & nitrogenase activity | *Oscillatoria williamsii* | |
| ***Bdellovibrio*-like bacteria** | Varese Penetration | *Microcystis aeruginosa* | |
| ***M. fulvus*** | Entrapment | *Phormidium luridum* | |
| ***Pseudomonas fluorescens*** | Indirect attack by alga-lytic substances | *Heterosigma akashiwo* | |
| ***Halobacillus* sp.** | Bio-flocculation | *Microcystis aeruginosa* | |
| Zoonplankton | | | |
| ***Daphnia ambigua*** | Grazing | *Microcystis aeruginosa* | (Richards, 2019) |
| ***Daphnia hyaline*** | Grazing | *Chlorella* | |
| ***D. galeata*** | Grazing | *Scenedesmus* | |
| ***Cyclops* sp.** | | | |
| ***Eudiaptomus gracilis*** | Grazing | *Chlorella* | |
| ***Eudiaptomus gracilis*** | Grazing | *Microcystis aeruginosa* | |
| ***Cyclopoid copepods*** | Grazing | *Anabaena, Microcystis* and Planktothrix species | |

*(Continued)*

TABLE 3 Continued

| Predatory bacteria | Mode of action | Major host | References |
|---|---|---|---|
| Algae | | | |
| ***Ankistrodesmus falcatus*** | Bioflocculation | *Chlorella vulgaris* | (Jalgaonwala, 2020) |
| ***Scenedesmus obliquus*** | Bioflocculation | *Chlorella vulgaris* | |
| ***Tetraselmis suecica*** | Bioflocculation | *Neochloris oleoabundans* | |
| ***Poterioochromonas*** | Grazing | *Microcystis aeruginosa* | |
| Fungi | | | |
| ***Trichaptum abietinum*** | Direct attack | *Microcystis aeruginosa* & *Microcystis flosaquae* | (Sun et al., 2018) |
| ***Lopharia spadicea*** | Direct attack | *Microcystis aeruginosa* | |
| ***Irpex lacteus, Trametes hirsute Trametes versicolor &Bjerkandera adusta*** | Direct attack | *Microcystis aeruginosa* | |
| Cyanophage | | | |
| **SM-1** | Species-specific interaction | *M. aeruginosa* | (Xu et al., 2020a) |
| **SM-2** | Species-specific interaction | *M. aeruginosa* | |
| **Ma-LBP** | Species-specific interaction | *M. aeruginosa* | |
| ***Cyanostyloviridae*** | Species-specific interaction | *Lyngbya majuscule* | |
| **Ma-LMM01** | Species-specific interaction | *M. aeruginosa* | |
| **S-PM2** | Species-specific interaction | *Synechococcus* | |
| **MaMV-DC** | Species-specific interaction | *M. aeruginosa* | |
| **MaCV-L** | Species-specific interaction | *M. aeruginosa* | |
| **SAM-1** | Species-specific interaction | *Broader host range* | |
| ***Myoviridae*** | Species-specific interaction | *M. aeruginosa* | |
| ***Siphoviridae*** | Bursts and virus lytic cycle | *C. raciborskii* | |
| **Ma-LEP** | Mechanical stiffness | *M. aeruginosa* | |
| Fish | | | |
| ***Hypophthalmichthys molitrix*** | Grazing | *Microcystis aeruginosa* | (Gu et al., 2021) |
| ***Aristichthys nobilis*** | Grazing | *Microcystis aeruginosa* | |
| ***Hyriopsis cumingii*** | Ingestion and digestion | *Microcystis aeruginosa* | |
| ***Oreochromisni loticus*** | Ingestion and digestion | *Microcystis aeruginosa* | |

accidental introduction of a microalgal biofuel species into the surrounding environment. Table 4 shows the number of chemicals that are potentially toxic for water and human food materials. Documentation and more studies are required to protect wildlife from HABs, the effects of red tides and freshwater cyanobacterial blooms in the future (Müller et al., 2020). Reducing fertilizer use, improving animal waste control, and sewage treatment should also reduce the population of toxic algal blooms. Tables 5, 3 listed various methods to control harmful algal blooms from water water and other water resources.

## 2.9 Biomass to biofuel conversions

Algal cultures are very dilute in nature necessitating dewatering, to produce an algal cake that can be readily handled manually or mechanically for conversion to biofuel (Tables 6, 7 and Figure 2). However, dewatering is expensive if done by current methods, accounting for approximately 20-40% of the energy required (Tan et al., 2020). Currently, commercial dewatering methodologies include centrifugation, flocculation, coagulation, flotation and sedimentation. Other harvesting techniques such as

TABLE 4 Potential biotoxin producers and human health implications of algal biomass.

| Algae | Toxins | Human health implication | References |
|---|---|---|---|
| ***Alexandrium catenella*, *A. minutum complex*, *A. ostenfeldii*, *A. tamarense*** | Saxitoxins, gonyautoxins | PSP | (Pang et al., 2017) |
| ***Chattonella antiqua*, *C. marina*** | Breve-like | NSP | |
| ***Coolia monotis*** | Uncertain | Uncertain | |
| ***Dinophysis acuta*, *D. acuminata*** | Okadaic acid; dinophysis toxin 2 (DTX2); pectenotoxin 2 | DSP | |
| ***G. mikimotoi* complex** | Breve-like | NSP, respiratory distress | (Niu et al., 2021) |
| ***Gyrodinium galatheanum*** | Breve-like | NSP | |
| ***Heterosigma akashiwo*** | Ichthyotoxic | Ass. with peppery taste | |
| ***Ostreopsis siamensis*** | Uncertain | Uncertain | |
| ***Prorocentrum lima*** | Okadaic acid; DTX1,4; diol esters | DSP | |
| ***Protoceratium reticulatum*** | Yessotoxin | Uncertain | (Zingone et al., 2020) |
| ***Pseudo-nitzschia australis*, *P. delicatissima*, *P. fraudulenta*, *P. multiseries*, *P. pseudodelicatissima*, *P. pungens*, *P. turgidula*** | Domoic acid | ASP | |
| ***Fibrocapsa japonica*** | Ichthyotoxic | None | |

TABLE 5 Various methods to control harmful algal blooms from water resources.

| Methods | Techniques | Advantages | Limitations | References |
|---|---|---|---|---|
| **Chemical methods** | Metals (Fe, Cu, Ca & Al) | Low cost and High residence time | Toxicity against non-target species and Accumulation in the environment | (Li et al., 2020a) |
| | Photosensitizers (hydrogen peroxide, phthalocyanines and titanium dioxide) | Low cost and Degradability | Risky manipulation and Coloration | |
| | Herbicides (diuron, endothall, atrazine and simazine) | Low cost and High residence time | Release of toxins | |
| **Physical methods** | Ultrasound techniques | Low impact on ecosystems and Contamination free | To be confirmed at up-scaled levels | (Kong et al., 2019) |
| | UV irradiation | Eco-friendly and Contamination free | High energy consumption and To be confirmed at up-scaled levels | |
| | Membrane filtration technology | Well-established technology and High stability | High cost | |
| | Adsorption | Eco-friendly and Contamination free | Costly and To be confirmed at up-scaled levels | |
| **Biology methods** | Aquatic plants | Technically simple reactor | Affect biodiversity and Deteriorate eutrophication | (Zerrifi et al., 2018) |
| | Aquatic animals | User-friendly and Environmentally sound | It will not work in oxygen-poor conditions, Affect biodiversity and Poor efficiency | |
| **Combined technologies** | Microorganisms | High specificity and High efficiency | High cost and To be confirmed at up-scaled levels | (Park et al., 2019) |
| | Ultrasonic radiation and jet circulation to flushing | High efficiency | High cost and To be confirmed at up-scaled levels | |
| | Combination of uniform design with artificial neural network coupling genetic algorithm | High efficiency and Low cost | To be confirmed at up-scaled levels | |

TABLE 6 Potential of different biofuels feedstocks on the basis of their oil yield for sustainable energy production.

| Species | Oil (%) | References |
|---|---|---|
| Soybean | 20 | (Giuffrè et al., 2020) |
| Palm oil | 30 | |
| Coconut | 63 | (Suryani et al., 2020) |
| Rapeseed | 38 | (Konur, 2021) |
| Sunflower | 25 | (Subaşı et al., 2020) |
| Peanut oil | 45 | (Dun et al., 2019) |
| Olive oil | 45 | (Giuffrè et al., 2020) |
| Cottonseed | 18 | (Riaz et al., 2021) |
| Halophytes | | |
| *Salicornia bigelovii* | 30 | (Zapata-Sifuentes et al., 2021) |
| *Cressa cretica* | 23 | (Afshari and Sayyed-Alangi, 2017) |
| *Suaeda salsa* | 22 | (Kefu et al., 2003) |
| *Haloxylon stocksii* | 23 | (Abbas et al., 2022) |
| *Kosteletzkya virginica* | 30 | (Ruan et al., 2008) |
| *Atriplex rosea* | 13 | (Abideen et al., 2015b) |
| *Ricinus communis* | 55 | (Salimon et al., 2010) |
| *Descurainaia sophia* | 44 | (Mokhtassi-Bidgoli et al., 2022) |
| *Suaeda torreyana* | 25 | (Arias-Rico et al., 2020) |
| *Crithmum maritimum* | 40 | (D'Agostino et al., 2021) |
| Algae | | |
| *Botryococcus braunii* | 25 | (Cheng et al., 2013) |
| *Chlorella* sp. | 28 | (Munir et al., 2022) |
| *Crypthecodinium cohnii* | 20 | (Li et al., 2015) |
| *Dunaliella salina* | 20 | (Yilancioglu et al., 2014) |
| *Nannochloropsis* sp. | 31 | (Pal et al., 2011) |
| *Neochloris oleoabundans* | 35 | (Tao et al., 2019) |
| *Nitzschia* sp. | 45 | (Sahin et al., 2019) |
| *Schizochytrium* sp. | 50 | (Ren et al., 2014) |

electrophoresis, electro-flotation, and ultra-sonication are used less frequently but require either prohibitive quantities of energy or harmful chemicals (Almomani, 2020).

Filtration using a suction pump with a filter of some sort can be used for dewatering. The advantage over other methods is that algal suspensions of low density can be harvested with very high efficiency. The main problem is clogging of the filter by the algae being harvested (Cha et al., 2020); this has to be tackled by frequent backwashing. Dewatering by centrifugation uses a centrifugal force that is a few orders of magnitude higher than the force of gravity (Hua et al., 2020) but has to be stopped periodically (batch mode) for the solids to be removed (Kong et al., 2020). Efficiency and reliability of centrifugation techniques are high, but so are the operating costs often negating the efficiency of the method. If good quality algae are to be continuously produced, continuous centrifugation (by solid ejecting-type or nozzle-type disc centrifuges) is recommended. These centrifuges, which are suitable for all microalgae, can be cleaned easily and sterilized. However, their cost of operation needs be compared with the value of the end product (He et al., 2020). Harvesting micro-algal biomass by chemical coagulation and flocculation is the most economical of the methods available. The advantage of chemical coagulation/flocculation is that large culture volumes can be collected and the methodology applied to a wide variety of species. Microalgal suspensions can be concentrated 20-100 times by this harvesting technique (Li et al., 2020c). Flocculation increases the effective size of the particles before dewatering and so reduces the energy cost. Coagulation/flocculation is generally followed by gravity sedimentation which is a low-cost method of harvesting microalgae. While coagulation involves adjusting the pH or adding an electrolyte, flocculation uses cationic polymers that are added to the broth (Pei et al., 2021). Liquid biphasic flotation system is a novel method of biomolecules extraction. The system is an integration of aqueous two-phase system with mass transfer mode of solvent sublation, which has been used in the downstream processing of microalgae biorefinery (Aron et al., 2022).

After harvesting, the dewatered cake is usually dried to improve the efficiency of the downstream processes (e.g., lipid extraction) (Najjar and Abu-Shamleh, 2020). Recent technologies have shown that biofuel production from algal biomass may not be energy efficient because the production process consumes more energy than that produced by combusting the resulting biofuel. The harvesting of small algae (usually between 10 and 30 µm in diameter) is laborious and the cheaper press method of extracting oil from oilseed plants is not applicable with algae, which adds to the production cost (Saengsawang et al., 2020). Extraction of the substrates (lipids and sugars) also requires rupturing of the cell walls through an energy intensive process, depending on the algal strains (Dharmaprabhakaran et al., 2020). Lowering harvesting costs is thus important for the sustainable production of micro-algal biomass. Optimizing the method of harvest depends on the characteristics of the alga and the nature of the end product. Harvesting half of algal biomass and allowing it to double again before each subsequent harvest has proven difficult to manage (Hirooka et al., 2020). To date, most of the techniques used to harvest algae have drawbacks, such as costs of operation that may be high, and low efficiencies producing a relatively poor quality product: mechanical processes involved in sedimentation, centrifugation, and filtration can result in cell rupture, leading to leakage of cell content and a low quality (Bošnjaković and Sinaga, 2020). It is suggested that microbes should be engineered to perform direct photosynthetic and conversion of carbon by

TABLE 7 List of halophytes used for lignocellulosic biomass cellulose, hemicellulose and lignin for bioethanol production.

| Species | Cellulose (%) | Hemicellulose (%) | Lignin (%) | References |
|---|---|---|---|---|
| *Calotropis procera* | 12 | 11 | 5 | (Narayanasamy et al., 2020) |
| *Suaeda monoica* | 10 | 11 | 2 | (Abideen et al., 2011) |
| *Panicum virgatum* | 45 | 13 | 12 | |
| *Suaeda fruticose* | 8 | 21 | 4 | (Abideen et al., 2012) |
| *Phragmites karka* | 26 | 29 | 10 | |
| *Arthrocnemum indicum* | 11 | 13 | 7 | (Munir et al., 2020) |
| *Sporobolus ioclados* | 15 | 30 | 2 | |
| *Desmostachya bipinnata* | 26 | 24 | 6 | (Abideen et al., 2022) |
| *Urochondra setulosa* | 25 | 25 | 6 | |
| *Aeluropus lagopoides* | 26 | 29 | 7 | (Attia-Ismail, 2016) |
| *Tamarix indica* | 12 | 24 | 3 | |
| *Cenchrus ciliaris* | 22 | 23 | 7 | (Zheng et al., 2007) |
| *Eleusine indica* | 22 | 29 | 7 | |
| *Salsola imbricate* | 9 | 18 | 2 | (Abideen et al., 2011) |
| *Lasiurus scindicus* | 24 | 29 | 6 | |

efficient nutrients and light energy capturing to produced algal biofuel and other industrial product.

## 3 Biofuel production from halophytes

Halophytes appear an ecologically and economically feasible alternative to agricultural crops for biofuel production (Figure 2), especially in arid and semi-arid regions, because of their ability to survive in saline habitats and tolerate extremes of temperature, high irradiance, and scarcity of water (Halat et al., 2020). Table 8 and Figure 3 illustrate the biofuel properties generated from halophytes and glycophytes. Conversion of lignocellulosic biomass to ethanol has been widely studied in past decades. New technologies are being proposed for lignocellulosic ethanol production, which includes mild torrefaction (is a mild form of pyrolysis at temperatures

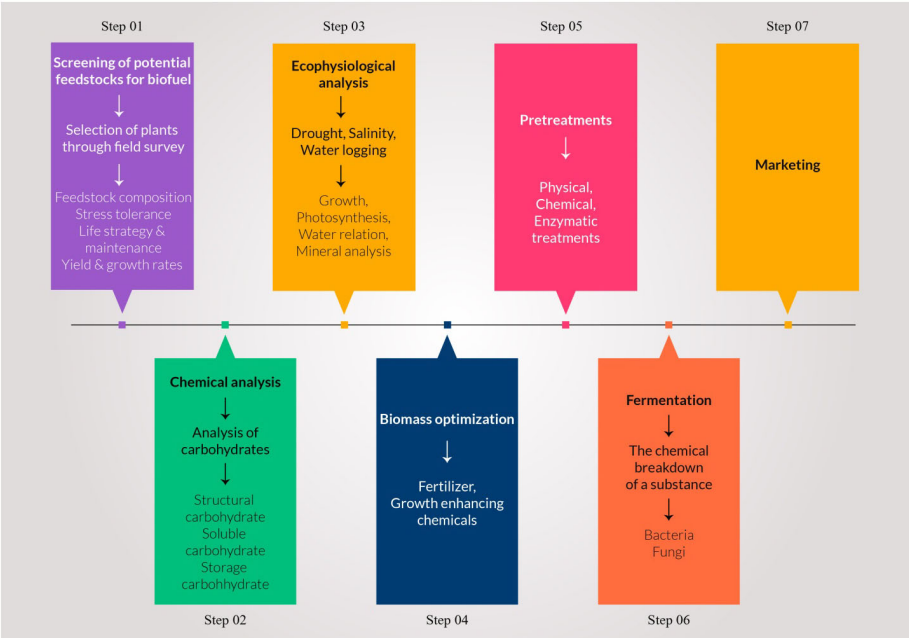


FIGURE 2
Different key steps of biomass to biofuel conversion form wild halophytic plants from screening to ethanol yield.

10.3389/fpls.2023.1026063

TABLE 8 Lignocellusic biomass (cellulose, hemicellulose and lignin composition of different plant feedstocks.

| Species | Example | Cellulose | Hemicellulose | Lignin | References |
|---|---|---|---|---|---|
| Edible crops | Sugar beet | 20.0 | 25.0 | 20.0 | (Câmara-Salim et al., 2021; Turcios et al., 2021) |
| | Sunflower | 25.0 | 17.0 | 17.0 | |
| | Maize | 33.8 | 25.4 | 8.6 | |
| | Corn stover | 38.0 | 28.0 | 7.0 | |
| | Alfalfa | 34.4 | 6.7 | 7.2 | |
| Halophytes | | | | | |
| | *Halopyrum mucronatum* | 37.0 | 28.7 | 5.0 | [31–33] |
| | *Panicum turgidum* | 28.0 | 28.0 | 6.0 | |
| | *Phragmites karka* | 26.0 | 29.0 | 10.3 | |
| | *Typha domingensis* | 26.3 | 38.7 | 4.7 | |
| | *Desmostachya bipinnata* | 26.7 | 24.7 | 6.7 | |

typically between 200 and 320°C). Different processing methods have also been proposed after a pretreatment step, which include separate hydrolysis and fermentation, simultaneous saccharification and fermentation, simultaneous saccharification and co-fermentation and consolidate bioprocessing. In consolidate bioprocessing, lignocellulosic materials are depolymerized into sugars and simultaneously enzymes that convert the sugars to ethanol or other products (Zoghlami and Paës, 2019). Brethauer and Wyman (2010) achieved 67% ethanol yield by dilute acid pretreatment of wheat straw using natural strains of microbes. For ethanol production, organosolv pretreatment using ethanol is preferred, as the ethanol used is recovered during distillation, when the final pure product is obtained (Liu et al., 2019).

Using plants has particular potential especially in areas where large populations of diverse halophytic species already grow and can be cultivated using saline water for irrigation without using existing arable lands or clearing forests to open new lands (Xu et al., 2020b). By providing a cover on barren lands, halophytes can reduce soil erosion and reduce greenhouse gases by C-sequestration; some halophytes are potential sources of oil seeds (Abideen et al., 2015b); others have value in medicines and various other purposes (see Figure 4) (Abideen et al., 2012; Abideen et al., 2014b; Yasin Ashraf et al., 2020). Many perennial halophytic grasses produce enough lignocellulosic biomass under saline conditions to warrant conversion into biofuel (Munir et al., 2021). In our preliminary study, *Halopyrum mucronatum*, *Desmostachya*

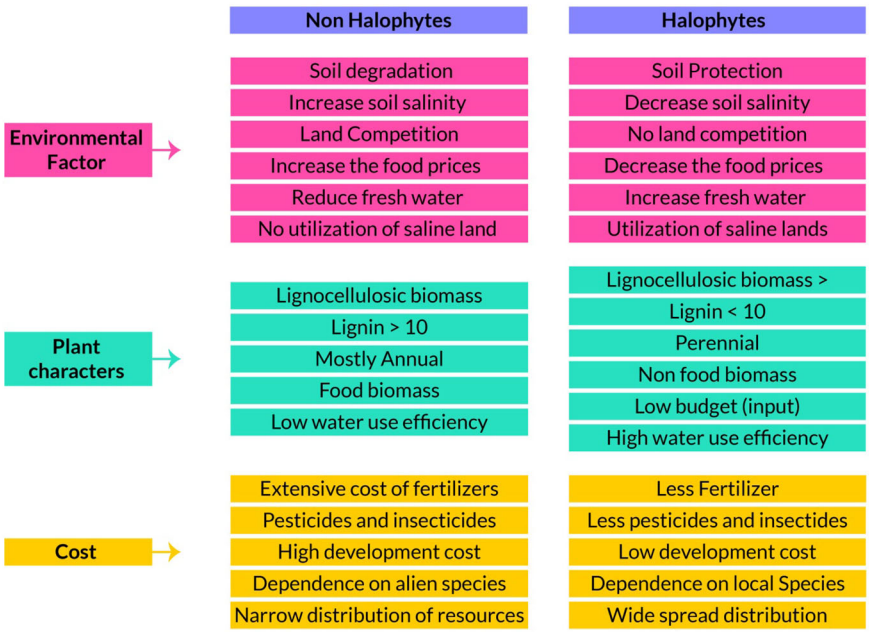


FIGURE 3
Comparisons of halophytes over non-halophytes as environment factors, plant biomass compositions and their cost effectiveness as energy source.

10.3389/fpls.2023.1026063


FIGURE 4
Application of salt resistant plant for different industrial purposes using saline land and brackish water.

*bipinnata*, *Typha domingensis*, *Phragmites karka* and *Panicum antidotale* emerged as suitable bioethanol candidates among halophytic grasses of coastal region of Pakistan (Toqeer et al., 2018). These species show high growth rates reaching up to a meter in height in 4-5 weeks and therefore can compete with conventional edible biofuel crops (Tipnee et al., 2015). These halophytes not only accumulate high biomass but also contain low lignin with high cellulose and hemicelluloses contents, which can make the hydrolysis of their biomass more efficient than that of the conventional biofuel crops (Table 8). Similarly halophytic plant species like *Salicornia fruticosa*, *Cressa cretica*, *Arthrocnemum macrostachyum*, *Alhagi maurorum*, *Halogeton glomeratus*, *Kosteletzkya virginica* and *Atriplex rosea* appear to be promising biodiesel candidates based on the quality and quantity of seed oil

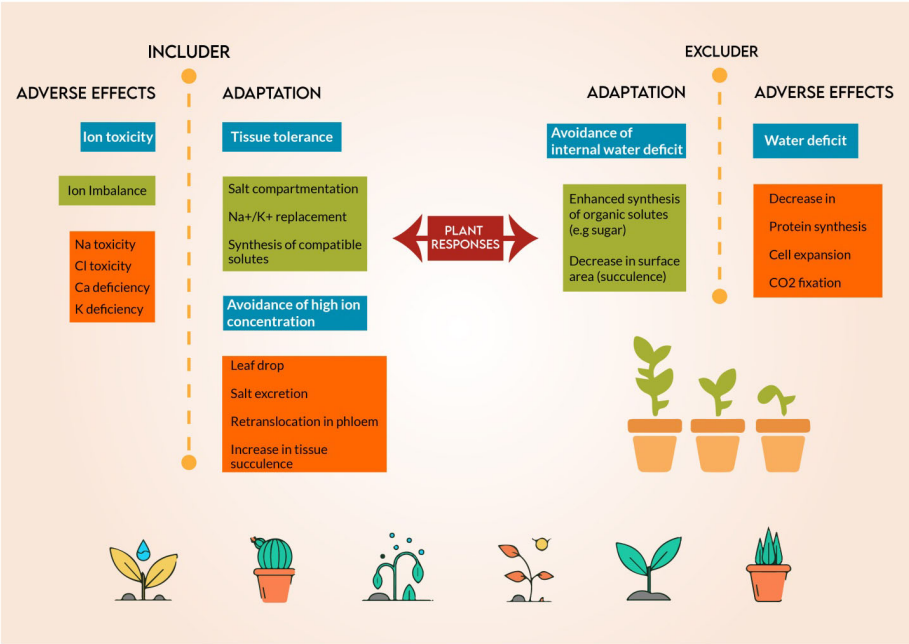


FIGURE 5
Salt tolerance machanisms and plant adaptaion of salt resitant plants to grow and complete their life cycle under saline medium.

(Abideen et al., 2015a). Further surveys are needed to identify other halophytes that have the potential to grow satisfactorily under saline/arid conditions and can be harvested for several years without replanting, thus making them more economical to grow than annual species. However, while producing biofuel from halophytes is attractive, halophytes will only serve as a supplement to existing sources and need research to solve various problems discussed below that might occur if adopted for industrial scale biofuel production. The steps of biofuel conversion from wild halophytic plants are described in detail in Figure 5.

## Ecological constraints

Experimental and circumstantial evidence proves the advantages of halophytes over the present day glycophytic crops in tolerating salinity stress. However, systematic research on halophytes has gained momentum only during the last 40-50 years and shows wide diversity in growth response to salt. Some halophytic seeds may germinate better in the absence of salinity but as plants, many require salt for optimum growth (Flowers and Colmer, 2015): the optimal growth of a number of halophytes, particularly dicotyledonous species, was obtained in about 200 mM salinity (Flowers et al., 2010). Halophytic grasses like *Halopyrum mucronatum*, *Aeluropus lagopoides*, *Sporobolus ioclados* show higher growth under fresh than salt water conditions (Abideen et al., 2014a). *Phragmites karka* and other halophytic grasses like *Phragmites australis*, *P. communis*, *Spartina maritima* and *Pennisetum clandestinum* show reduced growth as the concentration of NaCl increases (Faustino et al., 2020). *Arthrocnemum macrostachyum* exhibited extreme salt resistance by surviving in up to 1000 mM NaCl salinity (Gulzar and Khan, 2008).

To survive in saline conditions, plants must adjust osmotically to the low water potentials of their growth media by accumulating solutes in their organs. On average, dicotyledonous halophytes have higher ion concentrations in their above-ground biomass than do monocotyledonous halophytes, of which the family with most salt-tolerant species is the Poaceae (Santos et al., 2016). Since efficient biomass saccharification and pyrolysis depends upon a low salt load in the foliage, salt tolerant grasses are more suitable than dicotyledonous halophytes because of their ability to restrict ion uptake at the root level and reduce salt buildup in above-ground parts (Wang et al., 2020a). But this advantage of being a better feedstock carries the associated trait of decreasing growth with increasing root zone salinity. Combining a salt excluder grass for use as biofuel feedstock and a salt accumulator in the same saline land to reduce root zone salinity may offer a partial remedy but needs further study (Huang et al., 2020). Responses to saline substrates need to be analyzed on all halophytic species with potential as sources of biofuel and to uncover the mechanism of salt resistance and ascertain the optimum level of salinity to improve productivity and identify suitable candidate(s) for use (Figure 3) (Lu et al., 2020). It is worth mentioning here that research on the improvement of salt tolerance of conventional crops for the benefit of mankind has been attempted over thousands of years but with little significant progress; work on the domestication of halophytes is still very limited (Yeo et al., 1990).

### 3.1 Availability of seeds

Availability of good quality seed is a basic requirement for plant production, which is critical in the case of halophytes because, unlike conventional crops, seeds of halophytes are rarely available commercially but have to be collected from the wild populations (Lombardi and Bedini, 2020). Availability, collection and multiplication of seed is labor intensive and costly (Bhatt et al., 2020). The role of the plant breeding industry is not only to produce adequate quantity of seeds but also bring desirable changes in its characteristics, keeping in consideration the end use (Munir et al., 2020). Support will be required for examining the quality and type of seed for a particular region. This will require capacity building of public institutes to produce breeder seeds and to conserve genetic resources in seed production as well as harmonization of policies and regulatory frameworks for large-scale planting. Very large nurseries are needed requiring technical know-how and this will involve cost. Tissue culture techniques may help to meet the demand, although information in this regard is scanty. If adopted, tissue culture techniques will require hands-on practical and consultative training for interested seed multipliers (Palchetti et al., 2020). Seed coating technology can modify seed shape and size with improve delivery to sites mainly for small-seeded plants and for seeds with complex morphology (Staples et al., 2020). Seed coating of *P. spicata* improves seedling emergence and growth in crusting soil as well as improving handling and sowing efficiency of small seeds such as those of *Artemisia tridentata* (Serpe et al., 2020).

### 3.2 Agronomy and cultural practices

Crop cultivation requires detailed information about best cultural practices for optimum yield, information that is available for most of our current conventional crops. However, such information is rarely available for halophytes (Hanus-Fajerska et al., 2020). Halophytes are substantially different from other agricultural crops in their morphology, growth habit, nutrition pattern and a proper understanding of various aspects of their cultivation is required if yields are to be maximized. For instance, detailed information is needed about the planting density for optimum growth, fertilizer requirement, irrigation scheduling and harvesting interval (Andreotti et al., 2020). Chemical testing of soil has long been an accepted agricultural management practice to assess soil fertility, and avoid excess fertilizer application or pollution of the environment especially in deserts with very deep water tables (Koyro, 2003). For coastal regions, this information is generally missing for halophytic plants including those meant for use as biofuel crops. Interpretations and fertility recommendations based on soil analyses and the information on cropping systems, tillage practices, soil texture and structure and manure use can contribute to increased efficiency of biomass production in saline

lands (Maciel et al., 2020). Currently, the amount of land devoted to growing crops for energy is only 0.19% of the world's total land area and only 0.5–1.7% of global agricultural land. The wasted saline land could be used for halophyte cultivation which can reduce land competition and freshwater resources so there will be no competition with the cultivated lands.

## 3.3 Knowledge of plant diseases

Losses from insects and diseases range from 9 to 16% in major field crops (rice, barley, wheat, maize, potato, soybean, cotton) (Ahmad et al., 2020) and are a significant constraint to crop production that stands between the rapidly growing world population and starvation. Research on diseases in halophytic plants is limited but needs to be pursued to find suitable control measures using methods available in conventional agriculture (Tıpırdamaz et al., 2020). The techniques of molecular biology may be helpful in analysis of gene expression for responses to different biotic and abiotic stresses and potential trade-offs. Seed coating with predator repellents can reduce seed consumption by rodents (Carter et al., 2020). Seeds coated with salicylic acid improved growth of *Austrostipa scabra*, *Microlaena stipoides*, and *Rytidosperma geniculatum* as well as survival. Biological control is a very promising strategy to control plant diseases. *Coniothyrium minitans* and *Sporidesmium sclerotivorum* are used to control diseases caused by *Sclerotinia* sp. *Coniothyrium minitans* based products are available in the European market (Patel et al., 2021). *Pseudomonas fluorescens*, which produces toxins or secondary metabolites such as siderophores, phenazines and cyanide, can be used against *Gaeumannomyces graminis* and *Chalara elegans* (Martin-Rivilla et al., 2020). However, there are no such examples for halophytes.

## 3.4 Variable seed germination and propagation

Halophytes are plants of saline habitats that grow under conditions with variable stress and may change their responses rapidly between seed germination and later growth. Germination at high salinity may provide an advantage of high seedling population to start with but subsequent growth and biomass yield may not necessarily reflect tolerance to salinity during seed germination (Becerra-Vázquez et al., 2020). Seed dormancy is an important means of delaying seed germination and initiating growth under suitable conditions. Many halophytic species do not, however, possess such elaborate systems because they naturally propagate through ramets and have no ecological compulsions for seed germination. Seed priming technology is used to reduce variability in seed germination rate with constant and rapid germination within populations (Banerjee and Roychoudhury, 2018). Seed dormancy is an important means of delaying seed germination and initiating growth under suitable conditions. Many halophytic species do not, however, possess such elaborate systems because they naturally propagate through ramets and have no ecological compulsions for seed germination. Seed priming technology is used to reduce variability in seed germination rate with constant and rapid germination within populations. Priming can provide resistance to heat, moisture and osmoticum stresses (salt) (Banerjee and Roychoudhury, 2018). Seed priming improves germination in *Guazuma ulmifolia*, *Albizia saman* (Ibrahim and Hawramee, 2019), *Cedrela odorata*, *Enterolobium cyclocarpum* (Becerra-Vázquez et al., 2020), *Swietenia macrophylla* and also the performance of *E. cyclocarpum* (Pedrini et al., 2020). Seed priming improved fast emergence in seeds of *Poa fendleriana* and *P. spicata* (66–82%), while the density of *P. spicata* seedlings was 2.9-3.8 fold higher than non-treated seeds (Madsen et al., 2018).

## 3.5 Invasive potential

Biological invasions are an increasingly important threat to biodiversity and ecosystem functioning and a major component of global change worldwide. In addition to affecting ecosystems and contributing to the extinction of native species, invasive non-native species can also cause major socio-economic damage. Many species that are currently invasive were introduced without proper study of after-effects and many spread providing usually small benefits to a sector of society but with harmful (often irreversible) environmental consequences. Once introduced and established in a new region, plant species, are extremely difficult to eradicate or control. Next generation biofuel crops, whose production demands large biomasses, have the potential to become problematic and costly invasive species that if alien for an area; need to be closely watched. Characteristics like wide environmental resistance, ease of establishment, ability to re-sprout when harvested, fast growth rate, low demand or good quality water are precisely the traits that predispose species to become invasive (Hussain et al., 2020); see Figure 3 for comparison or similarities in biofuels and non-invasive properties. For example *Arundo donax*, *Phalaris arundinacea* and *Phragmites karka* are fast growing $C_3$ invasive species with tolerance to drought, salinity, and low-fertility soils (Abideen et al., 2012; Abideen et al., 2014a; Qasim et al., 2014). They should be targeted for cultivation in specific areas where they can flourish and produce lignocellulosic biomass without harming the ecosystem.

A prospect which is apparently yet to be examined is that harvesting biomass for conversion into biofuels could be used as a tool for controlling invasive species (Nayak et al., 2020). Imperata grasslands found in Indonesia could be harvested to provide biomass, and then exchanged with more productive crops (e.g. oil palm) or with native biomass feedstocks that are non-invasive. The major risk of this approach is that it could encourage planting and spread of invasive species (Duarte and Caçador, 2021). This risk could be reduced if it were managed specifically as a control strategy, with penalties for replanting. No attempt has been made to quantify actual, relative or potential invasiveness of terrestrial biofuel crops at an appropriate regional or international scale, and their planting continues to be largely unregulated. Scientist must assess ecological risks before suggesting a new biofuel crop, to avoid introducing an invasive species (Mao et al., 2020).

## 4 Comparison of algae vs halophytes as biofuel candidates: a summary

In spite of harmful environmental consequences, fossil fuels continue to be used extensively in our daily life. The recent discovery of alternate energy sources such as shale oil have raised confidence in the continued availability of fossil resources. This optimism has been strengthened further by access to deposit sites previously considered difficult to reach. Technological improvements, coupled with general inflation in prices, have been an impetus for pumping oil from depths previously uneconomical to drill. However, there are still forecasts that these developments will only delay the inevitable loss of supply for which there is need to explore other sources of energy like nuclear, wind, solar, tidal, plant biomass as potential alternates.

Commercial interest with the rising awareness for environmental and energy issues are strong catalysts for producing biofuels from non-food resources. Halophytes and algae may be suitable options for this purpose because they do not need arable land and the freshwater required for growing food crops - with additional benefit of carbon sequestration and removing greenhouse gases (GHG) from the atmosphere by consuming $CO_2$ for photosynthesis during growth. The seed germination dynamics and growth of halophytes are rarely well documented but there are examples where substantial improvement in growth can be achieved by applying different growth promoting agents such as biochip, compost and growth promoting bacteria. In the case of algae, there are a few studies that help in improvement of growth parameters; dry biomass accumulation is key factor. The major advantage that growing algae has over halophytes is the faster growth rate of the former than the latter, achieved with lower nutrient requirements. Halophytes need at least one month to establish their seedling in the saline soil. After establishment they can achieve fast growth, but seed is only produced once, or rarely twice, a year. The smaller seed size of most halophytes compared with glycophytes can reduce the efficiency of biodiesel production in halophytes compare to algal blooms. However, the feedstock from halophytes could be a good source of bioethanol production compared to algae. Halophytes can produce leaf and shoot biomass on large scale and their biomass saccharification and fermentation could give more sustainable bioethanol than other bioenergy resources including algal biomass. The cultivation of halophytes for biofuel on otherwise saline barren lands could develop the use of non-agricultural lands for industrial application, although the potential for invasiveness needs care. The pond system of cultivation of algal biomass can raise environmental problems due eutrophication following discharge of nutrient-rich water to the local water resources. The exploitation of algal biomass directly from the ocean can disturb the food web, nutrient cycling and cause ecosystem damage.

The technology of converting biofuels from non-food options is potentially sound but it is not ready for instant application and needs a cautious approach with a number of obstacles to overcome before large scale adoption. The oil contents of algal biomass sounds very appealing but starting from identifying suitable algal strains and their growth optimization under particular conditions followed by subsequent processing involving harvesting, dewatering and conversion to the end product involves covering a long, tedious and underexplored terrain. Halophytes too have several problems that need to be assessed. Starting from the difficulty of availability of seed in adequate quantities for planting on a commercial scale to dearth of information about the cultural practices for optimum biomass yield and all the intermediary management steps; there are many questions. Without answers There are also many risks and uncertainties, such as variable germination, problems with propagation, plant diseases, scaling up, processing plant biomass, market demand and economic competition with bulk-produced raw materials from other conventional crops already being used. Cost effectiveness will be the prime consideration which will be compromised if halophytic plants are grown under artificially controlled conditions such as in a green house. Plants which are growing naturally near the coast or on inland degraded areas and producing suitable feedstock with saline irrigations is likely to be a better option as such systems have other important advantages like soil protection against wind and water erosion, enhancing biodiversity, creation of habitats for animals and mitigating environmental degradation.

## 5 Conclusions

In spite of projected shortages of energy and harmful environmental consequences of their production, fossil fuels continue to be used extensively in our daily life. Commercial interest with the rising awareness for environmental and energy issues are strong catalysts for the initiative of producing biofuels from nonfood resources. Halophytes and algae may be suitable options for this purpose because they do not need the arable land and freshwater required for growing food crops with additional benefit of removing greenhouse gases from the atmosphere by consuming $CO_2$ for photosynthesis during growth. Potential food value of both algae and halophytes is very limited at least for the time being – except, perhaps, the use of halophytes as high-value foods and animal feed. The facilities to produce biofuel other by products such as protein and other useful substances from the post processing residue can decrease the total cost of biofuel production. It is worth mentioning that while some algal strains contain suitable forms of carbohydrates that can be fermented to bioethanol, oil in adequate quantities can be obtained from oilseed halophytes for conversion into biodiesel.

## 6 Future prospects

The oil contents of algal biomass seem very appealing but starting from identifying suitable algal strains and their growth optimization under particular conditions and subsequent

processing involving harvesting, dewatering and conversion to the end product involves covering a long, tedious and underexplored terrain. The use of halophytes also has problems that need to be assessed. Starting from the poor availability of seed in adequate quantities for planting on a commercial scale to the dearth of information about the cultural practices for optimum biomass yield and all the intermediary management steps, there are many unanswered questions. There are also many risks and uncertainties such as variable germination, problems with propagation, plant diseases, processing plant biomass, market demand and economic competition with bulk-produced raw materials from other conventional crops. Cost effectiveness will be the prime consideration, which will be compromised if halophytic plants are grown under artificially controlled conditions such as in a greenhouse. Domestication of these plants can be initiated by screening collections for the best genotypes and detailed chemical analysis to judge their suitability for particular purposes. This article has highlighted some of the stumbling blocks that may lie on the way but there may be more bottlenecks to remove for successful adoption of this novel approach. It is also evident that biofuels will not meet the total demand but will only be part of the future energy mix of liquid fuel.

## Author contributions

ZA and RA: Conceptualization, Investigation, Formal analysis, Methodology, Writing – original draft. MH: Conceptualization, Investigation, Formal analysis, Methodology, Writing – original draft. TF, H-WK, AE-K, MA, and MAK: Supervision, Conceptualization, Resources, Writing – review and editing, Funding acquisition. MH: Supervision, Conceptualization, Resources, Writing – review and editing, Funding acquisition. MA: Formal analysis. MH: Formal analysis. ZA: Conceptualization, Investigation, Formal analysis, Methodology, Writing – original draft, Formal analysis. All authors contributed to the article and approved the submitted version.

## Funding

The work in this article was supported by the Open Access Program from the American University of Sharjah.

## Conflict of interest

The authors declare that the research was conducted in the absence of any commercial or financial relationships that could be construed as a potential conflict of interest.

## Publisher's note

All claims expressed in this article are solely those of the authors and do not necessarily represent those of their affiliated organizations, or those of the publisher, the editors and the reviewers. Any product that may be evaluated in this article, or claim that may be made by its manufacturer, is not guaranteed or endorsed by the publisher.

## Author disclaimer

This paper represents the opinions of the authors and does not mean to represent the position or opinions of the American University of Sharjah.

## References

Abbas, S., Rasheed, A., Soriano, P., Estrelles, E., Gul, B., and Hameed, A. (2022). Moisture content and oxidative damage determine longevity of the seeds of potential cash crop halophyte *Haloxylon stocksii*. *Plant Biosyst. Int. J. Deal. all Asp. Plant Biol.* 156 (6), 1478–1484. doi: 10.1080/11263504.2022.2065378

Abideen, Z., Ansari, R., Gul, B., and Khan, M. A. (2012). The place of halophytes in pakistan's biofuel industry. *Biofuels* 3, 211–220. doi: 10.4155/bfs.11.158

Abideen, Z., Ansari, R., and Khan, M. A. (2011). Halophytes: potential source of ligno-cellulosic biomass for ethanol production. *Biomass Bioenergy* 35, 1818–1822. doi: 10.1016/j.biombioe.2011.01.023

Abideen, Z., Hameed, A., Koyro, H.-W., Gul, B., Ansari, R., and Khan, M. A. (2014a). Sustainable biofuel production from non-food sources-an overview. *Emirates J. Food Agric.* 26 (12), 1057–1066. doi: 10.9755/ejfa.v26i12.19107

Abideen, Z., Koyro, H.-W., Huchzermeyer, B., Ahmed, M. Z., Gul, B., and Khan, M. A. (2014b). Moderate salinity stimulates growth and photosynthesis of phragmites karka by water relations and tissue specific ion regulation. *Environ. Exp. Bot.* 105, 70–76. doi: 10.1016/j.envexpbot.2014.04.009

Abideen, Z., Koyro, H.-W., Huchzermeyer, B., Bilquees, G. U. L., and Khan, M. A. (2020). Impact of a biochar or a biochar-compost mixture on water relation, nutrient uptake and photosynthesis of *Phragmites karka*. *Pedosphere* 30, 466–477. doi: 10.1016/S1002-0160(17)60362-X

Abideen, Z., Koyro, H. W., Hussain, T., Rasheed, A., Alwahibi, M. S., Elshikh, M. S., et al. (2022). Biomass production and predicted ethanol yield are linked with optimum photosynthesis in *Phragmites karka* under salinity and drought conditions. *Plants* 11, 1657. doi: 10.3390/plants11131657

Abideen, Z., Qasim, M., Rasheed, A., Adnan, M. Y., Gul, B., and Khan, M. A. (2015a). Antioxidant activity and polyphenolic content of phragmites karka under saline conditions. *Pakistan J. Bot.* 47, 813–818.

Abideen, Z., Qasim, M., Rizvi, R. F., Gul, B., Ansari, R., and Khan, M. A. (2015b). Oilseed halophytes: a potential source of biodiesel using saline degraded lands. *Biofuels* 6, 241–248. doi: 10.1080/17597269.2015.1090812

Afshari, A., and Sayyed-Alangi, S. Z. (2017). Antioxidant effect of leaf extracts from *Cressa cretica* against oxidation process in soybean oil. *Food Sci. Nutr.* 5, 324–333. doi: 10.1002/fsn3.396

Ahmad, F., Hameed, M., Ahmad, M. S. A., and Ashraf, M. (2020). Ensuring food security of arid regions through sustainable cultivation of halophytes. *Handb. Halophytes From Mol. to Ecosyst. Towar. Biosaline Agric.*, 1–21. doi: 10.1007/978-3-030-17854-3_89-1

Alami, A. H., Alasad, S., Ali, M., and Alshamsi, M. (2021). Investigating algae for CO2 capture and accumulation and simultaneous production of biomass for biodiesel production. *Sci. Total Environ.* 759, 143529. doi: 10.1016/j.scitotenv.2020.143529

Almomani, F. (2020). Algal cells harvesting using cost-effective magnetic nano-particles. *Sci. Total Environ.* 720, 137621. doi: 10.1016/j.scitotenv.2020.137621

Almutairi, A. W., and Toulibah, H. E. (2017). Effect of salinity and ph on fatty acid profile of the green algae *Tetraselmis suecica*. *J. Pet. Environ. Biotechnol.* 8, 3–8. doi: 10.4172/2157-7463.1000333

Alzahrani, E. O., El-Dessoky, M. M., and Dogra, P. (2020). Global dynamics of a cell quota-based model of light-dependent algae growth in a chemostat. *Commun. Nonlinear Sci. Numer. Simul.* 90, 105295. doi: 10.1016/j.cnsns.2020.105295

Amiri, R., and Ahmadi, M. (2020). Treatment of wastewater in sewer by *Spirogyra* sp. green algae: effects of light and carbon sources. *Water Environ. J.* 34, 311–321. doi: 10.1111/wej.12463

Andreotti, V., Solimeno, A., Rossi, S., Ficara, E., Marazzi, F., Mezzanotte, V., et al. (2020). Bioremediation of aquaculture wastewater with the microalgae *Tetraselmis suecica*: semi-continuous experiments, simulation and photo-respirometric tests. *Sci. Total Environ.* 738, 139859. doi: 10.1016/j.scitotenv.2020.139859

Anton, A., Geraldi, N. R., Lovelock, C. E., Apostolaki, E. T., Bennett, S., Cebrian, J., et al. (2019). Global ecological impacts of marine exotic species. *Nat. Ecol. Evol.* 3, 787–800. doi: 10.1038/s41559-019-0851-0

Arias-Rico, J., Macías-León, F. J., Alanís-García, E., Cruz-Cansino, N., del, S., Jaramillo-Morales, O. A., et al. (2020). Study of edible plants: effects of boiling on nutritional, antioxidant, and physicochemical properties. *Foods* 9, 599. doi: 10.3390/foods9050599

Aron, N. S. M., Chew, K. W., Ang, W. L., Ratchahat, S., Rinklebe, J., and Show, P. L. (2022). Recovery of microalgae biodiesel using liquid biphasic flotation system. *Fuel* 317, 123368.

Aron, N. S. M., Khoo, K. S., Chew, K. W., Veeramuthu, A., Chang, J.-S., and Show, P. L. (2021). Microalgae cultivation in wastewater and potential processing strategies using solvent and membrane separation technologies. *J. Water Process Eng.* 39, 101701. doi: 10.1016/j.jwpe.2020.101701

Aston, J. E., Wahlen, B. D., Davis, R. W., Siccardi, A. J., and Wendt, L. M. (2018). Application of aqueous alkaline extraction to remove ash from algae harvested from an algal turf scrubber. *Algal Res.* 35, 370–377. doi: 10.1016/j.algal.2018.09.006

Attia-Ismail, S. A. (2016). Nutritional and feed value of halophytes and salt tolerant plants. halophytic salt-tolerant feed. *impacts Nutr. Physiol. Reprod. Livest.*, 348–357.

Azizi, S., Bayat, B., Tayebati, H., Hashemi, A., and Pajoum Shariati, F. (2020). Nitrate and phosphate removal from treated wastewater by *Chlorella vulgaris* under various light regimes within membrane flat plate photobioreactor. *Environ. Prog. Sustain. Energy*, e13519.

Banerjee, A., and Roychoudhury, A. (2018). "Seed priming technology in the amelioration of salinity stress in plants," in *Advances in seed priming* (Springer), 81–93.

Becerra-Vázquez, Á.G., Coates, R., Sánchez-Nieto, S., Reyes-Chilpa, R., and Orozco-Segovia, A. (2020). Effects of seed priming on germination and seedling growth of desiccation-sensitive seeds from Mexican tropical rainforest. *J. Plant Res.* 133, 855–872. doi: 10.1007/s10265-020-01220-0

Bélanger-Lépine, F., Tremblay, A., Huot, Y., and Barnabé, S. (2018). Cultivation of an algae-bacteria consortium in wastewater from an industrial park: effect of environmental stress and nutrient deficiency on lipid production. *Bioresour. Technol.* 267, 657–665. doi: 10.1016/j.biortech.2018.07.099

Bews, E., Booher, L., Polizzi, T., Long, C., Kim, J.-H., and Edwards, M. S. (2021). Effects of salinity and nutrients on metabolism and growth of *Ulva lactuca*: implications for bioremediation of coastal watersheds. *Mar. pollut. Bull.* 166, 112199. doi: 10.1016/j.marpolbul.2021.112199

Bhatt, A., Gairola, S., Carón, M. M., Santo, A., Murru, V., El-Keblawy, A., et al. (2020). Effects of light, temperature, salinity, and maternal habitat on seed germination of *Aeluropus lagopoides* (Poaceae): an economically important halophyte of arid Arabian deserts. *Botany* 98, 117–125. doi: 10.1139/cjb-2019-0096

Bologna, M., and Aquino, G. (2020). Deforestation and world population sustainability: a quantitative analysis. *Sci. Rep.* 10, 1–9. doi: 10.1038/s41598-020-63657-6

Bošnjaković, M., and Sinaga, N. (2020). The perspective of Large-scale production of algae biodiesel. *Appl. Sci.* 10, 8181. doi: 10.3390/app10228181

Brethauer, S., and Wyman, C. E. (2010). Continuous hydrolysis and fermentation for cellulosic ethanol production. *Bioresour. Technol.* 101, 4862–4874. doi: 10.1016/j.biortech.2009.11.009

Brindhadevi, K., Mathimani, T., Rene, E. R., Shanmugam, S., Chi, N. T. L., and Pugazhendhi, A. (2021). Impact of cultivation conditions on the biomass and lipid in microalgae with an emphasis on biodiesel. *Fuel* 284, 119058. doi: 10.1016/j.fuel.2020.119058

Brown, J. J. (2019). "Considerations for producing bioenergy from halophyte feedstocks," in *Biorefinery* (Springer), 657–668.

Câmara-Salim, I., Conde, P., Feijoo, G., and Moreira, M. T. (2021). The use of maize stover and sugar beet pulp as feedstocks in industrial fermentation plants–an economic and environmental perspective. *Clean. Environ. Syst.* 2, 100005. doi: 10.1016/j.cesys.2020.100005

Carter, S. K., Pilliod, D. S., Haby, T., Prentice, K. L., Aldridge, C. L., Anderson, P. J., et al. (2020). Bridging the research-management gap: landscape science in practice on public lands in the western united states. *Landsc. Ecol.*, 1–16. doi: 10.1007/s10980-020-00970-5

Cha, G., Choi, S., Lee, H., Kim, K., Ahn, S., and Hong, S. (2020). Improving energy efficiency of pretreatment for seawater desalination during algal blooms using a novel meshed tube filtration process. *Desalination* 486, 114477. doi: 10.1016/j.desal.2020.114477

Chen, Z., Shao, S., He, Y., Luo, Q., Zheng, M., Zheng, M., et al. (2020). Nutrients removal from piggery wastewater coupled to lipid production by a newly isolated self-flocculating microalga desmodesmus sp. PW1. *Bioresour. Technol.*, 302122806. doi: 10.1016/j.biortech.2020.122806

Cheng, P., Ji, B., Gao, L., Zhang, W., Wang, J., and Liu, T. (2013). The growth, lipid and hydrocarbon production of *Botryococcus braunii* with attached cultivation. *Bioresour. Technol.* 138, 95–100. doi: 10.1016/j.biortech.2013.03.150

Christiansen, A. H. C., Lyra, D. A., and Jørgensen, H. (2021). Increasing the value of *Salicornia bigelovii* green biomass grown in a desert environment through biorefining. *Ind. Crops Prod.* 160, 113105. doi: 10.1016/j.indcrop.2020.113105

Clements, C. S., Burns, A. S., Stewart, F. J., and Hay, M. E. (2020). Seaweed-coral competition in the field: effects on coral growth, photosynthesis and microbiomes require direct contact. *Proc. R. Soc B* 287, 20200366. doi: 10.1098/rspb.2020.0366

Correa, D. F., Beyer, H. L., Possingham, H. P., García-Ulloa, J., Ghazoul, J., and Schenk, P. M. (2020). Freeing land from biofuel production through microalgal cultivation in the Neotropical region. *Environ. Res. Lett.* 15, 94094. doi: 10.1088/1748-9326/ab8d7f

D'Agostino, G., Giambra, B., Palla, F., Bruno, M., and Badalamenti, N. (2021). The application of the essential oils of *Thymus vulgaris* l. and *Crithmum maritimum* l. as biocidal on two tholu bommalu indian leather puppets. *Plants* 10, 1508.

Dharmaprabhakaran, T., Karthikeyan, S., Periyasamy, M., and Mahendran, G. (2020). Combustion analysis of CuO2 nanoparticle addition with blend of *botryococcus braunii* algae biodiesel on CI engine. *Mater. Today Proc.* 33, 2874–2876. doi: 10.1016/j.matpr.2020.02.776

Duarte, B., and Caçador, I. (2021). Iberian Halophytes as agroecological solutions for degraded lands and biosaline agriculture. *Sustainability* 13, 1005. doi: 10.3390/su13021005

Dubey, D., and Dutta, V. (2020). "Nutrient enrichment in lake ecosystem and its effects on algae and macrophytes," in *Environmental concerns and sustainable development* (Springer), 81–126.

Dun, Q., Yao, L., Deng, Z., Li, H., Li, J., Fan, Y., et al. (2019). Effects of hot and cold-pressed processes on volatile compounds of peanut oil and corresponding analysis of characteristic flavor components. *Lwt* 112, 107648. doi: 10.1016/j.lwt.2018.11.084

Edrisi, S. A., Tripathi, V., Chaturvedi, R. K., Dubey, D. K., Patel, G., and Abhilash, P. C. (2020). Saline soil reclamation index as an efficient tool for assessing restoration progress of saline land. *L. Degrad. Dev.*

ElFar, O. A., Aron, N. S. M., Chew, K. W., and Show, P. L. (2022). "Sustainable management of algal blooms in ponds and rivers," in *Biomass, biofuels, biochemicals* (Elsevier), 431–444.

El-Katony, T. M., and El-Adl, M. F. (2020). Salt response of the freshwater microalga *Scenedesmus obliquus* (Turp.) kutz is modulated by the algal growth phase. *J. Oceanol. Limnol.* 38, 802–815. doi: 10.1007/s00343-019-9067-z

El Shenawy, E. A., Elkelawy, M., Bastawissi, H. A.-E., Taha, M., Panchal, H., kumar Sadasivuni, K., et al. (2020). Effect of cultivation parameters and heat management on the algae species growth conditions and biomass production in a continuous feedstock photobioreactor. *Renew. Energy* 148, 807–815. doi: 10.1016/j.renene.2019.10.166

Farooqi, Z. U. R., Ahmad, Z., Ayub, M. A., Umar, W., Nadeem, M., Fatima, H., et al. (2021). Threats to arable land of the world: current and future perspectives of land use. *Exam. Int. L. Use Policies Change Conflicts*, 186–209. doi: 10.4018/978-1-7998-4372-6.ch010

Faustino, M. V., Faustino, M. A. F., Silva, H., Silva, A. M. S., and Pinto, D. C. G. A. (2020). Lipophilic metabolites of *Spartina maritima* and *Puccinellia maritima* involved in their tolerance to salty environments. *Chem. Biodivers.* 17, e2000316. doi: 10.1002/cbdv.202000316

Flowers, T. J., and Colmer, T. D. (2015). Plant salt tolerance: adaptations in halophytes. *Ann. Bot.* 115, 327–331. doi: 10.1093/aob/mcu267

Flowers, T. J., Galal, H. K., and Bromham, L. (2010). Evolution of halophytes: multiple origins of salt tolerance in land plants. *Funct. Plant Biol.* 37, 604–612. doi: 10.1071/FP09269

Fong-Lee, N., Siew-Moi, P., Leong, L. B., Vineetha, K., Cheng-Han, T., Kian-Ted, C., et al. (2020). Optimised spectral effects of programmable LED arrays (PLA) s on bioelectricity generation from algal-biophotovoltaic devices. *Sci. Rep. (Nature Publ. Group)* 10 (1),16105.

Fork, M. L., Karlsson, J., and Sponseller, R. A. (2020). Dissolved organic matter regulates nutrient limitation and growth of benthic algae in northern lakes through interacting effects on nutrient and light availability. *Limnol. Oceanogr. Lett.* 5, 417–424. doi: 10.1002/lol2.10166

Galès, A., Triplet, S., Geoffroy, T., Roques, C., Carré, C., Le Floc'h, E., et al. (2020). Control of the pH for marine microalgae polycultures: a key point for CO2 fixation improvement in intensive cultures. *J. CO2 Util.* 38, 187–193. doi: 10.1016/j.jcou.2020.01.019

Gharbia, H.B., Laabir, M., Mhamed, A.B., Gueroun, S. K. M., Yahia, M. N. D., Nouri, H., et al. (2019). Occurrence of epibenthic dinoflagellates in relation to biotic substrates and to environmental factors in southern Mediterranean (Bizerte bay and lagoon,

tunisia): an emphasis on the harmful ostreopsis spp., *Prorocentrum lima* and *Coolia monotis*. *Harm. Algae* 90, 101704. doi: 10.1016/j.hal.2019.101704

Giuffrè, A. M., Capocasale, M., Macrì, R., Caracciolo, M., Zappia, C., and Poiana, M. (2020). Volatile profiles of extra virgin olive oil, olive pomace oil, soybean oil and palm oil in different heating conditions. *Lwt* 117, 108631. doi: 10.1016/j.lwt.2019.108631

Gour, R. S., Garlapati, V. K., and Kant, A. (2020). Effect of salinity stress on lipid accumulation in *Scenedesmus* sp. and *Chlorella* sp.: feasibility of stepwise culturing. *Curr. Microbiol.* 77 (5), 779-785,

Gressel, J., van der Vlugt, C. J. B., and Bergmans, H. E. N. (2013). Environmental risks of large scale cultivation of microalgae: mitigation of spills. *Algal Res.* 2, 286–298. doi: 10.1016/j.algal.2013.04.002

Gu, P., Li, Q., Zhang, W., Gao, Y., Sun, K., Zhou, L., et al. (2021). Biological toxicity of fresh and rotten algae on freshwater fish: LC50, organ damage and antioxidant response. *J. Haz. Mater.* 407, 124620. doi: 10.1016/j.jhazmat.2020.124620

Gulzar, S., and Khan, M. A. (2008). "Comparative salt tolerance of perennial grasses," in *Ecophysiology of high salinity tolerant plants* (Springer), 239–253.

Halat, L., Galway, M. E., and Garbary, D. J. (2020). Cell wall structural changes lead to separation and shedding of biofouled epidermal cell wall layers by the brown alga *Ascophyllum nodosum*. *Protoplasma* 257, 1319–1331. doi: 10.1007/s00709-020-01502-3

Hanus-Fajerska, E., Wiszniewska, A., Kamińska, I., and Koźmińska, A. (2020). Metallomic approach to enhance agricultural application of halophytes. *Handb. Halophytes From Mol. to Ecosyst. Towar. Biosaline Agric.*, 1–17. doi: 10.1007/978-3-030-17854-3_82-1

Hasnain, M., Abideen, Z., Hashmi, S., Naz, S., and Munir, N. (2023). Assessing the potential of nutrient deficiency for enhancement of biodiesel production in algal resources. *Biofuels* 14 (1), 1–34.

Hasnain, M., Abideen, Z., Naz, S., Roessner, U., and Munir, N. (2021). Biodiesel production from new algal sources using response surface methodology and microwave application. *Biomass Convers. Biorefinery*. doi: 10.1007/s13399-021-01560-4

He, J., Hong, B., Lu, R., Zhang, R., Fang, H., Huang, W., et al. (2020). Separation of saturated fatty acids from docosahexaenoic acid-rich algal oil by enzymatic ethanolysis in tandem with molecular distillation. *Food Sci. Nutr.* 8, 2234–2241. doi: 10.1002/fsn3.1462

Hirooka, S., Tomita, R., Fujiwara, T., Ohnuma, M., Kuroiwa, H., Kuroiwa, T., et al. (2020). Efficient open cultivation of cyanidialean red algae in acidified seawater. *Sci. Rep.* 10, 1–12. doi: 10.1038/s41598-020-70398-z

Ho, S.-H., Shimada, R., Ren, N.-Q., and Ozawa, T. (2017). Rapid *in vivo* lipid/carbohydrate quantification of single microalgal cell by raman spectral imaging to reveal salinity-induced starch-to-lipid shift. *Biotechnol. Biofuels* 10, 1–9.

Hua, L., Cao, H., Ma, Q., Shi, X., Zhang, X., and Zhang, W. (2020). Microalgae filtration using an electrochemically reactive ceramic membrane: filtration performances, fouling kinetics, and foulant layer characteristics. *Environ. Sci. Technol.* 54, 2012–2021. doi: 10.1021/acs.est.9b07022

Huang, J., Khan, M. T., Perecin, D., Coelho, S. T., and Zhang, M. (2020). Sugarcane for bioethanol production: potential of bagasse in Chinese perspective. *Renew. Sustain. Energy Rev.* 133, 110296. doi: 10.1016/j.rser.2020.110296

Hussain, M. I., Elnaggar, A., and El-Keblawy, A. (2020). Eco-physiological adaptations of *Salsola drummondii* to soil salinity: role of reactive oxygen species, ion homeostasis, carbon isotope signatures and anti-oxidant feedback. *Plant Biosyst. Int. J. Deal. all Asp. Plant Biol.*, 1–13.

Ibrahim, H. S., and Hawramee, o. (2019). Impact of acid scarification and cold mist stratification on enhancing seed germination and seedling early growth of *Albizia lebbeck* (L.) benth. *Mesopotamia J. Agric.* 47, 1–13. doi: 10.33899/magrj.2019.163175

Jacob, A., Ashok, B., Alagumalai, A., Chyuan, O. H., and Le, P. T. K. (2020). Critical review on third generation micro algae biodiesel production and its feasibility as future bioenergy for IC engine applications. *Energy Convers. Manage.*, 228, 113655.

Jalgaonwala, R. E. (2020). "Considering harmful algal blooms," in *Environmental change and sustainability* (IntechOpen).

Jazie, A. A., Abed, S. A., Nuhma, M. J., and Mutar, M. A. (2020). Continuous biodiesel production in a packed bed reactor from microalgae *Chlorella* sp. using DBSA catalyst. *Eng. Sci. Technol. an Int. J.* 23, 642–649. doi: 10.1016/j.jestch.2019.08.002

Jeon, H.-S., Park, S. E., Ahn, B., and Kim, Y.-K. (2017). Enhancement of biodiesel production in *Chlorella vulgaris* cultivation using silica nanoparticles. *Biotechnol. Bioprocess Eng.* 22, 136–141. doi: 10.1007/s12257-016-0657-8

Juneja, A., and Murthy, G. S. (2017). Evaluating the potential of renewable diesel production from algae cultured on wastewater: techno-economic analysis and life cycle assessment. *Aims Energy* 5, 239–257. doi: 10.3934/energy.2017.2.239

Kefu, Z., Hai, F., San, Z., and Jie, S. (2003). Study on the salt and drought tolerance of *Suaeda salsa* and *Kalanchoe claigremontiana* under iso-osmotic salt and water stress. *Plant Sci.* 165, 837–844. doi: 10.1016/S0168-9452(03)00282-6

Khuram, I., Muhammad, Z., Ahmad, N., Ullah, R., and Barinova, S. (2019). Green and charophyte algae in bioindication of water quality of the shah alam river (District peshawar, Pakistan). *Transylvanian Rev. Syst. Ecol. Res.* 21, 1–16. doi: 10.2478/trser-2019-0001

Koech, A. K., Kumar, A., and Siagi, Z. O. (2020). *In situ* transesterification of *Spirulina* microalgae to produce biodiesel using microwave irradiation. *J. Energy* 1-10. doi: 10.1155/2020/8816296

Kong, X., Ma, J., Le-Clech, P., Wang, Z., Tang, C. Y., and Waite, T. D. (2020). Management of concentrate and waste streams for membrane-based algal separation in water treatment: a review. *Water Res.* 183, 115969. doi: 10.1016/j.watres.2020.115969

Kong, Y., Peng, Y., Zhang, Z., Zhang, M., Zhou, Y., and Duan, Z. (2019). Removal of microcystis aeruginosa by ultrasound: inactivation mechanism and release of algal organic matter. *Ultrason. Sonochem.* 56, 447–457. doi: 10.1016/j.ultsonch.2019.04.017

Konur, O. (2021). "Rapeseed oil-based biodiesel fuels: a review of the research," in *Biodiesel fuels based edible nonedible feed. wastes, algae*, 497–514.

Koyro, H.-W. (2003). "Study of potential cash crop halophytes by a quick check system: determination of the threshold of salinity tolerance and the ecophysiological demands," in *Cash crop halophytes: recent studies* (Springer), 5–17.

Kumar, S., Jain, S., and Kumar, H. (2017). Process parameter assessment of biodiesel production from a jatropha–algae oil blend by response surface methodology and artificial neural network. *Energy sources Part A Recover. Util. Environ. Eff.* 39, 2119–2125.

Lee, J. W., Mets, L., and Greenbaum, E. (2002). "Improvement of photosynthetic CO 2 fixation at high light intensity through reduction of chlorophyll antenna size," in *Biotechnology for fuels and chemicals* (Springer), 37–48.

Leng, L., Wei, L., Xiong, Q., Xu, S., Li, W., Lv, S., et al. (2020). Use of microalgae based technology for the removal of antibiotics from wastewater: a review. *Chemosphere* 238, 124680. doi: 10.1016/j.chemosphere.2019.124680

Li, S., Hu, T., Xu, Y., Wang, J., Chu, R., Yin, Z., et al. (2020c). A review on flocculation as an efficient method to harvest energy microalgae: mechanisms, performances, influencing factors and perspectives. *Renew. Sustain. Energy Rev.* 131, 110005. doi: 10.1016/j.rser.2020.110005

Li, J., Niu, X., Pei, G., Sui, X., Zhang, X., Chen, L., et al. (2015). Identification and metabolomic analysis of chemical modulators for lipid accumulation in *Crypthecodinium cohnii*. *Bioresour. Technol.* 191, 362–368. doi: 10.1016/j.biortech.2015.03.068

Li, H., Watson, J., Zhang, Y., Lu, H., and Liu, Z. (2020a). Environment-enhancing process for algal wastewater treatment, heavy metal control and hydrothermal biofuel production: a critical review. *Bioresour. Technol.* 298, 122421. doi: 10.1016/j.biortech.2019.122421

Li, H., Yan, Z., Li, Y., and Hong, W. (2020b). Latest development in salt removal from solar-driven interfacial saline water evaporator: advanced designs and challenges. *Water Res.*, 115770. doi: 10.1016/j.watres.2020.115770

Liu, H., Lu, Q., Wang, Q., Liu, W., Wei, Q., Ren, H., et al. (2017). Isolation of a bacterial strain, acinetobacter sp. from centrate wastewater and study of its cooperation with algae in nutrients removal. *Bioresour. Technol.* 235, 59–69. doi: 10.1016/j.biortech.2017.03.111

Liu, C.-G., Xiao, Y., Xia, X.-X., Zhao, X.-Q., Peng, L., Srinophakun, P., et al. (2019). Cellulosic ethanol production: progress, challenges and strategies for solutions. *Biotechnol. Adv.* 37, 491–504. doi: 10.1016/j.biotechadv.2019.03.002

Lombardi, T., and Bedini, S. (2020). Seed germination strategies of Mediterranean halophytes under saline condition. *Handb. Halophytes From Mol. to Ecosyst. Towar. Biosaline Agric.* 1–19. doi: 10.1007/978-3-030-17854-3_119-1

Lu, L., Chen, X., Zhu, L., Li, M., Zhang, J., Yang, X., et al. (2020). NtCIPK9: a calcineurin b-like protein-interacting protein kinase from the halophyte *Nitraria tangutorum*, enhances *Arabidopsis* salt tolerance. *Front. Plant Sci.* 11, 1112. doi: 10.3389/fpls.2020.01112

Ma, J., Wang, Z., Zhang, J., Waite, T. D., and Wu, Z. (2017). Cost-effective *Chlorella* biomass production from dilute wastewater using a novel photosynthetic microbial fuel cell (PMFC). *Water Res.* 108, 356–364. doi: 10.1016/j.watres.2016.11.016

Maciel, E., Domingues, P., Domingues, M. R. M., Calado, R., and Lillebø, A. (2020). Halophyte plants from sustainable marine aquaponics are a valuable source of omega-3 polar lipids. *Food Chem.* 320, 126560. doi: 10.1016/j.foodchem.2020.126560

Madsen, M. D., Svejcar, L., Radke, J., and Hulet, A. (2018). Inducing rapid seed germination of native cool season grasses with solid matrix priming and seed extrusion technology. *PloS One* 13, e0204380. doi: 10.1371/journal.pone.0204380

Mao, X., Zhang, Y., Wang, X., and Liu, J. (2020). Novel insights into salinity-induced lipogenesis and carotenogenesis in the oleaginous astaxanthin-producing alga *Chromochloris zofingiensis*: a multi-omics study. *Biotechnol. Biofuels* 13, 1–24. doi: 10.1186/s13068-020-01714-y

Martin-Rivilla, H., Garcia-Villaraco, A., Ramos-Solano, B., Gutierrez-Manero, F. J., and Lucas, J. A. (2020). Improving flavonoid metabolism in blackberry leaves and plant fitness by using the bioeffector *Pseudomonas fluorescens* n 21.4 and its metabolic elicitors: a biotechnological approach for a more sustainable crop. *J. Agric. Food Chem.* 68, 6170–6180. doi: 10.1021/acs.jafc.0c01169

Mayer, A., Tavakoli, H., Fessel Doan, C., Heidari, A., and Handler, R. (2020). Modeling water-energy tradeoffs for cultivating algae for biofuels in a semi-arid region with fresh and brackish water supplies. *Biofuels Bioprod. Biorefining* 14, 1254–1269. doi: 10.1002/bbb.2137

Melis, A. (2009). Solar energy conversion efficiencies in photosynthesis: minimizing the chlorophyll antennae to maximize efficiency. *Plant Sci.* 177, 272–280. doi: 10.1016/j.plantsci.2009.06.005

Meyer, N., Bigalke, A., Kaulfuß, A., and Pohnert, G. (2017). Strategies and ecological roles of algicidal bacteria. *FEMS Microbiol. Rev.* 41, 880–899. doi: 10.1093/femsre/fux029

Miyauchi, H., Okada, K., Fujiwara, S., and Tsuzuki, M. (2020). Characterization of CO2 fixation on algal biofilms with an infrared gas analyzer and importance of a space-rich structure on the surface. *Algal Res.* 46, 101814. doi: 10.1016/j.algal.2020.101814

Mokhtassi-Bidgoli, A., AghaAlikhani, M., and Eyni-Nargeseh, H. (2022). Effects of nitrogen and water on nutrient uptake, oil productivity, and composition of *Descurainia sophia*. *J. Soil Sci. Plant Nutr.* 22, 59–70. doi: 10.1007/s42729-021-00633-7

Morales-Sánchez, D., Schulze, P. S. C., Kiron, V., and Wijffels, R. H. (2020). Production of carbohydrates, lipids and polyunsaturated fatty acids (PUFA) by the polar marine microalga *Chlamydomonas malina* RCC2488. *Algal Res.* 50, 102016. doi: 10.1016/j.algal.2020.102016

Muhammad, G., Alam, M. A., Mofijur, M., Jahirul, M. I., Lv, Y., Xiong, W., et al. (2021). Modern developmental aspects in the field of economical harvesting and biodiesel production from microalgae biomass. *Renew. Sustain. Energy Rev.* 135, 110209. doi: 10.1016/j.rser.2020.110209

Müller, M. N., Mardones, J. I., and Dorantes-Aranda, J. J. (2020). Harmful algal blooms (HABs) in Latin America. *Front. Mar. Sci.* 7, 34. doi: 10.3389/fmars.2020.00034

Munir, N., Abideen, Z., and Sharif, N. (2020). Development of halophytes as energy feedstock by applying genetic manipulations. *All Life* 13, 1–10. doi: 10.1080/21553769.2019.1595745

Munir, N., Hasnain, M., Roessner, U., and Abideen, Z. (2021). Strategies in improving plant salinity resistance and use of salinity resistant plants for economic sustainability. *Crit. Rev. Environ. Sci. Technol.* 52 (12), 2150–2196.

Munir, N., Hasnain, M., Sarwar, Z., Ali, F., Hessini, K., and Abideen, Z. (2022). Changes in environmental conditions are critical factors for optimum biomass, lipid pattern and biodiesel production in algal biomass. *Biologia* 77 (11), 3099–3124. 1–26. doi: 10.1007/s11756-022-01191-8

Mussgnug, J. H., Thomas-Hall, S., Rupprecht, J., Foo, A., Klassen, V., McDowall, A., et al. (2007). Engineering photosynthetic light capture: impacts on improved solar energy to biomass conversion. *Plant Biotechnol. J.* 5, 802–814. doi: 10.1111/j.1467-7652.2007.00285.x

Naira, V. R., Das, D., and Maiti, S. K. (2020). A novel bubble-driven internal mixer for improving productivities of algal biomass and biodiesel in a bubble-column photobioreactor under natural sunlight. *Renew. Energy* 157, 605–615. doi: 10.1016/j.renene.2020.05.079

Najjar, Y. S. H., and Abu-Shamleh, A. (2020). Harvesting of microalgae by centrifugation for biodiesel production: a review. *Algal Res.* 51, 102046. doi: 10.1016/j.algal.2020.102046

Narayanasamy, P., Balasundar, P., Senthil, S., Sanjay, M. R., Siengchin, S., Khan, A., et al. (2020). Characterization of a novel natural cellulosic fiber from *Calotropis gigantea* fruit bunch for ecofriendly polymer composites. *Int. J. Biol. Macromol.* 150, 793–801. doi: 10.1016/j.ijbiomac.2020.02.134

Nayak, S. S., Pradhan, S., Sahoo, D., and Parida, A. (2020). *De novo* transcriptome assembly and analysis of *Phragmites karka*, an invasive halophyte, to study the mechanism of salinity stress tolerance. *Sci. Rep.* 10, 1–12. doi: 10.1038/s41598-020-61857-8

Negi, S., Perrine, Z., Friedland, N., Kumar, A., Tokutsu, R., Minagawa, J., et al. (2020). Light regulation of light-harvesting antenna size substantially enhances photosynthetic efficiency and biomass yield in green algae. *Plant J.* 103, 584–603. doi: 10.1111/tpj.14751

Niu, X., Xu, S., Yang, Q., Xu, X., Zheng, M., Li, X., et al. (2021). Toxic effects of the dinoflagellate *Karenia mikimotoi* on zebrafish (Danio rerio) larval behavior. *Harm. Algae* 103, 101996. doi: 10.1016/j.hal.2021.101996

Norsker, N.-H., Barbosa, M. J., Vermuë, M. H., and Wijffels, R. H. (2011). Microalgal production–a close look at the economics. *Biotechnol. Adv.* 29, 24–27. doi: 10.1016/j.biotechadv.2010.08.005

Nouri, H., Mohammadi Roushandeh, J., Hallajisani, A., Golzary, A., and Daliry, S. (2021). The effects of glucose, nitrate, and pH on cultivation of *Chlorella* sp. microalgae. *Glob. J. Environ. Sci. Manage.* 7, 103–116.

Nyström, P. (2017). "Ecological impact of introduced and native crayfish on freshwater communities: European perspectives," in *Crayfish in Europe as alien species* (Routledge), 63–85.

Oostlander, P. C., van Houcke, J., Wijffels, R. H., and Barbosa, M. J. (2020). Microalgae production cost in aquaculture hatcheries. *Aquaculture* 525, 735310. doi: 10.1016/j.aquaculture.2020.735310

Pal, D., Khozin-Goldberg, I., Cohen, Z., and Boussiba, S. (2011). The effect of light, salinity, and nitrogen availability on lipid production by *Nannochloropsis* sp. *Appl. Microbiol. Biotechnol.* 90, 1429–1441. doi: 10.1007/s00253-011-3170-1

Palchetti, M. V., Llanes, A., Reginato, M., Barboza, G., Luna, V., and Cantero, J. J. (2020). Germination responses of lycium humile, an extreme halophytic *Solanaceae*: understanding its distribution in saline mudflats of the southern puna. *Acta Bot. Brasilica* 34, 540–548. doi: 10.1590/0102-33062020abb0034

Pang, M., Xu, J., Qu, P., Mao, X., Wu, Z., Xin, M., et al. (2017). Effect of CO2 on growth and toxicity of *Alexandrium tamarense* from the East China Sea, a major producer of paralytic shellfish toxins. *Harm. Algae* 68, 240–247. doi: 10.1016/j.hal.2017.08.008

Park, J., Son, Y., and Lee, W. H. (2019). Variation of efficiencies and limits of ultrasonication for practical algal bloom control in fields. *Ultrason. Sonochem.* 55, 8–17. doi: 10.1016/j.ultsonch.2019.03.007

Patel, D., Shittu, T. A., Baroncelli, R., Muthumeenakshi, S., Osborne, T. H., Janganan, T. K., et al. (2021). Genome sequence of the biocontrol agent *Coniothyrium minitans* conio (IMI 134523). *Mol. Plant-Microbe Interact.* 34, 222–225. doi: 10.1094/MPMI-05-20-0124-A

Pedrini, S., Balestrazzi, A., Madsen, M. D., Bhalsing, K., Hardegree, S. P., Dixon, K. W., et al. (2020). Seed enhancement: getting seeds restoration-ready. *Restor. Ecol.* 28, S266–S275. doi: 10.1111/rec.13184

Pei, X.-Y., Ren, H.-Y., and Liu, B.-F. (2021). Flocculation performance and mechanism of fungal pellets on harvesting of microalgal biomass. *Bioresour. Technol.* 321, 124463. doi: 10.1016/j.biortech.2020.124463

Petrie, J. R., Zhou, X.-R., Leonforte, A., McAllister, J., Shrestha, P., Kennedy, Y., et al. (2020). Development of a *Brassica napus* (Canola) crop containing fish oil-like levels of DHA in the seed oil. *Front. Plant Sci.* 11, 727. doi: 10.3389/fpls.2020.00727

Priyadharsini, P., Nirmala, N., Dawn, S. S., Baskaran, A., SundarRajan, P., Gopinath, K. P., et al. (2022). Genetic improvement of microalgae for enhanced carbon dioxide sequestration and enriched biomass productivity: review on CO2 bio-fixation pathways modifications. *Algal Res.* 66, 102810. doi: 10.1016/j.algal.2022.102810

Prudkin-Silva, C., Lanzarotti, E., Álvarez, L., Vallerga, M. B., Factorovich, M., Morzan, U. N., et al. (2021). A cost-effective algae-based biosensor for water quality analysis: development and testing in collaboration with peasant communities. *Environ. Technol. Innov.* 101479. doi: 10.1016/j.eti.2021.101479

Qasim, M., Abideen, Z., Adnan, M. Y., Ansari, R., Gul, B., and Khan, M. A. (2014). Traditional ethnobotanical uses of medicinal plants from coastal areas. *J. Coast. Life Med.* 2, 22–30.

Qiu, R., Gao, S., Lopez, P. A., and Ogden, K. L. (2017). Effects of pH on cell growth, lipid production and CO2 addition of microalgae *Chlorella sorokiniana*. *Algal Res.* 28, 192–199. doi: 10.1016/j.algal.2017.11.004

Rahman, A., Agrawal, S., Nawaz, T., Pan, S., and Selvaratnam, T. (2020). A review of algae-based produced water treatment for biomass and biofuel production. *Water* 12, 2351. doi: 10.3390/w12092351

Randhir, A., Laird, D. W., Maker, G., Trengove, R., and Moheimani, N. R. (2020). Microalgae: a potential sustainable commercial source of sterols. *Algal Res.* 46, 101772. doi: 10.1016/j.algal.2019.101772

Ren, L.-J., Sun, G., Ji, X.-J., Hu, X., and Huang, H. (2014). Compositional shift in lipid fractions during lipid accumulation and turnover in *Schizochytrium* sp. *Bioresour. Technol.* 157, 107–113. doi: 10.1016/j.biortech.2014.01.078

Resurreccion, E. P., Colosi, L. M., White, M. A., and Clarens, A. F. (2012). Comparison of algae cultivation methods for bioenergy production using a combined life cycle assessment and life cycle costing approach. *Bioresour. Technol.* 126, 298–306. doi: 10.1016/j.biortech.2012.09.038

Riaz, T., Iqbal, M. W., Mahmood, S., Yasmin, I., Leghari, A. A., Rehman, A., et al. (2021). Cottonseed oil: a review of extraction techniques, physicochemical, functional, and nutritional properties. *Crit. Rev. Food Sci. Nutr.* 63 (9), 1219–1237.

Richards, D. C. (2019). "Zooplankton assemblages in highly regulated Utah lake: 2015-2018," in *Prog. rep. to wasatch front water qual. counc* (Salt Lake City, UT: OreoHelix Consult. Vineyard, UT).

Rogers, M.-J. E., Craig, A. D., Colmer, T. D., Munns, R., Hughes, S. J., Nichols, P. G. H., et al. (2020). *Suitable species for the reclamation and sustainability of saline land in southern Australia*.

Roostaei, J., Zhang, Y., Gopalakrishnan, K., and Ochocki, A. J. (2018). Mixotrophic microalgae biofilm: a novel algae cultivation strategy for improved productivity and cost-efficiency of biofuel feedstock production. *Sci. Rep.* 8, 1–10. doi: 10.1038/s41598-018-31016-1

Ruan, C.-J., Li, H., Guo, Y.-Q., Qin, P., Gallagher, J. L., Seliskar, D. M., et al. (2008). *Kosteletzkya virginica*, an agroecoengineering halophytic species for alternative agricultural production in china's east coast: ecological adaptation and benefits, seed yield, oil content, fatty acid and biodiesel properties. *Ecol. Eng.* 32, 320–328. doi: 10.1016/j.ecoleng.2007.12.010

Saengsawang, B., Bhuyar, P., Manmai, N., Ponnusamy, V. K., Ramaraj, R., and Unpaprom, Y. (2020). The optimization of oil extraction from macroalgae, *Rhizoclonium* sp. by chemical methods for efficient conversion into biodiesel. *Fuel* 274, 117841.

Sahin, M. S., Khazi, M. I., Demirel, Z., and Dalay, M. C. (2019). Variation in growth, fucoxanthin, fatty acids profile and lipid content of marine diatoms *Nitzschia* sp. and *Nanofrustulum shiloi* in response to nitrogen and iron. *Biocatal. Agric. Biotechnol.* 17, 390–398. doi: 10.1016/j.bcab.2018.12.023

Salimon, J., Noor, D. A. M., Nazrizawati, A., and Noraishah, A. (2010). Fatty acid composition and physicochemical properties of Malaysian castor bean *Ricinus communis* l. seed oil. *Sains Malaysiana* 39.

Santos, J., Al-Azzawi, M., Aronson, J., and Flowers, T. J. (2016). eHALOPH a database of salt-tolerant plants: helping put halophytes to work. *Plant Cell Physiol.* 57 (1). doi: 10.1093/pcp/pcv155

Sero, E. T., Siziba, N., Bunhu, T., Shoko, R., and Jonathan, E. (2020). Biophotonics for improving algal photobioreactor performance: a review. *Int. J. Energy Res.* 44, 5071–5092. doi: 10.1002/er.5059

Serpe, M. D., Thompson, A., and Petzinger, E. (2020). Effects of a companion plant on the formation of mycorrhizal propagules in *Artemisia tridentata* seedlings. *Rangel. Ecol. Manage.* 73, 138–146. doi: 10.1016/j.rama.2019.09.002

Serrà, A., Artal, R., Garcia-Amoros, J., Gómez, E., and Philippe, L. (2020). Circular zero-residue process using microalgae for efficient water decontamination, biofuel production, and carbon dioxide fixation. *Chem. Eng. J.* 388, 124278. doi: 10.1016/j.cej.2020.124278

Severes, A., Hegde, S., D'Souza, L., and Hegde, S. (2017). Use of light emitting diodes (LEDs) for enhanced lipid production in micro-algae based biofuels. *J. Photochem. Photobiol. B Biol.* 170, 235–240. doi: 10.1016/j.jphotobiol.2017.04.023

Sharif, N., Munir, N., Hasnain, M., Naz, S., and Arshad, M. (2021). "Environmental impacts of ethanol production system," in *Sustainable ethanol and climate change* (Springer), 205–223.

Sheehan, C. E., Baker, K. G., Nielsen, D. A., and Petrou, K. (2020). Temperatures above thermal optimum reduce cell growth and silica production while increasing cell volume and protein content in the diatom *Thalassiosira pseudonana*. *Hydrobiologia* 847, 4233–4248. doi: 10.1007/s10750-020-04408-6

Sivakaminathan, S., Wolf, J., Yarnold, J., Roles, J., Ross, I. L., Stephens, E., et al. (2020). Light guide systems enhance microalgae production efficiency in outdoor high rate ponds. *Algal Res.* 47, 101846. doi: 10.1016/j.algal.2020.101846

Staples, T. L., Mayfield, M. M., England, J. R., and Dwyer, J. M. (2020). Comparing the recovery of richness, structure, and biomass in naturally regrowing and planted reforestation. *Restor. Ecol.* 28, 347–357. doi: 10.1111/rec.13077

Subaşı, B. G., Casanova, F., Capanoglu, E., Ajalloueian, F., Sloth, J. J., and Mohammadifar, M. A. (2020). Protein extracts from de-oiled sunflower cake: structural, physico-chemical and functional properties after removal of phenolics. *Food Biosci.* 38, 100749. doi: 10.1016/j.fbio.2020.100749

Sun, C.-H., Fu, Q., Liao, Q., Xia, A., Huang, Y., Zhu, X., et al. (2019). Life-cycle assessment of biofuel production from microalgae *via* various bioenergy conversion systems. *Energy* 171, 1033–1045. doi: 10.1016/j.energy.2019.01.074

Sun, R., Sun, P., Zhang, J., Esquivel-Elizondo, S., and Wu, Y. (2018). Microorganisms-based methods for harmful algal blooms control: a review. *Bioresour. Technol.* 248, 12–20. doi: 10.1016/j.biortech.2017.07.175

Suryani, S., Sariani, S., Earnestly, F., Marganof, M., Rahmawati, R., Sevindrajuta, S., et al. (2020). A comparative study of virgin coconut oil, coconut oil and palm oil in terms of their active ingredients. *Processes* 8, 402. doi: 10.3390/pr8040402

Talaei, M., Mahdavinejad, M., and Azari, R. (2020). Thermal and energy performance of algae bioreactive façades: a review. *J. Build. Eng.* 28, 101011. doi: 10.1016/j.jobe.2019.101011

Tan, X.-B., Meng, J., Tang, Z., Yang, L.-B., and Zhang, W.-W. (2020). Optimization of algae mixotrophic culture for nutrients recycling and biomass/lipids production in anaerobically digested waste sludge by various organic acids addition. *Chemosphere* 244, 125509. doi: 10.1016/j.chemosphere.2019.125509

Tao, R., Bair, R., Lakaniemi, A.-M., van Hullebusch, E. D., and Rintala, J. A. (2019). Use of factorial experimental design to study the effects of iron and sulfur on growth of *Scenedesmus acuminatus* with different nitrogen sources. *J. Appl. Phycol.*, 1–11. 32, 221–231.

Tipnee, S., Ramaraj, R., and Unpaprom, Y. (2015). Nutritional evaluation of edible freshwater green macroalga *Spirogyra varians*. *Emergent Life Sci. Res.* 1, 1–7.

Tıpırdamaz, R., Karakas, S., and Dikilitas, M. (2020). Halophytes and the future of agriculture. *Handb. Halophytes From Mol. to Ecosyst. Towar. Biosaline Agric.*, 1–15.

Toqeer, S., Qasim, M., Abideen, Z., Gul, B., Rasheed, M., and Khan, M. A. (2018). Chemical composition and antioxidant activity of seeds of various halophytic grasses. *J. Am. Oil Chem. Soc* 95, 1285–1295. doi: 10.1002/aocs.12099

Touliabah, H. E., Abdel-Hamid, M. I., and Almutairi, A. W. (2020). Long-term monitoring of the biomass and production of lipids by *Nitzschia palea* for biodiesel production. *Saudi J. Biol. Sci.* 27, 2038–2046. doi: 10.1016/j.sjbs.2020.04.014

Turcios, A. E., Cayenne, A., Uellendahl, H., and Papenbrock, J. (2021). Halophyte plants and their residues as feedstock for biogas production–chances and challenges. *Appl. Sci.* 11, 2746. doi: 10.3390/app11062746

Vadlamani, A., Viamajala, S., Pendyala, B., and Varanasi, S. (2017). Cultivation of microalgae at extreme alkaline pH conditions: a novel approach for biofuel production. *ACS Sustain. Chem. Eng.* 5, 7284–7294. doi: 10.1021/acssuschemeng.7b01534

Vo, H. N. P., Ngo, H. H., Guo, W., Chang, S. W., Nguyen, D. D., Chen, Z., et al. (2020). Microalgae for saline wastewater treatment: a critical review. *Crit. Rev. Environ. Sci. Technol.* 50, 1224–1265. doi: 10.1080/10643389.2019.1656510

Vu, H. P., Nguyen, L. N., Zdarta, J., Nga, T. T. V., and Nghiem, L. D. (2020). Blue-green algae in surface water: problems and opportunities. *Curr. pollut. Rep.* 6, 105–122. doi: 10.1007/s40726-020-00140-w

Wang, S., Liu, S., Wang, J., Yokosho, K., Zhou, B., Yu, Y.-C., et al. (2020b). Simultaneous changes in seed size, oil content and protein content driven by selection of SWEET homologues during soybean domestication. *Natl. Sci. Rev.* 7, 1776–1786. doi: 10.1093/nsr/nwaa110

Wang, J., Xiong, Y., Zhang, J., Lu, X., and Wei, G. (2020a). Naturally selected dominant weeds as heavy metal accumulators and excluders assisted by rhizosphere bacteria in a mining area. *Chemosphere* 243, 125365. doi: 10.1016/j.chemosphere.2019.125365

Wei, J., Gao, L., Shen, G., Yang, X., and Li, M. (2020). The role of adsorption in microalgae biological desalination: salt removal from brackish water using *Scenedesmus obliquus*. *Desalination* 493, 114616. doi: 10.1016/j.desal.2020.114616

Wei, L., Huang, X., and Huang, Z. (2015). Temperature effects on lipid properties of microalgae *Tetraselmis subcordiformis* and *Nannochloropsis oculata* as biofuel resources. *Chin. J. Oceanol. Limnol.* 33, 99–106. doi: 10.1007/s00343-015-3346-0

Xu, H., Liu, Y., Tang, Z., Li, H., Li, G., and He, Q. (2020a). Methane production in harmful algal blooms collapsed water: the contribution of non-toxic *Microcystis aeruginosa* outweighs that of the toxic variety. *J. Clean. Prod.* 276, 124280. doi: 10.1016/j.jclepro.2020.124280

Xu, Z., Shao, T., Lv, Z., Yue, Y., Liu, A., Long, X., et al. (2020b). The mechanisms of improving coastal saline soils by planting rice. *Sci. Total Environ.* 703, 135529. doi: 10.1016/j.scitotenv.2019.135529

Yasin Ashraf, M., Awan, A. R., Anwar, S., Khaliq, B., Malik, A., and Ozturk, M. (2020). Economic utilization of salt-affected wasteland for plant production: a case study from Pakistan. *Handb. Halophytes From Mol. to Ecosyst. Towar. Biosaline Agric.*, 1–24. doi: 10.1007/978-3-030-17854-3_87-1

Yeo, A. R., Yeo, M. E., Flowers, S. A., and Flowers, T. J. (1990). Screening of rice (*Oryza sativa* l.) genotypes for physiological characters contributing to salinity resistance, and their relationship to overall performance. *Theor. Appl. Genet.* 79, 377–384. doi: 10.1007/BF01186082

Yilancioglu, K., Cokol, M., Pastirmaci, I., Erman, B., and Cetiner, S. (2014). Oxidative stress is a mediator for increased lipid accumulation in a newly isolated *Dunaliella salina* strain. *PloS One* 9, e91957. doi: 10.1371/journal.pone.0091957

Yuasa, K., Shikata, T., Ichikawa, T., Tamura, Y., and Nishiyama, Y. (2020). Nutrient deficiency stimulates the production of superoxide in the noxious red-tide-forming raphidophyte *Chattonella antiqua*. *Harm. Algae* 99, 101938. doi: 10.1016/j.hal.2020.101938

Zamani-Ahmadmahmoodi, R., Malekabadi, M. B., Rahimi, R., and Johari, S. A. (2020). Aquatic pollution caused by mercury, lead, and cadmium affects cell growth and pigment content of marine microalga, *Nannochloropsis oculata*. *Environ. Monit. Assess.* 192, 1–11. doi: 10.1007/s10661-020-8222-5

Zapata-Sifuentes, G., Preciado-Rangel, P., Guillén-Enríquez, R. R., Bernal, F. S., Holguin-Peña, R. J., Borbón-Morales, C., et al. (2021). Lipid and yield evaluation in *Salicornia bigelovii* by the influence of chitosan-IBA, in conditions of the Sonora desert. *Agronomy* 11, 428. doi: 10.3390/agronomy11030428

Zedler, J. B., and Kercher, S. (2004). Causes and consequences of invasive plants in wetlands: opportunities, opportunists, and outcomes. *CRC. Crit. Rev. Plant Sci.* 23, 431–452. doi: 10.1080/07352680490514673

Zerrifi, S. E. A., El Khalloufi, F., Oudra, B., and Vasconcelos, V. (2018). Seaweed bioactive compounds against pathogens and microalgae: potential uses on pharmacology and harmful algae bloom control. *Mar. Drugs* 16, 55. doi: 10.3390/md16020055

Zhang, Y. F., Li, Y. P., Sun, J., and Huang, G. H. (2020). Optimizing water resources allocation and soil salinity control for supporting agricultural and environmental sustainable development in central Asia. *Sci. Total Environ.* 704, 135281. doi: 10.1016/j.scitotenv.2019.135281

Zhang, L., Pei, H., Chen, S., Jiang, L., Hou, Q., Yang, Z., et al. (2018). Salinity-induced cellular cross-talk in carbon partitioning reveals starch-to-lipid biosynthesis switching in low-starch freshwater algae. *Bioresour. Technol.* 250, 449–456. doi: 10.1016/j.biortech.2017.11.067

Zhao, L., Peng, C., Zhang, J., and Tang, Z. (2021). Synergistic effect of microbubble flow and light fields on a bionic tree-like photobioreactor. *Chem. Eng. Sci.* 229, 116092. doi: 10.1016/j.ces.2020.116092

Zheng, Y., Pan, Z., Zhang, R., Labavitch, J. M., Wang, D., Teter, S. A., et al. (2007). "Evaluation of different biomass materials as feedstock for fermentable sugar production," in *Applied biochemistry and biotecnology* (Springer), 423–435.

Zingone, A., Escalera, L., Aligizaki, K., Fernández-Tejedor, M., Ismael, A., Montresor, M., et al. (2020). Toxic marine microalgae and noxious blooms in the Mediterranean Sea: a contribution to the global HAB status report. *Harm. Algae*, 101843.

Zoghlami, A., and Paës, G. (2019). Lignocellulosic biomass: understanding recalcitrance and predicting hydrolysis. *Front. Chem.* 7, 874. doi: 10.3389/fchem.2019.00874

# Frontiers in
# Plant Science

**Cultivates the science of plant biology and its applications**

The most cited plant science journal, which advances our understanding of plant biology for sustainable food security, functional ecosystems and human health.

---

## Discover the latest Research Topics

See more →

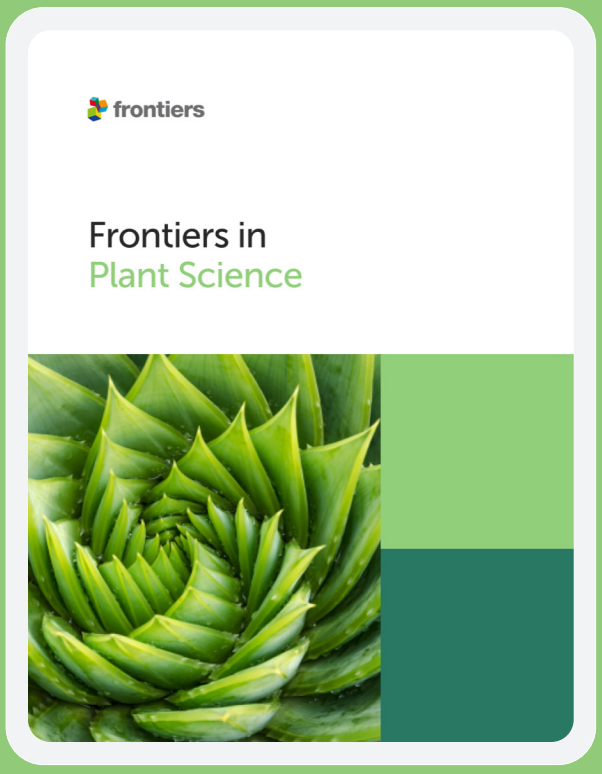


**Frontiers**

Avenue du Tribunal-Fédéral 34
1005 Lausanne, Switzerland
frontiersin.org

**Contact us**

+41 (0)21 510 17 00
frontiersin.org/about/contact